University of Alberta

Stratigraphy, paleogeography and tectonic evolution of early Paleozoic to Triassic pericratonic strata in the northern Kootenay Arc, southeastern Canadian Cordillera, British Columbia

by

Jamie Lorne Kraft

A thesis submitted to the Faculty of Graduate Studies and Research
in partial fulfillment of the requirements for the degree of

Doctor of Philosophy

Earth and Atmospheric Sciences

Spring 2013
Edmonton, Alberta

Abstract

The northern Kootenay Arc in southeastern British Columbia hosts a near-continuous succession of Cambrian to Permian strata that were deposited in overlapping marginal basins outboard of the Canadian Cordilleran miogeocline. The basinal strata of the Late Cambrian and younger Lardeau Group are conformably overlain by a succession of Devonian and Early Mississippian strata herein named the Mount Sproat assemblage. The Mount Sproat assemblage comprises an undated carbonaceous lower unit that passes upward into a lithologically diverse succession of siliciclastic, carbonate and mafic metavolcanic strata that have geochemical signatures recording a transition from non-arc to arc-related volcanism. Calc-alkaline basalt in the Mount Sproat assemblage yielded prismatic zircon dated at 367.2 ± 2 Ma. The Mount Sproat assemblage is truncated by an angular unconformity at the base of the Late Mississippian Milford Group. Lower stratigraphic levels of the Mount Sproat assemblage were deformed penetratively with the Lardeau Group prior to deposition of the Milford Group. The Thompson assemblage (new term) is a localized sedimentary succession between the Viséan Milford Group and the Broadview Formation (Lardeau Group) at Mount Thompson. It was deposited after Early Mississippian deformation of the Lardeau Group and was partially eroded into the overlying the Milford Group.

Detrital zircon dates in the intervals 2.8-2.6 Ga and 2.1-1.75 Ga link the Lardeau Group, Mount Sproat assemblage, Thompson assemblage and Milford

Group to the Canadian Cordilleran miogeocline. Detrital zircon data also reveal sources of zircon that were not available to the miogeocline. The Broadview Formation is interpreted to record uplift of an outer high of sialic North American crust that contained zircon in the intervals 1.48-1.41 Ga, 1.38-1.32 Ga, and 1.30-0.95 Ga in addition to ages typical of the adjacent miogeocline. Palinspastic restoration of this margin places the edge of attenuated North American cratonic crust near the present day coastline of southern British Columbia. In Late Devonian to Late Triassic time, detrital zircon grains with Neoproterozoic (700-550 Ma) and Silurian (ca. 420 Ma) dates appear in the dataset. These dates are interpreted to originate from an exotic terrane that docked in mid-Devonian time.

Acknowledgments

There is a very long list of people to whom I owe thanks for their various roles in helping me complete this project. I hope I cover most of them, but so many people have contributed – whether by inspiring me or encouraging me, teaching me or aiding me – that I simply cannot acknowledge them all here.

I would like to thank Bob Thompson for his mentorship, perennial encouragement, and friendship. This project was largely his creation and I wouldn't have spent three fantastic summers working in the Selkirks if not for his involvement. And I owe many thanks to Bryce Jablonski, Ryley Tapping, and Kyle Laird for putting up with long days, steep, bushy mountainsides, and bears (especially you Kyle: you definitely got the 'best' bear encounter) as my field assistants. You guys were a pleasure to work with so thanks for your part in this.

To my friends and colleagues at the University of Alberta, you truly enriched my experience and made grad school worth doing. Thank you Shawna for being my best friend. Thank you Brian and Christine for being the best housemates ever.

I wish to thank Tony Simonetti and Andy Dufrane for guiding me through the use of a first-class laser ablation lab and teaching me how to process the millions of pages of data (okay, thousands…). Thank you Tom Chacko and Larry Heaman for serving on my supervisory committee and for the important role each of you played.

Thanks Matt Callaghan at Arrow Helicopters, Revelstoke, and Mark Homis at Highland Helicopters, Nakusp, for delivering me to the middle of nowhere and bringing me safely home again.

Thank you to my supervisor, Philippe Erdmer, for teaching me how to write with half the words and twice the strength. I owe thanks to Bob Anderson and the Geological Survey of Canada for financial and logistical support for my field work.

Mom and Dad, thank you both for providing a perfect balance of loving encouragement and the odd gentle reminder to keep me going when my pace slowed. Thank you, Sarah, for being the perfect supportive partner and helping me succeed in the final months of this project. And finally, I extend my gratitude to my coworkers, managers, friends at Teck Resources for their support while I completed this project.

Thank you.

Table of Contents

Table of Figures

Chapter 1: Introduction

1.1 Purpose

This thesis examines the stratigraphy, geological relationships and detrital zircon provenance of early Paleozoic to Triassic metasedimentary and metavolcanic strata in the Selkirk Mountains of southeastern British Columbia. It aims to test hypotheses about Cordilleran evolution, which are outlined below, and to address unresolved questions about the tectonic evolution and paleogeography of the Paleozoic Cordilleran margin.

The Canadian segment of the Cordilleran orogen has been considered either as a type example of crustal growth by terrane accretion, whereby oceanic arcs were added to the edge of the North American plate (e.g. Monger et al., 1982), or alternatively as a heterogeneously extended and reworked plate margin upon which continental arcs formed (e.g. Struik, 1987; Thompson et al., 2006). Data from stratigraphic, tectonic, provenance, geochronological, paleomagnetic and paleontological studies have led to conflicting hypotheses regarding the paleogeographic evolution of the Canadian Cordillera (e.g., Monger and Price, 2002; Thompson et al., 2006; Wright and Wyld, 2006; Johnston, 2008; Colpron and Nelson, 2009) and the paleogeography of many of the Cordilleran rock assemblages remains uncertain (Figure 1-1). Thorough characterization of the inboard regions of the Cordillera – the pericratonic assemblages – provides an essential foundation from which to interpret the paleogeography and affinity of outboard assemblages and terranes. With a basic understanding of the pre-orogenic (pre-Jurassic) configuration of the Cordilleran margin one can begin to address the question of the degree to which Cordilleran crust has grown by accretion versus magmatic and tectonic reworking. I present below the questions about the pre-Jurassic history of the Canadian Cordillera that this research sought to address.

1.2 Research questions

Do equivalents of Late Devonian-Early Mississippian continental margin strata in the North Okanagan-Shuswap region ("Eagle Bay assemblage" of Schiarizza and Preto, 1987, and "Mount Ida Group" of Jones, 1959) exist in the northern Kootenay Arc as hypothesized by Thompson et al. (2006)?

Lemieux (2006) and Thompson et al. (2006) proposed that the late Paleozoic stratigraphy of the Vernon map area has equivalents in the Kootenay Arc near

Upper Arrow Lake. In addition to significant paleogeographic implications expounded below, this correlation would increase the interpreted economic prospectivity of the pericratonic rocks of the northern Selkirk Mountains, which are a target of modern base metal exploration. Estimation of the economic prospectivity of these Paleozoic strata relies on interpretations of depositional settings, regional correlations and tectonic history of the rocks.

How significant are the hypothetical terrane boundaries between upper Paleozoic rock assemblages of the southeastern Canadian Cordillera? Are these assemblages truly terranes in the sense of Coney et al. (1980)?

Upper Paleozoic rocks in the Selkirk Mountains and Okanagan-Shuswap region of British Columbia interpreted to have deposited in pericratonic basins have been assigned to as many as four different terranes (Klepacki, 1985; Monger and Berg, 1987; Wheeler and McFeely, 1991; Colpron and Nelson, 2009), despite a number of proposed correlations across hypothetical terrane boundaries (e.g. Klepacki, 1985; Thompson et al., 2006). These include the Kootenay, Slide Mountain, Okanagan, and Quesnel terranes depicted in Figure 1-2. The Milford Group is an assemblage of Carboniferous sedimentary and basaltic rocks that has been assigned in part to two different terranes (Figure 1-3). If the assemblages do not fit the definition of a terrane then nomenclature must be updated to match the present understanding of the geology of the region. The concept and definition of terranes is described below under Terminology and Definitions.

When were the extensional events attributed to Lardeau Group grits and volcanic rocks (e.g. Logan and Colpron, 2006)?

The Cambrian to pre-Late Mississippian Lardeau Group (Fyles and Eastwood, 1962; Read and Wheeler, 1976) is a deep-water volcanic-sedimentary succession that conformably overlies the Lower Cambrian miogeocline in southeastern British Columbia (Colpron and Price, 1995). It was deposited in a margin-parallel basin, called the Lardeau trough, outboard of coeval miogeoclinal sedimentary rocks (Figure 1-4A; Logan and Colpron, 2006). Two episodes of significant crustal extension or transtension interpreted from data of the Lardeau Group were inferred to have occurred in the early Paleozoic (Logan and Colpron, 2006); however age constraints available prior to this study (Read and Wheeler, 1976; Klepacki and Wheeler, 1985; Parrish, 1992; Logan and Colpron, 2006) allowed that these events could have occurred any time from the late Cambrian to the Late Devonian. In a conventional Wilson Cycle framework, the Cordilleran margin should have been tectonically passive in the interval between latest Proterozoic opening of the Cordilleran margin (at ca. 575 Ma; Bond and Kominz, 1984; Colpron et al., 2002) and mid- to Late Devonian initiation of convergence along western North America (Rubin et al., 1990). Evidence of Cambrian and Ordovician extension and mafic volcanism from the Cordilleran miogeocline (e.g., Cecile et al., 1997) support a hypothesis of intermittent extension during the 'drift' phase of Cordilleran margin evolution. Whether data from the Lardeau Group corroborates the idea of protracted extension into the early Paleozoic or instead records tectonism associated with Devonian initiation of an active margin cannot be determined from prior data.

When and how did the pre-Milford fabric in the Lardeau Group form? Was pre-Milford deformation in the Kootenay Arc a northern counterpart of the (Late Devonian-?) Early Mississippian Antler orogeny of the U.S. Cordillera (e.g. Smith et al., 1993), or other mid-Paleozoic Cordilleran events (e.g. Root, 1987; Colpron et al., 2006a), or does it record a separate event?

During the latest Devonian and Early Mississippian, the Antler (Poole, 1974; Smith and Ketner, 1977; Carpenter et al., 1993) and Ellesmerian (Thorsteinsson and Tozer, 1970; Trettin et al., 1991) orogenies simultaneously reworked the Arctic Canadian and central U.S. margins of the North American plate while the intervening segment in northern British Columbia and southern Yukon possibly experienced an extensional (Gordey et al., 1987) and (or) transtensional regime (Eisbacher, 1983). Some workers have argued that mid- and Late Devonian compression affected the entire Cordilleran margin (Smith et al., 1993; Root, 2001). The Lardeau Group uniquely preserves a fabric from a poorly understood pre-Late Mississippian Milford Group deformation event (Wheeler, 1968; Read and Wheeler, 1976; Klepacki, 1985) that has been speculatively correlated with the Antler orogeny (Smith et al., 1993). Alternatively, prior data permit that early deformation of the Lardeau Group was coeval with older compressional events documented within the Canadian Cordillera (Middle Devonian in the Purcell Mountains, Root, 1987; Early Paleozoic in Alexander terrane, Gehrels and Saleeby, 1987, and Chilliwack Composite terrane, Brown et al, 2010). Better constraint on the timing of the pre-Milford deformation is necessary to incorporate this event into models of Cordilleran evolution.

Why is pre-Milford fabric well developed in the Lardeau Group in the northern Kootenay Arc but absent from (or not evident in) pre-Lardeau strata and Lardeau Group *rocks to the north?*

The cause of pre-Milford deformation in the Lardeau Group is unclear because of a paucity of evidence constraining the timing, nature and extent of the deformation. The penetrative deformation associated with pre-Milford deformation of the Lardeau Group indicates a penetrative event affected the Cordilleran margin, but corroborating evidence from other parts of the southern Canadian Cordillera are sparse. Hypothesized Middle Devonian collision of an exotic terrane ("Okanagan terrane") has been suggested as a cause of pre-Milford deformation in the Kootenay Arc and Purcell Mountains (Colpron and Nelson, 2009), but no description of the event has been offered. Was the event regional or local in extent? In what tectonic environment did it take place?

Do Grenville-aged granitic clasts and detrital zircon grains in the southern Canadian Cordillera record an intra-Cordilleran block of Grenville-aged crust upon which late Paleozoic arcs formed (e.g. Erdmer et al., 2002; Lemieux et al., 2007), or was exotic Grenville-aged crust translated into the Cordilleran realm in the mid-Paleozoic (e.g. Colpron and Nelson, 2009)?

Modern studies of the North American Cordillera have shown that a small proportion of Cordilleran strata have features that are more similar to Iapetan geology in eastern North America and Europe than they are to western North America, suggesting an exotic affinity (Wright and Wyld, 2006; Grove et al., 2008; Colpron and Nelson, 2009; 2011). Detritus of Grenville province age (ca. 1.3-1.0 Ga) in particular is rare in the Cordilleran miogeocline between Mexico and Yukon but increasingly is being found in pericratonic and outboard assemblages in the Canadian Cordillera (Gehrels and Ross, 1998; Erdmer et al., 2002; Ross et al., 2005; Lemieux et al., 2007; Milidragovic et al., 2007). Evidence of exotic affinities of pre-Mississippian Cordilleran rocks include: detrital zircon populations similar to rocks of Iapetan or Siberian terranes and that cannot be attributed to known western North American sources, fossil faunal assemblages of Siberian or Appalachian affinity, Neoproterozoic and (or) Ordovician-Silurian arc magmatism (Colpron and Nelson, 2009), and Early Paleozoic compressional tectonism (Gehrels et al., 1983; Gehrels and Saleeby, 1987). Models involving translation of Iapetan, Baltican or Siberian terranes around the northern and southern margins of Laurentia into the Cordilleran realm have been proposed to explain these data (Figure 1-5). Alternatively, the presence of a source of atypical detrital zircon signatures within the Cordilleran realm has been proposed

(Lemieux et al., 2007). An emergent block of North American Precambrian crust has been hypothesized to have existed outboard of the Lardeau trough and formed the basement to Late Paleozoic and Mesozoic volcanic arcs (Figure 1-4B,C; Thompson et al., 2006). Was the Okanagan High the source of Grenville-aged detritus in the Paleozoic Cordilleran margin (e.g. Erdmer et al., 2002; Lemieux et al., 2007)? Iapetan-like detrital zircon signatures have been found mainly in rocks with unclear physical relationships to the ancient Cordilleran margin (e.g. Chilliwack Composite, Brown et al., 2010; Alexander, Gehrels et al., 1996; Eastern Klamath and Northern Sierra terranes; Wright and Wyld, 2006). The Devonian Chase Formation (Jones, 1959) in southeast British Columbia may be a critical exception in that its relations to the North American margin can be observed.

Does the Devonian Chase Formation record an intra-Cordilleran continental high (e.g Lemieux et al., 2007), or is it part of an exotic Okanagan terrane that was accreted in Devonian time (Colpron and Nelson, 2009)? If the former, why does its detrital zircon provenance contrast with that of the Cordilleran miogeocline? If the latter, from where and when did the terrane arrive in the southern Canadian Cordillera?

The Chase Formation is a regionally extensive calcareous quartzite marker horizon that has been mapped from Shuswap Lake to Upper Arrow Lake as the stratigraphic base of a pericratonic assemblage (Thompson et al., 2001, 2002, 2006; Glombick et al., 2006; Lemieux, 2006). Primarily on the basis of reinterpretation of detrital zircon data, Colpron and Nelson (2009) included the Devonian Chase and Silver Creek formations in their list of exotic terranes. They interpreted that the basement of the Quesnel arc (including the Chase Formation) was at least in part a fragment of Caledonian crust that collided with the southern Canadian Cordilleran margin in Middle and possibly Late Devonian time. Because arc magmatism at the Cordilleran margin began no earlier than Middle Devonian time (Rubin et al., 1990), evidence of a Silurian arc outboard of the Milford Group (Figure 1-4D; Roback et al., 1994) was used to support the introduction of exotic crust into the Cordilleran realm. Colpron and Nelson's (2009; 2011) exotic Okanagan terrane hypothesis dictates that: 1) the Chase and Silver Creek formations lack stratigraphic ties with the Cordilleran pericratonic assemblages, and 2) those formations were thrust against pericratonic rocks prior to Late Devonian arc magmatism. Interpretation of the affinity of the Chase Formation is therefore crucial to reconstructions of the mid-Paleozoic Cordilleran margin and the hypothesized emplacement of exotic Paleozoic terranes.

1.3 Methods and contributions

This study is based on eight months of regional and detailed geological bedrock mapping augmented with lithogeochemical and U-Pb zircon geochronological analyses of Cambrian to Permian strata in an area of approximately 2,000 km^2 in southeastern British Columbia. Field work was conducted in the northernmost segment of the Kootenay Arc (Hedley, 1955) – a Jurassic-Cretaceous structural belt in southeastern British Columbia. The northern Kootenay Arc-Upper Arrow Lake area was selected for study because it contains both lower and upper Paleozoic Kootenay Arc successions and the Chase-Silver Creek succession. The studied strata encompass pericratonic depositional settings from a nascent Eocambrian passive margin to a Late Triassic back-arc basin that only shortly preceded initiation of main Cordilleran orogenesis. Because the pericratonic assemblages were deposited along the western fringe (modern coordinates) of ancestral North America they are well situated to record the relationships between parauthochthonous miogeoclinal successions and outboard tectonic assemblages that have less clear geological affinity (Figure 1-1).

Chapter 2 presents field, geochemical and U-Pb zircon data to support the definition of a new mid-Paleozoic stratigraphic succession in the Kootenay Arc termed the Mount Sproat assemblage (MSA). The MSA is described here in terms of four stratigraphic members that are mutually conformable. The MSA is interpreted to conformably overlie the Broadview Formation of the Lardeau Group and to be unconformably overlain by the Upper Mississippian McHardy assemblage of the Milford Group (Kraft et al. (2011a,b). Volcanic lithogeochemical data show that Cambrian to Devonian(?) rift-related volcanism in the Lardeau Group and lowermost MSA was followed by arc-related magmatism in the MSA and back-arc basin magmatism in the Kaslo Group. A Late Devonian U-Pb zircon ID-TIMS age dates calc-alkaline volcanism in the MSA. New field observations and a revised interpretation of the geology of the Tenderfoot Lake area and implications for the Devonian Chase Formation are discussed.

Chapter 3 presents new field observations from Carboniferous strata of the northern Kootenay Arc. Field relations and sedimentological data from the Milford Group and a detailed description of the recently defined Thompson assemblage of Kraft et al. (2011a; 2011c) are presented. The Milford Group north of the Goat Range is interpreted here to correlate with the McHardy and Davis assemblages of Klepacki (1985). The Davis assemblage unconformably overlies the Thompson assemblage and the Broadview Formation throughout the Badshot Range. The McHardy assemblage overlies the Mount Sproat assemblage with angular unconformity in the Lardeau Range.

In Chapter 4, new structural geological observations are presented and used to discuss the tectonic evolution of northern Kootenay Arc strata. Tectonic implications of the revised stratigraphic framework presented in chapters 2 and 3 are discussed. The timing of mid-Paleozoic deformation in the region is constrained by observations from local strata to be latest Devonian or Early Mississippian in age, and the strain is shown to have been localized in the Lardeau Group and the lower Mount Sproat assemblage. The tectonic significance of faults such as the Stubbs fault, Standfast Creek fault and the Columbia River fault zone are discussed. Post-Jurassic folding and static amphibolite-facies metamorphism of rocks in the immediate hanging wall of the Columbia River fault zone are illustrated.

Chapter 5 uses a new detrital zircon data set to draw inferences about the pre-Jurassic paleogeography of the Cordilleran margin. Detrital zircon analysis has become a preferred method for terrane analysis and studies of paleogeography because of the relative ease with which vast amounts of useful provenance data can be generated with modern geochronological techniques. The data show both similarities and important differences in zircon provenance between pericratonic rocks and the miogeocline. The differences are used to infer the presence and character of emergent crust that was outboard of the Cordilleran miogeocline at various times in the Paleozoic.

1.4 Terminology and definitions

The Cordilleran miogeocline is an easterly-derived, east-tapering wedge of sedimentary rock that developed immediately outboard of the cratonic platform from Cryogenian to Jurassic time (Stewart, 1972; Monger and Price, 1979; Price, 1994). In the Kootenay Arc, the Lower Cambrian Hamill Group and Badshot Formation have been included in the Cordilleran miogeocline (Colpron and Price, 1995); all overlying units, including the Lardeau Group, have not.

In this thesis the term pericratonic refers to the rock assemblages that have stratigraphic and (or) isotopic similarities with the Cordilleran miogeocline but which have important stratigraphic, tectonic or magmatic distinctions from the miogeocline. Unless otherwise stated, Laurentia is the craton that is implied. Pericratonic assemblages are interpreted to have evolved on the periphery of the continent and were sufficiently isolated from the continental shelf and slope that they preserve geologic histories, typically from late Paleozoic and younger times, that are distinct from the miogeocline.

This research deals extensively with relations of successions of stratified rocks. Two important classification schemes for regional scale rock assemblages provide a framework for modern Cordilleran research.

The so-called tectono-stratigraphic assemblages (Monger and Price, 1979) or tectonic assemblages (Figure 1-6; Tipper et al., 1981; Wheeler and McFeely, 1991) are fundamental elements of the Cordillera and are defined as follows:

"The tectonic assemblages represent distinctive successions of stratified rocks, mainly bounded by unconformities or faults, deposited in specific tectonic environments during particular intervals of time," (Wheeler and McFeely, 1991).

The tectonic assemblages that constitute most of the Canadian Cordillera describe a generalized east to west transition from Neoproterozoic and younger continental shelf and rise successions (the miogeocline) to marginal basin deposits (pericratonic assemblages) to magmatic arc and oceanic assemblages that have uncertain paleogeography.

Another scheme groups one or more tectonic assemblages into terranes (Figure 1-2). The term terrane is used in this thesis to describe a fault-bounded fragment of crust that preserves a geologic record distinct from that of adjacent terranes (Coney et al., 1980; Gabrielse and Yorath, 1991). A terrane has been tectonically emplaced against adjacent or subjacent rocks. The terrane concept is used in the North American Cordillera to explain the juxtaposition of disparate geologic domains by plate tectonic processes (e.g Irwin, 1972; Coney et al., 1980; Monger et al., 1982). The terrane paradigm dictates that the relationship of adjacent but disparate terranes is considered suspect until a connection is demonstrated (Coney et al., 1980). Like tectonic assemblages, terranes have temporal extent. For example, hypothetical arc terrane X was transported on an oceanic plate and accreted to a continental margin at the end of the Cambrian. It was subsequently overlain by an Ordovician overlap assemblage. The overlap assemblage is part of a new tectonic assemblage because it formed in a different tectonic setting. The overlap assemblage is not part of terrane X because the arc was part of the same tectonic plate as the continent during deposition of the overlap assemblage. In a way, terrane X ceased to exist after its accretion to the continent and only rocks that were part of terrane X before accretion can be assigned to the terrane. Note also that the overlap assemblage is depositionally linked to both the continent and the arc rocks and therefore it cannot be called a terrane.

About 20 major terranes are shown in recent terrane maps of the Canadian Cordillera (Figure 1-2; Colpron et al., 2006). Since the application of terrane nomenclature to the Canadian Cordillera, depositional contacts have been reported between several terranes (ie. Quesnel and Slide Mountain terranes, Read and Okulitch, 1977; Kootenay terrane and miogeocline, Colpron and Price, 1995; Quesnel terrane and Yukon-Tanana terrane, Nelson and Friedman, 2004; unassigned terrane and miogeocline, Erdmer et al., 2005; Slide Mountain terrane and Yukon-Tanana terrane, Murphy et al., 2006; Kootenay terrane and miogeocline, Lemieux, et al., 2007). Because a terrane cannot be in depositional contact with an adjacent terrane, nomenclature must be updated in such instances.

Because the 'Kootenay terrane' represents off-shelf, lateral equivalents of the Cordilleran miogeocline that, at least locally, depositionally overlie the Cambrian miogeocline (Colpron and Price, 1995) indicates that 'Kootenay' is not a terrane (Thompson et al., 2006), but can be, in part, accurately described as a tectonic assemblage. Accordingly, the term 'Kootenay tectonic assemblage' is introduced and employed in this thesis to describe the Lardeau Group (Fyles and Eastwood, 1962) and equivalent strata in southeastern British Columbia.

1.5 Geological setting

The North American Cordillera is a ~7000 km long orogen that formed along the western margin of Laurentia (the North American craton; Hoffman, 1988) as a result of Proterozoic to modern interactions between western Laurentia and the lithosphere of easternmost Panthalassa and the Pacific Ocean. The Canadian segment of the Cordillera is largely a product of mid-Jurassic to Paleocene orogenesis and superposed Eocene crustal extension (e.g., Gabrielse et al., 1991 and references therein), but it records a protracted and complex Late Proterozoic and Paleozoic history.

The Cordilleran margin formed by the late Neoproterozoic break-up of the supercontinent Rodinia, during which a large continental mass rifted from the western side (modern coordinates) of the North American craton (Bond and Kominz, 1984; Dalziel, 1991; Hoffman, 1991; Colpron et al., 2002). Widespread and thick (6- 9 km) accumulations of predominantly immature siliciclastic Neoproterozoic (<780 Ma) strata throughout the North American Cordillera – the Windermere Supergroup (Stewart, 1972; c.f. Ross, 1991) – are interpreted as syn- and post-rift deposits from the partial and earlier of two phases of continental break-up along the western margin of Laurentia (Colpron et al., 2002). Ediacaran and Lower Cambrian siliciclastic deposits of the Gog Group in the southern Canadian Cordillera and its correlative strata are proposed to record a second and ultimate rifting event that likely initiated at ca. 575 Ma (Bond and Kominz, 1984; Colpron et al., 2002).

The Cordilleran margin from the Yukon to California existed for approximately 200 m.y. as a 'passive' margin that experienced intermittent pulses of crustal extension (Root, 1987; Cecile and Norford, 1993; Goodfellow et al., 1995; Lickorish and Simony, 1995; Cecile et al., 1997). During this period, continentally-derived siliciclastic detritus and carbonate deposits grew the continental margin sedimentary prism, or miogeocline.

The Cordilleran margin from the Yukon to Nevada transitioned from a passive to an active, predominantly convergent, plate boundary in Middle and Late Devonian time (Rubin et al., 1990; Monger and Nokleberg, 1996). In the northern Cordillera, a Late Devonian to Early Permian continental arc developed on Paleozoic, and possibly older, pericratonic rocks that today compose the basement to the Yukon-Tanana terrane (Nelson et al., 2006). A corresponding back-arc basin grew to become the Slide Mountain ocean – a seaway of uncertain breadth that separated Yukon-Tanana terrane from ancestral North America in Mississippian to Triassic time (Nelson, 1993; Nelson et al., 2006; Beranek et al., 2010a). The equivalent Slide Mountain ocean rocks in southern British Columbia separate a Devonian-Early Mississippian continental margin arc (e.g. Paradis et al., 2006) from the Mesozoic Quesnel arc to the west (Wheeler and McFeely, 1991). The suite of Late Devonian and Early Mississippian arc-related plutons and volcanic rocks occurs in the Adams Plateau and North Okanagan- Shuswap region of southeastern British Columbia occur in a succession of early and mid- to late Paleozoic strata traditionally referred to as the Eagle Bay assemblage (Schiarizza and Preto, 1987; Paradis et al., 2006).

1.5.1 Pericratonic assemblages

In Canada, the Cordilleran pericratonic assemblages (Figure 1-1) occur immediately west of the foreland, roughly along the interior metamorphic axis of the Canadian Cordillera (Omineca morphogeological belt of Monger et al. 1972). The pericratonic assemblages are referred to as the Yukon-Tanana terrane in the northern Cordillera (Coney et al., 1980; Nelson et al., 2006) and the former 'Kootenay terrane' ("Kootenay tectonic assemblage" and related strata here) in southern British Columbia (Wheeler and McFeely, 1991) where this study was conducted.

According to a synthesis by Colpron and Nelson (2009), Cordilleran Paleozoic assemblages that formed in the peri-Laurentian realm:

1. share stratigraphic similarities with the continental autochthon, especially in pre-Devonian strata;
2. contain detrital zircons with a primary mode from 2.0-1.8 Ga and smaller modes in the Archean and early Paleoproterozoic. Grenville-age (1.3-1.0 Ga) detrital zircons are minor and are inferred to represent far-travelled detritus from the Grenville orogen;
3. first developed continental arcs in Middle to Late Devonian time. Evidence of extensional and locally compressional tectonics in Middle Devonian and Carboniferous time is widespread;
4. lack evidence of subduction or arc magmatism from Neoproterozoic to Middle Devonian time.

1.6 Study area

Field investigations were conducted in the Selkirk Mountains south of Revelstoke and north of Nakusp, British Columbia (Figure 1-7). Ground access by highways and forest service roads was good to excellent in much of the area; helicopter access was used for remote locations. Much of the terrain is densely forested. Shoreline exposures along the Upper Arrow Lake hydroelectric reservoir were accessed by boat. The extent of geological mapping for this study and by previous workers is shown in Figure 1-8.

1.7 Conventions used

The geologic timescale of Walker and Geissman (2009) is used for all geologic intervals. Attitudes of planar data are reported in right-hand rule, whereby the strike is 90° counter-clockwise from the dip direction; strike and dip are separated by a forward slash (/). Linear data are presented as a trend and plunge separated by a comma (,). Units of distance and weight are standard SI units, for example metres, m.

1.8 Notes on appended material

The reader is referred to supplementary material in the pocket (and appended digitally) for geological maps, cross-sections and other information.

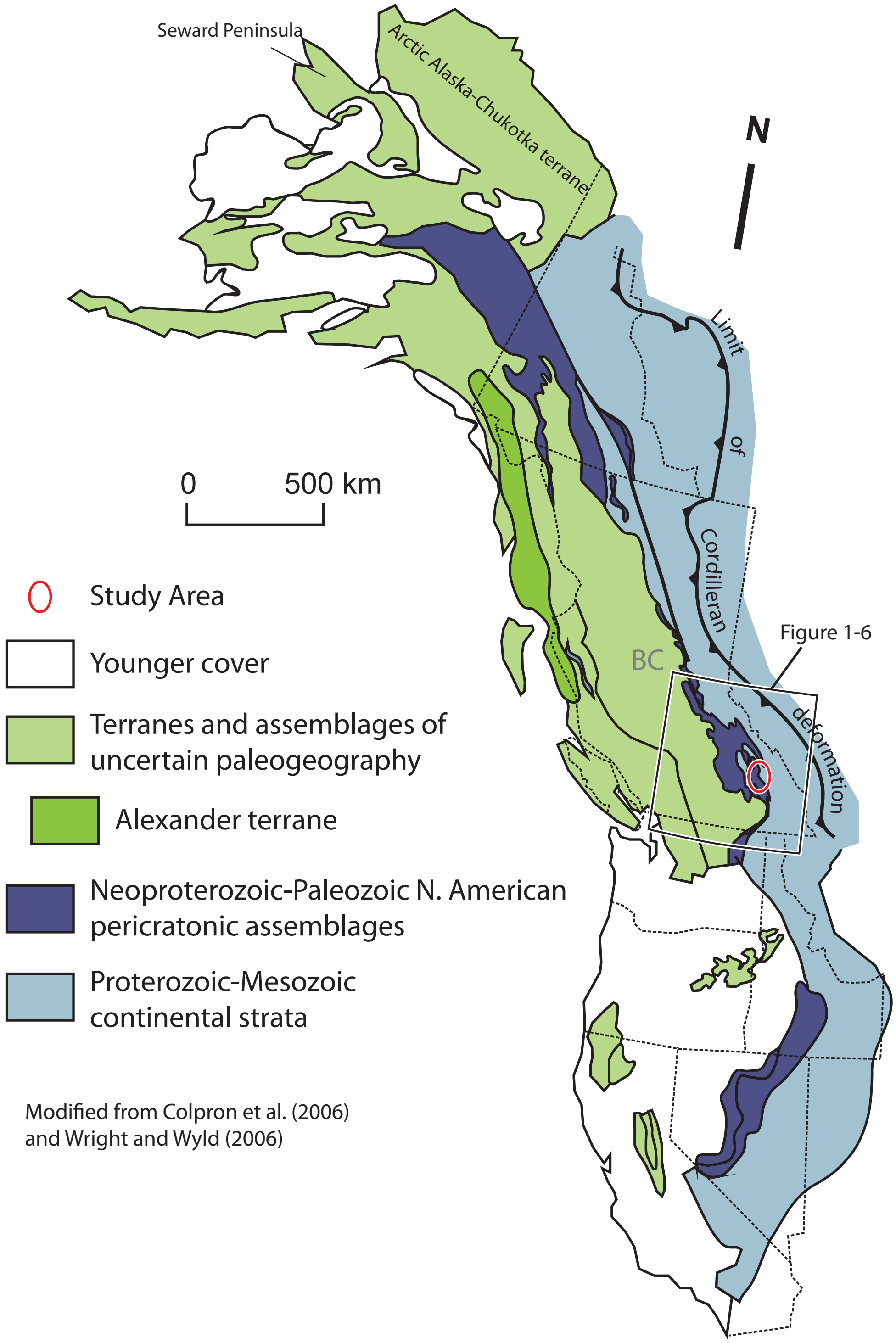

Figure 1-1. The North American Cordillera by geological affinity.
Areas in pale green are underlain by pericratonic and arc assemblages that have unclear or contested relations to the North American margin ro cks shown in blue. The area of study in southeast British Columbia is indicated in red. After Colpron et al. (2006b) and Wright and Wyld (2006).

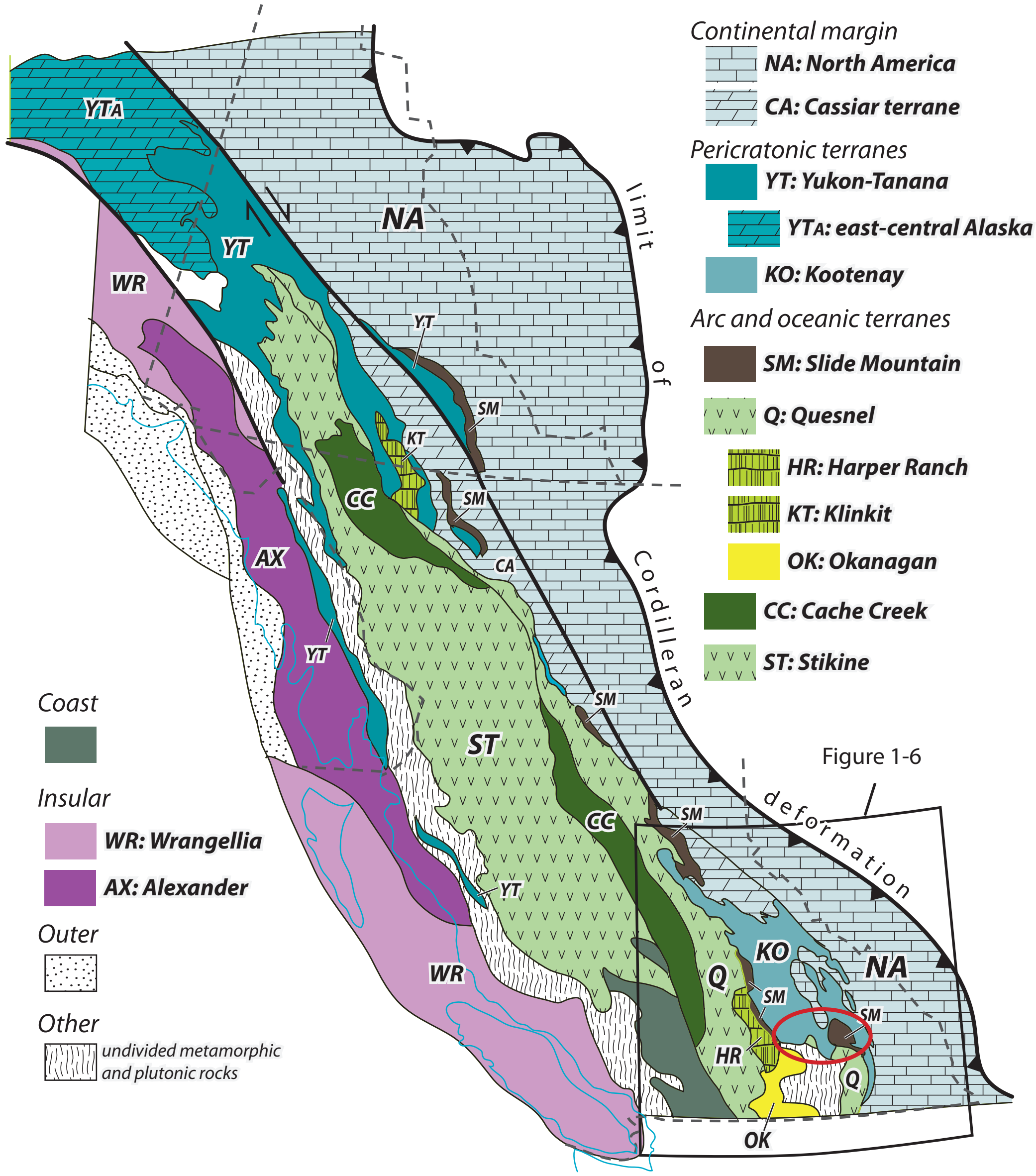

Figure 1-2. Terrane classifications of the Canadian Cordillera and parts of eastern Alaska.

According to this scheme the present study area (shown by red ellipse) involves rocks of the continental margin and Kootenay, Okanagan, Slide Mountain and Quesnel terranes. This terrane nomenclature, or variations thereof, is used widely but evidence from this research and prior investigation suggests a need to revise the terminology for the rocks of southeastern British Columbia. Simplified from Colpron et al. (2006b).

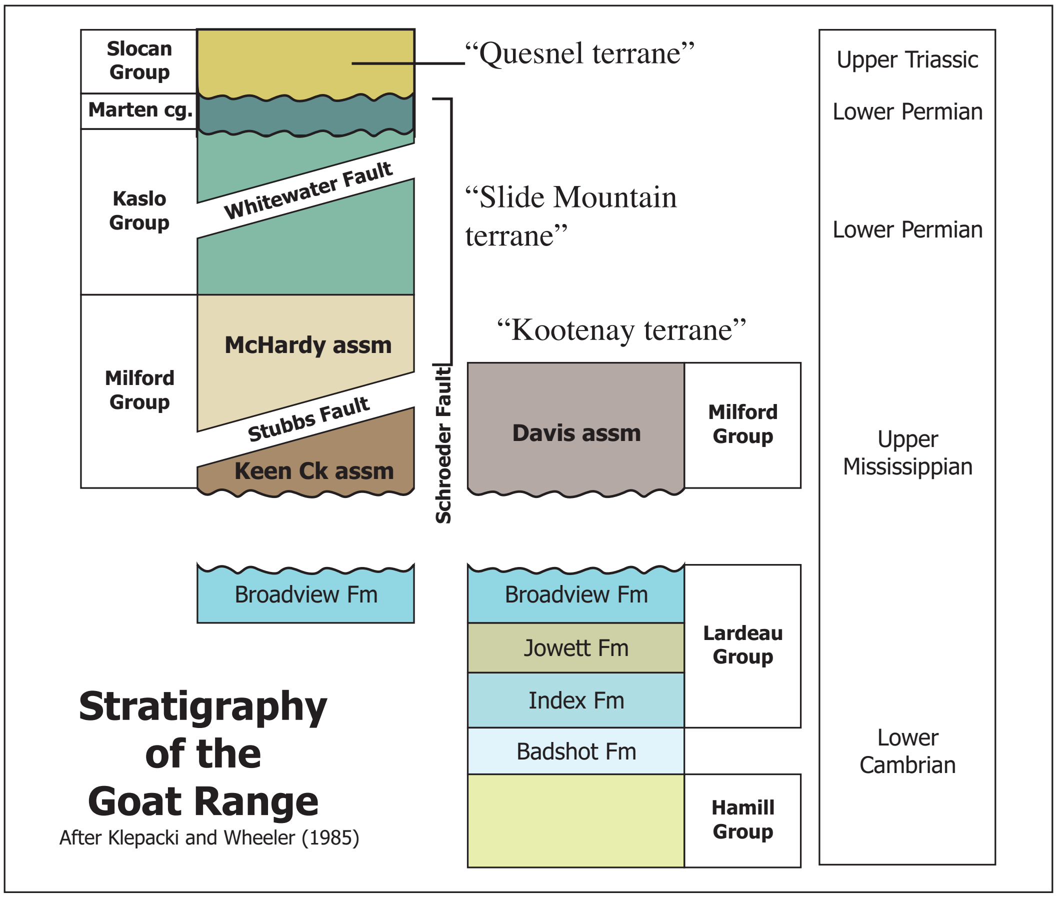

Figure 1-3. Stratigraphy of the Kootenay Arc in the Goat Range.
Two important elements of this framework are: 1) a major unconformity separates the lower Paleozoic Lardeau Group from overlying Milford Group rocks, and 2) the succession of "Slide Mountain terrane" and "Quesnel terrane" rocks, shown as McHardy assemblage to Slocan Group above, is in fault contact with other Milford strata and its basement is unknown. From Klepacki and Wheeler, 1985.

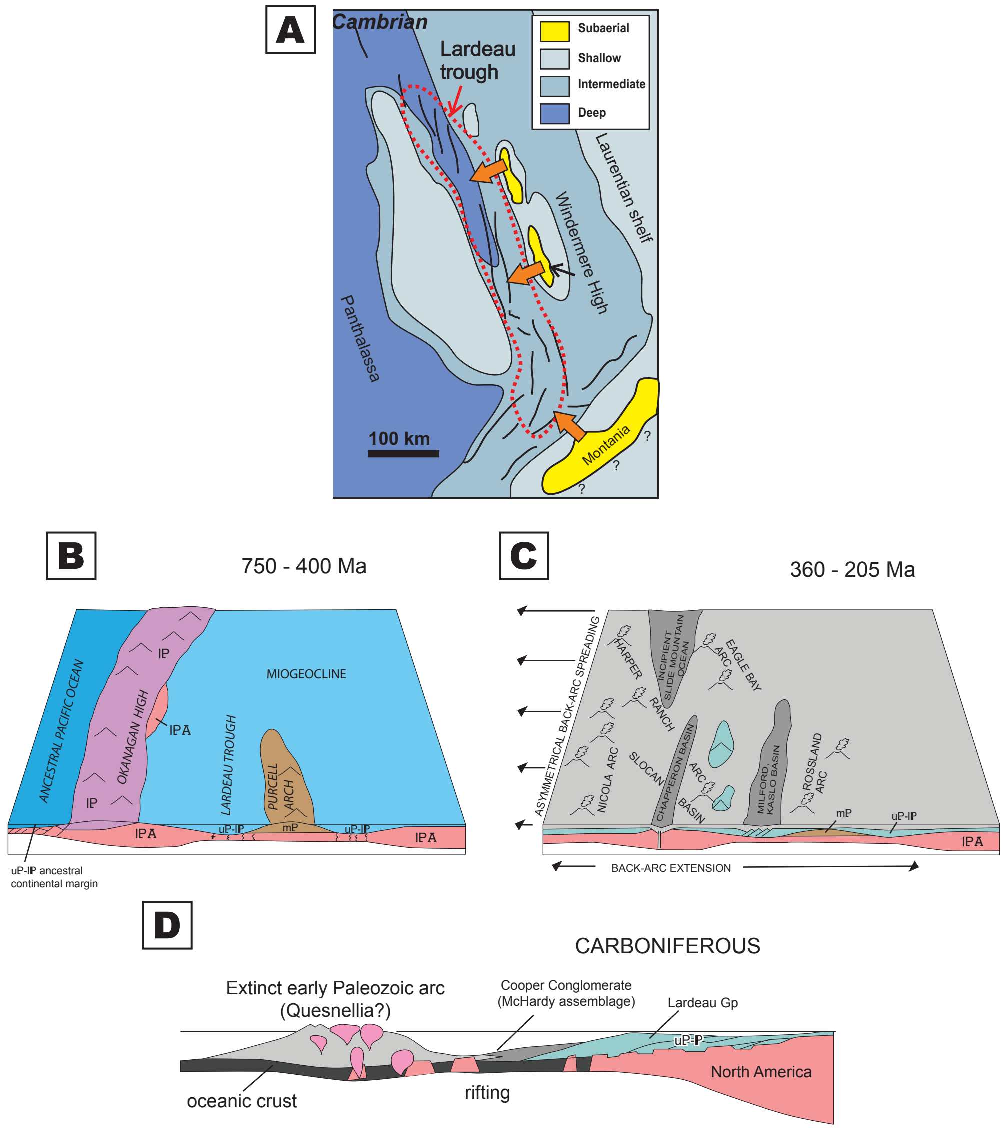

Figure 1-4. Previous models of the paleogeography of the Lardeau and Milford groups.
A) Depiction of the early Paleozoic Lardeau trough by Logan and Colpron (2006) that shows sediment originating from rift shoulders on the Purcell arch to the east and no emergent crust in the west. B) The Okanagan High model of Thompson et al. (2006) shows an emergent ribbon of North American Precambrian crust on the outboard margin of the early Paleozoic Lardeau trough. C) Carboniferous-Triassic phase of the Okanagan High model shows in situ development of several arcs on attenuated North American crust including the Okanagan High. D) Interpreted setting of the McHardy assemblage on transitional or ocean crust between an Early Paleozoic arc and the Lardeau Group (after Roback et al., 1994).

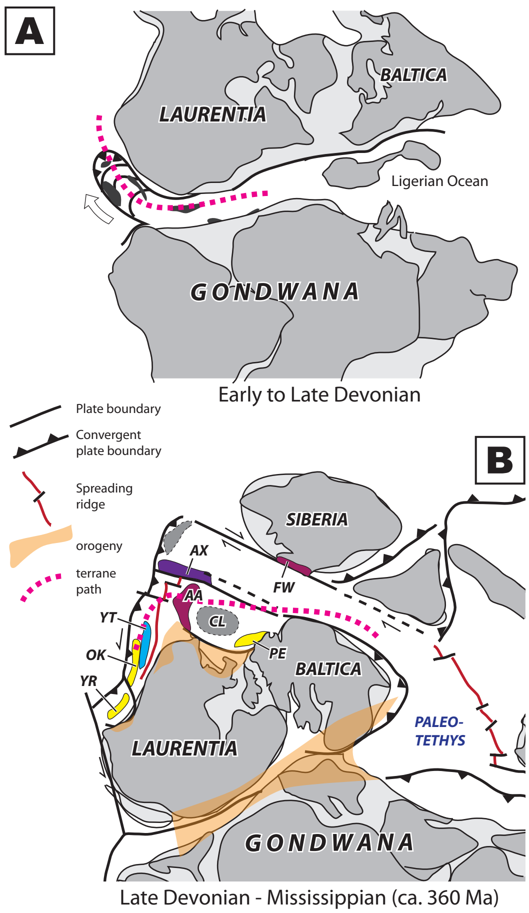

Figure 1-5. Hypothesized introduction of Appalachian/Baltican/Caledonian terranes into the North American Cordillera.

A) Wright and Wyld's (2006) 'southern passage' model in which terranes of Caledonian affinity were transported around the southern margin of Laurentia in Devonian time. B) "Northwest Passage" model of Colpron and Nelson (2009) whereby the Chase Formation ("Okanagan terrane") and other terranes of Caledonian, Baltican, and Siberian affinity were translated around the northern margin of Laurentia and emplaced along the Cordilleran margin in the Devonian. AA, Arctic Alaska, AX, Alexander; CL, Crocker Land; FW, Farewell, OK, Okanagan, PE, Pearya; YR, Yreka; YT, Yukon-Tanana. After Colpron and Nelson (2009).

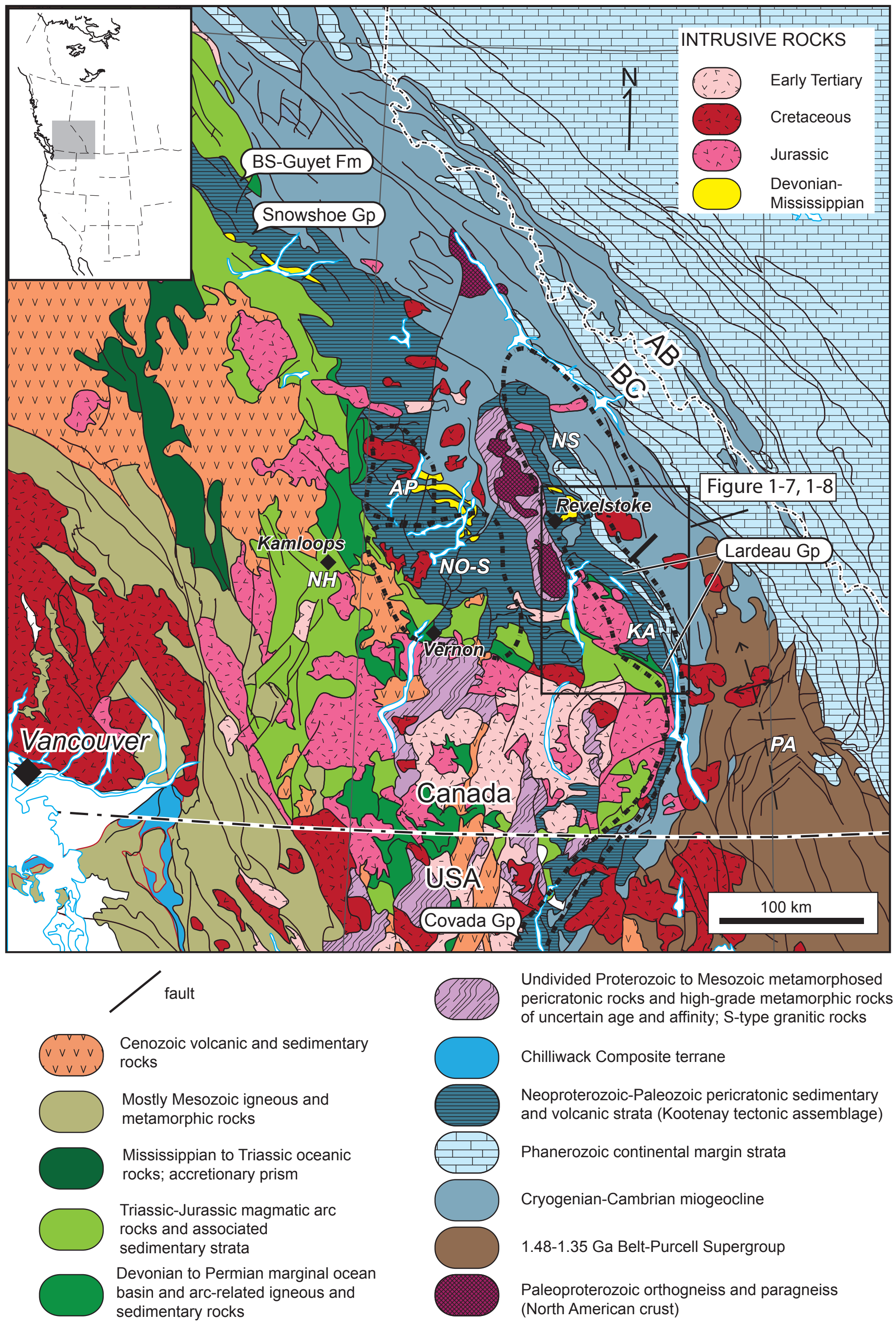

Figure 1-6. Tectonic assemblage map of the southern Canadian Cordillera. Modified from Wheeler and McFeely (1991), Glombick et al. (2006), Thompson et al. (2006), Brown et al. (2010). AP, Adams Plateau; KA, Kootenay Arc; NH, Nicola Horst; NS, Northern Selkirks; NO-S, North Okanagan-Shuswap region; PA, Purcell anticlinorium

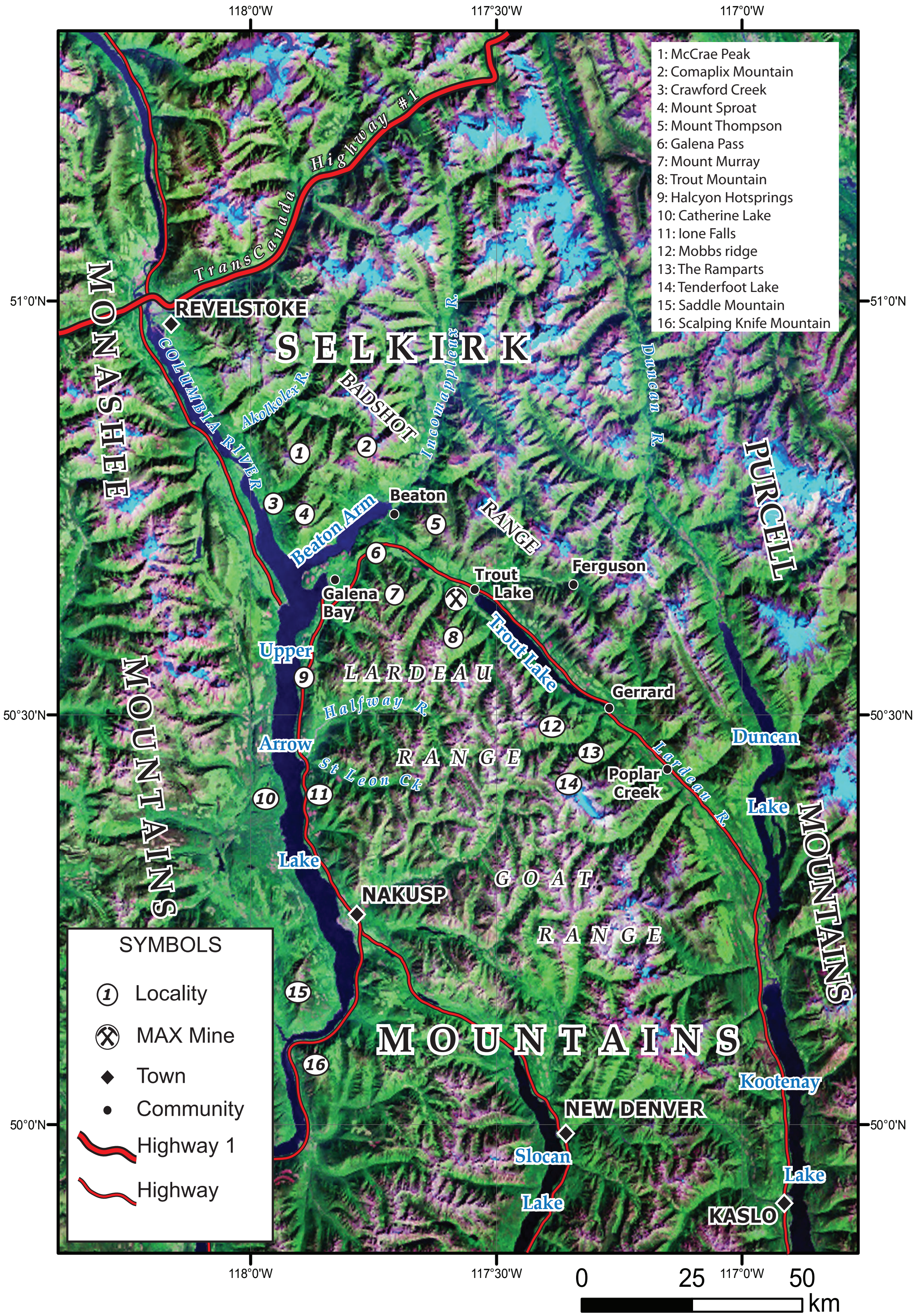

Figure 1-7: Geography of the Upper Arrow Lake-Trout Lake area. Numbers indicate localities referred to in this thesis.

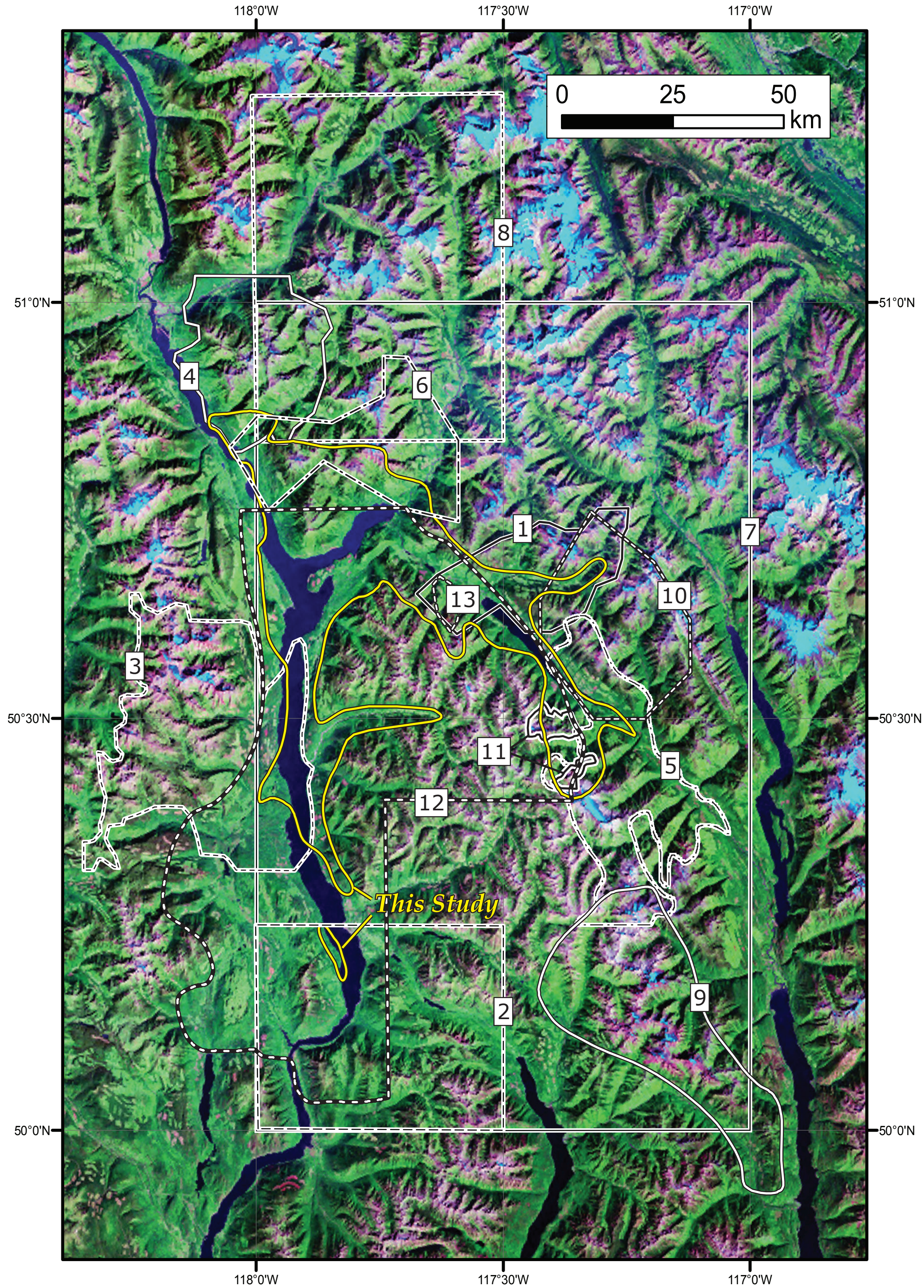

Figure 1-8: Extent of mapping from this and previous geological studies. This study, yellow; 1) Fyles and Eastwood, 1962; 2) Hyndman, 1968; 3) Reesor and Moore, 1971; 4) Thompson, 1978; 5) Read, 1973; 6) Read, 1975-1977; 7) Read and Wheeler, 1976; 8) Sears, 1979; 9) Klepacki, 1985; 10) Smith, 1990; 11) Roback, 1993; 12) Lemieux, 2006; 13) Read et al., 2009

References

Beranek, L., Mortensen, J., Orchard, M. J., and Ullrich, T., 2010, Provenance of North American Triassic strata from west-central and southeastern Yukon: correlations with coeval strata in the Western Canada Sedimentary Basin and Canadian Arctic Islands: Canadian Journal of Earth Sciences, v. 47, p. 53-73.

Bond, G., and Kominz, M. A., 1984, Construction of tectonic subsidence curves for the early Paleozoic miogeocline,southern Canadian Rocky Mountains: Implications for subsidence mechanisms, age of breakup and crustl thinning. Geological Society of America Bulletin, v. 95, p. 155-173.

Brown, E., Gehrels, G., and Valencia, V. A., 2010, Chilliwack composite terrane in northwest Washington: Neoproterozoic-Silurian passive margin basement, Ordovician-Silurian arc inception: Canadian Journal of Earth Sciences, v. 47, p. 1347-1366.

Carpenter, D.G., Carpenter, J.A., Dobbs, S.W., and Stuart, C.K., 1993, Regional structural synthesis of the Eureka fold and thrust belt, east-central Nevada, *in* Gillespie, C.W., ed., Structural and stratigraphic relation- ships of Devonian reservoir rocks, east-central Nevada: Reno, Nevada Petroleum Society, p. 59–72.

Cecile, M., and Norford, B.S., 1993, Ordovician and Silurian, *in* Sedimentary Cover of the North American Craton in Canada, Chapter 4c, D.F. Stott and J.D. Aitken, (eds.), Geological Survey of Canada, Geology of Canada No. 5, p. 125-149.

Cecile, M., Morrow, D., and Williams, G., 1997, Early Paleozoic (Cambrian to Early Devonian) tectonic framework, Canadian Cordillera: Bulletin of Canadian Petroleum Geology, v. 45, p. 54.

Colpron, M., and Price, R., 1995, Tectonic significance of the Kootenay terrane, southeastern Canadian Cordillera: An alternative model: Geology, v. 23, p. 25-28.

Colpron, M., and Nelson, J.L., 2009, A Palaeozoic Northwest Passage: incursion of Caledonian, Baltican and Siberian terranes into eastern Panthalassa, and the early evolution of the North American Cordillera: Geological Society London Special Publications, v. 318, p. 273–307, doi: 10.1144/SP318.10.

Colpron, M., and Nelson, J.L., 2011, Chapter 31: A Palaeozoic NW Passage and the Timanian, Caledonian and Uralian connections of some exotic terranes in the North American Cordillera: Geological Society, London, Memoirs, v. 35, p. 463–484, doi: 10.1144/M35.31.

Colpron, M., Logan, J., and Mortensen, J., 2002, U-Pb zircon age constraint for late Neoproterozoic rifting and initiation of the lower Paleozoic passive margin of western Laurentia: Canadian Journal of Earth Sciences, v. 39, p. 133–143.

Colpron, M., Mortensen, J.K., Gehrels, G.E. and Villeneuve, M., 2006a, Basement complex, Carboniferous magmatism and Paleozoic deformation in Yukon-Tanana terrane of central Yukon: Field, geochemical and geochronological constraints from Glenlyon map area, *in* Colpron, M. and Nelson, J.L., eds., Paleozoic Evolution and Metallogeny of Pericratonic Terranes at the Ancient Pacific Margin of North America, Canadian and Alaskan Cordillera: Geological Association of Canada, Special Paper 45, p. 131-151.

Colpron, M., Nelson, J. L., and Murphy, D. C., 2006b, A tectonostratigraphic framework for the pericratonic terranes of the northern Cordillera, *in* Colpron, M. and Nelson, J.L., eds., Paleozoic Evolution and Metallogeny of Pericratonic Terranes at the Ancient Pacific Margin of North America, Canadian and Alaskan Cordillera: Geological Association of Canada, Special Paper 45, 1–23.

Coney, P.J., Jones, D.L., and Monger, J.W.H. 1980. Cordilleran suspect terranes: Nature, v. 288: 329–333. doi:10.1038/288329a0.

Dalziel, I., 1991, Pacific margins of Laurentia and East Antarctica-Australia as a conjugate rift pair: evidence and implications for an Eocambrian supercontinent: Geology, v. 19, p. 598-601.

Eisbacher, G., 1983, Devonian-Mississippian sinistral transcurrent faulting along the cratonic margin of western North America: A hypothesis: Geology, v. 11, p. 7.

Erdmer, P., Moore, J., Heaman, L., Thompson, R., Daughtry, K., and Creaser, R., 2002, Extending the ancient margin outboard in the Canadian Cordillera: record of Proterozoic crust and Paleocene regional metamorphism in the Nicola horst, southern British Columbia: Canadian Journal of Earth Sciences, v. 39, p. 1605–1623.

Erdmer, P., Mihalynuk, M., Gabrielse, H., Heaman, L., and Creaser, R., 2005, Mississippian volcanic assemblage conformably overlying Cordilleran miogeoclinal strata, Turnagain River area, northern British Columbia, is not part of an accreted terrane: Canadian Journal of Earth Sciences, v. 42, p. 1449–1465.

Fyles, J.T. and Eastwood, G.E.P., 1962, Geology of the Ferguson area, Lardeau district, British Columbia: B.C. Department of Mines and Petroleum Resources, Bulletin 45, 92 p.

Gabrielse, H., and Yorath, C.J., eds., 1991, Geology of the Cordilleran orogen in Canada. Geological Survey of Canada, Geology of Canada, No. 5.

Gehrels, G.E., and Saleeby, J.B. 1987. Geologic framework, tectonic evolution, and displacement history of the Alexander terrane, Tectonics, v. 6, p. 151–173.

Gehrels, G., and Ross, G., 1998, Detrital zircon geochronology of Neoproterozoic to Permian miogeoclinal strata in British Columbia and Alberta: Canadian Journal of Earth Sciences, v. 35, p. 1380–1401.

Gehrels, G. E., Saleeby, J. B., and Berg, H. C., 1983, Preliminary description of the Late Silurian–Early Devonian Klakas orogeny in the southern Alexander terrane, *in* Stevens, C. H., ed., Pre-Jurassic rocks in western North American suspect terranes: Los Angeles, Pacific Section, Society of Economic Paleontologists and Mineralogists, p. 131–141.

Glombick, P., Thompson, R. I., Erdmer, P., Heaman, L., Friedman, R. M., Villeneuve, M., and Daughtry, K. L., 2006, U–Pb constraints on the thermotectonic evolution of the Vernon antiform and the age of the Aberdeen gneiss complex, southeastern Canadian Cordillera: Canadian Journal of Earth Sciences, v. 43, p. 213-244.

Goodfellow, W., Cecile, M., and Leybourne, M., 1995, Geochemistry, petrogenesis, and tectonic setting of lower Paleozoic alkalic and potassic volcanic rocks, Northern Canadian Cordilleran Miogeocline: Canadian Journal of Earth Sciences, v. 32, p. 2167–2167.

Gordey, S., Abbott, J., Tempelman-Kluit, D., and Gabrielse, H., 1987, " Antler" elastics in the Canadian Cordillera: Geology, v. 15, p. 103.

Grove, M., Gehrels, G.E., Cotkin, S.J., Wright, J.E. & Zou, H., 2008, Non-Laurentian cratonal provenance of Late Ordovician blueschists and a link to the Alexander terrane: *in* Wright, J.E. & Shervais, J.W., eds., Ophiolites, Arcs, and Batholiths. Geological Society of America, Special Papers, no. 438, p. 223–250.

Hedley, M.S., 1955, Lead-Zinc deposits of the Kootenay Arc: Western Miner, July, p. 31- 35.

Hoffman, P., 1988, United plates of America, the birth of a craton: Early Proterozoic assembly and growth of Laurentia: Annual Review of Earth and Planetary Sciences, v. 16, p. 543–603.

Hoffman, P., 1991, Did the breakout of Laurentia turn Gondwanaland inside-out?: Science, v. 252, p. 1409.

Irwin, W.P., 1972, Terranes of the western Paleozoic and Triassic belt in the southern Klamath Mountains, California. U.S. Geological Survey, Professional Paper 800-C, p. C103-111.

Johnston, S., 2008, The Cordilleran Ribbon Continent of North America: Annual

Reviews Earth and Planetary Science Letters, v. 36, p. 495-530, doi: 10.1146/annurev.earth.36.031207.124331

Jones, A.G., 1959, Vernon map-area, British Columbia. Geological Survey of Canada Memoir 296.

Klepacki, D.W., 1985, Stratigraphy and structural geology of the Goat Range area, southeastern British Columbia, Ph.D. thesis, Massachusetts Institute of Technology, Cambridge, Mass.

Klepacki, D.W., and Wheeler, J.O., 1985, Stratigraphic and structural relations of the Milford, Kaslo and Slocan Groups, Goat Range, Lardeau and Nelson map area, British Columbia: *in* Current Research, Part A. Geological Survey of Canada, Paper 85-1A, p. 277- 286.

Kraft, J. L., Thompson, R. I., and Dhesi, P. (compilers), 2011a, Geology, Beaton, British Columbia; Geological Survey of Canada, Open File, 6574, scale 1:50 000, doi: 10.4095/288009.

Kraft, J. L., Thompson, R. I., and Dhesi, P. (compilers), 2011b, Geology, Trout Lake, British Columbia; Geological Survey of Canada, Open File, 6572, scale 1:50 000, doi: 10.4095/288063.

Kraft, J. L., Thompson, R. I., and Dhesi, P. (compilers), 2011c, Geology, Camborne, British Columbia; Geological Survey of Canada, Open File, 6573, scale 1:50 000, doi: 10.4095/288064.

Lemieux, Y., 2006, Structure, geochronology and thermobarometry of the eastern flank of the Shuswap metamorphic complex in the Upper Arrow Lake area, southeastern British Columbia, Ph.D. thesis, University of Alberta, Edmonton, AB.

Lemieux, Y., Thompson, R., Erdmer, P., Simonetti, A., and Creaser, R., 2007, Detrital zircon geochronology and provenance of Late Proterozoic and mid-Paleozoic successions outboard of the miogeocline, southeastern Canadian Cordillera: Canadian Journal of Earth Sciences, v. 44, no. 12, p. 1675–1693.

Lickorish, W., and Simony, P. S., 1995, Evidence for late rifting of the Cordilleran margin outlined by stratigraphic division of the Lower Cambrian Gog Group, Rocky Mountain Main Ranges, British Columbia and Alberta: Canadian Journal of Earth Sciences, v. 32, p. 860-874.

Logan, J., and Colpron, M., 2006, Stratigraphy, geochemistry, syngenetic sulphide occurrences and tectonic setting of the lower Paleozoic Lardeau Group, northern Selkirk Mountains, British Columbia: *in* Colpron, M. and Nelson, J.L., eds., Paleozoic Evolution and Metallogeny of Pericratonic Terranes at the Ancient Pacific Margin of North America, Canadian and Alaskan Cordillera: Geological Association of Canada, Special Paper 45, v. 45, p. 361–382.

Milidragovic, D., Thorkelson, D. J., Davis, W. J., Marshal, D. D., and Gibson, H. D., 2011, Evidence for late Mesoproterozoic tectonism in northern Yukon and the identification of a Grenville-age tectonothermal belt in western Laurentia: Terra Nova, v. 23, p. 307-313, doi: 10.1111/j.1365-3121.2011.01015.x.

Monger, J., and Price, R., 1979, Geodynamic evolution of the Canadian Cordillera – progress and problems: Canadian Journal of Earth Sciences, v. 16, p. 770-791.

Monger, J., and Berg, H., C., 1987, Lithotectonic terrane map of western Canada and southeastern Alaska. United States Geological Survey, Miscellaneous Field Studies Map MF-1874-B.

Monger, J.W.H. and Nokleberg, W.J., 1996, Evolution of the northern North American Cordillera: Generation, fragmentation, displacement and accretion of successive North American plate-margin arcs: American Journal of Science, v. 272, p. 577-602.

Monger, J., and Price, R., 2002, The Canadian Cordillera: geology and tectonic evolution: Canadian Society of Economic Geophysicists Recorder, v. 27, p. 17–36.

Monger, J. W. H., Souther, J., and Gabrielse, H.,1972, Evolution of the Canadian Cordillera; a plate-tectonic model: American Journal of Science, v. 272, p. 577-602.

Murphy, D., 2006, Mid-Paleozoic to early Mesozoic tectonostratigraphic evolution of Yukon-Tanana and Slide Mountain terranes and affiliated overlap assemblages, Finlayson Lake massive sulphide district, southeastern Yukon: *in* Colpron, M. and Nelson, J.L., eds., Paleozoic Evolution and Metallogeny of Pericratonic Terranes at the Ancient Pacific Margin of North America, Canadian and Alaskan Cordillera: Geological Association of Canada, Special Paper 45, p. 75-106.

Nelson, J. L., 1993, The Sylvester Allochthon: upper Paleozoic marginal-basin and island-arc terranes in northern British Columbia: Canadian Journal of Earth Sciences, v. 30, p. 631-643.

Nelson, J.L., Colpron, M., Piercey, S.J., Dusel-Bacon, C., Murphy, D.C. and Roots, C.F., 2006, Paleozoic tectonic and metallogenic evolution of the pericratonic terranes in Yukon, northern British Columbia and eastern Alaska, *in* Colpron, M. and Nelson, J.L., eds., Paleozoic Evolution and Metallogeny of Pericratonic Terranes at the Ancient Pacific Margin of North America, Canadian and Alaskan Cordillera: Geological Association of Canada, Special Paper 45, p. 323-360.

Paradis, S., Bailey, S., Creaser, R., Piercey, S., and Schiarizza, P., 2006, Paleozoic magmatism and syngenetic massive sulphide deposits of the Eagle Bay assemblage, Kootenay terrane, southern British Columbia: *in* Colpron, M. and Nelson, J.L., eds., Paleozoic Evolution and Metallogeny of Pericratonic Terranes at the Ancient Pacific Margin of North America, Canadian and Alaskan Cordillera: Geological Association of Canada, Special Paper 45, p. 383-414.

Parrish, R. R., 1992, U-Pb ages of Jurassic-Eocene plutonic rocks in the vicinity of Valhalla complex, southeast British Columbia, *in* Radiogenic age and isotopic studies: Report 5, Geological Survey of Canada Paper 91-2, p. 115-134.

Poole, F.G., 1974, Flysch deposits of the Antler foreland basin, western United States: *in* Dickinson, W.R., ed., Tectonics and sedimentation: Society of Economic Paleontologists and Mineralogists Special Publication 22, p. 58–82.

Price, R., 1994, Cordilleran tectonics and the evolution of the Western Canada Sedimentary Basin: *in* Geological Atlas of the Western Canada Sedimentary Basin, Mossop, G. D., and Shetsen, I., eds., Calgary, Canadian Society of Petroleum Geologists and Alberta Research Council, Chapter 2.

Read, P.B., 1975, Lardeau Group, Lardeau map-area, west half (82K west-half), British Columbia. Geological Survey of Canada Paper 75-1, Part A, p. 29-30.

Read, P.B., and Wheeler, J.O., 1976, Geology, Lardeau west-half, British Columbia. Geological Survey of Canada Open File 432.

Read, P., and Okulitch, A., 1977, The Triassic unconformity of south-central British Columbia: Canadian Journal of Earth Sciences, v. 14, p. 606-638.

Roback, R., Sevigny, J., and Walker, N., 1994, Tectonic setting of the Slide Mountain terrane, southern British Columbia: Tectonics, v. 13, p. 1242–1242.

Root, K., 1987, Geology of the Delphine Creek area, southeastern British Columbia: Implications for the Proterozoic and Paleozoic development of the Cordilleran divergent margin: Ph.D. thesis, University of Calgary, Calgary, AB.

Root, K., 2001, Devonian Antler fold and thrust belt and foreland basin development in the southern Canadian Cordillera: implications for the Western Canada Sedimentary Basin: Bulletin of Canadian Petroleum Geology, v. 49, p. 7-36.

Ross, G., 1991, Tectonic setting of the Windermere Supergroup revisited: Geology, v. 19, p. 1125-1128.

Ross, G., Friedman, R., and Mortensen, J. K., 2005, Detrital zircon and monazite from the Hyland Group (northern Canadian Cordillera and Alaska): evidence for intra-Cordilleran “Grenville” basement: Geological Society of

America Abstracts with Programs, v. 37, p. 56.

Rubin, C. M., Miller, M. M., and Smith, G. M., 1990, Tectonic development of Cordilleran mid-Paleozoic volcano-plutonic complexes; Evidence for convergent margin tectonism: *in* Harwood, D. S. and Miller, M. M. (eds.) Paleozoic and early Mesozoic paleogeo- graphic relations; Sierra Nevada, Klamath Mountains, and related terranes. Geological Society of America, Special Paper 255, p. 1–16.

Schiarizza, P. and Preto, V.A., 1987, Geology of the Adams Plateau-Clearwater-Vavenby area: B.C. Geological Survey Branch, Paper 1987-2, 88 p.

Smith, M., Dickinson, W., and Gehrels, G., 1993, Contractional nature of Devonian-Mississippian Antler tectonism along the North American continental margin: Geology, v. 21, p. 21.

Smith, J.F., Jr., and Ketner, K.B., 1977, Tectonic events since early Paleozoic in the Carlin–Pinon Range area, Nevada: U.S. Geological Survey Professional Paper 876C, 18 p.

Stewart, J.H., 1972, Initial deposits in the Cordilleran geosyncline: Evidence of late Precambrian (<850 m.y.) continental separation: Geological Society of America Bulletin, v. 83, p. 1345-1360.

Struik, L., 1987, The ancient western North American margin: An Alpine rift model for the east-central Canadian Cordillera: Geological Survey of Canada Paper 87-15, p. 1–21.

Thompson, R. I., 1978, Geology of the Akolkolex River area: B.C. Ministry of Energy, Mines and Petroleum Resources, Bulletin 60, 77 p.

Thompson, R.I., Glombick, P., Daughtry, K.L. and Erdmer, P., 2001, Upper Paleozoic stratigraphic linkage between Kootenay Arc and “Vernon antiform”: New constraints on southern Canadian Cordilleran evolution: Slave- Northern Cordillera Lithospheric Evolution (SNORCLE) Transect and Cordilleran Tectonics Workshop Meeting, Program with Abstracts, Lithoprobe Report No. 79, p. 104-105.

Thompson, R.I., Glombick, P., Acton, S., Heaman, L., Friedman, R., Daughtry, K., Erdmer, P. and Paradis, S., 2002, New Constraints on the age and distribution of the Chase quartzite, Vernon (82L) and Lardeau (82K) map areas: Regional implications [abstract]: Slave-Northern Cordillera Lithospheric Evolution (SNORCLE) Transect and Cordilleran Tectonics Workshop Meeting, Lithoprobe Report No. 82, p. 91-94.

Thompson, R.I., Glombick, P., Erdmer, P., Heaman, L. M., Lemieux, Y., and Daughtry, K. L., 2006, Evolution of the ancestral Pacific margin, southern Canadian Cordillera: Insights from new geologic maps: *in* Colpron, M. and

Nelson, J.L., eds., Paleozoic Evolution and Metallogeny of Pericratonic Terranes at the Ancient Pacific Margin of North America, Canadian and Alaskan Cordillera: Geological Association of Canada, Special Paper 45, p. 433-482.

Thorsteinsson, R., and Tozer, E.T., 1970, Geology of the Arctic Archipelago: *in* Douglas, R.J.W, ed., Geology and Economic Minerals of Canada: Geological Survey of Canada Economic Geology Report 1, p. 547–590.

Tipper, H. W., Woodsworth, G. J., and Gabrielse, H., 1981, Tectonic assemblage map of the Canadian Cordillera and adjacent parts of the United States of America. Geological Survey of Canada, Map 1505A, scale 1 : 2 000 000.

Trettin, H.P., Okulitch, A.V., Harrison, J.C., Brent, T.A., Fox, F.G., Packard, J.J., Smith, G.P., and Zolnai, A.I., 1991, Silurian–early Carboniferous deformational phases and associated metamorphism and plutonism, Arctic Islands, *in* Trettin, H.P., ed., Geology of the Innuitian Orogen and Arctic Platform of Canada and Greenland: Geological Survey of Canada, Geology of Canada, v. 3, p. 293–341.

Walker, J.D., and Geissman, J.W., compilers, 2009, Geologic Time Scale: Geological Society of America, doi: 10.1130/2009.CTS004R2C.

Wheeler, J. O., 1968, Lardeau (west half) map-area, British Columbia (82K W112): *in* Report of Activities, Part A, Geological Survey of Canada, Paper 68-lA, p. 56-58.

Wheeler, J.O. and McFeely, P. (compilers), 1991, Tectonic assemblage map of the Canadian Cordillera and adjacent parts of the United States of America: Geological Survey of Canada, Map 1712A, 1:2,000,000.

Wright, J., and Wyld, S., 2006, Gondwanan, Iapetan, Cordilleran interactions: A geodynamic model for the Paleozoic tectonic evolution of the North American Cordillera: *in* Haggart, J., Enkin, R.J and Monger, J. W. H., eds., Paleogeography of the North American Cordillera: Evidence For and Against Large-Scale Displacements: Geological Association of Canada, Special Paper 46, p. 377-408.

Chapter 2: A revised stratigraphic framework for the northern Kootenay Arc: lower Paleozoic to Early Mississippian rocks

2.1 Introduction

The northern Kootenay Arc has long been interpreted to contain lower Paleozoic strata overlain with angular unconformity by Late Mississippian and younger strata (e.g Wheeler, 1968; Read and Wheeler, 1976; Klepacki, 1985; Smith and Gehrels, 1991). Recent geological studies, however, have argued that the Devonian Chase and Silver Creek formations (Jones, 1959) from the Vernon area have equivalents in the northern Kootenay Arc (Lemieux, 2006; Thompson et al., 2006; Lemieux et al., 2007). The map relations between the Devonian strata and the Kootenay Arc succession, however, were not demonstrated, and geological maps of the Upper Arrow Lake area (Lemieux, 2006; Thompson et al., 2009a) contained implicit contradictions in relative ages and structural relations. Re-interpretation of the Chase Formation as part of an allochthonous Okanagan terrane that was emplaced at the Cordilleran margin in the Middle Devonian (Colpron and Nelson, 2009) challenged the notion that the Chase and Silver Creek formations are depositionally linked to North American rocks. The map relations and correlations between the Chase-Silver Creek formations and the Kootenay Arc succession are therefore crucial to identifying the correct hypothesis.

The present research investigated the structural-stratigraphic relations, age and depositional setting of Paleozoic strata in the northern Kootenay Arc and sought to test proposed correlations between the Kootenay Arc and Chase-Silver Creek successions. Volcanic lithogeochemistry of mafic strata is used with sedimentological observations to infer tectonic settings. U-Pb zircon geochronology by isotope dilution thermal ionization mass spectrometry (ID-TIMS) of a greenstone unit improves constraint on the depositional ages of the stratigraphic succession.

This paper argues for reassignment of a large extent of strata in the Upper Arrow Lake area to a new stratigraphic division called the Mount Sproat assemblage. According to the revised relations, Devonian to Early Mississippian sedimentary and arc-related volcanic rocks of the Mount Sproat assemblage conformably overlie the Lardeau Group west of Trout Lake. Part of the Mount Sproat assemblage is correlated with the Silver Creek Formation but the Chase Formation does not occur in the Kootenay Arc succession.

2.2 Geological setting

The Kootenay Arc (Hedley, 1955) contains a large proportion of the Cordilleran pericratonic strata in southern British Columbia. The Kootenay Arc (Figure 2-1) is a convex-east, arcuate structural belt in which Late Proterozoic to Triassic strata were deformed and metamorphosed during Jurassic to Cretaceous phases of the main Cordilleran orogeny (e.g Archibald et al., 1983). It is the locus of transition from foreland to hinterland style deformation and its strata reflect an outboard, North American plate-margin tectonic and depositional setting between the Cordilleran miogeocline to the east and volcanic arc complexes to the west.

Pre-Carboniferous rocks in the northern Kootenay Arc bear a chlorite-grade transposition foliation absent from younger rocks (Read, 1973; Klepacki, 1985; Smith and Gehrels, 1992). All strata were deformed in the Mesozoic phases of the main Cordilleran orogeny partly synchronous with voluminous Early to Middle Jurassic plutonism (Roback, 1993) but prior to emplacement of the granitic ca. 162 Ma Galena Bay stock (Parrish and Armstrong, 1987). Jurassic (and possibly Cretaceous) metamorphism in the northern Kootenay Arc ranges from greenschist-facies in the Badshot Range to mid amphibolite-facies near Upper Arrow Lake (figures 1-7 and A1-1).

2.2.1 Lardeau Group

At its outer limit in southeastern British Columbia, the Lower Cambrian (Waucoban) miogeocline is conformably overlain by a lithologically diverse and laterally variable undated succession of deep-water sedimentary strata and rift-related mafic volcanic rocks named the Lardeau Group (Fyles and Eastwood, 1962; Colpron and Price, 1995). The Lardeau Group is isolated in surface exposure from coeval miogeoclinal successions by tectonically uplifted Proterozoic strata in the Purcell anticlinorium (e.g Wheeler and McFeely, 1991).

Fyles and Eastwood (1962) divided the Lardeau Group into six formations, in ascending order: grey and green phyllite, limestone, quartzite and metabasalt of the Index Formation; black siliceous argillite of the Triune Formation; grey quartzite of the Ajax Formation; black siliceous argillite of the Sharon Creek Formation; basaltic flows and mafic volcaniclastic rocks of the Jowett Formation; and grey and green gritty quartzite and phyllite of the Broadview Formation. The term ‘grit’ here describes poorly sorted, sandy to pebbly quartz- and feldspar-rich siliciclastic sedimentary rock. In the Badshot Range, the Jowett Formation comprises deformed, greenschist-facies alkaline mafic volcanogenic rocks with minor siliciclastic intervals (Fyles and Eastwood, 1962; Logan and Colpron, 2006). Primary volcanic textures and structures are common (Fyles and Eastwood, 1962). The Broadview Formation in the Trout Lake area is characterized by nearly ubiquitous ~1-4 mm blue-quartz granules. The Broadview Formation comprises predominantly coarse-grained, poorly sorted quartz wacke and sub-arkosic wacke that commonly form graded beds interlayered with grey and green phyllite, suggesting deposition in a submarine fan environment (Smith, 1990).

Previously available lithogeochemical data from volcanic rocks of the Lardeau Group have ocean island basalt (OIB) or enriched mid-ocean ridge basalt (E-MORB) composition indicating formation in a rift environment with along-strike variation in volcanic processes (Logan and Colpron, 2006). When combined with the occurrence of abundant coarse clastic units and sedimentary facies changes in the Lardeau Group, the data were interpreted to indicate deposition in a margin-parallel Early Paleozoic trough within a transtensional regime (Smith, 1990) similar to the modern day Gulf of California (Logan and Colpron, 2006).

Lardeau grits (Akolkolex and Broadview formations) and alkaline volcanism (Jowett Formation) have been regarded as products of lower Paleozoic (probably Ordovician) crustal extension (Zwanzig, 1973; Read, 1973; Klepacki, 1985; Smith and Gehrels, 1992; Logan and Colpron, 2006), although the ages of those formations is only loosely constrained.

In the northern Selkirk Mountains (Figure 2-1), two Early Mississippian granodiorite plutons (354 ± 1 Ma, Logan and Friedman, 1997; 358 ± 6 Ma, Parrish, 1992) intrude the lower Jowett Formation and Index Formation, constraining the age of the lower Lardeau Group to pre-Mississippian. The upper age limit of the Lardeau Group has been constrained by the unconformably overlying mid-Mississippian Milford Group (Read and Wheeler, 1976; Orchard, 1985).

2.2.2 Carboniferous rocks

Viséan and younger Carboniferous metasedimentary and metabasaltic strata of the Milford Group (Cairnes, 1934; Read and Wheeler, 1976, and Klepacki, 1985) unconformably overlie the Lardeau Group. The Milford Group comprises predominantly fine-grained siliciclastic rocks with local limestone and conglomerate near its base (Read and Wheeler, 1976; Klepacki, 1985). A sedimentary succession that occurs between the Davis assemblage and Broadview Formation north of Trout Lake was introduced as the Thompson assemblage by Kraft et al. (2011a). The Milford Group and Thompson assemblage are described in detail in Chapter 3.

The Catherine Lake phyllite (Thompson et al., 2006) is a poorly exposed succession of phyllite and limestone west of Upper Arrow Lake (Figure A1-1) that has yielded Famennian or Tournaisian conodonts (Orchard, 1985) and a ca. 359 Ma detrital zircon (Thompson et al., 2006).

2.2.3 Pre-Milford rocks in the Lardeau Range

Polydeformed strata beneath the Milford Group form an extensive belt in the eastern Lardeau Range of the Selkirk Mountains. Faults and Quaternary drift isolate them from the well-constrained stratigraphy in the Badshot Range. Following reconnaissance mapping, Fyles and Eastwood (1962) noted that these strata shared similarities with both the Lardeau and Milford groups, but due to important stratigraphic differences and a combination of structural complexity and poor exposure they did not suggest a correlation. On the basis of mesoscopic structures and the distribution of Jowett-like metabasaltic rocks, Read (1976) interpreted a kilometre-scale, pre-Carboniferous syncline to span from Trout Lake and Comaplix Mountain. He suggested that the pre-Milford strata in the eastern Lardeau Range represent a fold repetition of the Index and Badshot formations and Hamill Group, similar to the earlier regional interpretation by Walker and Bancroft (1929). On the basis of lithological and structural similarities and equivalent stratigraphic position beneath Mississippian rocks, Read and Wheeler (1976) and Read et al. (2009) assigned to the Lardeau Group all strata between the two belts of Milford Group strata north of Trout Lake (Figure A1-1). On the basis of lithologic similarity, Read et al. (2009) suggested correlations with the Jowett and Broadview and (or) Index formations of the Lardeau Group. Kraft et al. (2007) described the same strata, grouped them as the Northeast Arm assemblage, and correlated them with the lower half of the Lardeau Group, and possibly underlying Lower Cambrian units.

2.2.4 Chase and Silver Creek formations

Between Chase and Upper Arrow Lake, calcareous quartzite of the Chase Formation (Jones, 1959) has been interpreted as the Middle Devonian stratigraphic base of a succession of mid-Paleozoic supracrustal rocks (Figure 2-2; Glombick, 2005; Lemieux, 2006; Thompson et al., 2006). Although this succession was originally inferred to comprise Precambrian strata (Jones, 1959), its constituent formations (Silver Creek, Tsalkom, Sicamous and Eagle Bay) are now known to be Late Devonian and Mississippian in age (Erdmer et al., 2001; Thompson et al., 2006). The Chase Formation unconformably overlies paragneiss of probable Late Proterozoic age interpreted to have formed a topographic high, the Okanagan High, at the outer edge of the Cordilleran miogeocline (Thompson et al., 2006; Lemieux et al., 2007).

Calcareous quartzite at the base of the Milford Group at Tenderfoot Lake (Unit 18 of Read, 1973) was correlated with the Devonian Chase Formation by Thompson et al. (2006) and Lemieux et al. (2007) based on lithological and stratigraphic evidence. This correlation was presented as a stratigraphic link between the Chase Formation and the Cordilleran miogeocline (Thompson et al., 2006; Lemieux et al., 2007). In contrast, Colpron and Nelson (2009) proposed that a terrane boundary (major fault) separates the Chase and Silver Creek formations from all rocks east of their present exposures.

Amphibolite and amphibolitic schist at Tenderfoot Lake (Unit 13 of Read, 1973) and on Scalpingknife Mountain south of Nakusp (Figure 1-7; Unit 5 of Hyndman, 1968) were originally interpreted to pre-date the Milford Group, but were not correlated with known stratigraphic divisions. Lemieux (2006) and Thompson et al. (2006) interpreted these occurrences and amphibolitic schist along Upper Arrow Lake (Unit 3d of Lemieux, 2006) to represent a mid- or Late Devonian unit that stratigraphically overlies the Devonian Chase Formation and correlates with amphibolitic schist in the Silver Creek Formation.

2.3 Results of geological mapping

Field data were collected during 8 months of bedrock mapping in 2006, 2007 and 2008. A revised stratigraphic terminology is used here and in Kraft et al. (2011a; 2011b; 2011c) because previous stratigraphic nomenclature could not be reconciled with new observations. It includes a new stratigraphic division, the

Mount Sproat assemblage (Kraft et al., 2011a), for pre-Milford strata between Trout and Upper Arrow lakes. The relations and internal stratigraphy of the Mount Sproat assemblage are summarized below and described in detail in Appendix 1. Mapping results have been published in three 1:50 000 scale Geological Survey of Canada Open File maps (Kraft et al., 2011a; 2011b; 2011c), which are included in the appendix. Unpublished maps and descriptions of local stratigraphy in this thesis provide additional data.

2.3.1 Lardeau Group

The oldest rocks mapped for this study belong to the Lardeau Group.

Akolkolex Formation

The Akolkolex Formation (Logan and Colpron, 2006) is exposed north of Beaton Arm on Comaplix Mountain (Figure A-1). It comprises sharply interlayered grit and grey, tan, green and dark green phyllite that give a striped appearance to glaciated exposures. Beds are typically a few centimetres to about a metre thick. Grit is light brown or grey, has phyllitic to finely micaceous partings and contains well rounded sand to pebble size quartzofeldspathic granules and clasts. Size grading of grit layers was observed at several locations; fining direction at one locality was stratigraphically downward.

Jowett Formation

Near Comaplix Mountain, well preserved Jowett Formation (Fyles and Eastwood, 1962) strata are in the greenschist metamorphic facies. The Jowett Formation west of the Incomappleux River and north of the Beaton Arm of Upper Arrow Lake is dominantly massive or weakly foliated pale green greenstone. Phenocrysts of plagioclase and chloritized augite, pillows, flow-banding, vesicular texture and mafic dikes inferred to be subvolcanic feeders were observed on the west and south sides of Comaplix Mountain, in the hinge zone of the Holyk antiform. A few subordinate, possibly discontinuous, horizons of medium green to dark green phyllite are interlayered with greenstone. Horizons of similar pebbly grit and phyllite occur below (Akolkolex Formation) and above (Broadview Formation) at Comaplix Mountain (Figure 2-3). Both upper and lower contacts of the metavolcanic rocks are gradational and at least locally are either interlayered or repeated by folds.

The metavolcanic horizon was traced westward from Comaplix Mountain along the increasingly strained west limb of the Holyk antiform to McCrae Peak. Across this area, the Jowett Formation thins substantially and massive greenstone passes laterally into green phyllite and phyllitic greenstone (see description below under McCrae Peak succession).

Broadview Formation

In the Trout Lake area, the Broadview Formation (Fyles and Eastwood, 1962) can be subdivided into two units based on a predominance of either phyllite and schist or quartzite and grit.

North of Beaton Arm (Figure 2-11), the lower ~700-900 m of the Broadview Formation contains green and grey, commonly carbonaceous, phyllite (McCrae Peak and Comaplix Mountain; figures 1-7 and 2-3). Crystalline quartz veinlets or ‘sweats’ along the S1 transposition foliation are common, and infrequently define F1 rootless folds. Unlike carbonaceous phyllite in the Milford Group, the presence of D1 quartz veinlets in Broadview phyllite imparts a waviness or anastamosing nature to the dominant foliation (S2). North of Trout Lake, the phyllite-rich lower Broadview Formation is overlain by a laterally persistent unit of grit, which comprises pale green to light grey or white quartzite to sub-arkosic wacke with millimetric blue-quartz granules. Where exposure is adequate, graded bedding in gritty quartzite is apparent. Phyllitic parting surfaces often define millimetric laminations that parallel compositional layering. Laminated texture is especially strong on the west flank of Mount Thompson and occurs along strike at McCrae Peak. Identical laminated white quartzite forms an inlier on Trout Mountain and is here correlated with the Broadview Formation. Like the Jowett Formation, the Broadview Formation undergoes a lateral sedimentary facies change near McCrae Peak (see ‘McCrae Peak succession’ below).

McCrae Peak succession

Lithofacies of the Lardeau Group at the stratigraphic level of the Jowett and lower Broadview formations differ in the McCrae Peak area relative to localities along strike to the east and south, and are referred to here as the McCrae Peak succession (Figure 2-3).

Metabasalt of the Jowett Formation tapers from its regionally typical ~0.1 to >1 km thickness to a few metres of green phyllite and phyllitic volcaniclastic rocks on a ridge north of McCrae Peak (Figure 2-4A). Greenstone near Comaplix Mountain passes along strike into strongly dark green phyllite with rare agglomerate-like texture interpreted to represent a volcanic origin. Carbonaceous phyllite in the lower and mid-levels of the Broadview Formation between the mouth of the Incomappleux River and Comaplix Creek passes westward into a more diverse succession of green, grey and tan phyllite, quartzofeldspathic grit, marble and quartzite. An overlying quartzite and grit-dominated unit of the Broadview Formation traverses the McCrae Peak area uninterrupted from Mount Thompson to Upper Arrow Lake (Kraft et al., 2011a; 2011c). Unlike elsewhere in the study area, much of the quartzite at McCrae Peak is micaceous, tan coloured, and lightly rusty weathering, but retains its laminated and poorly sorted texture (figures 2-4E and 2-4F). Horizons of non-micaceous quartzite are lithologically indistinguishable from quartzite in the Broadview Formation at Mount Thompson.

Several metres of bedded barite occur within phyllite on McCrae Peak's north ridge (Figure 2-4C). Mapping from this study indicates that the barite occurs in the lower Broadview Formation roughly 140 m stratigraphically above the equivalent of the Jowett Formation. The barite is gradationally underlain successively by several metres each of flinty black quartzite (Figure 2-4B), carbonaceous slaty phyllite and sooty black phyllite. Distinctive rusty orange weathering iron carbonate-bearing phyllite to impure marble (Figure 2-4D) is common in the Lardeau Group between McCrae Peak and Comaplix Mountain.

2.3.2 Mount Sproat assemblage

The Mount Sproat assemblage (MSA) is a >4 km thick (present, composite thickness) succession of polydeformed phyllite, schist, marble, quartzite and mafic to intermediate metavolcanic rocks that unconformably underlies the Milford Group near Upper Arrow Lake. It includes strata that have previously been included in the Lardeau, Milford and Kaslo groups. The MSA is named for its most complete and accessible exposures on Mount Sproat. It is also readily observable on the shoreline of Upper Arrow Lake during low water levels. In their present state, lithological units range in thickness from ~1 m to >100 m and most rock types are repeated stratigraphically and (or) structurally several times.

Exposure of the MSA is generally poor below treeline, but road cuts, bluffs, shorelines, and ridges provide sufficient outcrop to correlate horizons along strike and delineate the general stratigraphy of the assemblage, which is illustrated in Figure A1-3. Although the MSA has been tightly folded, north of the Kuskanax batholith stratigraphic markers are traceable for up to several kilometres and the internal stratigraphic succession is generally consistent at map scale (Kraft et al. 2011a; 2011b). Along the eastern margin of the Kuskanax batholith the internal stratigraphy of the MSA has been significantly complicated by Mesozoic deformation.

Stratigraphy of the Mount Sproat assemblage

The Mount Sproat assemblage was mapped according to lithologically-defined subunits (Kraft et al., 2011a; 2011b; 2011c). Lithological trends and associations in the Mount Sproat assemblage form the basis for its subdivision into four members (Figure A1-3) described here and shown in map view in Figure A1-1. Some rock types transcend the boundaries of these members. Tight folding has transposed bedding. Way-up indicators were not identified, but the map pattern, contact relations and a transition from 'Lardeau-like' to 'Milford-like' lithofacies indicate that the following stratigraphic order is upright.

The Carbonaceous member is the structurally lowest member of the MSA; it forms the core of the Sproat antiform from Mount Sproat to the Jurassic Hadow stock. The Carbonaceous member comprises a mixed gradation of carbonaceous phyllite to banded fine-grained carbonaceous quartzite (figures 2-5A and 2-5B), limy carbonaceous phyllite and grey marble (Figure 2-5C), and quartzite (Figure 2-5D). Conspicuous white laminae and veinlets of quartz or calcite define a transposition foliation that is deformed by the regional mid-Jurassic fabric that controls the regional map pattern (Read et al., 2009). At 'The Ramparts' locality between Trout and Tenderfoot lakes, similar carbonaceous quartzite and argillaceous marble, which are interlayered with brown and purple gritty quartzite of the Broadview Formation (Read, 1973) in a fault-bound tectonic panel, are herein correlated with the Carbonaceous member.

The Heterolithic member of the MSA conformably overlies the Carbonaceous member between Mount Sproat and Trout Mountain. It is a sharply interbedded association of mafic metavolcanic strata, micaceous phyllite, fine-grained biotite schist, and white marble in addition to carbonaceous rocks like those in the underlying Carbonaceous member. The Heterolithic member is distinguished from the Carbonaceous member by the increased diversity of rock types that include metavolcanic rocks (Figure 2-5E), non-carbonaceous phyllite and semi-pelitic schist, and buff weathering marble (Figure 2-5F). The base of the Heterolithic member is placed at the lowest laterally extensive occurrences of metavolcanic or non-carbonaceous rocks in the MSA. Between Galena Pass and the Hadow stock, the Heterolithic member is truncated by the sub-Milford unconformity. North of Galena Pass, the Heterolithic member is overlain by the Amphibolitic Schist member.

The combined Heterolithic and Carbonaceous members are herein referred to informally as the lower Mount Sproat assemblage.

The Amphibolitic Schist member crops out in the hanging wall of the Columbia River fault zone from St. Leon Creek and Catherine Lake to Mount Sproat. It consists primarily of medium- to coarse-grained amphibole-plagioclase schist (± quartz ± calcite ± biotite ± chlorite ± epidote ± titanite) and greenstone (Figure 2-6). Subordinate marble, calc-silicate, semi-pelitic and pelitic schist interlayer with amphibolitic schist. Where rocks are in the greenschist-facies near Beaton Arm, mafic units of the Amphibolitic Schist are phyllitic and gradational with the Heterolithic member. The base is placed at a cobble conglomeratic greenschist (Figure 2-6A), stratigraphically above which amphibole and biotite become abundant in schist on the south flank of Mount Sproat. The Amphibolitic Schist member grades upward into the Upper Clastic member at Upper Arrow Lake and is absent beneath the sub-Milford unconformity in the eastern Lardeau Range.

The Upper Clastic member of the MSA gradationally overlies and interlayers with the Amphibolitic Schist member in the Beaton Arm and at St. Leon Creek (Figure A1-1). The Upper Clastic member comprises a mixed gradation of pelitic schist and phyllite, metasiltstone, metasandstone, amphibolitic schist and pebble to cobble polymict and oligomict conglomerate (Figure 2-7). Some rock types are similar to parts of the Milford Group, with which it has been correlated previously (Read and Wheeler, 1976). Unlike the overlying Milford Group, the Upper Clastic member contains a substantial amount of mafic to intermediate metavolcanic or metavolcaniclastic rocks (Figure 2-7D), and conglomerate (Figure 2-7E) is abundant throughout the member near St. Leon Creek. Amphibole- or biotite-rich schist and fragmental rocks indistinguishable from units in the underlying Amphibolitic Schist member are interlayered with metasandstone (Figure 2-7F) and metasiltstone of the Upper Clastic member near St. Leon Creek.

The upper contact with the Milford Group could not be observed due to cover; it is inferred to be an angular unconformity on the basis of the map pattern and for other reasons discussed in chapters 3 and 4.

The combined Amphibolitic Schist and Upper Clastic members are referred to herein as the upper Mount Sproat assemblage.

An isolated succession of biotite schist (± staurolite ± garnet), calc-silicate and marble on the western shoreline of Upper Arrow Lake across from the village of Nakusp (Figure 2-11) is correlated with the Upper Clastic member because of strong lithological similarity. The succession structurally overlies a domal culmination of Monashee cover sequence paragneiss (unit Pqfh of Lemieux, 2006 and Thompson et al., 2009a). The contact with paragneiss is obscured by drift on the shoreline. Because of omission of underlying strata of the Mount Sproat assemblage and Lardeau Group and the discordance between the contact and compositional layering, the contact is inferred to be a fault corresponding to the Columbia River fault zone. The relationship of this succession to rocks included in the Triassic Slocan Group to the north (Thompson et al., 2009a) was not observed and is inferred to be a fault.

Map relations of the Mount Sproat assemblage

The contact between the Mount Sproat assemblage and Broadview phyllite in the valley of Trout Lake is covered. Strong lithological similarities across the contact between Trout Lake and Beaton (Figure A1-1) give the appearance of a gradational transition, but truncation of markers in the MSA in the eastern limb of the Sproat antiform indicates a faulted contact, which is likely the northern extension of the post-80 Ma Adit fault (Read et al., 2009; Kraft et al., 2011a). On Trout Mountain (Figure 1-7), the Carbonaceous member gradationally overlies an inlier of distinctive gritty quartzite identical to the Broadview Formation (Figure 2-8). A gradational transition between Broadview phyllite and MSA rock types immediately west of Trout Lake, and similarities between Broadview quartzite and MSA quartzite at The Ramparts (Figure 1-7), support a conformable relationship.

Macrofossils have not been identified in rocks of the Mount Sproat assemblage and seven samples of crystalline limestone from the MSA were found to be barren of conodonts.

2.3.3 Milford and Kaslo groups in the Lardeau Range

Due to the inclusion of strata in the Mount Sproat assemblage, the Milford and Kaslo groups are here interpreted to occur in the Lardeau Range only in the Hill Creek syncline and south of St. Leon Creek. The Milford Group in the Lardeau Range comprises basal pebble conglomerate overlain by a 500 m to 1200 m thick interval of dark grey argillite and siltstone that is in turn capped by up to 500 m of rhythmically interbedded sandstone and siltstone. The upper sandstone unit interfingers with and is intruded by sills of greenstone of the Kaslo Group. The Kaslo Group consists of massive to moderately foliated greenstone and locally abundant gabbroic rocks. Near St. Leon Creek the base of the Milford Group is placed at a conglomerate that separates the lithologically diverse Upper Clastic member of the MSA from a structurally overlying argillite and sandstone succession (Milford Group) that directly underlies metabasalt of the Kaslo Group. Clasts within the conglomerate include amphibolitic schist similar to rocks in the Mount Sproat assemblage. The base of the conglomerate was not exposed. In the eastern Lardeau Range, the base of the Milford Group truncates strata of the Heterolithic member that bear two foliations (see Chapter 4). The conglomerate locally contains an abundance of clasts and matrix similar to silver-grey phyllite of the immediately underlying Heterolithic member or, rarely, blue-quartz granule grit characteristic of the Broadview Formation in the area. The reader is referred to Chapter 3 for further description of the Milford Group.

2.3.4 Re-evaluation of the Chase quartzite at Upper Arrow Lake

Investigation of exposures along new logging roads in the area of Halycon Hot Springs (Figure 1-7) showed that the Chase quartzite and overlying semi-pelitic paragneiss is separated from the Mount Sproat assemblage by tens of metres or more of strongly faulted rocks. The cataclastic nature and breadth of the fault zone and the apparent metamorphic contrast across it (migmatitic paragneiss in the footwall and epidote amphibolite-facies schist in the hanging wall) indicate the fault is part of the Eocene Columbia River fault zone (Read and Brown, 1981; Lane, 1984; Carr, 1991; Kraft et al., 2011a). This segment of the Columbia River fault zone is inferred to be truncated by or merge with the newly-identified Blind Bay fault, across which displacement is on the order of 50-250 metres based on the mapped offset of the Hill Creek syncline near Beaton Arm

(Figure A1-1).

2.3.5 Geology of the Tenderfoot Lake area

The Milford Group can be traced semi-continuously from the Lardeau Range into the Tenderfoot Lake area (Read and Wheeler, 1976; Kraft et al., 2011a; 2011b) where it contacts older and more highly strained rocks in the Falls antiform (Read, 1973). Metamorphic grade is higher (garnet zone; Read, 1973) and strain is greater at Tenderfoot Lake than in the Lardeau and Badshot ranges to the north, but superior exposure allows for more detailed observation of map relations near Tenderfoot Lake.

The Falls antiform east of Tenderfoot Lake (Figure A1-5) is cored by strongly rusty weathering medium- to coarse-grained quartzose biotite-muscovite schist (Figure 2-9). The schist is gradationally interlayered with quartzose carbonaceous biotite schist, banded garnet-biotite schist, and banded dark grey marble. Where it is quartz-rich, the schist preserves a penetrative spaced foliation, S1, defined by micaceous partings several millimetres apart. S1 has been crenulated and overprinted by the regional north-striking schistosity, S2 (Figure 2-9B). The spaced S1 foliation has been obliterated by S2 in more micaceous lithofacies (Figure 2-9C). Marble layers in the schist display colour banding that outlines convoluted, intensely deformed folds consistent with polydeformation (Figure 2-10E). The schist is interlayered across a 2 m zone with a horizon of medium-grained, strongly foliated amphibolite referred to here as the Tenderfoot amphibolite (figures 2-11D and 2-11E). Lithological boundaries at the interlayered contact are sharp to diffuse across a few centimeters and are transposed into the main schistosity, S2. The contact is locally intruded by a ~40 cm wide undeformed granitic sill inferred to be part of the Kuskanax suite.

On its western side the Tenderfoot amphibolite has a sharp, transposed contact with a calcareous quartzite and calc-silicate unit that grades westward into metasandstone, metasiltstone and calc-silicate rocks of the McHardy assemblage (Figure 2-10). The contact was observed in only a few metres of outcrop and is covered elsewhere. The calcareous quartzite and calc-silicate unit strikes north across Tenderfoot Lake into calcareous quartzite that was interpreted by Lemieux et al. (2007) to correlate with the Devonian Chase Formation.

Field relations are less clear north of Tenderfoot Lake due to increased structural complexity and inaccessibility due to steep terrain. The calcareous quartzite occurs at least 100 m up section from (west of) the lowest exposed McHardy assemblage rocks north of Tenderfoot Lake.

A rock succession ~100-150 m thick that occurs between clear Milford and pre-Milford rocks north of Tenderfoot Lake was examined. The succession comprises dark green, fine-grained foliated greenstone to amphibolite underlain by rusty weathering tuffaceous and conglomeratic metasandstone and sandy marble. One isolated 10x30 m outcrop of massive, anthophyllite-rich metamorphosed ultramafic rock was observed in the succession but its field relations are obscured by drift. Sandy marble, which contains ~30-60 modal percent coarse sand-sized quartz grains, is gradationally interbedded with metasandstone and is in sharp contact with amphibolitic greenstone correlated with the Tenderfoot amphibolite. The sandy marble also interlayers with a prominent, thick white marble unit that overlies (is west of) the amphibolitic greenstone and is similar to calcareous quartzite roughly 250 metres to the west. The contact of metasandstone with the Falls antiform schist was not seen.

2.4 Discussion of field data

2.4.1 Distinction of the MSA from the Lardeau Group

A number of characteristics distinguish the Carbonaceous and Heterolithic members of the MSA from the Lardeau Group, in which they were previously included (Read and Wheeler, 1976; Read et al., 2009).

1) The MSA includes no equivalent of the Akolkolex and Broadview formations. Coarse clastic rocks (“grit”) that dominate those extensive formations were observed in the Mount Sproat assemblage only where it interlayers with the Broadview Formation at The Ramparts, and in one horizon of phyllite with rare blue quartz granules in the Heterolithic member. Siliciclastic rocks in the Carbonaceous and Heterolithic members overwhelmingly are fine grained.

2) The stratigraphic context of metavolcanic rocks in the Heterolithic member is unlike those of the Lardeau Group. Metavolcanic rocks in the Lardeau Group are mostly restricted to the Jowett Formation and a few thinner horizons in the upper Index Formation (Fyles and Eastwood, 1962; Logan and Colpron, 2006). Neither the Carbonaceous nor Heterolithic member of the MSA contain an equivalent of the Jowett Formation. Rather, Heterolithic member volcanic units are thinner and interlayer with phyllite and marble similar to the upper Index

Formation. An analog of the Akolkolex or Triune-Ajax-Sharon Creek formations, which contact Index Formation metavolcanic rocks, does not occur in the MSA, however.

3) The conformable contact between the Carbonaceous member and quartzite of the Broadview Formation at Little Trout Mountain precludes correlation of the MSA with lower Lardeau Group or older strata.

4) Distinctive carbonaceous quartzite, white orthoquartzite, and differentially weathering marble in the Carbonaceous and Heterolithic members have no equivalents in the Lardeau Group.

Despite these differences, a stratigraphic connection between the lower MSA and Lardeau Group is indicated by the conformable transition between Broadview quartzite and the Carbonaceous member. Instead of the lateral equivalence with the Index Formation proposed by Kraft et al. (2007), the available field data lead to the interpretation that the Carbonaceous and Heterolithic members depositionally overlie the Broadview Formation, and thus, the MSA conformably overlies the Lardeau Group.

2.4.2 Distinction of the MSA from the Milford and Kaslo groups

The Amphibolitic Schist and Upper Clastic members are lithologically unlike the other MSA members, but field observations link them physically to the Heterolithic member of the MSA and distinguish them from the Kaslo and Milford groups. The Amphibolitic Schist member is not a lithological match with the uniformly basaltic and gabbroic Kaslo Group. Mafic rocks in the Amphibolitic Schist member are platy to schistose and they commonly have significantly more feldspar and biotite than Kaslo Group greenstone. Abundant biotite schist, calcareous amphibolitic schist and pelitic schist, and the gradational variations between them, are widespread in the Amphibolitic Schist member but are unknown in the Kaslo Group. Increased strain or metamorphism cannot produce the significant compositional differences. Additionally, the gradational relationship between the Heterolithic and Amphibolitic Schist members on Mount Sproat and the distribution of map units in the Upper Arrow Lake area show that the Amphibolitic Schist member stratigraphically underlies the Upper Clastic member and the Milford Group.

The contact between the Upper Clastic member and the Milford Group could not be observed, but outcrop distribution and map scale truncations lead to the interpretation that the contact is an angular unconformity. The contrasting deformation histories across the contact, which is most readily observed in the eastern Lardeau Range, are compatible with an unconformable relationship between Milford and MSA rocks, or a faulted contact. Milford Group strata overlie progressively deeper levels of the MSA from west to east, indicating angular discordance at the contact, e.g, an erosional onlap. The Upper Clastic member of the MSA contains a broader variety of rock types than the relatively monotonous Milford Group, although argillaceous layers and quartz pebble conglomerate in each are visually indistinguishable.

2.4.3 Chase Formation at Upper Arrow Lake

New mapping of the Chase Formation on Upper Arrow Lake showed that the brittle Blind Bay fault (Figure A1-1), which is interpreted as a splay of the Columbia River fault zone, juxtaposes the Chase Formation and overlying Silver Creek Formation rocks with roughly coeval but less metamorphosed rocks in the Mount Sproat assemblage. The trace of the Columbia River fault zone therefore coincides with the eastern limit of the Chase Formation. Assignment of amphibolitic schist on either side of the fault to the Silver Creek Formation, as proposed by Lemieux (2006) and supported by results of this study, suggests throw on the Columbia River fault zone at this location is hundreds of metres or less. This would refute interpretations of the Columbia River fault zone as a core complex-bounding detachment fault (Parrish et al., 1988) and instead indicates brittle fault offset of an attenuated metamorphic and structural gradient or ‘transition zone’ (Lemieux, 2006). Continuity of Mount Sproat assemblage strata in the eastern Beaton Arm shows that displacement on the Blind Bay fault diminishes to zero in the Beaton Arm (Figure A1-1; Kraft et al., 2011a).

2.4.4 Interpretations of Goat Range geology

Read (1973) placed the Jurassic Spyglass fault at Tenderfoot Lake between the Tenderfoot amphibolite (part of Read’s Unit 13) and the Milford Group. His map shows interfingering of those units east of the Spyglass fault in the hinge of the Falls antiform. In the core of the antiform, rusty weathering mica schist that directly underlies the Tenderfoot amphibolite was assigned to the Broadview Formation (Read, 1973; Roback, 1993).

Correlation of the Falls antiform schist and Tenderfoot amphibolite

Field investigation for this study found that polydeformed schist, marble and amphibolite in the core of the Falls antiform are lithologically more similar to the Mount Sproat assemblage than to the Lardeau Group in the Trout Lake area. The following observations were made: 1) grit and quartzite are minor in the Falls antiform rocks, 2) the association of quartzose carbonaceous schist, banded grey marble and mafic volcanic rocks interbedded with pelitic schist is a match for the Heterolithic member and is unlike the Broadview Formation, 3) rusty weathering pelitic schist is indistinguishable from schist transitional between the Broadview Formation and the Mount Sproat assemblage west of McCrae Peak, and 4) the rocks in the Falls antiform are similar to strata at The Ramparts (Figure A1-5) that are correlated with the Mount Sproat assemblage. On that basis, the rocks in the Falls antiform are assigned to the Mount Sproat assemblage, and are probably equivalent to the Heterolithic and Amphibolitic Schist members.

Closest to Tenderfoot Lake in the hinge zone of the Falls antiform, the succession of conglomerate, tuffaceous sandstone, marble and amphibolitic schist that structurally (and stratigraphically?) overlies the Falls antiform schist is similar to rocks in the Upper Clastic and Amphibolitic Schist members of the MSA. Except for the amphibolitic schist, these strata also resemble rock types in the McHardy assemblage. It is difficult to correlate those rocks with the McHardy assemblage, however, because of the intervening amphibolite horizon that is correlated with the Tenderfoot amphibolite south of Tenderfoot Lake. Calcareous quartzite similar to that in the McHardy assemblage appears to be infolded with this upper succession. Although more work is needed to resolve the map relations in the hinge zone of the Falls antiform, it is clear that the calcareous quartzite unit at Tenderfoot Lake is conformable within the McHardy assemblage.

The gradational interlayering between the Tenderfoot amphibolite and polydeformed schist is consistent with the depositional relationship implied by the map of Read (1973) and makes the Tenderfoot amphibolite older than the pre-Milford deformation. Roback (1993) re-interpreted the Tenderfoot amphibolite and associated clastic rocks as the Keen Creek assemblage of the Milford Group and equated a nearby segment of the Spyglass fault (Figure A1-1) with the Stubbs thrust, a hypothesized terrane-bounding fault that would place the McHardy assemblage over the Keen Creek assemblage in the southern Goat Range (Figure A1-1; Klepacki, 1985). Results of this study, however, favour Read's (1973) original interpretation that the Tenderfoot amphibolite pre-dates the Milford Group. It is correlated here with metavolcanic horizons in the Heterolithic member of the Mount Sproat assemblage. Presence of the Spyglass fault between the McHardy assemblage and the Tenderfoot amphibolite is not supported by new observations. In order for the contact between the Tenderfoot amphibolite and calcareous quartzite to be tectonic the fault would have to have been masked by subsequent strain and metamorphism. Such masking of a fault is considered unlikely because the Spyglass and other Jurassic faults in the area post-date the main schistosity-forming event and can be identified by zones of metamorphosed fault rock (Read, 1973). Read's (1973) map indicated that an alpine glacier would have, in the 1960's, concealed the outcrop in which the transposed contact between the Tenderfoot amphibolite and the McHardy assemblage was observed in this study. These observations suggest that the Spyglass fault does not exist north of the North Fork stock (Figure A1-1).

Calcareous quartzite at Tenderfoot Lake

Observations from this study support Read's (1973) interpretation that the calcareous quartzite is interbedded with mixed siliciclastic and calc-silicate strata in the McHardy assemblage. Although the quartzite is a lithological match for the Chase Formation, the succession of argillaceous, arenaceous and carbonate strata overlying the Tenderfoot quartzite is lithologically unlike the mixed pelitic, semi-pelitic and amphibolitic rocks that overlie the nearest Chase Formation equivalent at Upper Arrow Lake (Lemieux et al., 2004; Kraft et al., 2011a). The Tenderfoot quartzite's stratigraphic position between the Milford Group and the Tenderfoot amphibolite/Mount Sproat assemblage is inconsistent with the Chase quartzite, which underlies the pre-Milford amphibolitic schist unit west of Nakusp (Lemieux et al., 2006) and in the Okanagan-Shuswap region to the west (Thompson et al., 2002; 2006). Instead, the Tenderfoot Lake calcareous quartzite and calc-silicate horizon is inferred to correspond to a Late Mississippian carbonate at a comparable stratigraphic level a few kilometres to the south (Orchard, 1985) and to calcareous sandstone that occurs in lower exposures of the Milford Group and Thompson assemblage north of Trout Lake (see Chapter 3; Kraft et al., 2011a; 2011b).

2.5 Volcanic lithogeochemistry

Mafic volcanogenic strata occur throughout the area and at most stratigraphic levels spanning the Paleozoic Era. Whole-rock geochemistry of meta-igneous units of mafic composition is used here to describe the temporal trends of Paleozoic magmatism in the northern Kootenay Arc and to provide interpretations of the tectonic settings of stratigraphic constituents. The tectonic setting of samples analyzed in this study is interpreted using trace-element profiles modeled after Piercey et al. (2006) and a variety of tectonic discrimination diagrams (Wood, 1980; Shervais, 1982; Meschede, 1986; Pearce, 1996) that were generated from empirical studies of mafic magmatic rocks in well-constrained (usually modern) tectonic settings.

Principles

Empirical observation shows that magma composition varies systematically according to tectonic setting of emplacement (Pearce and Cann, 1973). Geochemical variations arise from differences in the processes that form and modify magmas in different tectonic environments. Trace-elements are particularly reflective of these differences because of their sensitivity to magmatic processes and low concentration. Trace-element profiles are drawn on primitive mantle-normalized multi-element diagrams that include rare earth elements, high field-strength elements and transition elements. The profiles are compared visually with those of reference compositions from modern environments. The Ti-Zr-Y diagram of Pearce and Cann (1973) is effective at distinguishing within plate basalt but other fields on the diagram are ambiguous. The Th-Hf-Ta diagram of Wood (1980) effectively identifies volcanic arc basalt and can subdivide arc basalt into tholeiitic and calc-alkaline basalt (CAB) series. The Ti-V diagram of Shervais (1982) has a theoretical and empirical basis for distinguishing arc tholeiite (IAT) from mid-ocean ridge basalt (MORB) and back-arc basin basalt (BABB) from ocean island basalt (OIB). Whereas titanium has one valence state, vanadium has three and they have significantly different partition coefficients in pyroxene and magnetite (Rollinson, 1993). Consequently, the chemical behaviour of vanadium is controlled by oxygen fugacity, which varies systematically across tectonic settings (Shervais, 1982). The Zr-Nb-Y diagram of Meschede (1986) subdivides MORB into 'normal' and 'enriched' varieties on the basis of niobium content, but it gives ambiguous classifications for most other compositions. These five plots are used in combination to interpret the tectonic affinity, which is indicated in the appended geochemical data tables (appendix A2-3).

Effects of metamorphism

Greenschist and higher metamorphism can mobilize most major elements (e.g. SiO_2, Na_2O, K_2O, and CaO) and low field strength elements (e.g. Cs, Rb, Ba, Sr, U; MacLean, 1990; Lentz, 1999; Large et al., 2001); thus their concentrations in metamorphic rocks may not accurately reflect protolith values. On the other hand, some major elements (Al_2O_3, TiO_2, $\pm P_2O_5$), transition elements (V, Ni, Cr, Co), high field strength elements (Nb, Ta, Zr, Hf, Y, Sc, Ga), rare earth elements (La, Ce, Pr, Nd, Sm, Gd, Tb, Dy, Er, Yb, Lu) and Th are relatively immobile under those conditions (Floyd and Winchester, 1978; Whitford et al., 1989; Pearce, 1996; Jenner, 1996; Barrett and MacLean, 1999). Geochemical studies of mafic rocks metamorphosed at amphibolite- and eclogite-facies have found coherent protolith geochemical signatures (Creaser et al., 1999; Dusel-Bacon and Cooper, 1999; Piercey et al., 2001; 2002; 2006). In light of these conclusions, measured concentrations of immobile, incompatible elements in this study are taken to reflect protolith characteristics. Metamorphism is assumed to be isochemical (at the scale of analyzed hand samples) with respect to the immobile elements in figure 2-14.

2.5.1 Sampling and analytical methods

Samples of all local Paleozoic meta-igneous and volcaniclastic units were collected during geological mapping. Sample sites within the map area are shown according to geochemical affinity in Figure 2-11. Additionally, three amphibolite horizons in the uppermost Hamill Group at Kootenay Lake were sampled for comparison. All samples have experienced regional metamorphism at greenschist to epidote amphibolite-facies conditions, except for mid-amphibolite grade samples from the Hamill Group and from the immediate footwall of the Columbia River fault zone near Halcyon Hot Springs.

Zones of visible post-metamorphic hydrothermal alteration, weathered surfaces and veins were excluded from samples. Samples were taken where evidence most supported an igneous protolith or where shearing was least intense. Many of the mafic rocks, however, are moderately to strongly foliated and all contain secondary mineral assemblages. Greenschist-facies samples comprise secondary or recrystallized: chlorite, actinolite, albite, quartz, ± biotite, ± epidote, and locally carbonate. Epidote amphibolite-facies amphibolitic schist from the Amphibolitic Schist member (uDMSas of Kraft et al., 2011a) comprises metamorphic hornblende ± biotite, plagioclase, epidote, minor titanite and, locally, carbonate. Units DMSv1 and uDMSas frequently have gradational contacts with metasedimentary rocks and are interpreted to have volcaniclastic or epiclastic protoliths. Mafic strata in the Lardeau Group, Thompson assemblage, Kaslo Group and units uDMSv2 and uDMSv3 each contain, at least locally, primary structure such as flow banding, amygdules or pillows.

Green phyllite is commonly interlayered with and (or) contains centimetre to metre-scale lenses of buff weathering dolomitic marble or calc-silicate, suggesting an extrusive, possibly volcaniclastic, origin. Some gradational contacts between green phyllite and grey phyllite or biotite schist indicate local sedimentary mixing and preclude an intrusive origin. A coarse-grained gabbroic unit in the Heterolithic member (uDMSv2) on the west flank of Trout Mountain that has unknown contact relations is inferred to be intrusive.

Laboratory methods

All samples were submitted to the Ontario Geoscience Laboratories in Sudbury, Ontario for geochemical analysis. Samples were crushed with a steel jaw-crusher and pulverized in an agate mill. Major elements were determined by XRF (x-ray fluorescence) on fused discs after samples were run for loss on ignition. Sample solutions were produced by closed vessel multi-acid digestion using the methods of Tomlinson et al. (1999). Solutions were analyzed for trace-elements using ICP-MS (inductively coupled plasma - mass spectrometry).

Measurements with values near detection limits were not plotted nor are they considered in the discussion. Duplicate and standard analyses were conducted for data quality control. Plots of various elemental ratios (e.g Ti/V, Zr/Y, La/Sm) and loss on ignition (LOI) against an alteration proxy (Al_2O_3/Na_2O) show no correlation (Appendix A2-3), suggesting that those ratios and LOI have not been biased by alteration processes.

2.5.2 Lithogeochemistry results

Seventy-three samples of mafic metamorphosed volcanic and plutonic rock were analyzed. Results are presented in groups according to map units in the appended Geological Survey of Canada Open File maps (Kraft et al., 2011a; 2011b; 2011c). Figure 2-12 shows tectonic discrimination diagrams for the Hamill, Lardeau and Kaslo groups. Figure 2-13 shows the same tectonic discrimination diagrams for samples of the Mount Sproat assemblage. Data from all map units are plotted in primitive mantle-normalized profiles in Figure 2-14. Classification of the samples into tectonic affinities is generally in agreement between the different tectonic discrimination diagrams and the trace-element profiles. Where discrepancies arise the samples are classified according to trace-element profiles. All data are tabulated in the Appendix (A2-2). Abbreviations in the text are: CAB, calc-alkaline basalt; E-MORB, enriched mid-ocean ridge basalt; IAT, island arc tholeiite; N-MORB, normal mid-ocean ridge basalt; OIB, ocean island basalt.

Hamill and Lardeau groups (lCHv, lPLJv, lPLv)

The Jowett Formation consists of greenschist-facies massive greenstone to green phyllite. Primary igneous textures including pillows, volcanic breccia or agglomerate, flow banding and pseudomorphs after feldspar and clinopyroxene phenocrysts were observed. At Comaplix Mountain, metabasaltic dikes cross-cut pillowed metabasaltic flows of similar composition and texture.

Amphibolite of the Hamill Group at Kootenay Lake and phyllitic to massive chloritic greenstone of the Jowett Formation are alkaline (Figure 2-12A) OIB-like basalt with one outlier plotting as E-MORB on tectonic discrimination diagrams (Figure 2-12). Trace-element profiles range continuously from E-MORB to OIB (Figure 2-14).

Mount Sproat assembage, Heterolithic member (DMSv1)

Green phyllite and massive to phyllitic greenstone forms several mappable horizons in the lower Mount Sproat assemblage. The lowermost metavolcanic horizons in the Mount Sproat assemblage are designated v1. Unit v1 predominantly has geochemical characteristics ranging between OIB and E-MORB, but two samples also yielded N-MORB-like patterns (Figure 2-14A). Three samples of epidote amphibolite from the Tenderfoot amphibolite unit are included in this unit and have trace-element lithogeochemical signatures of E-MORB.

Mount Sproat assemblage, Heterolithic member (DMSv2)

Although visually indistinguishable from unit v1, the uppermost volcanic horizon (or possibly horizons) of the Heterolithic member is geochemically distinct from underlying mafic units and has been distinguished as v2 on that basis. Three of four samples collected from unit v2 plot in the arc basalt field on the Th-Zr-Nb diagram of Wood (1980). Trace-element profiles of four samples have niobium depletions similar to island-arc tholeiite (Figure 2-14B).

Mount Sproat assemblage, Amphibolitic Schist member greenstone (uDMSv3)

Amphibolitic Schist member greenstone is massive to moderately foliated and locally contains centimetre-scale plagioclase phenocrysts. A fragmental, clinopyroxene-phyric phase of the Amphibolitic Schist member greenstone was sampled near Halfway River (Figure 2-6E). All samples from this unit have trace-element profiles of calc-alkaline basalt (figures 2-13C and 2-14B).

Mount Sproat assemblage, Amphibolitic Schist member amphibolitic schist (uDMSas)

Amphibolitic schist consistently yielded CAB signatures similar to associated greenstone unit v3 except one non-arc, OIB-like sample from the Galena Bay area. The Zr/TiO_2 versus Nb/Y diagram (Pearce, 1996) shows basaltic compositions close to the andesite and trachy-andesite fields.

Thompson assemblage (MTv)

A single sample of weakly metamorphosed amygdaloidal basalt from the Thompson assemblage has geochemical attributes similar to E-MORB (figures 2-14E and 2-15). The context of the sample is shown in appended Figure A1-4 and is described with the stratigraphy of the Thompson assemblage in Chapter 3.

Kaslo Group (PKv) and associated gabbro/diorite (Pd)

Kaslo Group samples are weakly to moderately foliated metabasalt (Figure 2-12A) that have mainly N-MORB affinities. Less common E-MORB and one sample of IAT from the contact with the McHardy assemblage were identified. The trace-element profiles of gabbroic sills, dikes and a pluton (Pd) that are associated with Kaslo Group greenstone are indistinguishable from those of the greenstone.

Monashee cover succession (Pqfba)

One sample of coarse grained amphibolite (*sensu stricto*) of late Proterozoic or early Paleozoic age (Lemieux et al., 2007) was collected from the paragneiss succession that immediately underlies the Chase Formation near Halcyon Hot Springs. The sample has an OIB-like alkaline basalt geochemical composition (figures 2-14 and 2-15).

Mantle array and contamination

A plot of Th/Yb versus Nb/Yb (Figure 2-15) shows crustal contamination and influence of subduction zone processes (Pearce and Peate, 1995). All samples follow the mantle array, which is a band of compositions that lack crustal or subduction-zone influence, except for the arc-related units of the Mount Sproat assemblage and two samples from the Kaslo Group. IAT of the Kaslo Group and Heterolithic member show subduction-zone enrichment of an N-MORB composition. Non-arc basalt of the Heterolithic member (unit v1) scatters along the mantle array, indicating no influence of crustal or subduction-zone enrichment. CAB in the Amphibolitic Schist member (amphibolitic schist and greenstone units) plot on a trajectory of subduction zone and (or) crustal contamination of the non-arc unit v1.

2.6 U-Pb zircon geochronology

2.6.1 Sample description and analytical methods

A sample interpreted as a weakly metamorphosed mafic volcaniclastic rock, possibly tuff, was selected from the Amphibolitic Schist unit to constrain the age of the Mount Sproat assemblage.

Zircon was extracted from a ~15 kg sample of chloritic greenstone of calc-alkaline basalt affinity (sample 06TWJK200) collected near the Beaton Arm of Upper Arrow Lake (Figure 2-11). The greenstone forms a massive layer several metres thick that occurs roughly 500 m stratigraphically above the member's basal conglomerate and not more than 100 m below phyllitic argillite of the McHardy assemblage. The greenstone unit ranges from massive to strongly foliated, is texturally homogeneous and it varies in colour from pale chlorite green to greenish grey (Figure 2-16). Millimetres- to centimetres-size lithic fragments of similar composition occur locally giving the rock a fragmental texture. Abundant fine biotite and chlorite can be seen with a hand lens. In thin section, the rock is fine grained, equigranular, and comprises biotite and chlorite in a very fine felsic groundmass (figures 2-16B and 2-16C). Igneous texture was not observed in the sampled locality, but greenstone along strike contains deformed 0.5-2 cm plagioclase crystals interpreted to be phenocrysts (Figure 2-6F).

U-Pb dating by isotope dilution – thermal ionization mass spectrometry (ID-TIMS) was carried out at the University of Alberta's Radiogenic Isotope Facility. The sample was sawn into blocks with a clean diamond saw and washed prior to pulverizing by standard techniques with a steel jaw crusher and disk mill. Methods to isolate and prepare analytical samples and measure the isotopic composition of zircon followed those of Heaman et al. (2002). This procedure utilizes a Wilfley table, magnetic separation techniques and heavy liquids to isolate zircon, and a VG354 thermal ionization mass spectrometer for measurements. The uranium decay constants recommended by Jaffey et al. (1971) were used with Isoplot software (Ludwig, 2003) in all calculations. Atomic ratios have been corrected for fractionation and initial common Pb using the lead evolution model of Stacey and Kramers (1975). Thorium concentration was calculated from the amount of ^{208}Pb and the ^{207}Pb/^{206}Pb age with a small correction. Results are tabulated in appendix A2-4.

2.6.2 Geochronology results

The heavy mineral concentrate from sample 06TWJK200 contained trace apatite and zircon in >99% pyrite. Most zircon grains were pink and sub-angular to well rounded, and are interpreted to be of detrital or xenocrystic origin. Three grains from a group of rare colourless, euhedral zircon and one angular anhedral crystal or fragment (Figure 2-16D) were selected for single grain analyses because they were considered most likely to indicate the eruptive or maximum age of the unit. Results are tabulated in the Appendix (A2-4) and plotted on a concordia diagram in Figure 2-16E.

Grain 1 was a colourless, irregularly shaped fragment with low U (98 ppm) and high Th/U (0.52). It yielded a strongly discordant result with a Neoarchean ^{207}Pb/^{206}Pb model date of ca. 2.70 Ga. Neoarchean grain 1 is interpreted to be either xenocrystic or detrital in origin because it is far older than the host rock.

Grains 2, 3 and 4 were tiny colourless prisms with aspect ratios of 2, 3 and 4:1, respectively, that each yielded discordant late Paleozoic U/Pb dates.

Of the three, the morphology and U/Pb systematics of grains 2 and 4 are most similar. They contained a moderate amount of uranium (300-350 ppm), had Th/U ratios of 0.30 and 0.42 and produced nearly identical $^{206}Pb/^{238}U$ dates with a weighted mean of 367.2 ± 2.0 Ma (2σ; probability of concordance = 0.97). Grain 3 had high uranium content (832 ppm), very low Th/U (0.09) and produced a 17% discordant result with apparent ages of 342.9 ± 0.6 Ma ($^{206}Pb/^{238}U$) and 414.2 ± 11.1 Ma ($^{207}Pb/^{206}Pb$).

If the round zircon crystals were xenocrysts, the sample may have been purely meta-igneous, but presence in the zircon concentrate of detrital zircon would indicate that siliciclastic detritus was incorporated into the unit. The locally fragmental texture of the sample may derive from sedimentary re-working of igneous and potentially other rocks. The prismatic, faceted morphologies of zircon grains 2, 3 and especially 4 indicates they are first cycle grains and experienced little or no sedimentary transport. Their rarity in the zircon separate is attributed to the mafic-intermediate composition of the sample. The relatively low Th/U ratios of grains 1, 2 and 3 are suggestive of a felsic igneous source (Belousova et al., 2002) unlike the bulk composition of the sample from which they were extracted. These zircon grains may therefore have originated in a small amount of felsic volcanic rock that was incorporated into the fragmental parts of this unit. Accordingly, zircon dates are interpreted to provide a maximum age of deposition.

The weighted mean $^{206}Pb/^{238}U$ date of 367.2 ± 2.0 Ma for grains 2 and 4 is taken as the best approximation of a shared crystallization age. The reliability of the result from grain 3 is less clear. Its Late Mississippian $^{206}Pb/^{238}U$ date is inconsistent with regional field relations that place the Amphibolitic Schist member stratigraphically below the Tournaisian (359-345 Ma; Orchard, 1985; Thompson et al., 2006) Catherine Lake limestone west of Nakusp. At the local scale, the Amphibolitic Schist member's position stratigraphically beneath the mid-Mississippian McHardy assemblage (Kraft et al., 2011a) requires a mid-Mississippian (ca. 340 Ma) minimum age. An alternative interpretation that the sampled greenstone belongs to the Mississippian McHardy assemblage or Permian Kaslo Group is not favoured because 1) the greenstone is visually and geochemically indistinguishable from rocks elsewhere in the Amphibolitic Schist member, 2) it maps laterally into a succession that is typical of the Mount Sproat assemblage, and unlike the Milford Group, 3) volcanic rocks have not been observed in the McHardy assemblage in the Lardeau Range, and 4) the unit is unlike metabasaltic rocks conformably overlying the McHardy assemblage (Kaslo Group), which are dark green to black, amphibolitic greenstone and gabbro with MORB geochemical affinity (see Chapter 2). The anomalously young $^{206}Pb/^{238}U$ date probably represents Pb loss expedited by the grain's high U content; the Late Silurian or Early Devonian $^{207}Pb/^{206}Pb$ date of grain 3 is favoured. The shared crystallization date of 367.2 ± 2.0 Ma for grains 2 and 4 is thus taken as the maximum age of the greenstone horizon in the Amphibolitic Schist member.

2.7 Discussion

2.7.1 Interpretations of volcanic lithogeochemistry

In addition to field observations that distinguish the MSA from the Lardeau Group, differences in trace-element geochemistry discriminate metavolcanic rocks of the MSA from those of the Lardeau Group. All samples from the Lardeau Group (23 from Logan and Colpron, 2006; 17 from this study) have either OIB or MORB geochemical affinities; all Jowett Formation samples are OIB-like. This contrasts markedly with the arc-related geochemical characteristics (especially increased Th:Nb ratio) of volcanic units of the Amphibolitic Schist and Heterolithic members of the MSA.

2.7.2 Interpretations of tectonic setting

Lithogeochemical results from the Lardeau Group are in agreement with prior data that indicate periodic eruption of mafic volcanic rocks with OIB and E-MORB geochemical affinities in the Lardeau trough occurred in an extensional or transtensional setting (Smith, 1990; Logan and Colpron, 2006).

Sedimentological and stratigraphic characteristics of the Mount Sproat assemblage are used here with lithogeochemical data to infer depositional environment. Horizons of poorly sorted quartzite that interlayer with fine grained lowermost Carbonaceous member strata are interpreted as the last sediment gravity flows associated with the Broadview Formation. Because the Carbonaceous member is inferred to have originated as carbonaceous shale and carbonate it is interpreted to have formed in a low energy, anoxic marine environment during tectonic quiescence that followed deposition of the Broadview Formation.

The transition to the Heterolithic member marked a new phase of widespread mafic volcanism and deposition of both carbonaceous and non-carbonaceous fine-grained siliciclastic and carbonate rocks. Geochemical data in stratigraphic context indicate a temporal trend in Heterolithic member volcanic affinities from mixed OIB and E-MORB to island arc tholeiite. The Heterolithic member thus records the initiation of arc-related magmatism along the axis of the Lardeau trough. The Heterolithic member is slightly older than but would be analogous to the ca. 360-365 Ma Fire Lake Formation, which records initiation of back-arc basin magmatism in the Yukon-Tanana terrane, Finlayson Lake region, Yukon (Piercey et al., 2004).

Widespread conglomerate in the Amphibolitic Schist and Upper Clastic members indicates that uplift was associated with arc-related basaltic volcanism during deposition of the upper part of the MSA. The predominance of undeformed quartzite and mafic to intermediate igneous clasts is interpreted to reflect a source comprising mature, continental strata upon which mafic to intermediate volcanism occurred.

2.7.3 Age of the Mount Sproat assemblage

The stratigraphic position of the MSA conformably above the Broadview Formation and unconformably beneath the Milford Group requires a mid-Paleozoic depositional age. A minimum depositional age of the Mount Sproat assemblage comes from Late Mississippian (Serpukhovian-Bashkirian) conodonts from the McHardy assemblage in the Goat Range (Orchard, 1985; Klepacki, 1985) because the McHardy assemblage unconformably overlies the MSA throughout the Lardeau Range.

Absolute ages are not available from the Heterolithic member but it is inferred to be older than the ca. 367 Ma Amphibolitic Schist member and younger than the Middle Devonian (ca. 385 Ma) initiation of subduction at the Cordilleran margin (Rubin et al., 1990). The oldest arc-related magmatic rocks known from southeastern British Columbia, which are only slightly older than the Amphibolitic Schist member (ca. 372-365 Ma; Okulitch, 1985; Slemko, 2000; Richards et al., 2002; Simony et al., 2006), are tentatively taken to approximate the age of the Heterolithic member. Because evidence of arc magmatism was not identified in the Carbonaceous member, it may pre-date initiation of subduction beneath the Cordilleran margin. Its age is constrained only by overlying Late Devonian strata and underlying Lower Cambrian Badshot Formation beneath the Lardeau Group.

The 367.2 ± 2.0 Ma zircons recovered from greenstone in the Amphibolitic Schist member provide a maximum depositional age for that horizon. As outlined above, the prismatic shapes and small size of the zircons is taken to reflect a volcanic origin and little or no sedimentary transport. As there is no likely source for these zircons in underlying strata, they are inferred to approximate the depositional age of the Amphibolitic Schist member.

The Catherine Lake phyllite has been interpreted as a western extension of the Milford Group (Reesor and Moore, 1971; Read and Wheeler, 1976; Orchard, 1985), or alternatively as a Late Devonian-Early Mississippian equivalent of similar rocks in the Vernon area (Bruen phyllite; Thompson et al., 2006). Because of 1) equivalent stratigraphic position immediately above the Amphibolitic Schist member, and 2) lithological similarities with the Upper Clastic member, the Catherine Lake phyllite is included here in the Upper Clastic member of the MSA. This results in a simpler map pattern in which stratigraphic younging is consistent in the rocks of the hanging wall of the Columbia River fault zone. Conodont elements (Orchard, 1985) and a ca. 359 Ma detrital zircon (Thompson et al., 2006) from the Catherine Lake phyllite constrain the succession, and the top Mount Sproat assemblage, to be Tournaisian.

2.7.4 Local correlations of the Mount Sproat assemblage

A post-Lardeau, pre-Milford thrust fault was postulated by Klepacki and Wheeler (1985) to explain their observation of upright marble and mafic volcanic rocks that structurally overlie the Broadview Formation southeast and east of Mount Buchanan in the Goat Range. An alternative, simpler explanation is that the marble and volcanic rocks are equivalent to the Mount Sproat assemblage, making a fault unnecessary. If the volcanic rocks have an arc-related geochemical affinity their correlation with the Mount Sproat assemblage is probable; MORB or OIB affinities would be consistent with either interpretation.

2.7.5 Regional correlations of the Mount Sproat assemblage

If rocks of the Mount Sproat assemblage are Devonian to Early Mississippian, a number of correlations may exist between these Kootenay Arc strata and mid-Paleozoic successions elsewhere in the North American Cordillera.

The ca. 367 Ma Amphibolitic Schist member is, within analytical error, coeval with a suite of Late Devonian arc plutons in southeastern British Columbia (Figure 2-17; Okulitch, 1985; Slemko, 2000; Simony et al., 2006). It is interpreted as a back-arc basin expression of the arc magmatism that generated those plutons.

Lemieux (2006) and Thompson et al. (2006) proposed a direct correlation between the Silver Creek Formation and rocks at Upper Arrow Lake that are included here in the Amphibolitic Schist and Upper Clastic members. The ca. 367 Ma Amphibolitic Schist member in the upper Mount Sproat assemblage is a close lithological match to parts of the Late Devonian Silver Creek Formation and the Spa Creek assemblage in the Vernon area (Thompson and Unterschutz, 2005; Thompson and Glombick, 2005; Thompson et al., 2006). All three amphibolitic schist units are constrained to overlapping Late Devonian time intervals and each is characterized by gradationally mixed amphibole-biotite-plagioclase schist, commonly with distinctive coarse, 'feathery' black metamorphic amphibole on foliation surfaces. Lemieux (2006) and Thompson et al. (2009b) also correlated with the Silver Creek Formation conglomerate and pelitic schist at St. Leon Creek that are here included in the Upper Clastic member of the Mount Sproat assemblage. Field relations and interpreted ages in this study support correlation of the amphibolitic schist at Upper Arrow Lake with the Silver Creek Formation; however, prior detrital zircon data show that the Catherine Lake phyllite (Upper Clastic member) is younger than the Bruen phyllite (Figure 2-17) and therefore cannot be correlated as suggested by Thompson et al. (2006).

If the Amphibolitic Schist member correlates with the Silver Creek Formation, as interpreted here, the stratigraphic relations of the Silver Creek Formation change significantly between the Vernon and Lardeau map areas, in that 1) a lithological match to the Chase Formation does not occur in or below the Mount Sproat assemblage, and 2) the lower MSA and Lardeau Group rocks are not represented in the Vernon area. Amphibolitic schist therefore forms an overlap assemblage that links older basinal (Lardeau trough) and platformal (Okanagan High and Chase platform) settings.

Thompson et al. (2006) correlated the Bob Lake assemblage in the Nicola Horst with the Spa Creek assemblage. The Bob Lake assemblage comprises metavolcanic schist, siliciclastic metaconglomerate, and mica ± garnet schist, phyllite and metasiltstone. If, as inferred by Thompson et al. (2006), the Bob Lake assemblage is Late Devonian or Carboniferous in age, it is a potential correlative of the Upper Clastic member of the Mount Sproat assemblage, also on the basis of lithostratigraphic similarity.

It has been suggested that the Chase Formation calcareous quartzite may have equivalents as far east as the Mount Forster Formation in the Purcell anticlinorium (Thompson et al., 2006). A combination of new (see Chapter 5) and previous U-Pb zircon data (Thompson et al., 2006) constrain deposition of the Chase Formation to the interval between 372.6 ± 5.2 Ma and 359 ± 0.8 Ma. Data from the Sicamous area (granodioritic pluton that cuts strata interpreted to overlie the Chase Formation; Slemko, 2000; Thompson et al., 2006) may place the minimum age of the Chase Formation at 365.9 ± 2.7 Ma. These data indicate that the Chase Formation is coeval with part of the Mount Sproat assemblage, although it has no lithological equivalent in the MSA. The platform on which the Chase Formation is interpreted to have been deposited (Thompson et al., 2006) was outboard of, and did not extend across, the Lardeau trough. Correlation of the Amphibolitic Schist member with the Silver Creek Formation implies that the Chase Formation would have passed laterally eastward into the Heterolithic or Carbonaceous members of the Mount Sproat assemblage.

Correlations in the northern Cordillera

The Mount Sproat assemblage may have correlatives in central and northern British Columbia. The Guyet Formation in the Cariboo Mountains (Figure 2-1) comprises a lower basalt flow and volcaniclastic unit and middle conglomerate overlain by the Mississippian to Permian Greenberry Limestone Member (Struik, 1981). Conglomerate in the Guyet Formation occurs in discontinuous bodies that pass laterally into pelitic and volcanic strata and contains sand to cobble size clasts of chert, pelite, basalt, sandstone and limestone (Struik, 1981). The Guyet Formation depositionally overlies and interfingers with mixed deep and shallow water siliciclastic and carbonate strata of the Early Devonian to Mississippian Black Stuart Formation. Similarities in age and lithostratigraphy suggest that the Guyet Formation may correlate with the Amphibolitic Schist and (or) the Upper Clastic member of the Mount Sproat assemblage. This would in turn correlate the Black Stuart Formation with older Mount Sproat assemblage strata.

2.7.6 New interpretation of the Lardeau Group

Presence of the Mount Sproat assemblage above the Broadview Formation is in agreement with a discovery by Hughes et al (2003) of ca. 360 Ma meta-tuff of magmatic arc affinity from a unit previously inferred to be a Thompson region equivalent of the Lardeau Group. Whereas Hughes et al. (2003) inferred the Late Devonian volcanic rocks to also date the Broadview Formation, field and lithogeochemical data presented above, and detrital zircon data reported in Chapter 5, suggest that the Broadview Formation was deposited prior to arc volcanism in the region.

The new interpretations of the stratigraphy of the northern Kootenay Arc presented here could reconcile apparent stratigraphic disparities between the Lardeau Group and northern Washington's Covada Group. The model of Smith and Gehrels (1992), which involves structural inversion of the Lardeau Group to better correlate it with the Covada Group, contradicts the conclusions of several studies that argue for or imply an upright Lardeau Group (Fyles and Eastwood, 1962; Read and Wheeler, 1976; Sears, 1979; Klepacki, 1985; Colpron and Price, 1995; Logan and Colpron, 2006). Evidence from this study supports the notion that the stratigraphy of the Lardeau Group as defined by Fyles and Eastwood (1962) is upright. Smith and Gehrels (1992) correlated Early Ordovician (Snook et al., 1981; Joseph, 1990) coarse clastic rocks of the Daisy Formation and conformably overlying alkaline basaltic rocks of the Early Ordovician Butcher Mountain Formation (Snook et al., 1981; Smith, 1990) with the Broadview and Jowett formations, thereby implying that the Lardeau Group had been tectonically inverted by cryptic thrusting. An alternative correlation of the Daisy Formation with the Akolkolex Formation (Logan and Colpron, 2006) is consistent with results of this study. If the Daisy-Butcher Mountain couplet correlates with the Akolkolex-Jowett couplet, then the Broadview Formation and Mount Sproat assemblage should be time-equivalent with strata that depositionally overlie the Butcher Mountain Formation: the Bradeen Hill assemblage (Smith, 1982; Smith and Gehrels, 1992). Unlike the Broadview Formation, however, the Bradeen Hill assemblage is characterized by fine-grained sedimentary rocks (chert, slate, argillite) and a paucity of quartzo-feldspathic detritus (Smith and Gehrels, 1992) except for a unit comprising several hundred metres of quartz arenite reported by Fullmer (1986). Quartz arenite, pillow basalt, chert pebble conglomerate, and limestone are locally common in the Bradeen Hill assemblage (Smith and

Gehrels, 1992). A close match of the Broadview Formation, therefore, does not appear to be represented in Washington. Abundant hemipelagic sedimentary rocks with limestone, quartz arenite, and basalt in the Bradeen Hill assemblage are, however, a potential match to the Mount Sproat assemblage. That correlation is supported by the Devonian depositional age inferred by Smith and Gehrels (1992) for at least part of the Bradeen Hill assemblage.

If the Carbonaceous member represents less than about 10 m.y., the Broadview Formation, and the inferred extensional episode that it represents, may have been as young as Early or Middle Devonian. Similarly, the Jowett Formation and stratiform barite in the McCrae Peak succession, which pass laterally into the Jowett and Broadview formations, may be Devonian features also. In this case, the upper Lardeau Group would be an equivalent of Devonian extension-related submarine fan deposits, bedded barite and alkaline magmatic rocks to the north in the Earn Group of the Selwyn Basin (Gordey et al., 1987).

2.7.7 Location of the ancient plate edge

That the MSA represents a back-arc basin has implications for the location of the edge of the North American plate at the time of deposition. In modern circum-Pacific subduction zones, the arc-trench gap ranges from about 120 km (e.g, Aleutian arc, Tonga-Kermadec arc) to over 300 km (Cascade arc); distances to back-arc basins, where they are present, are greater than 150 km. If the Late Devonian Cordilleran continental subduction zone was analogous to modern ones, the trench axis of the west-facing Late Devonian continental margin arc (Paradis et al., 2006) was ~150 km to 350 km outboard of the Lardeau trough. This leads to the interpretation that a ribbon of relatively strong crust of the North American plate existed outboard of the Lardeau trough.

2.8 Conclusions

The revised stratigraphic relations simplify the geologic map pattern of the Upper Arrow Lake area and eliminate structural and stratigraphic inconsistencies.

Field observations combined with volcanic lithogeochemistry and U-Pb zircon geochronology show that the Mount Sproat assemblage is distinct from the Lardeau, Milford and Kaslo groups. The Mount Sproat assemblage was deposited in the back-arc of an west-facing (east-dipping slab; modern coordinates) Late Devonian to Early Mississippian continental margin arc. This back-arc basin was superimposed on the Lardeau trough, into which the Lardeau Group was deposited. The Mount Sproat assemblage is included with the Lardeau Group in the Kootenay tectonic assemblage because it conformably overlies the Lardeau Group. That conformable relationship implies that the Jowett and Broadview formations and the McCrae Peak succession may be Early or mid-Devonian, which would make them southern equivalents of similar strata in the Earn Group of the Selwyn Basin.

The sub-Milford unconformity is an intra-Mississippian feature that is significantly shorter in duration than speculated previously.

Volcanic lithogeochemical data show a progression from rift-related volcanism in the Early to mid-Paleozoic Lardeau Group to arc-related volcanism in the Devonian and Early Mississippian Mount Sproat assemblage, followed by oceanic spreading-centre volcanism in the Permian Kaslo Group. Volcanic rocks have not been identified in the Milford Group north of Tenderfoot Lake. Within the Mount Sproat assemblage is a trend from OIB and E-MORB to IAT and then extensive calc-alkaline arc volcanism.

The Chase Formation is not present in the stratigraphic succession of the Kootenay Arc, contrary to previous proposals (Thompson et al., 2006; Lemieux et al., 2007), but the Silver Creek Formation has lithostratigraphic equivalents in the Mount Sproat assemblage. Because basinal strata of the Mount Sproat assemblage span the interval in which the Chase quartzite was deposited, the Late Devonian platform represented by the Chase Formation existed outboard of the Lardeau trough. The Silver Creek Formation and upper Mount Sproat assemblage represent an overlap assemblage that ties the 'Chase platform' to the Lardeau trough by ca. 367 Ma.

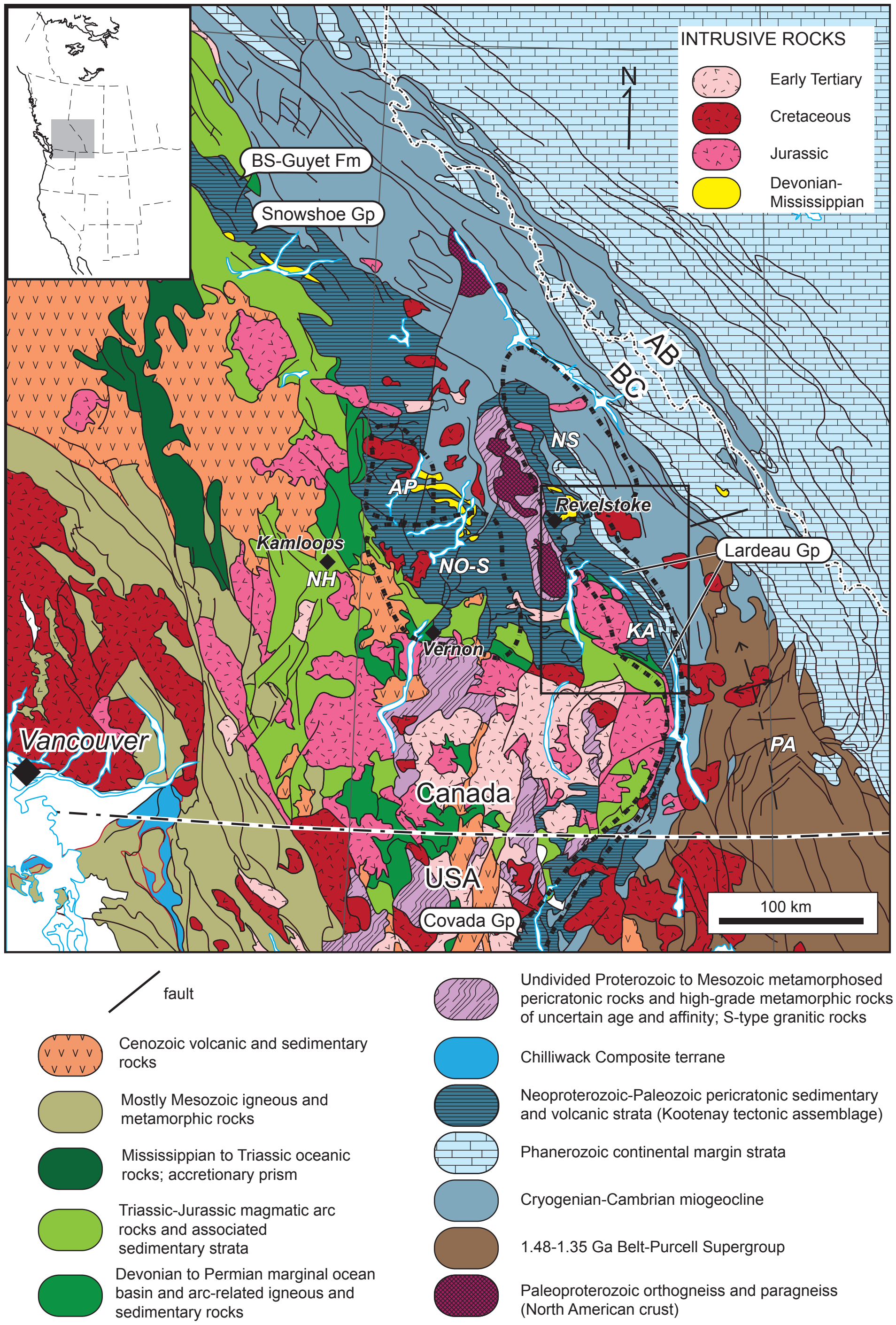

Figure 2-1. Tectonic assemblages of the southern Canadian Cordillera. Modified from Wheeler and McFeely (1991), Glombick et al. (2006), Thompson et al. (2006), Brown et al. (2010). AP, Adams Plateau; BS-Guyet Fm, Black Stuart and Guyet formations; KA, Kootenay Arc; NH, Nicola Horst; NS, Northern Selkirks; NO-S, North Okanagan-Shuswap region; PA, Purcell anticlinorium.

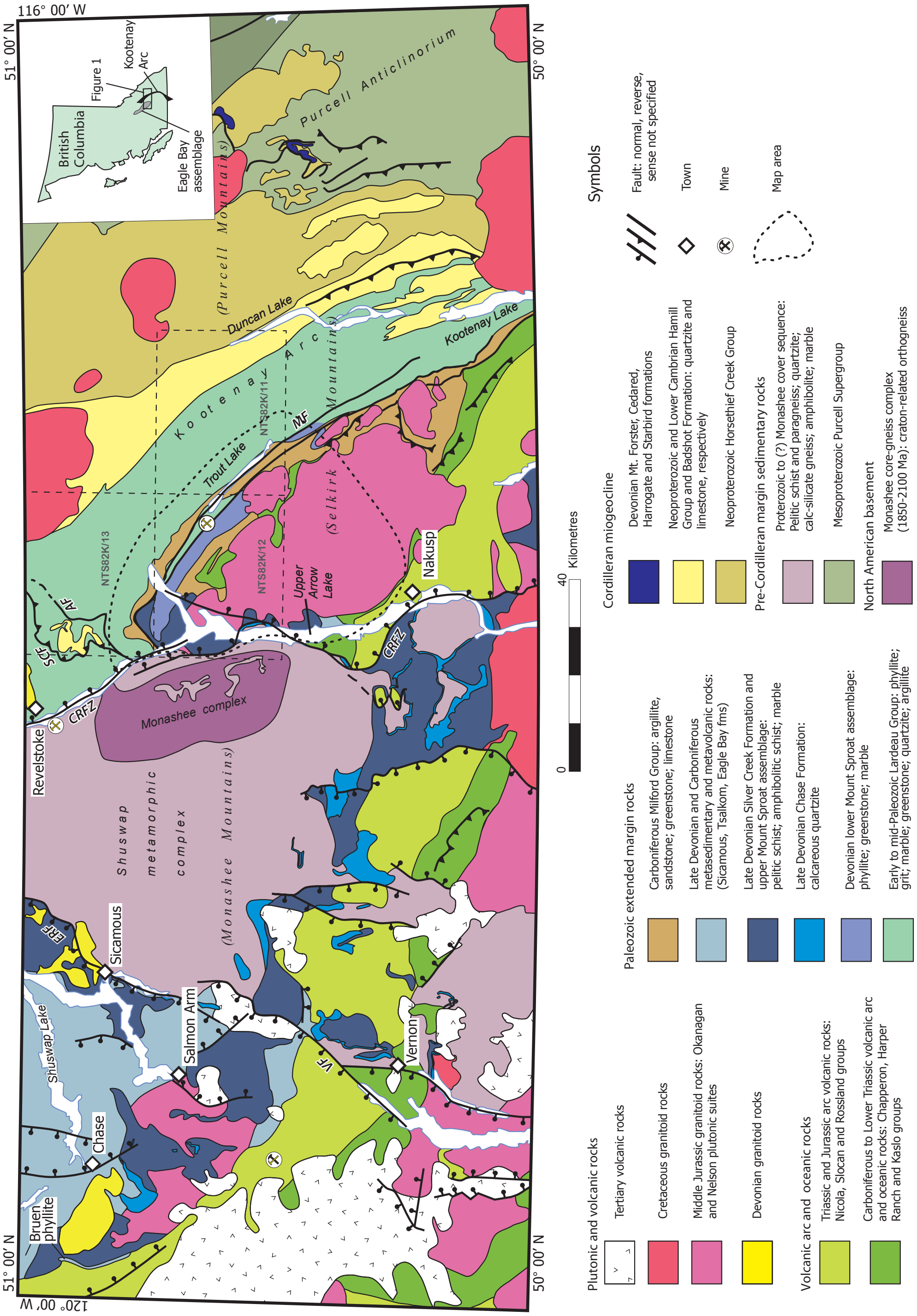

Figure 2-2. Geological compilation of the Vernon and Lardeau map areas. Simplified from Thompson et al. (2006) and modified to incorporate results of this study. Extent of new mapping and appended published maps (Kraft et al., 2011a; 2011b; 2011c) area indicated. This map shows the transitions from Neoproterozoic miogeocline to Mesozoic volcanic arc rocks. The Chase and Silver Creek formations span the Shuswap complex to Upper Arrow Lake.

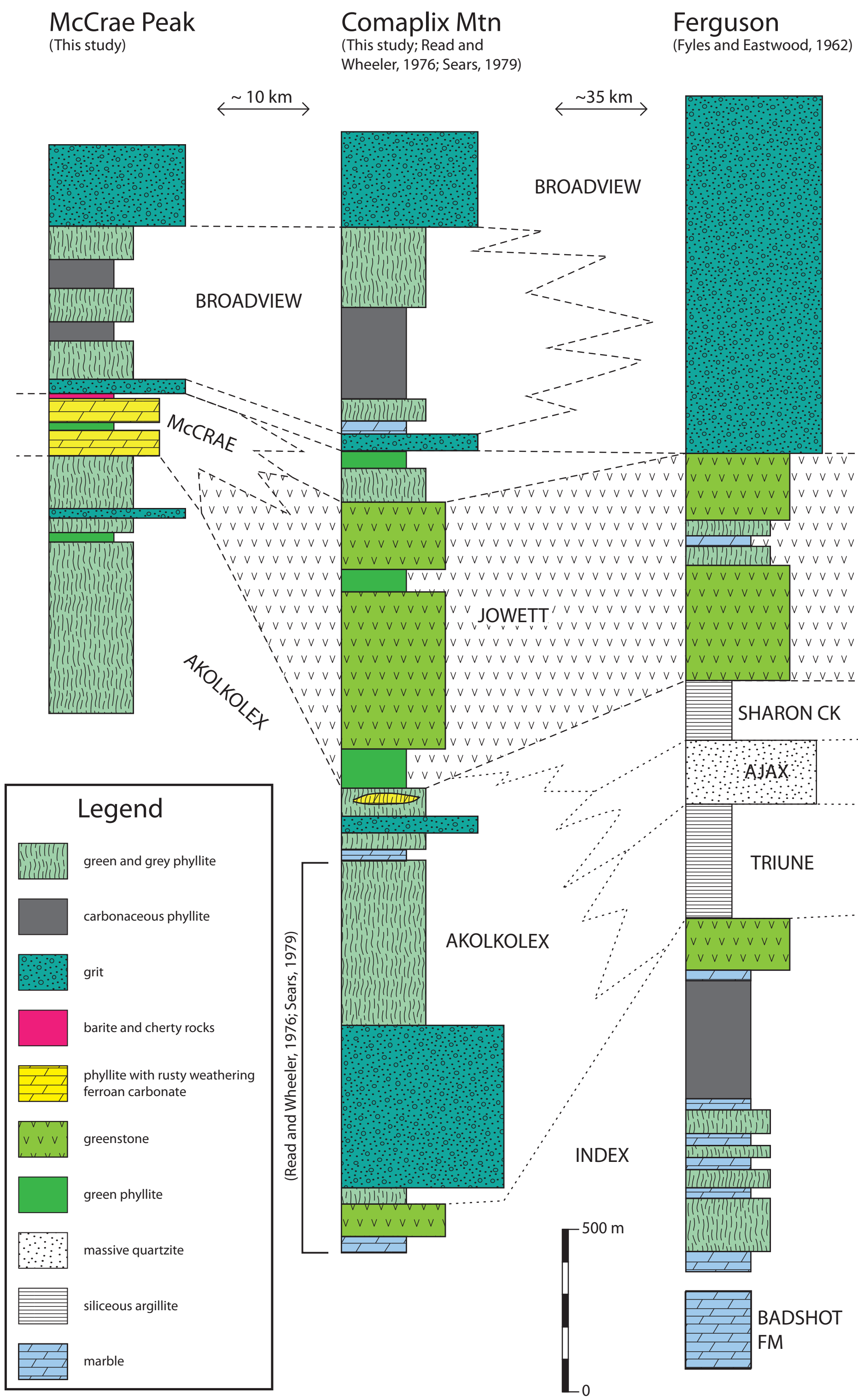

Figure 2-3. Correlations of Lardeau Group strata between McCrae Peak and Ferguson.
The McCrae Peak succession is an along-strike equivalent of the Jowett Formation and the lowermost Broadview Formation.

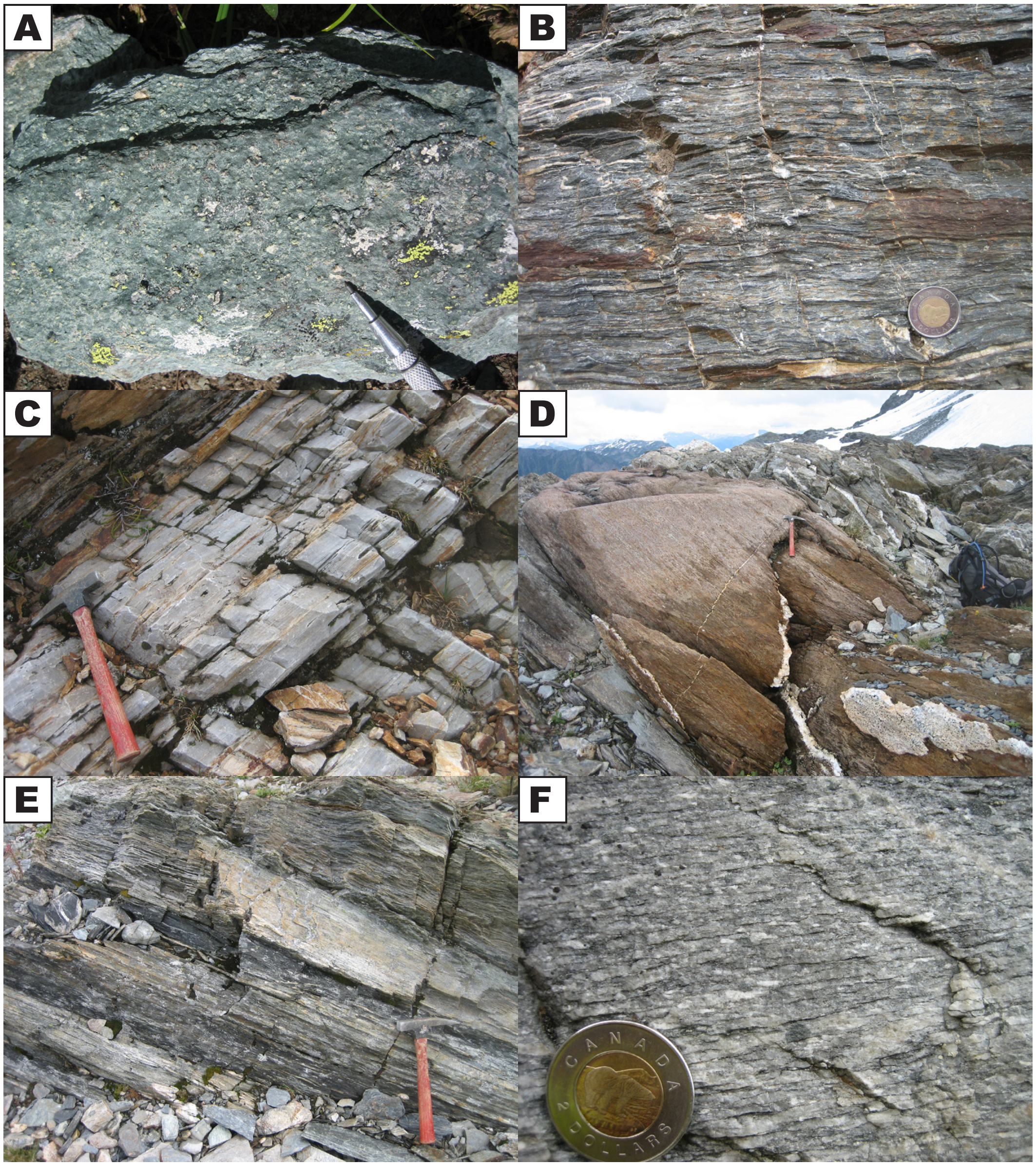

Figure 2-4. Field photographs of rock types in the McCrae Peak succession (Lardeau Group) at McCrae Peak.

From oldest to youngest: A) Green phyllite with feldspar grains interpreted to be phenocrysts. This unit passes laterally into the Jowett Formation. B) Dark grey siliceous rock that immediately underlies the barite. C) Part of the 2-3 m thick horizon of stratiform barite. D) Distinctly orange-brown layer of phyllite with abundant iron carbonate (possibly ankerite or siderite). E) Interbedded grit and black slaty phyllite. Passes laterally into the Broadview Formation. F) Gritty quartzite equivalent to the Broadview Formation.

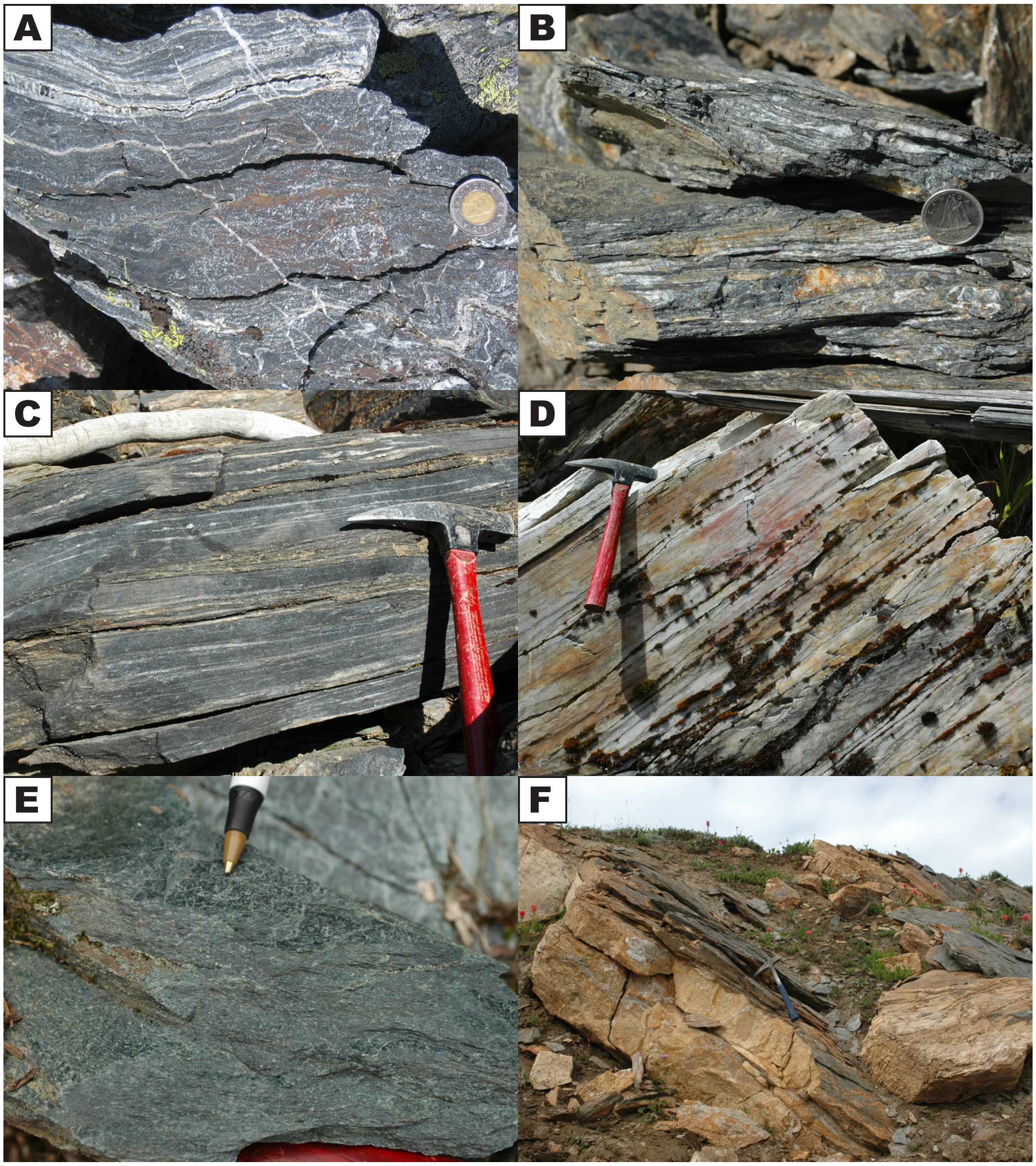

Figure 2-5. Field photographs of representative rock types of the lower Mount Sproat assemblage.

A) Carbonaceous quartzite, Carbonaceous member. B) Quartzose carbonaceous phyllite/schist, Carbonaceous member. Canadian dime for scale. C) Argillaceous marble, Carbonaceous member. D) White quartzite, Heterolithic member. E) Phyllitic greenstone, Heterolithic member. F) Dolomitic marble, Heterolithic member.

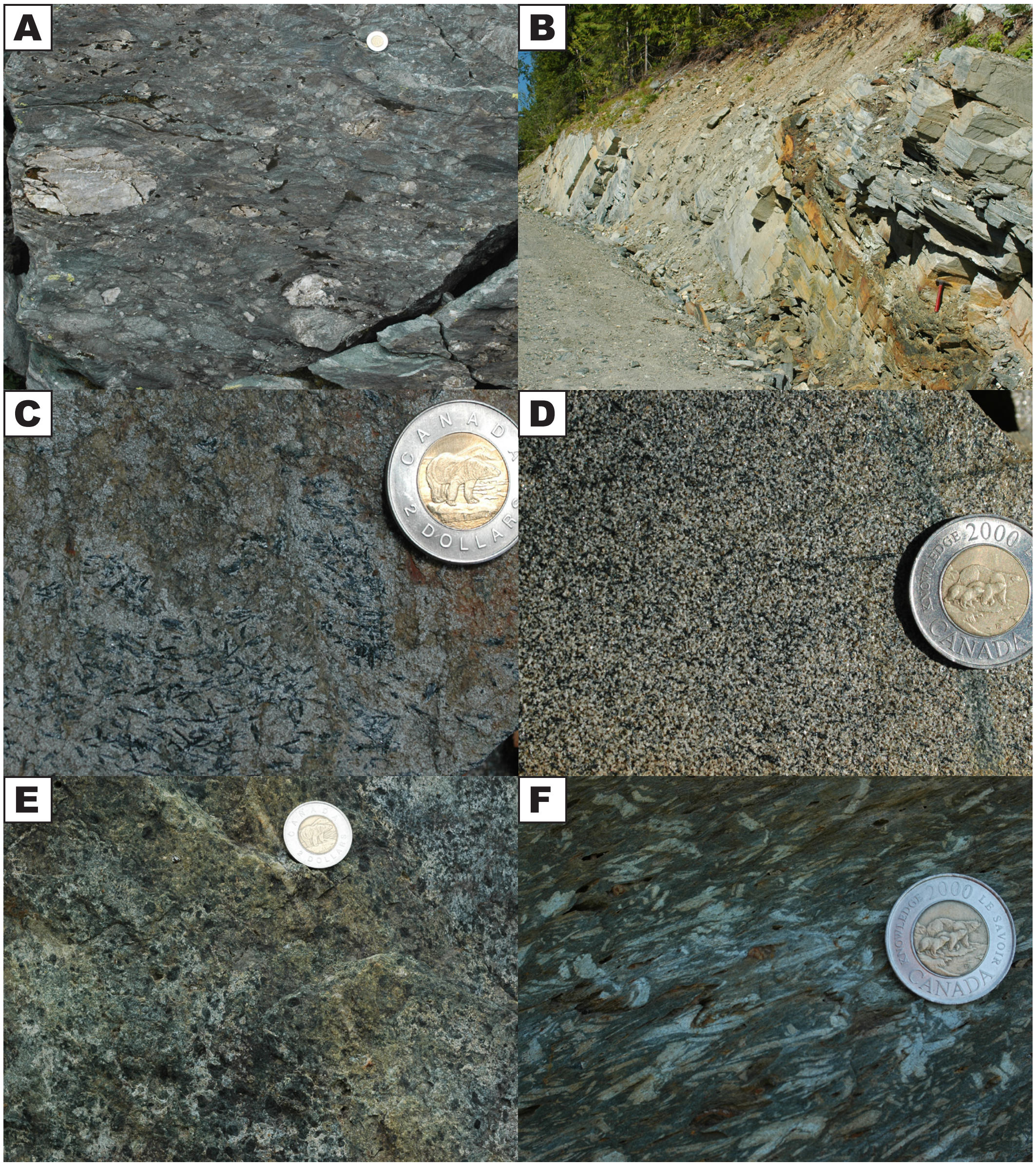

Figure 2-6. Field photographs of rock types in the Amphibolitic Schist member of the Mount Sproat assemblage.
A) Cobble conglomerate with a matrix of green phyllite that defines the base of the Amphibolitic Schist member on Mount Sproat. B) Roadcut showing the strongly foliated, platy habit of the Amphibolitic Schist member near Galena Bay. Rock hammer for scale. C) Hornblende-biotite schist. D) Biotite-plagioclase schist. E) Augite-phyric calc-alkaline metabasalt near Halfway River. F) Strained greenstone with relict plagioclase phenocrysts from the horizon sampled for zircon geochronology at Blind Bay. In each photo except B is a two-dollar coin for scale (28 mm diameter).

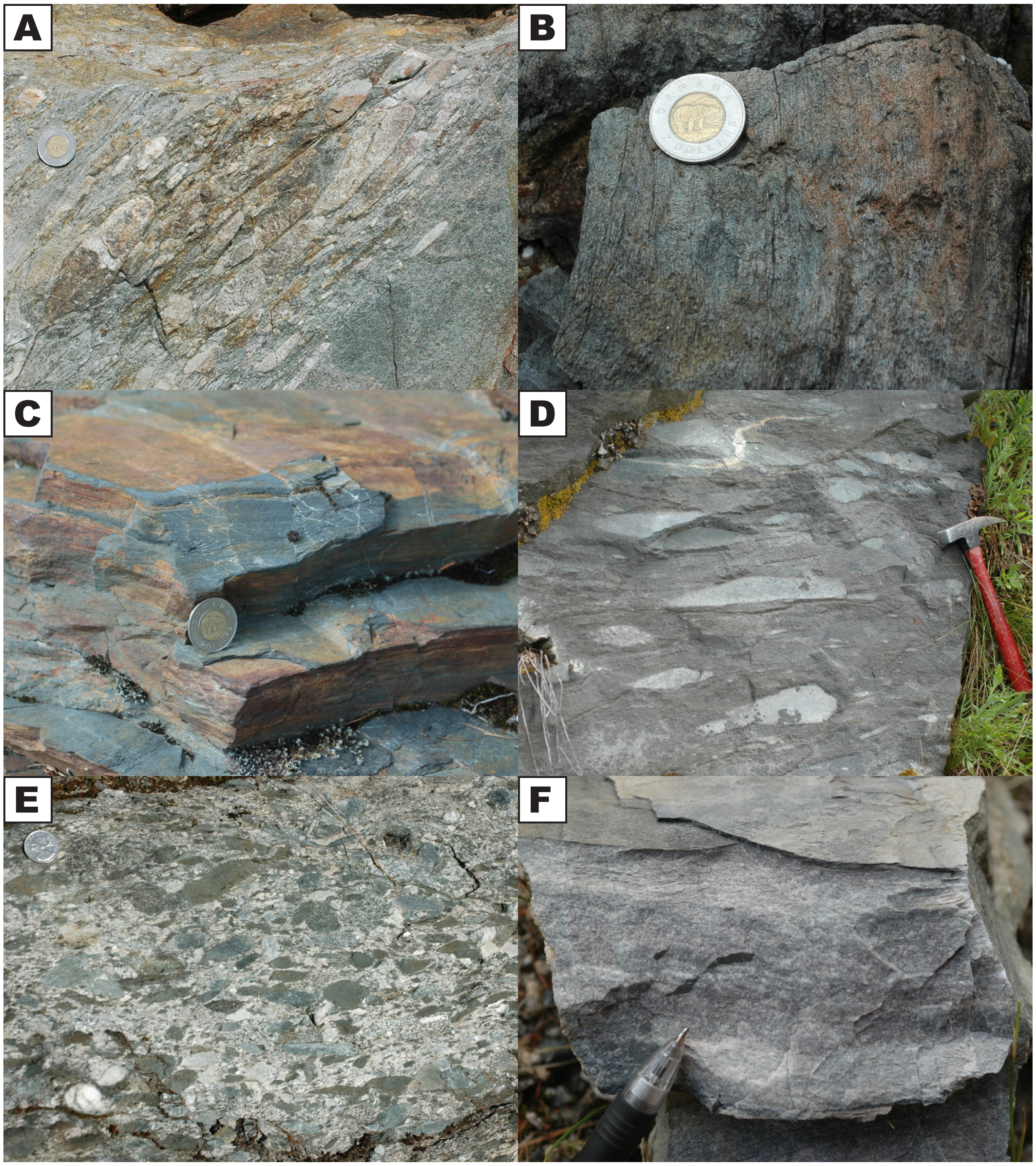

Figure 2-7. Field photographs of representative rock types of the Upper Clastic member.
A) Quartzite pebble conglomerate lens in quartz-muscovite schist that gradationally overlies the Amphibolitic Schist member at Beaton Arm. Detrital zircon ages from this conglomerate (sample 06TWJK138A) are presented in Chapter 5. B) Medium-grained biotite-muscovite schist typical of this member at Upper Arrow Lake. C) Argillaceous siltstone. D) Monomict paraconglomerate, interpreted as a metamorphosed volcaniclastic or pyroclastic deposit, that occurs at the interlayered transition with the Amphibolitic Schist member near St Leon Creek. E) Polymict orthoconglomerate comprising clasts of mafic and intermediate igneous rocks and quartzose sedimentary rocks in a sandy matrix. Quarter for scale at top left. F) Massive metasandstone with minor fine-grained biotite that imparts a purple-grey colour.

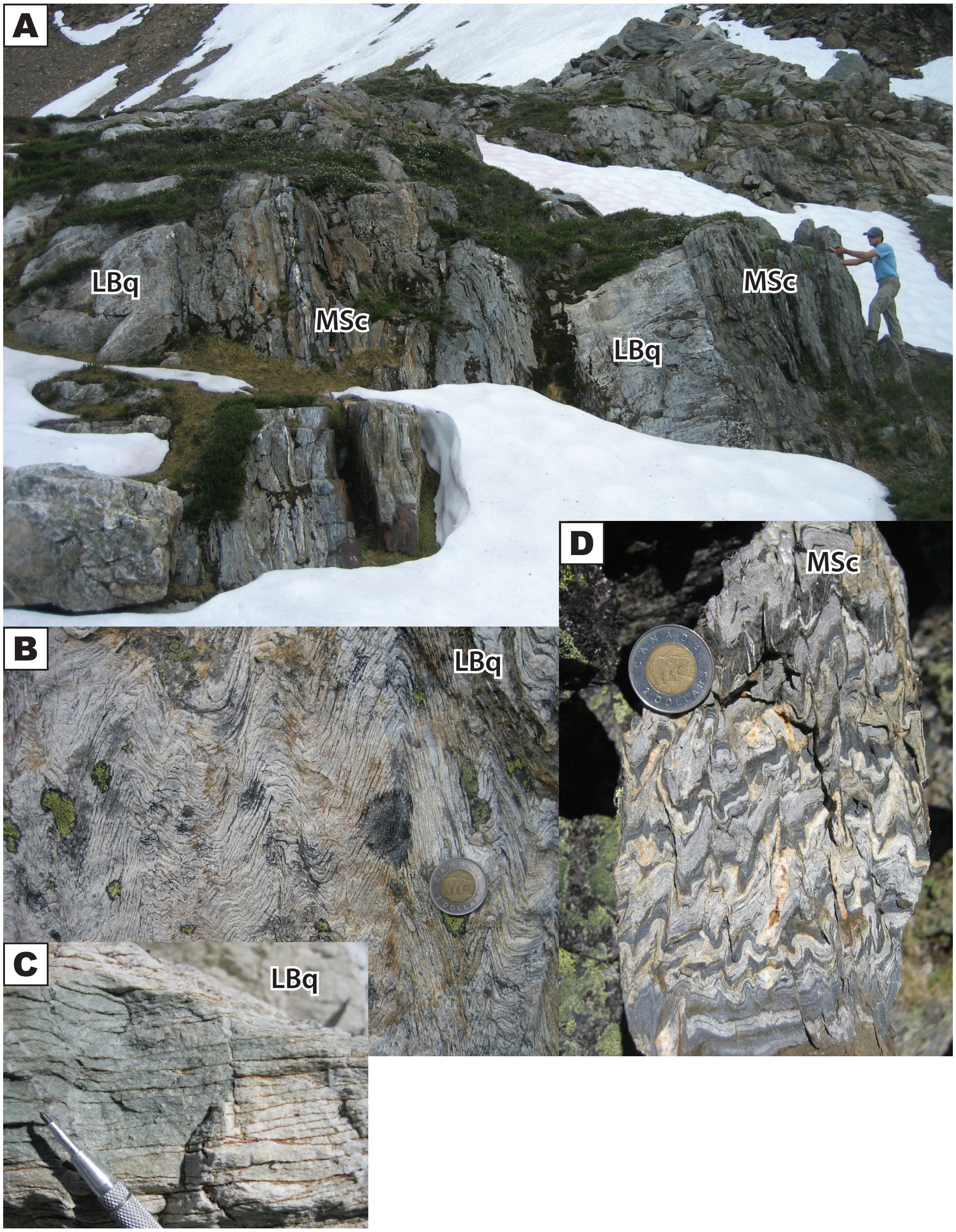

Figure 2-8. Field photographs of the interlayered contact between the Broadview Formation and Mount Sproat assemblage at Trout Mountain.
A) Outcrop in which metre-thick layers of Broadview quartzite (LBq) interlayers with banded quartzite of the Carbonaceous member (MSc). B) Close up of the gritty quartzite correlated with the Broadview Formation. C) Representative Broadview Formation quartzite from the Mount Thompson area. Quartzite at Trout Mountain (B) is correlated with the Broadview Formation because of the strong lithological and strain similarities. D) Banded quartzite of the Carbonaceous member near the interlayered contact at Trout Mountain.

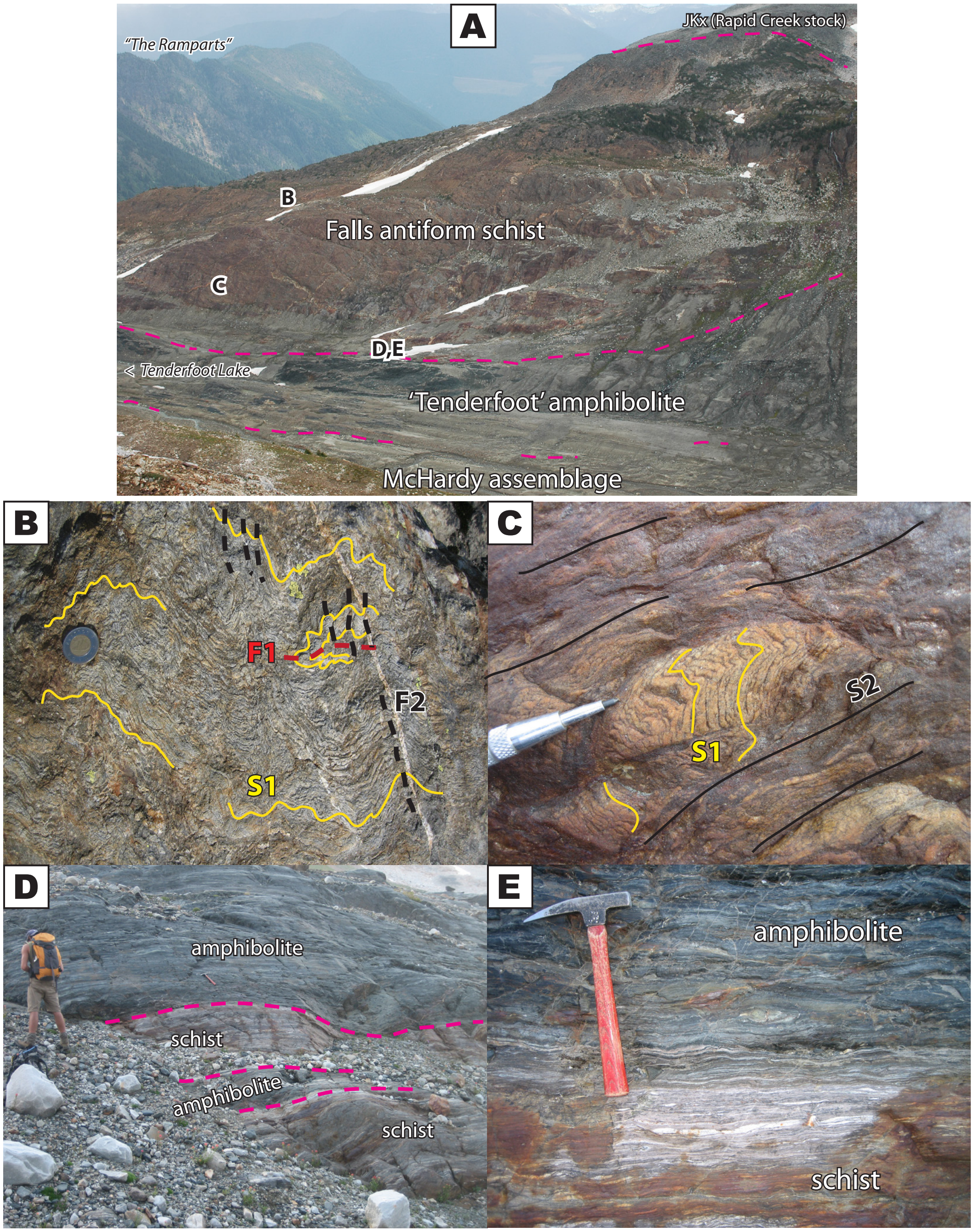

Figure 2-9. Photographs of the Falls antiform schist and its contact with the structurally overlying Tenderfoot amphibolite.
A) View of south side of Tenderfoot Lake, facing NE. Locations of photos B-E are indicated. B) F2 crenulation of S1 foliation and an F1 rootless fold hinge in Falls antiform schist. Axial planes of F2 are sub-parallel to surrounding and regional schistosity. C) Where the schist is mica-rich, S2 has fully overprinted S1. Relict S1 is preserved in this quartzose domain. D) Interfingering contact of Tenderfoot amphibolite and the Falls antiform schist. E) Close-up of the amphibolite/schist contact from (D).

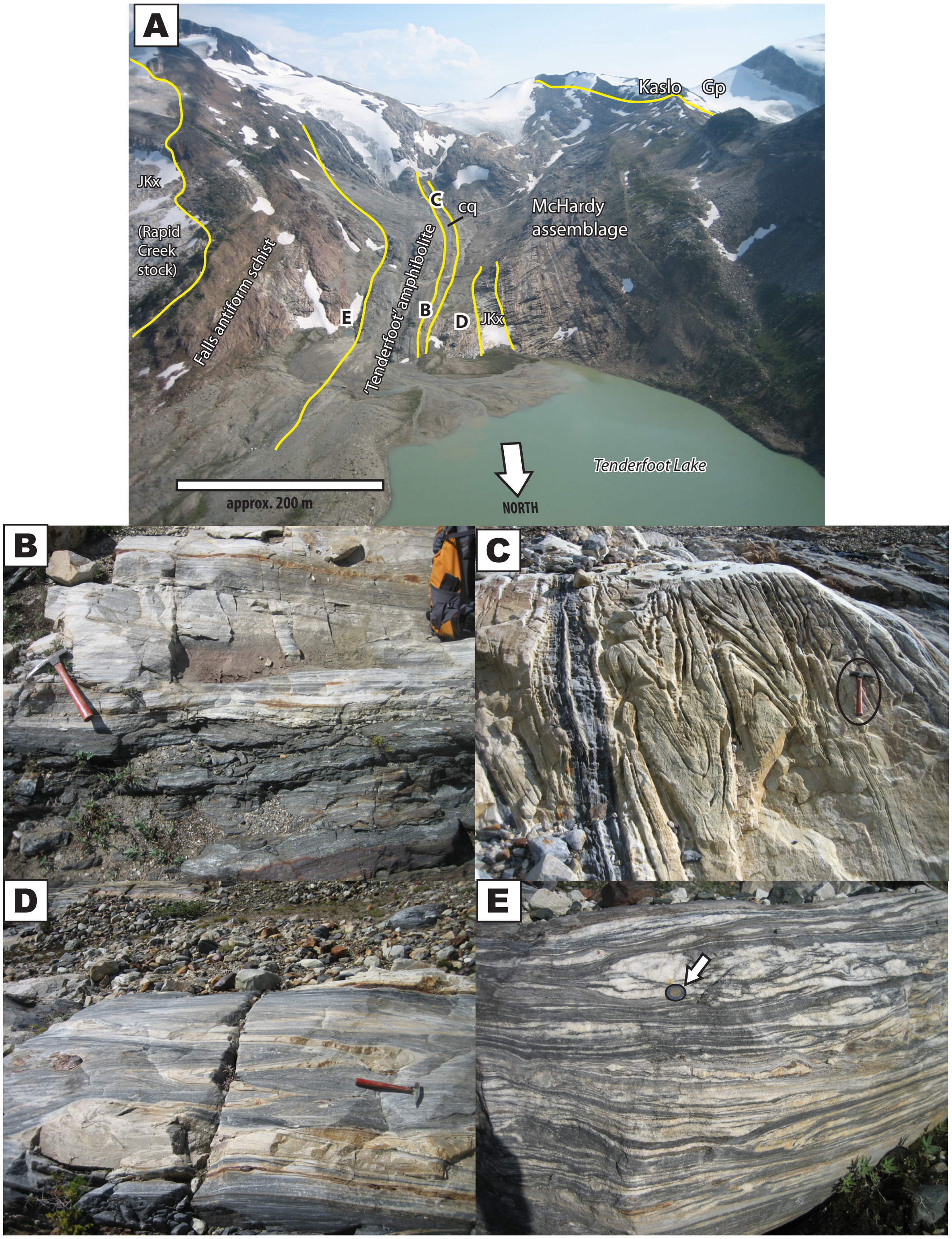

Figure 2-10. Photographs of calcareous quartzite at Tenderfoot Lake.
A) View of exposures south of Tenderfoot Lake, looking south. Locations of B-E are indicated. B) The lower/east contact of calcareous quartzite with Tenderfoot amphibolite is sharp and transposed. Looking west. C) Fold style and differential weathering in the calcareous quartzite unit. D) Folded quartzite layer in McHardy assemblage marble. Oblique section exaggerates fold amplitude. Note similarity of strain with (C). E) Strain in marble within the Falls antiform schist appears greater and more complex than in the McHardy assemblage rocks in photos (C) and (D). Two-dollar coin for scale.

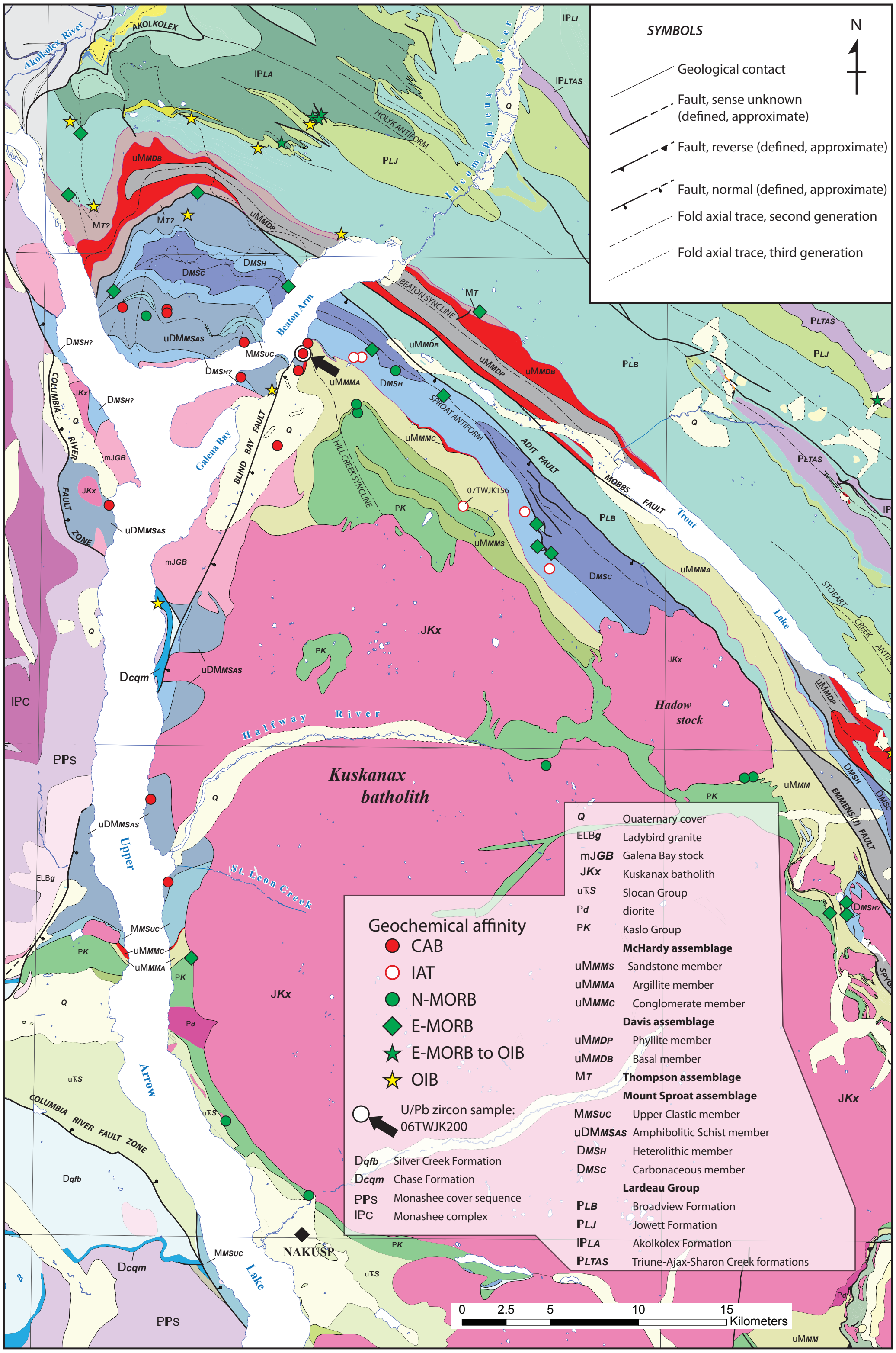

Figure 2-11. Volcanic lithogeochemistry sample sites on summary geologic map. Samples are symbolized according to interpreted geochemical affinity described in the text. There is a close correlation between lithogeochemistry and map units.

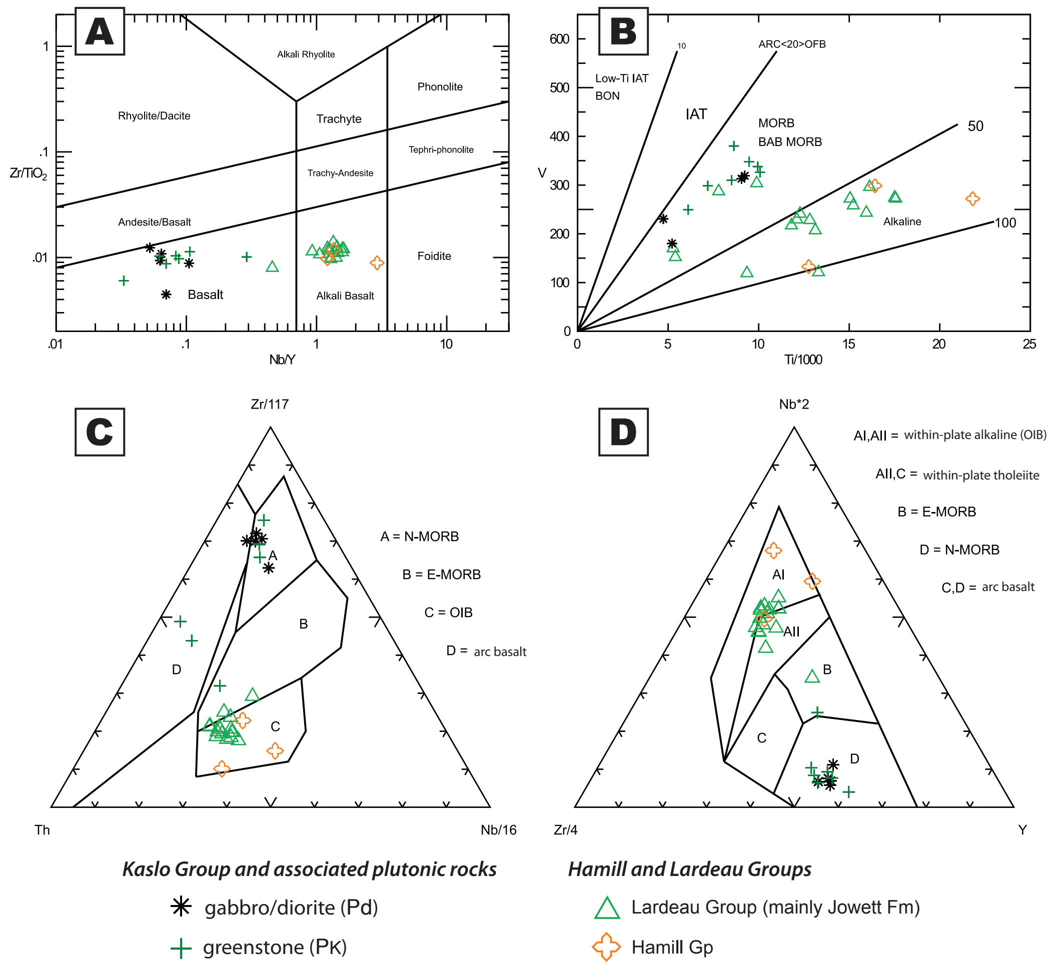

Figure 2-12. Tectonic discrimination diagrams with data from mafic rocks of the Hamill, Lardeau and Kaslo groups.

A) Zr/TiO_2 versus Nb/Y diagram of Pearce (1996; modified from Winchester and Floyd, 1977). B) Ti-V diagram of Shervais (1982). Abbreviations as in text except OFB = ocean floor basalt, BON = boninite. C) Th-Zr-Nb diagram of Wood (1980). D) Zr-Nb-Y diagram of Meschede (1986).

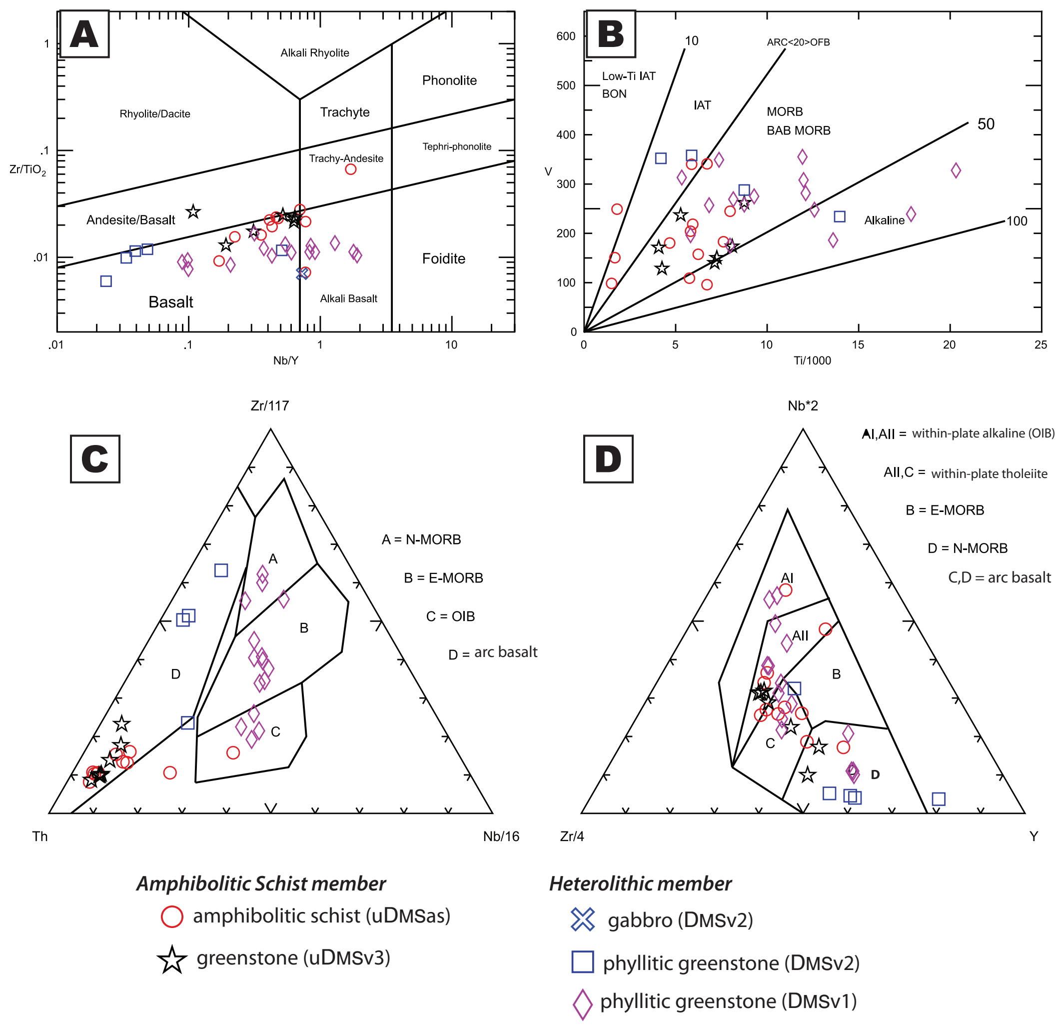

Figure 2-13. Geochemical trace element plots with data from mafic rocks of the Mount Sproat assemblage.
A) Zr/TiO2 versus Nb/Y diagram of Pearce (1996; modified from Winchester and Floyd, 1977). B) Ti-V diagram of Shervais (1982). Abbreviations as in text except OFB = ocean floor basalt, BON = boninite. C) Th-Zr-Nb diagram of Wood (1980). D) Zr-Nb-Y diagram of Meschede (1986).

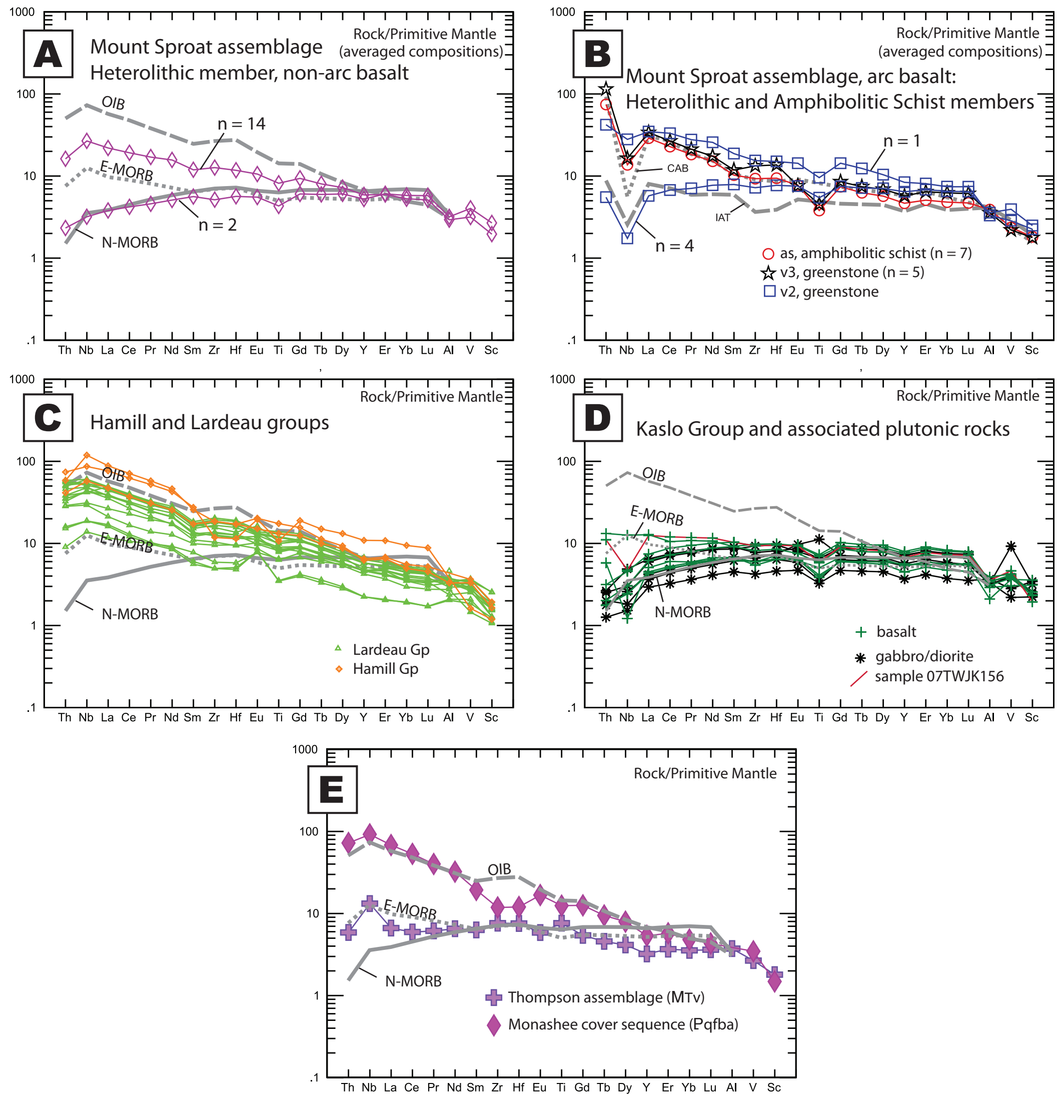

Figure 2-14. Primitive mantle-normalized trace element profiles of mafic rock units.

A) Averaged compositions of the lower mafic horizons in the Heterolithic member, which have E-MORB to OIB affinities. B) Averaged compositions of arc-related basalt suites in the MSA. Upper Heterolithic member greenstone (v2) has IAT and CAB signatures. Amphibolitic Schist member units (as, v3) are geochemically indistinguishable and plot as CAB. C) The Hamill and Lardeau groups range from E-MORB to OIB. D) The Kaslo Group and associated (cross-cutting) gabbroic rocks have similar compositions of N-MORB and minor E-MORB. Sample 07TWJK156 (red line) from the basal contact (see map figure 2-11) has IAT affinity. E) Single samples from the Thompson assemblage and amphibolite of unknown age in paragneiss immediately beneath the Chase Formation at Upper Arrow Lake. Reference compositions from modern environments are shown in grey. Sources: Primitive mantle, OIB, E-MORB, N-MORB, Sun and McDonough, 1989; IAT, Piercey et al., 2004; CAB, Stoltz et al., 1990.

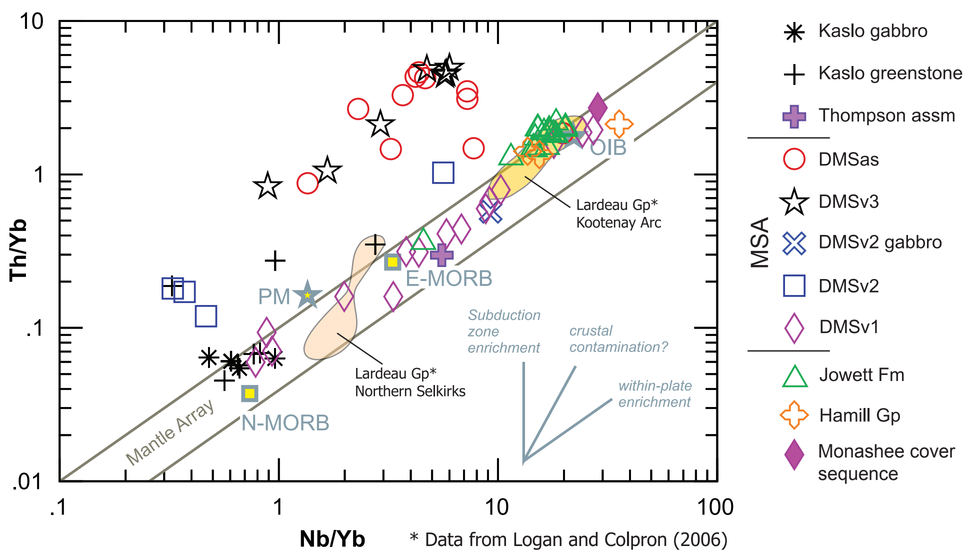

Figure 2-15. All mafic samples plotted with the mantle array on the Th/Yb vs. Nb/Yb diagram of Pearce and Peate (1995).

The only samples that plot away from the mantle array are from the Mount Sproat assemblage (samples other than unit DMSv1) and one from the Kaslo Group. These samples were influenced by subduction processes or crustal contamination. The Lardeau, Hamill and Kaslo groups plot along the mantle array at a position in agreement with results from the tectonic discrimination diagrams and spider plots. The Thompson assemblage basalt is E-MORB and amphibolite of the Monashee cover sequence that underlies the Chase Formation at Upper Arrow Lake is OIB. Published data from the Lardeau Group (Logan and Colpron, 2006) are plotted for comparison. Mantle reservoir values are from McDonough and Sun (1995).

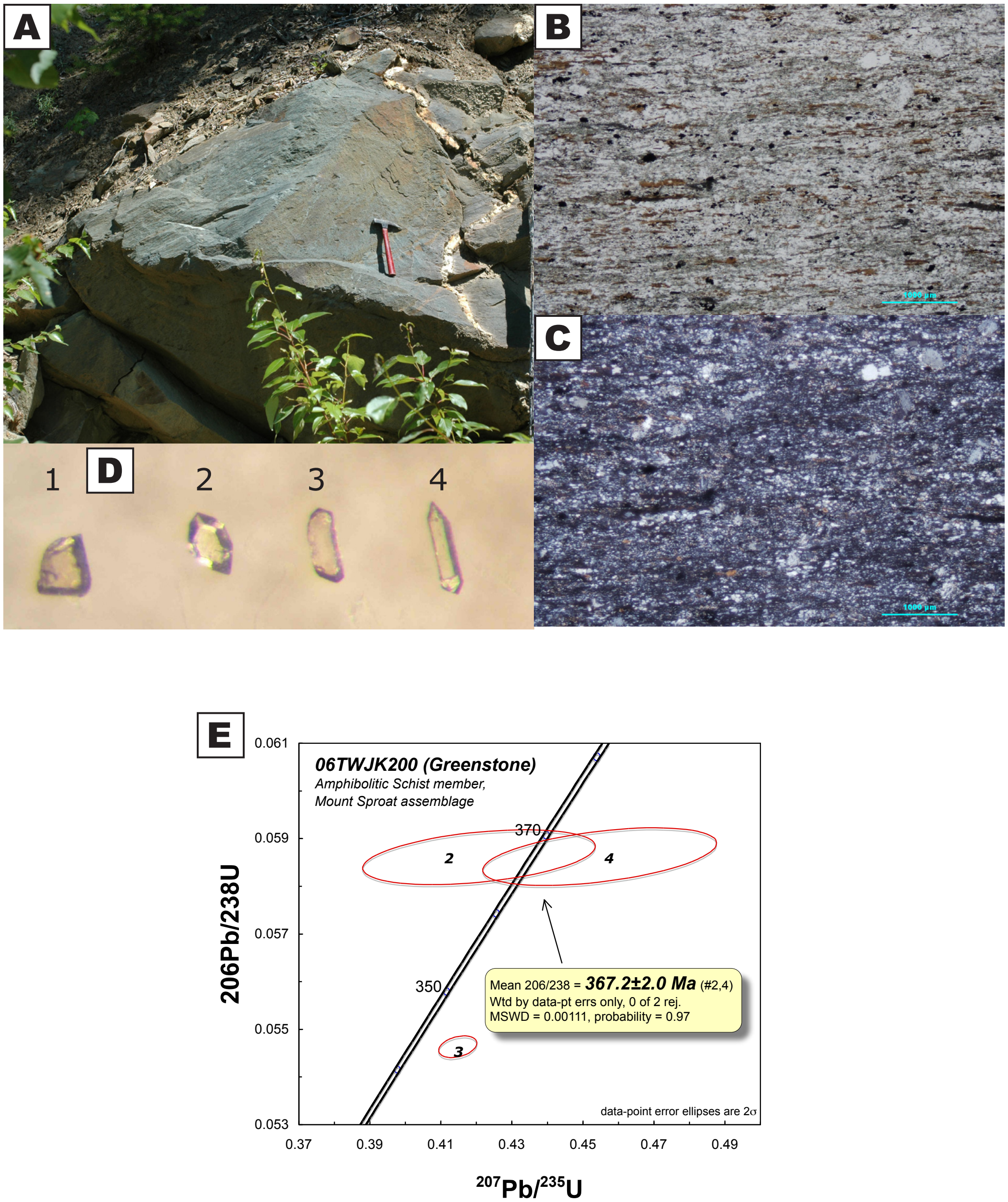

Figure 2-16. U-Pb zircon geochronology sample 06TWJK200 from the Mount Sproat assemblage.

A) Outcrop at sample site near Beaton Arm. B) Photomicrograph of a piece of the analyzed material. Transmitted, plane polarized light. C) Same as "B" but in cross-polarized light. D) Photograph of the four zircons selected for ID-TIMS analysis. Note that grains 2 and 4 are clear, faceted and lack signs of sedimentary transport. E) Concordia plot of the three Phanerozoic zircons (2, 3, and 4). Grains 2 and 4 share a Late Devonian 206Pb/238U age of ca. 367 Ma.

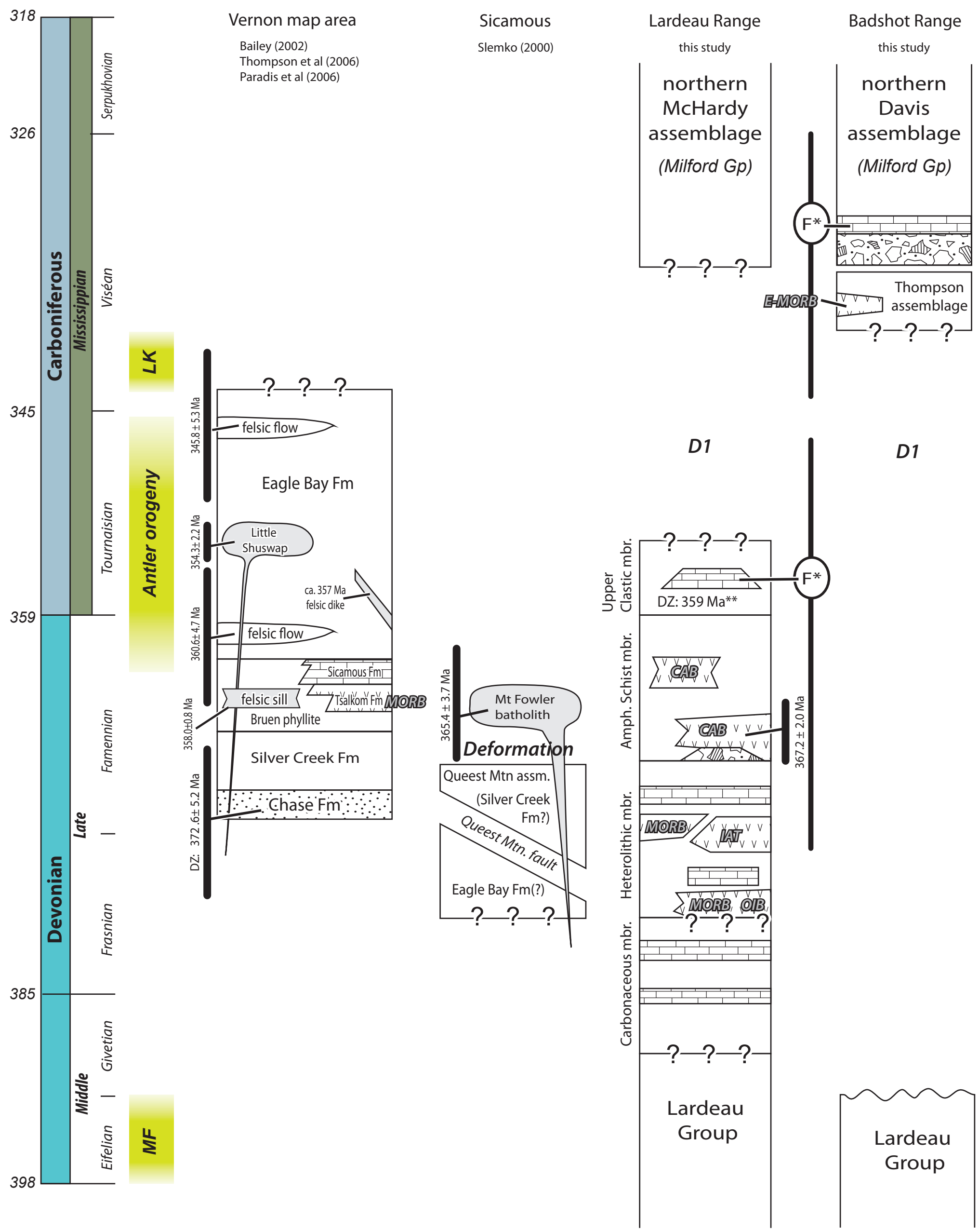

Figure 2-17. Stratigraphy of Devonian-Mississippian rocks from the North Okanagan-Shuswap region and Selkirk Mountains.

The Amphibolitic Schist member of the Mount Sproat assemblage overlaps the age range of the Silver Creek Formation. Abbreviations: DZ, detrital zircon date; LK, Little Kalzas orogeny (Colpron et al., 2006); MF, Mount Forster Formation deformation (Root, 1987); *conodont data from Orchard (1985); **U-Pb detrital zircon from Thompson et al. (2006)

References

Archibald, D.A., Glover, J.K., Price, R.A., Farrar, E., and Carmichael, D.M., 1983, Geochronology and tectonic implications of magmatism and metamorphism, southern Kootenay Arc and neighbouring regions, southeastern British Columbia. Part I : Jurassic to mid-Cretaceous: Canadian Journal of Earth Sciences, v. 20, p. 1891-1913.

Bailey, S., 2002, Geology and geochemistry of the Eagle Bay assemblage in the Johnson Lake area, Kootenay terrane, south-central British Columbia: M.Sc. thesis, University of Victoria, Victoria, British Columbia, Canada, 200 p.

Barrett, T.J., and MacLean, W.H., 1999, Volcanic sequences, lithogeochemistry, and hydrothermal alteration in some bimodal volcanic-associated massive sulfide systems: Reviews in Economic Geology, v. 8, p. 101–131.

Belousova, E.A., Griffin, W. L., O'Reilly, S. Y., and Fisher, N. I., 2002, Igneous zircon: trace element composition as an indicator of source rock type: Contributions to Mineralogy and Petrology, v. 143, p. 602-622, doi 10.1007/s00410-002-0364-7.

Brown, E., Gehrels, G., and Valencia, V. A., 2010, Chilliwack composite terrane in northwest Washington: Neoproterozoic-Silurian passive margin basement, Ordovician-Silurian arc inception: Canadian Journal of Earth Sciences, v. 47, p. 1347-1366.

Cairnes, C. E., 1934, Slocan Mining Camp, British Columbia; Geological Survey of Canada, Memoir 173.

Carr, S.D., 1991, Three crustal zones in the Thor-Odin – Pinnacles area, southern Omineca Belt, British Columbia. Canadian Journal of Earth Sciences, v. 28, 2003-2023.

Colpron, M., and Price, R., 1995, Tectonic significance of the Kootenay terrane, southeastern Canadian Cordillera: An alternative model: Geology, v. 23, p. 25.

Colpron, M., and Nelson, J.L., 2009, A Palaeozoic Northwest Passage: incursion of Caledonian, Baltican and Siberian terranes into eastern Panthalassa, and the early evolution of the North American Cordillera: Geological Society London Special Publications, v. 318, p. 273–307, doi: 10.1144/SP318.10.

Creaser, R. A., Goodwin-Bell, J. S., and Erdmer, P. E., 1999, Geochemical and Nd isotopic constraints for the origin of eclogite protoliths, northern Cordillera: Implications for the Paleozoic tectonic evolution of the Yukon-Tanana terrane: Canadian Journal of Earth Sciences, v. 36, p. 1697-1709.

Dusel-Bacon, C. and Cooper, K.M., 1999, Trace-element geochemistry of metabasaltic rocks from the Yukon-Tanana Upland and implications for the origin of tectonic assemblages in east-central Alaska: Canadian Journal of Earth Sciences, v. 36, p. 1671-1695.

Erdmer, P., Heaman, L., Thompson, R.I. and Daughtry, K.L, 2001, Eocambrian granite clasts in southern British Columbia shed light on Cordilleran hinterland crust: Canadian Journal of Earth Sciences, v. 38, p. 1007-1016.

Floyd, P.A. and Winchester, J.A., 1978, Identification and discrimination of altered and metamorphosed volcanic rocks using immobile elements: Chemical Geology, v. 21, p. 291-306.

Fullmer, C. Y., 1986, Geology of the SE1/4 of the Twin Lakes Quad- rangle, Ferry County, Washington. M.Sc. thesis, Eastern Washington University, Cheney

Fyles, J.T. and Eastwood, G.E.P., 1962, Geology of the Ferguson area, Lardeau district, British Columbia: B.C. Department of Mines and Petroleum Resources, Bulletin 45, 92 p.

Glombick, P., 2005, Mesozoic to early Tertiary metamorphic evolution of the Shuswap metamorphic complex in the Vernon area, southeastern Canadian Cordillera: Ph.D. Thesis, University of Alberta, Edmonton, Alberta, Canada, 417 p.

Glombick, P., Thompson, R. I., Erdmer, P., Heaman, L., Friedman, R. M., Villeneuve, M., and Daughtry, K. L., 2006, U–Pb constraints on the thermotectonic evolution of the Vernon antiform and the age of the Aberdeen gneiss complex, southeastern Canadian Cordillera: Canadian Journal of Earth Sciences, v. 43, p. 213-244.

Gordey, S., Abbott, J., Tempelman-Kluit, D., and Gabrielse, H., 1987, " Antler" elastics in the Canadian Cordillera: Geology, v. 15, p. 103.

Heaman, L.M., Erdmer, P., and Owen, J.V. 2002, U–Pb geochronologic constraints on the crustal evolution of the Long Range Inlier, Newfoundland: Canadian Journal of Earth Sciences, 39, p. 845–865.

Hedley, M.S., 1955, Lead-Zinc deposits of the Kootenay Arc: Western Miner, July, p. 31- 35.

Hughes, N. D., Sears, J. W., and Chamberlain, K. R., 2003, New Upper Devonian U-Pb date for Eagle Bay felsic volcanics in the distal Cordilleran miogeocline, Vavenby, British Columbia: Geological Society of America Abstracts with Programs, v. 35, p. 3.

Hyndman, D.W., 1968, Petrology and structure of Nakusp map-area, British Columbia: Geological Survey of Canada Bulletin 161.

Jaffey, A.H., Flynn, K.F., Glendenin, L.E., Bentley, W.C., and Essling, A.M., 1971, Precision measurement of half-lives and specific activities of 235U and 238U: Physical Review C, p. 1889-1906.

Jenner, G.A., 1996, Trace element geochemistry of igneous rocks: Geochemical nomenclature and analytical geochemistry: Geological Association of Canada Short Course Notes, v. 12, p. 51–77.

Jones, A.G., 1959, Vernon map-area, British Columbia. Geological Survey of Canada Memoir 296.

Joseph, N. L., 1990, Geologic map of the Nespelem 1:100,000 Quadrangle, Washington. Washington, Division of Geology and Earth Resources, Open-file Report 90-16.

Klepacki, D.W., 1985, Stratigraphy and structural geology of the Goat Range area, southeastern British Columbia. Ph.D. thesis, Massachusetts Institute of Technology, Cambridge, Mass.

Klepacki, D.W., and Wheeler, J.O., 1985, Stratigraphic and structural relations of the Milford, Kaslo and Slocan Groups, Goat Range, Lardeau and Nelson map area, British Columbia: in Current Research, Part A, Geological Survey of Canada Paper 85-1A, p. 277- 286.

Kraft, J.L., Thompson, R.I., and Erdmer, P., 2007, Geological relationships at Upper Arrow Lake, southeastern British Columbia: implications for the Milford and Kaslo groups; Geological Survey of Canada, Current Research 2007-A8, 12 p.

Kraft, J. L., Thompson, R. I., and Dhesi, P. (compilers), 2011a, Geology, Beaton, British Columbia; Geological Survey of Canada, Open File, 6574, scale 1:50 000, doi: 10.4095/288009.

Kraft, J. L., Thompson, R. I., and Dhesi, P. (compilers), 2011b, Geology, Trout Lake, British Columbia; Geological Survey of Canada, Open File, 6572, scale 1:50 000, doi: 10.4095/288063.

Kraft, J. L., Thompson, R. I., and Dhesi, P. (compilers), 2011c, Geology, Camborne, British Columbia; Geological Survey of Canada, Open File, 6573, scale 1:50 000, doi: 10.4095/288064.

Lane, L.S., 1984, Brittle deformation in the Columbia River fault zone near Revelstoke, southeastern British Columbia. Canadian Journal of Earth Sciences, v. 21, p. 584-598.

Large, R.R., Gemmell, J.B., Paulick, H., and Huston, D.L., 2001, The alteration box plot: A simple approach to understanding the relationships between alteration mineralogy and lithogeochemistry associated with VHMS deposits: Economic Geology, v. 96, p. 957–971.

Lemieux, Y., 2006, Structure, geochronology and thermobarometry of the eastern flank of the Shuswap metamorphic complex in the Upper Arrow Lake area, southeastern British Columbia. Unpublished Ph.D. thesis, University of Alberta, Edmonton, AB.

Lemieux, Y., Thompson, R.I., and Erdmer, P. 2004. Stratigraphic and structural relationships across the Columbia River fault zone, Vernon and Lardeau map areas, British Columbia. In Current Research. Geological Survey of Canada Paper 2004-A3.

Lemieux, Y., Thompson, R., Erdmer, P., Simonetti, A., and Creaser, R., 2007, Detrital zircon geochronology and provenance of Late Proterozoic and mid-Paleozoic successions outboard of the miogeocline, southeastern Canadian Cordillera: Canadian Journal of Earth Sciences, v. 44, no. 12, p. 1675–1693.

Lentz, D.R. 1999. Petrology, geochemistry and oxygen isotopic interpretation of felsic volcanic and related rocks hosting the Brunswick 6 and 12 massive sulfide deposits (Brunswick Belt), Bathurst Mining Camp, New Brunswick, Canada. Economic Geology, v. 94, 57–86.

Logan, J.M. and Friedman, R.M., 1997, U-Pb ages from the Selkirk allochthon, Seymour Arm map-area, southeast British Columbia (82M/8 and 9), in Lefebure, D.V., McMillan, W.J. and McArthur, J.G., eds., Geological Fieldwork 1996: B.C. Ministry of Employment and Investment, Energy and Minerals Division, Geological Survey Branch, Paper 1997-1, p. 17-23.

Logan, J., and Colpron, M., 2006, Stratigraphy, geochemistry, syngenetic sulphide occurrences and tectonic setting of the lower Paleozoic Lardeau Group, northern Selkirk Mountains, British Columbia: in Colpron, M. and Nelson, J.L., eds., Paleozoic Evolution and Metallogeny of Pericratonic Terranes at the Ancient Pacific Margin of North America, Canadian and Alaskan Cordillera: Geological Association of Canada, Special Paper 45, v. 45, p. 361–382.

Ludwig, K.R., 2003, Isoplot 3.0, a geochronological toolkit for Microsoft Excel. Berkeley Geochronological Centre Special Publication No. 4, 71 pp. (http://www.bgc.org/klprogrammenu.html).

MacLean, W.H., 1990, Mass change calculations in altered rock series: Mineralium Deposita, v. 25, p. 44–49.

Meschede, M., 1986. A method of discriminating between different types of mid-ocean ridge basalts and continental tholeiites with the Nb-Zr-Y diagram. Chemical Geology, v. 56, p. 207-218.

Okulitch, A.V., 1985, Paleozoic plutonism in southeastern British Columbia.

Canadian Journal of Earth Sciences, v. 22, p. 1409-1424.

Orchard, M.J., 1985, Carboniferous, Permian and Triassic conodonts from the Central Kootenay Arc, British Columbia : constraints on the age of the Milford, Kaslo, and Slocan groups. In Current Research, Part A. Geological Survey of Canada, Paper 85-1A, p. 287-300.

Paradis, S., Bailey, S., Creaser, R., Piercey, S., and Schiarizza, P., 2006, Paleozoic magmatism and syngenetic massive sulphide deposits of the Eagle Bay assemblage, Kootenay terrane, southern British Columbia: in Colpron, M. and Nelson, J.L., eds., Paleozoic Evolution and Metallogeny of Pericratonic Terranes at the Ancient Pacific Margin of North America, Canadian and Alaskan Cordillera: Geological Association of Canada, Special Paper 45, p. 383-414.

Parrish, R. R., 1992, U-Pb ages of Jurassic-Eocene plutonic rocks in the vicinity of Valhalla complex, southeast British Columbia, In Radiogenic age and isotopic studies: Report 5. Geological Survey of Canada, Paper 91-2, p. 115-134.

Parrish, R., and Armstrong, R.L., 1987, The ca. 162 Ma Galena Bay stock and its relationships to the Columbia River fault zone, southeast British Columbia. In Radiogenic Age and Isotopic Studies: Report 1, Geological Survey of Canada Paper 87-2, p. 25-32.

Pearce, J.A., 1996, A user's guide to basalt discrimination diagrams: Geological Association of Canada Short Course Notes, v. 12, p. 79–113.

Pearce J.A. and Cann, J.R., 1973. Tectonic setting of fasic volcanic rocks determined using trace element analyses. Earth and Planetary Science Letters, v. 19, p. 290-300.

Pearce, J.A., and Peate, D.W., 1995, Tectonic implications of the composition of volcanic arc magmas. Earth and Planetary Science Annual Review 23, p. 251–285.

Piercey, S.J., Murphy, D.C., Mortensen, J.K., and Paradis, S., 2001, Boninitic magmatism in a continental margin Yukon–Tanana Terrane, southeastern Yukon, Canada: Geology, v. 29, p. 731–734.

Piercey, S. J., Mortensen, J. K., Murphy, D. C., Paradis, S., and Creaser, R. A., 2002, Geochemistry and tectonic significance of alkalic mafic magmatism in the Yukon–Tanana terrane, Finlayson Lake region, Yukon: Canadian Journal of Earth Sciences, v. 39, p. 1729-1744.

Piercey, S. J., Murphy, D. C., Mortensen, J. K., and Creaser, R., 2004, Mid-Paleozoic initiation of the northern Cordilleran marginal back-arc basin: Geologic, geochemical, and neodymium isotope evidence from the oldest mafic magmatic rocks in Yukon-Tanana terrane, Finlayson Lake district, southeast Yukon, Canada, Geological Society of America Bulletin, v. 116, p. 1087–1106, doi:10.1130/B25162.1.

Piercey, S. J., Nelson, J. L., Colpron, M., Dusel-Bacon, C., Roots, C. F., and Simard, R.-L., 2006, Paleozoic magmatism and crustal recycling along the ancient Pacific margin of North America, northern Cordillera: *in* Colpron, M. and Nelson, J.L., eds., Paleozoic Evolution and Metallogeny of Pericratonic Terranes at the Ancient Pacific Margin of North America, Canadian and Alaskan Cordillera: Geological Association of Canada, Special Paper 45, p. 281–322.

Read, P.B. 1973, Petrology and structure of Poplar Creek map-area, British Columbia. Geological Survey of Canada Bulletin 193.

Read, P.B. 1976, Lardeau map-area (82K west half), British Columbia. Geological Survey of Canada, Paper 76-1, Part A, p. 95-96.

Read, P.B., and Wheeler, J.O., 1976, Geology, Lardeau west-half, British Columbia. Geological Survey of Canada Open File 432.

Read, P.B., and Brown, R.L., 1981, Columbia River fault zone: southeastern margin of the Shuswap and Monashee complexes, southern British Columbia: Canadian Journal of Earth Sciences, v. 18, p. 1127-1145.

Read, P.B., Psutka, J.F., Fyles, J.T., and MacLeod, R.F, 2009, Geology, MAX Molybdenum Mine area (NTS 82K/12), British Columbia; Geological Survey of Canada, Open file 6215, 2 sheets, 1:10 000 scale, and 1 report, 21 p.

Reesor, J.E., and Moore, J.M., 1971, Petrology and structure of Thor-Odin gneiss dome, Shuswap metamorphic complex, British-Columbia. Geological Survey of Canada Bulletin 195.

Richards, B.C., Ross, G.M. and Utting, J., 2002, U-Pb geochronology, lithostratigraphy and biostratigraphy of tuff in the upper Fammenian to Tournaisian Exshaw Formation: Evidence for a mid-Paleozoic magmatic arc on the northwestern margin of North America, in Hills, L.V., Henderson, C.M. and Bamber, E.W., eds, Carboniferous and Permian of the World: Canadian Society of Petroleum Geologists, Memoir 19, p. 158-207.

Roback, R.C., 1993, Late Paleozoic to middle Mesozoic tectonic evolution of the Kootenay arc, northeastern Washington and southeastern British Columbia: PhD thesis, University of Texas, Austin, Texas, 237 p.

Rollinson, H. R., 1993, Using Geochemical Data: Evaluation, Presentation, Interpretation. Longman, London.

Rubin, C. M., Miller, M. M., and Smith, G. M., 1990, Tectonic development of Cordilleran mid-Paleozoic volcano-plutonic complexes; Evidence for convergent margin tectonism: in Harwood, D. S. and Miller, M. M. (eds.) Paleozoic and early Mesozoic paleogeo- graphic relations; Sierra Nevada, Klamath Mountains, and related terranes. Geological Society of America, Special Papers, v. 255, p. 1–16.

Sears, J.W., 1979, Tectonic contrasts between the infrastructure and suprastructure of the Columbian orogen, Albert Peak area, western Selkirk Mountains, British Columbia: Ph.D. thesis, Queen’s University, Kingston, Ontario, 154 p.

Shervais, J.W., 1982. Ti-V plots and the petrogenesis of modern ophiolitic lavas: Earth and Planetary Science Letters, v. 59, p. 101-118.

Simony, P.S., Sevigny, J.H., Mortensen, J.K. and Roback, R.C., 2006, Age and origin of the Trail Gneiss Complex: Basement to Quesnel terrane near Trail, southeastern British Columbia, in Colpron, M. and Nelson, J.L., eds., Paleozoic Evolution and Metallogeny of Pericratonic Terranes at the Ancient Pacific Margin of North America, Canadian and Alaskan Cordillera: Geological Association of Canada, Special Paper 45, p. 505-515.

Slemko, N. M., 2000, Structural, Metamorphic, and Plutonic History o f Rocks Adjacent to Shuswap Lake, British Columbia: Evidence of Early to Middle Paleozoic Deformation: M.Sc. thesis, University of Alberta, Edmonton, AB.

Smith, B. L., 1982, Geology of the southeast portion of the Inchelium Quadrangle, Stevens County, Washington., M.Sc. thesis, Eastern Washington University, Cheney, WA.

Smith, M. T. 1990, Stratigraphic, structural, and U-Pb geochronologic investigation of lower Paleozoic eugeoclinal strata in the Kootenay Arc, southeastern British Columbia and northeastern Washington. Ph.D. dissertation, University of Arizona, Tucson, AZ.

Smith, M. T., and Gehrels, G. E., 1991, Detrital zircon geochronology of Upper Proterozoic to lower Paleozoic continental margin strata of the Kootenay Arc: implications for the early Paleozoic tectonic development of the eastern Canadian Cordillera: Canadian Journal of Earth Sciences, v. 28, p. 1271-1284.

Smith, M. T., and Gehrels, G. E., 1992a, Structural geology of the Lardeau Group near Trout Lake, British Columbia: implications for the structural evolution of the Kootenay Arc: Canadian Journal of Earth Sciences, v. 29, p. 1305-1319.

Smith, M. T., and Gehrels, G. E., 1992b, Stratigraphic comparison of the Lardeau and Covada groups: implications for revision of stratigraphic relations in the Kootenay Arc: Canadian Journal of Earth Sciences, v. 29, p. 1320-1329.

Snook, J. T., Lucas, H. E., and Abrams, M. J., 1981, A cross-section of a Nevada-style thrust in northeast Washington. Washington, Department of Natural Resources, Report of Investigations, no. 25.

Stacey, J. S., and Kramers, J. D., 1975, Approximation of terrestrial lead isotope evolution by a two-stage model: Earth and Planetary Science Letters, v. 26, p. 207-221.

Stoltz, A.J., Varne, R., Davies, G.R., Wheller, G.E., and Foden, J.D., 1990, Magma source components in an arc-continent collision zone: The Flores-Lembata sector, Sunda arc, Indonesia: Contributions to Mineralogy and Petrology, v. 105, p. 585–601.

Struik, L.C., 1981, A reexamination of the type area of the Devono-Mississippian Cariboo orogeny, central British Columbia: Canadian Journal of Earth Sciences, v. 18, p. 1767-1775.

Sun, S.S. and McDonough, W.F., 1989. Chemical and isotopic systematics of oceanic basalts: implications for mantel composition and processes. In Saunders, A.D. and Norry, M.J., eds., Magmatism in the Ocean Basins. Geological Society Special Publication 42, p. 313-345.

McDonough, W. F., and Sun, S.-s., 1995, The composition of the Earth: Chemical Geology, v. 120, p. 223-253.

Thompson, R.I., Glombick, P., Acton, S., Heaman, L., Friedman, R., Daughtry, K., Erdmer, P. and Paradis, S., 2002, New Constraints on the age and distribution of the Chase quartzite, Vernon (82L) and Lardeau (82K) map areas: Regional implications [abstract]: Slave-Northern Cordillera Lithospheric Evolution (SNORCLE) Transect and Cordilleran Tectonics Workshop Meeting, Lithoprobe Report No. 82, p. 91-94.

Thompson, R.I. and Glombick, P., 2005, Geology, Shuswap Falls, British Columbia: Geological Survey of Canada Open File 4376, 1:50,000.

Thompson, R.I. and Unterschutz, J.L., 2005, Geology, Vernon,, British Columbia: Geological Survey of Canada, Open File 4375, 1:50,000.

Thompson, R.I., Glombick, P., Erdmer, P., Heaman, L. M., Lemieux, Y., and Daughtry, K. L., 2006, Evolution of the ancestral Pacific margin, southern Canadian Cordillera: Insights from new geologic maps: in Colpron, M. and Nelson, J.L., eds., Paleozoic Evolution and Metallogeny of Pericratonic Terranes at the Ancient Pacific Margin of North America, Canadian and Alaskan Cordillera: Geological Association of Canada, Special Paper 45, p. 433-482.

Thompson, R. I., Lemieux, Y, Glombick, P, and Dhesi, P, 2009a, Geology, St Leon Creek, British Columbia: Geological Survey of Canada, Open File 6185, 2009; 1 sheet, doi:10.4095/247848

Thompson, R. I., Lemieux, Y, Glombick, P, and Dhesi, P, 2009b, Geology, Nakusp, British Columbia: Geological Survey of Canada, Open File 6186, 2009; 1 sheet, doi:10.4095/247849

Tomlinson, K.Y., Hughes, D.J., Thurston, P.C., and Hall, R.P., 1999, Plume magmatism and crustal growth at 2.9 to 3.0 Ga in the Steep Rock and Lumby Lake area, western Superior province: Lithos, v. 46, p. 103–136.

Walker, J. F., and Bancroft, M. F., 1929, Lardeau map-area, British Columbia: general geology; in Lardeau Map-area, British Columbia, (ed.) J.F. Walker and H.C. Gunning; Geological Survey of Canada, Memoir 161, p. 1–16.

Wheeler, J. O., 1968, Lardeau (west half) map-area, British Columbia (82K W112). In Report of activities, part A. Geological Survey of Canada, Paper 68-lA, p. 56-58.

Wheeler, J.O. and McFeely, P. (compilers), 1991, Tectonic assemblage map of the Canadian Cordillera and adjacent parts of the United States of America: Geological Survey of Canada, Map 1712A, 1:2,000,000.

Whitford, D.J., McPherson, W.P.A. and Wallace, D.B., 1989, Geochemistry of the host rocks of the volcanogenic massive sulfide deposit at Que River, Tasmania: Economic_Geology, v. 84, p. 1-21.

Wood., D.A., 1980. The application of the Th-Hf-Ta diagram to problems of tectonomagmatic classification and to establishing the nature of crustal contamination of basaltic lacas of the British Tertiary volcanic province. Earth and Planetary Science Letters, v. 50, p. 11-30.

Zwanzig, H. V., 1973, Structural transitions between the foreland zone and the core zone of the Columbian orogen, Selkirk Moun- tains, British Columbia. Ph.D. dissertation, Queen's University, Kingston, Ont.

Chapter 3: A revised stratigraphic framework for the northern Kootenay Arc: Upper Mississippian and Permian rocks

3.1 Introduction

The Milford Group (Cairnes, 1934; Read and Wheeler, 1976) is a Carboniferous sedimentary and volcanic succession in southeastern British Columbia that has been apportioned to two different terranes despite evidence that its constituent assemblages were deposited in the same continental margin basin (Klepacki, 1985; Smith and Gehrels, 1991; Roback et al., 1994) dubbed the Slide Mountain ocean (e.g. Nelson, 1993; Piercey et al., 2004). Rocks of the Slide Mountain terrane (Monger, 1984; Monger and Berg, 1987) are consistently thrust over continental margin rocks (e.g. Klepacki, 1985; Schiarizza and Preto., 1987; Wheeler and McFeely, 1991; Nelson, 1993; Murphy et al., 2006). But how significant is the terrane boundary hypothesized to dissect the Milford Group assemblages? Why, when the main regional unconformity in the nearby miogeocline is sub-Devonian, is the major unconformity in the northern Kootenay Arc beneath Late Mississippian strata? What more can be learned about the significance, depositional settings and regional correlations of these uncommon strata?

Previous investigations of the Milford Group were conducted in the Goat Range area (Figure 1-7) where strata are well exposed but are strongly deformed and metamorphosed to lower amphibolite facies (Read, 1973; Klepacki, 1985; Roback, 1993). This study involved detailed investigation of the Milford Group in the Lardeau and Badshot ranges, where rocks are less metamorphosed and deformed, allowing greater resolution of stratigraphic details and original sedimentology.

This chapter presents new detailed descriptions of the Milford Group north of the Goat Range and evidence of a new sedimentary succession, termed the Thompson assemblage (Kraft et al., 2011a), stratigraphically between the Milford and Lardeau groups north of Trout Lake.

3.2 Geological setting and previous work

3.2.1 Milford Group

The Viséan to Serpukhovian Milford Group (Cairnes, 1934; Read and Wheeler, 1976; Klepacki, 1985; Orchard, 1985) hosts the southernmost and most outboard pericratonic Carboniferous strata in the Canadian Cordillera that are in depositional contact with rocks of the ancestral North American margin

(Read and Wheeler, 1976; Colpron and Price, 1995). Milford strata crop out in the Kootenay Arc north of the city of Nelson. In contrast to the well-characterized and extensive cratonal and miogeoclinal rocks of the Western Canada Sedimentary Basin (Figure 3-1), Carboniferous strata exposed west of the Rocky Mountains such as the Milford Group exist as widely separated erosional remnants that have yielded little biostratigraphic data (Richards, 1989; Richards et al., 1994). Most have been interpreted to be deposited along the western side of a continent scale margin-parallel basin, the Prophet Trough, with the Carboniferous miogeocline deposited on the inboard eastern side (Figure 3-1; Richards, 1989). In contrast, the Milford Group was deposited outboard of the Prophet Trough at the inboard fringe of the late Paleozoic Slide Mountain marginal basin (Klepacki, 1985; Roback et al., 1994), where it overlapped oceanic and continental crust (Klepacki, 1985; Murphy et al., 1995) and possibly lay inboard of an Early Paleozoic volcanic arc (Figure 1-4D; Roback et al., 1994). Deposition has been interpreted to result from subsidence due to back-arc extension (Klepacki, 1985; Richards, 1989), although subsidence could have been associated with local compression or crustal loading, as in the Antler orogeny to the south (Richards et al., 1994).

Conodont biofacies from the Milford Group and coeval strata to the northwest (Eagle Bay Formation) are indicative of eastward shallowing and younging of Carboniferous strata consistent with transgressive onlapping of a topographic high in the east (Orchard, 1985). Proterozoic and possibly lower Paleozoic high grade gneiss of the Shuswap complex to the west presently separates the Milford Group from proposed correlative strata in the Eagle Bay Formation (Jones, 1959), which contains conodont fauna of the same age as those in the Milford Group (Okulitch and Cameron, 1976; Orchard, 1985).

Age of the Milford Group

Carboniferous coral, echinoderm and brachiopod fossils have long been recognized in Milford Group limestone (Bancroft, 1921; Cairnes, 1934; Read and Wheeler, 1976). Samples from the Milford Group, collected in the Goat Range have yielded Late Viséan to Bashkirian conodonts (Orchard, 1985). Four other samples from a site referred to in this study as Comaplix Ridge (Figure A1-1) yielded Viséan conodonts, marginally older than those from Milford strata in the Goat Range (Orchard, 1985). Due to imprecision of the reported site data, the location of the Comaplix Ridge samples could not be matched to the stratigraphy mapped in this study, but published descriptions suggest that they belong to strata referred to below as the northern Davis assemblage. The low diversity, *Cavusgnathus-Kladognathus* conodont biofacies reported from the site indicates a stressed environment, probably due to shallow-water, energetic and (or) brackish conditions (Orchard, 1985). Tournaisian phyllite and limestone (Orchard, 1985; Catherine Lake phyllite of Thompson et al., 2006) immediately west of Upper Arrow Lake have been included in the Milford Group (Read and Wheeler, 1976; Orchard, 1985) but, as discussed in Chapter 2, are here assigned to the Upper Clastic member of the Mount Sproat assemblage.

Milford Group in the Goat Range

The Milford Group as first described by Cairnes (1934) was redefined by Read and Wheeler (1976) to include only strata now known to be of Carboniferous age (Orchard, 1985). Detailed investigations of the Milford Group come from the Goat Range of the Selkirk Mountains, where polyphase folding, lower amphibolite-grade metamorphism and significant faulting along the southeast margin of the Kuskanax batholith (Read, 1973; Klepacki, 1985) have obscured primary relationships. In the Goat Range, the Milford Group comprises three fault-bounded assemblages of Late Viséan to Bashkirian (Upper Mississippian to Pennsylvanian) metasedimentary and metabasaltic rocks (figures 1-3 and A1-1; Klepacki, 1985; Orchard, 1985). From east to west they are: the mainly siliciclastic Davis assemblage, the tholeiitic Keen Creek assemblage, and the argillaceous McHardy assemblage. Although the assemblages are homotaxial and share certain lithological similarities, correlations were not proposed (Klepacki, 1985). The two eastern assemblages, Davis and Keen Creek, overlie unconformably previously deformed strata of the lower to mid-Paleozoic Lardeau Group (Figure A1-1; Read, 1973; Klepacki, 1985). The westernmost assemblage, McHardy, however, has been thrust eastward over the Keen Creek assemblage along the Stubbs fault and its basement is unknown; it was proposed to have been deposited on Devonian-Mississippian oceanic crust (Klepacki, 1985). Petrographic evidence (Klepacki, 1985) and detrital zircon dates (Roback et al., 1994) from the McHardy assemblage support derivation from the Lardeau Group, establishing an indirect stratigraphic link between the Milford assemblages. A conglomerate lens in the southern McHardy assemblage, the Cooper conglomerate, contains granitic clasts which have yielded concordant Silurian U-Pb zircon dates (431 ± 12 Ma and 418 ± 5 Ma; Roback et al., 1994).

Milford Group in the Lardeau and Badshot ranges

Milford Group strata in the vicinity of Trout and Upper Arrow lakes occur in Jurassic synclines (Read and Wheeler, 1976) that are separated by steeply dipping Jurassic and younger faults (Kraft et al., 2011a; 2011b;). The easternmost syncline forms a belt in the western Badshot Range in which Milford strata rest unconformably on grit of the lower or mid-Paleozoic Broadview Formation (Lardeau Group; Read and Wheeler, 1976). Western occurrences of Milford strata underlie the Lardeau Range west of Trout Lake and, along with conformably overlying Permian Kaslo Group metabasalt (Klepacki, 1985; Roback et al., 1994), surround the granodioritic Early to Middle Jurassic Kuskanax batholith (Read and Wheeler, 1976; Roback, 1993). Milford Group rocks in the western Badshot Range have been interpreted as the McHardy assemblage by Lemieux (2006) and Thompson et al. (2006), but their lithological characteristics and stratigraphic relationship with the Broadview Formation instead support correlation with the Davis assemblage. On the basis of map continuity and lithostratigraphy, Milford Group rocks in the Lardeau Range are considered in this study to be equivalents of the McHardy assemblage. The local stratigraphy is illustrated in Figure 3-2. The data are presented below.

Permian Kaslo Group

The McHardy assemblage is conformably overlain by a thick succession of Permian basaltic greenstone (Orchard, 1985) and local ultramafic bodies termed the Kaslo Group (Hyndman, 1968; Read and Wheeler, 1976). The McHardy assemblage and Kaslo Group were assigned to the oceanic Slide Mountain terrane (Monger, 1984; Klepacki, 1985; Monger and Berg; 1987), which has been interpreted as obducted vestiges of a Late Paleozoic marginal ocean basin that formed along the length of the Canadian Cordillera (Nelson et al., 2006; Figure 1-2).

3.3 New field data

Field investigations were conducted over a ~500 km^2 area that exposes all known Milford Group strata north of the Goat Range. Geology was mapped at 1:20 000-scale where exposure permitted. Reassignment of strata to the Mount Sproat assemblage (see Chapter 2) has decreased the interpreted extent of the Milford Group from that reported in previous work (i.e. Read and Wheeler, 1976).

3.3.1 Metamorphism and strain

Carboniferous rocks are preserved at greenschist facies in most of the study area, with local zones of increased metamorphism. From McCrae Peak to Gerrard, rocks of the Thompson assemblage and Milford Group were not significantly recrystallized by metamorphism. Sedimentary protoliths are readily identifiable and macrofossils in limestone are only weakly recrystallized. Pelite is phyllitic and may contain millimetre sized white mica, biotite or rarely garnet porphyroblasts within ~1 km of Jurassic plutons. The Thompson assemblage and Milford Group in the Badshot Range contain a cleavage that may be parallel or moderately oblique to bedding. Milford strata that encircle the Kuskanax batholith tend to contain a layer-parallel weak schistosity in place of cleavage. Between the Columbia River and McCrae Peak or Mount Sproat, pelitic rocks in the northern Davis and Thompson assemblages have been recrystallized to medium grained muscovite-biotite (±garnet ± kyanite ± staurolite) schist, and marble contains centimetre-scale radial sprays of tremolite. Because of uncertainties in primary features caused by increased metamorphism and strain, those strata are excluded from discussion of local stratigraphy.

3.3.2 Stratigraphic descriptions

Milford strata in the Lardeau and Badshot ranges are considered here to be correlative with two of the Goat Range Milford assemblages of Klepacki (1985), but distinctions exist (see below). The Milford assemblages north of the Goat Range (or ~ 50 deg 30′ N latitude) are referred to here as 'northern Davis' and 'northern McHardy'. Thicknesses of lithological units presented here are field or map-based estimates. The stratigraphy of Carboniferous strata described below is illustrated in the appended figure A1-4.

Thompson assemblage

Investigation of the sub-Milford unconformity north of Trout Lake allows differentiation of a sedimentary sequence between the northern Davis assemblage and the Broadview Formation. The sequence was named the Thompson assemblage by Kraft et al. (2011a). The strata were previously included in the Broadview Formation or in the Milford Group (Read and Wheeler, 1976). The description below builds on the original definition of Kraft et al. (2011a).

The Thompson assemblage reaches ~450 m thickness where it is best exposed on the southwest flank of Mount Thompson (figures 3-3 and 3-4). It is inferred to extend along strike to McCrae Peak and Upper Arrow Lake (Figure A1-1). Reconnaissance revealed similar rock types beneath Milford strata 2.5 km to the southeast, and identified a roughly 150 m thick section of potentially correlative strata immediately below the Milford Group farther south at Lardeau Creek. Equivalents of the Thompson assemblage have not been identified south of the community of Trout Lake.

Lithostratigraphy

The internal stratigraphy of the Thompson assemblage was compiled from exposures at Mount Thompson. The lower ~300 m of the Thompson assemblage is dominated by pale green, grey and maroon phyllite (Figure 3-5). The lowest observed unit, which sits on top of the Broadview Formation with presumed unconformity, is conglomeratic grey phyllite with angular pebble sized crystalline quartz clasts (Figure 3-5A). Discontinuous weakly strained purple and green amygdaloidal basalt (figures 3-5C, D) with enriched mid-ocean ridge basalt trace element geochemical traits (see Chapter 2) occurs approximately 120 m above the basal unconformity. Phyllitic paraconglomerate and a few metres of grey crystalline limestone overlie the basalt unit and are in turn overlain by mixed green and maroon phyllite to argillite and green grit. Phyllitic grit and wacke form decimetres-thick graded beds, locally with scoured bases, that fine upward toward Milford strata (figures 3-5E, F). Grit and phyllite are typically the same pale green colour as the underlying Broadview Formation and similarly contain millimetric blue-quartz granules.

Upper levels of the Mount Thompson assemblage (~300-450 m above the base) are characterized by carbonate beds and phyllitic argillite with lesser grit and rare centimetre-scale beds of ribbon chert in phyllite (Figure 3-6). Beds with thicknesses of several metres of moderately recrystallized grey limestone, sandy limestone to coarse calcite-cemented sandstone, and limestone-dolostone breccia interbedded with maroon phyllitic argillite are abundant in the uppermost ~75 m of exposure. Limestone breccia is clast supported and comprises moderately flattened, angular, cobble-size blocks of grey crystalline limestone and centimetre-scale angular dolostone fragments in a volumetrically minor dolostone matrix. Rare exposures of sharply interbedded, centimetre-scale beds of chert, limestone and green, grey and maroon laminated phyllite (Figure 3-6B) occur near the top of the section.

Because of stratigraphic position and occurrences of similar conglomeratic phyllite and sandy marble, grey phyllite and limestone (mica schist and marble where metamorphism is greater near Upper Arrow Lake) beneath Milford Group, conglomerate on Comaplix Ridge and McCrae Peak are tentatively assigned to the Thompson assemblage. At McCrae Peak, a succession below basal Milford conglomerate comprises tens to hundreds of metres of grey phyllite and medium grey, often mottled or fractured marble (Figure 3-7). Unlike at Mount Thompson, a discrete contact with the Lardeau Group could not be clearly identified. Pale green talc-rich layers occur gradationally within the sub-Milford phyllite on the western spine of the summit of McCrae Peak (Figure 3-7A). A single ramiform conodont element (conodont alteration index of 5.5) recovered from limestone indicates deposition in the interval Ordovician to Triassic (Orchard, report 008-MJO-2009; collection site UTM: 433997E, 5629280N). Similar talc-serpentine schist occurs on the west flank of Mount Sproat at the inferred faulted contact of the Mount Sproat assemblage and sub-Milford phyllite and marble. The talc schist and nearby phyllite and marble are correlated with similar rocks on McCrae Peak and are tentatively included in the Thompson assemblage because of their stratigraphic position. Rare crinoid ossicles occur in limestone assigned to the Thompson assemblage at Comaplix ridge (Figure 3-7C). Roughly 200 m of soft calcareous phyllite that commonly contains angular intraclasts of similar composition and colour that occurs below the basal Milford conglomerate near Beaton Arm may also be equivalent to the Thompson assemblage. Similarly, a few metres of calcareous phyllite was observed within interpreted Thompson assemblage strata immediately to the north at Comaplix Ridge.

Field relations

The contact with Broadview grit can be constrained within a few metres at Mount Thompson but was not found in outcrop. The upper contact of the Thompson assemblage with the overlying Milford Group Basal member is poorly exposed on the north side of Beaton Arm, where conglomeratic calcareous phyllite is in sharp contact with overlying Milford pebble conglomerate. Both lower and upper contacts of the Thompson assemblage are concordant with layering at outcrop scale. The lower contact with the Broadview Formation is slightly discordant at map-scale. A strong contrast in deformation histories across the contact (see Chapter 4) and inferred derivation of Thompson assemblage sedimentary rock from the Broadview Formation, using petrographic data above and detrital zircon data in Chapter 5, indicate an unconformable relationship between the Broadview Formation and Thompson assemblage.

Northern Davis assemblage (Milford Group)

The northern Davis assemblage forms a 50 km long synclinal belt that follows the northwesterly regional strike from the south end of Trout Lake to McCrae Peak, where it deflects westward. The belt terminates in Upper Arrow Lake and is interpreted to be truncated by a normal fault associated with the Columbia River fault zone (Kraft et al., 2011c). At its southern limit near Gerrard, the northern Davis assemblage belt is truncated by the Mobbs fault (Kraft et al., 2011b). The most complete exposures of the basal units occur on a ridge that connects Comaplix and Sproat mountains, referred to here as Comaplix Ridge (Figure A1-1), and on the west flank of Mount Thompson. Good exposures can also be found on McCrae Peak, in logging road cuts south of the mouth of the Incomappleux River, near the mouth of Lardeau Creek east of the community of Trout Lake, and on West Trout logging road west of Gerrard (Figure 1-7). The top of the assemblage is not exposed. Assuming a tight to isoclinal Beaton syncline (as map patterns indicate), the present deformed thickness of the northern Davis assemblage is at least 1000 m.

The northern Davis assemblage is divided here into a Basal member and an overlying Phyllite member.

Basal member

The Basal member comprises conglomerate with minor sandstone or sandy phyllite beds (figures 3-8 and 3-9) overlain by interlayered limestone and phyllite. The composition of clasts and matrix in the conglomerate varies along strike and commonly reflects the composition of underlying strata. Clasts of grit identical to underlying Broadview Formation grit and white crystalline quartz are ubiquitous and dominant. Less common clasts include quartzite, orange-weathering carbonate, chert, and argillite. At Gerrard, the conglomerate matrix is chloritic and compositionally mirrors the alkaline basalt of underlying Jowett Formation strata (sample 08TWJK362, appendix A2-2). Quartzite clasts contain rare quartz veins that do not enter the conglomerate matrix. Basal conglomerate at Mount Thompson is the thickest of the observed sites. There it comprises diamictite with sub-rounded boulders of foliated grit up to 40 cm across. Lack of sorting and presence of flow top boulders in diamictite beds indicate deposition as debris flows (figures 3-8A, B). Thin, sandy beds are graded and fine away from the Thompson assemblage.

The ~100 m thick basal conglomerate at Mount Thompson is exposed for 3 km along strike. Carbonate forms the basal unit to the northwest and southeast of the conglomerate. In the southeast, the basal carbonate is a metres-thick carbonate breccia/rudstone containing unsorted angular blocks of massive grey limestone up to 30 cm across in a dolostone matrix (Figure 3-10). The breccia is similar to rudstone in the uppermost Thompson assemblage. Massive micritic limestone overlying the breccia contains at least two ~1 m thick horizons of subangular quartz pebbles and abundant bioclasts.

Relative to conglomerate on the eastern limb of the syncline, conglomerate on the western limb has smaller clasts (<~4 cm) and a better sorted sandy matrix, are thinner (decimetres- to metres thick), and are more repetitively interbedded with sandstone, siltstone and phyllite (Figure 3-9).

Basal conglomerate is consistently overlain by one or more grey fossiliferous or rarely pebbly limestone horizons that vary greatly in thickness from a few metres to >75 m. Multiple carbonate horizons that overlie the basal conglomerate at Mount Thompson lack fragmental or conglomeratic textures and commonly contain intact macrofossils. Rounded vein quartz pebbles and quartz sands in northern Davis assemblage limestone (figures 3-10A ,B) were observed at Comaplix Ridge and McCrae Peak. In the northern Davis assemblage, all fossils observed have been disarticulated and (or) depositionally transported. In decreasing abundance, macrofossils observed are crinoids (common, Figure 3-10E), solitary rugose corals, bryozoans (rare, Figure 3-10F), and gastropods, brachiopods and syringopora (trace). The greatest diversity and abundance of body macrofossils was observed at Mount Thompson. The diversity and along-strike variability of the Basal member are indicative of a complex basin with local carbonate build-ups that were proximal to a high-energy coastline comprising quartzofeldspathic crust.

Phyllite member

An abrupt upward disappearance of coarse clastic- and carbonate-rich units marks the transition from the Basal member to the Phyllite member, which is composed almost entirely of soft, fissile, medium grey silty or sandy phyllite with local cubic pyrite up to 1 cm (Figure 3-11). One or more horizons of 1-10 m of bedded grey chert and cherty quartzite (figures 3-11A, B, C) occur in the lower 50-200 m of the Phyllite member at several localities across the study area. At Mount Thompson, chert is immediately overlain by a 1.5 m bed of orthoquartzite sampled for detrital zircons (see Chapter 5; sample 08TWJK309). Two layers (or one folded layer) of grey micritic limestone occur(s) at Mount Thompson roughly 150-200 m above the chert horizon. Planar bedded rhythmite comprising silty grey phyllite and tan weathering very fine sandstone (Figure 3-11F) was observed at the highest exposed stratigraphic level between Mount Thompson and Trout Lake on the Peek Forest Service Road. Sandstone is minor or absent from the Phyllite member; several hundred metres of well-bedded metasandstone with phyllite present in a fault-bounded panel of the Davis assemblage between Mobbs Ridge and Tenderfoot Lake is inferred to be age-equivalent to the Phyllite member.

Field relations

The lower contact of the northern Davis assemblage in the east limb of the syncline is covered. The western limb is faulted against polydeformed grit of the Broadview Formation by Jurassic Mobbs fault (Figure 3-12; Read, 1973; Kraft et al., 2011a; see description below). The Mobbs and Adit faults (Kraft et al., 2011c) separate the northern Davis assemblage from the Davis assemblage where it was defined in the Goat Range (Klepacki, 1985).

Northern McHardy assemblage (Milford Group)

In the Lardeau Range, the northern equivalent of the McHardy assemblage of the Goat Range documented by Klepacki (1985) occurs in two belts separated by the Late Cretaceous or younger Adit fault (Read et al., 2009). West of the Adit fault, northern McHardy strata and overlying Kaslo Group metabasalt envelop the Kuskanax batholith and form the limbs of the overturned Hill Creek syncline (Figure A1-1). The northern McHardy assemblage is about 500 m thick at the west margin of the Kuskanax batholith near Ione Falls, and approximately 1,500-2,000 m thick north of the Kuskanax batholith. Northern McHardy assemblage strata terminate in the southeast against the mid-Jurassic Hadow stock (Klepacki, 1985; Roback, 1993). Overlying Permian Kaslo basalt continues uninterrupted into the Goat Range (Read and Wheeler, 1976). A belt of at least 500 m of argillaceous rocks correlated with the northern McHardy assemblage occurs between the Adit and Mobbs faults along the west side of Trout Lake.

The northern McHardy assemblage is subdivided here, in ascending order, into the Conglomerate, Argillite, and Sandstone members.

Conglomerate member

The conglomerate-rich lower member (Figure 3-13) ranges in thickness from approximately 200 m at Mount Murray to zero near Trout Mountain and in Galena Pass. At Mount Murray, the Conglomerate member is mainly pebbly grit with white crystalline quartz clasts and argillite fragments interpreted as mud rip-up clasts. Quartz sandstone interlayers with the grit. The lowermost horizon has a uniquely micaceous matrix (Figure 3-13B) similar in colour and composition to micaceous phyllite in the immediately underlying Mount Sproat assemblage (Heterolithic member).

Argillite member

The relatively thick middle interval of the northern McHardy assemblage is dominated by fine-grained carbonaceous siliciclastic rocks (Figure 3-14). Medium to dark grey, and sometimes black, siliceous phyllite and siliceous argillite with only rare compositional banding are most abundant, but thinner intervals with planar and lenticular laminated striped metasiltstone, fine-grained sandstone and lithic wacke are common. Dark grey to black siliceous argillite is common but less abundant than medium and dark grey phyllite. Phyllite in the northern McHardy assemblage tends to be more siliceous and darker coloured than that of the northern Davis assemblage, but medium grey phyllite in the Argillite member, especially at its northern limit of exposure, is indistinguishable from rocks in the northern Davis assemblage. Siltstone, sandstone and wacke form a mappable horizon near the middle of the Argillite member in the eastern Lardeau Range. Colour banded grey crystalline limestone roughly 25 m thick occurs near the top of the Argillite member near Trout Mountain. Three 1-4 metre-thick layers of coarse crystalline white marble in the Argillite member are exposed along Upper Arrow Lake near Ione Falls.

Sandstone member

This member encompasses the variable thickness of the uppermost northern McHardy assemblage that is dominated by rhythmically interbedded feldspathic metasandstone and metasiltstone (Figure 3-15). Sandstone is consistently beige to faintly purple in colour, equigranular, medium-grained and forms beds ~5-10 cm thick, and rarely greater. Faint, gently undulating or lenticular laminations interpreted as bedforms are visible (Figure 3-15C). Near Mount Murray lenses of calcite-cemented clast-supported sandy pebble conglomerate and argillaceous medium to dark grey limestone occur at the transition from the Argillite member to the Sandstone member. Several metres of calcite cemented pebble conglomerate with clasts of feldspathic sandstone, possibly intraclasts, occur at the upper limit of the Sandstone member near the nose of the Hill Creek syncline.

Field relations

The northern McHardy assemblage overlies various rock types in the Mount Sproat assemblage north of the Kuskanax batholith. The lower contact is less clear near Ione Falls where it is assumed to be at the base of conglomerate that separates the lithologically diverse succession (Upper Clastic member) from a succession of argillite and siltstone with minor marble (northern McHardy assemblage). The lower contact of the northern McHardy assemblage rocks on the west shore of Upper Arrow Lake is covered by drift. At the upper limit of the northern McHardy assemblage, the Sandstone member appears to interfinger with Kaslo Group greenstone across > 100 m in the hinge of the Hill Creek syncline and near Ione Falls and over about 10 m near Mount Murray, although the contact is not exposed. Immediately north of Mount Murray, layering in the Sandstone member is about 20 degrees discordant to the contact with massive greenstone suggesting that the contact is faulted.

Fossils from the northern McHardy assemblage

Macrofossils are unknown in the northern McHardy assemblage. A carbonate sample, sample 06TWJK183B, was taken from a lens of grey limestone within black siliceous argillite on Bigger Creek FSR approximately 7.5 km down the west side of Trout Lake. The lens occurs in argillite near the upper contact of a laterally persistent massive grey limestone layer at or near the base of the northern McHardy assemblage. The sampled lens sits within 50-300 metres of the unconformable contact (which is not exposed) with underlying Mount Sproat assemblage or Broadview Formation rocks. Recovered *Idioprioniodus*?, *Idiognathodus*? and other fossils are poorly preserved (conodont alteration index 6-7), and indicate only a probable Carboniferous age (M.J. Orchard, GSC Report

MJO-2007-28). These conodont taxa are cosmopolitan and thus insufficient to constrain the environment of deposition of the limestone; the lack of shallow water conodont fauna, such as cavusgnathids, is consistent with a deep water setting (M.J. Orchard, personal communication, 2011).

Kaslo Group and associated gabbroic rocks

In the Lardeau Range, the Kaslo Group comprises metamorphosed basalt and gabbroic rocks (Figure 3-16). Metabasalt occurs as weakly to moderately recrystallized, massive chlorite-actinolite greenstone or amphibolite depending on local metamorphic grade. Pillow texture is preserved locally. Unlike the Mount Sproat assemblage, little metasedimentary rock occurs in the Kaslo Group. Poorly exposed horizons of tuffaceous sandstone interfinger with greenstone at its lower contact with the McHardy assemblage near Upper Arrow Lake. In the northern Goat Range the Kaslo Group is interlayered with the McHardy assemblage (Klepacki, 1985), but the Kaslo-McHardy contact at Mount Wilkie appears to be discordant to bedding in the McHardy assemblage (Figure 3-17A).

3.3.3 Faults that juxtapose Carboniferous strata

Adit fault

The Adit fault is inferred to extend north and south of the MAX Molybdenum Mine where it was defined by Read et al. (2009). The Adit fault truncates the ca. 80 Ma Trout Lake stock at the MAX Mine (Read et al., 2009; Lawley et al., 2010) and is the youngest known fault in the Trout Lake area. It is difficult to correlate stratigraphy across the Adit fault (Read et al., 2009) but rocks on both sides are part of the northeast limb of a large second phase antiform (Read et al., 2009) referred to here as the Sproat antiform. Map relations indicate that the Adit fault has west-side-down throw of hundreds of metres near Trout Lake, which is in agreement with earlier interpretation (Read et al 2009).

The Adit fault was not observed along strike to the north, but its presence is inferred from truncation of strata on the northeast limb of the Sproat antiform (Kraft et al., 2011a; Figure A1-1). Map control along strike shows that either displacement diminishes to zero near Mount Sproat or the Adit fault has been folded by late megascopic recumbent (F3) folds between Beaton Arm and the Akolkolex River.

Mobbs fault

A significant fault interpreted to bound the western edge of the northern Davis assemblage from Beaton Arm to Mobbs Creek is inferred to be an extension of the Mobbs fault of Read (1973) mapped in the Goat Range. Construction of the MAX Mine tailings pond temporarily uncovered the fault zone: it consists of 2-3 m of intensely sheared and moderately quartz veined dark grey quartzose phyllite (Figure 3-12). In the west wall of the Mobbs fault to the south, the Broadview Formation, and possibly a thin succession of the Mount Sproat assemblage, is overlain by a thick and uniform succession of rusty weathering siliceous dark grey argillite. The argillite is assigned here to the northern McHardy assemblage because it contrasts with the northern Davis assemblage rocks in the east wall of the Mobbs fault. Those are neither carbonaceous nor rusty weathering and include medium grey silty phyllite, chert, fossiliferous grey limestone, minor banded siltstone and basal pebble conglomerate. A gently northwest-plunging synform-antiform pair outlined by Davis assemblage strata near Gerrard, which appears to be parasitic to the Jurassic Silvercup anticline, is truncated by the Mobbs fault. The Mobbs fault is truncated by, or merges with, the Adit fault north of Beaton Arm. Its surface trace suggests that it is steeply dipping to vertical. The Mobbs fault corresponds to an east-verging thrust inferred by Wheeler and McFeely (1991), however evidence for its sense of displacement is lacking (Read, 1973).

Emmens fault

The Emmens fault (Read 1973), which juxtaposes the Davis assemblage (west) against the Broadview Formation (east) in the Goat Range, may continue north of Mobbs Creek and correspond to a fault that is truncated by or merges with the Adit fault near the Hadow stock. The Emmens fault is inferred at Mobbs Ridge (Roback, 1993) from the juxtaposition of Davis assemblage metasandstone and phyllite (east wall) with a structural slice of the McHardy assemblage (west wall; Figure 3-17B).

3.4 Discussion

3.4.1 Thompson assemblage: age and correlation

The Thompson assemblage is similar to parts of the Mount Forster

Formation (Root, 1987), suggesting similar environments of deposition. Because the Thompson assemblage post-dates early deformation of the Broadview Formation (see Chapter 4), the Thompson assemblage could be contemporaneous with the Eifelian Mount Forster Formation only if the first phase transposition fabric in the Broadview Formation is older than Middle Devonian. Regional data and evidence presented in Chapter 4, however, suggest that early transposition in the Broadview Formation occurred in the Early Mississippian. The Thompson assemblage was therefore deposited in the mid- or Late Mississippian and is not substantially older than the Milford Group. No lithostratigraphic equivalent of the Thompson assemblage is known in southern British Columbia.

3.4.2 Depositional setting

Thompson assemblage

The preponderance of green and maroon mudstone in the Thompson assemblage indicates a low energy depositional setting. Mudstone has little organic carbon and appears to have been deposited in a relatively oxidized setting. The basal phyllitic conglomerate bed is interpreted as a transgressive lag deposit. Massive and graded beds of grit with scoured basal surfaces are interpreted as submarine fan deposits. Interruption of hemipelagic sedimentation by submarine fans, eruption of tholeiitic (E-MORB) basalt, and occurrence of conglomeratic phyllite at mid levels of the Thompson assemblage may record activity on extension faults in and around the basin. Lateral changes in strata of the Thompson assemblage may similarly reflect either syn-depositional normal faulting or (and) deposition on a surface with moderate topographic relief.

Because a deepening trend is not apparent in its strata, sedimentation in the Thompson assemblage kept pace with, or outpaced, subsidence. Sharply and thinly interbedded micritic limestone, chert and argillite at the top of the succession were probably deposited in a protected, low energy marine environment below fair-weather wave base and the effects of tidal currents. Sandy marble layers and rudstones, however, indicate that the area was within reach of storms that mobilized beach or eolian sand and fragments of nearby carbonate buildups, respectively. Calcareous green and grey phyllite in lateral equivalents of the Thompson assemblage between Mount Thompson and McCrae Peak indicate a similarly low energy setting that received mixed carbonate and siliciclastic sediment input. The paucity of body and ichnofossils (bioturbation) is interpreted to reflect a stressed depositional environment, perhaps due to brackish conditions.

The Thompson assemblage appears to represent relatively shallow water deposition during a period of marine transgression and (or) slow subsidence, possibly induced by extensional tectonism. Similarities to the Broadview Formation suggest that Thompson assemblage grit and phyllite were probably largely derived from the underlying Broadview Formation. It is distinguished from the Broadview Formation by the absence of a regional phase 1 transposition foliation (see also Chapter 4) and presence of rock types not found in the Broadview Formation.

Northern Davis assemblage

Like other parts of the Milford Group (Monger, 1977; Klepacki, 1985), the northern Davis assemblage exhibits a fining upward and deepening succession of conglomerate and limestone overlain by minor chert, siltstone and monotonous, thick pelite.

Basal northern Davis assemblage conglomerate records derivation from underlying strata. At Mount Thompson, the basal boulder conglomerate is interpreted to have deposited as debris flows because of the unsorted and wide range of clast sizes and the presence of flow top boulders. (figures 3-7A, B). A nearby fault scarp is interpreted to be the source for the boulder conglomerate and the cause of the change in depositional setting compared with underlying (Thompson assemblage) and overlying strata. Observations in this study are in agreement with previous interpretations that boulder-size clasts were derived from the underlying Broadview Formation and were foliated prior to formation of the conglomerate (Wheeler, 1968; Read and Wheeler, 1976). Subordinate lenses of pebble breccia in the Basal member of the northern Davis assemblage at Mount Thompson contain abundant clasts of rock types (maroon argillite, white chert) that occur in the Thompson assemblage but not in other pre-Milford units in the region. Parts of the Thompson assemblage, therefore, were eroded from a consolidated state and resedimented during initial deposition of the northern Davis assemblage. This observation and the unconformable nature and slight discordance of the Thompson/Milford contact is interpreted to result from uplift and tilting of the Thompson assemblage by extensional faults during deposition of the northern Davis assemblage.

Lenses of graded conglomerate and grit in pyritic dark grey phyllite at the MAX Mine tailings pond on the western edge of the belt (Figure 3-8A) are interpreted to represent distributary channels in anoxic mud, potentially in a submarine or a fluvial setting. The latter is consistent with the location of the conglomerate at the base of a transgressive succession, but occurrence of limestone immediately above similar conglomerate along strike instead indicates a marine setting. Differences in the Basal member on the west side of the syncline, including smaller clast sizes, thinner bedding, increased sand and phyllite component, greater size sorting, and paucity of rock types indicative of shallow marine settings, appear to reflect east to west changes in depositional setting. Northern Davis assemblage strata in the east limb are interpreted to have been more proximal than those in the western limb of the Beaton syncline.

Rapid lateral changes in thickness in the lithostratigraphy of the Basal member indicate deposition on a high relief surface and (or) influence of syndepositional faults. Sedimentological features of units in the Basal member reflect shallow marine settings with intermittent high energy events. Event beds, interpreted as tempestites, within micritic limestone near Mount Thompson indicate that the Basal member was deposited below fair-weather wave-base but above storm wave-base – a range of water depth from approximately 10-50 m (Tucker and Wright, 1990; p. 103-107). The presence of quartzite pebbles in the event beds indicates proximity to a high-energy shoreline with siliciclastic input. Trough cross-bedded sandy marble at Comaplix ridge formed in a high energy marine environment, such as a tidal channel, also in proximity to a source of quartz sand. The moderate abundance and diversity of bioclasts in limestone indicates habitable settings for coral, echinoderms, and other organisms.The preponderance of fissile grey phyllite and a persistent occurrence of chert in the Phyllite member indicate a transition to hemipelagic sedimentation in a low energy setting. Northern Davis assemblage phyllite is interpreted as metamorphosed claystone and silty claystone that was deposited during a period of increasing accommodation space. Such an increase in accommodation space could be produced by tectonic subsidence such as by normal faulting in the basin. Outcrops of planar laminated siltstone and very fine sandstone (Figure 3-10F) that were observed at locations in the Phyllite member are interpreted to have formed as distal turbidites.

Northern McHardy assemblage

The northern McHardy assemblage formed in environments that were somewhat deeper and more prone to turbidite deposition than the northern Davis assemblage. Like the northern Davis assemblage, basal conglomerate is highly variable in thickness and character. The lowermost few metres that locally reflect the composition of underlying strata are interpreted as transgressive lag deposits. Overlying thick beds of quartz-rich pebbly grit with mud rip up clasts at Mount Murray are interpreted to have formed by strong currents, perhaps channels in a submarine fan. The thick intervals of variably carbonaceous mudstone with intervals of feldspathic sandstone, lithic wacke and banded siltstone that comprise the Argillite member likely reflect a moderately deep marine basin setting that experienced intermittent pulses of siliciclastic sedimentation by turbidity currents. Although equivocal, new conodont data from the northern McHardy assemblage are consistent with a deep water setting. Even at upper levels of the assemblage, however, the northern McHardy assemblage was within reach of debris flows of pebbly quartz-rich conglomerate mixed with carbonate from a high energy, probably near-shore environment. Although limestone is rarer than in the northern Davis assemblage, local limestone beds greater than 20 m thick in the uppermost Argillite member are consistent with proximity to a small carbonate platform. Sedimentary facies appear to become more similar to those of the northern Davis assemblage's Phyllite member north of the Kuskanax batholith. This is consistent with a general northward shallowing trend away from the deep basinal chert and argillite of the McHardy assemblage in the Goat Range (Klepacki, 1985).

Rhythmically planar bedded sandstone and siltstone in the Sandstone member at the top of the assemblage are interpreted as thin-bedded turbidites. The insignificance of mudstone intervals in the Sandstone member leads to the interpretation that sedimentation was rapid and frequent, possibly due to increased tectonism or a drop in relative sea level. That the Sandstone member immediately preceded, and interlayers with, eruption of MORB (Kaslo Group) leads to interpretation of increased extension as the primary cause.

3.4.3 Links between the Milford assemblages

Continuity of the Kaslo Group and lithological similarities in Milford rocks across the Hadow stock suggest that the northern McHardy assemblage and McHardy assemblage were continuous prior to emplacement of the stock. Because of strong lithological similarities and equivalent relations to the Lardeau Group, the northern Davis assemblage is here considered to be a continuation of the Davis assemblage in the Goat Range.

As in the Goat Range (Klepacki, 1985), specific correlations between the Davis and McHardy assemblages in the Lardeau and Badshot ranges cannot be made. Strong similarities in several rock types exist and it is inferred that the ranges of depositional settings of these assemblages overlapped. The northern Milford assemblages, therefore, were probably deposited in only slightly different parts of the same basin and have less significant primary differences than their counterparts (Davis and McHardy assemblages) in the Goat Range.

3.4.4 Is a Slide Mountain terrane obduction surface present?

Several faults truncate and juxtapose Late Paleozoic rocks in the study area. Are any of them potential obduction surfaces for a Slide Mountain terrane comprising the McHardy assemblage and Kaslo Group?

Talc-serpentinite lenses outcropping near Crawford Creek north of Beaton Arm (Bancroft, 1921; Read and Wheeler, 1976) were cited as evidence of an obduction surface along which the oceanic [northern] McHardy assemblage was thrust over the [northern] Davis assemblage (Klepacki, 1985; p. 117). New mapping, however, indicates that the northern McHardy assemblage does not outcrop north of Beaton Arm (Kraft et al., 2011a; 2011c). Instead, serpentinite and talc schist occur at or near the base of a sequence of phyllite and marble correlated with the Thompson assemblage, or possibly the Mount Sproat assemblage. The talc-serpentinite lenses cannot have accommodated obduction of the McHardy assemblage. The new interpretation places the serpentinite at the inferred fault contact between the Thompson and Mount Sproat assemblages. The contact corresponds to the mid-Jurassic Mobbs fault in a segment that may have been reactivated by the Adit fault (Kraft et al., 2011a).

The Mobbs fault is the most significant in the Poplar Creek map area (Read, 1973) and from Poplar Creek to the Beaton Arm. Both the McHardy and Davis assemblages, and the Lardeau Group, occur west of the Mobbs fault (Klepacki, 1985; Kraft et al., 2011b), however, so it cannot be a thrust on which the Slide Mountain terrane was obducted. Moreover, the Mobbs fault truncates Middle Jurassic F2 folds (Read, 1973) and is therefore too young to have accommodated hypothesized obduction of the Slide Mountain terrane. Designation of carbonaceous Milford strata on the west shore of Trout Lake as the McHardy assemblage (Kraft et al., 2011a; 2011b) implies that all faults west of those rocks, including the Adit fault (Read et al., 2009), Emmens fault (Read, 1973; Roback 1993), Spyglass fault (Read, 1973) and the northern extension of the Stubbs thrust inferred at Tenderfoot Lake (Roback, 1993) cannot be surfaces on which the McHardy assemblage was obducted. In summary, the northern Kootenay Arc lacks a surface that could separate a hypothesized Slide Mountain terrane from Lardeau rocks that have previously been shown to depositionally overlie the miogeocline along strike to the north (Colpron and Price, 1995).

3.4.5 Nomenclature advances

Application of the tectonic assemblage concept to the northern Kootenay Arc and the revised structural and stratigraphic relations described here and in Chapter 2 leads to several important modifications of the nomenclature that describes the geology of the northern Kootenay Arc (Figure 3-17). As concluded in Chapter 2, the Kootenay tectonic assemblage comprises strata of the Lardeau trough (Lardeau Group) and a superimposed Devonian to Early Mississippian back-arc basin (Mount Sproat assemblage). A major angular unconformity separates the Kootenay tectonic assemblage from overlying strata.

Those overlying rocks – the Milford and Kaslo groups and the Thompson assemblage – constitute a conformable or near conformable succession that was deposited at the inboard margin of the Slide Mountain ocean basin during tectonically controlled subsidence and transgression onto deformed Kootenay tectonic assemblage strata. The Thompson-Milford-Kaslo succession therefore constitutes a tectonic assemblage that is distinct from the Kootenay tectonic assemblage, and, because it depositionally overlies its basement "Slide Mountain" in the northern Kootenay Arc, is not a terrane. The term Slide Mountain tectonic assemblage is proposed here to describe the Thompson assemblage, Milford and Kaslo Groups (Figure 3-17). The term Slide Mountain terrane should be reserved for rocks of the Slide Mountain ocean that have no stratigraphic link to the continental margin.

3.5 Conclusions

A newly recognized sedimentary sequence, the Thompson assemblage, is present immediately beneath the northern Davis assemblage north of Trout Lake.

Carboniferous strata of the Milford Group in the northern Kootenay Arc are inboard parts of assemblages defined in the Goat Range by Klepacki (1985). Depositional environments preserved in both the northern Davis and northern McHardy assemblages are interpreted to be shallower and more proximal than their southern equivalents in the Goat Range. As in the Goat Range, the Davis assemblage north of Trout Lake unconformably overlies the Lardeau Group. In the Lardeau Range, the northern McHardy assemblage unconformably overlies Late Devonian and Early Mississippian continental back-arc basin strata of the Mount Sproat assemblage and is overlain conformably by the Kaslo Group.

A period of transgression with minimal tectonic activity during deposition of the Thompson assemblage was followed in Mississippian (Milford) time by increased subsidence and normal faulting. Fault scarps inferred to have produced basal Milford boulder conglomerate may have also uplifted the Thompson assemblage. Extensional tectonism appears to have continued to drive subsidence and turbidite deposition in the Milford Group (McHardy assemblage) until eruption of Kaslo Group basalt in a basin without significant clastic input.

New mapping demonstrates that northern Kootenay Arc strata previously assigned to the Slide Mountain terrane depositionally overlie continental margin rocks in the Lardeau Range and are therefore not part of a terrane. The Milford Group and Kaslo Groups (and Thompson assemblage) are assigned here to the Slide Mountain tectonic assemblage (new term), which represents transgressive Late Paleozoic pericratonic strata that onlap continental margin strata on the inboard edge of the Slide Mountain marginal ocean basin. Consequently, faults in the Goat Range that place Slide Mountain tectonic assemblage rocks over continental margin strata, such as the Stubbs thrust, have relatively minor displacement. They are interpreted to have accommodated shortening and closure of the marginal basin but not obduction of a terrane.

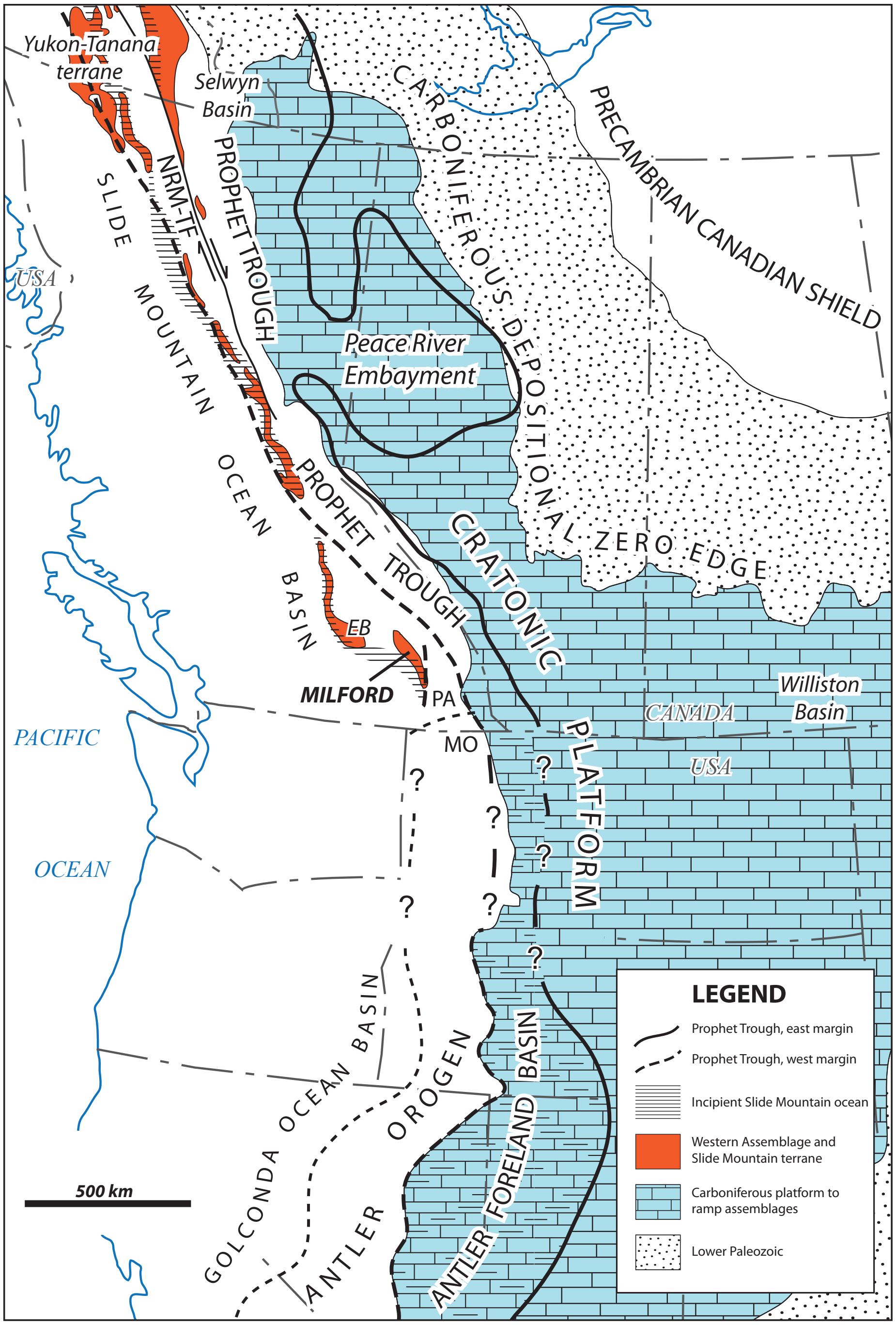

Figure 3-1: Map of Carboniferous strata and basins of central western North America.

The Western Assemblage is closely associated with Slide Mountain terrane strata in scattered outliers. The Milford Group was isolated from the Prophet Trough by highlands that may have been contiguous with the Antler orogen. The Prophet Trough may have merged with the Antler Foreland Basin. Adapted from Richards et al. (1994) and Colpron et al. (2006). Abbreviations: EB, Eagle Bay Formation; MO, Montania; PA, location of former Purcell Arch; NRM-TF, Northern Rocky Mountain Trench - Tintina Fault

ERA	PERIOD OR EPOCH	GROUP, FORMATION, MEMBER, OR MAP UNIT			THICKNESS	
CENOZOIC	QUATERNARY			glacial deposits, alluvium, colluvium	-	
MESOZOIC	LOWER TO MIDDLE JURASSIC		Galena Bay stock[3]	muscovite-biotite quartz monzonite, granodiorite and monzogranite with rare garnet	-	
MESOZOIC	LOWER TO MIDDLE JURASSIC		Kuskanax suite intrusions[2]	multi-phase batholith and satellite stocks, dikes and sills. Biotite or augite granodiorite; leuco-quartz monzonite; minor leucosyenite and leucogranite	-	
MESOZOIC	UPPER TRIASSIC		SLOCAN GROUP[2]	fine-grained siliciclastic rocks and carbonate. Dark grey argillite and phyllite; grey metasiltstone; metasandstone; minor volcanic rocks	>100 m	**Quesnellia**
	unconformity					
PALEOZOIC	PERMIAN		Pd	medium- to coarse-grained hornblende meta- gabbro or diorite	-	***Slide Mountain tectonic assemblage***
PALEOZOIC	PERMIAN		KASLO GROUP[2]	metamorphosed basalt flows with mid-ocean ridge geochemical affinity. Massive amphibolitic or chloritic greenstone; pillow basalt	> 1000 m	***Slide Mountain tectonic assemblage***
PALEOZOIC	UPPER MISSISSIPPIAN TO PENNSYLVANIAN	MILFORD GROUP	McHardy assemblage 700-2000 m: **Sandstone member**	sandstone and siltstone rhythmite; 50 - >600 m		***Slide Mountain tectonic assemblage***
PALEOZOIC	UPPER MISSISSIPPIAN TO PENNSYLVANIAN	MILFORD GROUP	McHardy assemblage: **Argillite member**	argillite; siltstone; wacke; 400-1000 m		***Slide Mountain tectonic assemblage***
PALEOZOIC	UPPER MISSISSIPPIAN TO PENNSYLVANIAN	MILFORD GROUP	McHardy assemblage: **Conglomerate member**	quartz pebble conglomerate; limestone; 0 - 200 m		***Slide Mountain tectonic assemblage***
PALEOZOIC	UPPER MISSISSIPPIAN TO PENNSYLVANIAN	MILFORD GROUP	Davis assemblage >1000 m: **Phyllite member**	silty medium grey phyllite; rare sandstone, limestone >1000 m		***Slide Mountain tectonic assemblage***
PALEOZOIC	UPPER MISSISSIPPIAN TO PENNSYLVANIAN	MILFORD GROUP	Davis assemblage: **Basal member**	pebble to boulder conglomerate; fossiliferous limestone; chert; phyllite 50 - 700 m		***Slide Mountain tectonic assemblage***
	unconformity (locally conformable?)					
PALEOZOIC	MID- or UPPER MISSISSIPPIAN		**Thompson assemblage**	green phyllitic grit; green, grey and maroon phyllitic argillite; crystalline limestone; limestone breccia; amygadaloidal basalt; sandy marble; chert	0 - 450 m	***Slide Mountain tectonic assemblage***
	angular unconformity					
PALEOZOIC	LOWER MISSISSIPPIAN	**MOUNT SPROAT ASSEMBLAGE**	**Upper Clastic member**	metamorphosed siliciclastic rocks: basal quartz pebble conglomerate; laminated black siltstone; argillite; biotite-muscovite ± garnet ± staurolite schist; metasandstone; igneous cobble conglomerate; coarse crystalline marble	800 m*	***Kootenay tectonic assemblage***
PALEOZOIC	UPPER DEVONIAN AND/OR LOWER MISSISSIPPIAN	**MOUNT SPROAT ASSEMBLAGE**	**Amphibolitic Schist member**	metamorphosed calc-alkaline basaltic to andesitic flows and volcaniclastic rocks with minor pelitic schist and carbonate: hornblende ± biotite schist; chloritic greenstone; amphibolite; sericite-chlorite schist; mafic cobble conglomerate and agglomerate; biotite ± garnet ± muscovite ± staurolite schist; banded marble; buff dolomitic marble	2000 m - 4000 m*	***Kootenay tectonic assemblage***
PALEOZOIC	LOWER CAMBRIAN TO UPPER DEVONIAN	**MOUNT SPROAT ASSEMBLAGE**	**Heterolithic member**	metamorhosed siliciclastic, carbonate and volcanic strata: grey and green phyllite; fine-grained biotite schist; alkaline and tholeiitic basalt flows and tuff; white and buff crystalline limestone and dolostone; grey marble; white to grey quartzite; micaceous quartzite. Lithologies are stratigraphically and structurally repeated layers 1 to >50 m thick.	1500 m*	***Kootenay tectonic assemblage***
PALEOZOIC	LOWER CAMBRIAN TO UPPER DEVONIAN	**MOUNT SPROAT ASSEMBLAGE**	**Carbonaceous member**	carbonaceous fine-grained quartzite to carbonaceous phyllite; dark grey crystalline limestone and limy carbonaceous phyllite; carbonaceous fine-grained biotite schist; fine-grained white quartzite	2000 m*	***Kootenay tectonic assemblage***
PALEOZOIC	LOWER CAMBRIAN TO UPPER DEVONIAN	LARDEAU GROUP	Broadview Fm[1]	green and grey phyllitic grit; green, grey and white quartzite with blue-quartz granules; tan weathering micaceous quartzite	>1500 m*	***Kootenay tectonic assemblage***
PALEOZOIC	LOWER CAMBRIAN TO UPPER DEVONIAN	LARDEAU GROUP	Jowett Fm[1] 0 - 1000 m*	metamorphosed alkaline basalt flows and volcaniclastic rocks; green phyllite		***Kootenay tectonic assemblage***
PALEOZOIC	LOWER CAMBRIAN TO UPPER DEVONIAN	LARDEAU GROUP	**McCrae Peak succession** 0 - 250 m	green and grey phyllite and grit; ferroan marble; stratiform barite and chert; gritty grey quartzite		***Kootenay tectonic assemblage***
PALEOZOIC	LOWER CAMBRIAN TO UPPER DEVONIAN	LARDEAU GROUP	Index, Triune, Ajax and Sharon Creek formations[1]	Index: grey and green phyllite, slaty phyllite, dark grey crystalline limestone, and mafic volcanic rocks; Triune: siliceous phyllite and argillite; Ajax: massive grey quartzite; Sharon Creek: siliceous phyllite and argillite		***Kootenay tectonic assemblage***
PALEOZOIC	LOWER CAMBRIAN		Badshot Formation[1]	grey and white marble; rare archeocyathids		**miogeocline**

Figure 3-2. Revised table of units for the Lardeau and Badshot ranges.

Suggested classification of tectonic assemblages in the right-hand column. Units in boldface are terms introduced in this thesis (of which Mount Sproat and Thompson assemblages were defined by Kraft et al., 2011a). Symbolized divisions as per definitions of: [1]Fyles and Eastwood, 1962; [2](Hyndman, 1968); ‡ (Kuskanax, Galena Bay stock); (*) indicates an approximation of present deformed thickness in strongly deformed rocks.

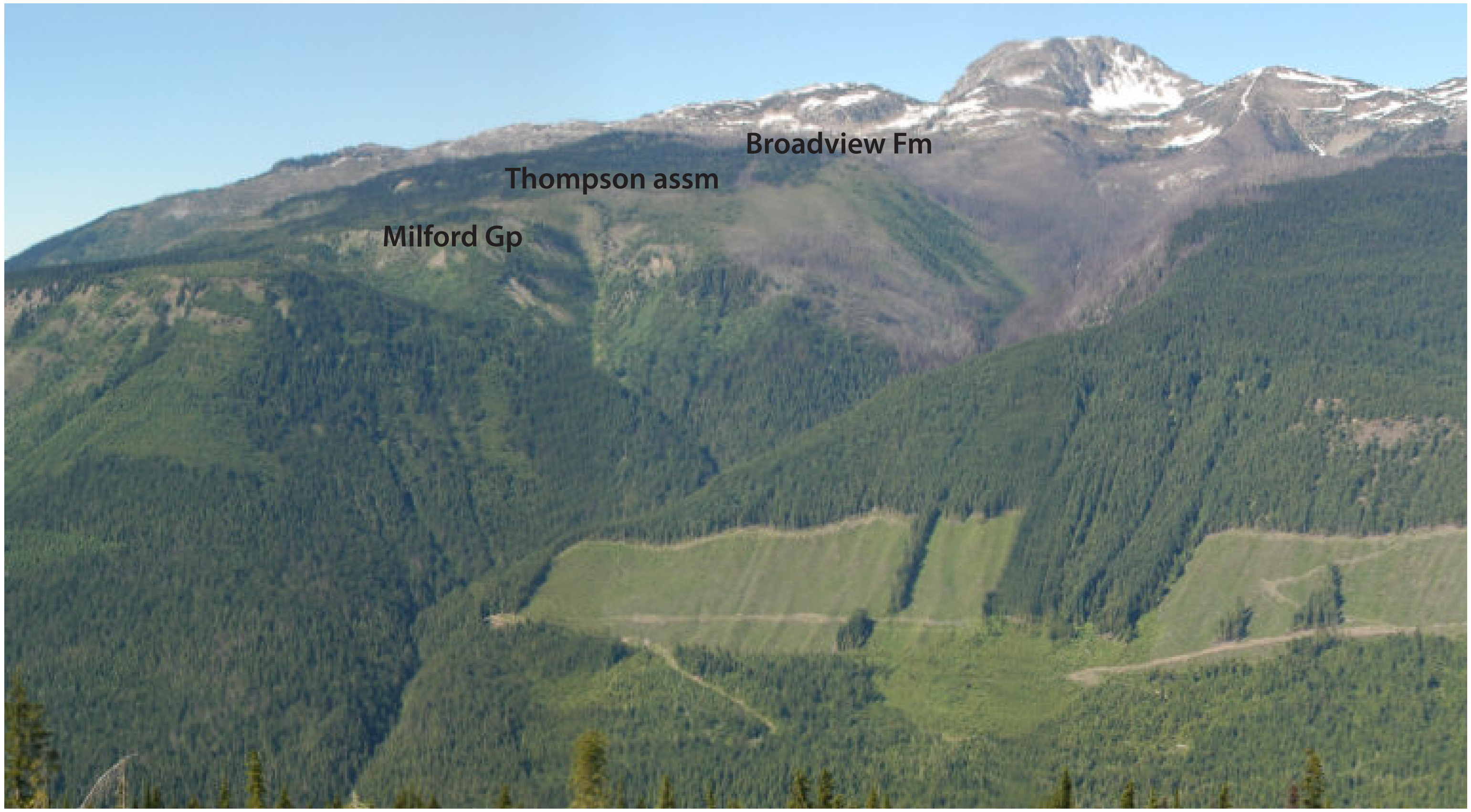

Figure 3-3. View of Mount Thompson - the type locality of the Thompson assemblage.
Approximate locations of the three main stratigraphic units are as labeled. Photo looks northeast.

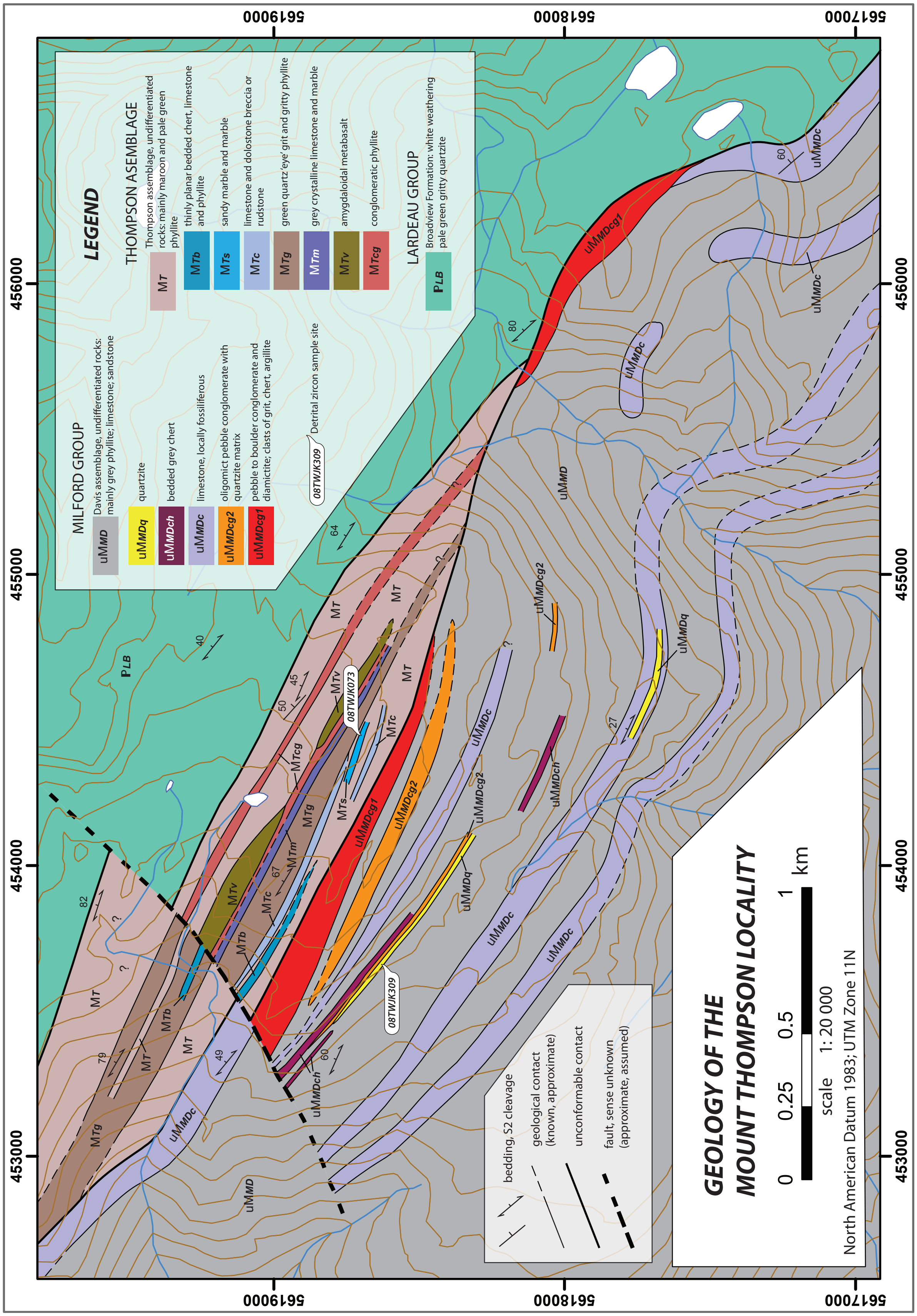

Figure 3-4. Geologic map of the Mount Thompson locality.

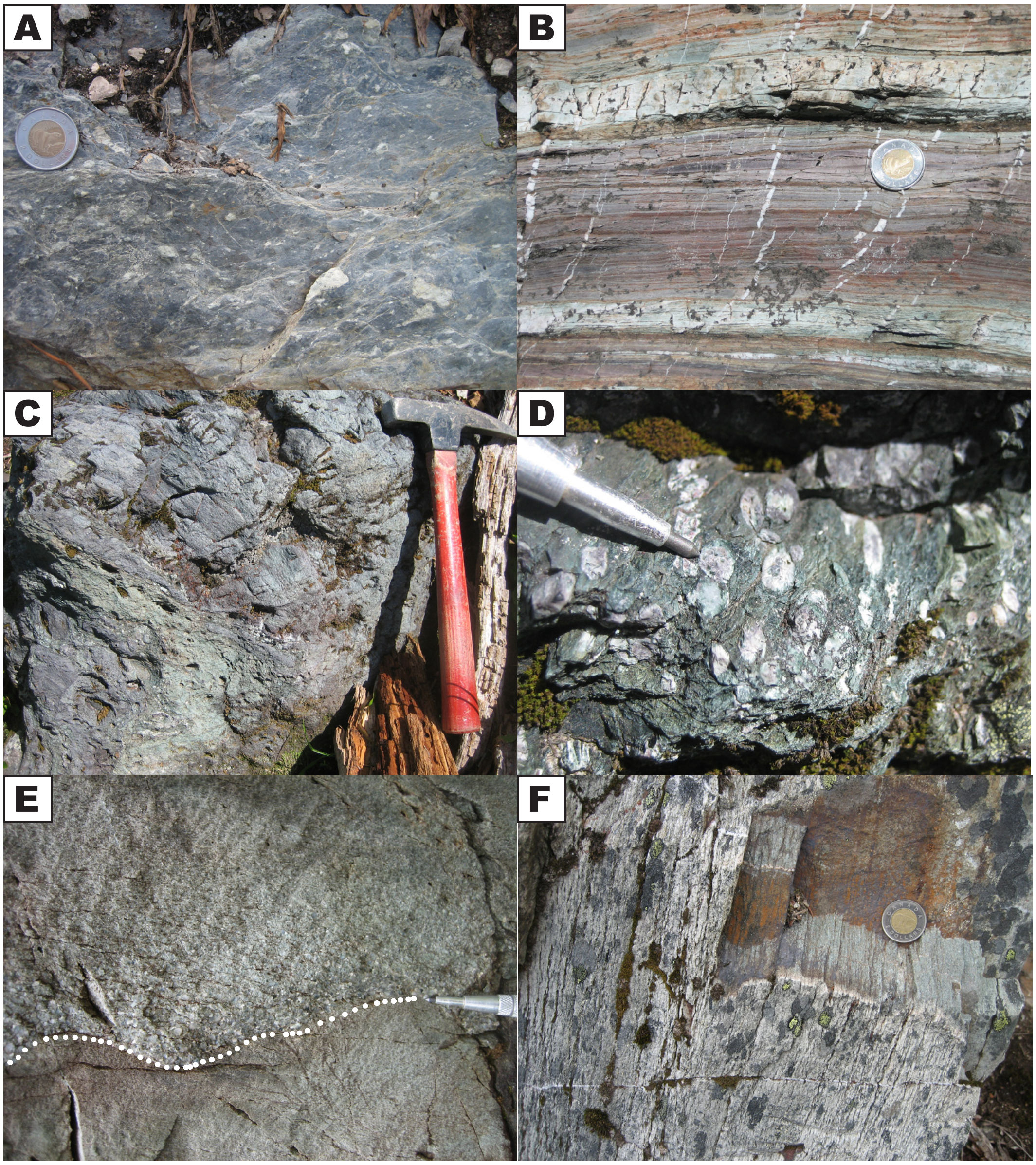

Figure 3-5. Field photographs of rock types in the lower Thompson assemblage at Mount Thompson.
A) Phyllitic paraconglomerate that immediately overlies the Broadview Formation. Contact is concealed. B) Banded maroon and green phyllite. C) Amydaloidal and fragmental metabasalt. D) Amygdules and weak foliation in metabasalt. E) Scoured base of a graded bed of quartz eye grit that fines toward the Milford Group (up in photo). F) Pale green grit with well developed cleavage.

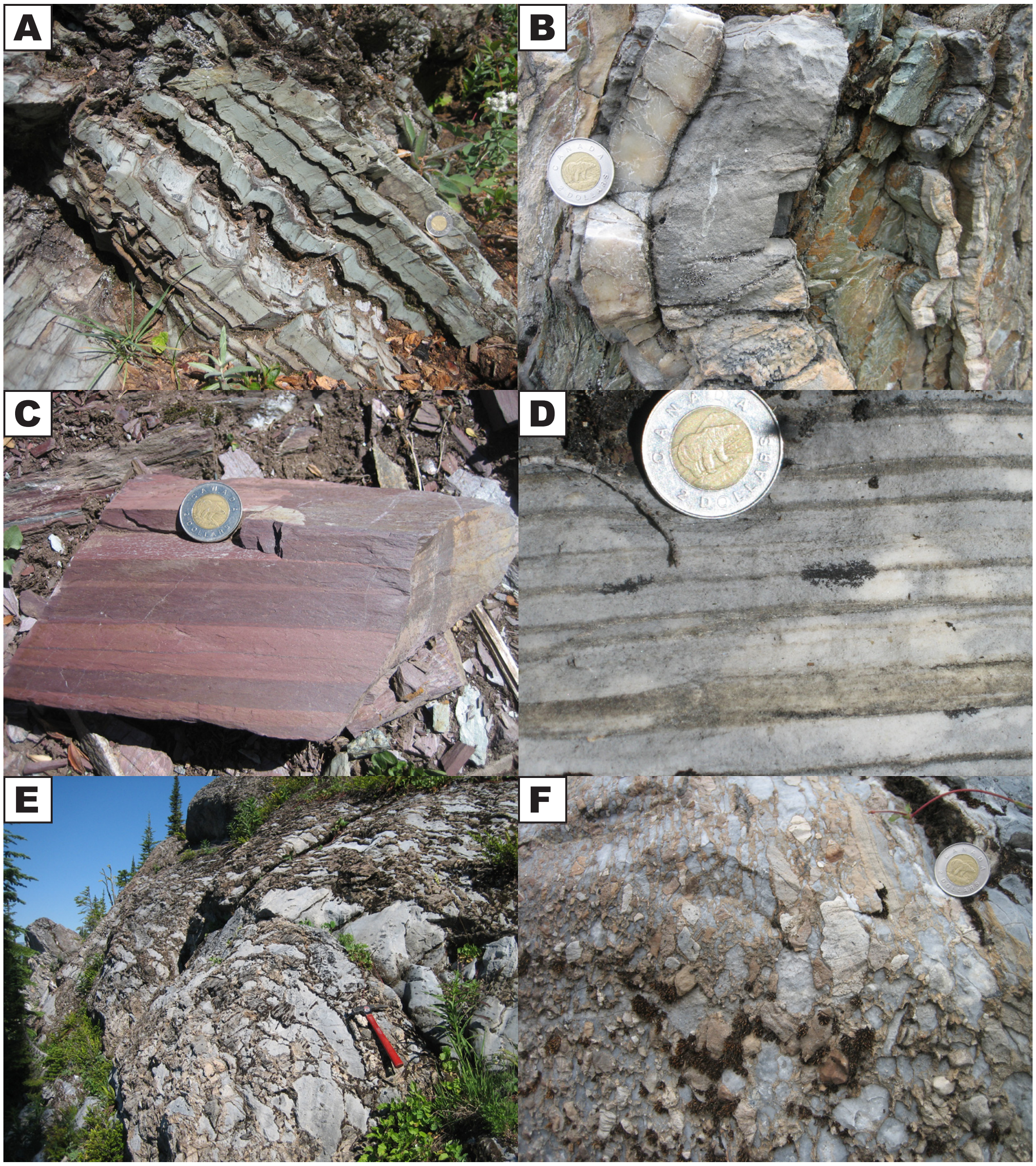

Figure 3-6. Field photographs of rock types in the upper Thompson assemblage at Mount Thompson.

A) Interbedded green argillite and limestone disrupted by cleavage. B) Thin beds of white chert (under coin), grey limestone (centre), green argillite (right) and limestone (far right). C) Colour banded maroon phyllitic argillte. D) White marble with (darker) planar sandy laminations. E) Carbonate breccia or rudstone comprising clasts of micritic limestone in fragmental dolostone matrix. F) Rudstone with fragments of dolostone and limestone.

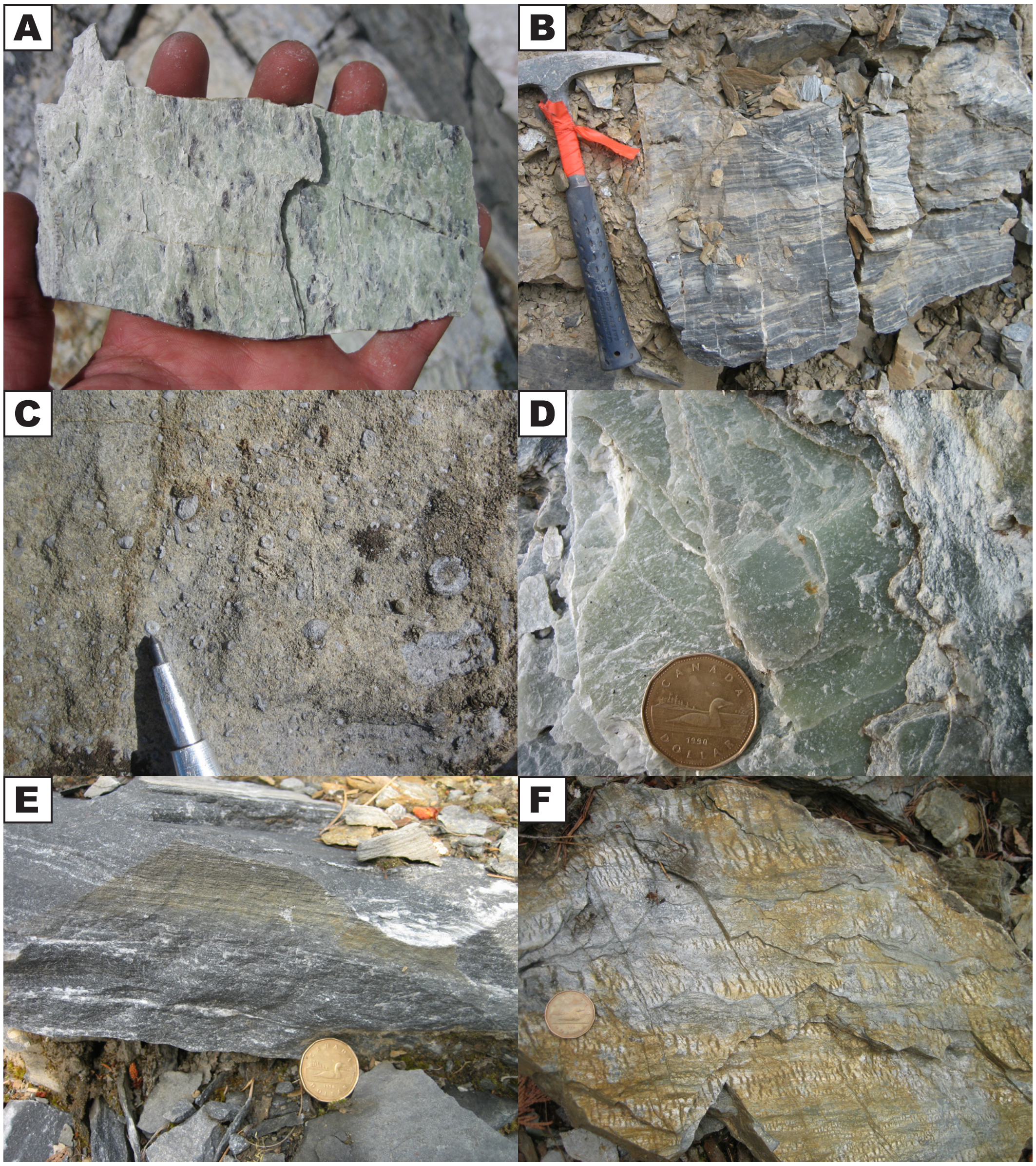

Figure 3-7. Field photographs of possible lateral equivalents of the Thompson assemblage near Mount Sproat and McCrae Peak.
A) Talc schist from one of several metre-thick horizons in a succession of grey phyllite and marble (B) stratigraphically between Milford conglomerate and rocks of the Lardeau Group. B) Mottled texture in sub-Milford marble at McCrae Peak. C) Crinoid ossicles in probable Thompson assemblage strata at Comaplix ridge. D) Talc schist from a roadcut on Dupont forest service road on Mount Sproat. The talc schist occurs adjacent to >100 m of interlayered E) marble and F) phyllite stratigraphically below unambigous Milford strata, in inferred tectonic contact with the Mount Sproat assemblage.

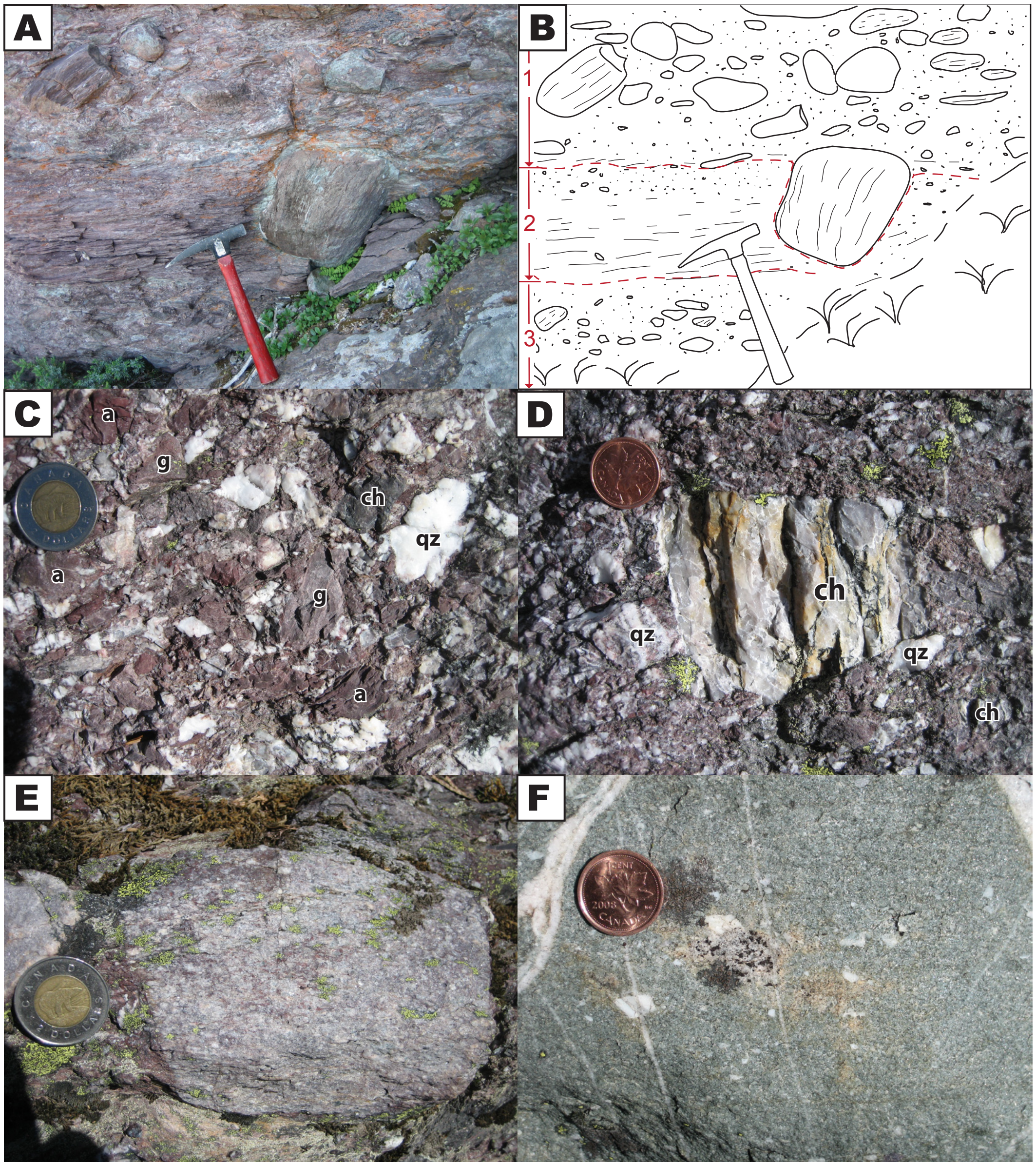

Figure 3-8. Field photographs of northern Davis assemblage conglomerate at Mount Thompson.

A) Boulders of foliated grit in diamictite. B) Interpretation of photo (A) as three distinct beds. Size grading in bed 2 indicates the sequence is inverted here, which is consistent with the site's location on an overturned fold limb. The boulder protruding from bed 1 indicates deposition as a debris flow. C) Sedimentary breccia with angular clasts of maroon argillite (a), crystalline quartz (qz), quartzose grit (g), and chert (ch). The Thompson assemblage is the only known potential source of maroon argillite and chert. D) Angular clast of white chert identical to ribbon chert in underlying Thompson assemblage (Figure 3.5B). E) Clast of red stained gritty quartzite interpreted to come from the underlying Broadview Formation. F) Close-up of a pale green gritty quartzite bed stratigraphically overlying the boulder conglomerate. Colour and texture mimic the underlying Broadview grit.

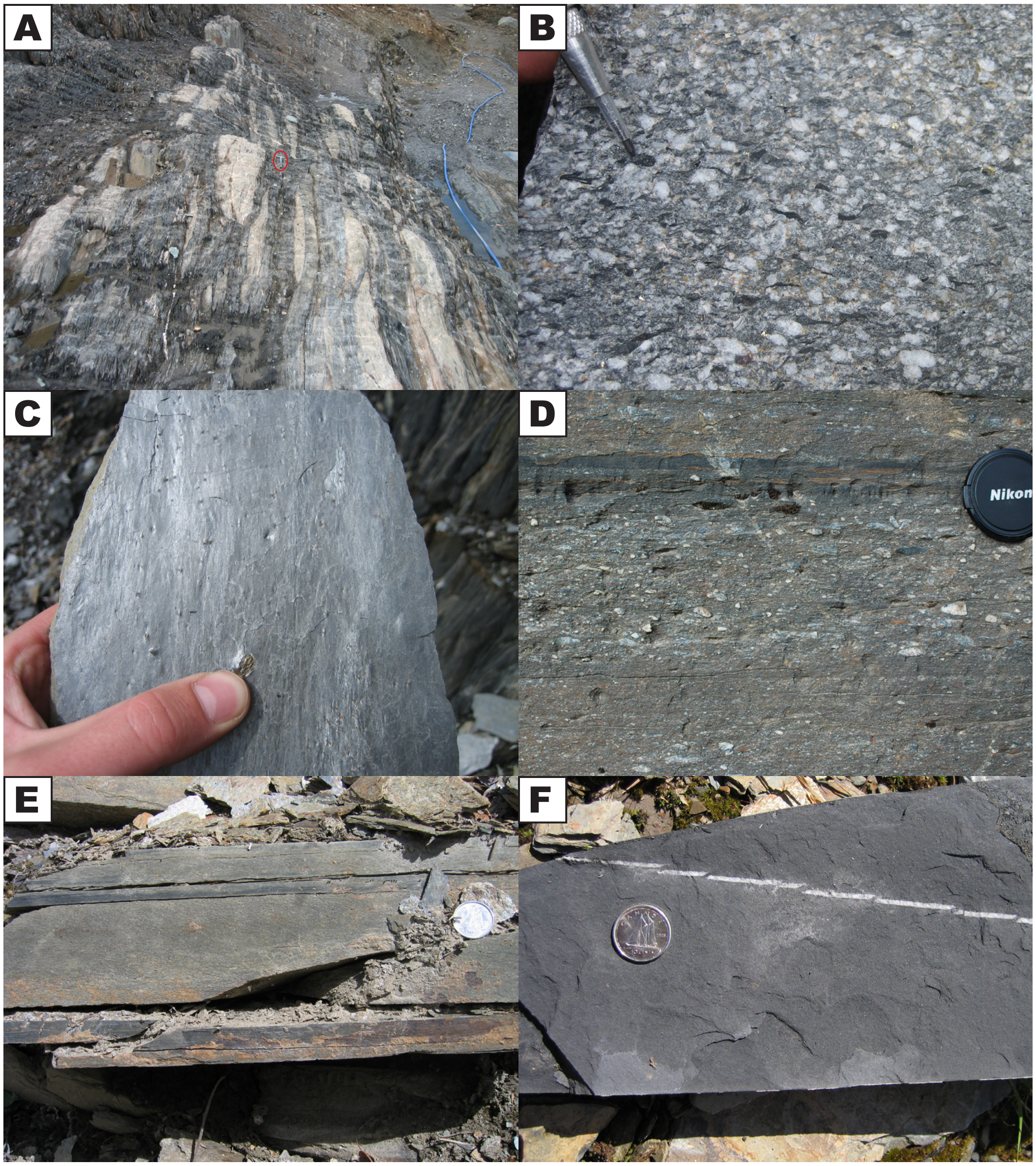

Figure 3-9. Photographs of the Basal member of the northern Davis assemblage on the west limb of the Beaton syncline.
A) Lenses of conglomerate in grey phyllite at the MAX Mine tailings pond interpreted as distributary submarine channels. Left (west) edge is the Mobbs fault. Red ellipse around hammer for scale. B) Oligomict grit/conglomerate with angular argillaceous fragments (indicated by scribe) that may be mud rip-ups. C) Phyllite associated with conglomerate lenses. Note irregularities cause by cubic pyrite. D) Diffusely bedded phyllitic conglomerate and grit on Hwy 31 north of Trout Lake. E) Fine sandstone and phyllite that interfinger with conglomerate lenses between Trout Lake and Beaton. F) Dark grey platy limestone that overlies basal conglomerate near Armstrong Lake.

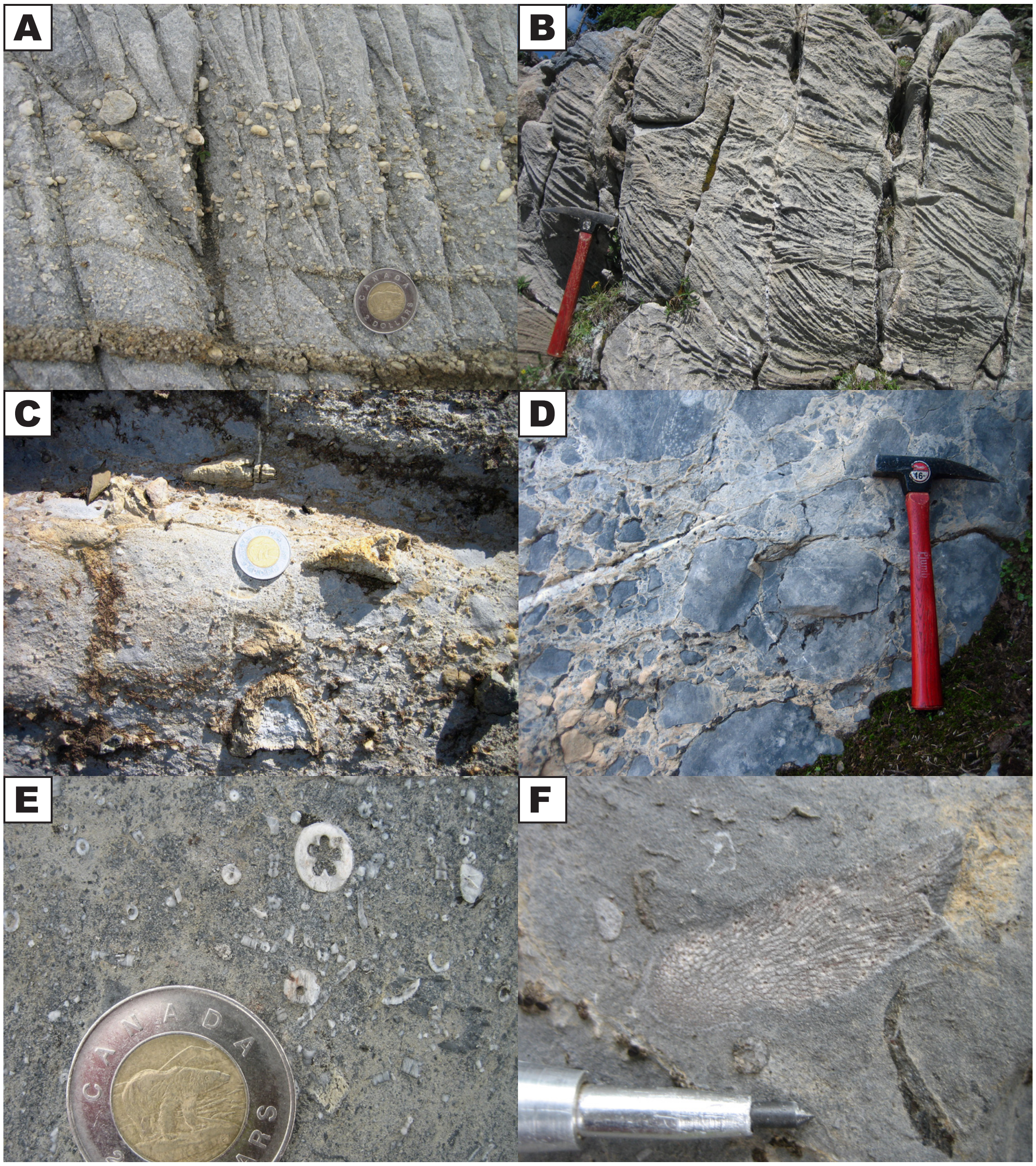

Figure 3-10. Field photographs of limestones in the northern Davis assemblage. A) Planar sandy to pebbly beds with well-rounded crystalline quartz pebbles, McCrae Peak. B) Trough cross-bedded sandy marble that overlies basal conglomerate, Comaplix ridge. Bulk strain may have increased the angularity of truncations. C) Bioclasts including solitary rugose corals in an event bed within micritic limestone, Mount Thompson. D) Rudstone with intraclasts of grey limestone in a dolostone matrix, Mount Thompson. E) The most common body fossil in the northern Davis assemblage: disarticulated crinoid ossicles, McCrae Peak. F) Bryozoan fossil at Mount Thompson illustrates quality of preservation in the area.

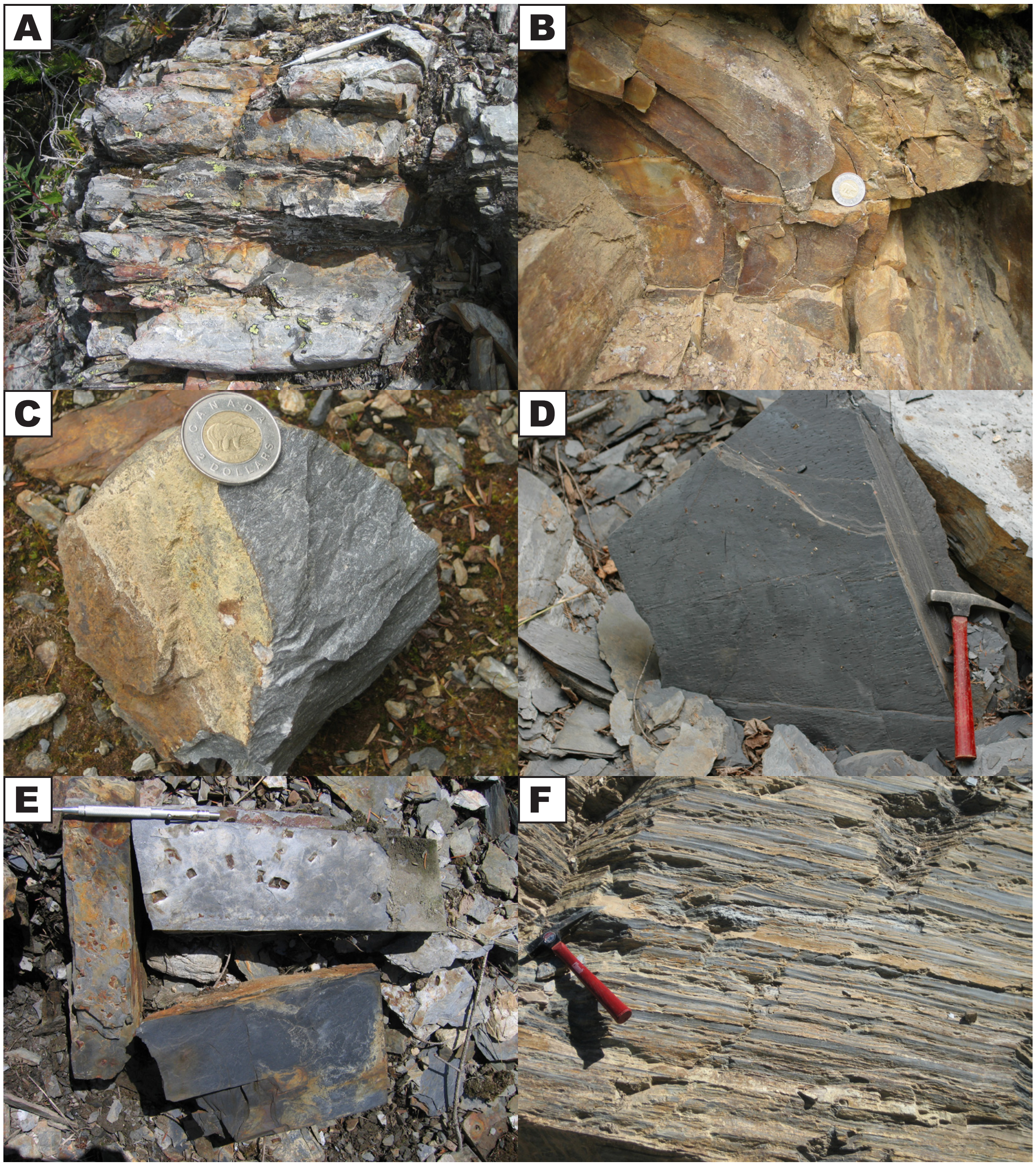

Figure 3-11. Field photographs of chert and phyllite in the Phyllite member of the northern Davis assemblage.
A) ~10 cm thick beds of light grey chert with thinner phyllite interbeds, Mount Thompson. B) Gently folded bedded chert with rusty weathered surface, Gerrard. C) Rusty weathering cherty quartzite, Gerrard. D) and E) Fissile medium grey silty phyllite with cubic pyrite, Beaton. F) Planar bedded rhythmite of silty phyllite (grey) and very fine sandstone (tan) 5 km south of Mount Thompson. Note the absence of bioturbation; ichnofossils were not found in the Milford Group.

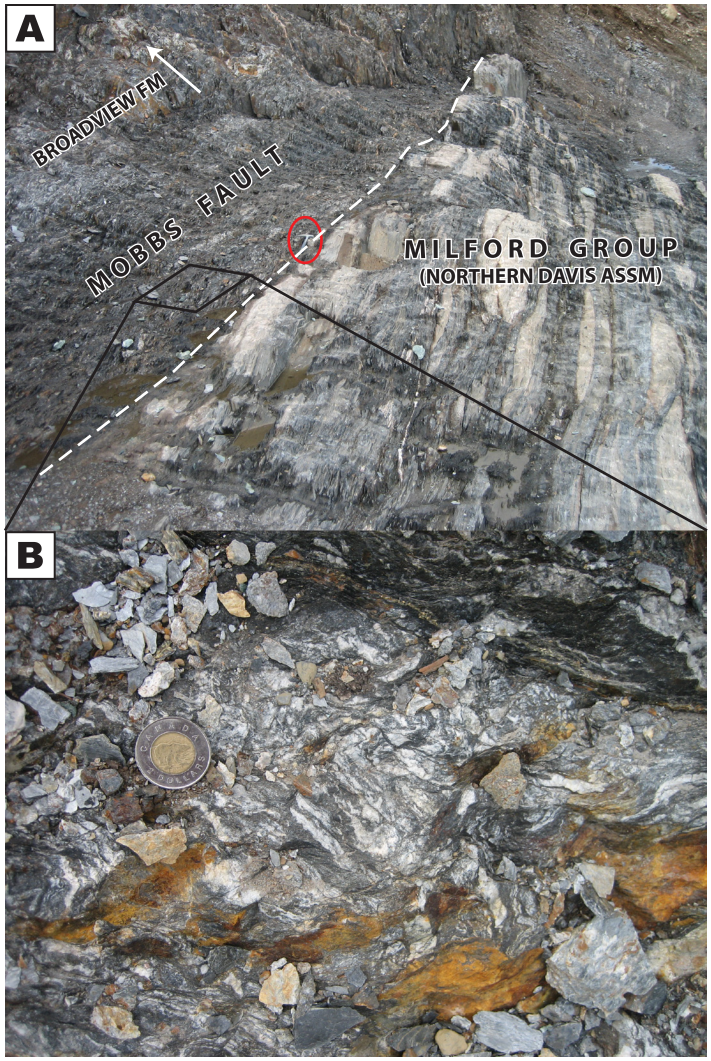

Figure 3-12. Field photographs of the Mobbs fault.
This site was temporarily uncovered during construction of the MAX Molybdenum Mine tailings pond. A) View of the faulted southwest margin of the northern Davis assemblage, which youngs toward the fault zone. Severity of shearing diminishes gradually over several metres within Broadview phyllitic grit at the top left corner of the photo. Looking northwest. Hammer in red ellipse for scale. B) Contorted, quartz veined fault rock in the fault zone.

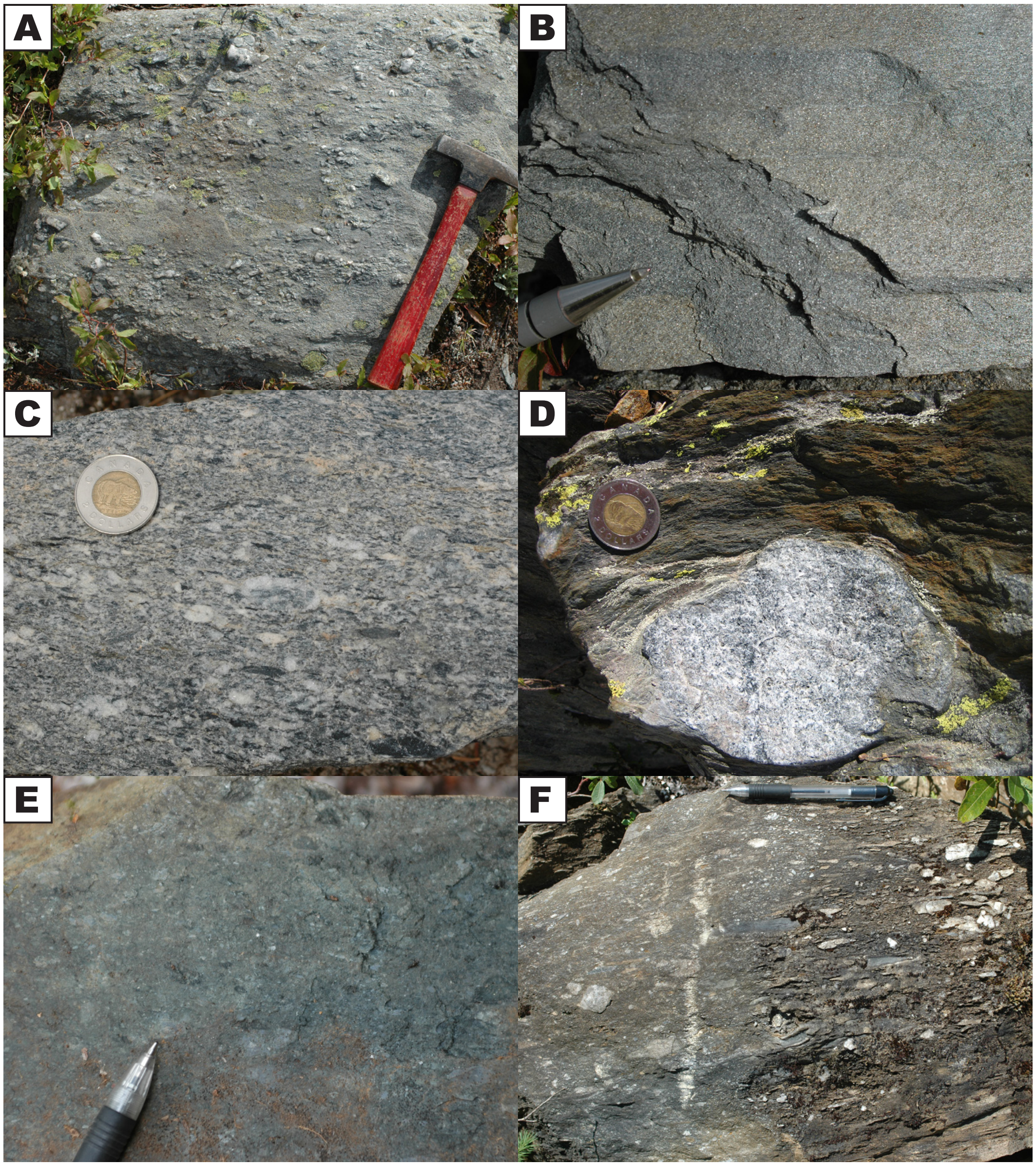

Figure 3-13. Field photographs of the Conglomerate member of the northern McHardy assemblage.

A) Quartz pebble paraconglomerate with a medium grey micaceous matrix similar in composition to directly underlying micaceous phyllite in the Mount Sproat assemblage, Mount Murray area. B) White mica in phyllite associated with (A). C) Oligomict grit with angular argillaceous clasts interpreted to be mud rip clasts, Mount Murray area. D) Clast of poorly sorted quartzite within a horizon of lithic wacke and grit, Mount Murray area. E). Pebble breccia comprising igneous clasts and matrix similar to directly underlying Mount Sproat assemblage volcanic rocks, Blind Bay. F) Quartz pebbles in grey limestone at the base of the northern McHardy assemblage near Asher Creek on the west shore of Trout Lake.

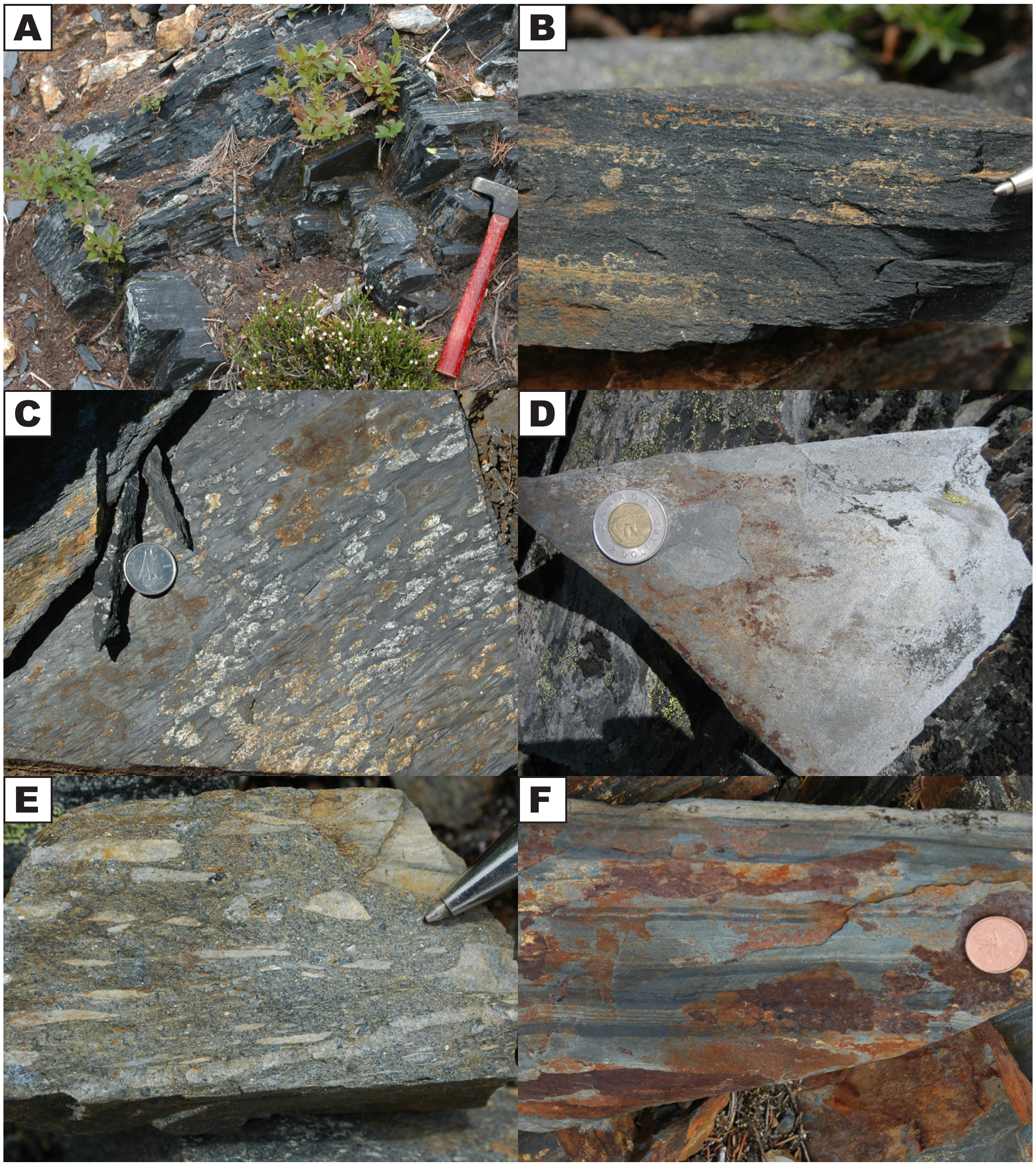

Figure 3-14. Field photographs of the Argillite member of the northern McHardy assemblage.

A) Carbonaceous siliceous argillite near Mount Murray. B) Matte black silty argillite with rusty oxidation staining, eastern Lardeau Range. C) Matte, dark grey argillite with patches of white mica on foliation surfaces, west side of Trout Lake. D) Shiny medium grey phyllite, eastern Lardeau Range E) Lithic wacke from a persistent horizon of similar immature clastic rocks and sandstone, eastern Lardeau Range. F) Rusty weathering planar laminated siltstone (dark) and very fine sandstone (light), Mount Murray.

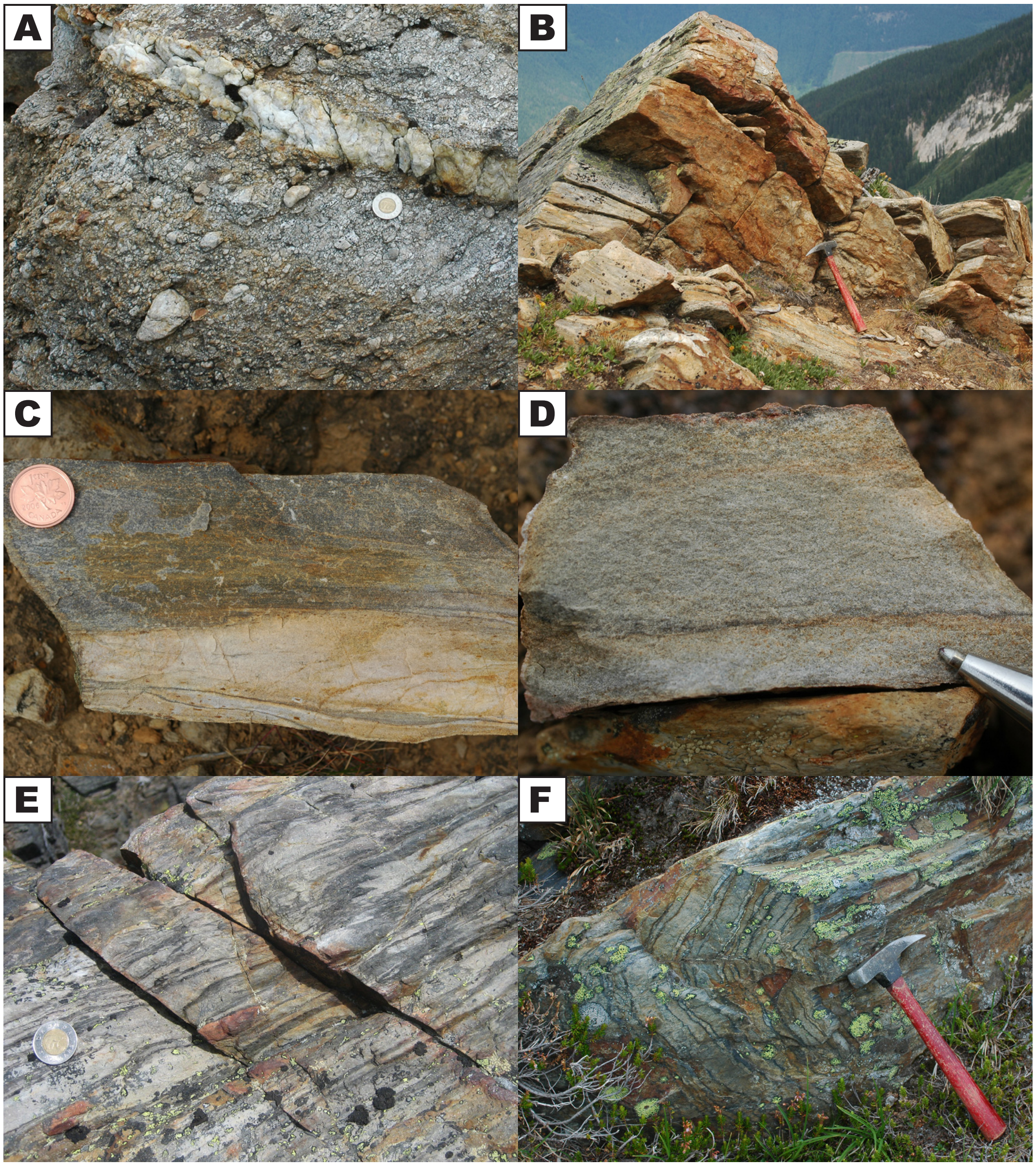

Figure 3-15. Field photographs of the Sandstone member of the northern McHardy assemblage.
A) Calcite-cemented quartz pebble conglomerate at the transition from Argillite to Sandstone members. B) Distinctive weathering of the sandstone unit. C-D) Fresh surfaces of sandstone. E-F) Deformed, rhythmically banded sandstone with finer grey siltstone layers.

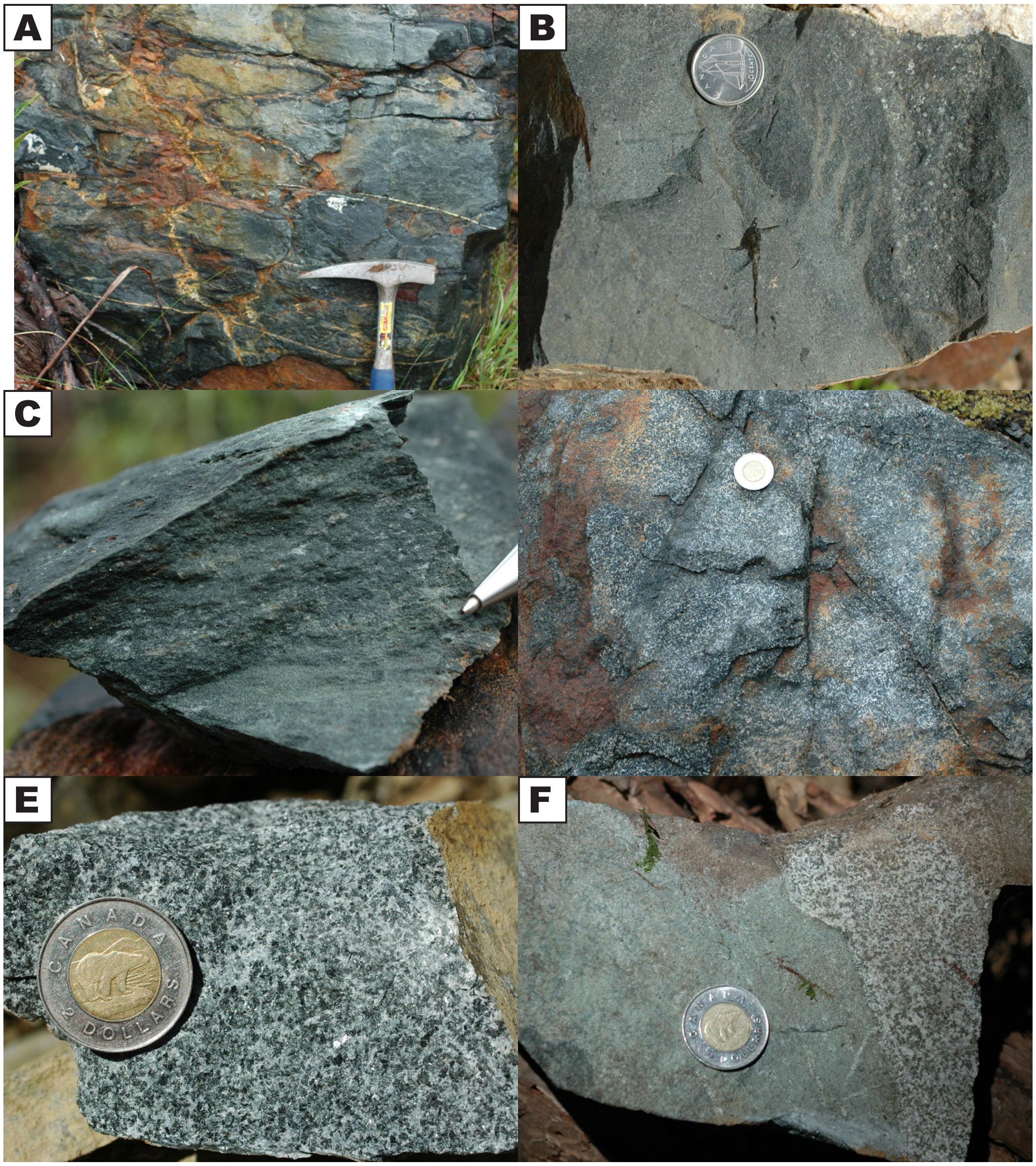

Figure 3-16. Field photographs of the Kaslo Group and associated gabbro.
A) Boulder from a pendant or raft of greenstone in the Kuskanax batholith near the headwaters of Kuskanax Creek. B) Fresh surface of greenstone near Nakusp. C) Fresh surface of chlorite-actinolite greenstone, Kuskanax Creek. D) Massive gabbro that is spatially associated with the Kaslo Group between Nakusp and St. Leon Creek. E) Fresh surface of gabbro that occurs with Kaslo metabasalt, Hill Creek. F) Intrusive contact between greenstone and gabbro, Hill Creek.

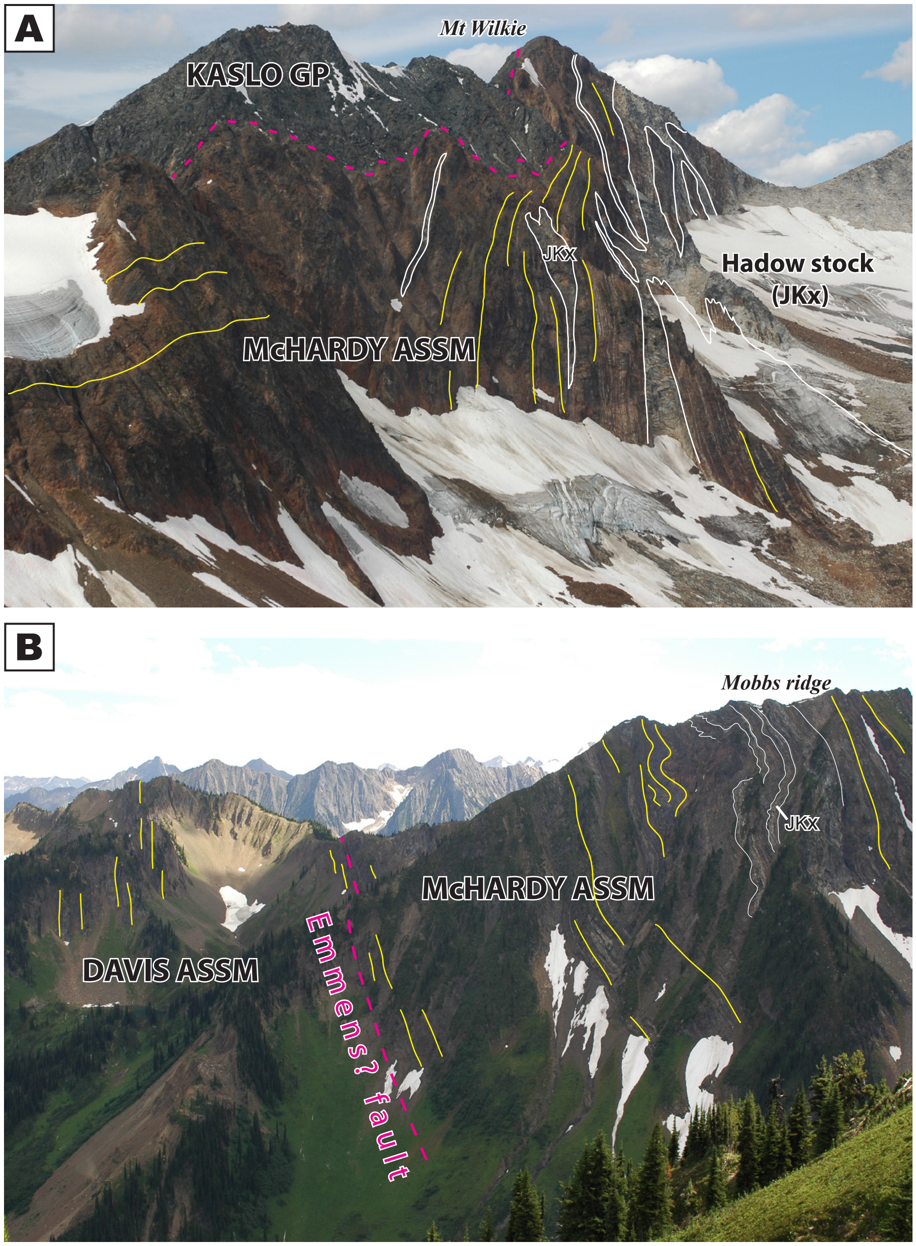

Figure 3-17. Field photographs of the Kaslo and Milford groups in the northern Goat Range.
A) Greenstone of the Kaslo Group overlying the McHardy assemblage at Mount Wilkie. This contact appears to be discordant to layering in the McHardy assemblage. Photo looks west. B) The concealed contact (pink) between the McHardy and Davis assemblages at Mobbs Ridge is inferred to be a northern continuation of the Emmens fault (Roback, 1993). Photo looks south. Yellow lines indicate trace of bedding. White lines trace Jurassic igneous contacts.

References

Bancroft, M. F., 1921, Lardeau Map Area, B.C., Geological Survey of Canada Reports 1920, pt. A, p. 94-102.

Cairnes, C. E., 1934, Slocan Mining Camp, British Columbia; Geological Survey of Canada, Memoir 173.

Colpron, M., and Price, R., 1995, Tectonic significance of the Kootenay terrane, southeastern Canadian Cordillera: An alternative model: Geology, v. 23, p. 25-28.

Jones, A.G., 1959, Vernon map-area, British Columbia. Geological Survey of Canada Memoir 296.

Hyndman, D.W. 1968. Petrology and structure of Nakusp map-area, British Columbia. Geological Survey of Canada Bulletin 161.

Klepacki, D.W., 1985, Stratigraphy and structural geology of the Goat Range area, southeastern British Columbia. Ph.D. thesis, Massachusetts Institute of Technology, Cambridge, Mass.

Kraft, J. L., Thompson, R. I., and Dhesi, P. (compilers), 2011a, Geology, Beaton, British Columbia; Geological Survey of Canada, Open File, 6574, scale 1:50 000, doi: 10.4095/288009.

Kraft, J. L., Thompson, R. I., and Dhesi, P. (compilers), 2011b, Geology, Trout Lake, British Columbia; Geological Survey of Canada, Open File, 6572, scale 1:50 000, doi: 10.4095/288063.

Kraft, J. L., Thompson, R. I., and Dhesi, P. (compilers), 2011c, Geology, Camborne, British Columbia; Geological Survey of Canada, Open File, 6573, scale 1:50 000, doi: 10.4095/288064.

Lawley, C. J. M., Richards, J. P., Anderson, R. G., Creaser, R. A., and Heaman, L. M., 2010, Geochronology and Geochemistry of the MAX Porphyry Mo Deposit and its Relationship to Pb-Zn-Ag Mineralization, Kootenay Arc, Southeastern British Columbia, Canada: Economic Geology, v. 105, p. 1113-1142

Lemieux, Y., 2006, Structure, geochronology and thermobarometry of the eastern flank of the Shuswap metamorphic complex in the Upper Arrow Lake area, southeastern British Columbia. Unpublished Ph.D. thesis, University of Alberta, Edmonton, AB.

Monger, J.W.H., 1977, Upper Paleozoic rocks of the western Canadian Cordillera and their bearing on Cordilleran evolution: Canadian Journal of Earth

Sciences, v. 14, p. 1832-1859.

Monger, J.W.H., 1984, Cordilleran tectonics: A Canadian perspective: Bulletin de la Société Géologique de France, v. 26, p. 255-278.

Monger, J., and Berg, H., C., 1987, Lithotectonic terrane map of western Canada and southeastern Alaska. United States Geological Survey, Miscellaneous Field Studies Map MF-1874-B.

Murphy, D.C., van der Heyden, P., Parrish, R.R., Klepacki, D.W., McMillan, W., Struik, L.C. and Gabites, J., 1995, New geochronological constraints on Jurassic deformation of the western edge of North America, southeastern Canadian Cordillera, in Miller, D.M. and Busby, C., eds., Jurassic Magmatism and Tectonics of the North American Cordillera: Geological Society of America, Special Paper 299, p. 159-171.

Murphy, D., 2006, Mid-Paleozoic to early Mesozoic tectonostratigraphic evolution of Yukon-Tanana and Slide Mountain terranes and affiliated overlap assemblages, Finlayson Lake massive sulphide district, southeastern Yukon: *in* Colpron, M. and Nelson, J.L., eds., Paleozoic Evolution and Metallogeny of Pericratonic Terranes at the Ancient Pacific Margin of North America, Canadian and Alaskan Cordillera: Geological Association of Canada, Special Paper 45, p. 75-106.

Nelson, J. L., 1993, The Sylvester Allochthon: upper Paleozoic marginal-basin and island-arc terranes in northern British Columbia: Canadian Journal of Earth Sciences, v. 30, p. 631-643.

Nelson, J.L., Colpron, M., Piercey, S.J., Dusel-Bacon, C., Murphy, D.C. and Roots, C.F., 2006, Paleozoic tectonic and metallogenic evolution of the pericratonic terranes in Yukon, northern British Columbia and eastern Alaska, *in* Colpron, M. and Nelson, J.L., eds., Paleozoic Evolution and Metallogeny of Pericratonic Terranes at the Ancient Pacific Margin of North America, Canadian and Alaskan Cordillera: Geological Association of Canada, Special Paper 45, p. 323-360.

Okulitch, A.V. and Cameron, B.E.B., 1976, Stratigraphic revisions of the Nicola, Cache Creek and Mount Ida groups based on conodont collections from the western margin of the Shuswap Metamorphic Complex, south-central British Columbia: Canadian Journal of Earth Sciences, v. 13, p. 44-53.

Orchard, M.J. 1985, Carboniferous, Permian and Triassic conodonts from the Central Kootenay Arc, British Columbia: constraints on the age of the Milford, Kaslo, and Slocan groups, *in* Current Research, Part A. Geological Survey of Canada, Paper 85-1A, p. 287-300.

Piercey, S. J., Murphy, D. C., Mortensen, J. K., and Creaser, R. 2004, Mid- Paleozoic initiation of the northern Cordilleran marginal back-arc basin: Geologic, geochemical, and neodymium isotope evidence from the oldest mafic magmatic rocks in Yukon-Tanana terrane, Finlayson Lake district, southeast Yukon, Canada, Geological Society of America Bulletin, v. 116, 1087–1106, doi:10.1130/B25162.1.

Read, P.B. 1973, Petrology and structure of Poplar Creek map-area, British Columbia. Geological Survey of Canada Bulletin 193.

Read, P.B., and Wheeler, J.O., 1976, Geology, Lardeau west-half, British Columbia. Geological Survey of Canada Open File 432.

Read, P.B., Psutka, J.F., Fyles, J.T., and MacLeod, R.F, 2009, Geology, MAX Molybdenum Mine area (NTS 82K/12), British Columbia; Geological Survey of Canada, Open file 6215, 2 sheets, 1:10 000 scale, and 1 report, 21 p.

Richards, B.C., 1989, Upper Kaskaskia sequence - uppermost Devonian and Lower Carboniferous: *in* Western Canada sedimentary basin, a case history. B.D. Rickets, ed., Canadian Society of Petroleum Geologists, Calgary, Alberta, p. 165-201.

Richards, B.C, Barclay, J. E., Bryan, D., Hartling, A., Henderson, C. M., and Hinds, R. C., 1994, Carboniferous strata of the Western Canada Sedimentary Basin. In: Geological Atlas of the Western Canada Sedimentary Basin. Mossop G.D., and Shetsen I., compilers, Calgary, Canadian Society of Petroleum Geologists and Alberta Research Council, Chapter 14.

Roback, R.C., 1993, Late Paleozoic to middle Mesozoic tectonic evolution of the Kootenay arc, northeastern Washington and southeastern British Columbia: PhD thesis, University of Texas, Austin, Texas, 237 p.

Roback, R., Sevigny, J., and Walker, N., 1994, Tectonic setting of the Slide Mountain terrane, southern British Columbia: Tectonics, v. 13, p. 1242–1242.

Root, K., 1987, Geology of the Delphine Creek area, southeastern British Columbia: Implications for the Proterozoic and Paleozoic development of the Cordilleran divergent margin: unpublished Ph.D. thesis, University of Calgary, Calgary, AB.

Schiarizza, P. and Preto, V.A., 1987, Geology of the Adams Plateau-Clearwater-Vavenby area: B.C. Geological Survey Branch, Paper 1987-2, 88 p.

Smith, M. T., and Gehrels, G. E., 1991, Detrital zircon geochronology of Upper Proterozoic to lower Paleozoic continental margin strata of the Kootenay Arc: implications for the early Paleozoic tectonic development of the eastern Canadian Cordillera: Canadian Journal of Earth Sciences, v. 28, p. 1271- 1284.

Thompson, R.I., Glombick, P., Erdmer, P., Heaman, L. M., Lemieux, Y., and Daughtry, K. L., 2006, Evolution of the ancestral Pacific margin, southern Canadian Cordillera: Insights from new geologic maps: in Colpron, M. and Nelson, J.L., eds., Paleozoic Evolution and Metallogeny of Pericratonic Terranes at the Ancient Pacific Margin of North America, Canadian and Alaskan Cordillera: Geological Association of Canada, Special Paper 45, p. 433-482.

Tucker, M.E., and Wright, V. P., 1990, Carbonate sedimentology: Blackwell Science, Oxford.

Wheeler, J. O., 1968, Lardeau (west half) map-area, British Columbia (82K W112). In Report of activities, part A. Geological Survey of Canada, Paper 68-lA, p. 56-58.

Wheeler, J.O. and McFeely, P. (compilers), 1991, Tectonic assemblage map of the Canadian Cordillera and adjacent parts of the United States of America: Geological Survey of Canada, Map 1712A, 1:2,000,000.

Chapter 4: Mid-Paleozoic deformation in the Canadian Cordillera: new evidence from the northern Kootenay Arc

4.1 Introduction

The Cordilleran margin of Laurentia – the North American craton (Hoffman, 1988) – existed as an active plate boundary for ~200 m.y. before initiation of Cordilleran orogenesis in the late Early Jurassic (Brown et al., 1986; Murphy et al., 1995). Constraints on the tectonic evolution of the Cordillera during this significant early time interval remain relatively sparse due mainly to overprinting effects of the main Cordilleran orogeny. Some of the clearest evidence that the mid-Paleozoic North American margin experienced an episode of penetrative deformation comes from the Paleozoic rocks of the northern Kootenay Arc (Wheeler, 1968; Read, 1975; Klepacki, 1985). Temporal context of that evidence has remained poorly constrained to an interval from Ordovician to Mississippian time (Read and Wheeler, 1976; Logan and Colpron, 2006), diminishing its usefulness to tectonic models. Both Middle Devonian (Root, 1987) and Late Devonian to Early Mississippian compressional events (Antler orogeny; Roberts et al., 1958) are known from the central North American Cordillera. Whether mid-Paleozoic deformation in the Kootenay Arc was coeval with, and therefore potentially related to, either of these events has been uncertain. Although workers have consistently concluded that early Paleozoic rocks in the northern Kootenay Arc were deformed prior to the Viséan (mid-Mississippian; Wheeler, 1968; Read, 1975; Klepacki, 1985; Smith, 1990), none have proposed a mechanism for the event.

Studies of the Canadian Cordillera have found evidence for extensional (e.g. Gordey et al., 1987), compressional (e.g. Root, 1987), and transcurrent (Eisbacher, 1983) tectonic regimes in the Devonian to Mississippian continental margin. Also during this time, the Ellesmerian (Thorsteinsson and Tozer, 1970; Trettin et al., 1991) and Antler (Roberts et al., 1958; Johnson and Pendergast, 1981) orogenies are interpreted to have involved thrusting of pericratonic successions onto adjacent continental shelves (Figure 4-1). The coeval geodynamic setting of the intervening Canadian Cordillera, however, remains less well characterized, due in part to overprinting effects of Jurassic to Paleocene Cordilleran orogenesis and Eocene extensional events.

This paper uses structural geological observations in the context of the revised stratigraphic framework presented in chapters 2 and 3 to constrain the distribution and timing of mid-Paleozoic deformation in the northern Kootenay Arc. Paleozoic strata there were affected by post-Mississippian strain and metamorphism to a far lower degree than other exposures in the Kootenay Arc and, because of the relative completeness of the stratigraphic record there, the timing and spatial extent of Paleozoic deformation can be more closely resolved. I propose a model in which Cambrian to Devonian strata of the Lardeau trough were penetratively strained in a broad shear zone that formed in the hanging wall of a contractional fault in Early Mississippian and possibly also Late Devonian time.

4.2 Geological setting and previous work

Root (1987) reported syn-depositional folds and faults in Eifelian (Middle Devonian) sedimentary rocks in the Purcell Mountains. Smith et al. (1993) postulated that a pre-Viséan foliation in the Lardeau Group resulted from deformation associated with the Late Devonian and Early Mississippian Antler orogeny of the western U.S.A., and that the entire western margin of Laurentia experienced Antler-age compression. Both Smith et al. (1993) and Root (2001) proposed that Late Devonian rocks in the Western Canada Sedimentary Basin represent a foreland basin. Root (2001) interpreted a margin-parallel Middle Devonian arch, called the West Alberta ridge (Grayston et al., 1965), as a forebulge that separated foredeep deposits exposed today in the Purcell Mountains (Mount Forster Formation and related strata) from a Middle Devonian distal foreland basin within the cratonic Western Canada Sedimentary Basin. In contrast, lithostratigraphy, alkaline volcanism and exhalative mineralization in the Selwyn Basin in Yukon have led to the suggestion of Devonian-Mississippian extensional or continental rift settings in the northern Canadian Cordillera (Gordey et al., 1987; Nelson et al., 2006).

Other evidence of mid-Paleozoic tectonism in southern British Columbia comes from metasedimentary rocks in the Shuswap Lake area that record metamorphism and gneissosity development, folding and extensional faulting that were interpreted to pre-date intrusion of a 365.9 ± 2.7 Ma granodioritic pluton (Slemko, 2000).

4.2.1 Local geology

Chapters 2 and 3 concluded that the northern Kootenay Arc contains two main stratigraphic successions that are divided by an intra-Mississippian angular unconformity. The Lardeau Group and conformably overlying Mount

Sproat assemblage span lower Cambrian (Fyles and Eastwood, 1962; Read and Wheeler, 1976) through Early Mississippian time. In the northern Kootenay Arc, the basal contact of the Lardeau Group with the Lower Cambrian miogeocline (Badshot Formation) is a shear zone called the Lardeau shear zone (Smith and Gehrels, 1992), whereas the same contact in the Northern Selkirk Mountains is a conformable transition (Colpron and Price, 1995). The Lardeau shear zone comprises an up to 200 km long faulted contact between the Index Formation and the Badshot Formation and numerous Mesozoic mylonitic normal and dextral shear zones that occur in the Index Formation within a few kilometres of the Badshot Formation (Smith and Gehrels, 1992). Smith and Gehrels (1992) interpreted juxtaposition of the Index Formation on the Badshot Formation to have occurred prior to the Jurassic on the basis of stratigraphic correlations between the Lardeau and Covada Groups but found no local evidence for or against displacement older than the regional Jurassic D2 deformation.

Carboniferous strata of the Thompson assemblage and Milford Group unconformably overlie the Lardeau Group (Chapter 3; Klepacki, 1985). An early greenschist-facies (qtz-ab-mu-chl facies; Read, 1973) transposition fabric, S1, and rootless F1 isoclines occur in the Lardeau Group but not in the Milford Group (Read, 1973; Read, 1975; Klepacki, 1985; Smith and Gehrels, 1992). Klepacki (1985) reported from the Lardeau Group F1 folds and D1 thrusts that have been truncated by the sub-Milford unconformity.

4.2.2 Mesozoic deformation

Mesozoic structures associated with the main Cordilleran orogenesis dominate the structural geology of the northern Kootenay Arc (Read and Wheeler, 1976). Second generation (F2) folds in the Badshot Range are open to tight and have northeast dipping axial surfaces and gently northwest or southeast plunging hinges (Read and Wheeler, 1976; Smith and Gehrels, 1992). A third generation of mesoscopic folds coaxial with F2 occurs locally south of Trout Lake (Read, 1973). Megascopic F2 folds control the structural map pattern east and north of the Kuskanax batholith (Read and Wheeler, 1976). Geological relationships and geochronology in rocks of the Selkirk and Cariboo mountains constrain the timing of regional Jurassic deformation to a ca. 10 Myr interval that straddles the Early-Middle Jurassic boundary (Roback, 1993; Murphy et al., 1995). Regional D2 deformation along the northeastern margin of the Kuskanax batholith affected early, 196 Ma to 187 Ma phases of the batholith but not phases younger than 180 Ma (Roback, 1993). Field relations on the west side of the Kuskanax batholith near Upper Arrow Lake indicate that deformation occurred during or after emplacement of early phases and ceased prior to late dikes and sills; however radiometric ages are not available for Kuskanax rocks in that area. On the basis of crosscutting relations, the ca. 162 Ma peraluminous Galena Bay stock post-dates penetrative deformation of its Paleozoic host strata (Parrish and Armstrong, 1987).

4.3 Field data

4.3.1 Strain in rocks below the Mississippian unconformity

D1 features in the Lardeau Group

The oldest preserved fabric in the Lardeau Group, S1, is a greenschist-grade foliation that is defined by the orientation of fine-grained phyllosilicates and is everywhere parallel to compositional layering at the scale of laminations to map-scale layers (Figure 4-2). S1 is also defined by flattened primary features (examples below). Carbonaceous phyllite and schist commonly contain conspicuous discontinuous millimetre- to centimetre-scale white quartz veinlets or 'sweats' in the S1 foliation (Figures 4-2C and 4-3). S1 occurs in all parts of the Lardeau Group in the study area. It can be distinguished from the younger regional fabric, S2, in F2 hinge zones, but it is commonly transposed into S2 on F2 fold limbs in less competent rock types such as phyllite. The intensity of post-D1 strain, and consequently the preservation of D1 features, varies considerably in the study area as a function of location and rock type. Competent rock types such as grit and greenstone commonly preserve S1 (figures 4-2 and 4-4). L1 lineations cannot be reliably distinguished because of overprinting coaxial episodes of deformation (Read, 1973).

Examples of D1 transposition in the Lardeau Group are clear at Mount Thompson and Comaplix Mountain. Graded beds of quartzofeldspathic grit in the Broadview Formation at Mount Thompson have a strong, closely spaced foliation, S1, defined by phyllitic partings that are parallel to transposed bedding (Figure 4-2B). S1 is axial planar to tightly folded contacts with rare phyllite interbeds (Figure 4-2A). A less developed phyllitic spaced cleavage, S2, which is parallel to the regional structural grain, transects S1. In the exceptionally well exposed, kilometres-wide hinge zone of the F2 Holyk anticline on Comaplix Mountain, rocks of the Lardeau Group (Akolkolex Formation) contain a strong greenschist-facies foliation (S1) that is parallel to compositional layering and the long axes of flattened clasts (Figure 4-4). S1 in Jowett Formation metabasalt on the west flank of Comaplix Mountain is defined by flattening of igneous structures and textures in greenstone and by phyllitic parting in green phyllite (Figure 4-5). A metabasaltic dike within foliated metabasalt outlines tight, metres-scale folds in which S1 is axial planar and local S2 spaced cleavage is oblique by ~30º (Figure 4-6). On the basis of local reversals of fining direction in graded beds, isoclinal F1 folding is present at a scale of tens to one hundred metres within the Akolkolex Formation on Comaplix Mountains, but hinges were not observed. Centimetre-scale rootless folds intrafolial to S1 were observed infrequently in moderately competent banded units, usually in phyllitic rocks, but also in quartzite and marble.

D1 features in the Mount Sproat assemblage

Greenschist-facies Mount Sproat assemblage strata, which occur between the Hadow stock and Mount Sproat, bear a transposition foliation, S1, that has been overprinted by the regional S2 cleavage in the same way as rocks of the Lardeau Group (Figure 4-7). Quartzose units in the Carbonaceous and Heterolithic members often record superposition of S2 on S1. Phyllitic greenstone, marble and low-silica phyllite, which collectively dominate the lower two members of the MSA, typically preserve one planar strain fabric, which is parallel to layering and S2. Rootless folds intrafolial within S1 in banded quartzite of the Heterolithic member have been crenulated by centimetric F2 folds with steeply dipping S2 cleavage parallel to the regional strike of ~320º (Figure 4-8). Carbonaceous quartzose schist frequently contains contorted and tightly appressed quartz veinlets as are characteristic of similar rocks in the Lardeau Group. S2 surfaces in most MSA phyllites are undulatory or anastamosing, interpreted to be due to interference of S1. Carbonates in the MSA are significantly recrystallized.

Mesoscopic phase one structures are less abundant in the Heterolithic member than in the Carbonaceous member and the Lardeau Group. Commonly only layer-parallel S2 cleavage is apparent in the Heterolithic member. S1 is locally crenulated by S2 in banded quartzite and quartzose schist in the Heterolithic member at Galena Pass and Beaton Arm.

The westernmost observations of a transposition foliation that pre-dates the regional S2 foliation were made in the uppermost strata of the Heterolithic member near the hinge of the Hill Creek syncline at Galena Pass. Discontinuous streaky S1 banding oblique to, and crenulated by, S2 has been preserved in calcareous biotite schist (figures 4-7E, F). As described below, foliation that pre-dates the Jurassic S2 schistosity could not be distinguished in the Mount Sproat assemblage between Galena Bay and Nakusp.

D2 features

S2 is the main fabric in rocks throughout most of the Lardeau Group and Mount Sproat assemblage, with notable exceptions as described here. The regionally predominant phase of compressional deformation, which included formation of upright to inclined folds that control the map pattern is referred to here, and by previous workers, as D2. D2 fabric and associated metamorphism vary from chlorite zone cleavage to garnet zone schistosity in the study area; both generally increase westward. West of the axial trace of the Hill Creek syncline and the Kuskanax batholith (Figure A1-1), S2 is a layer-parallel biotite- to garnet-zone schistosity to gneissosity in the Mount Sproat assemblage and S1 is not apparent (Figure 4-9). East of the axis of the F2 Hill Creek syncline, all strata are affected by S2 cleavage or schistosity that is axial planar to other megascopic F2 folds such as the Holyk anticline. Because of interference effects of the pre-existing S1 foliation, S2 is irregular or wavy in phyllitic Lardeau and Mount Sproat assemblage strata. In the hinge zone of the Holyk anticline, S2 is an axial planar spaced cleavage (Figure 4-4). Layering attitudes in the Holyk anticline (Figure 4-10) reflect the observed close to tight folding of S1 about an axis that plunges about 35° toward ~125°. The orientation of S2 cleavage (weighted mean of ~312º/80º using the right-hand rule) is consistent throughout the anticline. In thin section, S2 cleavage in phyllite is a crenulation of fine mica, carbonaceous bands, and quartz and feldspar grains, with little D2 recrystallization (figures 4-4E, F). Thick layers of greenstone have no expression of S2 (Figure 4-5).

On limbs of macroscopic F2 folds, S2 is better developed and largely or fully obscures S1 in incompetent rock types such as phyllite. On the limbs of the isoclinal F2 Sproat antiform near Mount Sproat (see cross-section A-B on Figure A1-2), felsic dikes inferred to derive from the mid-Jurassic Kuskanax suite have been strongly boundinaged in the combined S1/S2 layer-parallel foliation (Figure 4-7D).

Mesoscopic F2 folds are common in well-layered units of the Lardeau Group and Mount Sproat assemblage. In the Broadview Formation, F2 folds are generally similar folds outlined by transposed layering, S1, in grit (Figure 4-11).

Conglomerate clasts (long axes from ~1 cm to 50 cm) in the lowermost Amphibolitic Schist member at Mount Sproat consist of massive quartzite and quartzofeldspathic grit, are elongate along a local NNE stretching direction and lack internal foliation (Figure 4-12). Metamorphic grade increases steadily to the west of Mount Sproat; S2 changes gradually from spaced cleavage to penetrative schistosity associated with metamorphic biotite, amphibole and muscovite. In the transition zone, biotite in fine-grained biotite schist (Heterolithic member) in Galena Pass is strongly aligned in S2, which is axial planar to F2 crenulations of the compositional banding (figures 4-7E, F). Semi-continuous exposures along the north shore of Beaton Arm show a gradually westward increasing grain size of metamorphic minerals and apparent strain interpreted to be associated with D2.

D3 features

Gently inclined and open F3 folds deform map-scale F2 folds in the hanging wall of the Akolkolex and Standfast Creek faults at Mount Sproat and McCrae Peak (Figure A1-2, cross-section A-C). S3 crenulation cleavage to schistosity is axial planar to F3 folds. The Akolkolex fault (Thompson, 1978; Sears, 1979) separates F3 folds from the similarly oriented but nappe-like Akolkolex anticline (Thompson, 1978). D3 structures are minor or absent in the study area outside of the Mount Sproat-McCrae Peak area. Local gentle kink folding inferred from alternations of dip direction in subvertical layering in the eastern Lardeau Range and south of Trout Lake (Figure A1-2, cross section E-E’) has an unconstrained relationship to F3 folds. Further discussion of D3 structures is beyond the scope of this paper.

4.3.2 Strain in rocks above the intra-Mississippian unconformity

Descriptions in this section pertain to rocks exposed between Mobbs Creek in the south and McCrae Peak in the north unless otherwise stated. Because of strong post-Middle Jurassic metamorphism and strain, rocks west of McCrae Peak and Mount Sproat (Crawford Creek area) are not discussed.

Thompson assemblage

Argillite and grit in the Thompson assemblage display a phyllitic cleavage that dips moderately to steeply toward 030º. Bedding dips steeply toward 210º or 030º and commonly defines megascopic open to tight folds in which the cleavage is axial planar. Mesoscopic folds occur in outcrops containing strata with strong competence contrasts (Figure 4-13). Bedding/cleavage relations and fold asymmetry indicate that the Mount Thompson locality is on an overturned limb with a syncline to the southwest. This is consistent with graded beds that fine downward to the southwest and toward the axial surface of the Beaton syncline. Rare quartz filled tension gashes in the Thompson assemblage are orthogonal to the local F2 fold axis.

The Thompson assemblage has a high level of preservation of primary features (Figure 4-14). Mudstone has phyllitic lustre and basaltic rocks have been only partially chloritized. Carbonate units appear to be moderately recrystallized to medium grain size. Relative to the underlying Lardeau Group, Thompson assemblage strata have a high level of preservation of primary features. Sedimentary breccia texture in limestone (rudstone) and amygdaloidal fragmental texture in metabasalt are weakly to moderately deformed, without penetrative foliation. Grit compositionally and texturally similar to underlying Broadview strata is cleaved at a low angle to bedding. Basal surfaces of graded grit beds locally preserve scour marks.

Milford Group

Milford strata display slaty cleavage in phyllite and spaced cleavage in metasandstone or limestone. Cleavage is commonly parallel to compositional layering but bedding and cleavage are discordant at numerous localities across the study area (Figure 4-15). The transposition foliation in underlying Broadview grit (S1) does not occur in the Milford Group. Where cleavage is oblique to layering in the northern Davis and northern McHardy assemblages, there is no bedding-parallel tectonic fabric. In the hinge zone of the Hill Creek syncline, cleavage – whether parallel or oblique to layering – is axial planar. Banded sandstone compositionally similar to quartzite that clearly record two phases of deformation in the Mount Sproat assemblage (see above) lacks rootless intrafolial folds and the early foliation observed in the Mount Sproat assemblage. Angular lithic fragments in wacke in the northern McHardy assemblage near Mount

Murray (Figure 4-15A) are not obviously deformed. Rare rootless folds in banded argillite indicate partial transposition of bedding into S2 (Figure 4-15C).

Macrofossils in northern Davis assemblage limestone are variably recrystallized, but syringopora, brachiopods, gastropods, solitary rugose corals and bryozoans at Mount Thompson and McCrae peak are undeformed to weakly deformed (Figure 4-15F). The strong contrast in finite strain of carbonates on either side of the intra-Mississippian unconformity is shown in Figure 4-16.

A clear example of a clast of grit with pre-depositional foliation in basal Milford conglomerate that corroborates prior work is shown in Figure 4-17.

4.3.3 Sub-Milford unconformity

Nowhere in the study area could the sub-Milford unconformity be observed in outcrop. In the updated geologic map, angularity of the sub-Milford unconformity is most apparent beneath the McHardy assemblage in the Lardeau Range, where McHardy strata overlie progressively deeper levels of the Mount Sproat assemblage from west to east (Figure 4-18). The same eastward down-cutting by the unconformity is implied by the absence of the Mount Sproat assemblage beneath the Davis assemblage.

4.3.4 Faults

On the basis of map patterns and observed fault rock, three significant faults have been interpreted in the Trout Lake area: the Adit (Read et al., 2009; Kraft et al., 2011a), Blind Bay (Kraft et al., 2011a), and Mobbs (Read, 1973; Kraft et al., 2011a) faults. As described in Chapter 3, each of these faults truncate F2 folds and (or) Milford Group rocks.

4.4 Discussion

4.4.1 Interpretations of field data

Aspects of D1 deformation

Fabric

The first phase of deformation in the Lardeau Group and Mount Sproat assemblage imparted a strong layer-parallel greenschist-facies foliation that locally contains rootless folds and is commonly marked by discontinuous or disrupted banding (Read, 1973; Klepacki, 1985; Smith and Gehrels, 1992; this study). These strata were sufficiently ductile to fold but were sufficiently brittle to form ubiquitous quartz veins during D1. The S1 greenschist-facies mineral assemblage in the Lardeau Group (qtz-ab-mu-chl; Read, 1973) and structural style are consistent with deformation at conditions near the brittle-ductile transition (e.g. Scholz, 1988).

S1 is readily observed in most rock types of the Lardeau Group and appears to diminish in intensity in the Mount Sproat assemblage. The unambiguous presence of S1, where a transposition foliation is overprinted by S2, was not observed in the Amphibolitic Schist or Upper Clastic members. Inability to identify S1 in the Amphibolitic Schist and Upper Clastic members may be attributable to overprinting by the greater Jurassic and younger metamorphism and strain along Upper Arrow Lake where the Amphibolitic Schist and Upper Clastic members are exposed. Nonetheless, the weak strain in some areas and the failure to identify S1 or rootless isoclines in the Amphibolitic Schist and Upper Clastic members are interpreted to indicate that D1 did not pervasively deform the upper members of the Mount Sproat assemblage.

Folds

Expressions of pre-Milford age folds in the Lardeau Group are not present in the geologic map pattern of the study area (Figure A1-1). Large, recumbent phase 1 fold nappes reported to occur on Trout Mountain (Roback, 1993) are inconsistent with new mapping in that area that reports steeply dipping layers in subvertical structural panels (Read et al.., 2009; Kraft et al., 2011a). Read (1976) interpreted metabasaltic rocks immediately beneath the Davis assemblage on Mount Thompson and near Beaton Arm to indicate a first phase (pre-Milford) syncline that repeated the Jowett Formation. Mapping during this study shows that 1) Broadview strata are distinctly asymmetric between the two greenstone localities, with a thick lower section of carbonaceous phyllite overlain by quartzite and grit (Kraft et al., 2011a), and 2) Read's (1976) western repeat of the Jowett Formation has alternative possible correlations in the lower Mount Sproat assemblage. Moreover, discontinuous metabasaltic units occur nearby within the Broadview Formation (Read and Wheeler, 1976). The first phase fold interpretation is not required and a simpler interpretation that the western volcanic rocks are younger than the Jowett Formation is preferred. The lateral continuity of marker horizons and consistency of the stratigraphic succession in both the Lardeau Group and Mount Sproat assemblage (i.e. Fyles and Eastwood, 1962; Read and Wheeler, 1976; this study) indicate that D1 did not duplicate or affect the order of the lithostratigraphic succession.

Faults

Layer-parallel faults attributed to D1 have been reported from the Lardeau Group near Ferguson (Smith and Gehrels, 1992) and in the Goat Range (Klepacki, 1985); however, all faults mapped in this study are younger than the Milford Group and therefore cannot be attributed to a pre-Milford event. As noted above, the Lardeau shear zone (Figure A1-2, cross-section D-D') was active in the Jurassic but displacement may have occurred as early as mid-Paleozoic time (Smith and Gehrels, 1992).

Timing of D1

As is the case for the Lardeau Group (e.g. Wheeler, 1968; Read and Wheeler, 1976; Smith and Gehrels, 1992), the lower Mount Sproat assemblage is interpreted here to have been deformed prior to deposition of the Milford Group on the basis of the following evidence:

1) The lower Mount Sproat assemblage contains fabrics and folds analogous to D1 features in the Lardeau Group, which are absent from the Milford Group and Thompson assemblage. Phase one folds and fabrics occur in strata west of the Adit fault (Read et al., 2009) that were reassigned to the Mount Sproat assemblage in Chapter 2.
2) The Mount Sproat assemblage conformably overlies the Lardeau Group.

The strong layer-parallel phyllitic foliation observed in lower stratigraphic levels of the Mount Sproat assemblage are interpreted to originate from the same pre-Milford deformation that affected the Lardeau Group. Absence of S1 transposition foliation and superior preservation of primary features such as macrofossils indicate that the Thompson assemblage did not experience the pre-Milford deformation that affected the Lardeau Group.

Because unequivocal evidence of penetrative D1 strain has not been identified in the Amphibolitic Schist and Upper Clastic members of the Mount Sproat assemblage, the timing of D1 relative to deposition of those members is less certain. If D1 preceded deposition of the ca. 367 Ma Amphibolitic Schist member, its basal contact with the Heterolithic member would be an angular unconformity. Observations of that transition in semi-continuous exposures on Mount Sproat, however, showed 1) no contrast in structural style or finite strain, 2) that the contact is concordant, and 3) that similar rock types occur across the transition (Figure A1-3, see Chapter 2). The same argument is true for the contact between the Upper Clastic and Amphibolitic Schist members. The conformable nature of the entire Mount Sproat assemblage combined with the angular truncation of its strata by the unconformity separating it from the northern McHardy assemblage lead to the interpretation that D1 post-dated deposition of the youngest member of the Mount Sproat assemblage – the Upper Clastic member. This relative timing of D1 is consistent with the observation that the first conglomerate cobbles with a pre-depositional foliation in this region occur in the Milford Group.

The maximum age of D1 is therefore constrained by the ca. 359 Ma detrital zircon reported from the Catherine Lake phyllite (Thompson et al., 2006), which was correlated with the Upper Clastic member in Chapter 2. If the Catherine Lake phyllite is not correlative with the Upper Clastic member and instead corresponds to an older part of the Milford Group (e.g. Orchard, 1985), the next maximum age constraint of D1 is the ca. 367 Ma Amphibolitic Schist member. A third upper limit on the timing of D1 is the initiation of arc magmatism in the region because S1 affects metavolcanic strata with arc-related geochemical traits (unit DMSv2 in the Heterolithic member, Chapter 2). The oldest arc-related magmatic rocks known from southeastern British Columbia are Late Devonian – only slightly older than the Amphibolitic Schist member (ca. 372-365 Ma; Okulitch, 1985; Slemko, 2000; Richards et al., 2002; Simony et al., 2006).

The minimum age of D1 remains the Viséan (345-326 Ma) base of the Milford Group (e.g. Read and Wheeler, 1976; Klepacki, 1985; Orchard, 1985; Smith and Gehrels, 1992).

Although the conformable nature of the Mount Sproat assemblage and its contact with the Broadview Formation indicate that no major break occurred during deposition of the Lardeau Group and Mount Sproat assemblage, sedimentological features of MSA rocks do, however, reflect change in the tectonic setting of the basin during deposition of the MSA (see Chapter 2). The first conglomerate in the MSA, at the base of the Amphibolitic Schist member, closely overlies the lowest metavolcanic layers with geochemical characteristics of arc volcanism, indicating that uplift of the conglomerate's mixed quartzofeldspathic and mafic source shortly followed the first arc-related magmatism in the Lardeau trough. The abundance of conglomerate in the Upper Clastic member is interpreted to reflect tectonic instability that persisted into the Early Mississippian.

4.4.2 A model for Paleozoic (D1) deformation in the Lardeau trough

A model of D1 deformation in the northern Kootenay Arc must account for the following observations:

1) S1 is a greenschist-facies transposition foliation (Read, 1973);

2) Mesoscopic tight to isoclinal F1 folds are common;

3) The stratigraphic sequence was not structurally repeated prior to D2;

4) Formation of quartz veins and 'sweats' was significant during D1;

5) D1 strain is intense in the Lardeau Group, present in the lower Mount Sproat assemblage and minor or absent in the upper Mount Sproat assemblage;

6) D1 strain has not been reported from rocks stratigraphically below the Lardeau Group (Fyles and Eastwood, 1962; Fyles, 1964; Read and Wheeler, 1976; Smith, 1990);

7) The Lardeau Group lacks D1 structures and fabric in the northern Selkirk Mountains (Wheeler, 1963; Brown et al., 1983; Colpron, 1996; Gibson et al., 2005).

It is also noteworthy that the geographic extent along which the contact between the Index Formation-Badshot Formation is a fault (the northern Kootenay Arc) corresponds to the region in which the Lardeau Group has yielded evidence of D1 strain. The Lardeau shear zone may therefore be integral to D1 deformation.

D1 strain affected a kilometres-thick stratigraphic interval that had a discrete lower boundary at the Index Formation/Badshot Formation contact (the Lardeau shear zone) and an upper boundary inferred to be a broad strain gradient in the lower Mount Sproat assemblage (Figure 4-19). Because neither stratigraphic duplication older than D2 nor fold interference patterns are evident in the Lardeau Group and Mount Sproat assemblage, D1 did not involve large amplitude folds or repetition of strata by discrete thrust faults. Rather, brittle-ductile strain formed centimetre and metre-scale intrafolial and rootless folds and layer-parallel foliation in Lardeau Group and lower Mount Sproat assemblage rocks. The greenschist-facies, semi-brittle nature of D1 fabrics in the Lardeau Group indicates that strain occurred under conditions near the brittle-ductile transition. Semi-brittle, greenschist-facies conditions in the Lardeau Group are inferred to have existed from a combination of depositional burial beneath the >5 km thick Mount Sproat assemblage, tectonic thickening and a relatively high geothermal gradient beneath the Lardeau trough owing to its location on attenuated crust in a back-arc setting (e.g. Hyndman and Lewis, 1999; Currie et al., 2004). Early Mississippian deformation of the rocks of the Lardeau trough, therefore, took place in a broad, internally-deforming thrust sheet that detached from underlying competent miogeoclinal strata along the argillaceous Index Formation, causing early displacement on the Lardeau shear zone of Smith and Gehrels (1992). Analogous models of internally deformed thrust sheets, in which distributed strain produced isoclinal folds and transposition foliation at low metamorphic grade, are known in basinal strata from similar geological settings elsewhere in the North American Cordillera (Schoonover sequence, Nevada: Miller et al., 1984; Robert Service thrust, Yukon: Mair et al., 2006). This contrasts with the predominantly brittle style of deformation that affected the Mount Forster Formation farther to the east, which is interpreted to have overlain thicker continental crust in the Purcell Arch and was not buried depositionally beneath a significant thickness of strata (Root, 1987).

4.4.3 Devonian-Mississippian tectonism in the southern Canadian Cordillera

The Early Mississippian timing of D1 deduced above differs with the timing of other hypothesized compressional events in the southern Canadian Cordillera. Eifelian folds and thrusts on the Purcell Arch (Root, 1987; 2001) would have formed during deposition of the upper Lardeau Group or lower Mount Sproat assemblage in the Lardeau trough. If the Lardeau Group was situated on the outer flank of the Purcell Arch, as map relations strongly suggest, uninterrupted sedimentation in the Lardeau Group indicates that syn-depositional deformation in the Mount Forster Formation was not part of an orogenic event of sufficient magnitude to generate a foreland basin as proposed by Root (2001). Alternatively, the Lardeau trough was not outboard of the Purcell Arch but was farther south along the Cordilleran margin where compression did not begin until latest Devonian or Early Mississippian time (Johnson and Pendergast, 1981; Miller et al., 1984). Strong map control that physically links the Lardeau trough to the Purcell Arch via the Cordilleran miogeocline (Colpron and Price, 1995) indicates that the latter scenario is unlikely. Eifelian deformation on the Purcell Arch is interpreted to have been localized to an area inboard of the Lardeau trough and therefore reflects heterogeneity in the tectonic regimes along the Devonian Cordilleran margin.

Amphibolite-facies schistosity and a major normal fault (Queest Mountain fault of Johnson, 1994) in Lardeau Group- or Silver Creek Formation-equivalent rocks at Sicamous (Queest Mountain assemblage of Slemko, 2000) were interpreted to have formed prior to a ca. 366 Ma intrusion (Slemko, 2000) and thus would have formed during deposition in the Lardeau trough. The timing of this event is consistent with the Eifelian deformation of the Mount Forster Formation (Root, 1987), but the hinterland style of the hypothesized event, which involved burial to 6.9 kbar pressures before tectonic exhumation (Slemko, 2000) cannot be easily reconciled with data from this study and from Struik (1981), which argue for uninterrupted deposition of basinal Paleozoic pericratonic rocks through the Silurian and Devonian. Furthermore, other structural-metamorphic studies have found no evidence of pre-Mesozoic metamorphism or ductile strain in the pericratonic rocks of southern British Columbia outside of the northern Kootenay Arc (Okulitch, 1985; Schiarizza and Preto, 1987; Thompson et al., 2006), including studies of equivalents of the Queest Mountain assemblage (Glombick et al., 2006; Johnson, 2006). The cross-cutting relations reported by Slemko (2000) cannot be reconciled with evidence from this study unless the Lardeau trough and Queest Mountain assemblage were separated by a much larger distance than the present 100 km separation, which is considered to be unlikely because of stratigraphic correlations between the regions (e.g. Silver Creek Formation; Slemko, 2000; Thompson et al., 2001; Thompson et al., 2006). If the Queest Mountain assemblage does preserve a pre-365 Ma schistosity, the assemblage may have experienced the same early Paleozoic high-grade metamorphic event as the Chilliwack Composite terrane, and thus was likely outside the pericratonic realm during the Ordovician to Early Devonian.

The hypothesized Cariboo orogeny (White, 1959) and interpretations of the Lower Mississippian Guyet Formation conglomerate as a synorogenic deposit (Campbell et al., 1973; Smith et al., 1993) were contradicted by the observations of Struik (1981), who found no evidence of mid-Paleozoic deformation in the Cariboo Mountains and reported that the Guyet conglomerate resides in an unbroken sequence of Ordovician to Permian sedimentary and volcanic strata that unconformably overlies the Ediacaran-Cambrian Cordilleran miogeocline. The Guyet conglomerate and underlying Black Stuart Formation are correlated with the Mount Sproat assemblage in Chapter 2. The conclusions of Struik (1981) preclude the notion that the Mississippian deformation event manifested in the Kootenay Arc also affected similar marginal basin strata presently 400 km to the north and instead invoke periodic extensional settings. Gordey et al. (1987) similarly interpreted an extensional setting for Late Devonian and Mississippian coarse clastic sedimentation and tectonic subsidence in the Selwyn Basin. The variations in interpreted timing and nature of tectonism in the Devonian and Mississippian Cordilleran margin is considered here to reflect real heterogeneities in the tectonic setting of the margin.

That D1 structures have been observed in only the northern Kootenay Arc segment of the Lardeau Group is taken to indicate that shortening was a local phenomenon due to heterogeneity of the back-arc environment. Shortening may have been accommodated by relatively weak and hot crust due to a change at the plate boundary such as an increase in convergence rate or change in obliquity of subduction. Paleozoic deformation of the Lardeau Group was not associated with a major orogenic event in the sense of the Antler orogeny. The coincidence in timing does, however, leave room for speculation that deformation in the Kootenay Arc was a peripheral manifestation of the Antler orogeny.

4.5 Conclusions

The two lower members of the Mount Sproat assemblage were deformed with the Lardeau Group during regional D1 prior to deposition of the Thompson assemblage and Milford Group. The Amphibolitic Schist and Upper Clastic members of the Mount Sproat assemblage were not deformed penetratively by D1. Because of the conformable nature of the Mount Sproat assemblage, they are, however, interpreted to have been deposited prior to cessation of D1 strain in underlying rocks.

Tilting and erosional unroofing of the Mount Sproat assemblage and Lardeau Group took place after deposition of the Upper Clastic member of the Mount Sproat assemblage, which in Chapter 3 was assigned an age of Early Mississippian (Tournaisian). Penetrative D1 strain affects Heterolithic member metavolcanic strata with arc volcanic geochemical signatures (Chapter 2) and therefore took place or persisted after initiation of subduction-related magmatism, which is inferred to be ca. 375 Ma based on U/Pb ages of arc-related plutonic rocks in southeast British Columbia (Slemko, 2000; Simony et al., 2006). D1 strain in the Lardeau Group was significantly younger than Eifelian (398 Ma to 392 Ma) contraction in the Mount Forster Formation but was contemporaneous with the Antler orogeny (*sensu stricto*) in Nevada.

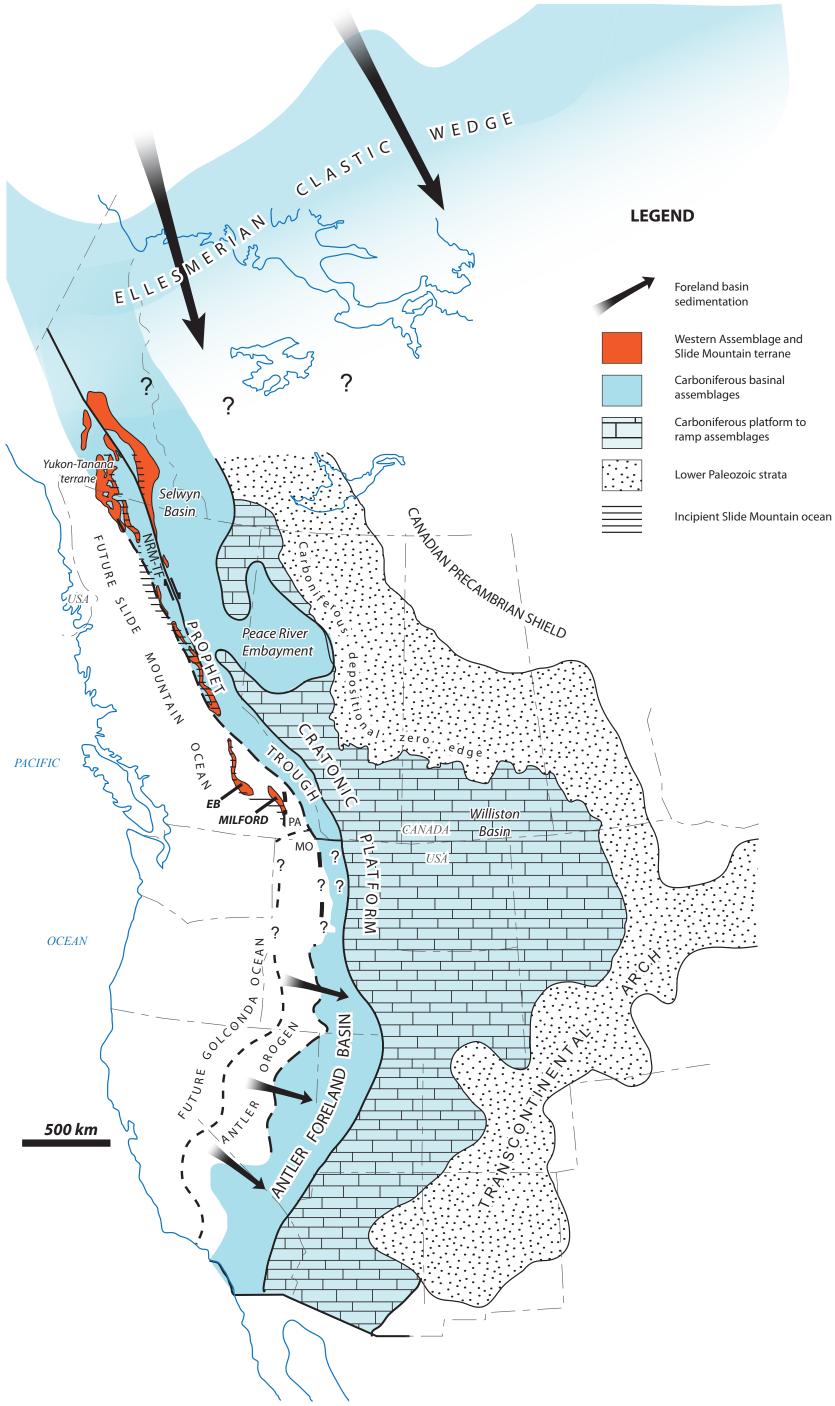

Figure 4-1. Map of western North American Late Devonian-Mississippian assemblages and basins.

Modified from Richards et al. (1994) and Beranek et al. (2010). The Ellesmerian and Antler orogenies during this time involved thrusting of basinal strata onto adjacent continental platform successions. The evolution of the intermediate segment of the Cordillera is less clear, having yielded evidence of both compressional and extensional tectonics from this interval.

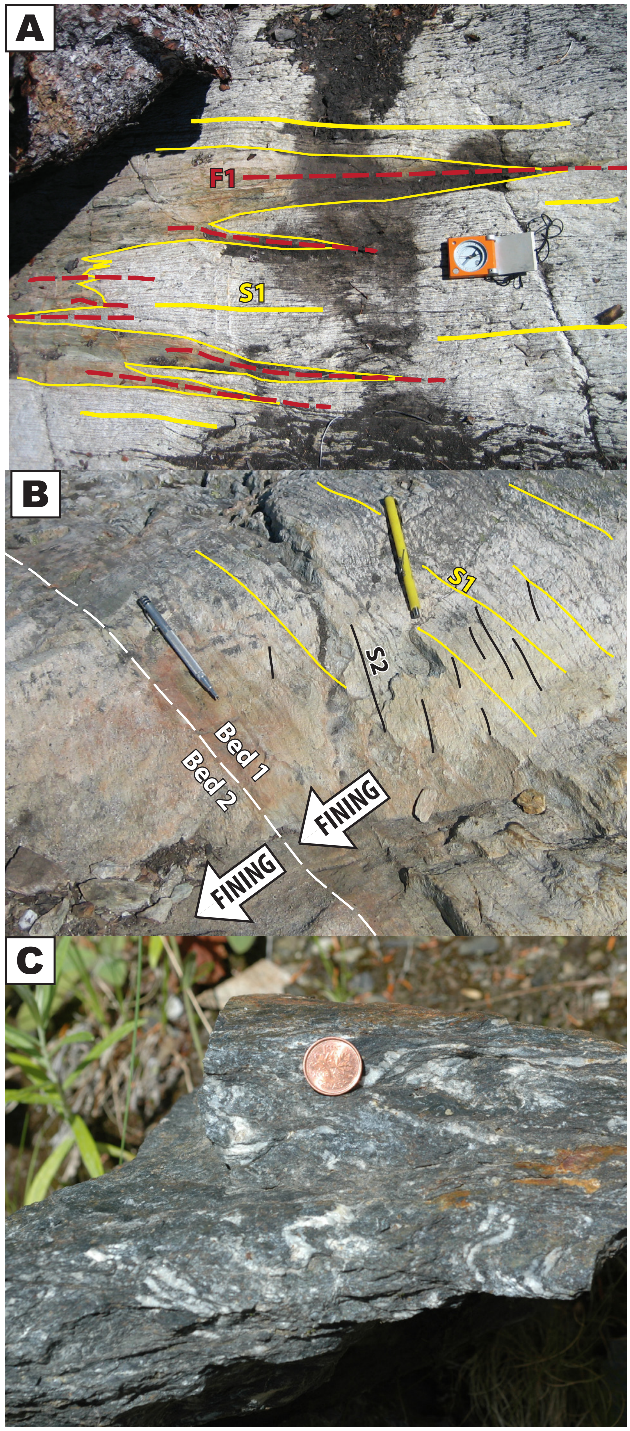

Figure 4-2. Phase 1 fabrics in the Broadview Formation at Mount Thompson.

A) Tight folds, F1, to which the transposition foliation, S1, is axial planar. Note: surface is an oblique section that exaggerates fold amplitude. B) Compositional layering from graded beds is parallel to the S1 foliation. Weaker spaced S2 cleavage transects S1 at a moderate angle. C) Quartz ‘sweats’ in carbonaceous schist outline the trace of S1, which, in this sample, was strongly deformed during D2. Sample from the southwest wall of the Mobbs fault near Mount Thompson.

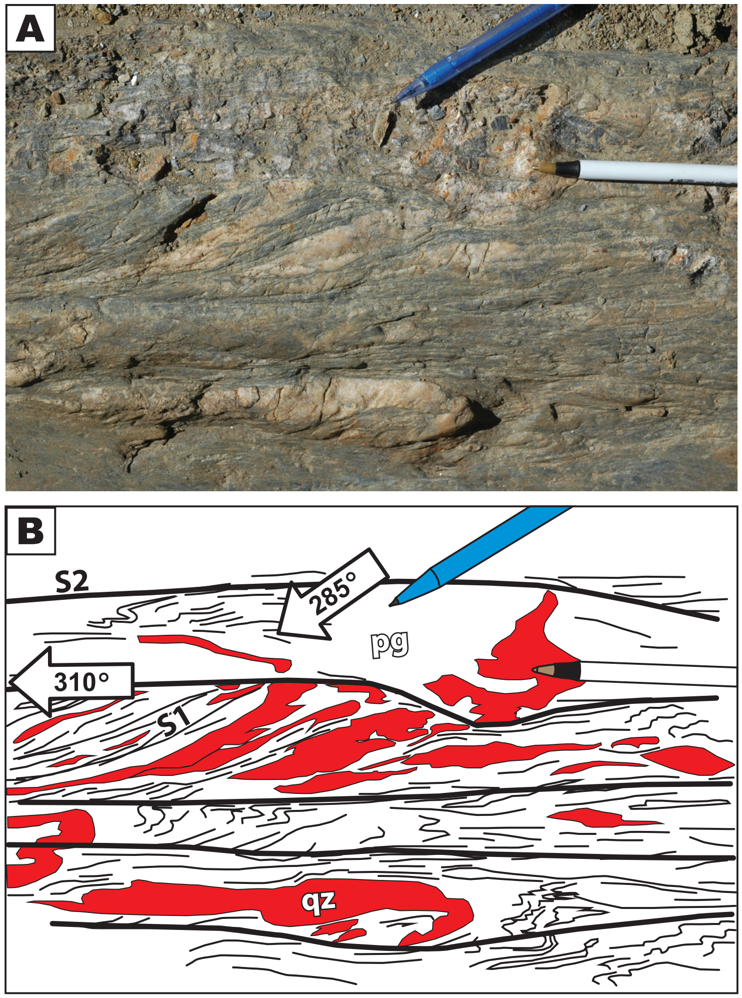

Figure 4-3. Overprinting fabrics in the Broadview Formation near the MAX Mine mill site.
A) Plan view photograph of phyllitic grit with deformed quartz veins. B) Interpretation of (A): quartz veins (red) have been transposed into a closely spaced early fabric (S1) indicated by fine black lines. S1 is deflected by a wider spaced foliation, S2 (heavy lines), which parallels the local structural trend. Small folds of S1 are inferred to be F2. Abbreviations: pg, phyllitic grit; qz, cystalline quartz.

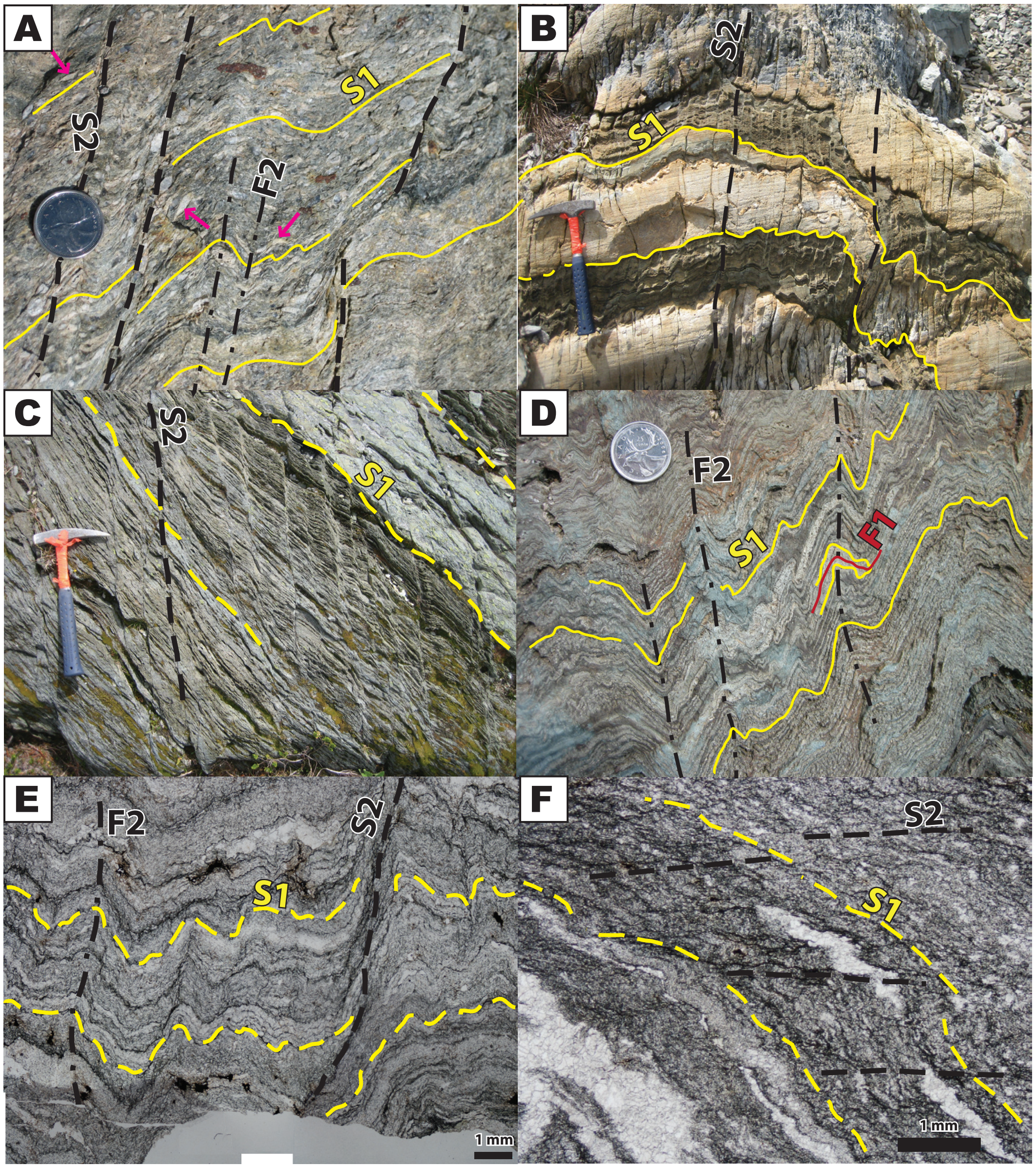

Figure 4-4. Folds and superposition of fabrics in the Akolkolex Formation in the Holyk antiform, Comaplix Mountain.

A) Upright inclined F2 folds and S2 cleavage overprint layer-parallel foliation in a graded bed of grit. Note flattening of pebbles into the transposition foliation, S1, indicated by pink arrows. B) S2 cleavage orthogonal to transposed bedding, S1, in interlayered grit and phyllite. C) S2 spaced cleavage overprints S1 transposition foliation. D) Small F2 folds that deform S1 in finely banded phyllite. A probable F1 hinge is indicated in red. E) Photomicrograph of carbonaceous phyllite showing F2 crenulations and partial development of spaced S2 cleavage parallel to F2 axial planes. Plane polarized light. F) Photomicrograph of phyllite in which S2 is weakly but penetratively developed at sub-1 mm scale. S1 is outlined by compositional layering. Plane polarized light.

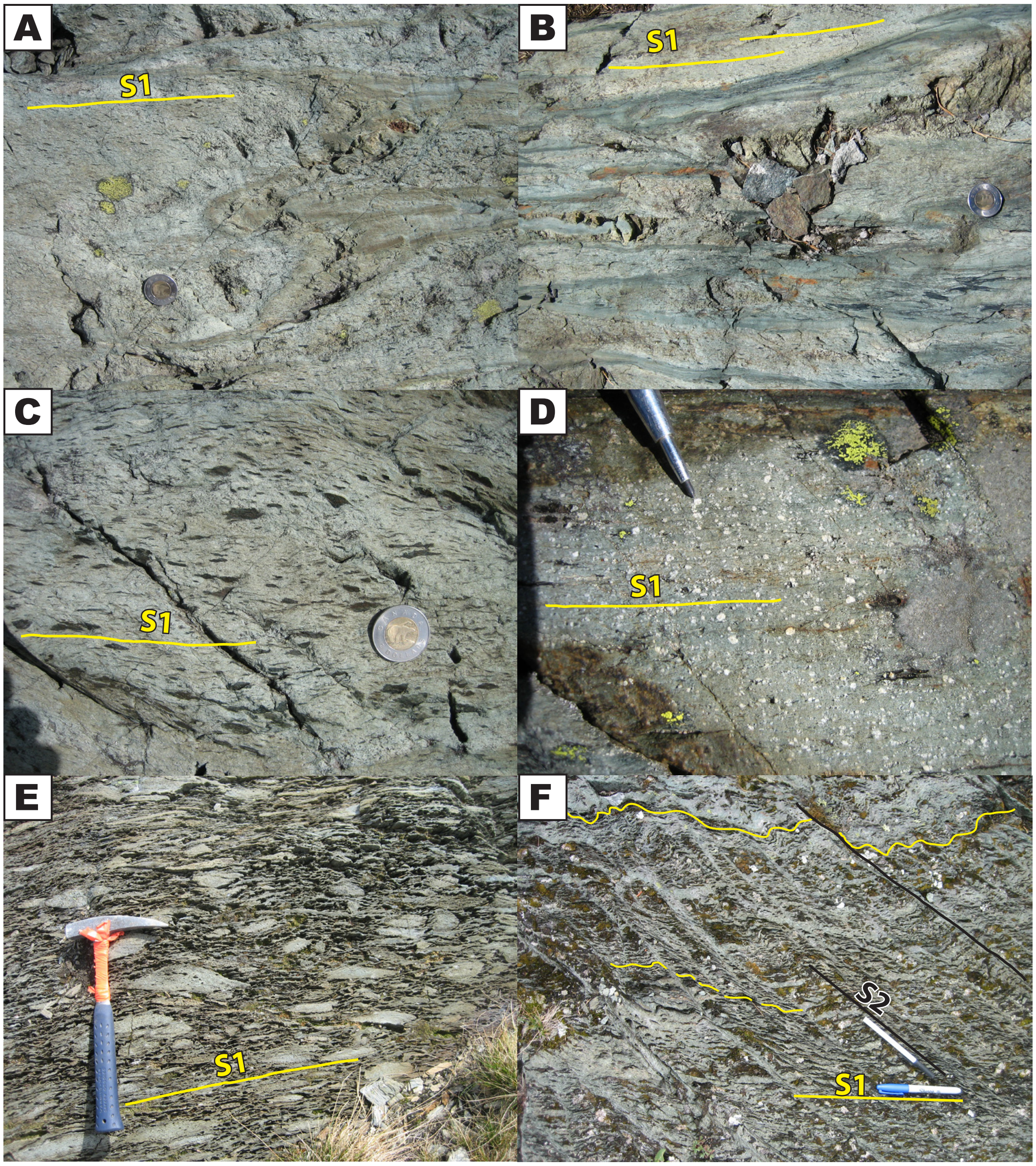

Figure 4-5. Development of S1 in different lithofacies of the Jowett Formation in the Holyk antiform, Comaplix Mountain.

A) Weakly sheared pillowed greenstone. Darker bands are interpreted as relict pillow selvages. B) Moderately foliated greenstone with banding possibly from pillow selvages or primary fragmental texture. C) S1 foliation defined by flattened clots of chlorite inferred to have replaced a primary phenocrystic phase such as clinopyroxene. D) Weak S1 foliation in greenstone groundmass. Feldspar phenocrysts appear undeformed. E) Basaltic clasts flattened into S1 in a fragmental facies with a deeply weathered phyllitic matrix. F) Crenulation of S1 by S2 cleavage, which is axial planar to the F2 Holyk antiform.

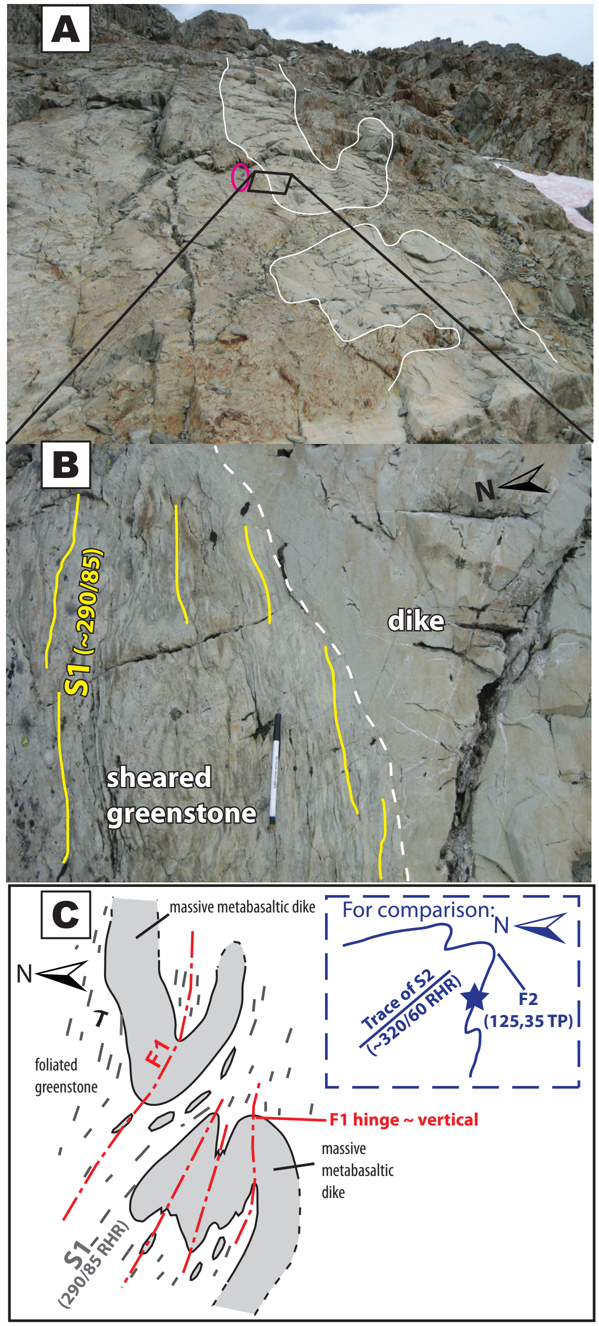

Figure 4-6. F1 folds in the Jowett Formation, Comaplix Mountain.
A) Folded mafic dike in sheared fragmental greenstone. Hammer in pink ellipse for scale. Black rectangle indicates location of (B). B) Angular relationship of S1 fabric to a dike margin. C) Digitized plan view field sketch of (A). Foliation, S1, is axial planar to the vertical folds, which are therefore F1. Blue inset shows plan view of orientations of D2 Holyk antiform structures in the area for comparison (refer also to Figure 4-10). The blue star indicates relative location of these F1 folds on the F2 Holyk antiform. Note the discordance of S1/F1 to S2/F2. RHR, right hand rule; TP, trend and plunge.

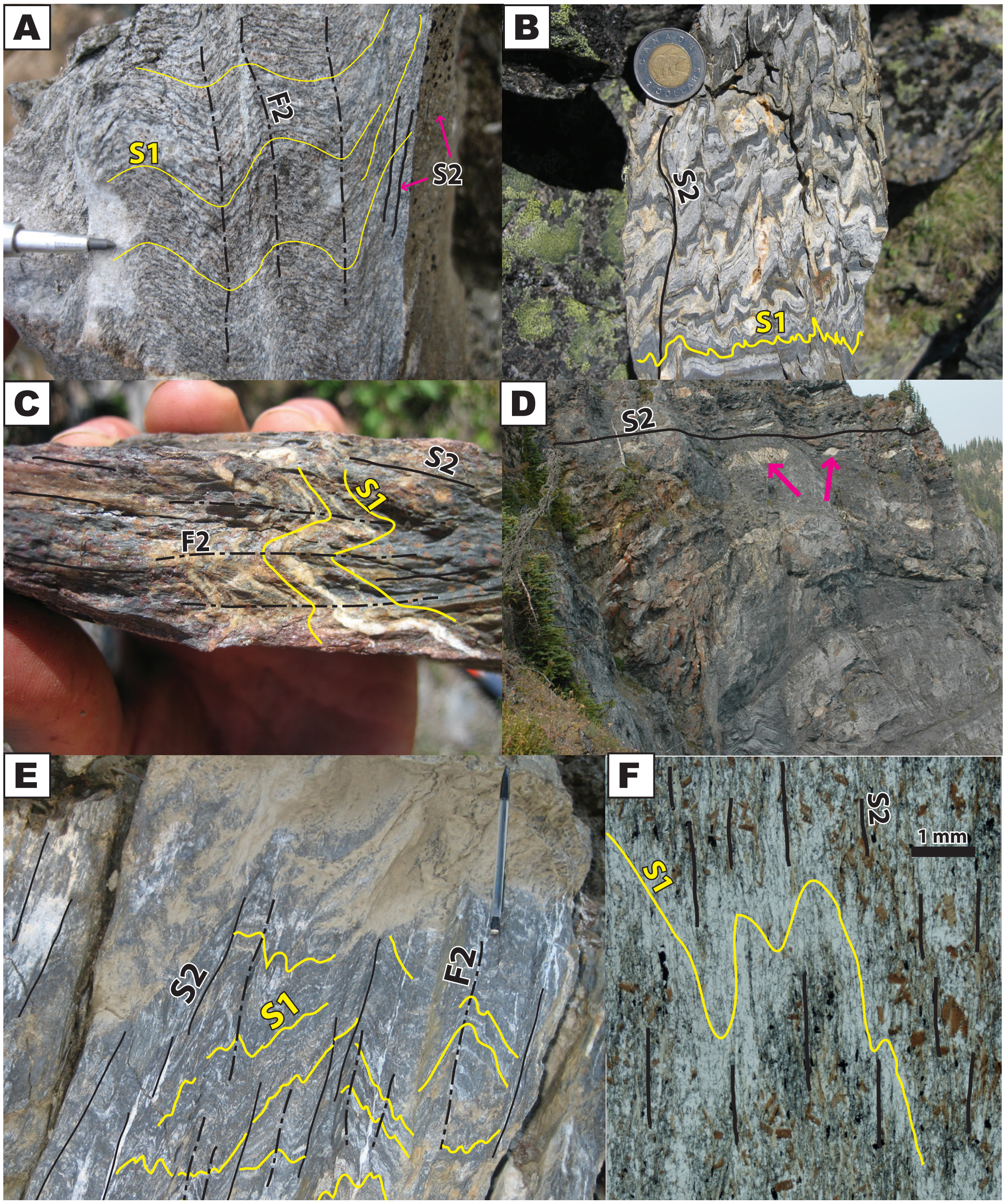

Figure 4-7. Fabrics in the lower Mount Sproat assemblage.
A) Deformation of S1 transposition by F2 folds in quartzite at the interlayered contact of the Broadview Formation and Carbonaceous member near Trout Mountain. B) Crenulation of S1 by F2 in banded quartzite of the lowermost Carbonaceous member near Trout Mountain. C) F2 folds and axial planar S2 cleavage deform the transposition foliation S1, which contains quartz veinlets in quartzose phyllite from the Carbonaceous member. D) Boudinaged Jurassic (?) sills in Heterolithic member limy phyllite where S2 is parallel to S1 near Mount Sproat. E) S2 cleavage overprints compositional banding (S1) in calcareous muscovite-biotite schist in the upper Heterolithic member at Galena Pass. F) Photomicrograph (plane polarized light) of sample from (E) shows alignment of micas in the S2 plane axial planar to a fold outlined by a lamination.

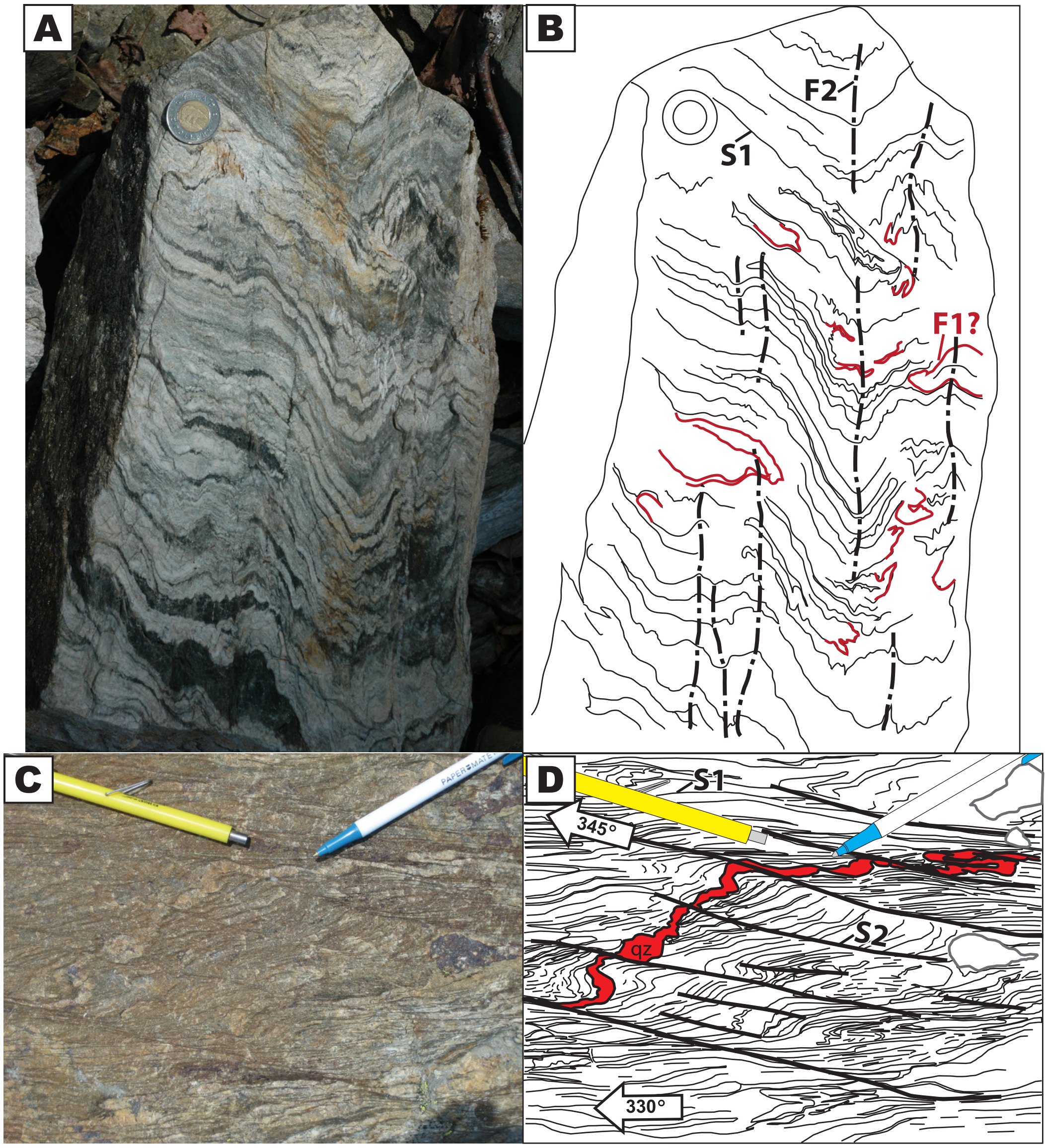

Figure 4-8. Superposed deformation in quartzite samples from the lower Mount Sproat assemblage.

A) Banded phyllitic quartzite, Heterolithic member at Beaton Arm. B) Interpretation of (A): S1 transposed layering and F1 isoclines have been crenulated by F2 folds. C) Quartzite at the Broadview Formation/Carbonaceous member contact at Trout Mountain. D) Interpretation of (C): A quartz vein (red) has been isoclinally folded and transposed into S1 (fine lines). Spaced S2 foliation (heavy lines) offsets the vein and S1 transposition foliation. S2 is parallel to the regional structural grain (azimuth 345 degrees).

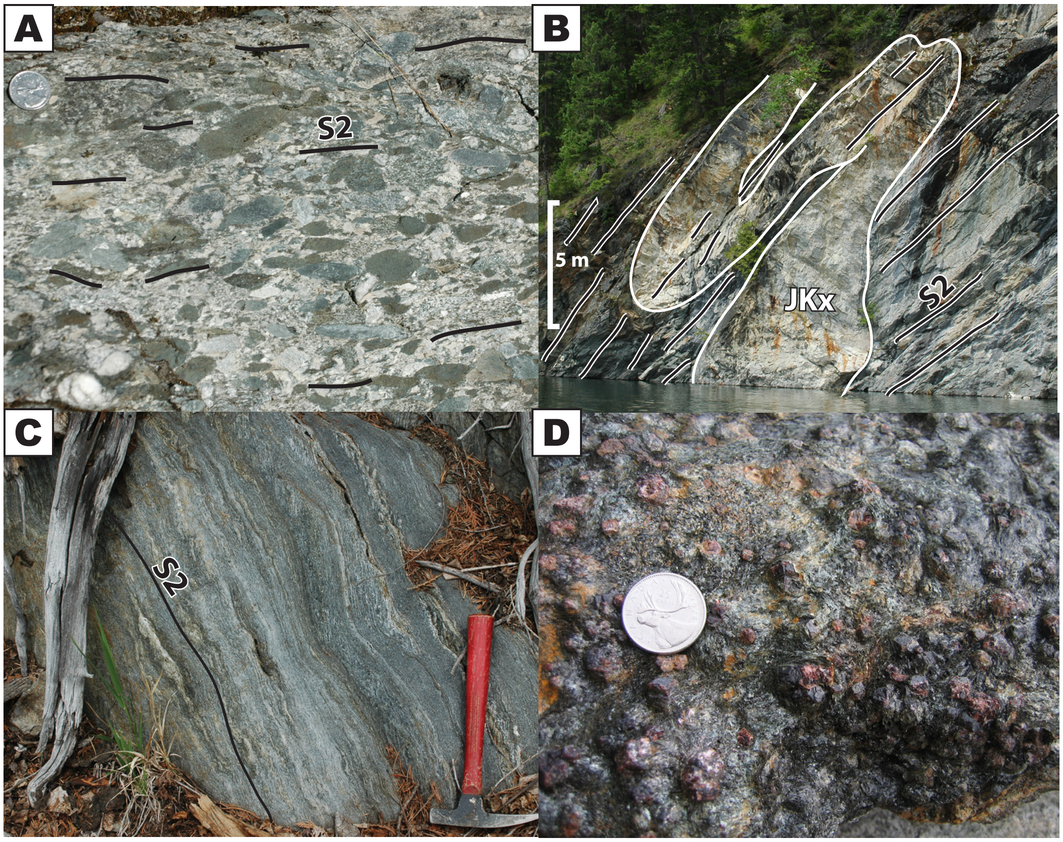

Figure 4-9. Strain and fabrics in the upper Mount Sproat assemblage.
A) Weak flattening of clasts in Upper Clastic member conglomerate, St Leon area. B) Isoclinally folded dike peripheral to the Kuskanax batholith or Galena Bay stock demonstrates intensity of post-Early Jurassic strain associated with S2. Host rock is calcareous amphibolitic schist of the Amphibolitic Schist member, Beaton Arm. C) S2 gneissosity in amphibolitic schist where D2 strain and metamorphism are greatest at the mouth of Beaton Arm. D) Garnet-biotite-muscovite schist from a metamorphosed equivalent of the Heterolithic member or a pelitic layer in the Amphibolitic Schist member, Halcyon Hot Springs. Mesozoic recrystallization is most significant in the Mount Sproat assemblage along Upper Arrow Lake.

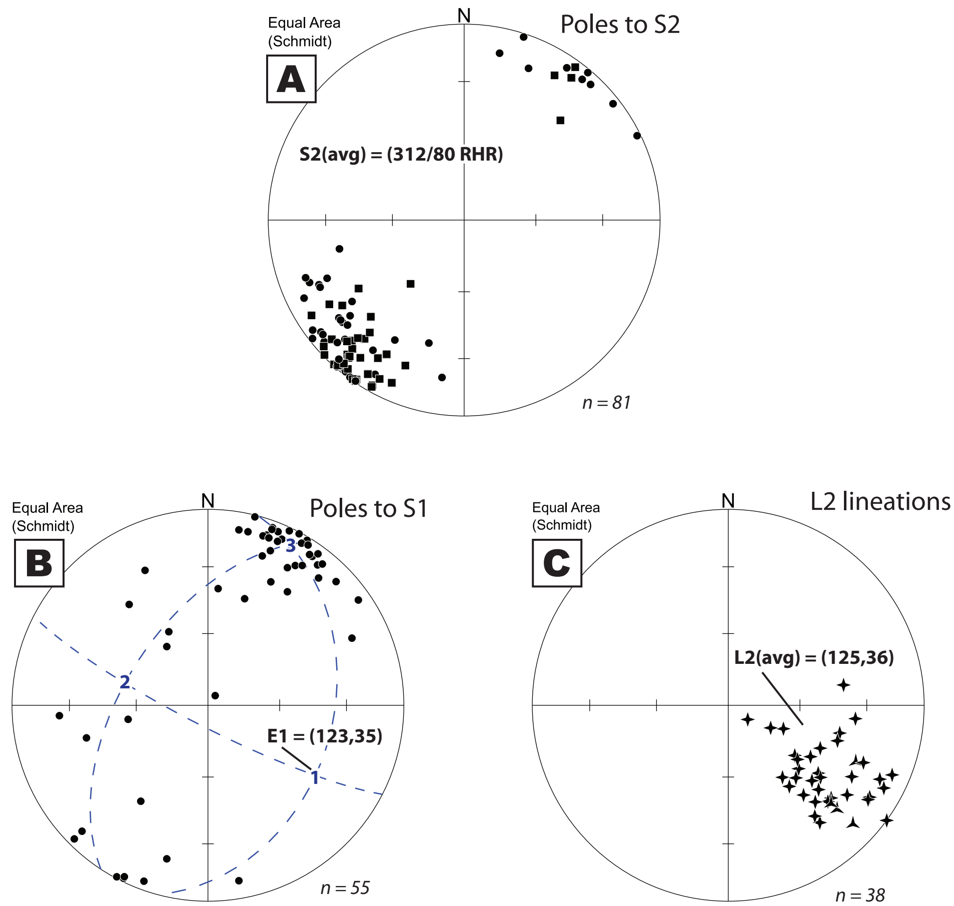

Figure 4-10. Equal area stereoplots of structural data from the Holyk antiform near Comaplix Mountain.
A) Poles to S2 cleavage, which is axial planar to the parasitic F2 folds. Weighted mean orientation is (312/80) in right-hand rule notation. Squares indicate measurements where S1 was not preserved. B) Poles to transposition foliation, S1. Although they are mainly clustered some measurements define a girdle. Eigenvector 1, the pole to the girdle and the fold axis, is (123,35). C) All F2 fold hinges and S1/S2 intersection lineations. Weighted average orientation is (125,36) - subparallel to the fold axis calculated from orientations of S1 in (B).

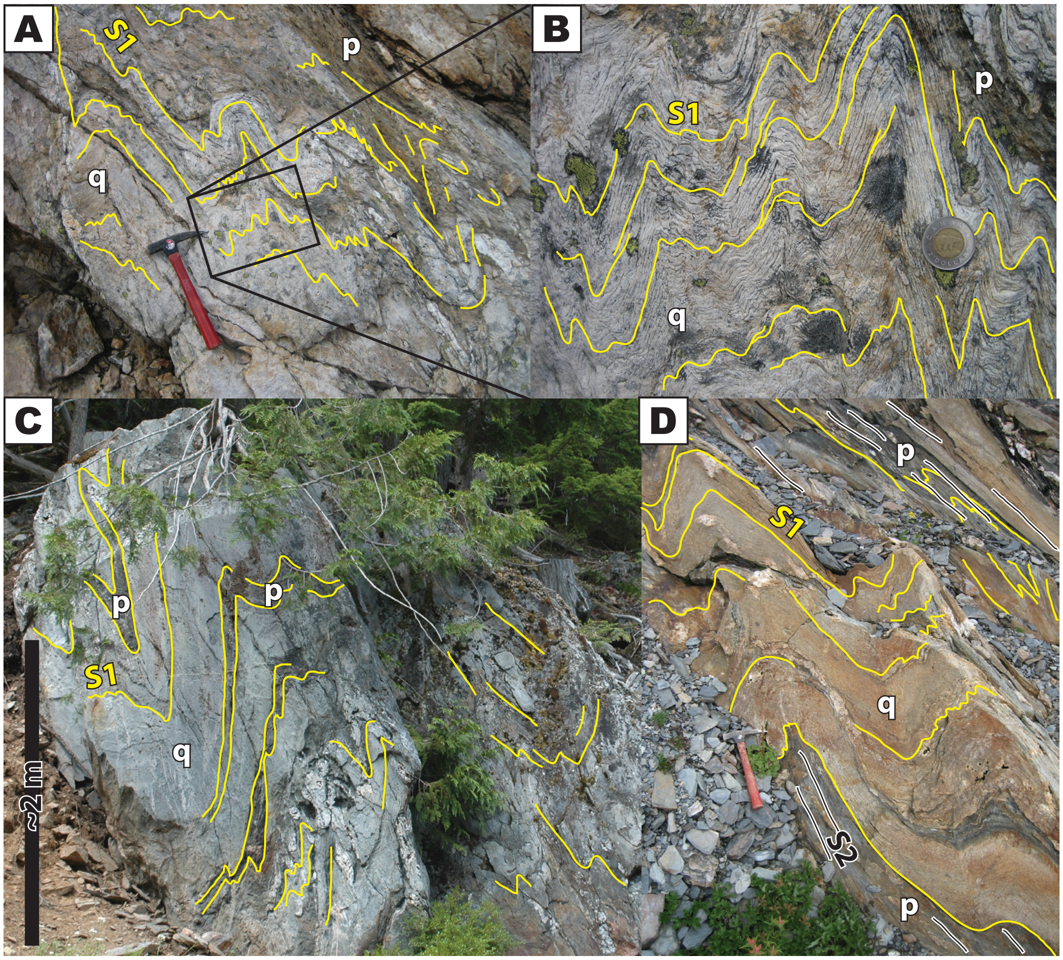

Figure 4-11. Mesoscopic F2 folds in the Broadview Formation.
Axial planar S2 cleavage is strong in interbedded phyllite but tends not to be well developed in quartzitic beds. A) Pseudo-laminated white weathering gritty quartzite in an inlier of Broadview Formation near Trout Mountain. B) Close-up of (A) showing distinctive phyllitic partings that define S1. The partings merge and terminate along distances of tens of cm's. C) Gritty quartzite with phyllitic bands in Asher Creek west of Trout Lake. D) Tan weathering gritty quartzite with phyllitic interbeds at McCrae Peak. Abbreviations: q, quartzite-grit; p, phyllite. Yellow lines trace S1 transposition foliation.

Figure 4-12. Strain in Mount Sproat assemblage conglomerate at Mount Sproat. A) Representative clast of massive quartzofeldspathic grit (or felsic igneous rock?) that lacks foliation. Unlike Milford conglomerate, no pre-depositionally foliated clasts were found in conglomerate in the MSA. B) View of a joint surface orthogonal to stretching lineation in the conglomerate. Green phyllitic matrix is strongly cleaved but quartzofeldspathic clasts appear to have little to zero tectonic flattening. Except for the pinched shape of clast above hammer, indicating moderate flattening into the cleavage. Stretching of a loose clast is indicated by the pink arrow. This outcrop is on the limb of the tight to isoclinal F2 Sproat antiform therefore S1 is parallel to, and has been transposed into, S2 here.

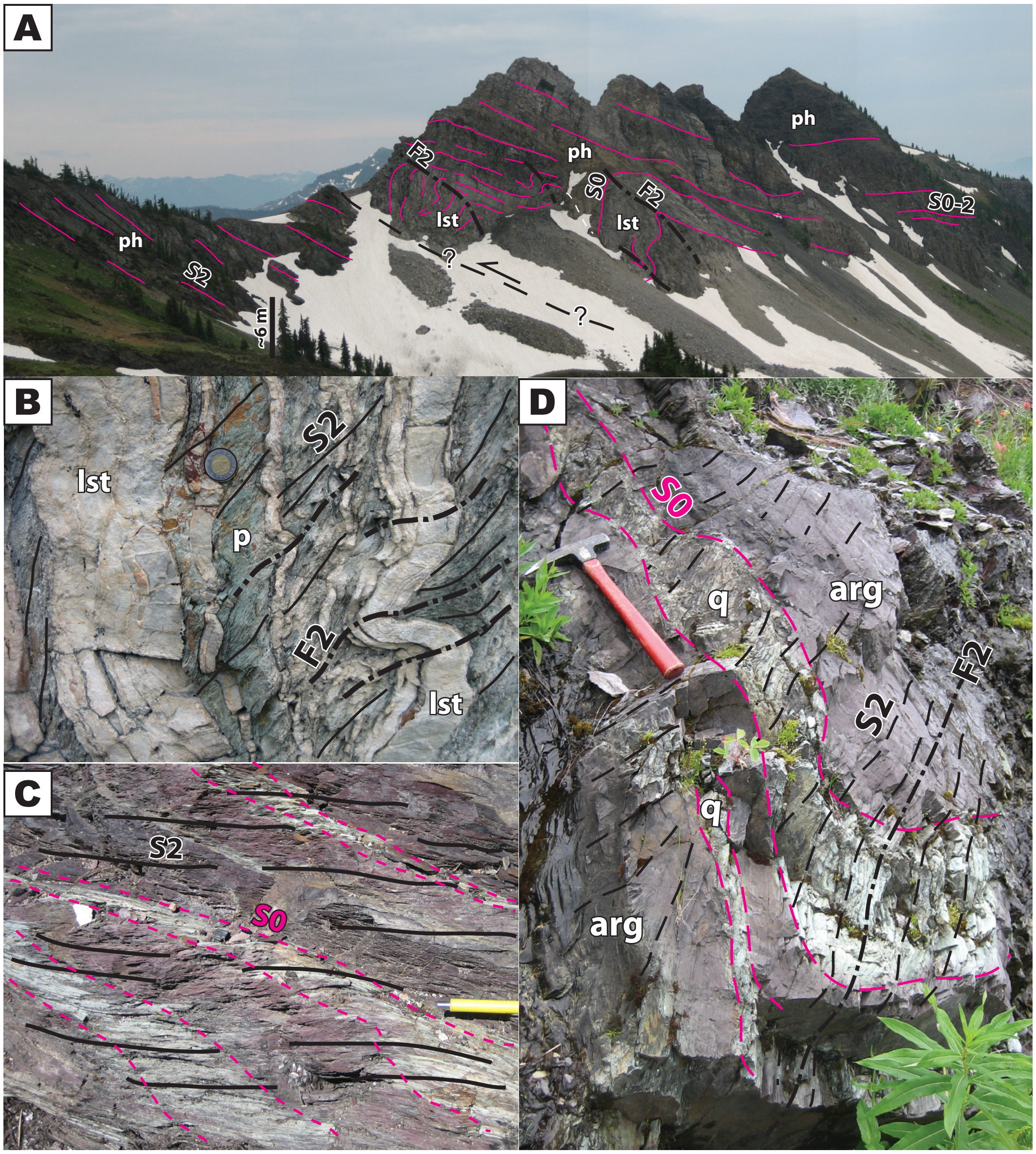

Figure 4-13. F2 folds in Mississippian strata in the Badshot Range.
A) Large (wavelength 20-30 m) asymmetric F2 folds outlined by limestone beds in the northern Davis assemblage at McCrae Peak. Asymmetry is consistent with location on the upright northern limb of the regional-scale Beaton syncline. Looking southeast. B) Disharmonically folded limestone beds in cleaved green phyllite, upper Thompson assemblage at Mount Thompson. Looking southeast. Asymmetry is consistent with location on the northeast limb of the F2 Beaton syncline. Coin for scale. C) Slaty cleavage, S2, is oblique to colour banding inferred to be relict bedding in maroon and pale green phyllite, Thompson assemblage. Colour banding where this unit is less strained corresponds to bedding. Tip of pen magnet for scale. D) Gently folded quartzite and maroon argillite in the Thompson assemblage have a well-developed axial planar cleavage, S2, and lack bedding-parallel foliation. Abbreviations: arg, argillite; lst, limestone; p, phyllite; q, quartzite.

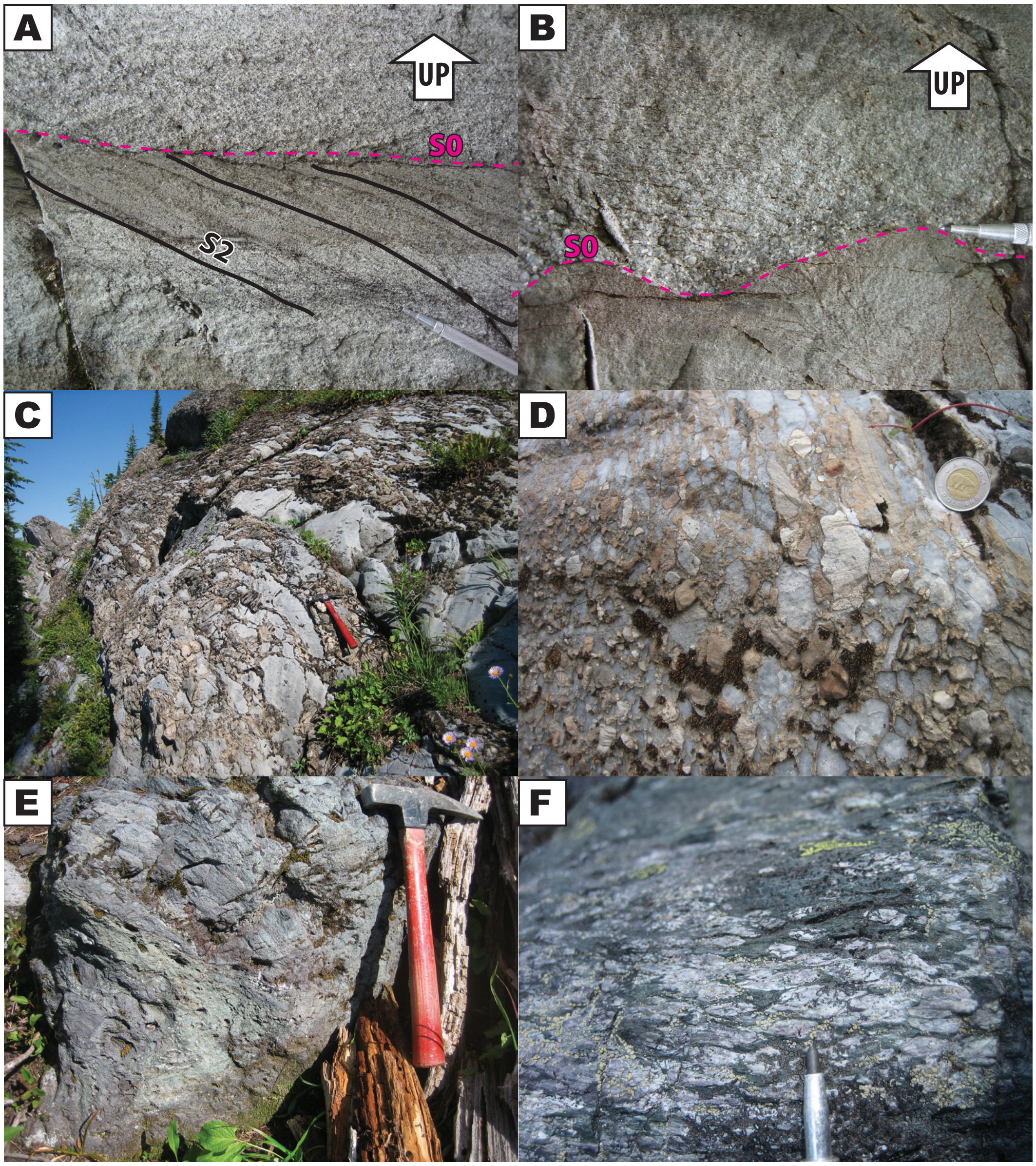

Figure 4-14. Primary features preserved in the Thompson assemblage at Mount Thompson.

A) Cleavage oblique to the bedding surface (in pink) between two normally graded beds. S2 cleavage formed only in the finer grained top of the lower bed. There is no foliation parallel to bedding. B) Undulating base of a graded bed of grit interpreted as a current scour mark, which appears undeformed. Foliation has not formed in this part of the outcrop, probably because of relatively coarse grain size. C) and D) Elongated fragments in rudstone or carbonate breccia. Flattening is minimal, unlike in the Lardeau Group. E) Igneous texture in weakly metamorphosed basalt. F) Strained amygdules in metabasalt.

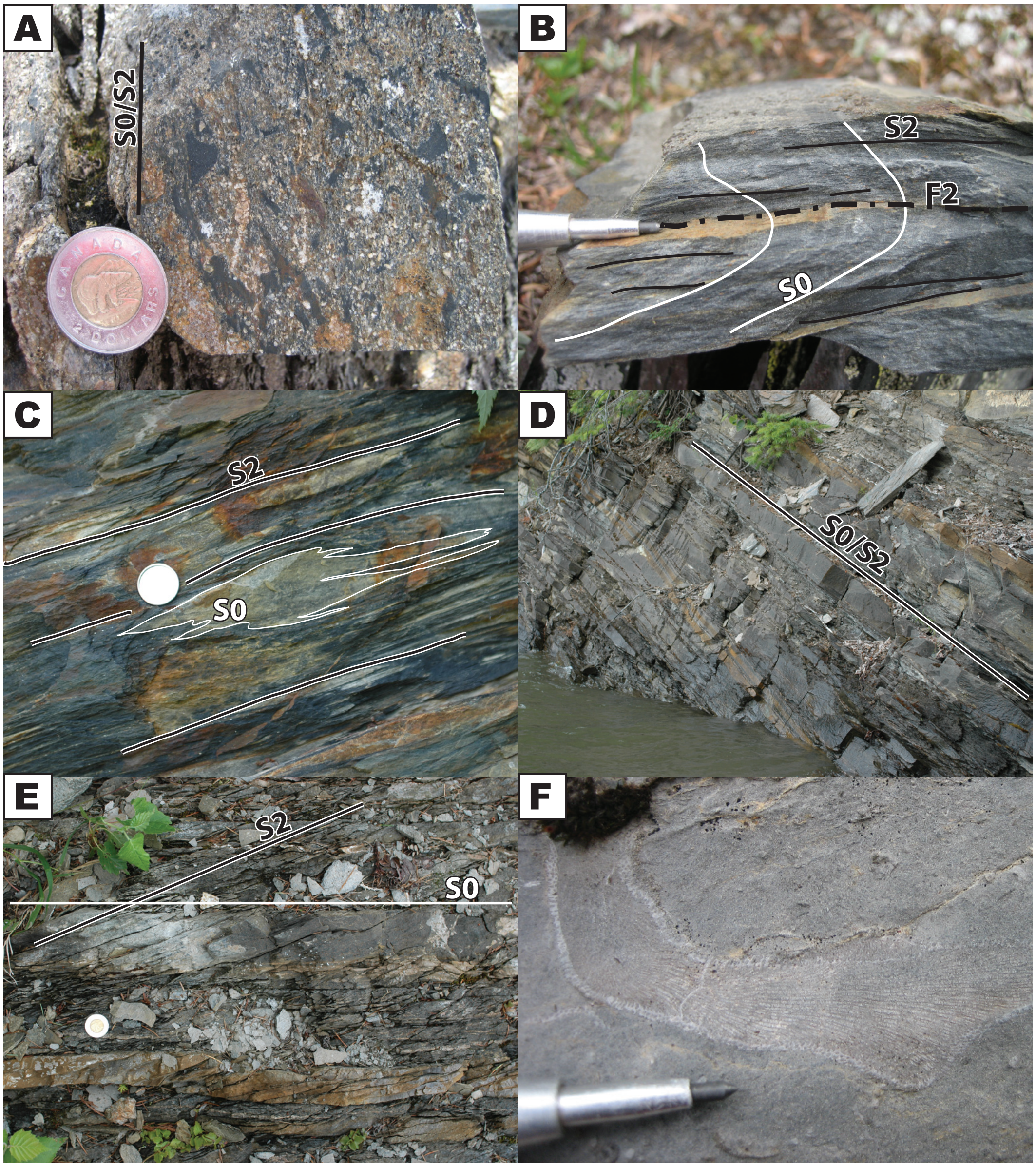

Figure 4-15. Strain in the Milford Group.
A) Lithic wacke with mudstone fragments shows only weak foliation parallel to layering (S0/S2). Northern McHardy assemblage, Trout Mountain area. B) Rare parasitic fold in laminated silty mudstone illustrates axial planar relationship of S2 to F2. Banding does not have a parallel tectonic fabric. Northern McHardy assemblage, Mount Murray area. C) Rootless folds and transposition of layering in argillite by a single fabric, S2. McHardy assemblage, Hill Creek area. D) Cleavage parallel to relatively undisturbed bedding in the northern Davis assemblage, Beaton Arm. E) Local discordance of S2 cleavage and bedding in the northern Davis assemblage, Beaton Arm. F) Delicate features of a bryozoan preserved in northern Davis assemblage limestone, Mount Thompson.

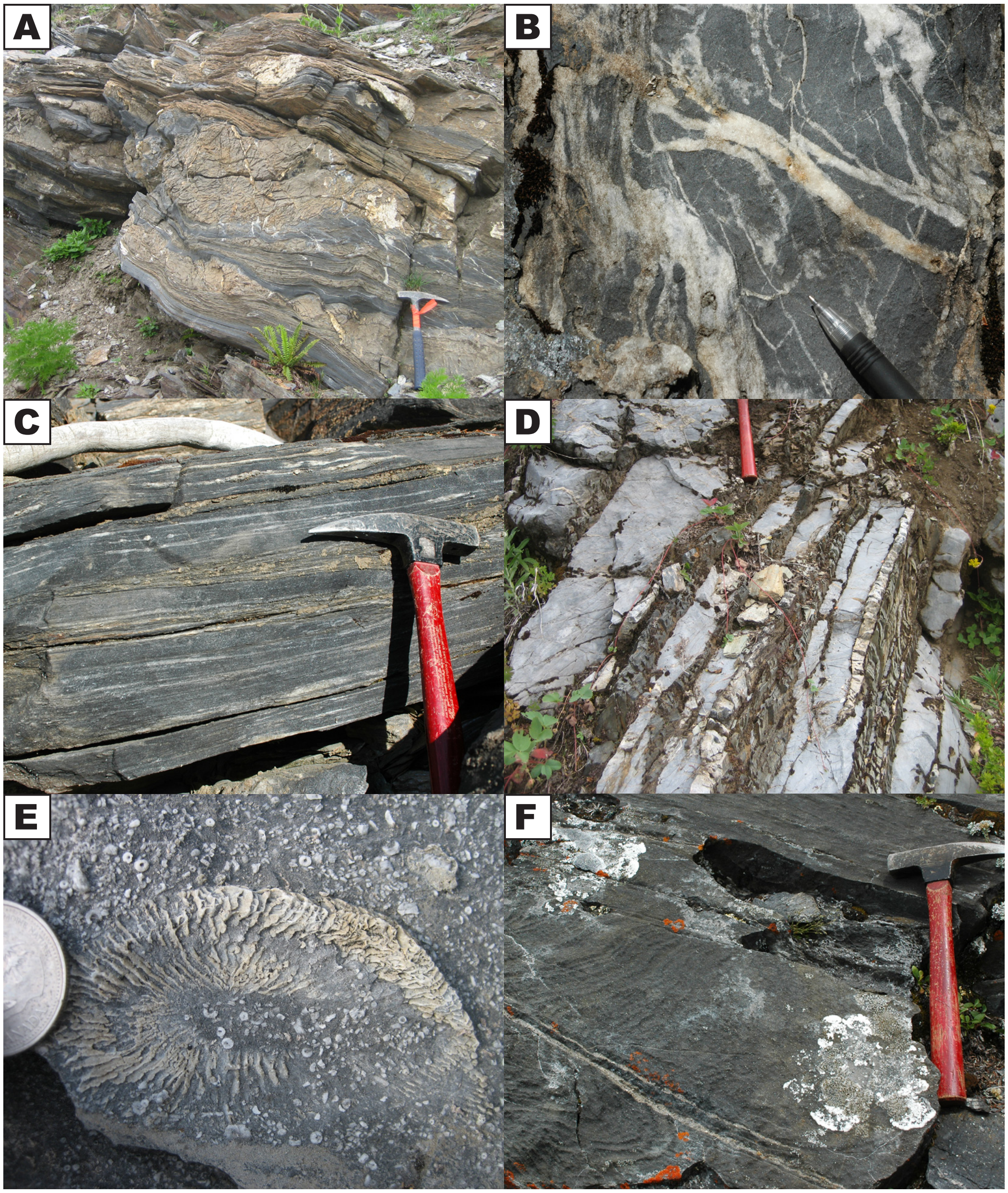

Figure 4-16. Contrasting recrystallization of carbonate units across the sub-Mississippian unconformity.

Below unconformity: A) Marble in the Broadview Formation at McCrae Peak. Dolomitic layers behaved more competently than dark grey calcitic marble. B) Carbonaceous marble with white calcite veins, Broadview Formation on the west shore of Trout Lake. C) Typical streaky foliation in carbonaceous marble in the Heterolithic member of the Mount Sproat assemblage at Beaton Arm.

Above unconformity: D) Light grey limestone with ribbon chert beds in the Thompson assemblage, Mount Thompson. E) Small crinoid ossicles and rugose coral in northern Davis limestone at McCrae Peak. F) Argillaceous limestone in the northern McHardy assemblage, Mount Murray.

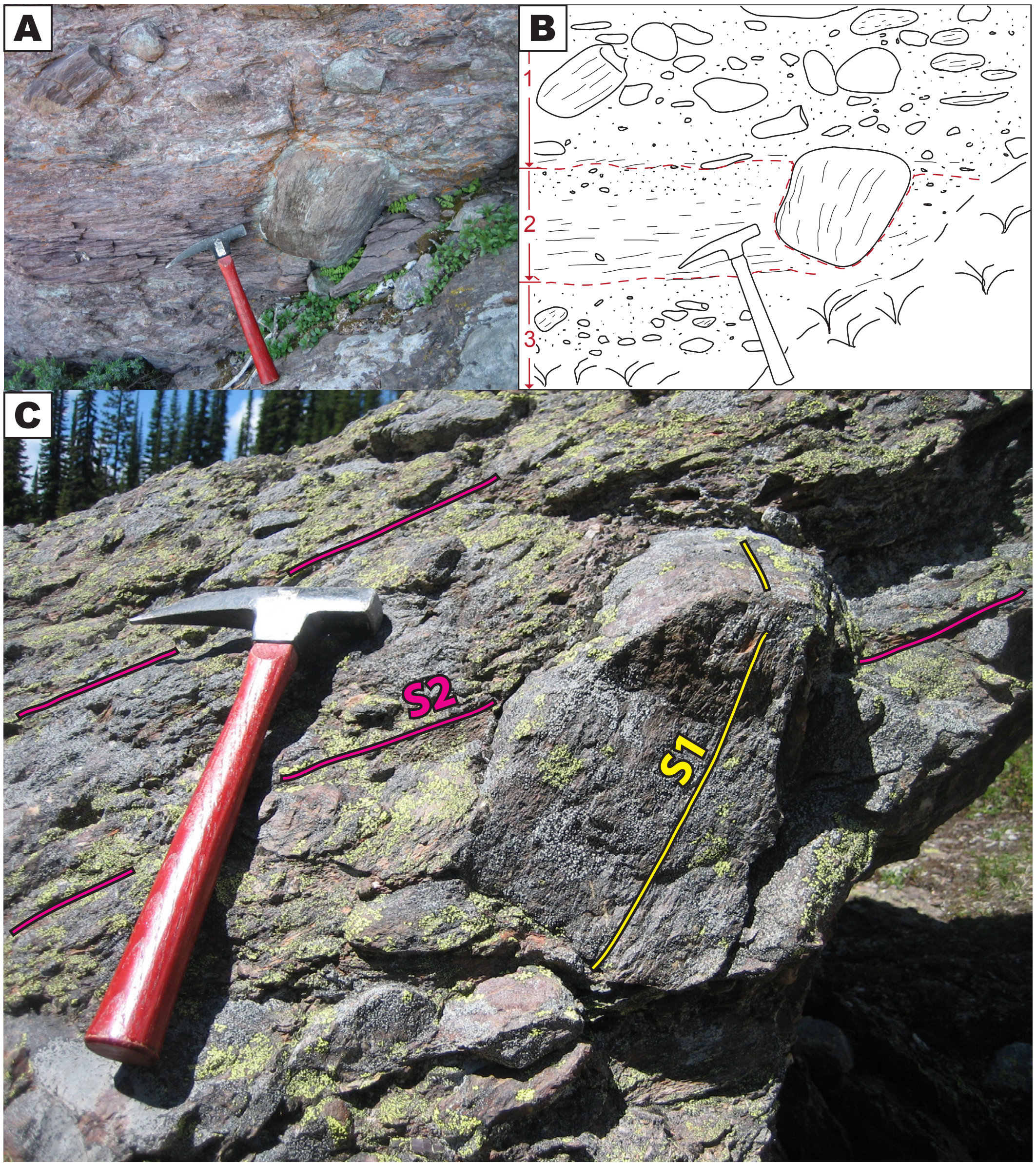

Figure 4-17. Clasts of Broadview Formation grit in the basal conglomerate of the northern Davis assemblage at Mount Thompson.

A) Structurally overturned sequence of three beds of Milford conglomerate. B) Interpretation of (A) that highlights the angularity of foliation within grit clasts relative to the cleavage in the matrix (subhorizontal). C) Well-developed foliation in a boulder of gritty quartzite is highly oblique to cleavage in the incompetent phyllitic matrix of the basal Milford conglomerate.

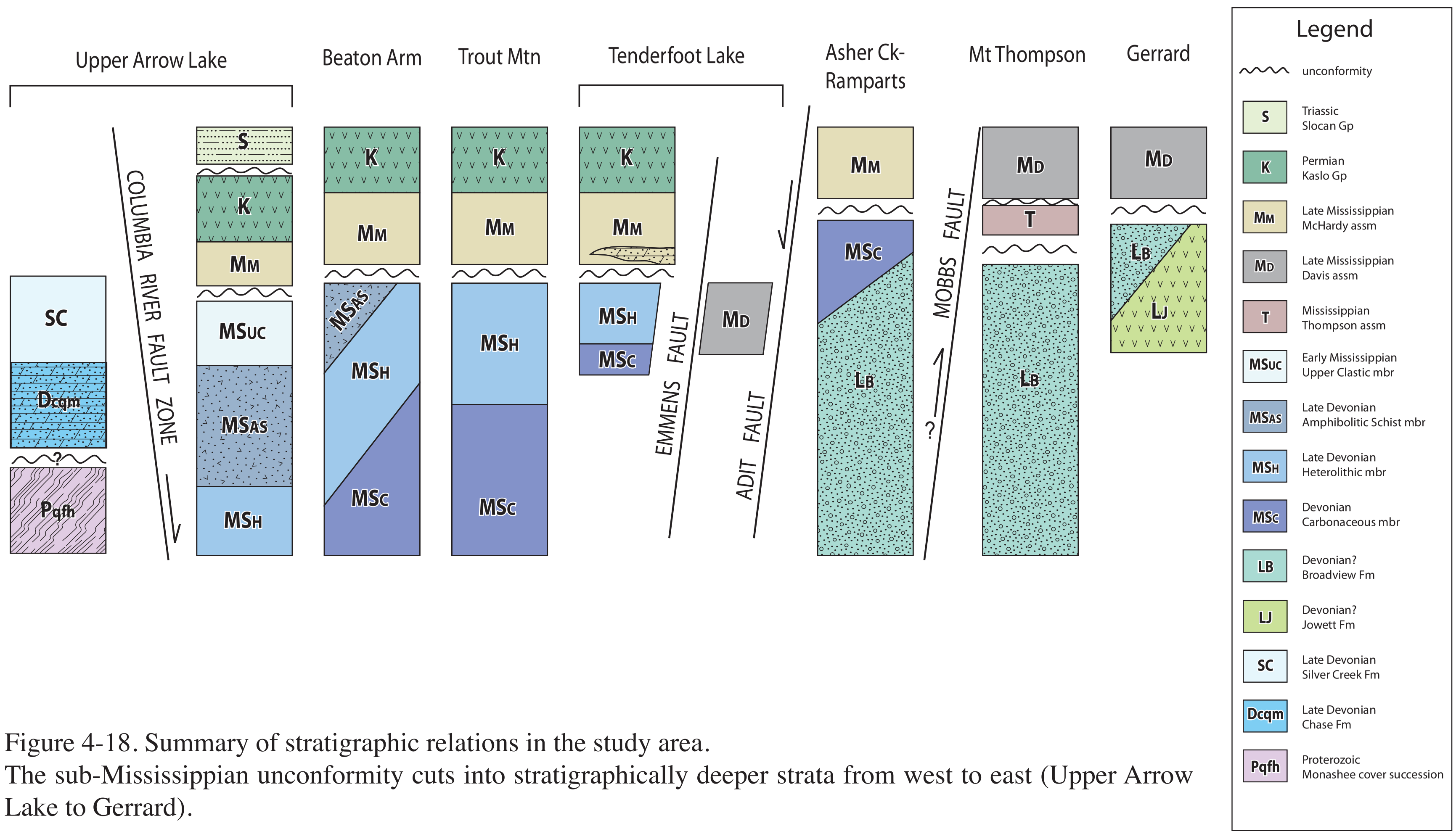

Figure 4-18. Summary of stratigraphic relations in the study area.
The sub-Mississippian unconformity cuts into stratigraphically deeper strata from west to east (Upper Arrow Lake to Gerrard).

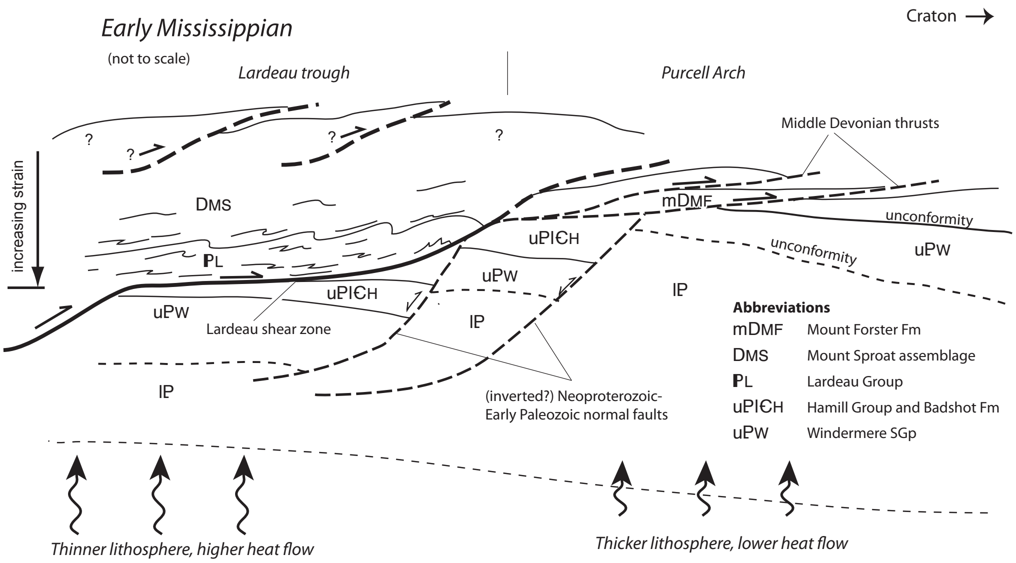

Figure 4-19. Interpreted nature of Mississippian deformation in the northern Kootenay Arc.

Penetrative, brittle-ductile deformation in the Lardeau trough contrasts with older brittle deformation of Devonian rocks atop the Windermere High. Strain is maximal in the Lardeau Group and diminishes upward becoming minor in the upper Mount Sproat assemblage. Shortening of Lardeau and MSA rocks was accommodated by displacement on the underlying Lardeau shear zone, which may have acted as a bedding-parallel detachment in the argillaceous Index Formation. Modest burial under the Mount Sproat assemblage, tectonic thickening and relatively high heat flow due to crustal attenuation and mantle convection in the back-arc beneath the Lardeau trough are inferred to have created brittle-ductile conditions of deformation and greenschist-facies metamorphism. Shortening concentrated in the Lardeau trough owing to 1) its relatively thin and weak lithosphere, which was weakened by Late Devonian back-arc extension and high heat flow, and 2) buttressing of Lardeau trough strata against the western flank of the Purcell Arch.

References

Beranek, L. P., Mortensen, J. K., Lane, L. S., Allen, T. , Fraser, T., Hadlari, T., and Zantvoort, W., 2010, Detrital zircon geochronology of the western Ellesmerian clastic wedge, northwestern Canada: Insights on Arctic tectonics and the mid-Paleozoic evolution of the northern Cordilleran miogeocline, Geological Society of America Bulletin, v. 122, p. 1899–1911, doi:10.1130/B30120.1.

Brown, R.L., Lane, L.S., Psutka, J.F. and Read, P.B., 1983, Stratigraphy and structure of the western margin of the northern Selkirk Mountains: Downie Creek map area, British Columbia: Geological Survey of Canada, Paper 83-1A, p. 203-206.

Brown, R.L., Journeay, J.M., Lane, L.S., Murphy, D.C. and Rees, C.J., 1986, Obduction, back folding and piggyback thrusting in the metamorphic hinterland of the southeastern Canadian Cordillera: Journal of Structural Geology, v. 8, p. 255-268.

Campbell, R.B., Mountjoy, E.W., and Young, F.G., 1973, Geology of the McBride map area, British Columbia: Geological Survey of Canada Paper 72-35, 104 p.

Colpron, M., 1996, Stratigraphy, structure and thermotectonic evolution of the western flank of the Selkirk fan structure, northern Selkirk Mountains, British Columbia: Ph.D. thesis, Queen's University, Kingston, Ontario, 162 p.

Colpron, M. and Price, R.A., 1995, Tectonic significance of the Kootenay terrane, southeastern Canadian Cordillera: An alternative model: Geology, v. 23, p. 25-28.

Currie, C.A., Wang, K., Hyndman, R.D., and He, J., 2004, The thermal effects of slab driven mantle flow above a subducting plate: The Cascadia subduction zone and backarc: Earth and Planetary Science Letters, v. 223, p. 35–48, doi: 10.1016/j.epsl.2004.04.020.

Eisbacher, G.H., 1983, Devonian-Mississippian sinistral transcurrent faulting along the cratonic margin of western North America: A hypothesis: Geology, v. 11, p. 7-10.

Fyles, J.T., 1964, Geology of the Duncan Lake area, Lardeau District, British Columbia: British Columbia Department of Mines and Petroleum Resources, Bulletin 49, 87 p.

Fyles, J.T. and Eastwood, G.E.P., 1962, Geology of the Ferguson area, Lardeau district, British Columbia: B.C. Department of Mines and Petroleum

Resources, Bulletin 45, 92 p.

Glombick, P., Thompson, R. I., Erdmer, P., Heaman, L., Friedman, R. M., Villeneuve, M., and Daughtry, K. L., 2006, U–Pb constraints on the thermotectonic evolution of the Vernon antiform and the age of the Aberdeen gneiss complex, southeastern Canadian Cordillera: Canadian Journal of Earth Sciences, v. 43, p. 213-244.

Gordey, S., Abbott, J., Tempelman-Kluit, D., and Gabrielse, H., 1987, " Antler" elastics in the Canadian Cordillera: Geology, v. 15, p. 103.

Grayston, L.D., Sherwin, D.F., and Allan, J.F., 1965, Middle Devonian; *in* Geological History of Western Canada, Alberta Society of Petroleum Geologists, p. 49-59

Hoffman, P., 1988, United plates of America, the birth of a craton: Early Proterozoic assembly and growth of Laurentia: Annual Review of Earth and Planetary Sciences, v. 16, p. 543–603.

Hyndman, R.D., and Lewis, T.S., 1999, Geophysical conse- quences of the Cordillera-Craton thermal transition in S.W. Canada: Tectonophysics, v. 306, p. 397–422, doi: 10.1016/ S0040-1951(99)00068-2.

Johnson, B. J., 2004, Structure and tectonic setting of the Okanagan Valley fault system in the Shuswap Lake area, southern British Columbia, Ph.D. thesis, Carleton University, Ottawa, ON.

Johnson, B. J., 2006, Extensional shear zones, granitic melts, and linkage of overstepping normal faults bounding the Shuswap metamorphic core complex, British Columbia: Geological Society of America Bulletin, v. 118, p. 366-382, doi: 10.1130/B25800.1

Johnson, J. G., and Pendergast, A. 1981, Timing and mode of emplacement of the Roberts Mountains allochthon, Antler orogeny: Geological Society of America Bulletin, v. 92, p. 648-658.

Klepacki, D.W., 1985, Stratigraphy and structural geology of the Goat Range area, southeastern British Columbia. Ph.D. thesis, Massachusetts Institute of Technology, Cambridge, Mass.

Kraft, J. L., Thompson, R. I., and Dhesi, P. (compilers), 2011, Geology, Beaton, British Columbia; Geological Survey of Canada, Open File, 6574, scale 1:50 000, doi: 10.4095/288009.

Logan, J., and Colpron, M., 2006, Stratigraphy, geochemistry, syngenetic sulphide occurrences and tectonic setting of the lower Paleozoic Lardeau Group, northern Selkirk Mountains, British Columbia: *in* Colpron, M. and Nelson, J.L., eds., Paleozoic Evolution and Metallogeny of Pericratonic Terranes at the Ancient Pacific Margin of North America, Canadian and Alaskan Cordillera: Geological Association of Canada, Special Paper 45, v. 45, p. 361–382.

Mair, J. L., Hart, C. J. R., and Stephens, J. R., 2006, Deformation history of the northwestern Selwyn Basin, Yukon, Canada: Implications for orogen evolution and mid-Cretaceous magmatism: Geological Society of America Bulletin, v. 118, p. 304-323, doi: 10.1130/B25763.1

Miller, E.L., Holdsworth, B.K., Whiteford, W.B., and Rogers, D., 1984, Stratigraphy and structure of the Schoonover sequence, northeastern Nevada: Implications for Paleozoic plate margin tectonics: Geological Society of America Bulletin, v. 95, p. 1063-1076.

Murphy, D.C., van der Heyden, P., Parrish, R.R., Klepacki, D.W., McMillan, W., Struik, L.C. and Gabites, J., 1995, New geochronological constraints on Jurassic deformation of the western edge of North America, southeastern Canadian Cordillera, *in* Miller, D.M. and Busby, C., eds., Jurassic Magmatism and Tectonics of the North American Cordillera: Geological Society of America, Special Paper 299, p. 159-171.

Nelson, J.L., Colpron, M., Piercey, S.J., Dusel-Bacon, C., Murphy, D.C. and Roots, C.F., 2006, Paleozoic tectonic and metallogenic evolution of the pericratonic terranes in Yukon, northern British Columbia and eastern Alaska: *in* Colpron, M. and Nelson, J.L., eds., Paleozoic Evolution and Metallogeny of Pericratonic Terranes at the Ancient Pacific Margin of North America, Canadian and Alaskan Cordillera: Geological Association of Canada, Special Paper 45, p. 323-360.

Okulitch, A. V., 1985, Stratigraphy and structure of the western margin of the Shuswap metamorphic complex, Vernon (82L) and Seymour Arm (82M) map-areas, British Columbia, Geological Survey of Canada Paper 75-1, Part A, p. 27-28.

Orchard, M.J. 1985, Carboniferous, Permian and Triassic conodonts from the Central Kootenay Arc, British Columbia : constraints on the age of the Milford, Kaslo, and Slocan groups. *In* Current Research, Part A. Geological Survey of Canada, Paper 85-1A, p. 287-300.

Parrish, R., and Armstrong, R.L. 1987, The ca. 162 Ma Galena Bay stock and its relationships to the Columbia River fault zone, southeast British Columbia: *in* Radiogenic Age and Isotopic Studies: Report 1, Geological Survey of Canada Paper 87-2, p. 25-32.

Read, P.B., 1973, Petrology and structure of Poplar Creek map-area, British Columbia. Geological Survey of Canada Bulletin 193.

Read, P.B. 1975. Lardeau Group, Lardeau map-area, west half (82K west half), British Columbia. Geological Survey of Canada, Paper 75-1, Part A, p. 29-30.

Read, P.B. 1976, Lardeau map-area (82K west half), British Columbia. Geological Survey of Canada, Paper 76-1, Part A, p. 95-96.

Read, P.B., and Wheeler, J.O., 1976, Geology, Lardeau west-half, British Columbia. Geological Survey of Canada Open File 432.

Read, P.B., Psutka, J.F., Fyles, J.T., and MacLeod, R.F, 2009, Geology, MAX Molybdenum Mine area (NTS 82K/12), British Columbia; Geological Survey of Canada, Open file 6215, 2 sheets, 1:10 000 scale, and 1 report, 21 p.

Richards, B.C, Barclay, J. E., Bryan, D., Hartling, A., Henderson, C. M., and Hinds, R. C., 1994, Carboniferous strata of the Western Canada Sedimentary Basin: *in* Geological Atlas of the Western Canada Sedimentary Basin. Mossop, G. D. and Shetsen I. (compilers), Calgary, Canadian Society of Petroleum Geologists and Alberta Research Council, Chapter 14.

Richards, B.C., Ross, G.M. and Utting, J., 2002, U-Pb geochronology, lithostratigraphy and biostratigraphy of tuff in the upper Fammenian to Tournaisian Exshaw Formation: Evidence for a mid-Paleozoic magmatic arc on the northwestern margin of North America, *in* Hills, L.V., Henderson, C.M. and Bamber, E.W., eds, Carboniferous and Permian of the World: Canadian Society of Petroleum Geologists, Memoir 19, p. 158-207.

Roback, R.C., 1993, Late Paleozoic to middle Mesozoic tectonic evolution of the Kootenay arc, northeastern Washington and southeastern British Columbia: PhD thesis, University of Texas, Austin, Texas, 237 p.

Roberts, R.J., Hotz, P.E., Gilluly, J., and Furgusan, H.G., 1958, Paleozoic rocks of north central Nevada: American Association of Petroleum Geologists Bulletin, v. 42, p. 2813-2857.

Root, K., 1987, Geology of the Delphine Creek area, southeastern British Columbia: Implications for the Proterozoic and Paleozoic development of the Cordilleran divergent margin: unpublished Ph.D. thesis, University of Calgary, Calgary, AB.

Root, K., 2001, Devonian Antler fold and thrust belt and foreland basin development in the southern Canadian Cordillera: implications for the Western Canada Sedimentary Basin: Bulletin of Canadian Petroleum Geology, v. 49, p. 7-36.

Schiarizza, P. and Preto, V.A., 1987, Geology of the Adams Plateau-Clearwater-Vavenby area: B.C. Geological Survey Branch, Paper 1987-2, 88 p.

Scholz, C. H., 1988, The brittle-plastic transition and the depth of seismic faulting:

Geologisches Rundschau, v. 77, p. 319-328.

Sears, J.W., 1979, Tectonic contrasts between the infrastructure and suprastructure of the Columbian orogen, Albert Peak area, western Selkirk Mountains, British Columbia: Ph.D. thesis, Queen's University, Kingston, Ontario, 154 p.

Simony, P.S., Sevigny, J.H., Mortensen, J.K. and Roback, R.C., 2006, Age and origin of the Trail Gneiss Complex: Basement to Quesnel terrane near Trail, southeastern British Columbia, *in* Colpron, M. and Nelson, J.L., eds., Paleozoic Evolution and Metallogeny of Pericratonic Terranes at the Ancient Pacific Margin of North America, Canadian and Alaskan Cordillera: Geological Association of Canada, Special Paper 45, p. 505-515.

Slemko, N. M., 2000, Structural, Metamorphic, and Plutonic History o f Rocks Adjacent to Shuswap Lake, British Columbia: Evidence of Early to Middle Paleozoic Deformation: M.Sc. thesis, University of Alberta, Edmonton, AB.

Smith, M. T. 1990, Stratigraphic, structural, and U-Pb geochronologic investigation of lower Paleozoic eugeoclinal strata in the Kootenay Arc, southeastern British Columbia and northeastern Washington. Ph.D. dissertation, University of Arizona, Tucson.

Smith, M. T., and Gehrels, G. E., 1992, Structural geology of the Lardeau Group near Trout Lake, British Columbia: implications for the structural evolution of the Kootenay Arc. Canadian Journal of Earth Sciences, v. 29, p. 1305- 1319.

Smith, M., Dickinson, W., and Gehrels, G., 1993, Contractional nature of Devonian-Mississippian Antler tectonism along the North American continental margin: Geology, v. 21, no. 1, p. 21.

Struik, L.C., 1981, A reexamination of the type area of the Devono-Mississippian Cariboo orogeny, central British Columbia: Canadian Journal of Earth Sciences, v. 18, p. 1767-1775.

Thompson, R. I., 1978, Geology of the Akolkolex River area: B.C. Ministry of Energy, Mines and Petroleum Resources, Bulletin 60, 77 p.

Thompson, R.I., Glombick, P., Daughtry, K.L., and Erdmer, P. 2001. Upper Paleozoic stratigraphic linkage between Kootenay Arc and "Vernon Antiform": new constraints on southern Canadian Cordilleran evolution: *in* Proceedings of the 2001 SNORCLE Transect and Cordilleran Tectonics Workshop, Sidney, B.C., 25–27 February 2001. Lithoprobe Secretariat, The University of British Columbia, Vancouver, BC, Lithoprobe Report 79, p. 104–105.

Thompson, R.I., Glombick, P., Erdmer, P., Heaman, L. M., Lemieux, Y., and Daughtry, K. L., 2006, Evolution of the ancestral Pacific margin, southern Canadian Cordillera: Insights from new geologic maps: *in* Colpron, M. and

Nelson, J.L., eds., Paleozoic Evolution and Metallogeny of Pericratonic Terranes at the Ancient Pacific Margin of North America, Canadian and Alaskan Cordillera: Geological Association of Canada, Special Paper 45, p. 433-482.

Thorsteinsson, R., and Tozer, E.T., 1970, Geology of the Arctic Archipelago: *in* Douglas, R.J.W, ed., Geology and Economic Minerals of Canada: Geological Survey of Canada Economic Geology Report 1, p. 547–590.

Trettin, H.P., Okulitch, A.V., Harrison, J.C., Brent, T.A., Fox, F.G., Packard, J.J., Smith, G.P., and Zolnai, A.I., 1991, Silurian–early Carboniferous deformational phases and associated metamorphism and plutonism, Arctic Islands, *in* Trettin, H.P., ed., Geology of the Innuitian Orogen and Arctic Platform of Canada and Greenland: Geological Survey of Canada, Geology of Canada, v. 3, p. 293–341.

Wheeler, J.O., 1963, Rogers Pass map-area, British Columbia and Alberta (82N west-half): Geological Survey of Canada, Paper 62-32, 32 p.

Wheeler, J. O., 1968, Lardeau (west half) map-area, British Columbia (82K W112). *In* Report of activities, part A**.** Geological Survey of Canada, Paper 68-lA, p. 56-58.

White, W.H., 1959, Cordilleran tectonics in British Columbia: American Association of Petroleum Geologists Bulletin, v. 43, p. 60-100.

Chapter 5: Detrital zircon provenance of Cryogenian to Triassic Cordilleran pericratonic rocks of southeastern British Columbia: implications for paleogeography

5.1 Introduction

This study investigates the detrital zircon provenance of pericratonic strata in southeastern British Columbia interpreted to have formed in Cryogenian to Triassic basins on the ancestral Pacific margin of North America. These rocks represent the most distal North American continental strata of their ages preserved in the southern Canadian Cordillera and are therefore ideally suited to studying the ancestral plate margin.

The Devonian Chase Formation quartzite in the North Okanagan-Shuswap region has been described as a parautochthonous outboard facies equivalent of the Cordilleran miogeocline that depositionally overlies Proterozoic North American rocks (Thompson et al., 2006; Lemieux et al., 2007). Its detrital zircon characteristics (Lemieux et al., 2007), however, are unique in the southern Canadian Cordillera and can be interpreted to reflect an origin not within western Laurentia (Colpron and Nelson, 2009). With the Chase Formation detrital zircon data, Grenville-age and late Ediacaran granitic clasts in the Nicola Horst (Erdmer et al., 2002) have been used as evidence that an exotic terrane underlies the Mesozoic Quesnel arc in southern British Columbia (Colpron and Nelson, 2009).

Detrital zircon age analysis is used to make inferences about paleogeography because it can establish depositional links between sedimentary strata and potential sediment source regions (e.g. Fedo et al., 2003; Cawood et al., 2007). In the study of accretionary orogens this can be useful to identify possible clastic input from continents or arcs that may have no obvious geological connection to far-travelled terranes (e.g. Wright and Wyld, 2006; Nelson and Gehrels, 2007; Grove et al., 2008). Previous detrital zircon studies in southeastern British Columbia were performed by resource-intensive isotope dilution – thermal ionization mass spectrometry (ID-TIMS) age determinations on both multi-grain and single grain fractions of zircon (Figure 5-2; e.g., Ross and Bowring, 1990; Smith and Gehrels, 1991). Consequently, earlier datasets are limited in their analytical statistics relative to newer studies, which typically utilize faster and more economical laser ablation inductively-coupled plasma mass spectrometry (LA-ICP-MS), the method that was employed in this study. This paper presents over 1200 detrital zircon U-Pb dates measured by laser ablation ICP-MS from thirteen samples of outer miogeocline and pericratonic strata from southeastern British Columbia. The samples include ten from the northern Kootenay Arc, one from the type locality of the Late Devonian Chase Formation near Shuswap

Lake and one sample each from the Cryogenian Toby Formation (Windermere Supergroup) and the Middle Devonian Mount Forster Formation.

This study aimed to enhance a previously sparse dataset of detrital zircon dates from southeastern British Columbia to better constrain the paleogeography of pericratonic rocks exposed there and, in particular, address the question of the Chase Formation's origin. Investigation of the Lardeau Group sought to test the hypothesis that emergent continental crust existed outboard of the southern British Columbia miogeocline during the Paleozoic (e.g., Struik, 1987; Unterschutz et al., 2002; Erdmer et al., 2002; Thompson et al., 2006; Lemieux et al., 2007). The new zircon data show that the Paleozoic pericratonic rocks of southeastern British Columbia share a significant component of zircon provenance with nearby miogeoclinal rocks, but have additional zircon populations that are interpreted here to reflect crustal sources outboard of rocks preserved today in the Kootenay Arc.

5.2 Previous work

The ancient edge of the North American craton

Palinspastic restoration of the Rocky Mountain fold and thrust belt places pericratonic Kootenay Arc strata outboard of a geophysically-imaged crustal ramp located near the Okanagan valley that has been inferred to be the edge of the North American craton (Price, 1994; Price, 2007). Alternatively, interpretation of deep seismic crustal profiles led Cook et al. (1992; 2005) to conclude that attenuated North American crust presently extends hundreds of kilometres outboard of that crustal ramp and that Cordilleran orogenesis may have shortened rather than added to the western edge of the North American plate.

On the basis of lithostratigraphic, isotopic, geochronological, and geochemical characteristics of pericratonic rocks in southeastern British Columbia, Precambrian sialic crust is hypothesized to have formed an offshore continental block or ribbon west of the Cordilleran miogeocline and to have been buried either depositionally or tectonically beneath Late Paleozoic and younger arc and basinal rocks (e.g., Read and Wheeler, 1976; Okulitch, 1984; Struik, 1987; Unterschutz et al., 2002; Erdmer et al., 2002; Thompson et al., 2006; Lemieux et al., 2007). Thompson et al. (2006) and Read and Wheeler (1976) proposed that the lower to mid-Paleozoic Lardeau Group in the Kootenay Arc of southeastern

British Columbia was sourced from this outboard high, which was dubbed the Okanagan high by Thompson et al. (2006; Figure 1-4). Devonian calcareous quartzite of the Chase Formation in southern British Columbia has also been interpreted to derive from erosion of the Okanagan high (Thompson et al., 2006; Lemieux et al., 2007).

Previous detrital zircon data

Dates of detrital zircon from strata of the Neoproterozoic and Early Paleozoic Cordilleran miogeocline have been interpreted to reflect the ages of basement domains in the adjacent Precambrian shield (Ross and Bowring, 1990; Gehrels and Ross, 1998; Stewart et al., 2001). In the southern Canadian Cordillera, this 'signature' is a bimodal distribution of Paleoproterozoic (~2.0-1.75 Ga; dominant group) and Neoarchean (~2.9-2.55 Ga; subordinate group) dates that is considered to mirror the Precambrian basement buried beneath younger cover rocks in western Canada (Ross and Bowring, 1990; Gehrels and Ross, 1998).

The previous nine single grain detrital zircon dates from the Lardeau Group (Ajax and Broadview formations; Smith and Gehrels, 1991) and 57 dates from the Milford Group in the northern Goat Range (McHardy assemblage; Roback et al., 1994; Lemieux et al., 2007, sample 04TWL072 interpreted to be Chase Formation) were interpreted to have ultimate derivation from the adjacent Alberta basement. Unlike the McHardy assemblage samples, the Davis assemblage yielded zircons from 1.6-1.2 Ga in addition to Paleoproterozoic and Archean dates. Detrital zircons and granitoid boulders from the lithologically unique Cooper conglomerate in the Milford Group show that Silurian felsic plutons were a significant source of detritus for at least part of the Milford Group (Figure 5-1; Roback et al., 1994).

Thompson et al. (2006) presented 2 near concordant ID-TIMS dates for detrital zircons (ca. 423 Ma and 1000 Ma) from the type locality of the Chase Formation. Lemieux et al. (2007) reported 50 additional LA-ICP-MS detrital zircon dates (<10% discordant) from three samples of the Chase Formation in the Monashee Mountains and at Upper Arrow Lake. Although limited in statistics, the distribution of zircon dates in the three Chase Formation samples is broadly consistent. Collectively, those data form a broad distribution of Late Paleoproterozoic to Early Neoproterozoic dates, plus several Silurian grains (Figure 5-2). A fourth sample attributed to the Chase Formation by Lemieux et al. (2007) came from a horizon of calcareous quartzite that in Chapter 2 was shown to occur within the Late Mississippian Milford Group near Tenderfoot Lake. This 'Tenderfoot quartzite' sample yielded Paleoproterozoic and Archean detrital zircon dates similar to miogeoclinal rocks and unlike the Chase Formation (Figure 5-2). Amphibolite-facies biotite-quartz-feldspar paragneiss that underlies the Chase Formation-equivalent in the Monashee Mountains has a dominant mode at 1.80 Ga plus trace Neoarchean and Grenville-age zircons (Lemieux et al., 2007).

Mesoproterozoic crust in the Canadian Cordillera?

Mesoproterozoic igneous and metamorphic rocks from the period 1.3-1.0 Ga are widespread globally in major orogenic belts formed by assembly of the hypothesized supercontinent Rodinia (e.g. Grenville, Sunsas, Sveconorwegian, Sibao orogens), but basement rocks of that age appear not to occur in northwestern Laurentia (Hoffman, 1988; Ross et al., 1991; Ross, 1991) and are unknown in the North American Cordillera north of Mexico. Samples from drill core that penetrated the Alberta basement (Ross et al., 1991) and the near absence of Grenville-age detrital zircons in the clastic rocks of the Western Canada Sedimentary Basin (Gehrels and Ross, 1998; Gehrels, unpublished data) indicate that a significant volume of Grenville-age crust does not occur in the Precambrian basement of western Canada. Nonetheless, Grenville-age zircons have been reported from diverse sources in the Canadian Cordillera, including: Paleozoic clastic metasedimentary strata (e.g., Ross et al., 2005; Lemieux et al., 2007; Brown et al., 2010), granitic cobbles in conglomerate (Figure 5-1; Erdmer et al., 2002; D. Murphy, unpublished data), lower crustal granitic xenoliths (Jefferson and Parrish, 1989; Mortensen and Colpron, 1998), lower crustal gneissic xenoliths (Milidragovic et al., 2011) and in the form of xenocrysts in diatremes (Parrish and Reichenbach, 1991). The extent and origin of buried Grenville-age crust in the Canadian Cordillera is not yet clear. Colpron and Nelson (2009) proposed that Grenville-age crust in the Canadian Cordillera originated as a terrane of Caledonian affinity that was transported around the northern edge of Laurentia and into the Cordilleran realm during the mid-Paleozoic. Alternatively, Milidragovic et al. (2011) interpreted gneissic xenoliths from a Cambrian lamprophyre in Yukon as a vestige of a late Mesoproterozoic orogenic belt that remained, in part, in western Laurentia following rifting of Rodinia.

5.4 New detrital zircon U-Pb data

5.4.1 Sampling and analytical methods

Detrital zircon data from 13 samples of Neoproterozoic to Triassic strata of southeastern British Columbia are presented here. Ten samples collected from the Kootenay Arc represent each of the local stratigraphic divisions from Cambrian or Ordovician to Triassic depositional ages (figures 5-3 and 5-4). For each sample, roughly 10-15 kg of material was collected as several large fragments from single outcrops. This composite sampling technique was adopted to maximize probabilities of identifying the largest number of detrital zircon age groups. From outside the Kootenay Arc, Cryogenian Toby Formation conglomerate from the base of the Windermere Supergroup was collected near Kootenay Lake, and two samples of Devonian arenite – the Middle Devonian Mount Forster Formation in the northern Purcell Mountains and the Late Devonian Chase Formation from the North Okanagan – were analyzed for comparison (Figure 5-1).

Samples were prepared using standard crushing and separation techniques described in the appendix (A2-5). Zircon grains were handpicked and sorted in all samples except for the Toby Formation and Slocan Group samples. Although picking zircons can introduce an element of sample bias, it was necessary to isolate zircon from other minerals in most samples. Measures to mitigate this bias are described in the appendix. Selected samples were sorted by grain morphology and colour. These data are listed with isotopic ratios and dates in the appendix.

U-Pb isotopic dating of detrital zircon was performed by laser ablation multi-collector inductively-coupled plasma mass spectrometry (LA-MC-ICP-MS) at the Radiogenic Isotope Facility, University of Alberta. Grains were ablated with a 40 micron beam at grain centre using a Nu Plasma multi-collector inductively-coupled plasma mass spectrometer (MC-ICP-MS) coupled to a frequency quintupled Nd:YAG laser ablation system (New Wave Research). Analyses were conducted using a standard-sample-standard protocol similar to that of Simonetti et al. (2005) with modifications described in appendix A2-5.

5.4.2 Detrital zircon samples and results

Zircon dates presented in the text and diagrams are less than 10%

discordant unless otherwise specified. All U-Pb data, including strongly discordant results and sample site coordinates, are tabulated in Appendix A2-6. Plots utilize $^{207}Pb/^{206}Pb$ model ages when that value is greater than 800 Ma. For grains with $^{207}Pb/^{206}Pb$ ages younger than 800 Ma the $^{206}Pb/^{238}U$ age is presented as the most reliable date because it more accurately reflects crystallization ages of young, slightly discordant zircons (e.g. Gehrels et al., 2000). Selected grains were analyzed with multiple spots to improve precision; a weighted mean or concordia age is presented in such cases.

Toby Formation (Cryogenian; sample 08JK-TOBY)

The Toby Formation is the conglomeratic base of the Windermere Supergroup in southern British Columbia. A bulk sample was taken from a highway cut on the east side of Kootenay Lake in the west limb of the Purcell anticlinorium (Figure 5-1; Reesor, 1996). The sample comprises monomict white quartzite cobble paraconglomerate with a quartzofeldspathic matrix. At the regional scale, the Toby Formation overlies the Mount Nelson Formation with angular unconformity, although the contact locally has the appearance of a mixed gradation (Reesor, 1973; Root, 1987). Syndepositional normal faulting was an important control on deposition of the Toby Formation (Freiholz, 1983; Root, 1987; Smith et al., 2011). The Toby Formation has been interpreted to include glaciogenic diamictite associated with widespread Cryogenian glaciations (Smith et al., 2011). Toby Formation conglomerate commonly is unimodal and contains clasts apparently derived from the Mount Nelson Formation (Root, 1987).

The sample yielded abundant, moderately to well-rounded zircon grains from which 109 near-concordant dates were obtained. The grains were not sorted and morphological data were not recorded for this sample. The oldest zircons analyzed cluster at ca. 2.7 Ga and 1.85-1.7 Ga (Figure 5-5A). A well-defined and prominent mode occurs at ~1770 Ma. Eleven grains fall in the interval 1.47-1.4 Ga and six cluster, within error, at 1.33 Ga. Thirty percent of the grains ($n = 31$) range from 1.3-1.0 Ga, with a concentration at 1.10-1.15 Ga. The youngest zircon is an outlier with a $^{206}Pb/^{238}U$ age of 734 ± 37 Ma and a $^{207}Pb/^{206}Pb$ age of 758 ± 28 Ma (3.5% discordant; Figure 5-5B).

Mount Forster Formation (Eifelian; sample DMF-5s)

The Mount Forster Formation forms outliers of Middle Devonian sedimentary strata that lie unconformably, and locally tectonically, on the Neoproterozoic Horsethief Creek Group (Windermere Supergroup) in the northern Purcell Mountains of southeastern British Columbia (Root, 1987). This sample was quartzite from Root's (1987) unit Dmf-5 in the upper Mount Forster Formation near Delphine Creek. The following contextual data for the sample come from Root (1987). The Mount Forster Formation near Delphine Creek was deposited on the Purcell Arch during a regional transgression, probably in a half-graben bounded to the northeast by a syndepositional normal fault. It lies with profound unconformity on the Neoproterozoic Horsethief Creek Group. Petrological data and field relations indicate that the clastic units of the Mount Forster Formation were derived from erosion of nearby Ordovician-Silurian Beaverfoot Formation and Horsethief Creek Group rocks. Paleocurrent data in the upper Mount Forster Formation are east- or west-directed with a slight predominance to the east-northeast.

Recovered zircon grains were well rounded except a small number of angular or fragmented grains. Colour ranged from pink to colourless. Seventy-six near-concordant dates were obtained from 87 zircon grains (Figure 5-5A). A primary cluster of dates at 1910-1670 Ma and a smaller mode at 2100-1970 Ma compose 70% (n = 54) of the results. Most of the remaining dates (n = 20) are spread sub-equally in the Neoarchean (2960-2530 Ma) and early Paleoproterozoic (2410-2230 Ma). Two outliers at 0.99 Ga and 1.18 Ga are the youngest zircons in the sample.

Lardeau Group, Akolkolex Formation (lower Paleozoic; sample 07TWJK567)

The Akolkolex Formation (Logan and Colpron, 2006) occurs in the Lardeau Group immediately beneath the Jowett Formation north of the Beaton Arm of Upper Arrow Lake. Detrital zircon sample 07TWJK567 is from a metre-thick bed of coarse-grained quartzofeldspathic grit approximately 140 m stratigraphically below the lowest metabasaltic rocks of the Jowett Formation at Comaplix Mountain. The sampled horizon occurs in a well-exposed succession of massive and graded beds of grit that are sharply interlayered with laminated green and grey phyllite. The setting is interpreted as a submarine fan deposit derived from recycled quartzofeldspathic sedimentary rocks and (or) felsic plutonic rocks.

Zircon extracted from the Akolkolex Formation included euhedral prismatic, fragmented and rounded grains that were colourless to pink. Zircon dates (n = 74) form a strongly bimodal distribution with primary and secondary clusters at 1900-1720 Ma and ~2850-2550 Ma, respectively (Figure 5-6). The most prominent age-probability peaks occur at ~1770 Ma, ~1815 Ma and ~1885 Ma. Approximately 14% of the ages are scattered in the intervals 2500-2350 Ma and 2140-1940 Ma. Old and young outliers occur at ca. 3.0 Ga and 789 ± 18 Ma.

Lardeau Group, Broadview Formation (lower or mid-Paleozoic; samples 08TWJK043 and 07TWJK516)

The Broadview Formation overlies the Jowett Formation and older units of the Lardeau Group through much of the Kootenay Arc. Detrital zircon samples were collected from the formation's type locality near Ferguson (Fyles and Eastwood, 1962) and at its northern limit of exposure between the Columbia River and McCrae Peak 48 km northwest of Ferguson.

From the Ferguson area, sample 08TWJK043 comprised several blocks of blue-grey quartzite with rare smoky quartz granules taken roughly 800 metres above the Jowett Formation (present deformed thickness). The composite sample came from several quartzite horizons interlayered with phyllite in a 4 m roadcut on the Gainer Creek logging road.

From the Columbia River area west of McCrae Peak, sample 07TWJK516 comprised sorted micaceous quartzite collected from a roadcut along the Crawford Forest Service Road north of Crawford Creek. Although moderately recrystallized at garnet-zone conditions, millimetric quartz and feldspar granules coarser than the matrix are preserved. The sampled horizon is part of a succession of several hundred metres of interlayered quartzite and metapelite that can be traced eastward across McCrae Peak and into the Broadview Formation at the Beaton Arm of Upper Arrow Lake (Kraft et al., 2011a). Both samples of the Broadview Formation are interpreted as submarine fan deposits derived from a coarse-grained felsic plutonic source and (or) texturally immature coarse clastic sedimentary rocks (Smith, 1990; this study).

Zircon grains in both samples of Broadview quartzite were predominantly rounded with less abundant subrounded and angular fragments. Pink zircon is common and yellow is rare in sample 08TWJK043; the opposite was true of 07TWJK516. Results of both samples are plotted in Figure 5-6. The Broadview Formation from its type locality near Ferguson (08TWJK043; n = 108) has a bimodal detrital zircon signature with ~80% of dates defining Paleoproterozoic

(1935-1650 Ma) and Neoarchean (2720-2510 Ma) clusters mirroring results from the older Akolkolex Formation. The remaining 20% of dates are scattered thinly in the intervals 2410-2010 Ma and 1560-800 Ma. Three grains fall within the 1600-1490 Ma NAMG of Van Schmus et al. (1993) – an interval in which magmatic rocks and high-grade metamorphic events are extremely rare in Laurentia. The northwestern Broadview sample (07TWJK516; n = 128) has Paleoproterozoic (2000-1700 Ma) and Neoarchean (2700-2630 Ma) date peaks coincident with those of the sample from the type locality, but those modes are dominated by the 70% of the grains that fall between 1470 Ma and 940 Ma, forming age-probability peaks, in diminishing proportion, at 1045 Ma, 1155 Ma, and 1315 Ma. Four early Paleoproterozoic zircons with dates of ca. 2490 Ma, ca. 2300 Ma, and ca. 2180 Ma were identified. The age spectrum has a gap from 1630-1470 Ma coincident with the NAMG.

Mount Sproat assemblage (Late Devonian; sample 06TWJK138A)

The Mount Sproat assemblage is interpreted to conformably overlie the Broadview Formation in the eastern Lardeau Range. Due to their generally fine-grained nature, rock types in the Mount Sproat assemblage suitable for recovering detrital zircons occur only near the basal contact with Broadview quartzite and in the Upper Clastic member – the youngest part of the assemblage. Quartzite pebble paraconglomerate at the base of the Upper Clastic member was sampled where it conformably overlies amphibolitic schist in the Beaton Arm of Upper Arrow Lake. Clasts comprise rounded white and grey quartzite and (or) vein quartz pebbles in a matrix of quartzose muscovite schist. One granitoid pebble was identified in the outcrop but none were observed in the sample. Clasts have elongated aspect ratios of ~2-5:1 and have long axes up to ~10 cm. Conglomerate occurs in several lenses in a 10 m section of quartzose muscovite schist that grades into garnet-muscovite schist and dark grey banded metasiltstone. The conglomerate is interpreted as a submarine debris flow deposit derived from a nearby high-energy shoreline dominated by continentally derived siliciclastic sediment.

The Upper Clastic member conglomerate (06TWJK138A) yielded numerous highly rounded and some prismatic zircon grains of pink, yellow or no colour. Near-concordant zircon dates (n = 120) define three major clusters at 2750-2580 Ma, 1960-1750 Ma, and 1250-1020 Ma, between which most remaining dates are scattered (Figure 5-6). The Paleoproterozoic cluster has one dominant mode at 1890-1850 Ma. Smaller clusters of dates occur in the intervals: 1710-1650, 1520-1450 Ma, and 1380-1330 Ma. Eleven dates span uniformly from 2460 Ma to 2010 Ma. The lone Paleozoic grain – the youngest in the sample – has a $^{206}Pb/^{238}U$ age of 484 ±15 Ma, which is interpreted to underestimate the crystallization age due to its 9% discordance; the grain is interpreted to be Cambrian or older.

Thompson assemblage (Mississippian; sample 08TWJK073)

The unconformity-bounded Thompson assemblage is enveloped between a thick succession of older Broadview grits and the younger northern Davis assemblage of the Milford Group at Mount Thompson. This sample came from a 1.5 m-thick horizon of sandy marble that occurs 70-100 m stratigraphically beneath the basal Davis assemblage conglomerate at Mount Thompson and overlies several hundred metres of phyllite and grit, also of the Thompson assemblage (Figure A1-4). Grit in the Thompson assemblage appears to have derived from erosion of the immediately underlying Broadview Formation (see Chapter 3). Limestone breccia and maroon and green phyllitic argillite are interbedded with and overlie the sandy marble layer. The sample comprises crystalline calcite with ~30-40% coarse sand size quartz and feldspar grains that define diffuse layer-parallel banding on differentially weathered surfaces. The sandy marble is interpreted to represent an influx of mature beach or aeolian sand onto a small carbonate platform in a tectonically quiescent setting that closely preceded deposition of the Davis assemblage (see Chapter 3 for more).

The sample returned a low yield of zircon grains, of which most were well rounded; prismatic to sub-rounded grains, however, were also recovered and analyzed. The grains were not sorted and morphological context was not recorded. The detrital zircon spectrum (n = 98) for this unit of the Thompson assemblage bears main date groups at 2840-2580 Ma and 1880-1750 Ma (Figure 5-7), similar to the underlying Lardeau Group. Unlike the Broadview and Akolkolex formations, the Thompson assemblage sample contains a significant detrital zircon mode (n = 12) at 2000 Ma. Four zircons fall in the interval 1480-1450 Ma and two other Mesoproterozoic grains (1318 ± 18 Ma and 1150 ± 23 Ma) were identified. The youngest zircon is an outlier with a $^{207}Pb/^{206}Pb$ age of 656 ± 23 Ma and $^{206}Pb/^{238}U$ age of 678 ± 44 Ma (4% reversely discordant)

Milford Group, northern Davis assemblage (Late Mississippian; samples 07TWJK104B, 08TWJK309)

In the study area, the northern Davis assemblage of the Milford Group unconformably overlies the Broadview Formation of the upper Lardeau Group and, at least locally, the Thompson assemblage. Sample 07TWJK104B was collected from a conglomerate lens in the lowermost ~100 m of the Davis assemblage near the tailings pond at the MAX Molybdenum Mine near Trout Lake. Stratigraphic height above the basal unconformity could not be determined; it is estimated at roughly 50 m. The conglomerate is in sharp contact with light grey foliated quartz wacke; both are surrounded by strongly sheared, pyritic argillaceous phyllite. Clasts are size-sorted and compositionally bimodal, comprising 70-90% white, rounded, polycrystalline quartz pebbles less than 1 cm across. Angular and tabular fragments of black argillite interpreted as rip-up clasts compose the rest. Conglomerate is clast-supported with a matrix of fine quartz, carbonaceous material and secondary pyrite. Five hundred metres along strike to the southeast, temporary exposure examined during construction of a mine tailings pond revealed many similar lenses of massive or graded conglomerate (see Figure 3-8A). The lenses are interpreted as distributary channels in anoxic mud, probably associated with intermediate submarine debris flows sourcing quartzose continental detritus.

Sample 08TWJK309 comprises quartzite collected approximately 300 m above the base of the northern Davis assemblage on the flank of Mount Thompson. The sampled horizon is a 1.5 m thick massive grey quartzite bed with a pebbly base that occurs at the top of the lithologically diverse Basal member (limestone, conglomerate, chert and phyllite) and is overlain by the mudstone-dominated Phyllite member.

Conglomerate from the western limb (07TWJK104B) and quartzite from the eastern limb (08TWJK309) of a syncline of the northern Davis assemblage north of Trout Lake yielded rounded and prismatic zircons with similar detrital zircon ages, which mimic the results from the underlying Broadview Formation. Both samples have a distinctive major population of 1800-1900 Ma zircons, and subordinate groups in the intervals 2800-1900 Ma, 1800-1600 Ma, 1500-1350 Ma, and 1300-900 Ma (Figure 5-7). The western conglomerate sample has well defined date peaks at 1950 Ma and 2700 Ma, and one 3380 Ma zircon. One grain produced a 6% discordant result with a $^{207}Pb/^{206}Pb$ age of 672 ± 34 Ma. The quartzite yielded five slightly discordant Late Silurian zircons (weighted mean $^{206}Pb/^{238}U$ age of 422.6 ± 5.4 Ma) and one Early Devonian or Late Silurian zircon ($^{206}Pb/^{238}U$ age of 405 ± 16 Ma; 7% discordant).

No near-concordant Paleozoic dates were found in the northern Davis conglomerate; however two imprecise Early Paleozoic lower discordia intercept ages from multiple analyses of single grains are consistent with results from other samples. From two data points, zircon 66 yields a discordia with intercepts at 2045 ±19 Ma and 520 ± 150 Ma (Figure 5-8B). Two data points from zircon 23 define a tenuous discordia with intercepts at 1029 ± 970 Ma and 489 ± 140 Ma (Figure 5-8A). A possible interpretation is that zircons 66 and 23 have Early Paleozoic crystallization ages with inheritance of ca. 2 Ga and ca. 1 Ga lead, respectively.

Milford Group, northern McHardy assemblage (Late Mississippian; samples 07TWJK153, 06TWJK176D)

The northern McHardy assemblage of the Milford Group lies with angular unconformity on different levels of the Mount Sproat assemblage. Immediately east of these sample sites the northern McHardy assemblage overlies the Heterolithic member of the lower Mount Sproat assemblage; to the west it overlies the two upper members of the Mount Sproat assemblage: the Amphibolitic Schist and Upper Clastic members.

Lithic quartz wacke sample 07TWJK153 comes from an interval of coarse siliciclastic rocks approximately 1300 m above the base and 500 metres below the top of the northern McHardy assemblage on a ridge northwest of Wilkie Creek in the eastern Lardeau Range. The sample comprised poorly sorted, carbonaceous quartz wacke with <10% millimetric angular lithic and quartz fragments and shale fragments inferred to be rip-up clasts. The sampled layer occurs in a ~50 m thick interval of interbedded massive quartz wacke, planar bedded and cross-stratified quartz arenite, and carbonaceous phyllite in a succession otherwise dominated by carbonaceous mudstone. The sample is interpreted to represent thin-bedded turbidite in a deep basinal setting. The quartz wacke (sample 07TWJK153; n = 115) produced a generally bimodal Paleoproterozoic (ca. 2.1-1.74 Ga) and Archean (ca. 2.8-2.5 Ga) date-probability distribution with a pronounced peak at 1.80 Ga (Figure 5-7). Six grains occupy the interval 2.49-2.23 Ga. Two Mesoproterozoic grains of 1.32 Ga and 1.24 Ga dates were identified. A group of 7 zircons range from 695-645 Ma. The youngest zircon in this sample yielded a date of 644 ± 21 Ma.

Sample 06TWJK176D was collected from a layer of tuffaceous metasandstone where the uppermost northern McHardy assemblage interfingers with metabasalt of the Kaslo Group in the valley of Hill Creek in the northern Lardeau Range. The well-sorted, medium-grained metasandstone is interbedded at centimetre-scale with finer-grained white meta-tuff containing random hornblende needles inferred to be porphyroblasts. Contact relations with surrounding metabasalt are obscured by colluvium. Few zircons were recovered from the tuffaceous sandstone at the northern McHardy/Kaslo contact (sample 06TWJK176D) and only six grains were analyzed (yielding seven dates because one grain was zoned; Appendix A2-6). Because of the low yield, results as much as 15% discordant are considered for interpretation (with their percent discordance listed in parentheses below). Three Paleoproterozoic grains [1.99 Ga (14%), 1.85 Ga (-14%), 1.61 Ga (-1%)] and two Mesoproterozoic grains [1.16 Ga (8%), 1.13 Ga (-7%)] were identified (Figure 5-7). Another zircon contained two distinct age domains that, in different parts of one analytical cycle, produced concordant results with $^{206}Pb/^{238}U$ dates of 328 ± 33 Ma (-3%) and 593 ± 57 Ma (0%). The results are interpreted to represent rim and core crystallization ages, respectively.

Chase Formation (Late Devonian; sample 'Chase quartzite')

The Chase Formation (Jones, 1959) is a laterally persistent horizon of prominently differentially weathering calcareous quartzite that regionally overlies Neoproterozoic or early Paleozoic paragneiss of the Monashee cover succession between Chase, British Columbia and Upper Arrow Lake (Thompson and Daughtry, 2000; Thompson et al., 2006; Lemieux et al., 2007). Near Nakusp, the Chase Formation's basal contact is sharp and parallel to schistosity and compositional layering in the Chase quartzite and the underlying paragneiss (Lemieux, 2006). Amphibolite-facies Late Devonian and Mississippian metasedimentary and metavolcanic rocks are interpreted to conformably overlie the Chase Formation (Glombick et al., 2004; Thompson et al., 2006; Lemieux, 2006). The Chase Formation is interpreted to have formed on a shallow-water marine platform that received detritus from ancient sialic crust and (or) quartzofeldspathic strata to the west (in present coordinates; Thompson et al., 2006). Its relationship to coeval basinal rocks in either the upper Lardeau Group or Mount Sproat assemblage is uncertain, but an indirect stratigraphic link via overlapping Late Devonian and Mississippian rocks was proposed in Chapter 3.

This sample of calcareous quartzite was collected from the formation's type locality near Chase, British Columbia. Thompson et al. (2006) previously reported five single grain ID-TIMS dates from the sample, of which two were less than 10% discordant (424 ± 13 Ma; 1008 ± 2 Ma). In this study more than 100 additional detrital zircons were analyzed by LA-MC-ICPMS.

Zircon grains from the Chase Formation are highly rounded and colourless to pink. New U-Pb dates (n=92) are strongly scattered from ca. 2.0 Ga to 930 Ma plus a significant group of Early Paleozoic dates and several Neoarchean dates (Figure 5-9A). Proterozoic zircons cluster loosely at ca. 1720 Ma, 1640-1600 Ma, 1500-1460 Ma, 1380-1320 Ma, 1220-1110 Ma, and 1080-950 Ma. Six Archean zircons form minor populations at 2.95 Ga, 2.81 Ga, and 2.67 Ga. Paleozoic zircons yielded the following dates: mid-Cambrian (508 ± 10 Ma), Late Ordovician or Early Silurian (two dates with a weighted mean $^{206}Pb/^{238}U$ age of 446 ± 17 Ma), Late Silurian (five with a weighted mean $^{206}Pb/^{238}U$ age of 420 ± 4 Ma), Middle Devonian (396 ± 12 Ma) and Late Devonian (372.6 ± 5.2 Ma; weighted mean $^{206}Pb/^{238}U$ age from two near-concordant analyses of one grain; Figure 5-9B). The youngest apparent age is from a slightly discordant analysis (4.3%) with Mississippian model ages of 325 ± 8 Ma ($^{206}Pb/^{238}U$) and 339 ± 17 Ma ($^{207}Pb/^{206}Pb$).

Slocan Group (Late Triassic; sample 08TWJK357)

Late Triassic phyllite and silt- to sandstone in the Selkirk Mountains have been assigned to the Slocan Group (Hyndman, 1968). The Slocan Group unconformably overlies Permian metabasalt of the Kaslo Group (Hyndman, 1968; Klepacki, 1985). The Slocan Group is considered an eastern facies of the Nicola Group – an extensive succession of Late Triassic volcanic and sedimentary rocks deposited on the Quesnel arc in south-central British Columbia (Preto, 1979; Moore and Pettipas, 1990).

From the Slocan Group, medium-grained sandstone with diffuse light and medium grey colour bands was collected at a roadcut on Turner Road north of Nakusp. The sandstone occurs in a discontinuously exposed succession of siltstone, argillite, sandstone and limestone that overlies the Kaslo Group near Nakusp (Figure 5-3).

The sample yielded a similar number of well-rounded and sub-rounded elongate zircon grains, and relatively few prismatic grains. Forty-two of 140 analyses produced results greater than 10% reversely discordant (see appended data tables in appendix A2-6). These strongly reversely discordant results predominantly had low ^{206}Pb count rates ($<10^5$ counts per second) and they produced $^{206}Pb/^{238}U$ model ages between 220 Ma and 375 Ma and ten as old as 640 Ma. Observed non-linear behaviour between the IC0 and IC1 ion counters' relative gain at low Pb count rates (A. Dufrane, personal communication 2011) means that $^{207}Pb/^{206}Pb$ ratios were incorrectly normalized using the standard zircon grains with much higher Pb count rates. The IC0-Faraday gain, however, behaved linearly in tests over a larger range of Pb count rates (A. Dufrane, personal communication 2011), in which case the $^{206}Pb/^{238}U$ ratio is accurately normalized in this sample.

Detrital zircon data for this sample are plotted with and without the 42 reversely discordant dates in Figure 5-9 to illustrate the changes to the signature by using the discordant data. The differences are almost entirely in the Phanerozoic grains. The detrital zircon spectrum (n = 109) of this Triassic sandstone is significantly different from all older units in the area. The sample is multi-modal and contains relatively few Paleoproterozoic or older zircons and many Neoproterozoic and Paleozoic grains. Only four zircons older than 1800 Ma were identified. A Paleoproterozoic age cluster spans 1780-1620 Ma and a major mode occurs at 1440-1390 Ma. Twenty-five zircons are spread from 1360 Ma to 820 Ma. Another 18 grains range from 680 Ma to 470 Ma, including modes of: 586 ± 18 Ma (n = 4) and 552 ± 18 Ma (n = 4). All weighted mean ages have probabilities greater than 90% unless otherwise stated. A cluster of ten Middle Devonian to Pennsylvanian dates (400 Ma to 310 Ma) contains weighted mean $^{206}Pb/^{238}U$ age modes at 369 ± 10 Ma (n = 5) and 310 ± 12 Ma (n = 2). Twenty-two zircons are Permian or Triassic, with modes at 296 ± 12 Ma (n = 3), 246 ± 8 Ma (n = 4) and 221 ± 7 Ma (n = 4).

5.5 Discussion

5.5.1 Sampling bias

As described in the appendix, measures were taken to minimize sampling bias from hand-picking of zircon; however, a degree of bias is probably present because of hand-sorting and use of the magnetic separation technique. Hand-picking would preferentially select large, rounded and coloured grains over smaller, prismatic grains and magnetic separation selectively removes magnetic grains.

To evaluate the potential for bias from hand picking, zircon dates from the three samples with the greatest variety of zircon dates have been plotted in probability density diagrams according to morphology (Figure 5-10) and colour (Figure 5-11). The plots show weak or no correlations between zircon date and morphology (which is also a crude proxy for size in these samples) or zircon date and colour. Although most Paleozoic zircons were faceted, many faceted and prismatic zircons were Mesoproterozoic and Paleoproterozoic. The presence of faceted or prismatic Archean and Paleoproterozoic zircons leads to the suggestion that the grains have not been recycled or transported extensively and may be in their first sedimentary cycle. A secondary complementary relationship is apparent in the Mount Sproat assemblage sample (06TWJK138A), wherein Paleoproterozoic grains are more abundant in the least rounded groups and Mesoproterozoic grains are predominant in the rounded zircon groups. If the angular fragments were produced during pulverization, this relationship would indicate that Paleoproterozoic zircons were the largest. Alternatively, the Paleoproterozoic grains were not rounded by sedimentary transport. An unconstrained factor is the bias away from smaller grains. Only grains larger than the 40 micron beam diameter could be analyzed therefore it is possible that populations of very small zircon have not been detected. Of the grains for which analysis is possible, the minimal correlation between zircon morphology and age, especially with respect to Precambrian zircons, allows the interpretation that a bias by handpicking is negligible in these samples. Recovered proportions of Precambrian zircons are therefore considered to approximate true proportions.

5.5.2 Interpretation of 'atypical' zircon ages

I discuss below potential sources for detrital zircons in this study that are not within the typical northwestern Laurentian basement age range of 3.5-1.7 Ga. A chart illustrating the occurrences of these and other key zircon age groups by sample is shown in Figure 5-12.

Ca. 1.48-1.32 Ga zircon

Two groups of Early Mesoproterozoic zircon dates were identified: ca. 1.48-1.41 Ga and ca. 1.38-1.32 Ga. These groups tend to occur in the same units, which include the Toby Formation, Broadview Formation, Mount Sproat assemblage, Chase Formation and Slocan Group, plus minor occurrences in the Milford Group and Thompson assemblage. Figure 5-13 shows the distribution of so-called 'anorogenic' 1.50-1.40 Ga granites in the southern U.S.A where they intrude predominantly ca. 1.72-1.62 Ga crust. The abundance of pre-1.75 Ga zircon and paucity of 1.72-1.62 Ga zircon in these samples are inconsistent with a source in that part of Laurentia, thus an alternative source of 1.48-1.41 Ga zircon is needed.

Detrital zircons from 1.48-1.41 Ga in these samples may have originated from the 1.48-1.40 Ga Moyie sills and related igneous rocks in the underlying Belt-Purcell Supergroup (Anderson and Davis, 1995; Doughty and Chamberlain, 1996; Sears et al., 1998; Evans et al., 2000; Doughty and Chamberlain, 2008). Detrital zircons of this age range are also represented in the detrital zircon record of upper Purcell Supergroup strata (Gardner, 2008); however Purcell strata that contain 1.47-1.41 Ga detrital zircon have significant numbers of zircon grains in the range 1.6-1.49 Ga (Figure 5-14; Gardner, 2008), which are rare to absent in the samples from this study. The 1.48-1.41 Ga zircon grains in the studied units are therefore interpreted to derive from an unknown igneous source associated with the Moyie sills and not erosion of the upper Purcell Supergroup. Other evidence of a local source of this age comes from two samples of pelitic schist from the Valhalla complex ("Passmore schist") that have yielded a unimodal detrital zircon population comprising only 1430 ± 30 Ma grains, reflecting a homogeneous source rock (Ross and Parrish, 1991).

Plutonic rocks associated with the 1.37-1.32 Ga East Kootenay orogeny (White, 1959; Obradovich and Peterman, 1968; Schandl et al., 1993; Doughty and Chamberlain, 1996; McFarlane and Pattison, 2000) may have produced the zircons of that age range found in this study. A regional thermal and felsic plutonic event at ca. 1.37-1.34 Ga in the lowermost Belt-Purcell Supergroup ("Kootenay orogeny"; Evans and Fischer, 1986; Evans and Zartman, 1990; Ross et al., 1992; Schandl et al., 1993; McFarlane and Pattison, 2000; Doughty and Chamberlain, 1996; Mortensen, personal communication to Doughty and Chamberlain, 1996) may have produced the sources of zircon of that age in the Broadview Formation.

1.3-0.9 Ga zircon

The Toby Formation and all pericratonic units sampled for this study except the Akolkolex Formation and Thompson and McHardy assemblages yielded significant (>5%) modes of 1.3-0.9 Ga detrital zircon indicating a sizable source was available in the southern Canadian Cordillera during the Paleozoic.

During this time, the Transcontinental Arch and broad epeiric seas, into which the Western Canada Sedimentary Basin deposited, would have represented effective barriers to sediment dispersal from the Grenville province and Appalachian orogen to the southern Canadian Cordilleran margin (Figure 5-13). Furthermore, the well-characterized Alberta basement (e.g. Ross et al., 1991), basement exposures in the eastern Cordillera (Parrish and Armstrong, 1983; Parrish and Ross, 1990; Parrish, 1995; Crowley, 1999; Gervais et al., 2010) and detrital zircon characteristics of the Canadian Cordilleran miogeocline (e.g. Ross and Bowring, 1990; Gehrels and Ross, 1998; Gehrels, unpublished data) indicate that basement domains in western Canada are overwhelmingly ca. 1.7 Ga and older. These evidences indicate that Grenville-age zircon in the studied pericratonic rocks did not come from the east, and therefore originated outboard of the miogeocline.

A 1.19 Ga granite clast in Windermere conglomerate in the Cariboo Mountains (D. Murphy, unpublished data; Figure 5-1) and 1.45-1.01 Ga detrital zircons in latest Precambrian or Lower Cambrian Hyland Group turbidite of the Selwyn Basin (Ross et al., 2005) were interpreted as first-cycle, proximal sediments and require that Grenville-age crust was present near these sequences during latest Proterozoic rifting of the Cordilleran margin. From the Nicola Horst near Kamloops, another Grenville-age (1.04 Ga) clast of granite, kilograms in size, was recovered from meta-conglomerate that is intruded by early Late Triassic Quesnel arc rocks (Erdmer et al., 2002). Two discrete modes of Grenville-age zircons in the Ordovician Mount Wilson Formation in eastern British Columbia indicate plutons of ca. 1030 and 1053 Ma ages were present, but not dominant, in the quartzite's source region, which was interpreted to be the Peace River Arch (Gehrels and Ross, 1998).

Grenville-age detrital zircon dominates the dataset from the Ruby terrane of western Alaska (Figure 5-15; Bradley et al., 2007) and is a characteristic of a number of northern Cordilleran terranes thought to have Baltican or Caledonian affinity (Colpron and Nelson, 2009; 2011). The presence of locally derived Grenville-age detritus in the late Neoproterozoic and early Cambrian rift successions (Ross et al., 2005; D. Murphy, unpublished data), however requires that Grenville-age crust was near the rift that formed the Cordilleran margin.

Grenville-age detritus in the studied pericratonic rocks may therefore derive from either intra-Cordilleran or exotic sources.

Neoproterozoic and Cambrian zircon

The Chase Formation, upper Mount Sproat assemblage and the Slocan Group yielded Neoproterozoic and Cambrian zircons, for which known potential sources are not obvious because in situ crystalline rocks of that age are not known in the region. The small group of angular and sub-rounded 650-700 Ma zircon in wacke from the northern McHardy assemblage is interpreted to reflect a local source because of its unique abundance relative to other samples and the low degree of rounding of the grains. Counterparts were identified, one grain each, in the Slocan Group (689 ± 41 Ma) and northern Davis assemblage (672 ± 34 Ma). Other occurrences of zircon of similar ages in the region include a discordant 650-700 Ma detrital zircon from the Broadview Formation (Smith and Gehrels, 1991), a ca. 650 Ma detrital zircon from quartzite in the Monashee cover sequence (Parrish et al., 1989) and a dominant mode of 670-590 Ma detrital zircons in Neoproterozoic or Paleozoic quartzite from the Grand Forks metamorphic complex (Ross and Parrish, 1991).

A swath of Ediacaran and early Paleozoic zircon (616 ± 44 Ma to 496 ± 34 Ma) was identified in the Slocan Group, including a four grains with a weighted mean $^{206}Pb/^{238}U$ age of 552 ± 18 Ma that matches, within error, ca. 555 Ma granite boulders recovered from Paleozoic conglomerate in the Spa Creek assemblage near Vernon (Erdmer et al., 2001) and 553 ± 20 Ma detrital zircons in the Chilliwack Composite terrane (Brown et al., 2010). Ediacaran granitic crust was therefore present in or near the Quesnel arc and its basement in Devonian and Triassic time. Another mode of 586 ± 18 Ma (n = 4) zircon from the Slocan Group sandstone is similar in age to one zircon of seven from the uppermost McHardy assemblage (sample 06TWJK176D) that has a 593 ± 57 Ma core overgrown by a 328 ± 33 Ma rim. The rim is inferred to be magmatic because Mississippian igneous rocks are common in potential source areas nearby (e.g. Paradis et al., 2006) and Carboniferous metamorphic zircon is unknown in the southern Canadian Cordillera. The core-rim relationship from the McHardy assemblage grain is tentatively interpreted to suggest that ca. 590 Ma zircon was present in rocks that were the basement to local Mississippian arc magmatism. Based on sample locations, the ca. 550 Ma and ca. 590 Ma zircon source rocks are inferred to have been outboard of the Lardeau trough.

Late Neoproterozoic (700-540 Ma) magmatism is characteristic of Colpron and Nelson's (2009) terranes of Siberian, Baltican and Caledonian affinities. In the Cordillera, these ages are not found in the Cordilleran miogeocline outside of local alkaline basaltic units but they are representative of the basement of the Arctic Alaska-Chukotka terrane in northern Alaska (Figure 1-1; Amato et al., 2009; McClelland et al., 2006). Circa 680-670 Ma and ca. 560-540 Ma gneiss and igneous rock in northwest Alaska (Seward Peninsula; Patrick and McClelland, 1995; Amato et al., 2009) and ca. 554 Ma arc rocks in the Alexander terrane (Wales Group; Gehrels et al., 1996) correspond with the ages of detritus in the pericratonic rocks discussed above.

Silurian zircon

Silurian (ca. 420 Ma) detrital zircons are common to the Chase Formation and Davis assemblage and constitute the only significant Phanerozoic zircon population from those units (Figure 5-16).

Silurian zircon dates are rare in the Canadian Cordillera outside of the Alexander terrane (Gehrels et al., 1996; G. Gehrels, unpublished data, 2011), which is believed to have been outside the Cordilleran realm prior to the Mesozoic (Gehrels et al., 1996; Colpron and Nelson, 2011; Beranek et al., 2013). From the southern Canadian Cordillera, Silurian detrital zircon has previously been reported from the Late Devonian-Early Mississippian Bob Lake assemblage in the Nicola Horst near Kamloops (434.2 ± 19.1 Ma; Erdmer et al., 2002) and the Pennsylvanian Spray Lakes Group of the southern Alberta miogeocline (427 ± 5 Ma and 431 ± 4 Ma, Gehrels and Ross, 1998). Provenance data therefore indicate that sources of ca. 420 Ma and 430 Ma zircon shed detritus into the pericratonic rocks of the southern Canadian Cordillera in Late Devonian and Mississippian time and, by Pennsylvanian time, into the adjacent miogeocline.

Silurian granitoid boulders that occur in the southern McHardy assemblage (418 ± 5 Ma and 431 ± 31 Ma, Roback et al., 1994) and other occurrences of Silurian detrital zircons in the southern Canadian Cordillera could not be linked to a source in the Cordilleran realm (Colpron and Nelson, 2009) until identification of an *in situ* suite of ca. 418 Ma magmatic arc-related intrusions in the Chilliwack Composite terrane (Figure 5-1; Brown et al., 2010) of northwestern Washington State. Circa 430 Ma and 550 Ma detrital zircons were recovered from Late Devonian strata of the Chilliwack Composite terrane indicating proximity to igneous and (or) metamorphic rocks of those ages (Brown et al., 2010).

The expanded detrital zircon dataset presented here shows that Silurian zircons are not ubiquitous in the analyzed units that contain them. The Milford and McHardy assemblages have yielded Silurian zircon in some samples and not others. The source of Silurian zircons in these strata therefore appears to have been inconsistently available (or prominent) in space and time, and presumably formed a point source close to the depositional site of the Milford Group owing to the kilograms-size of Silurian boulders in McHardy assemblage (Roback et al., 1994). Moreover, occurrence of the Silurian granite clasts with clasts derived from the Lardeau Group implies proximity of the Silurian intrusions and Lardeau strata in Late Mississippian time.

Gehrels and Ross (1998) interpreted Silurian and Grenville-age detrital zircon in the Spray Lakes Group to have derived from Arctic Canada or Alaska, where detrital zircons of those ages are known (McNicoll et al., 1995; Gehrels et al., 1999; Beranek et al., 2010). Other detrital zircon in the Spray Lakes Group sample with dates of ~1365 Ma, ~1576 Ma and ~1611 Ma were inferred to derive from sources to the southeast (Gehrels and Ross, 1998). Given the presence of boulders of Silurian granite in the McHardy assemblage, which require local derivation, and the increased knowledge of detrital zircons of Silurian and Grenville ages in the southern Canadian Cordillera presented in this study, I suggest an alternative hypothesis in which the Silurian, Grenville-age and ~1576 Ma and ~1611 Ma detrital zircon in the Spray Lakes Group derived from outboard pericratonic sources in the southern Canadian Cordillera and that the hypothesized long transport distance from the Arctic and the mixing of provenance from opposite directions are not required. On the basis of the Chilliwack Composite terrane's affinity with the Cordilleran margin (Brown et al., 2010) and its modern day proximity to southeastern British Columbia, the Silurian igneous rocks represented in the Chilliwack Composite terrane are interpreted here as the potential source of ca. 420 Ma detritus in the Milford Group and the Chase Formation and ca. 430 Ma detrital zircons in the Spray Lakes Group and Bob Lake assemblage.

But, did Silurian magmatism in the Chilliwack Composite terrane take place along the Canadian Cordilleran margin? Detrital zircon dates from the metamorphic basement (Yellow Aster Complex) of the Chilliwack Composite terrane match those of Late Proterozoic and Early Paleozoic Cordilleran margin strata, including the paragneiss basement of the Chase Formation (Lemieux et al., 2007) indicating the terrane was in the Canadian Cordilleran realm in Late Proterozoic and (or) early Paleozoic time (Brown et al., 2010). Similar basement domain ages are present throughout Canada, however (Figure 5-13), so the data are also consistent with an origin north of the Yukon-Tanana terrane or even in northeastern North America. The Chilliwack Composite terrane is presently separated from the miogeocline and pericratonic rocks by numerous faults and Mesozoic plutonic rocks in the Coast Plutonic Complex (e.g. Wheeler and McFeely, 1991), therefore its relationship to the continental margin cannot be fully ascertained. Detrital zircon data discussed above indicate sedimentary linkages between the Chilliwack Composite terrane and the southern Canadian Cordilleran margin during deposition of the Yellow Aster Complex protoliths in between 1000 Ma and 418 Ma and in the Late Devonian and Carboniferous. Field relations of the Chase Formation indicate it was deposited on continental margin rocks (Thompson et al., 2006; Lemieux et al., 2007), therefore, a Silurian magmatic arc represented by the Chilliwack Composite terrane was adjacent to the Cordilleran margin (Okanagan High) since deposition of the Chase Formation at ca. 375 Ma. The absence of Silurian grains from the upper Lardeau Group, MSA and Thompson assemblage means there is no evidence that detritus from the Silurian arc reached the Lardeau trough/Milford depositional site prior to Late Mississippian time. By Pennsylvanian time, detritus from the Silurian arc was being transported as far inboard as the Spray Lakes Group in the miogeocline.

5.5.3 Interpretation of provenance by unit

Provenance of the Toby Formation conglomerate

Archean and Paleoproterozoic zircons from the Toby conglomerate match the age of basement provinces of western Laurentia from which much of the lower Purcell Supergroup (Ross and Villeneuve, 2003), Windermere Supergroup (Smith and Gehrels, 1991; Gehrels and Ross, 1998; G. Gehrels, personal communication 2011) and the Paleozoic southern Canadian Cordilleran miogeocline (Gehrels and Ross, 1998) are interpreted to be derived. The Toby Formation therefore was also most likely derived primarily from western Laurentian rocks.

The Toby Formation also received a significant influx of Grenville-age detrital zircons that, on the basis of sedimentological and stratigraphic data, are interpreted to come from recycled older sedimentary rocks. Because the source rocks contained 1.0 Ga zircon, they must have been deposited in the interval 1.0-

0.75 Ga, which is "Sequence B" of Young et al. (1979). The alternative that 1.3-1.0 Ga zircon in the Toby sample derived directly from Grenville-age crust and mixed with older detritus cannot be excluded but is considered less likely here because of the textural maturity of arenite in the Toby conglomerate, the lack of angular or prismatic detrital zircon in the sample and the mixing of Mesoproterozoic zircon with Paleoproterozoic and Archean zircon.

Other Windermere strata in southern British Columbia share only the Paleoproterozoic and Archean (Ross and Bowring, 1990; Ross and Parrish, 1991; Gehrels and Ross, 1998; Gehrels, unpublished data) date clusters seen in the Toby Formation; however Windermere Supergroup rocks in Idaho have yielded Mesoproterozoic detrital zircons at ca. 1.37 and 1.25-1.1 Ga (Buffalo Hump Formation, Ross et al., 1992; Syringa metamorphic complex, Lewis et al., 2010) in addition to Paleoproterozoic and Archean modes (Figure 5-14). An absence of zircons between 1.6-1.49 Ga (NAMG, North American magmatic gap of Van Schmus et al., 1993) indicates that the significant volume of Belt-Purcell strata characterized by non-Laurentian detrital zircons (Prichard, Revett, Wallace formations; Ross and Villeneuve, 2003; Lewis et al., 2010) were not sources for these samples of the Windermere Supergroup.

Although the underlying Mount Nelson Formation is a potential local sediment source, its detrital zircon characteristics where they are known 150 km to the northeast are clearly not a match to the Toby Formation's (Figure 5-14). The Mount Nelson Formation has been interpreted to be older than 1.3 Ga (Ross and Villeneuve, 2003; Gardner and Johnston, 2008), but on the basis of stratigraphic relations, Root (1987) proposed that the Mount Nelson Formation might correlate with 1.0-0.78 Ga "Sequence B" sedimentary successions in northwestern Canada. Gardner (2008) reported from the Mount Nelson Formation one detrital zircon grain with a nearly concordant $^{207}Pb/^{206}Pb$ date of 1219 ± 41 Ma, and interpreted the Mount Nelson to have deposited at ca. 1.35 Ga. Alternatively, I interpret the Mount Nelson Formation to be younger than the ca. 1.2 Ga detrital zircon it contains (Gardner, 2008) and interpret new data from the Toby conglomerate to indicate that Sequence B strata were present near the depositional site of the Toby Formation during the Cryogenian. The Mount Nelson Formation may be a vestige of that succession.

The presence of a ca. 750 Ma detrital zircon supports the previously proposed Cryogenian age of the base of the Windermere Supergroup in southern

British Columbia (Ross et al., 1995) and is consistent with ages of correlative strata in northern British Columbia (<755 ± 18 Ma Rapitan Group; Ross and Villeneuve, 1997), central British Columbia (<728 ± 9 Ma Misinchinka Group; Evenchick et al., 1984) and Idaho (ca. 710-667 Ma Pocatello Formation; Fanning and Link, 2004).

Provenance of the Mount Forster Formation

Detrital zircon dates from the Mount Forster Formation have the characteristic northwestern Laurentia bimodal distribution of ages from 2.8-2.6 Ga and 1.9-1.75 Ga. Additional scattered dates from 2.5-1.9 Ga indicate a link to crust of that age, which, in North America, is known only in the basement beneath northern Alberta and the Northwest Territories (Ross et al., 1991; Figure 5-13). The Ksituan (1900-1987 Ma), Buffalo Head (1990-2324 Ma), Thorsby (1950-2380 Ma) and Chinchaga (2088-2186 Ma) provinces in the central Alberta basement (Hoffman, 1989; Ross, 1991; Villeneuve et al., 1993) are proposed ultimate sources of 2.38-1.90 Ga detrital zircons in the Mount Forster Formation. Local 2.50-2.38 Ga basement is not known, but has been inferred previously from detrital zircons of that age in Neoproterozoic and Cambrian miogeoclinal strata (Ross and Bowring, 1990; Ross and Parrish, 1991; Gehrels and Ross, 1998). The Peace River arch of northern Alberta is the only known potential source area of 2.5-2.0 Ga zircons in the Cordilleran margin (Figure 5-13).

The detrital zircon population of the Mount Forster Formation could be produced by mixing of detrital zircon from the Horsethief Creek Group and Cordilleran Ordovician strata (Figure 5-17). The zircon provenance data therefore corroborate Root's (1987) interpretation – made on the basis of petrographic and field data – that Horsethief Creek and Ordovician strata from uplifted exposures on the Purcell Arch were recycled into the Mount Forster Formation. The two youngest zircons (0.99 Ga and 1.18 Ga) may be far-travelled multi-cycle grains originating in a Grenville-age orogenic belt or, alternatively, could reflect closer sources of granitic crust such as was hypothesized to have shed 1.03 Ga and 1.05 Ga zircon into the nearby Ordovician Mount Wilson Formation (Gehrels and Ross, 1998).

Provenance of the Lardeau Group and Mount Sproat assemblage

The predominant, texturally immature grit in the Broadview and Akolkolex Formations (Fyles and Eastwood, 1962; Sears, 1979; Smith, 1990; Logan and Colpron, 2006) indicates that source areas were likely proximal (e.g., near the basin margin, not a cratonic interior) and were being uplifted. The coarse-grained, quartzofeldspathic nature of the Broadview Formation is inconsistent with derivation from the finer-grained Belt-Purcell Supergroup.

All three samples from the Lardeau Group (Akolkolex and Broadview formations) produced prominent clusters of 2.8-2.5 and 2.0-1.75 Ga detrital zircons (Figure 5-18) that corroborate prior detrital zircon data (Smith and Gehrels, 1991) and field evidence (Colpron and Price, 1995) that the Lardeau Group was depositionally linked to the southern Canadian Cordilleran miogeocline. As in the Mount Forster Formation, a spread of zircon dates from 2.5-1.9 Ga in all three Lardeau Group samples indicates ultimate derivation from a source similar to the basement of northern Alberta, which during the Paleozoic was exposed in the Peace River Arch (Ricketts, 1989). Detrital zircon data and the proximity to source indicated by the textural and compositional immaturity of Lardeau grits are interpreted here to indicate that the Lardeau trough was adjacent to sub-aerially exposed crust of similar ages and character to the Peace River Arch.

The Akolkolex Formation (07TWJK567) and Ferguson area Broadview Formation (08TWJK043) samples share a primary mode at 1.77 Ga that is not known in northwestern North American basement but is interpreted here to occur beneath Phanerozoic cover in western Canada. The 1.77 Ga zircon mode also forms the dominant mode in the Toby Formation sample. A relative abundance of 1.80-1.74 Ga detrital zircon grains also occurs in the Neoproterozoic and Cambrian miogeocline of southern British Columbia, and has been interpreted to indicate that plutonic rocks of that age are buried beneath the Western Canada Sedimentary Basin (Ross and Parrish, 1991; Gehrels and Ross, 1998; G. Gehrels, personal communication 2011). Rare 1.50-1.56 Ga detrital zircon grains in the Ferguson area Broadview sample are interpreted to originate from an unknown source of zircons of equivalent age in the upper Purcell Supergroup (Gardner, 2008). A small scattering of Mesoproterozoic zircon grains in the Broadview Formation at Ferguson indicates a minor contribution from a Grenville-age orogenic belt or crust.

The detrital zircon characteristics of the northwestern Broadview Formation are more similar to those of the overlying Mount Sproat assemblage than to the sample of Broadview grit from Ferguson. The relative abundance of Mesoproterozoic zircon in both the northwestern Broadview Formation and the Mount Sproat assemblage contrasts with other Lardeau Group, and with miogeoclinal rocks throughout the Canadian Cordillera. The pre-1.6 Ga zircon data for the Mount Sproat assemblage conglomerate and both samples of the Broadview Formation closely mirror those of the Akolkolex Formation and the southern B.C. miogeocline, leading to the interpretation of shared provenance and a stratigraphic connection (Figure 5-18).

Approximately 70% of the near concordant analyses in the northwestern Broadview Formation sample, however, yielded dates between 940 Ma and 1470 Ma. These dates are resolvable into modes, in diminishing proportion, at 1220-940 Ma, 1375-1250 Ma, and 1480-1420 Ma. The abundance of detrital zircons between 900 Ma and 1600 Ma in these samples is inconsistent with the provenance implicit in prior paleogeographic models of Kootenay Arc strata (Figure 1-4), which predict the Broadview Formation either derived from the Purcell Arch and would therefore have the same zircon provenance as the adjacent miogeocline (Logan and Colpron, 2006) or would have contained early Paleozoic detrital zircons (Roback et al., 1994) or only pre-1.7 Ga detrital zircon (Thompson et al., 2006). The 1.6-0.9 Ga zircons indicate additional sources that did not feed the Akolkolex Formation and miogeocline and are unknown in the basement of northwestern Laurentia.

The combined Archean, Paleoproterozoic and Mesoproterozoic zircon dates in the Broadview Formation and Mount Sproat assemblage are like those in the Toby Formation sample described above, however. That similarity leads to the suggestion that the source of Grenville-age zircon in the Toby conglomerate may also have supplied sediment to younger strata of the Lardeau Group and to the Mount Sproat assemblage.

New zircon dates from the Broadview Formation invalidate the hypothesis of Hughes et al (2003) that the Broadview Formation was derived from erosion of Late Devonian volcanic rocks to the west. That hypothesis implies that a significant population of Devonian detrital zircon would be present in the Broadview Formation. The absence of Paleozoic zircon and a diversity of zircon dates that match known units in the region is considered to result from derivation from heterogeneous Precambrian crystalline crust and (or) immature coarse siliciclastic strata to the west.

Considering near-concordant detrital zircon dates at one standard deviation margin of error, only 2 of 236 dates from the Broadview Formation and 3 of 120 from the Mount Sproat assemblage plot within the so-called 'North American magmatic gap' from 1.61-1.49 Ga (NAMG; an interval in which magmatic activity was rare in North American rocks; Van Schmus et al., 1993). Rare grains in the NAMG could derive either from recycled sediments of the Belt-Purcell Supergroup (Figure 5-14; Ross and Villeneuve, 2003; Gardner, 2008) or from the source of Belt-Purcell strata. The detrital zircon provenance of the Lardeau Group and Mount Sproat assemblage are consistent with derivation entirely from sources that were present in western Laurentia during the Paleozoic.

Provenance of the Thompson assemblage

Detrital zircon dates from the Thompson assemblage are similar to those in strata of the southern Canadian Cordilleran miogeocline, and are a close match to those in the Davis assemblage (Figure 5-19). The paucity of Mesoproterozoic and 1770 Ma zircons in the Thompson assemblage might indicate derivation was not entirely from the Broadview Formation; however the zircon characteristics of the Broadview Formation are known from only two sample localities. These detrital zircon data are consistent with the notion based on petrological and field data data presented in Chapter 3 that the Thompson assemblage is at least partially derived from sedimentary recycling of the underlying Broadview Formation. Because Mesoproterozoic zircon is not ubiquitous in the Lardeau Group, the Thompson assemblage is interpreted to derive from Lardeau strata that lacked zircon of that age range.

Provenance of the Davis assemblage

The two samples from the Viséan Davis assemblage (Milford group) have similar detrital zircon characteristics that mirror the underlying eastern Broadview Formation (Figure 5-19), which is consistent with observations of Broadview-like clasts and quartz 'eyes' in the Davis assemblage (Wheeler, 1968; Read and Wheeler, 1976; Klepacki, 1985; Roback, 1993; this study, Chapter 3). The basal conglomerate sample best matches the Broadview Formation and is therefore probably locally derived. The stratigraphically higher quartzite sample has a similar distribution of zircon dates but also contains Silurian zircon. Because Silurian zircon has not been identified in the Broadview Formation, another source, probably from the west, is interpreted to have contributed a small amount of Silurian detritus to the Davis assemblage. Potential sources of Silurian zircon were discussed above.

Provenance of the McHardy assemblage

The detrital zircon distribution from wacke in the upper half of the McHardy assemblage (Milford Group) matches northwestern Laurentian zircon ages and, more specifically, resembles the provenance data from Ordovician strata throughout the North American Cordillera suggesting a possibility of shared provenance. The proportion of 2.1-2.0 Ga zircon in the McHardy assemblage wacke is significantly greater than presently available data suggest would have occurred in potential source rocks to the east (the Windermere Supergroup, Hamill Group and Lardeau Group) and instead is characteristic of strata interpreted to derive from the Peace River Arch (Ross et al, 1993; Gehrels and Ross, 1998). Thirty kilometres along strike at Tenderfoot Lake, calcareous quartzite at least 100 m above the base of the McHardy assemblage has broadly similar detrital zircon characteristics (Lemieux et al., 2008;). The near absence of 1.5-1.0 Ga zircons in the McHardy assemblage is inconsistent with its main derivation from the Broadview Formation, Mount Sproat assemblage, or the source of those units.

The uniquely prominent cluster of Cryogenian detrital zircons (ca. 700-650 Ma) are interpreted to reflect a local source of that age, as discussed above.

Provenance of the Chase Formation

The Late Devonian detrital zircon date of 372.6 ± 5.2 Ma is consistent with map relations and age constraints from other sources (Thompson et al., 2006) and is considered here to be a maximum depositional age for the Chase Formation. The Mississippian $^{206}Pb/^{238}U$ model age of 325 ± 8 Ma of a discordant (4.3%) zircon presented above conflicts with a crosscutting relationship reported by Thompson et al. (2006), which establishes a minimum depositional age of 358 ± 0.8 Ma for the Chase Formation. Mesozoic or younger lead loss is interpreted to have produced an erroneously young date for this zircon. The paucity of Devonian zircons in the Chase Formation indicates Devonian felsic magmatic rocks of the Cordilleran margin arcs (e.g. Paradis et al., 2006) were not significant sediment sources. The compositional maturity of the Chase Formation and the highly rounded detrital zircon grains of diverse ages within it are interpreted to indicate it is a multi-cycle sedimentary unit.

Detrital zircon dates from the type locality of the Chase Formation presented here are similar to results from three occurrences of Chase quartzite in the Monashee Mountains by Lemieux et al. (2007) and support derivation from a source other than the known basement of western Laurentia or the Cordilleran miogeocline. As discussed in Chapter 2, a sample from Tenderfoot Lake reported as Chase Formation by Lemieux et al. (2007; sample 04TWL072) is probably part of the Mississippian Milford Group and is therefore not considered here. A significant proportion of 2.0-1.7 Ga zircon – the common thread of zircon provenance for western Laurentia – has not been identified in the Chase Formation. Instead, the Chase Formation is characterized by a broadly scattered distribution of detrital zircon from ca. 1.8-0.9 Ga with a few notable early Paleozoic grains and rare Neoarchean and ca. 2.0 Ga zircons.

The cluster of zircon dates of 1.2-0.9 Ga grains suggests proximity to a Grenville-age orogenic belt that also has a significant amount of 900-1000 Ma crust. The conspicuous gap of ages from 1.32-1.22 Ga is unlike sedimentary units in southwestern Laurentia (Figure 5-15; Talavera-Mendoza et al., 2005) or Early Neoproterozoic (Sequence B) strata of northwest Laurentia (Rainbird et al., 1997) that are interpreted to derive from erosion of the Grenville orogen.

Twelve of 142 zircon grains from the Chase Formation (Lemieux et al., 2007; this study) lie in the North American magmatic gap of Van Schmus et al. (1993), primarily in the range 1.55-1.48 Ga. Although these ages are not characteristic of North America, detrital zircons of this age occur in trace amounts in the Broadview Formation (this study) and the Belt-Purcell Supergroup (Ross and Villeneuve, 2003; Gardner, 2008) and therefore are not compelling evidence of exotic provenance of the Chase Formation. The presence of Phanerozoic zircon and a significant number of ca. 1.64-1.60 Ga zircon, and the scarcity of pre-1.75 Ga zircon are significant differences in the Chase Formation data relative to the Lardeau Group, Mount Sproat assemblage and miogeoclinal rocks. Its detrital zircon characteristics are inconsistent with primary derivation from the known Precambrian basement of northwestern North America, the Cordilleran miogeocline, or the pericratonic rocks in the Kootenay Arc. The Chase Formation was derived from crust that is not typical of northwestern Laurentia or other strata in the Cordillera.

Constraints presented in this thesis show that the Chase Formation was deposited around the time of the first local Devonian magmatism and ~5-20 Myr before phase 1 deformation in the adjacent Kootenay Arc. Correlation of the Mount Sproat assemblage with the Silver Creek Formation means that the amphibolitic schist overlap assemblage tied the Chase Formation to the Lardeau trough immediately after the Chase quartzite was deposited. Moreover, the paragneiss basement to the Chase Formation (Unit 1 of Lemieux et al., 2007; Pqfh in Figure A1-1) has detrital zircon attributes of the southern Canadian Cordilleran miogeocline (Lemieux et al., 2007) and is considered to be part of the Cordilleran margin (e.g. Wheeler and McFeely, 1991). The Chase Formation, therefore, is too young to have been accreted to the Cordilleran margin in mid-Devonian time as proposed by Colpron and Nelson (2009). Age and field data are most readily explained by a parautochthonous origin for the Chase Formation.

If the correlation between the Mount Sproat assemblage and the Silver Creek Formation is erroneous, however, it remains possible that the paragneiss basement of the Chase Formation existed outside the Cordilleran pericratonic realm in early Paleozoic to Devonian time, and that its tectonic relationship with the Cordilleran margin has been obscured by intense strain and metamorphism in the Shuswap metamorphic complex. A similar evolution is proposed below (see "5.5.5 Introduction of exotic crust?") for the paragneiss basement of the Chilliwack Composite terrane (Yellow Aster complex), which has yielded detrital zircon dates similar to the Chase Formation's basement and the Cordilleran miogeocline.

Based on the available evidence from detrital zircon analysis, field relations, and correlation of the Mount Sproat assemblage with the Silver Creek Formation, I interpret that the Chase Formation was deposited on an outboard Cordilleran margin platform (Okanagan High) and the source of its atypical provenance was present in the Cordilleran realm by Late Devonian time (ca. 375 Ma). Although the weight of evidence points to an autochthonous origin for the basement of the Chase Formation, the possibility that this paragneiss and (or) the Yellow Aster complex comprise rifted fragments of North American crust that evolved outside the Cordilleran realm in early Paleozoic time is a subject that warrants further investigation.

Provenance of the Slocan Group

The analyzed sample of Late Triassic Slocan Group sandstone has an abundance of Phanerozoic zircons showing that its provenance differs from other units. It received a large proportion of Triassic and Permian zircon plus some

Mississippian, Devonian and Silurian grains. These zircon groups are inferred to derive from magmatic arc rocks in the Quesnel arc and its basement. The Cordilleran miogeocline or its cratonic source were not measurable contributors of detrital zircon to the Slocan Group. Instead, a close match in zircon date distributions indicates Precambrian zircon (Ediacaran, Mesoproterozoic, and ca. 1640 Ma) in the Slocan Group sandstone probably came from the same source as that of the Chase Formation. The Slocan Group is therefore interpreted to have derived from erosion of a diverse suite of Silurian to Late Triassic igneous rocks in the Quesnel arc to the west, including the same Precambrian rocks that sourced the Chase Formation. Because the Slocan Group can be tied to the continental margin by an unbroken (e.g. without faulted contacts) stratigraphic succession, derivation of Slocan Group detritus from the Nicola arc unambiguously links the arc to the continental margin during Late Triassic deposition of the Slocan Group.

5.5.4 A continental high outboard of the miogeocline

Prior reference datasets (e.g. Gehrels and Ross, 1998) and new data from the Mount Forster Formation show that miogeoclinal rocks in British Columbia have a predictable bimodal detrital zircon signature with ~2.8-2.5 Ga and ~2.0-1.75 Ga zircons and a notable paucity of zircons younger than 1.7 Ga. All of the pericratonic strata in this study other than the Akolkolex Formation, which was derived from erosion of the Purcell Arch, contain detrital zircon populations indicative of sources that were not available to the easterly-derived miogeocline, and were therefore outboard of the miogeocline. These outboard sources provided to Paleozoic pericratonic strata in southern British Columbia detrital zircons in the ranges: 1480-1410 Ma, 1380-1320 Ma, 1300-900 Ma, 680-650 Ma, 550 Ma, and 430 Ma and 420 Ma. Importantly, all of the pericratonic unit samples except the Chase Formation and Slocan Group share the characteristic western Laurentian signature of Paleoproterozoic (2.0-1.75 Ga) and Neoarchean (2.8-2.5 Ga) ages, and therefore contained a mixture of zircon from ‘typical’ western Laurentian crust and outboard sources of the ages listed above.

The source that provided 1480-1410 Ma, 1380-1320 Ma, and 1300-1000 Ma detritus to the Toby Formation was short-lived and was replaced by easterly derived first cycle sediment from the Alberta basement that deposited as turbidite in the overlying Horsethief Creek Group (Ross and Bowring, 1990). More outboard in the Lardeau trough, pericratonic strata continued to receive detritus containing zircon of these ages into mid-Paleozoic time from an outboard source.

New zircon provenance data from the Lardeau Group and Mount Sproat assemblage indicates that the continental crust outboard of the Lardeau trough (Okanagan High) contained typical northwest Laurentian Precambrian zircon as well as rocks that provided 1480-1410 Ma, 1380-1320 Ma, and 1300-900 Ma detrital zircon.

5.5.5 Introduction of exotic crust?

From Late Devonian to Triassic time, and apparently not before the Late Devonian, sources of ca. 1.64 Ga, Ediacaran and Silurian zircon, and possibly Mesoproterozoic zircon-bearing rocks, were available to the pericratonic rocks of southeastern British Columbia. With current data (Ross et al., 1993; Gehrels and Ross, 1998), these sources have no manifestation in the Cordilleran margin prior to deposition of the Chase Formation in the Late Devonian. Neither Ediacaran crust nor Silurian arc activity is known from the Cordilleran margin in rocks older than Late Devonian. Although the Chilliwack Composite terrane was interpreted to originate at the Canadian Cordilleran margin in the early Paleozoic or late Proterozoic (Brown et al. 2010), early Paleozoic deformation and metamorphism in its basement (Brown et al., 2010) is at odds with the passive to extensional setting of the early Paleozoic Cordilleran margin (e.g. Cecile et al., 1997). Instead, the Chilliwack Composite terrane shares early and mid-Paleozoic features with, and probably was linked to, the Alexander terrane prior to the Late Devonian (Brown et al., 2010).

Prismatic ca. 556 Ma detrital zircons in the Paleozoic Spa Creek conglomerate northwest of Vernon were interpreted by Erdmer et al. (2002) as representative of granite related to terminal rifting of the Cordilleran margin. This date is approximately 20 Myr younger than the estimated onset of passive margin subsidence in the miogeocline (575 Ma; Bond and Kominz, 1984; Colpron et al., 2002) and would therefore represent granitic plutonism in a passive margin setting. There is presently no corroborating evidence of felsic magmatic activity of this age in the Canadian Cordillera; detrital zircon analysis of Ediacaran and Paleozoic strata in the eastern Canadian Cordillera, including the nearby Lardeau trough analyzed in this study, have found no suggestion of felsic magmatic activity in the Late Precambrian (Ross and Bowring, 1990; Ross and Parrish, 1991; Smith and Gehrels, 1991; Ross et al., 1993; Gehrels and Ross, 1998; Devine et al., 2006; Nelson and Gehrels, 2007; Piercey and Colpron, 2009; G. Gehrels, unpublished data). The Spa Creek conglomerate stratigraphically overlies the Silver Creek

Formation (Erdmer et al., 2002) and therefore had the potential to receive sediment from the same sources as the deeper underlying Chase Formation. This leads to an alternative interpretation that the anomalous Ediacaran zircon in the Spa Creek conglomerate originated from the same atypical source terrain as the Chase Formation.

The above detrital zircon ages cannot be matched to sources known to have Cordilleran origins, but are equivalent to characteristic domains in the terranes of the Arctic Realm of Colpron and Nelson (2011; Alexander, Arctic Alaska-Chukotka and Farewell terranes; see above). Beranek et al. (2013) recently characterized Cambrian-Ordovician sandstone of the Alexander terrane in the Saint Elias Mountains and identified dominant groupings of ca. 1650 Ma, 1450 Ma, 1250-1000 Ma and 760-565 Ma, which they linked to sources of coeval rocks in the Timanide Orogen and Baltican Shield of northern Eurasia. These groupings are a good fit to the ca. 1640 Ma, 1250-950 Ma, 700-650 Ma, 600-500 Ma zircon groupings in the Slocan Group and Chase Formation and in other scattered occurrences (700-650 Ma in McHardy assemblage; ca. 556 Ma zircon in Spa Creek conglomerate, Erdmer et al., 2001; ca. 555 Ma detrital zircon in Chilliwack Composite terrane, Brown et al., 2010; 1.04 Ga cobble in Nicola Horst, Erdmer et al., 2002). Combined with the appearance of associated Silurian detrital zircon and granite cobbles in Late Devonian time – after the Cordilleran margin became an active plate boundary – these data corroborate the hypothesis of Colpron and Nelson (2009; 2011) in which sources of late Paleoproterozoic, Ediacaran and Silurian zircon in the southern Canadian Cordillera derive from fragments of allochthonous crust (terranes) that were introduced into the Cordillera from the north in mid-Devonian time. Because of the disparity between the Early Paleozoic evolution of the Chilliwack Composite terrane and the Cordilleran margin, and the similarities with Alexander terrane in that period, I favour the interpretation that the Chilliwack Composite terrane was far north of its present Cordilleran residence during Ordovician to Early Devonian time. It may represent a rifted fragment of the northwest Laurentian margin that evolved in isolation from the Canadian Cordilleran margin in Early Paleozoic time. It was emplaced at the Cordilleran margin in the mid-Devonian time.

Paleogeographic maps illustrating this scenario and a best fit for provenance and regional geological data are presented in Chapter 6.

Interpretations of this study predict that other pericratonic strata in the

Canadian Cordillera also contain mixed populations of northwest Laurentian ages (2.8-2.5 Ga and 2.0-1.7 Ga) and Mesoproterozoic, Cryogenian, and Silurian detrital zircons similar to strata investigated in this study. Silurian and Neoproterozoic zircon are anticipated in pericratonic rocks younger than Middle Devonian, but Mesoproterozoic zircon should occur in a broad range of Phanerozoic pericratonic strata. Detrital zircon analysis of Silurian and Early Devonian strata of the Cordillera margin would offer a test of the exotic Okanagan terrane hypothesis. Presently the provenance dataset for such rocks is limited to only a few samples from the miogeocline (Ross et al., 1993; Gehrels et al., 1993; G. Gehrels, unpublished data). The presence of significant numbers of Silurian zircon in sediments of this age that were deposited at the Cordilleran margin would invalidate the hypothesis.

5.6 Conclusions

Early Neoproterozoic strata containing detritus from a Grenville-age orogenic belt were present near the depositional site of the Toby Formation.

The Broadview Formation records an important shift in provenance in the Lardeau trough with the introduction of abundant Mesoproterozoic zircon. This provenance shift is interpreted to reflect a change in the Lardeau trough to westerly provenance. The western source contained abundant detrital zircons in the ranges 1480-1410 Ma, 1380-1320 Ma, and 1300-1000 Ma in addition to ca 1.7-1.9 Ga and Neoarchean zircons interpreted to derive from the northwest Laurentian basement. Mount Sproat assemblage quartzofeldspathic conglomerate shares the provenance seen in the Broadview Formation and is interpreted to have derived from the same outboard source.

Zircon characteristics of the Thompson assemblage and Milford Group mimic the underlying Lardeau Group. The Davis assemblage of the Milford Group also contains sporadic occurrences of Silurian detrital zircon of the same age as granitic clasts reported from the McHardy assemblage by Roback et al. (1994).

Both in situ and allochthonous sources of Grenville-age crust are present in the Canadian Cordillera. Allochthonous crust arrived prior to Late Devonian time (ca. 375 Ma) with sources of the late Paleoproterozoic, Mesoproterozoic, Ediacaran and Silurian detrital zircon in the Chase Formation, Slocan Group and other rocks associated with the Quesnel arc. Cryogenian, Ediacaran and Silurian zircon in the Milford Group and Silurian zircon in the Spray Lakes Group came from this exotic source. The Chilliwack Composite terrane in northwestern Washington State is a surface representation of this allochthonous crust. There is currently no evidence that a Silurian arc shed detritus into Cordilleran marginal basins prior to deposition of the Late Devonian Chase Formation.

Devonian and Mississippian volcanic arc rocks in southeastern British Columbia were not significant sources of detritus to the studied Late Paleozoic strata.

The Triassic Slocan Group sandstone was derived from a source with diverse Late Paleozoic to Late Triassic crystalline rocks inferred to represent the Quesnel arc and its basement. Eastern provenance is not apparent.

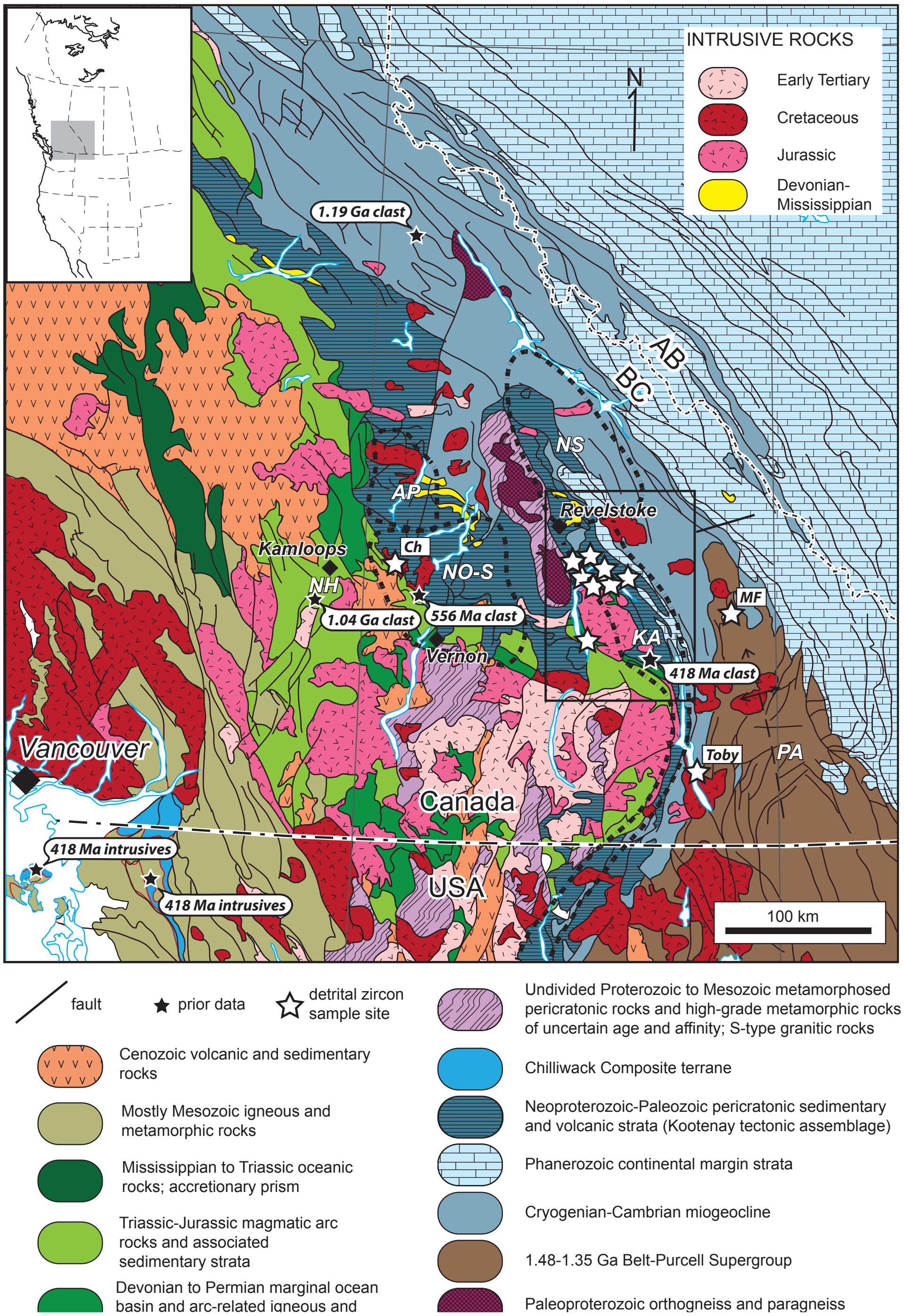

Figure 5-1. Sample sites and regional localities discussed in the text.
Refer to Figure 5-3 for sample sites in the Kootenay Arc. Abbreviations: Ch, Chase Formation; CM, Cariboo Mountains; EBA, Eagle Bay assemblage; KA, Kootenay Arc; MF, Mount Forster Formation; MO, Monashee complex; NH, Nicola Horst; NS, Northern Selkirk Mountains. (modified from Wheeler and McFeely, 1991) Data sources: Roback et al. (1994); Erdmer et al. (2001, 2002); Brown et al. (2010); D. Murphy (unpublished data).

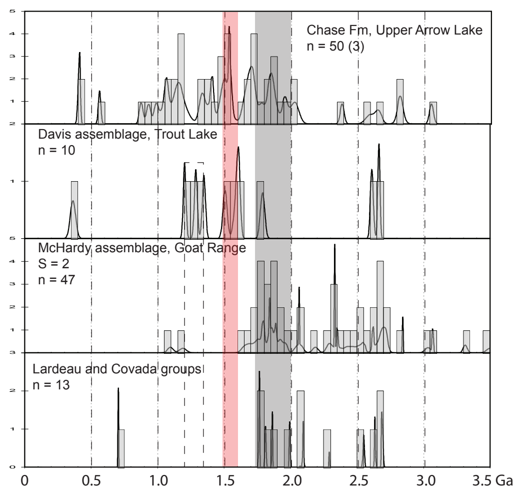

Figure 5-2. Previous detrital zircon data from the Kootenay Arc and Upper Arrow Lake area.

Sources are: Davis assemblage (Lemieux, 2006); McHardy assemblage (Roback, 1993; Lemieux et al., 2007 - note that they called it Chase Formation); Chase Formation (Lemieux et al., 2007); Lardeau and Covada groups (Smith and Gehrels, 1991)

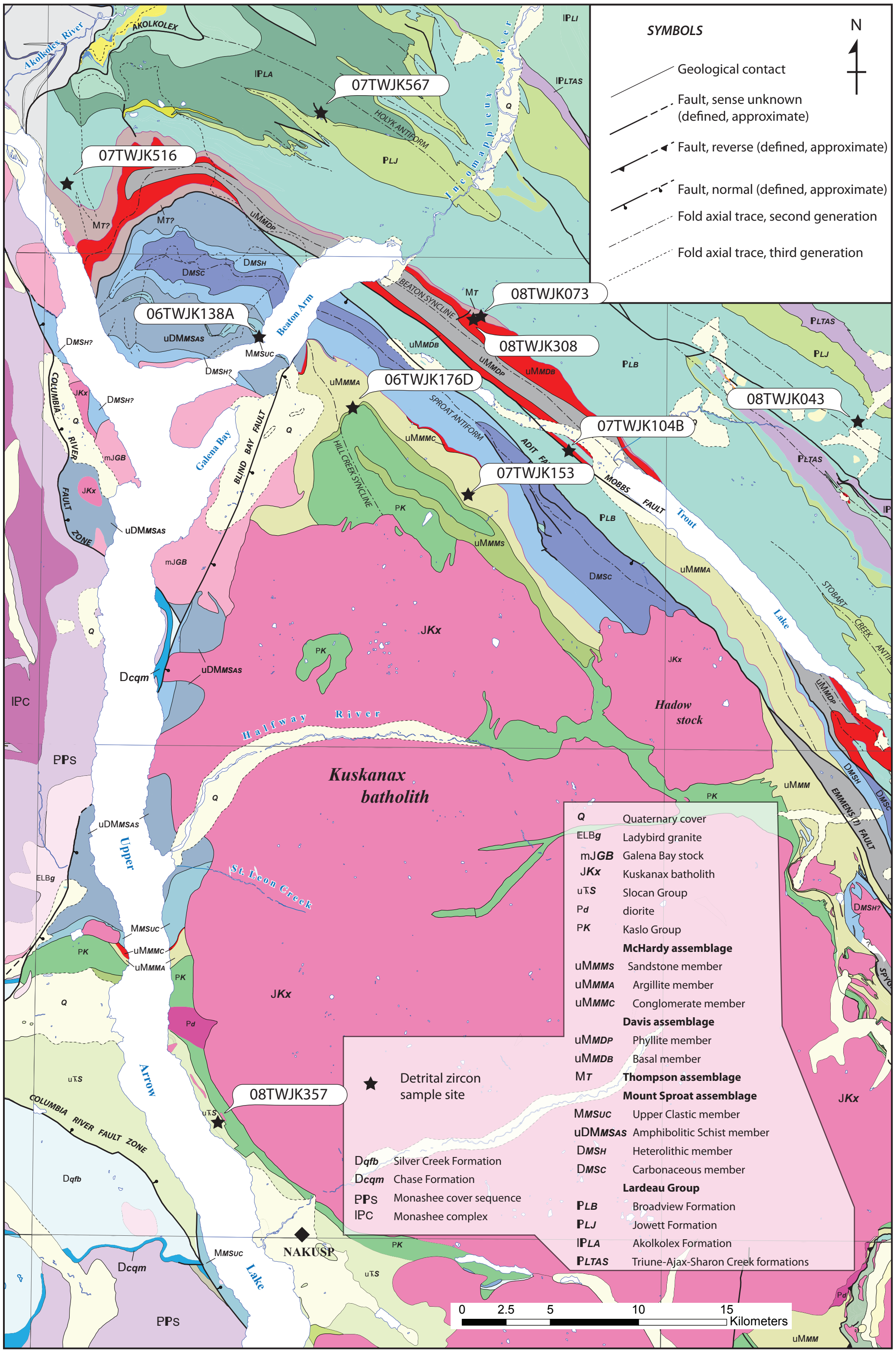

Figure 5-3. Detrital zircon samples sites in the northern Kootenay Arc.

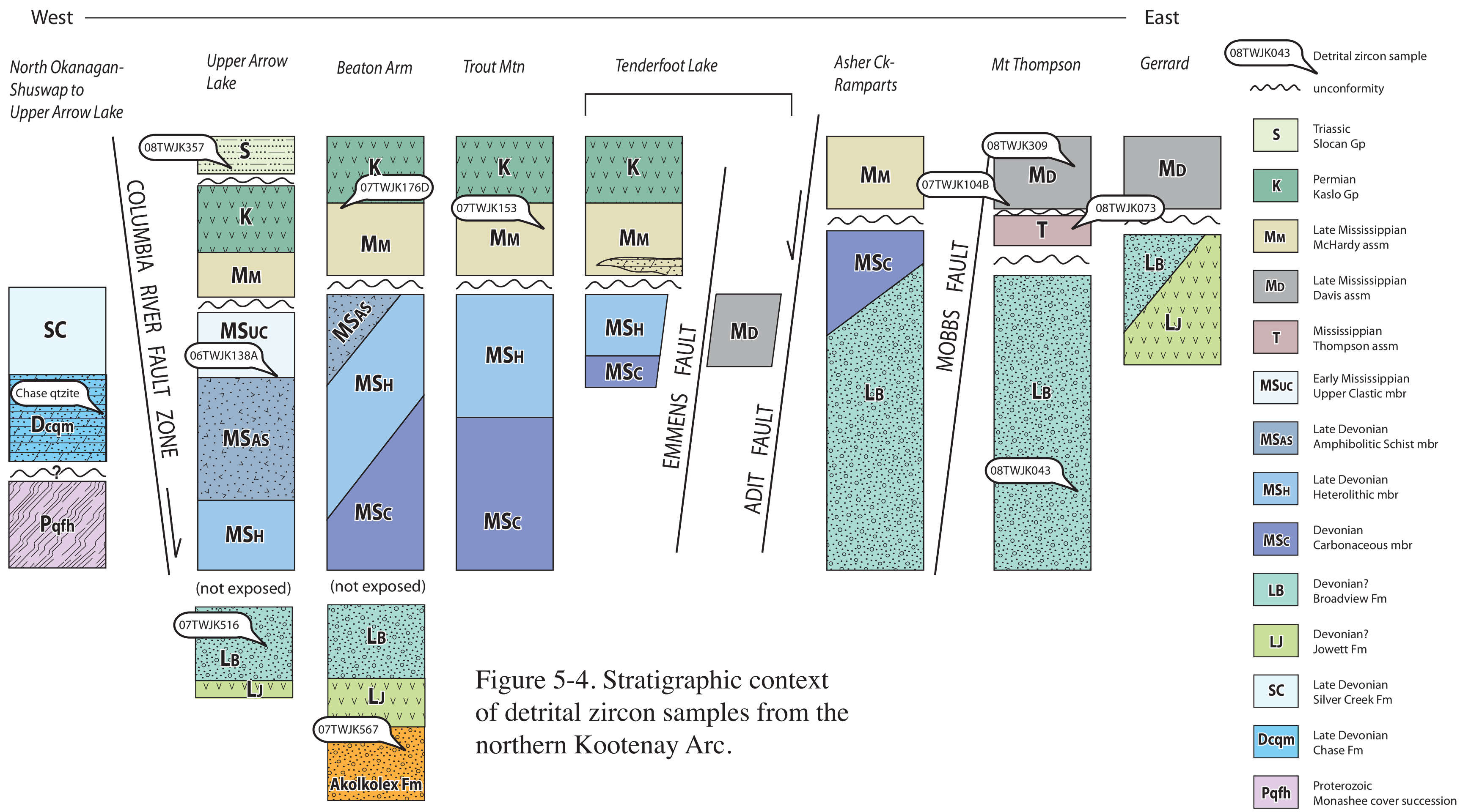

Figure 5-4. Stratigraphic context of detrital zircon samples from the northern Kootenay Arc.

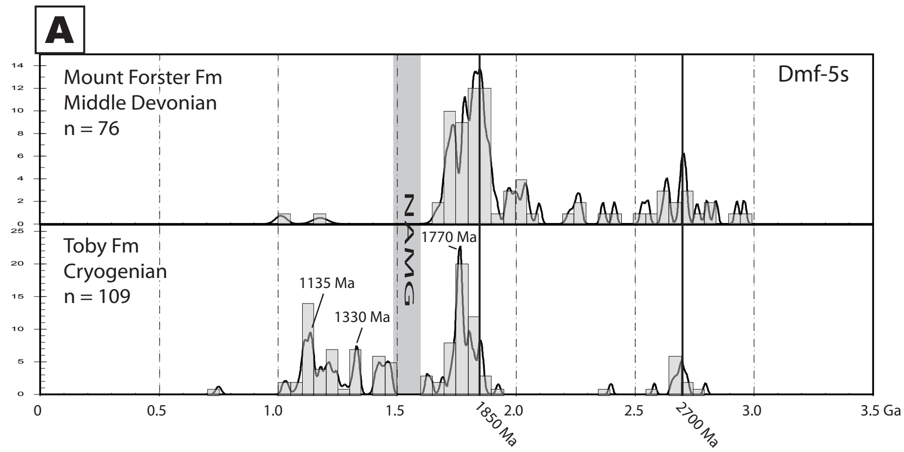

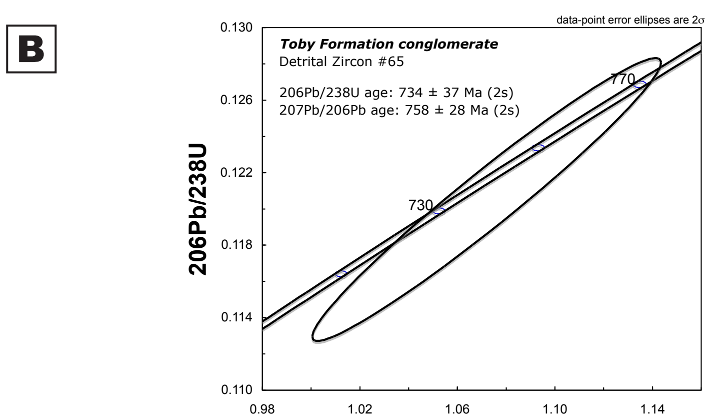

Figure 5-5. Detrital zircon data from the Toby and Mount Forster formations. A) Combined histogram and probability density plots. B) Concordia plot of the youngest zircon recovered from the Toby Formation. The interpreted age of 734 ± 37 Ma is the maximum depositional age of the conglomerate. NAMG is the North American magmatic gap - an interval in which zircon ages are rare in North America (Van Schmus et al., 1993).

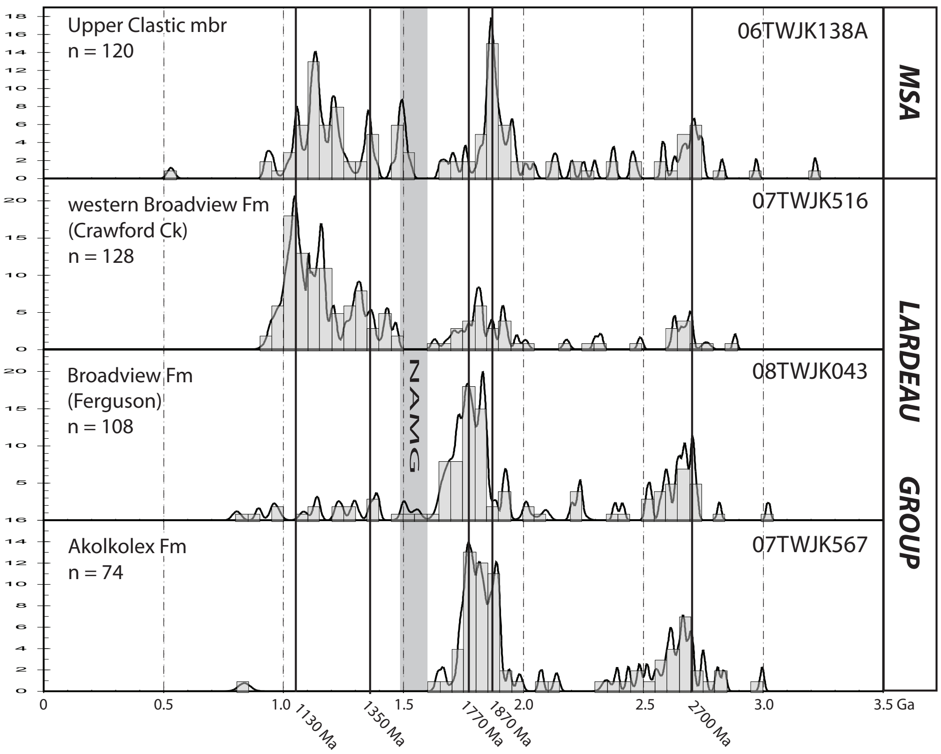

Figure 5-6. Combined histogram and probability density plots of new detrital zircon data from the Lardeau Group and Mount Sproat assemblage.

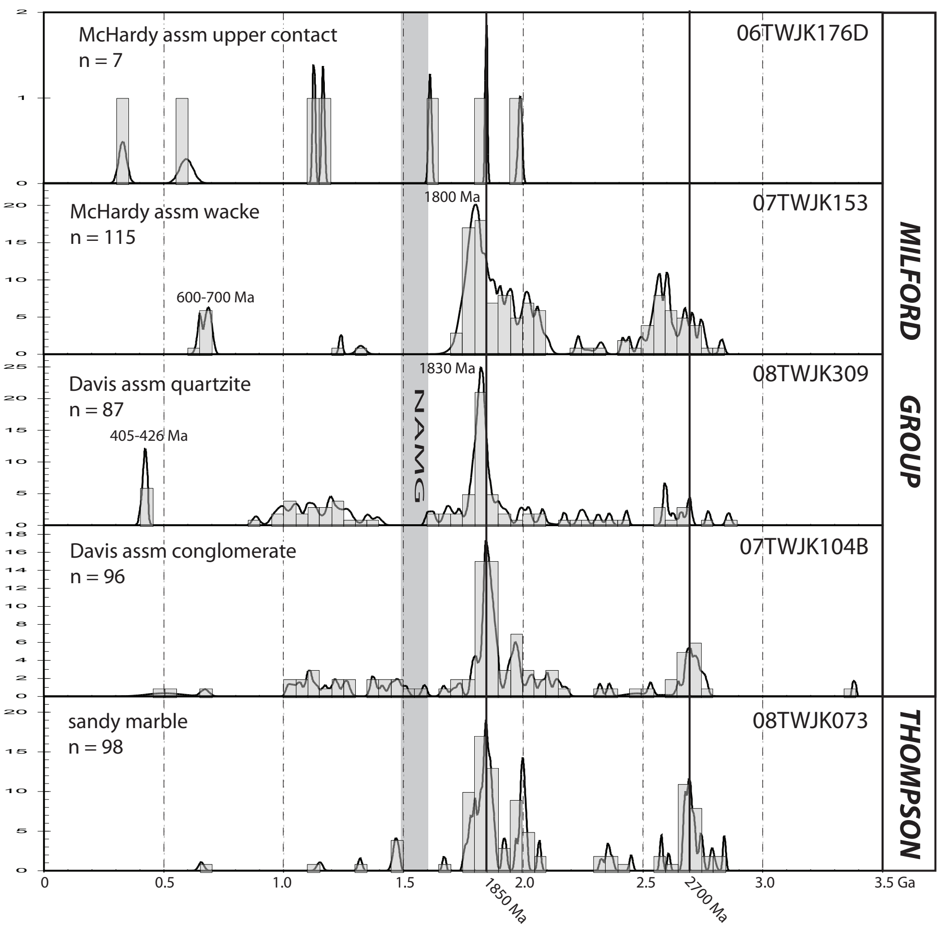

Figure 5-7. Combined histogram and probability density plots of detrital zircon data from the Thompson assemblage and Milford Group.

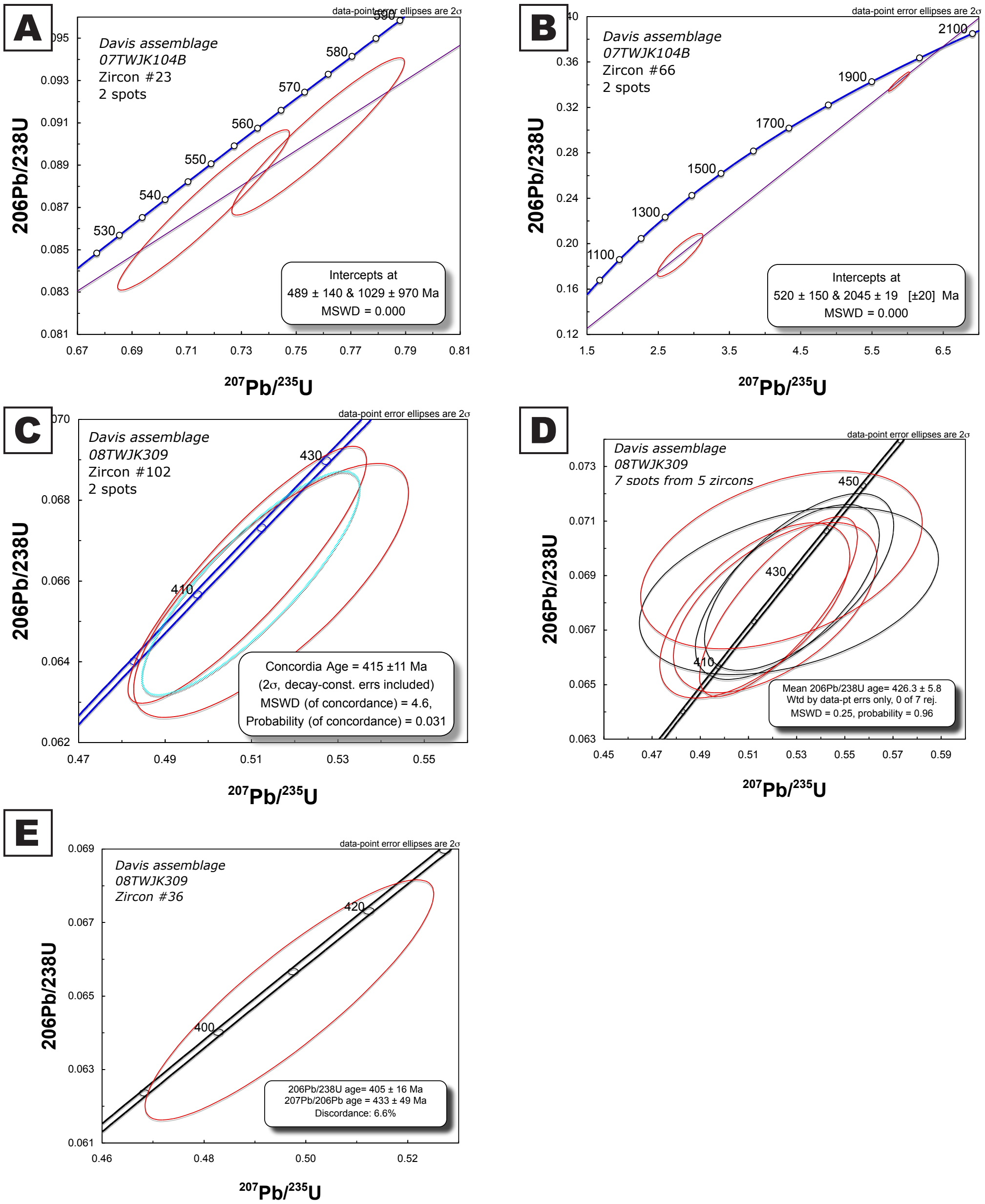

Figure 5-8. Concordia plots of select detrital zircon analyses from the Milford Group.

A) and B) are similar examples of grains for which two ablation spots define discordia with Early Paleozoic lower intercepts and Proterozoic upper intercepts. These results could be produced by Early Paleozoic zircon with inherited Mesoproterozoic (A) and Paleoproterozoic (B) lead. C) A detrital grain from which two ablation spots produced the same discordant Silurian (ca. 415 Ma) crystallization age. Blue ellipse represents the concordia age. D) Near concordant analyses from 5 Silurian zircons with a weighted mean 206Pb/238U age of ca. 426 Ma. Three black ellipses are from grain 49. Red ellipses are single spots on the other 4 zircons. E) Single spot analysis of a Silurian zircon in the Davis assemblage.

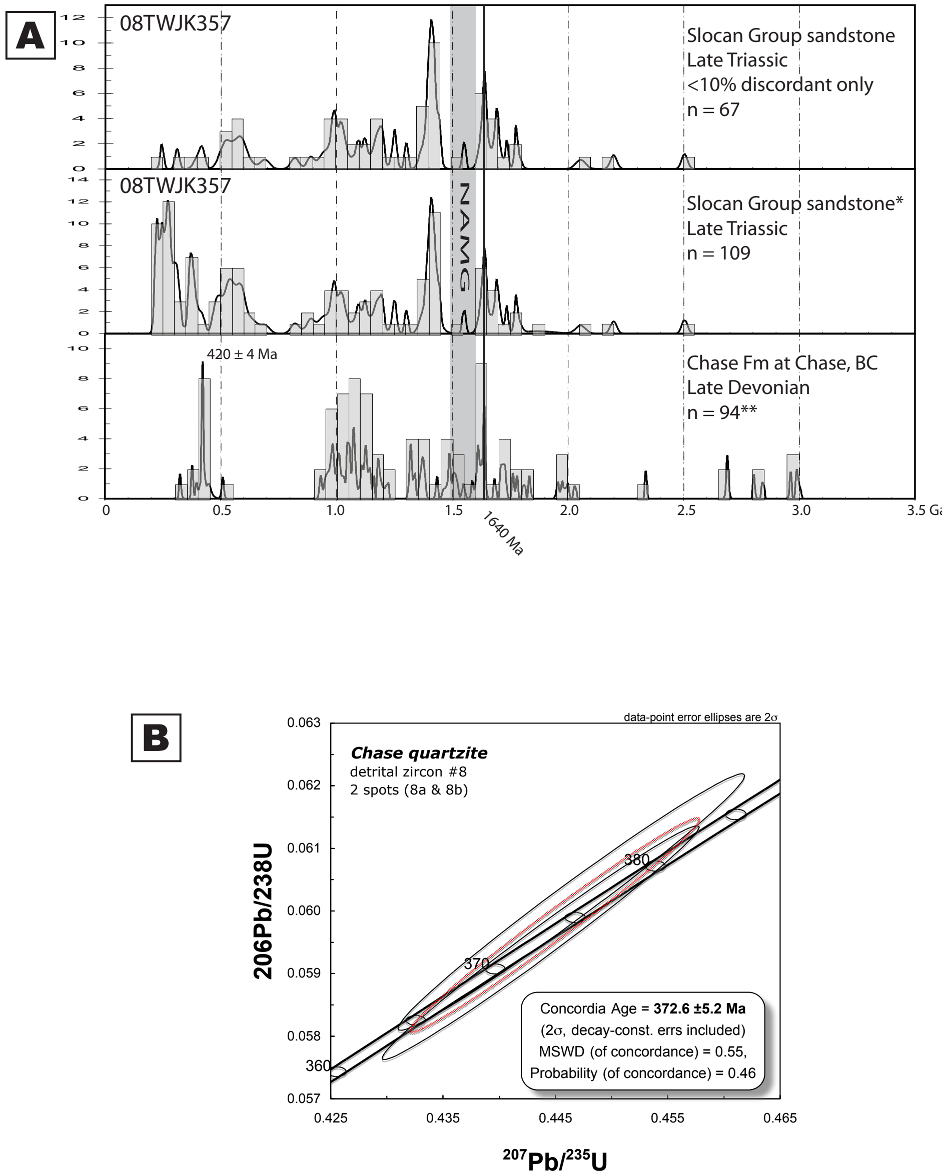

Figure 5-9. New detrital zircon data from the Slocan and Chase formations. A) Combined histogram and probability density plots of detrital zircon data from the Chase Formation and Slocan Group. B) Concordia plot of the youngest robust zircon age from the Chase Formation. Two ablation spot analyses on one zircon grain agree within error and yield a nearly concordant concordia age (red ellipse) of 372.6 ± 5.2 Ma (2σ). The Chase Formation is therefore no older than 378 Ma. * includes data less than 10% normally discordant and all reversely discordant data. **includes two U-Pb dates from Thompson et al. (2006) from the same sample.

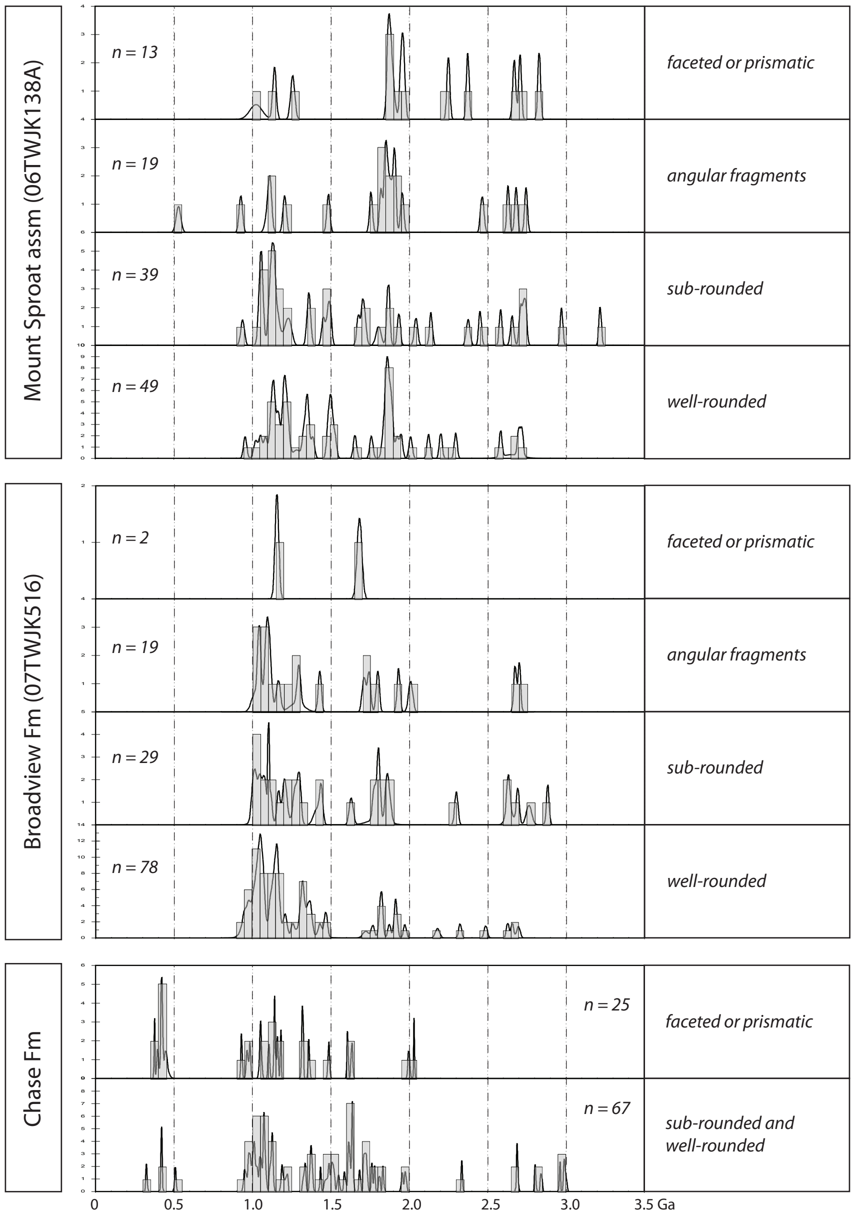

Figure 5-10. Comparison of detrital zircon signatures of 3 samples sorted by zircon morphology.
There is little correlation between the ages of these detrital zircons and their morphology.

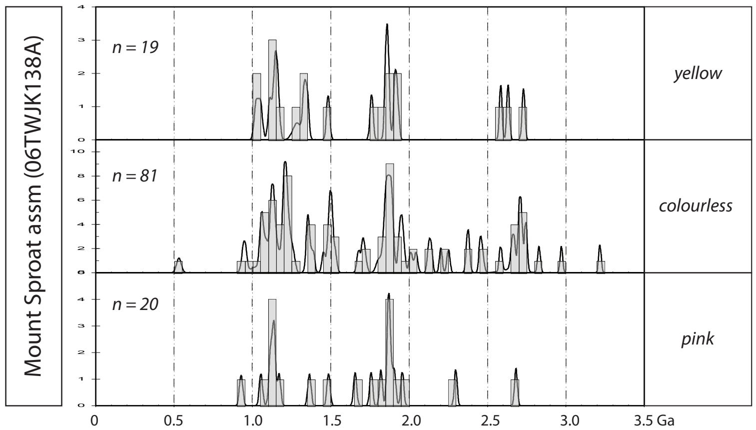

Figure 5-11. Comparison of detrital zircon signatures for different colour groups in sample 06TWJK138A.
There is little correlation between the colour of these detrital zircons and their age.

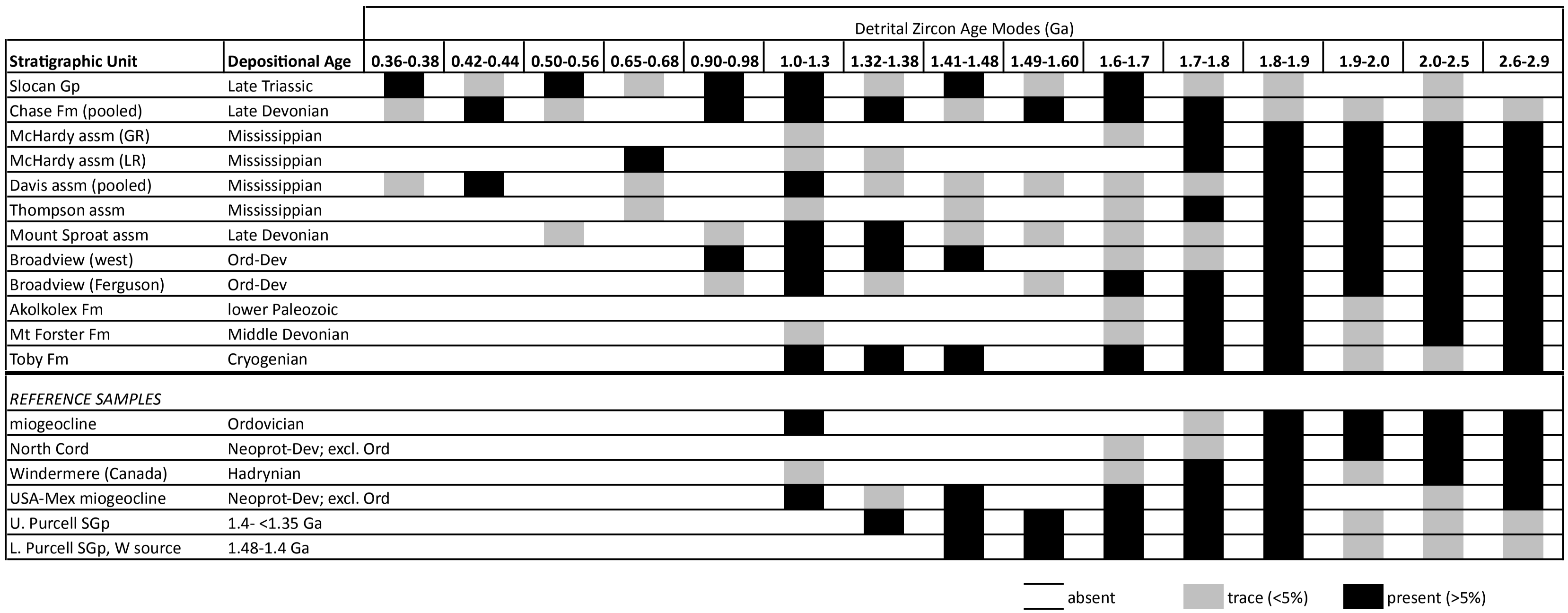

Figure 5-12. Plot showing distribution of the key zircon age groups in samples from this study compared with reference samples from potential miogeoclinal source or correlative rocks.

Abbreviations: GR, Goat Range; LR, Lardeau Range; North Cord; Northern Canadian Cordilleran miogeocline. Reference data sources: Gardner, 2008; Gehrels and Dickinson, 1995; Gehrels and Ross, 1998; Gehrels and Stewart, 1998, G. Gehrels, unpublished data; Ross and Parrish, 1991; Ross and Villeneuve, 2003, Stewart et al. 2001

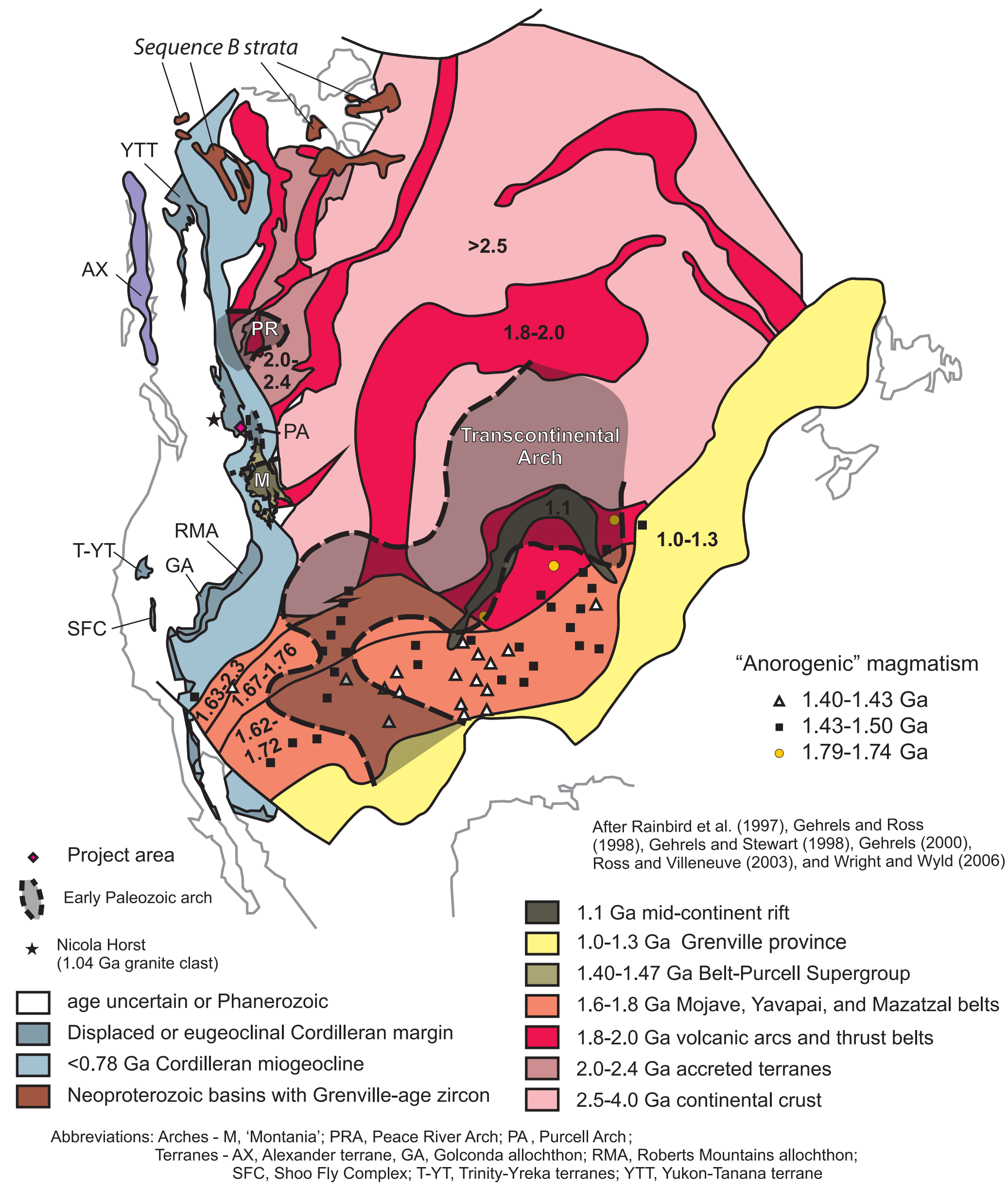

Figure 5-13. Map of the basement provinces of North America.
Note the absence of Mesoproterozoic crust in modern day northwestern North America where the present study was conducted.

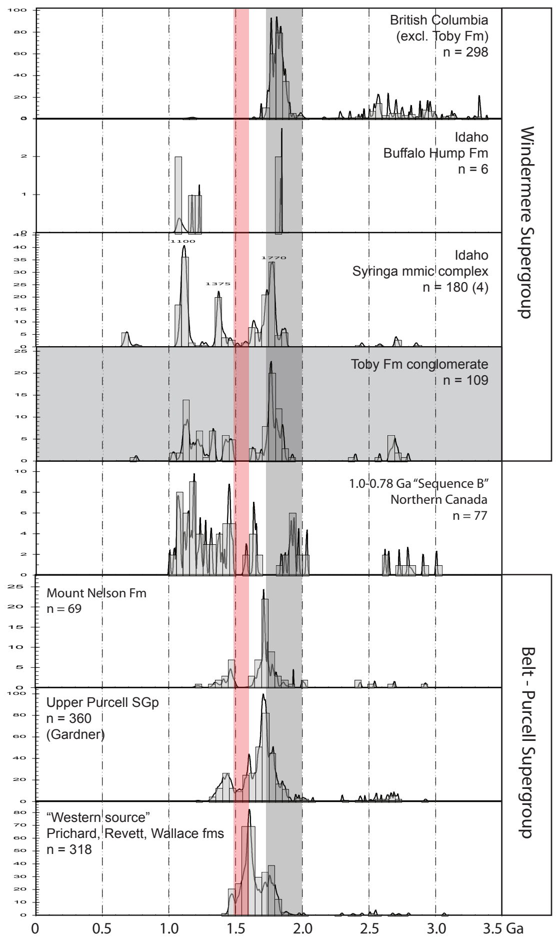

Figure 5-14: Comparisons of detrital zircon data from the Toby Formation, other Windermere strata and potential sources.

The provenance of the Toby conglomerate is similar to Windermere strata in Idaho and to older Sequence B strata in northwestern Laurentia. This is in contrast to higher strata of the Windermere Supergroup in British Columbia, which lack the Mesoproterozoic zircons. Belt-Purcell strata have different zircon provenance and therefore are probably not a significant source of detritus. Note that data from this study are shown in shaded boxes in this and later figures. Reference data sources: this study, Gardner, 2008; Gehrels and Ross, 1998; G. Gehrels, unpublished data; Lewis et al, 2010; Rainbird et al., 1997; Ross and Bowring, 1990; Ross and Villeneuve, 2003; Ross et al 1992.

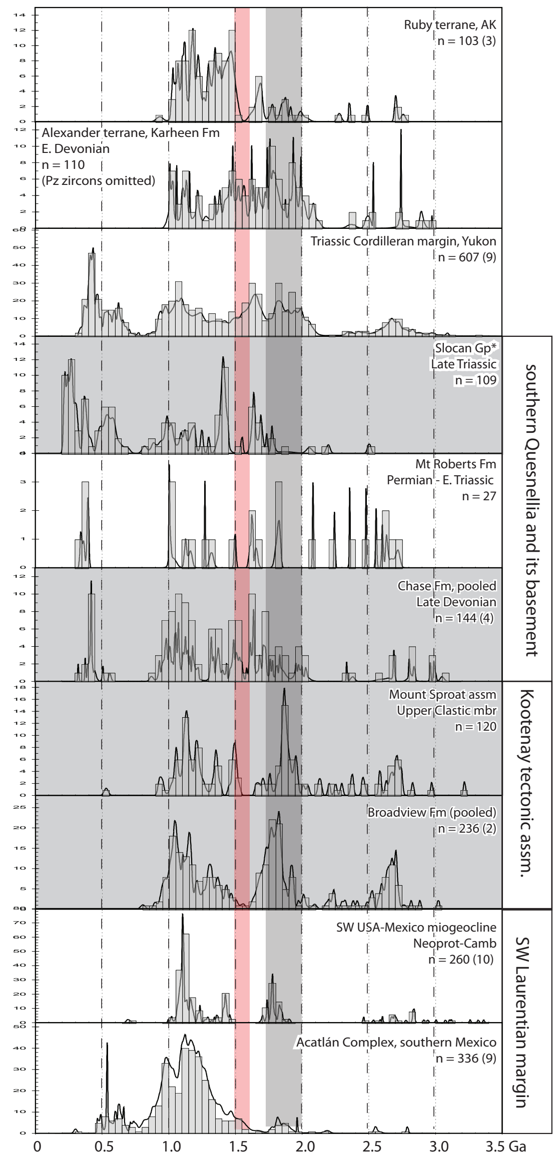

Figure 5-15. Detrital zircon data from Quesnellia (Quesnel arc and its basement) and Kootenay tectonic assemblage rocks compared with other strata of the North American Cordillera.

Data from this study are shown with grey backgrounds. See text for discussion. Reference data sources: Beranek et al., 2010b; Bradley et al., 2007; Gehrels and Ross, 1998; Gehrels et al., 1996; Gehrels and Stewart, 1998; G. Gehrels, unpublished data; Roback et al., 2005; Stewart et al., 2001; Talavera-Mendoza et al., 2005.

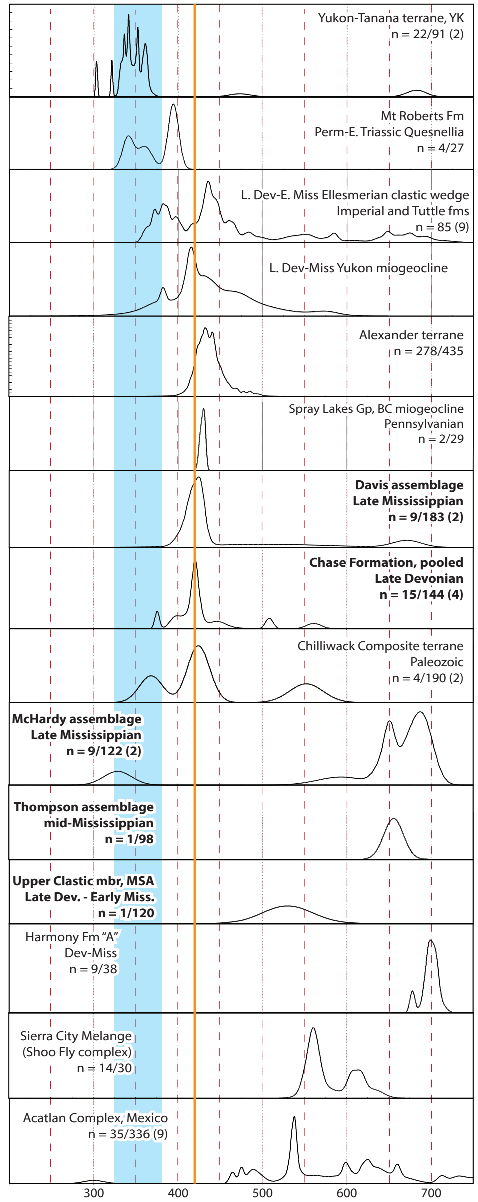

Figure 5-16. Detrital zircon data in the interval 200 Ma to 750 Ma from this study and select samples from the North American Cordillera.

Silurian (ca. 410-440 Ma) detrital zircons may link certain pericratonic and miogeoclinal strata with the Alexander terrane and (or) Chilliwack Composite terrane by Carboniferous time. Other post-750 Ma zircon populations do not correlate well across these samples. Blue bar indicates the interval of arc magmatism in Cordilleran pericratonic rocks. Samples from this study in boldface. Orange line is the ca. 420 Ma age of arc-related intrusions in the Chilliwack Composite terrane. See text for more discussion. Reference data sources: Beranek et al., 2010a; Brown et al., 2010; Devine et al., 2006; Gehrels and Kapp, 1998; Gehrels and Ross, 1998; Gehrels et al., 1996; Gehrels, umpublished data; Harding et al., 2000; Roback et al., 1995; Smith and Gehrels, 1994; Talavera-Mendoza et al., 2005.

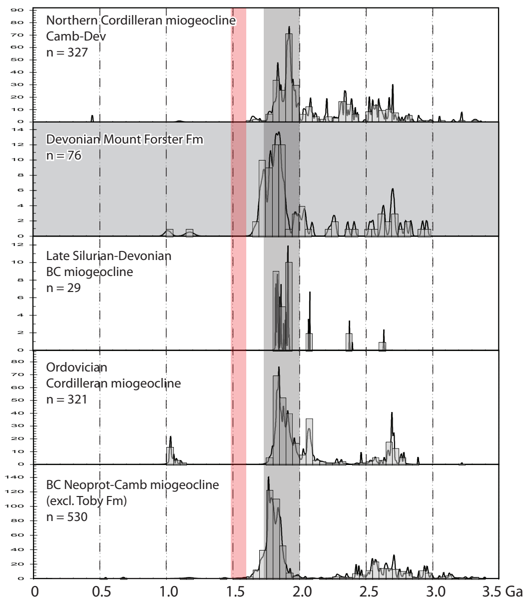

Figure 5-17. Comparison of the Middle Devonian Mount Forster Formation with other miogeoclinal strata and potential source rocks.
The Mount Forster quartzite appears to have a strong zircon provenance link to the northern Cordilleran miogeocline and to Ordovician strata found along the length of the North American Cordillera. Reference data sources: Gehrels and Dickinson, 1995; Gehrels and Ross, 1998; Gehrels and Stewart, 2001; G. Gehrels, unpublished data; Ross and Bowring, 1990; Ross and Parrish, 1991; Ross et al., 1993; Smith and Gehrels, 1991.

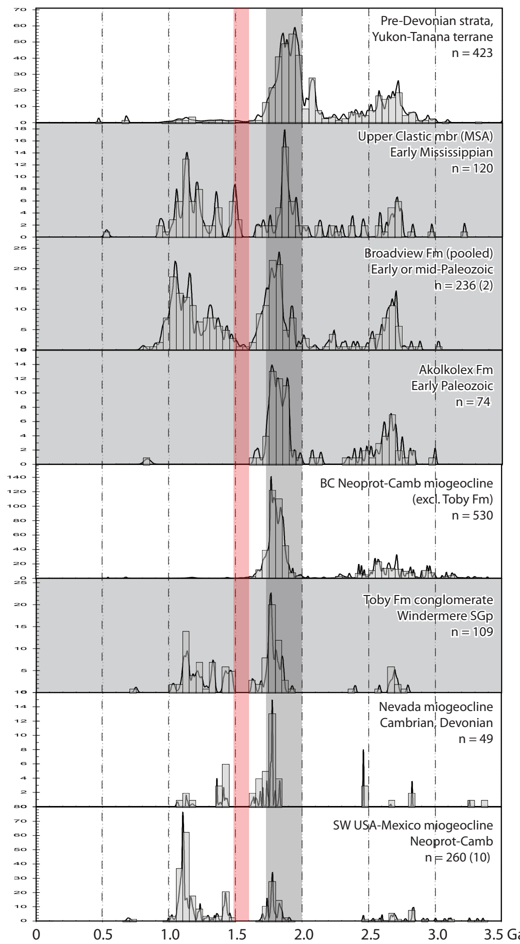

Figure 5-18. Comparison of the Lardeau Group and Mount Sproat assemblage with potential sources and select Paleozoic strata of the North American Cordillera.

Pre-1.7 Ga zircons from Lardeau and MSA strata are similar to those of the Canadian Cordilleran miogeocline and pre-Devonian strata of the Yukon-Tanana terrane. Post-1.7 Ga zircons indicate a major component of Mesoproterozoic zircon input that has not been found in the Cordillera except in certain Windermere strata and the miogeocline of southwest Laurentia. Reference data sources: Gehrels and Dickinson, 1995; Gehrels and Ross, 1998; G. Gehrels, unpublished data; Piercey and Colpron, 2009; Ross and Bowring, 1990; Ross and Parrish, 1991; Stewart et al., 2001.

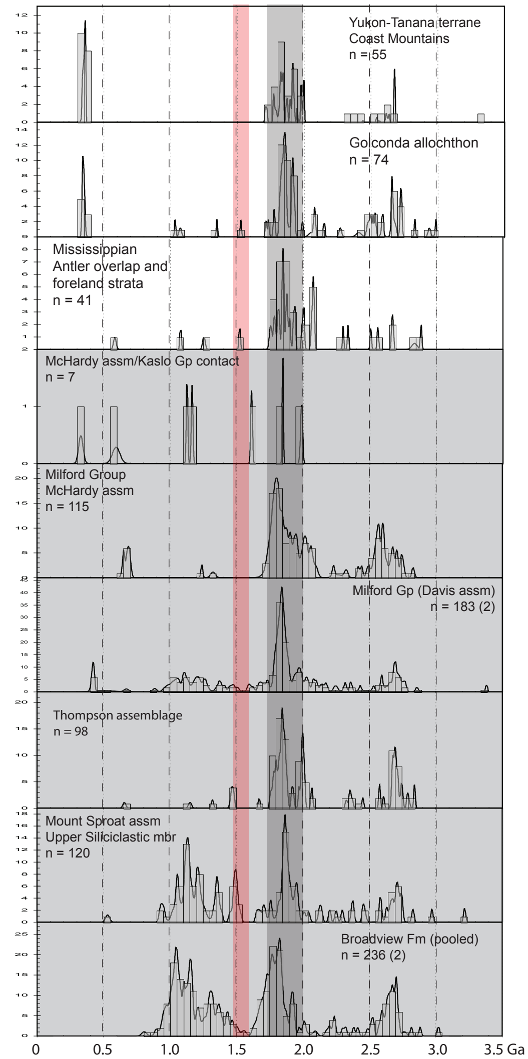

Figure 5-19. Comparison of the detrital zircon characteristics of the Milford Group and Thompson assemblage with underlying units and coeval strata in other parts of the North American Cordillera.

The Thompson, Davis, and McHardy assemblages mimic the zircon signatures of underlying strata, although with fewer Mesoproterozoic zircons than occur in the Broadview Formation and Mount Sproat assemblage. A similar nearly bimodal distribution occurs in Carboniferous rocks of the Antler orogen (Nevada) and the Yukon-Tanana terrane (northern British Columbia). Minor populations of post-700 Ma zircon are not readily matched between the Carboniferous assemblages except Late Devonian-Mississippian zircons in Yukon-Tanana terrane, Golconda allochthon and McHardy assemblage. Reference data sources: Gehrels and Kapp, 1998; Gehrels and Dickenson, 1995; Riley et al., 2000.

References

Amato, J.M., Toro, J., Miller, E.L., Gehrels, G.E., Farmer, G.L., Gottlieb, E.S., and Till, A.B., 2009, Late Proterozoic-Paleozoic evolution of the Arctic Alaska-Chukotka terrane based on U-Pb igneous and detrital zircon ages: Implications for Neoproterozoic paleogeographic reconstructions: Geological Society of America Bulletin, v. 121, p. 1219–1235, doi: 10.1130/B26510.1.

Anderson, H. E., and Davis, D. W., 1995, Purcell Supergroup, southeastern British Columbia: implications for the Mesoproterozoic geological history of the Purcell (Belt) basin: Canadian Journal of Earth Sciences, v. 32, p. 1180-1193.

Beranek, L., Mortensen, J., Lane, L. S., Allen, T. L., Fraser, T. A., Hadlari, T., and Zantvoort, W. G., 2010a, Detrital zircon geochronology of the western Ellesmerian clastic wedge, northwestern Canada: Insights on Arctic tectonics and the evolution of the northern Cordilleran miogeocline: Geological Society of America Bulletin, v. 122, 13 p. doi: 10.1130/B30120.1.

Beranek, L., Mortensen, J. K., Orchard, M. J., and Ullrich, T., 2010b, Provenance of North American Triassic strata from west-central and southeastern Yukon: correlations with coeval strata in the Western Canada Sedimentary Basin and Canadian Arctic Islands: Canadian Journal of Earth Sciences, v. 47, p. 53-73, doi:10.1139/E09-065.

Beranek, L.P., van Staal, C.R., McClelland, W.C., Israel, S., and Mihalynuk, M.G., 2013, Baltican crustal provenance for Cambrian-Ordovician sandstones of the Alexander terrane, North American Cordillera: evidence from detrital zircon U-Pb geochronology and Hf isotope geochemistry: Journal of the Geological Society, v. 170, p. 7–18, doi: 10.1144/jgs2012-028.

Bond, G., and Kominz, M. A., 1984, Construction of tectonic subsidence curves for the early Paleozoic miogeocline,southern Canadian Rocky Mountains: Implications for subsidence mechanisms, age of breakup and crustl thinning. Geological Society of America Bulletin, v. 95, p. 155-173.

Bradley, D.C., McClelleland, W. C. 2007. Detrital zircon geochronology of some Neoproterozoic to Triassic rocks in interior Alaska. D.C., McClelland, W.c., Wooden, I.L., Till, A.B., Roeske, S.M., Miller, M.L., Karl, S.M., and Abbott, J.G., 2007, Detrital zircon geochronology o f some Neoproterozoic to Triassic rocks in interior Alaska: *In* Ridgway, K. D., Trop, J.M., Glen, J.M.G. & O'neill, J.M. (eds) Tectonic Growth of a Collisional Continental Margin: Crustal evolution of Southern Alaska. Geological Society of America, Special Papers, v. 431, 155–189.

Brown, E., Gehrels, G., and Valencia, V. A., 2010, Chilliwack composite terrane in northwest Washington: Neoproterozoic-Silurian passive margin basement, Ordovician-Silurian arc inception: Canadian Journal of Earth Sciences, v. 47, p. 1347-1366.

Cawood, P., Nemchin, A., Strachan, R., Prave, T., and Krabbendam, M., 2007, Sedimentary basin and detrital zircon record along East Laurentia and Baltica during assembly and breakup of Rodinia: Journal of the Geological Society, v. 164, p. 257.

Cecile, M., Morrow, D., and Williams, G., 1997, Early Paleozoic (Cambrian to Early Devonian) tectonic framework, Canadian Cordillera: Bulletin of Canadian Petroleum Geology, v. 45, p. 54.

Colpron, M., and Price, R., 1995, Tectonic significance of the Kootenay terrane, southeastern Canadian Cordillera: An alternative model: Geology, v. 23, p. 25.

Colpron, M., and Nelson, J.L., 2009, A Palaeozoic Northwest Passage: incursion of Caledonian, Baltican and Siberian terranes into eastern Panthalassa, and the early evolution of the North American Cordillera: Geological Society London Special Publications, v. 318, no. 1, p. 273–307, doi: 10.1144/SP318.10.

Colpron, M., and Nelson, J.L., 2011, Chapter 31 A Palaeozoic NW Passage and the Timanian, Caledonian and Uralian connections of some exotic terranes in the North American Cordillera: Geological Society, London, Memoirs, v. 35, p. 463–484, doi: 10.1144/M35.31.

Colpron, M., Logan, J., and Mortensen, J., 2002, U-Pb zircon age constraint for late Neoproterozoic rifting and initiation of the lower Paleozoic passive margin of western Laurentia: Canadian Journal of Earth Sciences, v. 39, no. 2, p. 133–143.

Cook, F.A., Varsek, J.L., Clowes, R.M., Kanasewich, E.R., Spencer, C.S., Parrish, R.R., Brown, R.L., Carr, S.D., Johnson, B.J., and Price, R.A. 1992. Lithoprobe crustal reflection cross section of the southern Canadian Cordillera, 1, Foreland thrust and fold belt to Fraser River fault: Tectonics, v. 11, 12-35.

Cook, F., and Erdmer, P., 2005, An 1800 km cross section of the lithosphere through the northwestern North American plate: lessons from 4.0 billion years of Earth's history: Canadian Journal of Earth Sciences, v. 42, p. 1295–1311.

Crowley, J.L., 1999, U-Pb geochronological constraints on Paleoproterozoic tectonism in the Monashee complex, Canadian Cordillera: Elucidating an overprinted geologic history: Geological Society of America Bulletin, v. 111, p. 560-577.

Devine, F., Carr, S. D., Murphy, D. C., Davis, W. J., Smith, S., and Villeneuve, M., 2006, Geochronological and geochemical constraints on the origin of the Klatsa metamorphic complex: Implications for Early Mississippian highpressure metamorphism within Yukon-Tanana terrane: *in* Colpron, M. and Nelson, J.L., eds., Paleozoic Evolution and Metallogeny of Pericratonic Terranes at the Ancient Pacific Margin of North America, Canadian and Alaskan Cordillera: Geological Association of Canada, Special Paper 45, p. 107-130.

Doughty, P., and Chamberlain, K., 2008, Protolith age and timing of Precambrian magmatic and metamorphic events in the Priest River complex, northern Rockies: Canadian Journal of Earth Sciences, v. 45, p. 99-116.

Doughty, P., and Chamberlain, K., 1996, Salmon River Arch revisited: new evidence for 1370 Ma rifting near the end of deposition in the Middle Proterozoic Belt basin: Canadian Journal of Earth Sciences, v. 33, p. 1037-1052.

Erdmer, P., Heaman, L., Thompson, R.I. and Daughtry, K.L, 2001, Eocambrian granite clasts in southern British Columbia shed light on Cordilleran hinterland crust: Canadian Journal of Earth Sciences, v. 38, p. 1007-1016.

Erdmer, P., Moore, J., Heaman, L., Thompson, R., Daughtry, K., and Creaser, R., 2002, Extending the ancient margin outboard in the Canadian Cordillera: record of Proterozoic crust and Paleocene regional metamorphism in the Nicola horst, southern British Columbia: Canadian Journal of Earth Sciences, v. 39, no. 11, p. 1605–1623.

Evans, K. V., and Fischer, L. B., U-Pb geochronology of two augen gneiss terranes, Idaho-new data and tectonic implications: Canadian Journal of Earth Sciences, v. 23, p. 1919-1927.

Evans, K. V., and Zartman, R. E., 1990, U-Th-Pb and Rb-Sr geochronology of the middle Proterozoic granite and augen gneiss, Salmon River Mountains, east-central Idaho: Geological Society of America Bulletin, v. 102, p. 63-73.

Evans, K., and Aleinikoff, J., 2000, SHRIMP U-Pb geochronology of volcanic rocks, Belt Supergroup, western Montana: evidence for rapid deposition of sedimentary strata: Canadian Journal of Earth Sciences, v. 37, p. 1287-1300.

Evenchick, C. A., Parrish, R. P., and Gabrielse, H., 1984, Precambrian gneiss and late Proterozoic sedimentation in north-central British Columbia. Geology, v. 12, p. 233 -237.

Fanning, C., and Link, P., 2004, U-Pb SHRIMP ages of Neoproterozoic (Sturtian) glaciogenic Pocatello Formation, southeastern Idaho: Geology, v. 32, p. 881.

Fedo, C., Sircombe, K., and Rainbird, R., 2003, Detrital zircon analysis of the sedimentary record: Reviews in Mineralogy and Geochemistry, v. 53, p. 277.

Freiholz, G., 1983, The stratigraphic and structural setting or a lead-zinc occurrence near Invermere, southeastern British Columbia; M.Sc. thesis, University of Calgary, Calgary, AB.

Fyles, J.T. and Eastwood, G.E.P., 1962, Geology of the Ferguson area, Lardeau district, British Columbia: B.C. Department of Mines and Petroleum Resources, Bulletin 45, 92 p.

Gardner, D., 2008, Sedimentology, stratigraphy, and provenance of the upper Purcell Supergroup, southeastern British Columbia, Canada: implications for syn-depositional tectonism, basin models, and paleogeographic reconstructions. M.Sc. thesis, University of Victoria, Victoria, B.C.

Gardner, D.W. and Johnston, S.T., 2007, Sedimentology, correlation, and depositional environment of the upper Purcell Supergroup, northern Purcell Basin, southeastern British Columbia; Geological Survey of Canada, Current Research 2007-A6, 13 p.

Gehrels, G.E., 2000, Introduction to the detrital zircon studies of Paleozoic and Triassic strata in western Nevada and northern California: *in* Soreghan. MJ., and Gehrels, G.E., eds., Paleozoic and Triassic Paleogeography and Tectonics of Western Nevada and Northern California: Geological Society of America Special Paper 347, p. 1- 17.

Gehrels, G.E., and Kapp, P.A., 1998, Detrital zircon geochronology and regional correlation of metasedimentary rocks in the Coast Mountains, southeastern Alaska: Canadian Journal of Earth Sciences, v. 35, p. 269-279.

Gehrels, G., and Ross, G., 1998, Detrital zircon geochronology of Neoproterozoic to Permian miogeoclinal strata in British Columbia and Alberta: Canadian Journal of Earth Sciences, v. 35, p. 1380–1401.

Gehrels, G.E. and Saleeby, lB., 1987, Geologic Iramework. tectonic evolution and displacement history of the Alexander terrane: Tectonics, v. 6, p. 151-173.

Gehrels, G., and Stewart, J., 1998, Detrital zircon U-Pb geochronology of Cambrian to Triassic miogeoclinal and eugeoclinal strata of Sonora, Mexico: Journal of Geophysical Research, no. B2, v. 103, p. 2471-2487.

Gehrels, G. E., and Dickinson, W. R., 1995, Detrital zircon provenance of Cambrian to Triassic miogeoclinal and eugeoclinal strata in Nevada: American Journal of Science, v. 295, p. 18-48.

Gehrels, G.E., Butler, R.E and Bazard, D.R., 1996, Detrital zircon geochronology of the Alexander terrane, southeastern Alaska: Geological Society o f America Bulletin. v. 108, p. 722-734.

Gehrels, G. E., Johnsson, M. J. and Howell, D. G. 1999. Detrital zircon geochronology of the Adams Argillite and Nation River Formation,east–central Alaska, U.S.A.: Journal of Sedimentary Research, v. 69, p. 135-144.

Gervais, F., Brown, R., and Crowley, J., 2010, Tectonic Implications for A Cordilleran orogenic base in the Frenchman cap dome, southeastern Canadian Cordillera: Journal of Structural Geology, v. 32, p. 941-959, doi:10.1016/j.jsg.2010.05.006

Glombick, P., Thompson, R.I., and Daughtry, K.L. 2004. Geology of the Oyama map area, British Columbia (NTS 82L/03). Geological Survey of Canada, Open File 4370, scale 1 : 50 000.

Grove, M., Gehrels, G.E., Cotkin, S.J., Wright, J.E. & Zou, H., 2008, Non-Laurentian cratonal provenance of Late Ordovician blueschists and a link to the Alexander terrane: *in* Wright, J.E. & Shervais, J.W., eds., Ophiolites, Arcs, and Batholiths. Geological Society of America, Special Paper 438, p. 223–250.

Harding, IP., Gehrels, G.E., Harwood, D.S. and Girty, G.H., 2000, Detrital zircon geochronology of the Shoo Fly complex, northern Sierra terrane, northeastern California. *in* Soreghan, M. J. and Gehrels, G.E., eds., Paleozoic and Triassic Paleogeography and Tectonics of Western Nevada and Northern California: Geological Society of America, Special Paper 347, p. 43-56.

Hoffman, P., 1988, United plates of America, the birth of a craton: Early Proterozoic assembly and growth of Laurentia: Annual Review of Earth and Planetary Sciences, v. 16, p. 543–603.

Hoffman, P.F. 1989. Precambrian geology and tectonic history of North America: *in* The geology of North America—an overview. Bally, A. W. and Palmer, A. R., eds., Geological Society of America, The Geology of North America, vol. A, p. 447–512.

Hughes, N. D., Sears, J. W., and Chamberlain, K. R., 2003, New Upper Devonian U-Pb date for Eagle Bay felsic volcanics in the distal Cordilleran miogeocline, Vavenby, British Columbia: Geological Society of America Abstracts with Programs, v. 35, p. 3.

Hyndman, D.W. 1968. Petrology and structure of Nakusp map-area, British Columbia. Geological Survey of Canada Bulletin 161.

Jefferson CW, Parrish RR. 1989. Late Proterozoic stratigraphy, U-Pb zircon ages, and rift tectonics, Mackenzie Mountains, northwestern Canada. Canadian Journal of Earth Sciences, v. 26, p. 1784–801.

Jones, A.G., 1959, Vernon map-area, British Columbia. Geological Survey of Canada Memoir 296.

Klepacki, D.W., 1985, Stratigraphy and structural geology of the Goat Range area, southeastern British Columbia. Ph.D. thesis, Massachusetts Institute of Technology, Cambridge, Mass.

Kraft, J. L., Thompson, R. I., and Dhesi, P. (compilers), 2011, Geology, Camborne, British Columbia; Geological Survey of Canada, Open File, 6573, scale 1:50 000, doi: 10.4095/288064.

Lemieux, Y., 2006, Structure, geochronology and thermobarometry of the eastern flank of the Shuswap metamorphic complex in the Upper Arrow Lake area, southeastern British Columbia: Ph.D. thesis, University of Alberta, Edmonton, AB.

Lemieux, Y., Thompson, R., Erdmer, P., Simonetti, A., and Creaser, R., 2007, Detrital zircon geochronology and provenance of Late Proterozoic and mid-Paleozoic successions outboard of the miogeocline, southeastern Canadian Cordillera: Canadian Journal of Earth Sciences, v. 44, p. 1675–1693.

Lewis, R., Vervoort, J., Burmester, R., and Oswald, P., 2010, Detrital zircon analysis of Mesoproterozoic and Neoproterozoic metasedimentary rocks of north-central Idaho: implications for development of the Belt-Purcell basin: Canadian Journal of Earth Sciences, v. 47, p. 1383–1404.

Logan, J., and Colpron, M., 2006, Stratigraphy, geochemistry, syngenetic sulphide occurrences and tectonic setting of the lower Paleozoic Lardeau Group, northern Selkirk Mountains, British Columbia: *in* Colpron, M. and Nelson, J.L., eds., Paleozoic Evolution and Metallogeny of Pericratonic Terranes at the Ancient Pacific Margin of North America, Canadian and Alaskan Cordillera: Geological Association of Canada, Special Paper 45, p. 361–382.

McFarlane, C., and Pattison, D., 2000, Geology of the Matthew Creek metamorphic zone, southeast British Columbia: A window into Middle Proterozoic metamorphism in the Purcell Basin: Canadian Journal of Earth Science, v. 37, p. 1073-1092.

McClelleland, W. C., Schmidt, J. M., and Till., A. B., 2006, New SHRIMP ages from Devonian felsic volcanic and Proterozoic plutonic rocks of the southern Brooks Range, Alaska. Geological Society of America, Abstracts with Programs, v. 38, p. 12.

McNicoll, V. J., Harrison, J.C., Trettin, H.P., and Thorsteinsson, R., 1995, Provenance of the Devonian clastic wedge of Arctic Canada: Evidence provided by detrital zircon ages, *in* Dorobek, S.L., and Ross, G.M., eds., Stratigraphic Evolution of Foreland Basins: Society of Economic Paleontologists and Mineralogists Special Publication 52, p. 77–93.

Moore, J. M., and Pettipas, A.R., 1990, Geological studies in the Nicola Lake region (92-!/SE); Part A *in* Nicola Lake Region Geology and Mineral Deposits; British Columbia geological Survey Branch, Ministry of Energy, Mines and

Petroleum Resources, Paper 1989-1, p. 93-98.

Mortensen J. K., Colpron M. 1998. Geochronological and geochemical studies of the Coates Lake Diatreme, southern MacKenzie Mountains, western N.W.T.: *in* Slave-Northern Cordilleran Lithospheric Evolution (SNORCLE) and Cordilleran Tectonics Workshop, Cook, F. A., and Erdmer, P., eds., Lithoprobe Report 64, p. 278.

Nelson, J., and Gehrels, G., 2007, Detrital zircon geochronology and provenance of the southeastern Yukon-Tanana terrane: Canadian Journal of Earth Sciences, v. 44, p. 297-316.

Obradovich, J.D., and Peterman, Z.E., 1968, Geochronology of the Belt Series, Montana: Canadian Journal of Earth Sciences, v. 5, p. 737-747.

Okulitch, A.V., 1984, The role of the Shuswap metamorphic complex in Cordilleran tectonism: a review: Canadian Journal of Earth Sciences, v. 21, p. 1171-1193.

Paradis, S., Bailey, S., Creaser, R., Piercey, S., and Schiarizza, P., 2006, Paleozoic magmatism and syngenetic massive sulphide deposits of the Eagle Bay assemblage, Kootenay terrane, southern British Columbia: *in* Colpron, M. and Nelson, J.L., eds., Paleozoic Evolution and Metallogeny of Pericratonic Terranes at the Ancient Pacific Margin of North America, Canadian and Alaskan Cordillera: Geological Association of Canada, Special Paper 45, p. 383-414.

Parrish, R.R., 1995, Thermal evolution of the southeastern Canadian Cordillera: Canadian Journal of Earth Sciences, v. 32, p. 1618-1642.

Parrish, R. R., and Armstrong, R. L., 1983, U-Pb zircon age and tectonic significance of gneisses in structural culminations of the Omineca Crystalline Belt, British Columbia: Geological Society of America, Abstracts with Programs, v. 15, p. 324.

Parrish, R. R., and Ross, G. M., 1990, Review of the Precambrian basement of the Cordillera: Geological Association of Canada, Program with Abstracts, v. 15, p. 324.

Parrish, R. R., and Reichenbach, I., 1991, Age of xenocrystic zircon from diatremes of western Canada. Canadian Journal of Earth Sciences, v. 28, p. 1232–1238.

Parrish, R. R., Ross, G. M., Carr, S. D., Coleman, V., and Journeay, J. M., 1989, Single grain U-Pb provenance ages of detrital zircons from metaquartzites of the southern Omenica belt, British Columbia. Geological Society of America, Abstracts with Programs, v. 21, p. 127-128.

Patrick, B. E., and McClelland, W. C., 1995, Late Proterozoic granitic magmatism on Seward Peninsula and a Barentian origin for Arctic Alaska–Chukotka.

Geology, 23, 81–84.

Piercey, S., and Colpron, M., 2009, Composition and provenance of the Snowcap assemblage, basement to the Yukon-Tanana terrane, northern Cordillera: Implications for Cordilleran crustal growth: Geosphere, v. 5, p. 439- 464, doi: 10.1130/GES00505.1.

Preto, V. A., 1979, Geology of the Nicola Group between Merritt and Princeton: British Columbia Ministry of Energy, Mines and Petroleum Resources, Bulletin 69.

Price, R., 1994, Cordilleran tectonics and the evolution of the Western Canada Sedimentary Basin: *in* Geological Atlas of the Western Canada Sedimentary Basin. Mossop, G.D. and Shetsen, I. (compilers), Calgary, Canadian Society of Petroleum Geologists and Alberta Research Council, Chapter 2, p. 13-24.

Price, R. A., 2007, Whence the Southeastern Canadian Cordillera: Palinspastic Restorations Linking Displaced Supracrustal Rocks to Crustal Structure: Edmonton Geological Society presentation abstract, 4 p.

Rainbird, R., McNicoll, V., Theriault, R., Heaman, L. M., Abbott, J. G., Long, D. G. F., and Thorkelson, D. J., 1997, Pan-continental river system draining the Grenville Orogen recorded by U-Pb and Sm-Nd geochronology of Neoproterozoic quartzarenites and mudrocks, northwestern Canada: The Journal of Geology, vol. 105, no. 1, p. 1-17:

Read, P.B., and Wheeler, J.O., 1976, Geology, Lardeau west-half, British Columbia: Geological Survey of Canada Open File 432.

Reesor, J.E. 1973. Geology of the Lardeau map-area, east half, British Columbia: Geological Survey of Canada Memoir 369.

Reesor, J. E. (compiler), 1996, Geology, Kootenay Lake, British Columbia: Geological Survey of Canada Map 1864A, scale 1:100 000.

Ricketts, B. D., (ed.), 1989, Western Canada Sedimentary Basin: A case history: Canadian Society of Petroleum Geologists (book).

Riley, B. C. D., Snyder, W. S., and Gehrels, G. E., 2000, U-Pb detrital zircon geochronology of the Golconda allochthon, Nevada: *in* Soreghan. M. J., and Gehrels, G. E., eds., Paleozoic and Triassic Paleogeography and Tectonics of Western Nevada and Northern California: Geological Society of America Special Paper 347, p. 65-75.

Roback, R.C., 1993, Late Paleozoic to middle Mesozoic tectonic evolution of the Kootenay arc, northeastern Washington and southeastern British Columbia: PhD thesis, University of Texas, Austin, Texas, 237 p.

Roback, R. C., Sevigny, J., and Walker, N., 1994, Tectonic setting of the Slide Mountain terrane, southern British Columbia: Tectonics, v. 13, p. 1242–1242.

Roback, R. C., and Walker, N., 1995, Provenance, detrital zircon U-Pb geochronometry, and tectonic significance of Permian to Lower Triassic sandstone in southeastern Quesnellia, British Columbia and Washington: Geological Society of America Bulletin, v. 107, p. 665.

Root, K., 1987, Geology of the Delphine Creek area, southeastern British Columbia: Implications for the Proterozoic and Paleozoic development of the Cordilleran divergent margin: Ph.D. thesis, University of Calgary, Calgary, AB.

Ross, G. M., and Bowring, S., 1990, Detrital zircon geochronology of the Windermere Supergroup and the tectonic assembly of the southern Canadian Cordillera: The Journal of Geology, v. 98, p. 879-893.

Ross, G. M., and Parrish, R., 1991, Detrital zircon geochronology of metasedimentary rocks in the southern Omineca Belt, Canadian Cordillera: Canadian Journal of Earth Sciences, v. 28, p. 1254-1270.

Ross, G. M. & Villeneuve, M. E. 1997. U–Pb geochronology of stranger stones in Neoproterozoic diamictites, Canadian Cordillera; implications for provenance and ages of deposition. Geological Survey of Canada Paper 1997-F, p. 141–155.

Ross, G. M., and Villeneuve, M., 2003, Provenance of the Mesoproterozoic (1.45 Ga) Belt basin (western North America): Another piece in the pre-Rodinia paleogeographic puzzle: Geological Society of America Bulletin, v. 115, p. 1191.

Ross, G. M., Parrish, R.R., and Villeneuve, M.E., 1991, Geophysics and geochronology of the crystalline basement of the Alberta Basin, western Canada - Canadian Journal of Earth Sciences: Canadian Journal of Earth Sciences, v. 28, p. 512-522.

Ross, G. M., Parrish, R., and Winston, D., 1992, Provenance and U-Pb geochronology of the Mesoproterozoic Belt Supergroup (northwestern United States): Implications for age of deposition and pre-Panthalassa plate reconstructions: Earth and Planetary Science Letters, v. 113, p. 57–76.

Ross, G. M., McNicoll, V., Geldsetzer, H., Parrish, R., Carr, S., and Kinsman, A., 1993, Detrital zircon geochronology of Siluro-Devonian sandstones, Rocky Mountains, northeastern British Columbia: Bulletin of Canadian Petroleum Geology, v. 41, p. 349.

Ross, G. M., Parrish, R. R., and Winston, D., 1992, Provenance and U-Pb geochronology of the Mesoproterozoic Belt Supergroup (northwestern

United States): implications for age of deposition and pre-Panthalassa plate reconstructions: Earth and Planetary Science Letters, v. 113, p. 57-76.

Ross, G. M., Friedman, R., and Mortensen, J. K., 2005, Detrital zircon and monazite from the Hyland Group (northern Canadian Cordillera and Alaska): evidence for intra-Cordilleran "Grenville" basement: Geological Society of America Abstracts with Programs, v. 37, p. 56.

Schandl, E., Davis, D., and Gorton, M., 1993, The Pb-Pb age of metamorphic titanite in the chlorite-pyrite altered footwall of the Sullivan Zn-Pb SEDEX Deposit, B.C. and its relationship to the Ore: Geological Association of Canada-Mineralogical Association of Canada Programs with Abstracts, p. 1–2.

Sears, J.W., 1979, Tectonic contrasts between the infrastructure and suprastructure of the Columbian orogen, Albert Peak area, western Selkirk Mountains, British Columbia: Ph.D. thesis, Queen's University, Kingston, Ontario,

Sears, J. W., Chamberlain, K., and Buckley, S. N., 1998, Structural and U-Pb geochronological evidence for 1.47 Ga rifting in the Belt basin, western Montana: Canadian Journal of Earth Sciences, v. 35, p. 467-475.

Smith, M. T. 1990, Stratigraphic, structural, and U-Pb geochronologic investigation of lower Paleozoic eugeoclinal strata in the Kootenay Arc, southeastern British Columbia and northeastern Washington: Ph.D. dissertation, University of Arizona, Tucson.

Smith, M. T., and Gehrels, G. E., 1991, Detrital zircon geochronology of Upper Proterozoic to lower Paleozoic continental margin strata of the Kootenay Arc: implications for the early Paleozoic tectonic development of the eastern Canadian Cordillera: Canadian Journal of Earth Sciences, v. 28, p. 1271- 1284.

Smith, M. T., and Gehrels., G. E., 1994, Detrital zircon geochronology and the provenance of the Harmony and Valmy Formations, Roberts Mountains allochthon, Nevada: Geological Society of America Bulletin, v. 106, p. 968.

Smith, M. D., Arnaud, E., Arnott, R. W. C., and Ross, G. M., 2011, Chapter 37: The record of Neoproterozoic glaciations in the Windermere Supergroup, southern Canadian Cordillera: *in* Arnaud, E., Halverson, G. P., and Shields-Zhou, G., eds., The Geological Record of Neoproterozoic Glaciations, Geological Society of London Memoirs, v. 36, p. 413-423.

Stewart, J., Gehrels, G., and Barth, A., 2001, Detrital zircon provenance of Mesoproterozoic to Cambrian arenites in the western United States and northwestern Mexico: Geological Society of America Bulletin, v. 113, p. 1343-1356.

Struik, L., 1987, The ancient western North American margin: An Alpine rift model for the east-central Canadian Cordillera: Geological Survey of Canada Paper 87-15, p. 1–21.

Talavera-Mendoza, O., Ruiz, J., Gehrels, G.E., Meza-Figueroa, D.M., Vega-Granillo, R., and Campa-Uranga, M.F., 2005, U–Pb geochronology of the Acatlán Complex and implications for the Paleozoic paleogeography and tectonic evolution of southern Mexico: Earth and Planetary Science Letters, v. 235, p. 682–699, doi: 10.1016/j.epsl.2005.04.013.

Thompson, R., and Daughtry, K., 2000, Stratigraphic linkage of carbonate-rich units across east-central Vernon map area, British Columbia: are Kingfisher (Colby) and Big Ledge zinc-lead occurrences part of the same regional marker succession?: Geological Survey of Canada, Current Research 2000-A18, 5 p.

Thompson, R.I., Glombick, P., Erdmer, P., Heaman, L. M., Lemieux, Y., and Daughtry, K. L., 2006, Evolution of the ancestral Pacific margin, southern Canadian Cordillera: Insights from new geologic maps: *in* Colpron, M. and Nelson, J.L., eds., Paleozoic Evolution and Metallogeny of Pericratonic Terranes at the Ancient Pacific Margin of North America, Canadian and Alaskan Cordillera: Geological Association of Canada, Special Paper 45, p. 433-482.

Unterschutz, J., Creaser, R., Erdmer, P., Thompson, R., and Daughtry, K., 2002, North American margin origin of Quesnel terrane strata in the southern Canadian Cordillera: Inferences from geochemical and Nd isotopic characteristics of Triassic metasedimentary rocks: Geological Society of America Bulletin, v. 114, p. 462.

Van Schmus, W.R., Bickford, M.E., Anderson, J.L., Bender, E.E., Anderson, R.R., Bauer, P.W., Robertson, J.M., Bowring, S.A., Condie, K.C., Denison, R.E., Gilbert, M.C., Grambling, J.A., Mawer, C.K., Shearer, C.K., Hinje, W.J., Karlstrom, K.E., Kisvarsanyi, E.B., Lidiak, E.G., Reed, J.C., Jr., Sims, P.K., Tweto, O., Silver, L.T., Treves, S.B., Williams, M.L., and Wooden, J.L., 1993, Transcontinental Proterozoic provinces: *in* Reed, J. C. Jr, Bickford, M. E., Houston, R. S., Link, P. K., Rankin, D. W., Sims, P. K., and Van Schmus, W. R. (eds) Precambrian Conterminous US. Geological Society of America, The Geology of North America, C-2, p. 171–334.

Villeneuve, M.E., Ross, G.M., Parrish, R.R., Theriault, R.J., Miles, W., and Broome, J., 1993, Geophysical subdivision, U-Pb geochronology and Sm-Nd isotope geochemistry of the crystalline basement of the Western Canada sedimentary basin, Alberta and northeastern British Columbia: Geological Survey of Canada Bulletin 447, 86 p.

Wheeler, J. O., 1968, Lardeau (west half) map-area, British Columbia (82K W112). *In* Report of activities, part A**.** Geological Survey of Canada, Paper 68-lA, p. 56-58.

Wheeler, J.O. and McFeely, P. (compilers), 1991, Tectonic assemblage map of the Canadian Cordillera and adjacent parts of the United States of America: Geological Survey of Canada, Map 1712A, 1:2,000,000.

White, W. H., 1959, Cordilleran tectonics in British Columbia: American Association of Petroleum Geologists Bulletin, v. 43, p. 60-100.

Wright, J., and Wyld, S., 2006, Gondwanan, Iapetan, Cordilleran interactions: A geodynamic model for the Paleozoic tectonic evolution of the North American Cordillera: *in* Haggart, J., Enkin, R.J and Monger, J. W. H., eds., Paleogeography of the North American Cordillera: Evidence For and Against Large-Scale Displacements: Geological Association of Canada, Special Paper 46, p. 377-408.

Young, G.M., Jefferson, C.W., Long, D.G.F., Delaney, G.D., and Yeo, G.M., 1979, Middle and Late Proterozoic evolution of the northern Canadian Cordillera and Shield: Geology, v. 7, p. 125–128.

Chapter 6: Summary Discussion and Conclusions

6.1 Responses to research questions

Evidence presented in chapters 2-5 bear on the questions regarding Cordilleran evolution that were posed in Chapter 1 as follows:

Do equivalents of Late Devonian-Early Mississippian continental margin strata in the North Okanagan-Shuswap region ("Eagle Bay assemblage" of Schiarizza and Preto, 1987, and "Mount Ida Group" of Jones, 1959) exist in the northern Kootenay Arc as hypothesized by Thompson et al. (2006)?

Yes, the Amphibolitic Schist member of the Mount Sproat assemblage is correlative with the Silver Creek Formation of the North Okanagan-Shuswap region as suggested previously (Lemieux, 2006; Thompson et al., 2006). The Late Devonian Chase Formation, however, has no lithostratigraphic equivalent in the Kootenay Arc. Because the Chase Formation was deposited during deposition of the Mount Sproat assemblage, the disparity is interpreted to reflect a facies change between the Chase platform on the Okanagan High and the basinal Lardeau trough. Foundering of the Chase platform was coeval with the onset of local arc volcanism, which led to deposition of volcanic and volcaniclastic rocks in the overlying Silver Creek Formation and equivalent rocks in the ca. 367 Ma Amphibolitic Schist member of the Mount Sproat assemblage. The Tournaisian Catherine Lake phyllite and the Upper Clastic member of the Mount Sproat assemblage, with which it was correlated in Chapter 2, are coeval with part of the Eagle Bay assemblage and not the Bruen phyllite based on previously reported cross-cutting relations (Thompson et al., 2006).

How significant are the hypothetical terrane boundaries between Upper Paleozoic rock assemblages of the southeastern Canadian Cordillera? Are these assemblages truly terranes in the sense of Coney et al. (1980)?

A terrane boundary was hypothesized to separate assemblages of the Carboniferous Milford Group (Cairnes, 1934; Read and Wheeler, 1976) because of the contrasting depositional settings and map relations of its fault-bounded assemblages in the Goat Range (Klepacki, 1985). Its two eastern assemblages unconformably overlie the Lardeau Group and were included in the Kootenay terrane (Klepacki, 1985; Wheeler and McFeely, 1991). Alternatively, the McHardy assemblage and depositionally overlying MORB-type basalt of the Kaslo Group have been detached from their basement by the Stubbs fault and were assigned to the Slide Mountain terrane (Klepacki, 1985), which comprises vestiges of a Late

Paleozoic marginal ocean basin that have been obducted onto the continental margin (Monger, 1984; Monger and Berg, 1987; Nelson, 1993; Piercey et al., 2004). Previous study has shown indirect stratigraphic linkages between the McHardy assemblage and continental margin strata to the east (Klepacki, 1985; Roback et al., 1994). New mapping of the Milford Group north of the Goat Range has shown that the northern continuation of the McHardy assemblage is depositionally linked to its Late Devonian and Early Mississippian basement, the Mount Sproat assemblage, which in turn was deposited on the Lardeau Group. A surface along which the McHardy assemblage and Kaslo Group could have been obducted is not present in the Lardeau Range. Consequently, the Slide Mountain terrane in this area depositionally onlapped the continental margin and does not satisfy the definition of a terrane (Coney et al., 1980; Gabrielse and Yorath, 1991). As an alternative, the term Slide Mountain tectonic assemblage is proposed to include the Milford and Kaslo Groups. This does not preclude the existence of a Slide Mountain terrane in other parts of the Cordillera, but it does demonstrate that the inboard crust of the Slide Mountain ocean was part of the North American plate.

When were the extensional events attributed to Lardeau Group grits and volcanic rocks (e.g. Logan and Colpron, 2006)?

A revised interpretation of the stratigraphy of the Trout Lake area presented in Chapter 2 dictates that the Broadview Formation is conformably overlain by the Mount Sproat assemblage, which comprises an undated Carbonaceous member and a Late Devonian to Early Mississippian back-arc basin succession. The tectonism inferred to have caused deposition of the submarine fan deposits in the Broadview Formation is interpreted here to result from Middle Devonian initiation of the active plate boundary at the Cordilleran margin. Whether the uplift of the source region was due to extension or compression is unknown. Deposition of the Broadview Formation was potentially coeval with, and related to, syndepositional deformation of the Mount Forster Formation on the adjacent Purcell Arch. The Broadview Formation and the associated McCrae Peak succession is considered as a southern equivalent to Devonian submarine fan deposits and barite in the Earn Group of the Selwyn Basin (Gordey et al., 1987). As previously proposed (Logan and Colpron, 2006), the older Akolkolex Formation is inferred to relate to Ordovician extensional activity recorded in the adjacent miogeocline (Root, 1987).

When and how did the pre-Milford fabric in the Lardeau Group form? Was pre-

Milford deformation in the Kootenay Arc a northern counterpart of the (Late Devonian-?) Early Mississippian Antler orogeny of the U.S. Cordillera (e.g. Smith et al., 1993) or other mid-Paleozoic Cordilleran events (e.g. Root, 1987; Colpron et al., 2006) or does it record a separate event?

Interpretations of the Mount Sproat assemblage presented in chapters 2 and 4 offer an improved upper limit for the timing of pre-Milford deformation in the northern Kootenay Arc. This deformation event post-dated deposition of the Upper Clastic member of the Mount Sproat assemblage, which overlies the ca. 367 Ma Amphibolitic Schist member and is correlated with the Tournaisian (Orchard et al., 1985; Thompson et al., 2006) Catherine Lake phyllite, and was therefore Early Mississippian. This event was 40-50 Myr later than syn-depositional deformation in the Mount Forster Formation (Root, 1987) and was at least partly coeval with emplacement of the Roberts Mountains allochthon during the Antler orogeny (Roberts et al., 1958; Johnson and Pendergast, 1981; Miller et al., 1984). Importantly, deformation of the Lardeau Group and lower Mount Sproat assemblage occurred at least 5 Myr, and probably about 15 Myr, after deposition of the Chase Formation. Because the hypothesized Okanagan terrane was a sediment source of the Chase Formation, the terrane was emplaced at the Cordilleran margin before phase 1 deformation in the Lardeau Group and therefore was not the origin of the pre-Milford deformation as previously speculated (Colpron and Nelson, 2009). Alternatively, the deformation is inferred to result from changes at the plate boundary such as an increase in convergence rate or subduction of oceanic islands, which affected the stress regime of the back-arc environment in which the Lardeau trough existed. Shortening of the basin was accommodated by the weakened state of the thin and hot crust beneath the Lardeau trough following Late Devonian subduction beneath the edge of the North American plate.

Why is pre-Milford fabric well developed in the Lardeau Group in the northern Kootenay Arc but absent from (or not apparent in) underlying strata and Lardeau Group rocks to the north?

Pre-Milford deformation in the Lardeau trough affected the Lardeau Group and lower members of the Mount Sproat assemblage but has not been identified in underlying strata (Fyles and Eastwood., 1962; Fyles, 1964; Reesor, 1973) or in the Lardeau Group to the north (Wheeler, 1963; Colpron, 1996; Logan and Colpron, 2006). The localization of strain is interpreted to relate to the small scale of the deformation event described above, which did not involve obduction of an allochthon such as occurred in the larger Antler orogeny to the south (Johnson and Pendergast, 1981). The apparent absence of D1 strain in rocks underlying the Lardeau Group is interpreted to result from detachment of the Lardeau Group from the more competent Badshot Formation and Hamill Group. D1 strain was concentrated in the relatively incompetent Lardeau Group in the hanging wall of this detachment – the Lardeau shear zone of Smith and Gehrels (1992).

Do Grenville-age granitic clasts and detrital zircons in the southern Canadian Cordillera record an intra-Cordilleran block of Grenville-age crust upon which late Paleozoic arcs formed (e.g. Erdmer et al., 2002; Lemieux et al., 2007) or was exotic Grenville-age crust translated into the Cordilleran realm in the mid-Paleozoic (e.g. Colpron and Nelson, 2009)? Does the Devonian Chase Formation record an intra-Cordilleran continental high (i.e. Lemieux et al., 2007) or is it part of an exotic Okanagan terrane that was accreted in Devonian time (Colpron and Nelson, 2009)? If the former, why does its detrital zircon provenance contrast with that of the Cordilleran miogeocline? If the latter, from where and when did the terrane arrive in the southern Canadian Cordillera?

Two very different hypotheses have been forwarded to explain the presence of unexpected granitic clasts and detrital zircons in the pericratonic assemblages of the southern Canadian Cordillera. These include 1040 Ma and 555 Ma granitic clasts in late Paleozoic conglomerate (Erdmer et al., 2001; 2002) and a detrital zircon signature in the Chase Formation that comprises a swath of Mesoproterozoic zircon with lesser Late Paleoproterozoic, early Paleozoic and Archean grains (Lemieux et al., 2007).

Field relations of the Chase Formation were used by Lemieux et al. (2007) to argue that a source of atypical detrital zircon patterns was native to the southern Canadian Cordillera. Contrarily, Colpron and Nelson (2009; 2011) showed strong linkages between the atypical zircon ages in southern B.C. and several allochthonous terranes of the northern Cordillera and, ultimately, the Caledonian, Baltican and Siberian shields. They proposed that the exotic crust, which they called the Okanagan terrane, occurs in the basement of the Quesnel arc. Narrowing of the depositional age constraints on the Chase Formation and generation of a broader provenance database in this study led to a new interpretation in Chapter 5 in which the Chase Formation was deposited at the Cordilleran margin and was derived from previously emplaced exotic crust. This scenario is consistent with field relations and available detrital zircon data.

Unequivocal evidence of Grenville-age granite in the Cordillera at the time of Rodinia rifting has been identified previously (Ross et al., 1995; D. Murphy, unpublished date of granite clast 1.19 Ga in the Windermere Supergroup). New data presented in Chapter 5 were interpreted to show that Neoproterozoic strata containing a major proportion of Grenville-age detritus, and possibly Grenville crust also, were exposed west of the Lardeau trough in the mid- to late Paleozoic. Detrital zircons of Ediacaran (ca. 550 Ma) and Silurian age (ca. 430 Ma and 418 Ma) identified in this and prior studies appear to manifest at the Cordilleran margin no earlier than the Late Devonian. This sudden appearance shortly after the Cordilleran margin became an active plate boundary and the close matches in age with rocks characteristic of the allochthonous or distant terranes (Alexander, Arctic Alaska-Chukotka, Seward, Farewell) strongly supports Colpron and Nelson's (2009; 2011) notion of an allochthonous Okanagan terrane originating north of Laurentia. The stratigraphic link between the Chase Formation and the southern Canadian Cordilleran margin reported by Lemieux (2006) and Lemieux et al. (2007), and supported by interpretations in Chapter 2, can be reconciled with the exotic Okanagan terrane hypothesis if the Okanagan terrane was adjacent to the Chase platform at the Cordilleran margin during the Late Devonian and was the source of sediment in the Chase Formation.

Grenville-age zircons in, and possibly crust beneath, the Canadian Cordillera therefore include both original intra-Cordilleran sources and crust introduced in the Devonian. The distinction between these sources might be made by identification of associated Neoproterozoic or Silurian magmatic arc rocks or detrital zircon, which are exclusively of exotic origin (with the exception of trace amounts of zircon that may have been generated by Neoproterozoic rift-related rocks in the Cordillera).

6.2 Paleozoic paleogeography of the southern Canadian Cordillera: a model

The interpretations presented above and in chapters 2 to 5 have been compiled with previous work to create a series of diagrams (figures 6-1 to 6-9) that schematically illustrate the interpreted paleogeography of the Cordilleran margin in southern Canada from its formation in Cryogenian time to the Late Triassic configuration that shortly preceded initiation of the main Cordilleran orogeny. The outer limit of the miogeocline comes from palinspastic restoration of the Rocky Mountain fold and thrust belt (Price, 2007; 2009). The location and activity on the Purcell Arch is based primarily on the work of Root (1987).

This model shows that the southern Canadian Cordilleran margin was significantly attenuated by protracted rifting of the supercontinent Rodinia and subsequent extension in the back-arc of a Late Paleozoic subduction zone. The edge of Precambrian North American crust in early Paleozoic time is interpreted to have been approximately on strike with the outer edge of the Montana block or "Montania". The presence of multiple marginal basins and topographic highs that were sub-parallel to the plate edge suggests this segment was attenuated by a series of normal faults similar to the lower plate margin of the asymmetric rift model of Lister et al. (1986). This is in contrast to a relatively abrupt break with less crustal attenuation in an upper plate zone (Lister et al., 1986). Similar attenuation in a lower plate zone occurred in the northern British Columbia and Yukon segment of the Cordilleran margin on which the Selwyn Basin developed subsequently (Cecile et al., 1997). Strike-slip transfer zones that separate upper plate zones from more attenuated lower plate zones occur along the length of western North America (Cecile et al., 1997; Lund et al., 2010). The northern edge of Montania, which corresponds to a major crustal structure called the Vulcan low in the Alberta basement (Price, 1996) is interpreted here to be one such transfer structure that separated the long-lived positive relief of the Montana block in the south from the series of marginal basins (White River Trough/ Golden Embayment/Prophet Trough and Lardeau trough) and emergent blocks (Purcell and Dogtooth arches and Okanagan High) of the southern Canadian Cordillera (Figure 6-2). Periodic extension in the Early Paleozoic (Figure 6-3; Root, 1987; Cecile et al., 1997; Logan and Colpron, 2006) is interpreted here to have reactivated normal faults and generated alkaline magmatism in deep basins but did not significantly affect the width or geometry of the margin. This contrasts with the model of Logan and Colpron (2006) in which they likened the Lardeau trough to the transtensional Gulf of California.

That the Okanagan High was a site of deposition during the Late Devonian suggests exotic crust introduced in mid-Devonian time added to the edge of the North American plate and was not obducted over the Okanagan

High. Both accreted and *in situ* continental crust, and oceanic crust along strike to the south (e.g. Trail Gneiss complex, Simony et al., 2006; Figure 6-6) formed the basement to a series of overlapping Late Devonian to Triassic and younger continental margin magmatic arcs. East-dipping (modern coordinates) Late Devonian to Permian subduction beneath the Cordilleran margin is interpreted to have caused episodic contraction and extension of the relatively weak crust in the southern Canadian Cordillera, including Early Mississippian deformation of Late Cambrian to Late Devonian strata in the Lardeau trough (figures 6-5 to 6-8). The Late Triassic Slocan Group was the distal back-arc portion of a broad overlap assemblage that blanketed the Cordilleran margin from the location of the former Lardeau trough to the Nicola arc.

The strong map control that precludes formation of oceanic crust inboard of the Okanagan High leads to the interpretation that shortly before the onset of the main Cordilleran orogeny, attenuated Precambrian crust extended approximately to the edge of the Montania block, similar to its limit in Late Cambrian time. Much of the upper crust comprised Late Paleozoic and Triassic arc complexes that were built on (Erdmer et al., 2002) and accreted to the outer edge of Precambrian crust. This is in agreement with interpretations of deep seismic data that show North American Precambrian crust extending to the west edge of the Okanagan valley beneath a cover of Late Paleozoic and younger arc complexes (Cook et al., 1992; 2005). The edge of the North American plate (the subduction trench axis west of the Nicola arc) was outboard of the limit of Precambrian crust at a distance from the craton not significantly different from the modern day plate edge (Figure 6-9). The interpreted paleogeography of Paleozoic pericratonic strata indicates that the southern Canadian Cordilleran margin, in Paleozoic and Triassic time, grew by tectonic and magmatic reworking of a heterogeneously extended margin and by accretion of allochthonous terranes.

6.3 Future work and unresolved issues

The Mount Sproat assemblage is a new source of information about the Late Devonian evolution of the southern Canadian Cordilleran margin and is strong new evidence for Late Devonian subduction-related magmatism in the region. Future mapping and geochronological study along strike to the south in the Kootenay Arc and near Upper Arrow Lake may identify additional Late Devonian strata and shed more light on this dynamic period of Cordilleran evolution.

The map framework established in this work will facilitate an in-depth stratigraphic, sedimentologic and paleontologic analysis of the Milford Group and the Thompson assemblage. Especially in the Badshot Range, application of such data to measured stratigraphic sections would substantially augment the level of understanding of the pericratonic Carboniferous assemblages. The proposed Mississippian age of the Thompson assemblage remains to be tested. As a minimum age constraint for D1 deformation in the Broadview Formation, the Thompson assemblage offers a test of the Early Mississippian timing of D1 proposed here.

The detrital zircon dataset for the Canadian Cordillera is still at a reconnaissance level of resolution. The hypotheses presented above will be tested by expansion of the provenance database for the pericratonic rocks in the British Columbia Cordillera. In particular, work should focus on Silurian to Triassic rocks that formed outboard of the Cordilleran miogeocline, including strata in the Vernon area ("Eagle Bay assemblage") and the rocks that are commonly referred to as the Quesnel and Slide Mountain terranes in southern British Columbia. Detrital zircon provenance of the Black Stuart Formation and Guyet conglomerate will reveal more about the origin of the Guyet conglomerate and perhaps better constrain the timing and extent of exotic crust that arrived in the Cordillera in mid-Paleozoic time. The apparent Cordilleran affinity of the basement of the Chilliwack Composite terrane warrants further investigation of the geologic history and characteristics of that terrane. Either the Chilliwack Composite terrane records an Ordovician-Silurian connection between the Cordilleran margin and the Alexander terrane or paragneiss that would be interpreted as peri-Laurentian based on detrital zircon data (Yellow Aster complex) is in fact exotic to the Cordillera. If the latter, perhaps similar paragneiss elsewhere in the Cordillera (e.g. basement of Chase Formation; Queest Mountain assemblage; basement of Yukon-Tanana terrane) is less reliably of Cordilleran affinity than previously thought.

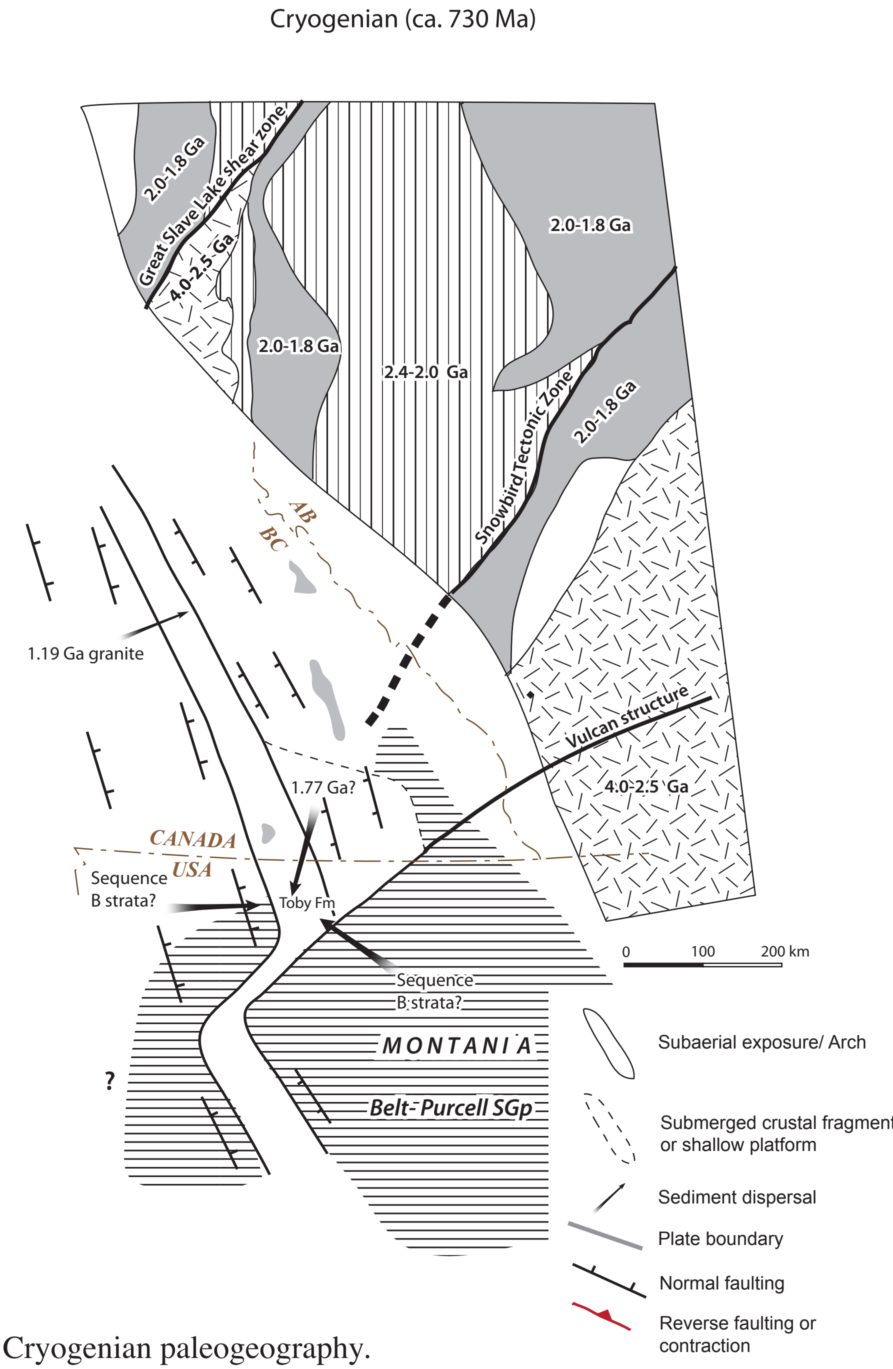

F igure 6-1. Cryogenian paleogeography.

Incipient rifting of the Cordilleran margin and deposition of the Toby Formation conglomerate. A local source of early Neoproterozoic sandstone derived in part from the Grenville province is inferred to have been near the Toby conglomerate sample, either overlying the Belt-Purcell Supergroup or northwest of it. Circa 1.77 Ga granitic crust, possibly from the north or west, was a major sediment source. A cobble of 1.2 Ga granite was deposited in the new rift basin (D. Murphy, unpublished data), probably from the west. Sources: Gehrels and Ross, 1998; Ross and Villeneuve, 2003; Price, 2007; Lund et al., 2010.

Early Cambrian

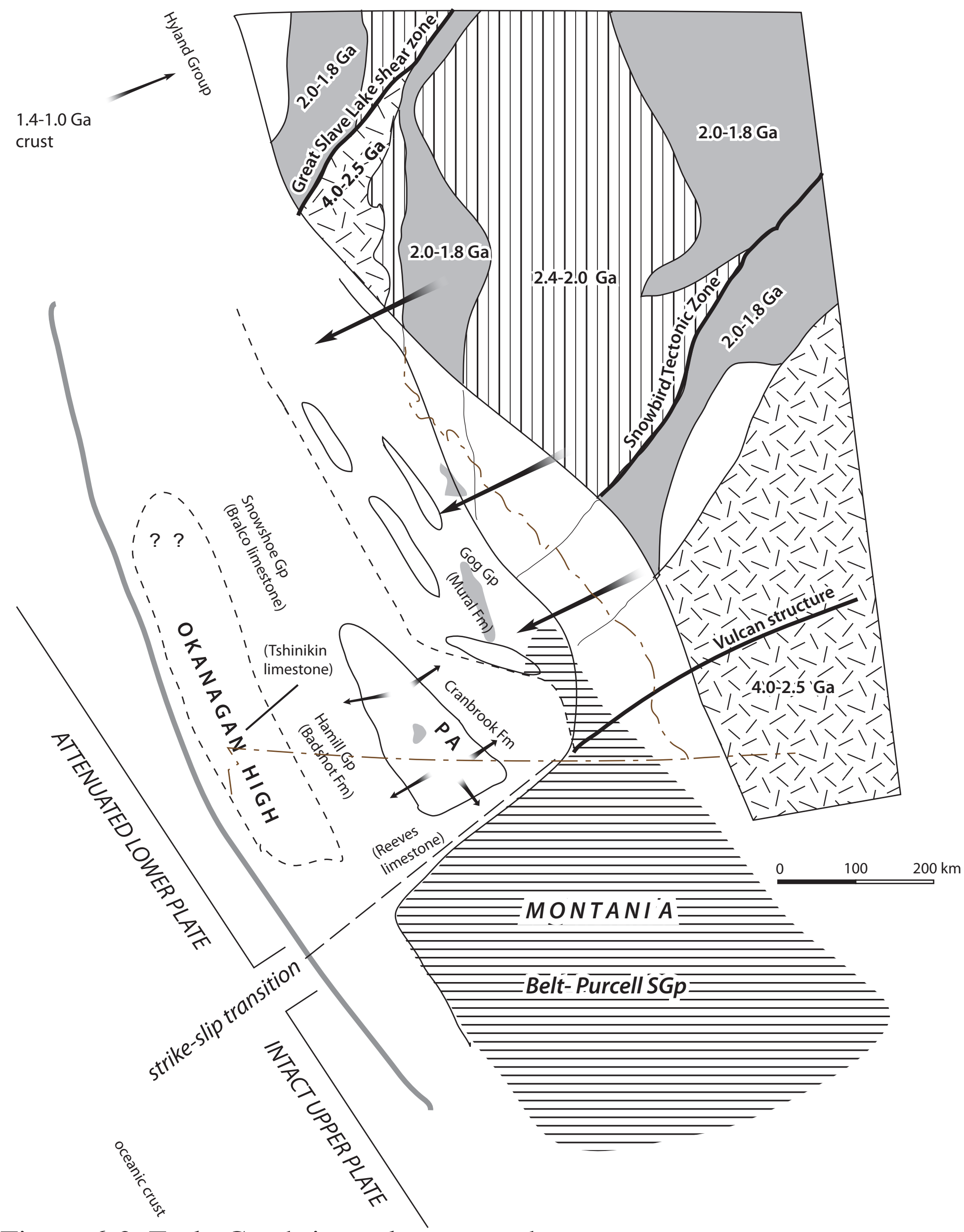

Figure 6-2. Early Cambrian paleogeography.

Cryogenian and Early Cambrian rifting left a highly attenuated lower plate-type (Lister et al., 1986) continental margin north of the less-attenuated block, Montania. Horsts or half-grabens of Precambrian continental crust include the Purcell Arch (PA) and the Okanagan High (Thompson et al., 2006). Prior data indicate Early Cambrian strata, including the Hamill Group, were derived from uplifted Hadrynian rift strata (Windermere Supergroup) and possibly crystalline basement to the northeast (Gehrels and Ross, 1998). A late Early Cambrian carbonate platform (Tshinikin limestone-Bralco limestone-Badshot Fm-Mural Fm-Reeves limestone) overlaps pericratonic and miogeoclinal rocks.

Middle Ordovician

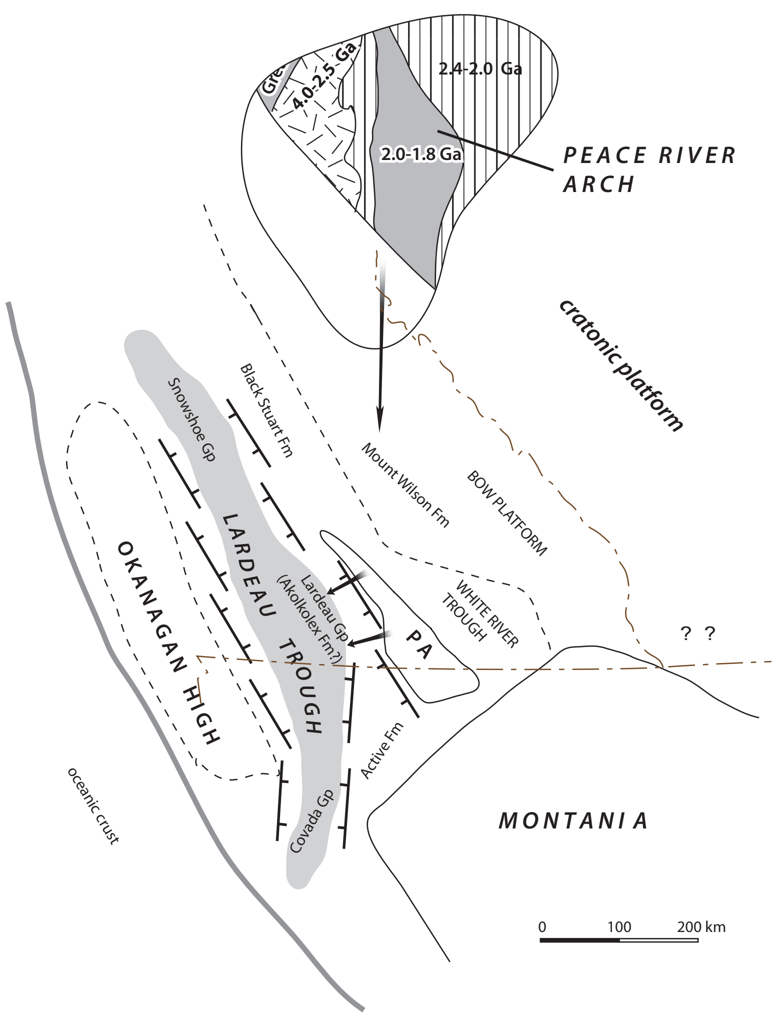

Figure 6-3. Mid-Cambrian to Ordovician paleogeography.
Subsidence is driven by normal faulting in the outer margin forms the Lardeau trough (Smith, 1990) between the Purcell Arch and the Okanagan High (Thompson et al., 2006). The Akolkolex Formation is interpreted to record Ordovician extension and uplift on the Purcell Arch (Logan and Colpron, 2006). Circa 1.77 Ga crust exposed on the Purcell Arch may have contributed detritus to the Akolkolex Formation. Alkaline basaltic magmatism occurs periodically in the Lardeau trough and elsewhere in the Cordilleran margin (Cecile et al., 1997). Abbreviations: PA, Purcell Arch.

Middle Devonian

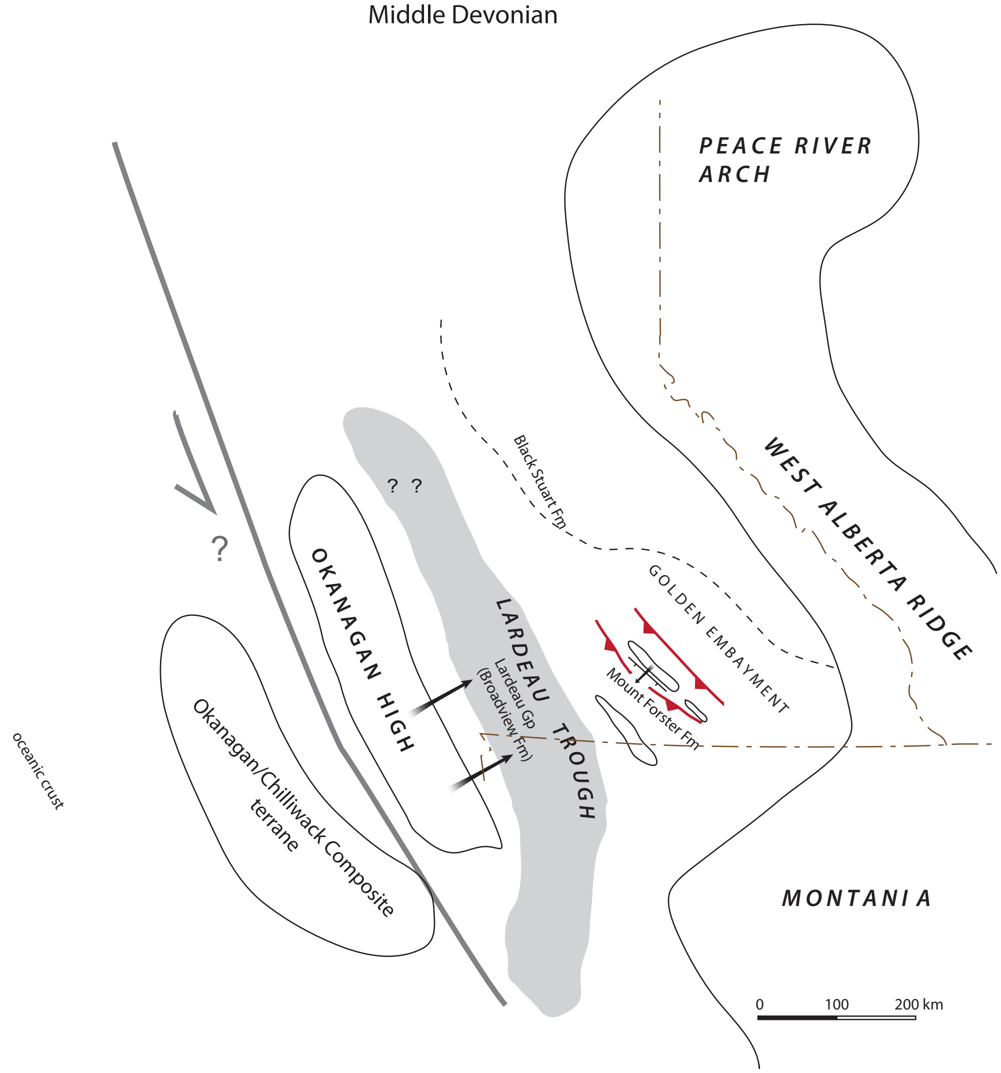

Figure 6-4. Middle Devonian paleogeography.
The Mount Forster Formation was deposited in a half graben on the crest of the predominantly submerged Purcell Arch (Root, 1987). Detrital zircons from this study and petrographic evidence from Root (1987) show that it was derived from nearby uplifted Horsethief Creek and Ordovician strata. A short pulse of deformation, probably compressional, folded and faulted the Mount Forster Formation during its deposition (Root, 1987). The Black Stuart Fm deposited with no evidence of compressional deformation 400 km to the north (Struik, 1981). The McCrae Peak succession is deposited in the Lardeau trough. Devonian tectonism associated with initiation of the active plate boundary caused influx of coarse clastic detritus from the Okanagan High to form the Broadview Formation. A source of Silurian, Eocambrian and Mesoproterozoic zircon and igneous rock entered the southern Canadian Cordilleran realm. The allochthonous terrane is represented today by the Okanagan and Chilliwack Composite terranes.

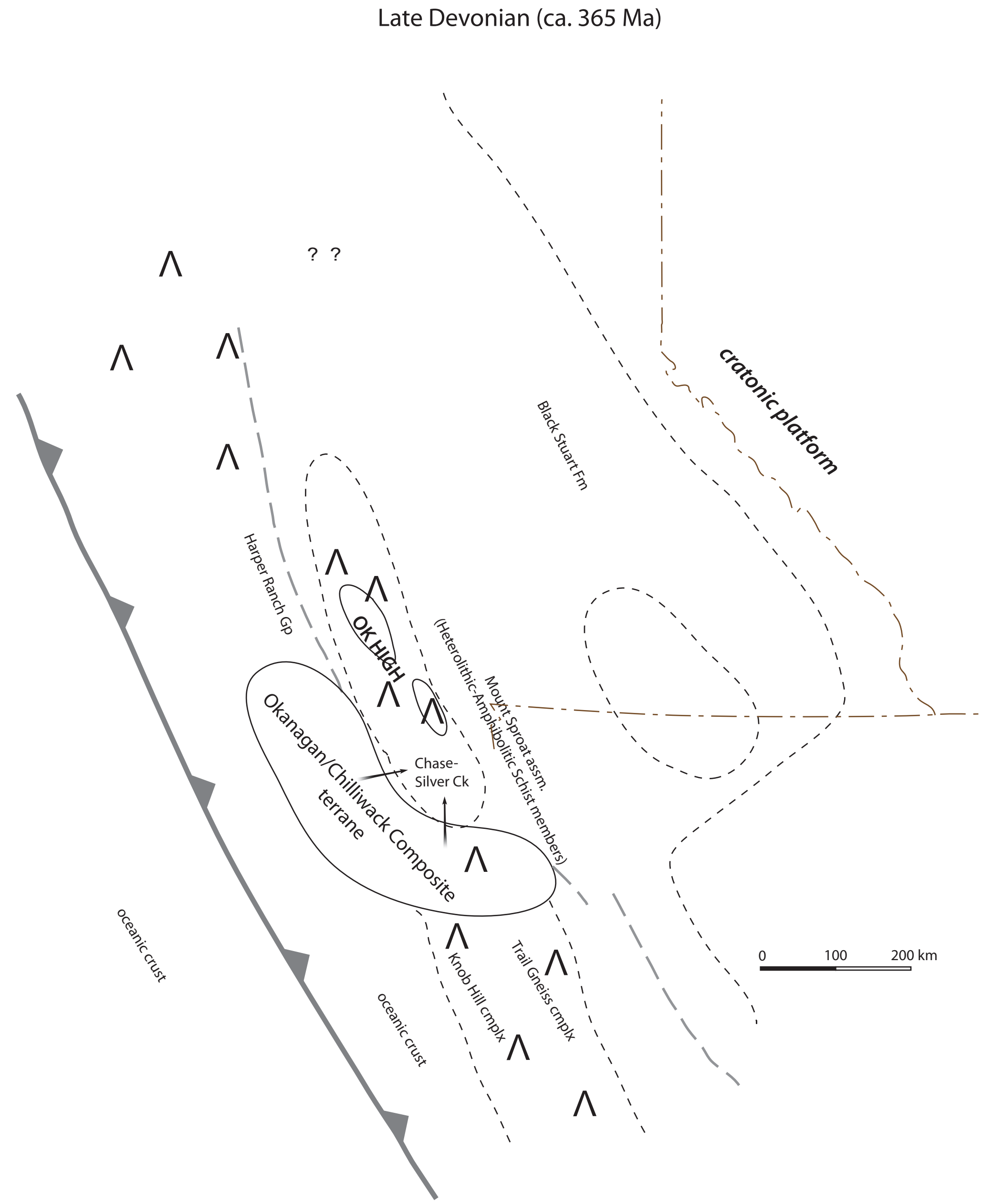

Figure 6-5. Late Devonian paleogeography.
Basinal deposition persists in the Lardeau trough. Initiation of subduction causes renewed magmatism that trends from OIB and MORB to IAT. The Chase Formation is deposited on Proterozoic strata on the Okanagan High (OK High), being derived from an exotic terrane comprising the Okanagan and Chilliwack Composite terranes. The Chase platform founders as volcanism becomes significant (Thompson et al., 2006). A continental margin arc is built across extended continental crust (Eagle Bay arc, Paradis et al., 2006) and on oceanic crust (Trail Gneiss complex, Simony et al., 2006; Harper Ranch Group, Danner and Orchard, 2000). Amphibolitic Schist in the Silver Creek Formation and Mount Sproat assemblage links the Okanagan High and the Lardeau trough.

Early Mississippian (ca. 350 Ma)

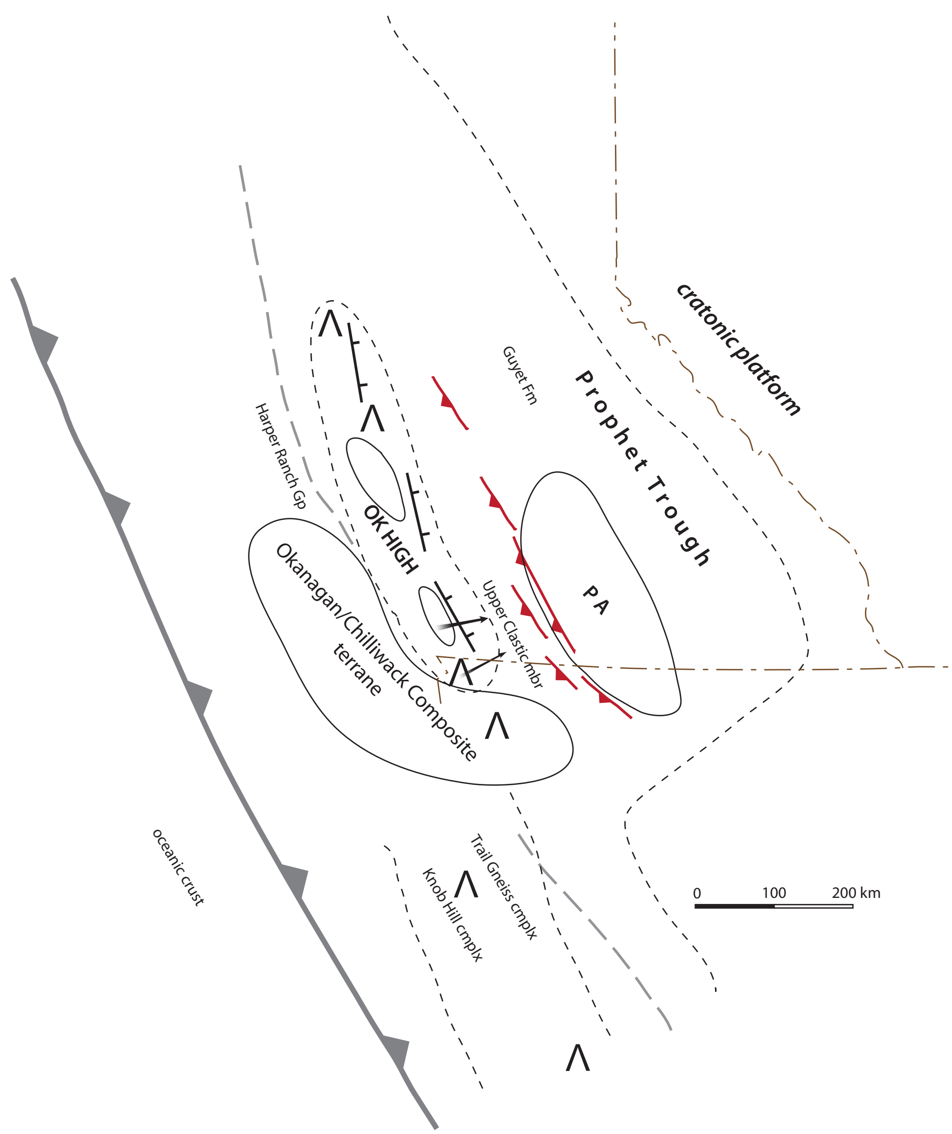

Figure 6-6. Early Mississippian paleogeography.

The Upper Clastic member (Mount Sproat assemblage) is deposited in a tectonically active back-arc setting, derived from a combination of uplifted continental rocks on the Okanagan High and igneous rocks from the magmatic arc that was forming on the Okanagan High. Local extension (Struik, 1986) or compression (Campbell et al., 1973) to the north uplifted outer margin rocks and caused deposition of the Guyet conglomerate. Inboard of the Okanagan High, the back-arc changed to a compressional environment, causing the thin crust under the Lardeau trough to shorten and deforming the Lardeau Group and older rocks of the Mount Sproat assemblage against a buttress in the Purcell Arch (see Chapter 4).

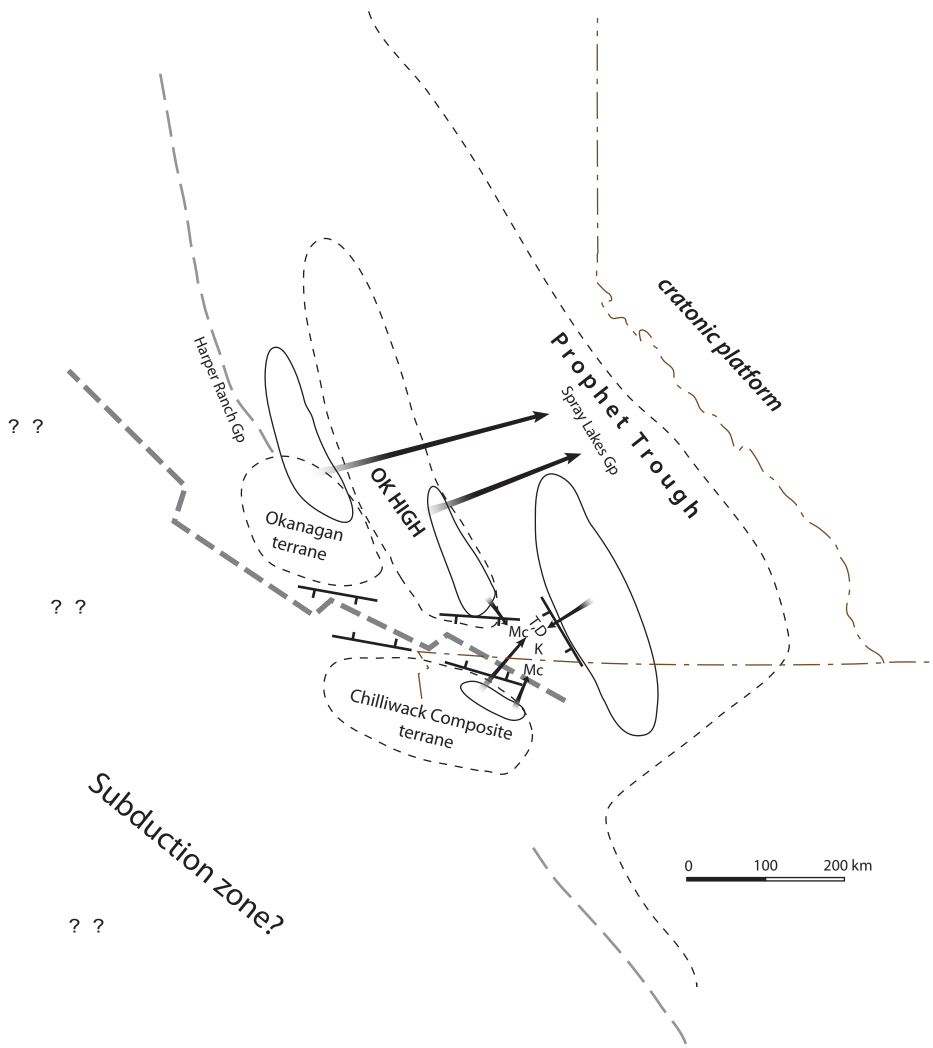

Figure 6-7. Late Mississippian to Pennsylvanian paleogeography.
Arc magmatism in the pericratonic rocks has waned or ceased. Rifting oblique to the margin forms a narrow trough into which the Thompson assemblage (T) and Milford Group (Slide Mountain tectonic assemblage) begin to deposit. The Thompson assemblage and basal Davis assemblage (D) conglomerate derive from uplifted Lardeau strata to the east. On the southwest side of the incipient rift the McHardy assemblage (Mc) receives boulders of Silurian granite from the adjacent Chilliwack composite terrane (CCT). Farther north, the McHardy assemblage is derived mainly from the Okanagan High or (and) parts of the CCT that have a typical northwest Laurentian signature. Quartzite higher in the Davis assemblage (D) receives a small amount of Silurian zircon from the CCT to the west.

Early Permian

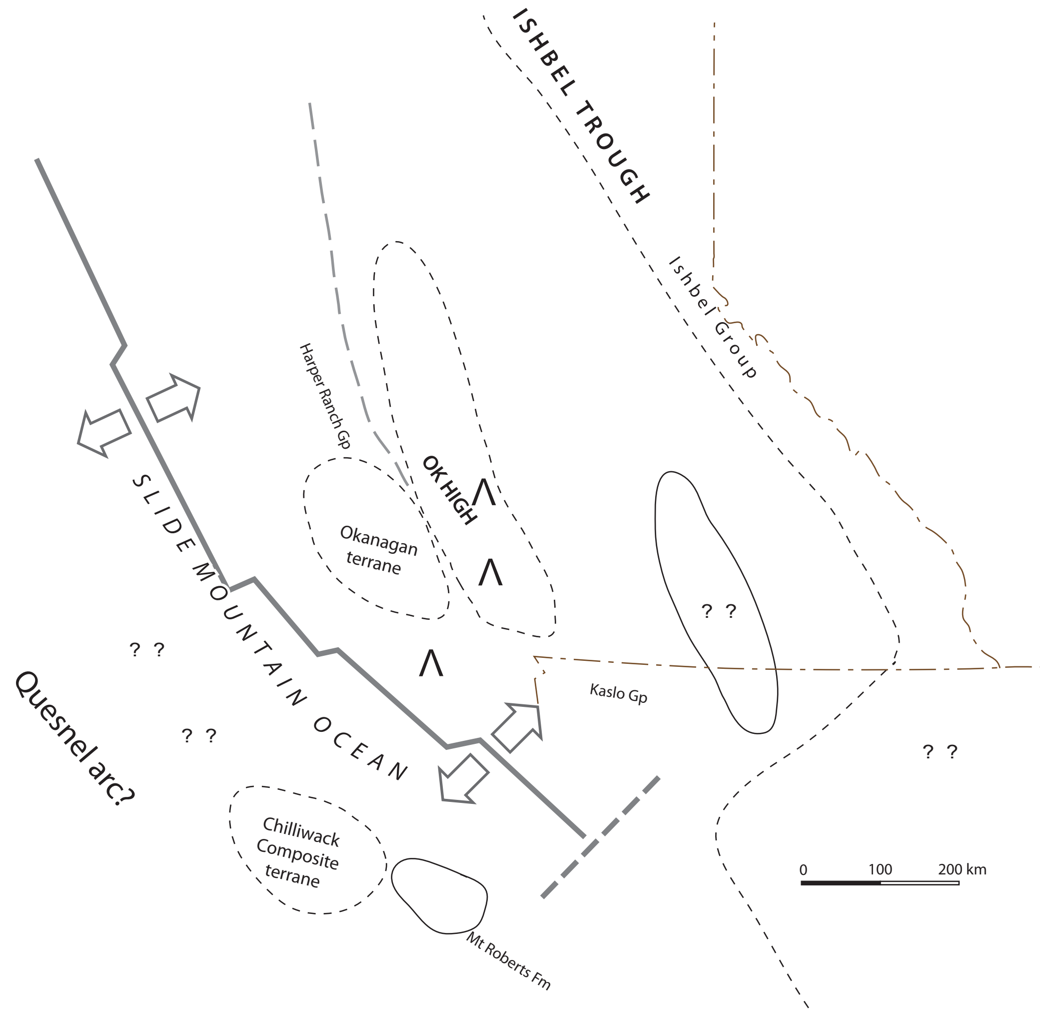

Figure 6-8. Early Permian paleogeography.
Rifting that formed the Milford Group has progressed to seafloor-spreading and has dissected the Late Devonian-Early Mississippian arc. The basin is part of the Slide Mountain marginal ocean (Klepacki, 1985). The Kaslo Group onlaps the inboard margin of the basin and also forms juvenile oceanic crust farther outboard. The width of the Slide Mountain basin is inferred here to be no more than a few hundred kilometres, or potentially much less, because the Chilliwack composite terrane returns to a similar location on the margin following closure of the basin.

Late Triassic

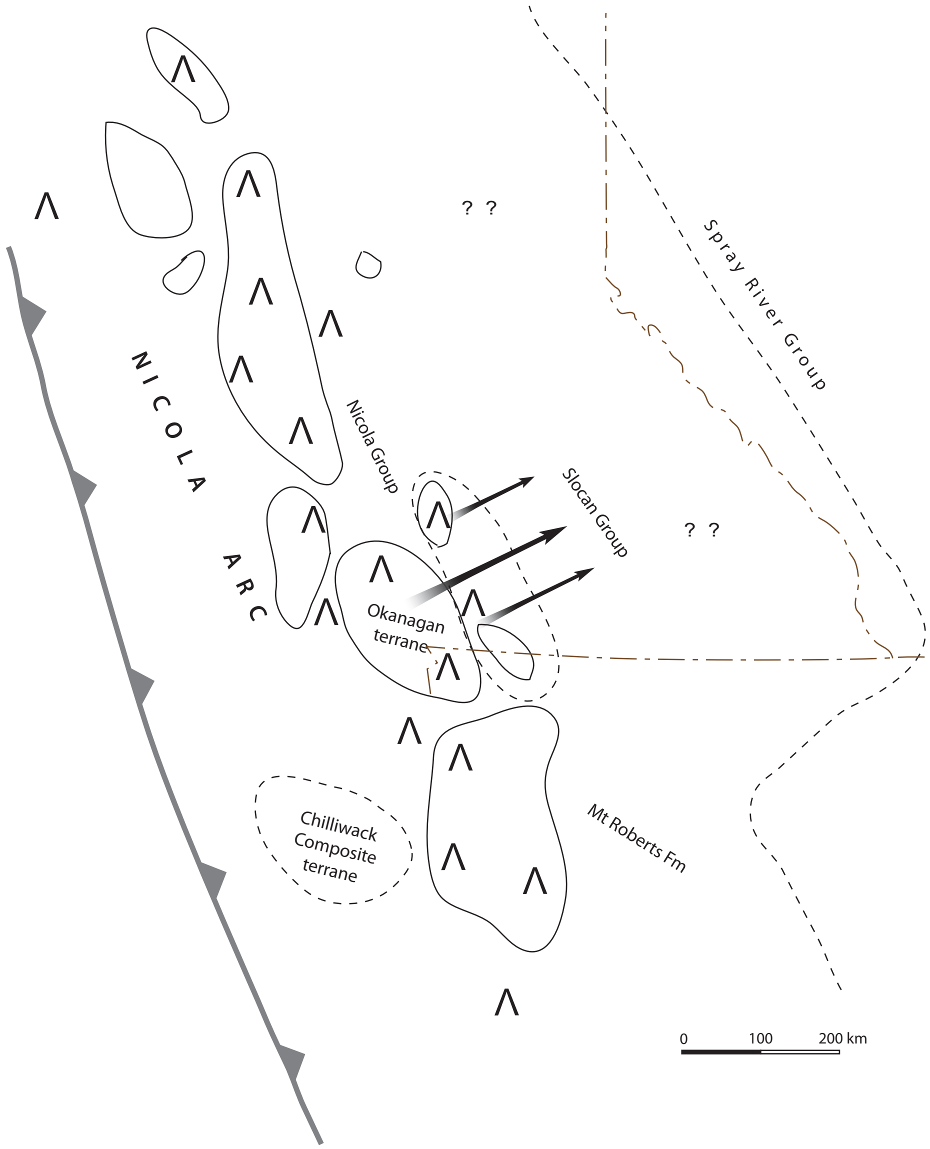

Figure 6-9. Late Triassic paleogeography.
The Slide Mountain ocean has closed and the Nicola Arc forms on a heterogeneous basement of late Paleozoic continental and arc rocks (Beatty et al., 2006). The Slocan Group deposits inboard of and is derived from the Nicola arc and its basement. The diverse sources are a mixture of ages found in the Chase Formation, Chilliwack Composite terrane and the Devonian to Triassic arcs. The Okanagan High was not a source, presumably because it was covered by Devonian to Triassic rocks.

References

Cairnes, C. E., 1934, Slocan Mining Camp, British Columbia; Geological Survey of Canada, Memoir 173.

Cecile, M., Morrow, D., and Williams, G., 1997, Early Paleozoic (Cambrian to Early Devonian) tectonic framework, Canadian Cordillera: Bulletin of Canadian Petroleum Geology, v. 45, p. 54.

Colpron, M., 1996, Stratigraphy, structure and thermotectonic evolution of the western flank of the Selkirk fan structure, northern Selkirk Mountains, British Columbia: Ph.D. thesis, Queen's University, Kingston, Ontario, 162 p.

Colpron, M., and Nelson, J.L., 2009, A Palaeozoic Northwest Passage: incursion of Caledonian, Baltican and Siberian terranes into eastern Panthalassa, and the early evolution of the North American Cordillera: Geological Society London Special Publications, v. 318, p. 273-307, doi: 10.1144/SP318.10.

Colpron, M., and Nelson, J.L., 2011, Chapter 31 A Palaeozoic NW Passage and the Timanian, Caledonian and Uralian connections of some exotic terranes in the North American Cordillera: Geological Society, London, Memoirs, v. 35, p. 463–484, doi: 10.1144/M35.31.

Colpron, M., Mortensen, J.K., Gehrels, G.E. and Villeneuve, M., 2006, Basement complex, Carboniferous magma- tism and Paleozoic deformation in Yukon-Tanana terrane of central Yukon: Field, geochemical and geochronological constraints from Glenlyon map area, in Colpron, M. and Nelson, J.L., eds., Paleozoic Evolution and Metallogeny of Pericratonic Terranes at the Ancient Pacific Margin of North America, Canadian and Alaskan Cordillera: Geological Association of Canada, Special Paper 45, p. 131-151.

Coney, P.J., Jones, D.L., and Monger, J.W.H., 1980, Cordilleran suspect terranes. Nature, v. 288, p. 329–333 doi:10.1038/288329a0.

Cook, F.A., Varsek, J.L., Clowes, R.M., Kanasewich, E.R., Spencer, C.S., Parrish, R.R., Brown, R.L., Carr, S.D., Johnson, B.J., and Price, R.A., 1992, Lithoprobe crustal reflection cross section of the southern Canadian Cordillera I: foreland thrust and fold belt to Fraser River fault: Tectonics, v. 11, p. 12–35.

Cook, F.A. and Erdmer, P., 2005, An 1800-km cross section of the lithosphere through the northwestern North American plate: Lessons from 4.0 billion years of Earth's history: Canadian Journal of Earth Sciences, v. 42, p. 1295-1311.

Erdmer, P., Heaman, L., Thompson, R.I. and Daughtry, K.L, 2001, Eocambrian granite clasts in southern British Columbia shed light on Cordilleran hinterland crust: Canadian Journal of Earth Sciences, v. 38, p. 1007-1016.

Erdmer, P., Moore, J., Heaman, L., Thompson, R., Daughtry, K., and Creaser, R., 2002, Extending the ancient margin outboard in the Canadian Cordillera: record of Proterozoic crust and Paleocene regional metamorphism in the Nicola horst, southern British Columbia: Canadian Journal of Earth Sciences, v. 39, p. 1605–1623.

Fyles, J.T., 1964, Geology of the Duncan Lake area, Lardeau District, British Columbia: British Columbia Department of Mines and Petroleum Resources, Bulletin 49, 87 p.

Fyles, J.T. and Eastwood, G.E.P., 1962, Geology of the Ferguson area, Lardeau district, British Columbia: B.C. Department of Mines and Petroleum Resources, Bulletin 45, 92 p.

Gabrielse, H., and Yorath, C.J., eds., 1991, Geology of the Cordilleran orogen in Canada. Geological Survey of Canada, Geology of Canada, No. 5.

Gordey, S., Abbott, J., Tempelman-Kluit, D., and Gabrielse, H., 1987, " Antler" elastics in the Canadian Cordillera: Geology, v. 15, p. 103.

Johnson, J. G., and Pendergast, A., 1981, Timing and mode of emplacement of the Roberts Mountains allochthon, Antler orogeny: Geological Society of America Bulletin, v. 92, p. 648-658.

Jones, A.G., 1959, Vernon map-area, British Columbia. Geological Survey of Canada Memoir 296.

Klepacki, D.W., 1985, Stratigraphy and structural geology of the Goat Range area, southeastern British Columbia. Ph.D. thesis, Massachusetts Institute of Technology, Cambridge, Mass.

Lemieux, Y., 2006, Structure, geochronology and thermobarometry of the eastern flank of the Shuswap metamorphic complex in the Upper Arrow Lake area, southeastern British Columbia. Ph.D. thesis, University of Alberta, Edmonton, AB.

Lemieux, Y., Thompson, R., Erdmer, P., Simonetti, A., and Creaser, R., 2007, Detrital zircon geochronology and provenance of Late Proterozoic and mid-Paleozoic successions outboard of the miogeocline, southeastern Canadian Cordillera: Canadian Journal of Earth Sciences, v. 44, p. 1675–1693.

Lister, G.S., Etheridge, M.A., and Symonds, P.A., 1986, Detachment faulting and the evolution of passive continental margins: Geology, v. 14, p. 246–250, doi: 10.1130/ 0091-7613(1986)14<246:DFATEO>2.0.CO;2.

Logan, J., and Colpron, M., 2006, Stratigraphy, geochemistry, syngenetic sulphide occurrences and tectonic setting of the lower Paleozoic Lardeau Group, northern Selkirk Mountains, British Columbia: *in* Colpron, M. and Nelson, J.L., eds., Paleozoic Evolution and Metallogeny of Pericratonic Terranes at the Ancient Pacific Margin of North America, Canadian and Alaskan Cordillera: Geological Association of Canada, Special Paper 45, v. 45, p. 361–382.

Lund, K., Aleinikoff, J. N., Evans, K. V., duBray, E. A., Dewitt, E. H., and Unruh, D. M., 2010, SHRIMP U-Pb dating of recurrent Cryogenian and Late Cambrian–Early Ordovician alkalic magmatism in central Idaho: Implications for Rodinian rift tectonics: Geological Society of America Bulletin, v. 122, p. 430-453, doi: 10.1130/B26565.1.

Miller, E.L., Holdsworth, B.K., Whiteford, W.B., and Rogers, D., 1984, Stratigraphy and structure of the Schoonover sequence, northeastern Nevada: Implications for Paleozoic plate margin tectonics: Geological Society of America Bulletin, v. 95, p. 1063-1076.

Monger, J.W.H., 1984, Cordilleran tectonics: A Canadian perspective: Bulletin de la Société Géologique de France, v. 26, p. 255-278.

Monger, J., and Berg, H., C., 1987, Lithotectonic terrane map of western Canada and southeastern Alaska. United States Geological Survey, Miscellaneous Field Studies Map MF-1874-B.

Nelson, J. L., 1993, The Sylvester Allochthon: upper Paleozoic marginal-basin and island-arc terranes in northern British Columbia: Canadian Journal of Earth Sciences, v. 30, p. 631-643.

Orchard, M.J. 1985, Carboniferous, Permian and Triassic conodonts from the Central Kootenay Arc, British Columbia : constraints on the age of the Milford, Kaslo, and Slocan groups. In Current Research, Part A. Geological Survey of Canada, Paper 85-1A, p. 287-300.

Piercey, S. J., Murphy, D. C., Mortensen, J. K., and Creaser, R. 2004, Mid- Paleozoic initiation of the northern Cordilleran marginal back-arc basin: Geologic, geochemical, and neodymium isotope evidence from the oldest mafic magmatic rocks in Yukon-Tanana terrane, Finlayson Lake district, southeast Yukon, Canada, Geological Society of America Bulletin, v. 116, p. 1087–1106, doi:10.1130/B25162.1.

Price, R. A., 1996, Tectonic heredity of the Crowsnest Pass cross-strike discontinuity: Mesozoic-Cenozoic tectonic inversion of Paleozoic structures with Eocambrian, Neoproterozoic, Mesoproterozoic and Archaen antecedents, in F. Cook and P. Erdmer (compilers_, Lithoprobe Slave-Northern Cordilleran Lithospheric Evolution and Cordilleran Tectonics Workshohp, Lithoprobe Report no. 50, p. 155.

Price, R. A., 2007, Whence the Southeastern Canadian Cordillera: Palinspastic Restorations Linking Displaced Supracrustal Rocks to Crustal Structure: Edmonton Geological Society presentation abstract, 4 p.

Price, R. A., 2009, Paleozoic paleogeography of the western margin of Laurentia as recorded in the displaced rocks of foreland thrust and fold belt of the southeastern Canadian Cordillera: Geological Society of America, Abstracts with Programs, 1 p.

Read, P.B., and Wheeler, J.O., 1976, Geology, Lardeau west-half, British Columbia. Geological Survey of Canada Open File 432.

Reesor, J.E. 1973. Geology of the Lardeau map-area, east half, British Columbia. Geological Survey of Canada Memoir 369.

Roback, R., Sevigny, J., and Walker, N., 1994, Tectonic setting of the Slide Mountain terrane, southern British Columbia: Tectonics, v. 13, p. 1242–1242.

Roberts, R.J., Hotz, P.E., Gilluly, J., and Furgusan, H.G., 1958, Paleozoic rocks of north central Nevada: American Association of Petroleum Geologists Bulletin, v. 42, p. 2813-2857.

Root, K., 1987, Geology of the Delphine Creek area, southeastern British Columbia: Implications for the Proterozoic and Paleozoic development of the Cordilleran divergent margin: Ph.D. thesis, University of Calgary, Calgary, AB.

Ross, G., Friedman, R., and Mortensen, J. K., 2005, Detrital zircon and monazite from the Hyland Group (northern Canadian Cordillera and Alaska): evidence for intra-Cordilleran "Grenville" basement: Geological Society of America Abstracts with Programs, v. 37, p. 56.

Schiarizza, P. and Preto, V.A., 1987, Geology of the Adams Plateau-Clearwater-Vavenby area: B.C. Geological Survey Branch, Paper 1987-2, 88 p.

Simony, P.S., Sevigny, J.H., Mortensen, J.K. and Roback, R.C., 2006, Age and origin of the Trail Gneiss Complex: Basement to Quesnel terrane near Trail, southeastern British Columbia, *in* Colpron, M. and Nelson, J.L., eds., Paleozoic Evolution and Metallogeny of Pericratonic Terranes at the Ancient Pacific Margin of North America, Canadian and Alaskan Cordillera: Geological Association of Canada, Special Paper 45, p. 505-515.

Smith, M. T., and Gehrels, G. E., 1992, Structural geology of the Lardeau Group near Trout Lake, British Columbia: implications for the structural evolution of the Kootenay Arc: Canadian Journal of Earth Sciences, v. 29, p. 1305- 1319.

Smith, M., Dickinson, W., and Gehrels, G., 1993, Contractional nature of Devonian-Mississippian Antler tectonism along the North American continental margin: Geology, v. 21, p. 21.

Thompson, R.I., Glombick, P., Daughtry, K.L., and Erdmer, P. 2001. Upper Paleozoic stratigraphic linkage between Kootenay Arc and “Vernon Antiform”: new constraints on southern Canadian Cordilleran evolution: *in* Proceedings of the 2001 SNORCLE Transect and Cordilleran Tectonics Workshop, Sidney, B.C., 25–27 February 2001. Lithoprobe Secretariat, University of British Columbia, Vancouver, BC, Lithoprobe Report 79, p. 104–105.

Wheeler, J.O., 1963, Rogers Pass map-area, British Columbia and Alberta (82N west-half): Geological Survey of Canada, Paper 62-32, 32 p.

Wheeler, J.O. and McFeely, P. (compilers), 1991, Tectonic assemblage map of the Canadian Cordillera and adjacent parts of the United States of America: Geological Survey of Canada, Map 1712A, 1:2,000,000.

Appendix 1: Oversize maps, sections and stratigraphic columns

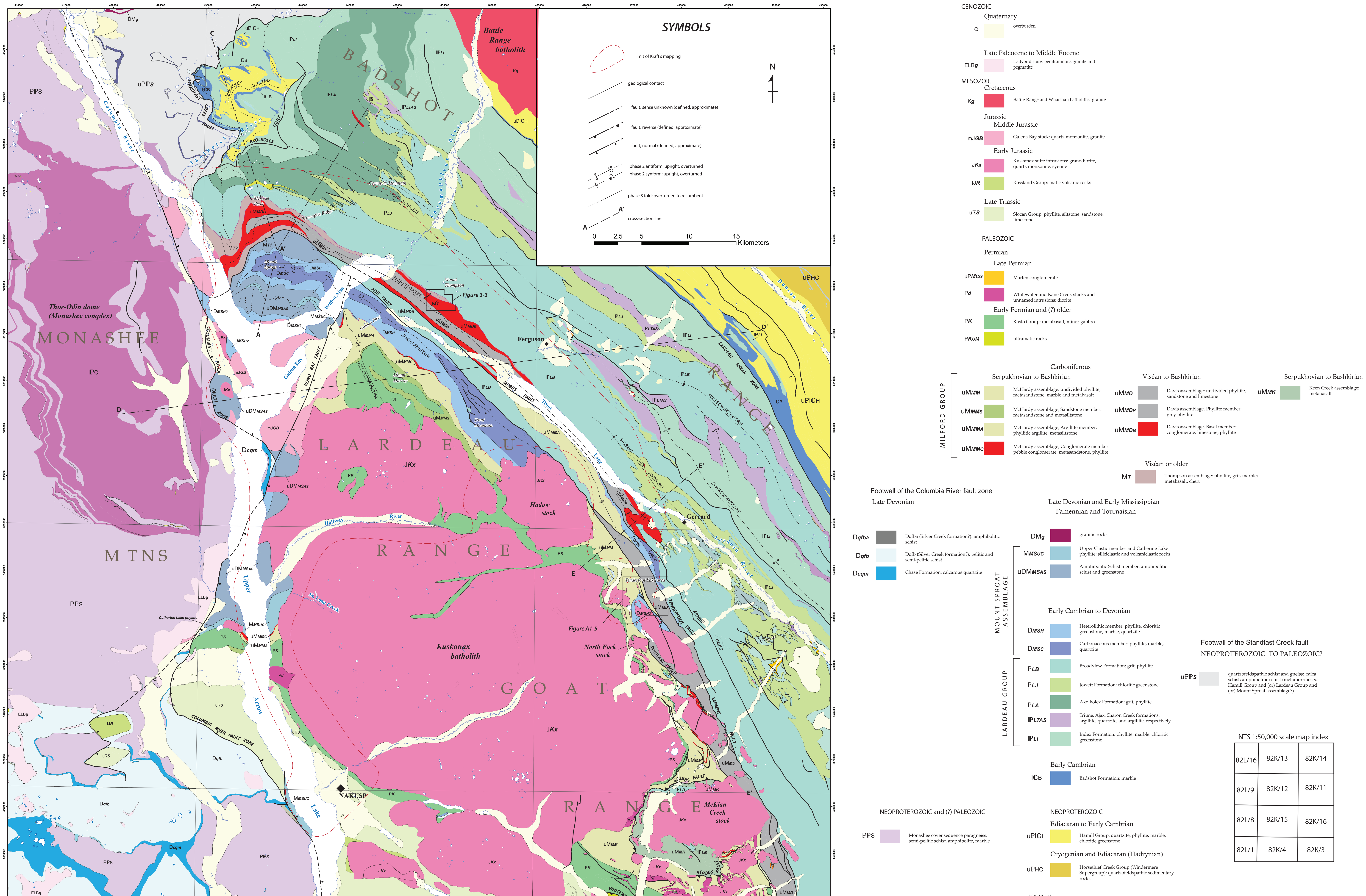

SOURCES:
Kraft, J. L., Thompson, R. I., and Dhesi, P. (compilers), 2011a, Geology, Beaton, British Columbia; Geological Survey of Canada, Open File, 6574, scale 1:50 000, doi: 10.4095/288009.
Kraft, J. L., Thompson, R. I., and Dhesi, P. (compilers), 2011b, Geology, Trout Lake, British Columbia; Geological Survey of Canada, Open File, 6572, scale 1:50 000, doi: 10.4095/288063.
Kraft, J. L., Thompson, R. I., and Dhesi, P. (compilers), 2011c, Geology, Camborne, British Columbia; Geological Survey of Canada, Open File, 6573, scale 1:50 000, doi: 10.4095/288064.
Thompson, R. I., Glombick, P., and Lemieux, Y., (compilers), 2004, Geology, Eureka Mountain, British Columbia, Geological Survey of Canada Open File 4370, scale 1:50 000.
Thompson, R. I., Glombick, P., and Lemieux, Y., (compilers), 2004, Geology, Mount Fosthall, British Columbia, Geological Survey of Canada Open File 4377, scale 1:50 000, doi:10.4095/215826.
Thompson, R. I., and Dhesi, P. (compilers), 2009, Geology, Poplar Creek, British Columbia, Geological Survey of Canada Open File 6184, scale 1:50 000.
Thompson, R. I., and Dhesi, P. (compilers), 2009, Geology, Duncan Lake, British Columbia, Geological Survey of Canada Open File 6183, scale 1:50 000.
Thompson, R. I., and Dhesi, P. (compilers), 2009, Geology, Rosebery, British Columbia, Geological Survey of Canada Open File 6187, scale 1:50 000.
Thompson, R. I., and Dhesi, P. (compilers), 2009, Geology, Lardeau Creek, British Columbia, Geological Survey of Canada Open File 6188, scale 1:50 000.
Thompson, R. I., Lemieux, Y, Glombick, P, and Dhesi, P, 2009, Geology, Nakusp, British Columbia: Geological Survey of Canada, Open File 6186, 2009; scale 1:50 000

Figure A1-1: COMPILED GEOLOGY OF THE UPPER ARROW LAKE-TROUT LAKE AREA

UTM Zone 11, North American Datum 1983

scale 1: 200 000

J. L. Kraft, 2013

Structural cross-sections of the Lardeau and Badshot ranges (1:100 000 and 1: 50 000 scale)

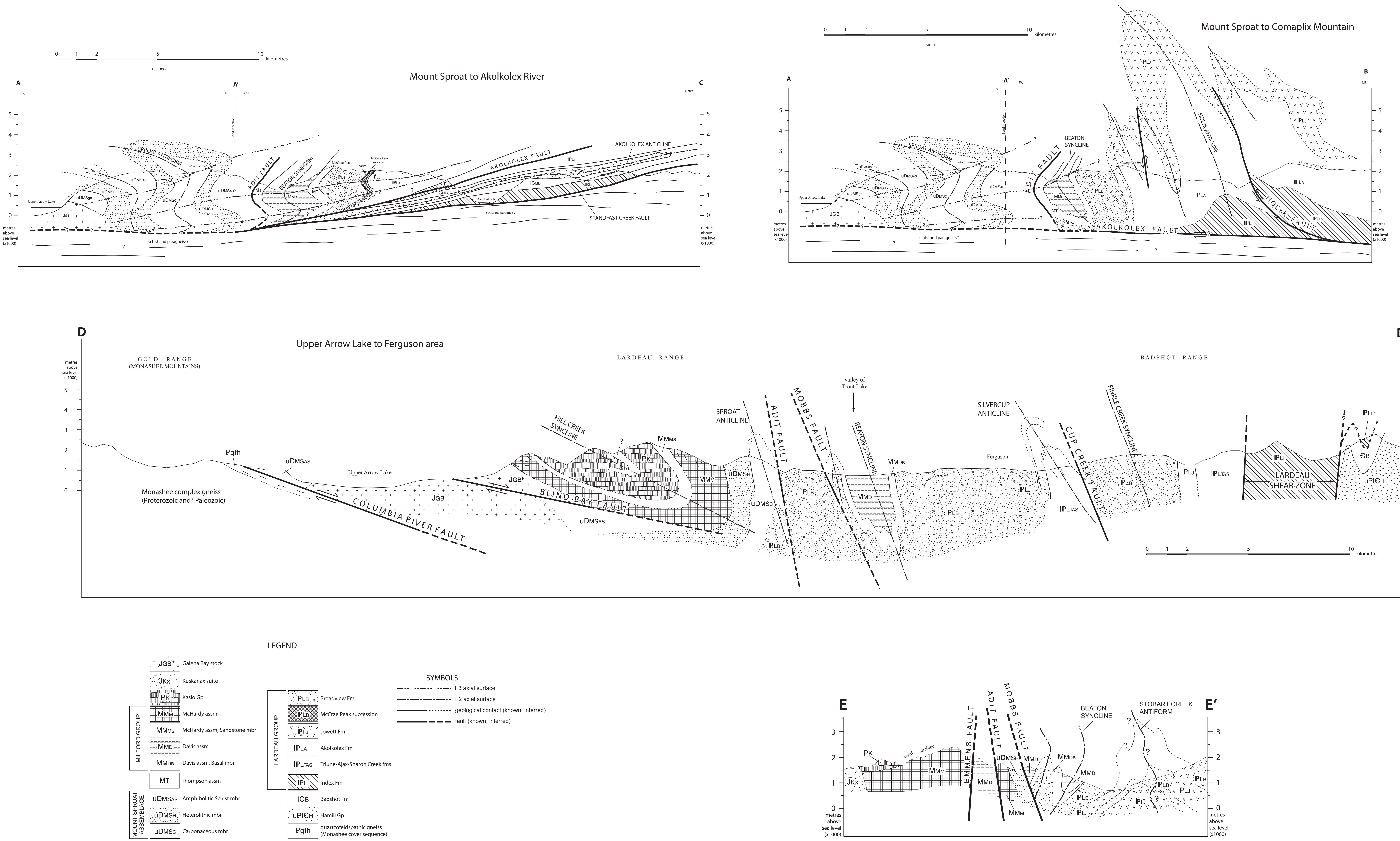

A1-2. Structural cross-sections of the Lardeau and Badshot ranges (1:100 000 and 1: 50 000 scale)

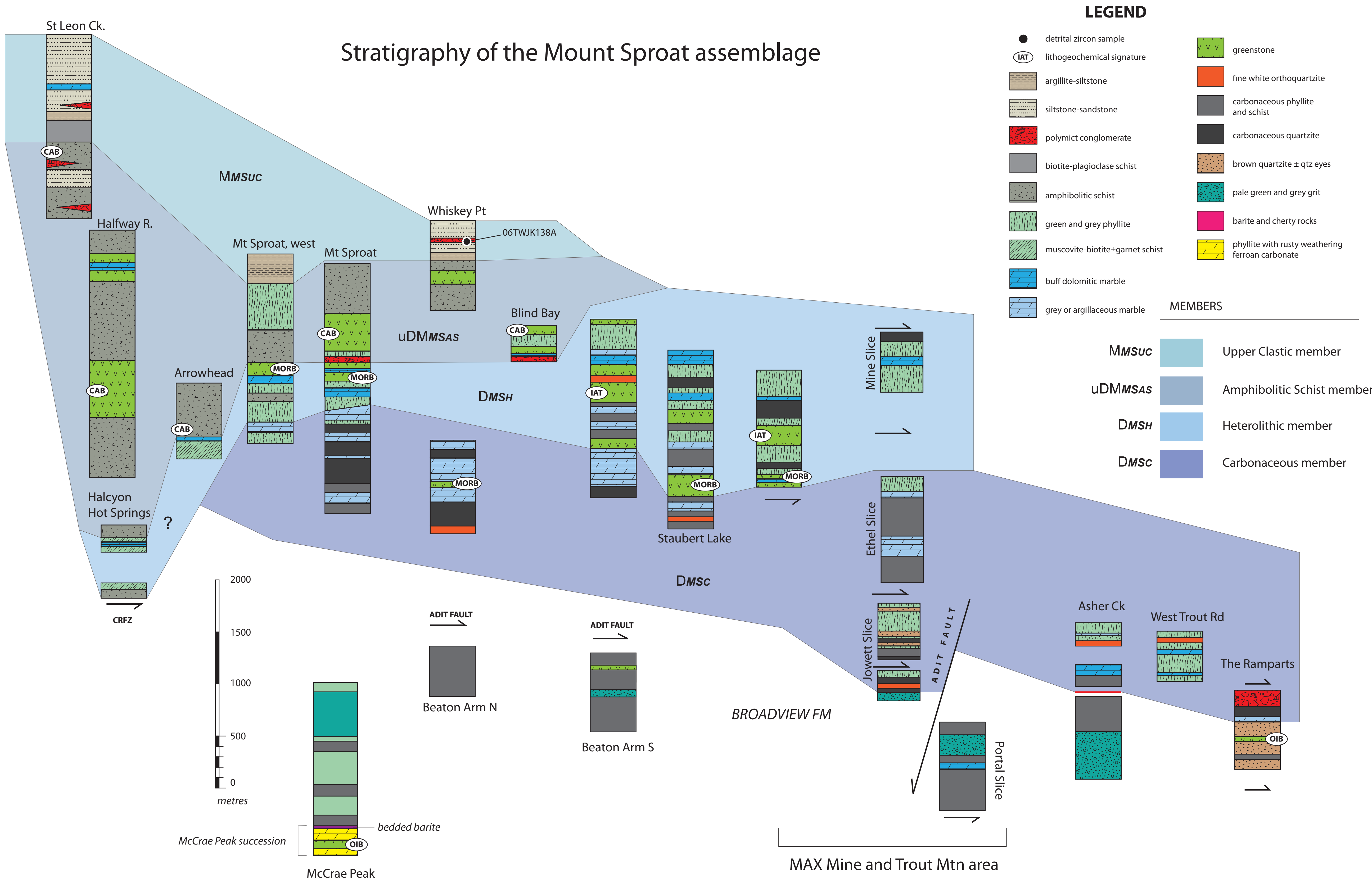

A1-3. Stratigraphy of the Mount Sproat assemblage

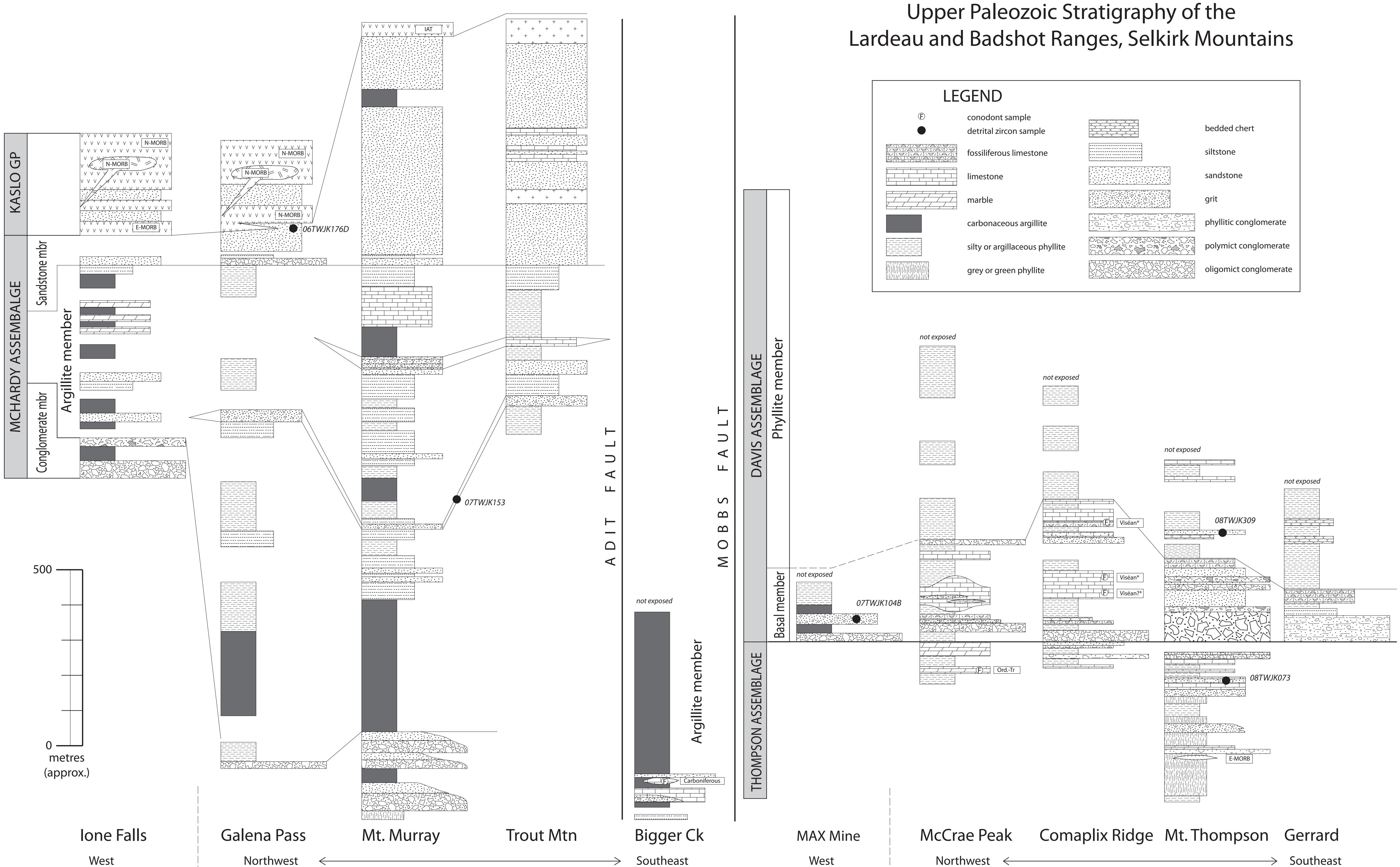

A1-4. Upper Paleozoic stratigraphy of the Lardeau and Badshot ranges, Selkirk Mountains

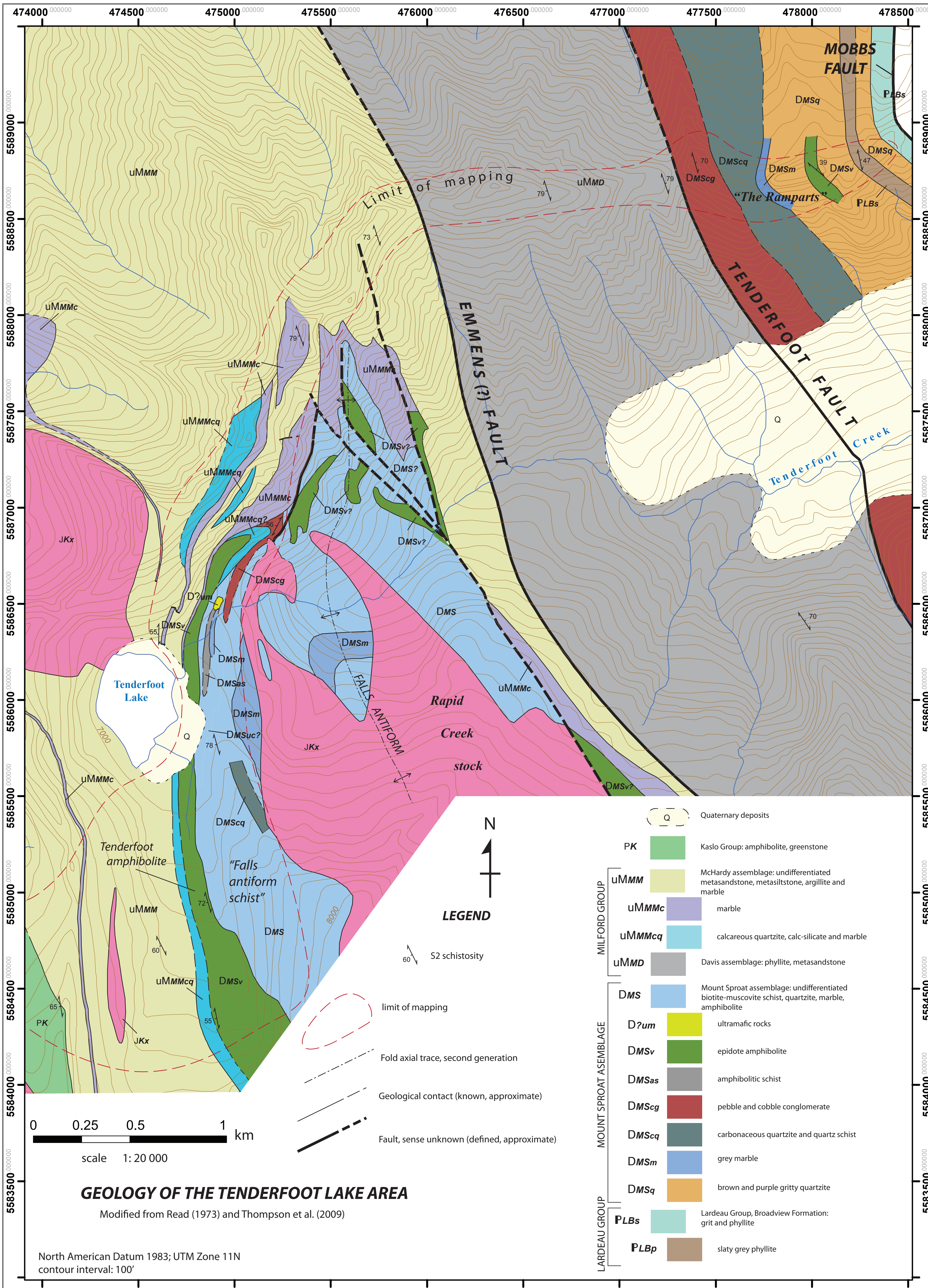

A1-5. Geology of the Tenderfoot Lake area

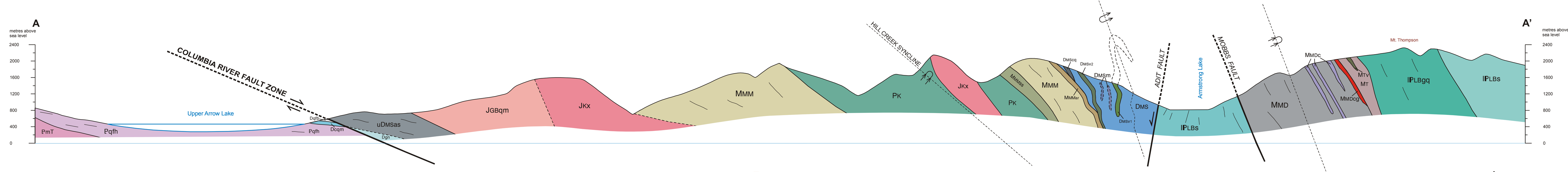

Natural Resources Canada / Ressources naturelles Canada

GEOLOGICAL SURVEY OF CANADA — COMMISSION GÉOLOGIQUE DU CANADA

REFERENCES

Vanderhaeghe, O. and Teyssier, C.
2001: Crustal-scale rheological transitions during late-orogenic collapse. Tectonophysics, v. 335, pp. 211-228.

Wheeler, J.O.
1966: Eastern tectonic belt of western Cordillera in British Columbia. In Tectonic history and mineral deposits of the western Cordillera. Canadian Institute of Mining and Metallurgy Special Volume 8, pp. 27-45.

Canadian Geochronology Knowledgebase: http://gdr.nrcan.gc.ca/geochron/index_e.php

MINERAL OCCURRENCE INDEX

MINFILE #	NAME	COMMODITY
082KNW002	STAUBERT LAKE	PB,ZN
082KNW003	LUCKY BOY (L.5423)	AG,PB,CU,ZN,WO,AU,MO
082KNW004	COPPER CHIEF (L.4584)	AG,PB,CU,WO,ZN,MO,AU
082KNW005	FISSURE	AG,CU,ZN,FE
082KNW030	TRUE FISSURE (L.1097)	AG,PB,ZN,AU,CU
082KNW040	BEATRICE (L.4586)	AG,PB,ZN,AU
082KNW059	ETHEL	AG,PB,ZN
082KNW061	GREAT NORTHERN (L.1099)	AG,AU,PB,ZN,CU
082KNW062	ST. ELMO, (L.4581)	AG,AU,PB,ZN,CU
082KNW087	MAX	MO,WO,PB,ZN,CU
082KNW088	VMS 9	CU
082KNW089	VMS 19, 20	CU
082KNW090	VMS 21	PB,ZN,CU
082KNW091	VMS 23	PB,ZN,MO
082KNW092	VMS 1	PB,ZN,AG
082KNW093	VMS 2	PB,ZN,MO,AG
082KNW096	MURRAY	CU,AU,PB,ZN
082KNW097	MIKE	PB,ZN,AG,AU
082KNW101	SILVER DOLLAR	AG,PB,ZN,AU,CU
082KNW105	MAR	MO,PB
082KNW123	HOMESTAKE	PB
082KNW127	GILLMAN	AU,AG,PB,ZN
082KNW131	MO,UNTAIN BOY (L. 2495)	AG,PB
082KNW136	IRON DOLLAR (L.7059)	PB,AU,AG,CU
082KNW147	CRAIG	AG,PB,AU
082KNW149	RAINY DAY	CU
082KNW189	ROYAL CANADIAN	AU
082KNW213	GREAT WESTERN (L.4503)	PB,AG
082KNW224	UPPER ARROW TALC	TC
082KNW226	SIDMO,UTH	LS,MB,BS
082KNW228	RATH	PB,ZN,AG
082KNW229	LEMAR	MO
082KNW230	POLLMAN CREEK	PB
082KNW231	STAU,BERT TRENCH	PB,ZN
082KNW233	HALCYON HOT SPRINGS	HS
082KNW234	HALFWAY RIVER HOTSPRINGS	HS
082KNW235	UPPER HALFWAY RIVER HOTSPRINGS	HS
082KSW099	PINGSTON	ZN,AG,PB,CU

* Abbreviations for commodities: AG – silver; AU - gold; BS - building stone; CU - copper; FE - iron; HS - hotspring; LS - limestone; MB - marble; MO - molybdenum; PB - lead; SB - antimony; TC - talc SN - tin; TC - talc; TE - tellurium; WO - tungsten; ZN - zinc

Source: British Columbia Ministry of Energy and Mines, MINFILE database available at: http://www.em.gov.bc.ca/Mining/Geolsurv/Minfile/

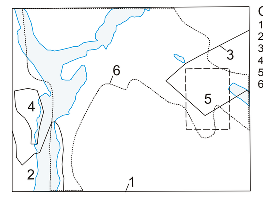

COMPILATION SOURCES:
1. Read and Wheeler (1976)
2. Reesor and Moore (1971)
3. Fyles and Eastwood (1962)
4. Kraft (2005)
5. Read et al. (2009)
6. Kraft (2011)

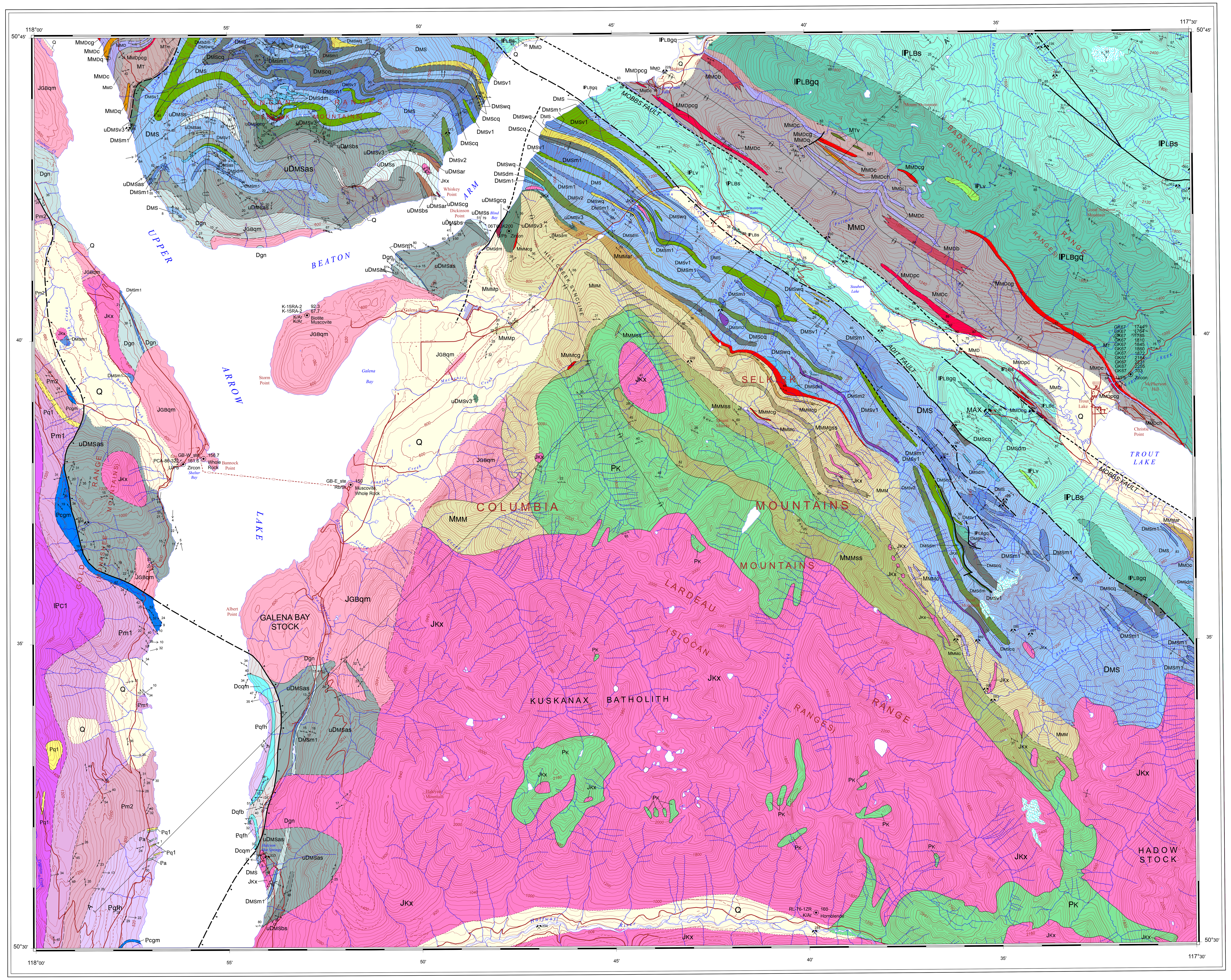

This publication is available from the Geological Survey of Canada Bookstore (http://gsc.nrcan.gc.ca/bookstore_e.php). It can also be downloaded free of charge from GeoPub (http://geopub.nrcan.gc.ca/).


LOCATION MAP

OPEN FILE 6574

GEOLOGY

BEATON

BRITISH COLUMBIA

Scale 1:50 000/Echelle 1/50 000

kilometres 1 0 1 2 3 4 kilomètres

Universal Transverse Mercator Projection
North American Datum 1983

Projection transverse universelle de Mercator
Système de référence géodésique nord-américain 1983

Compilers: J.L. Kraft, R.I. Thompson and P. Dhesi

Geology by: J.E. Reesor and J.M. Moore, 1963-65; J.O. Wheeler, 1965,67; P.B Read 1971-76; R.I. Thompson, 2002-04, Y. Lemieux, 2003-06; J.L. Kraft, 2004, 2006-08

Geological compilation by R.I. Thompson, 2002 and J. Kraft, 2010

Digital cartography by P. Dhesi, Geological Survey of Canada, Pacific Division

Any revisions or additional information known to the user would be welcomed by the Geological Survey of Canada

Digital base map from data compiled by Geomatics Canada, modified by the Geological Survey of Canada - Pacific Division

Magnetic declination 2011, 16°43' E, decreasing 13.3' annually

Elevations in metres above mean sea level
Contour interval 40 metres

Universal Transverse Mercator Grid
North American Datum 1983
Zone 11

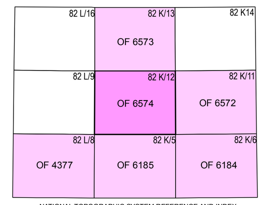

SYMBOLS

LEGEND

CENOZOIC

Q — *Unconsolidated sediments; glacial deposits, colluvium and alluvium; few if any outcrops*

MESOZOIC
JURASSIC
MIDDLE JURASSIC

JGBm — *Galena Bay Stock: muscovite-biotite quartz monzonite, granodiorite and monzogranite*

EARLY AND MIDDLE JURASSIC

JKx — *Kuskanax batholith: biotite or augite granodiorite; leuco-quartz monzonite; minor leucosyenite and leucogranite*

PALEOZOIC
PERMIAN
KASLO GROUP

PK — *Meta-basalt flows; minor volcanic breccia and tuff; local gabbro*

CARBONIFEROUS
UPPER MISSISSIPPIAN AND PENNSYLVANIAN
MILFORD GROUP (MCHARDY ASSEMBLAGE)

MMMss — *Banded tan, purple and white metasandstone, commonly rhythmically interbedded with thinner layers of black metasiltstone at centimetres- to decimetres-scale.*

MMM — *Medium grey to black phyllite and bedded or massive metasiltstone; argillaceous phyllite*

MMMgss — *Poorly sorted lithic metasandstone and grit; local conglomerate lenses*

MMMar — *Carbonaceous and siliceous argillite and metasiltstone weathering rusty brown and orange; pyritiferous*

MMMc — *Medium grey to black crystalline limestone or argillaceous limestone*

MMMcg — *Oligomict pebble orthoconglomerate with argillaceous clasts; grey quartzite*

DEVONIAN
UPPER DEVONIAN
MOUNT SPROAT ASSEMBLAGE

uDMSs — *Pelitic schist and phyllite: fine grained quartzose muscovite schist; black laminated metasiltstone and phyllite; garnet-hornblende-muscovite schist; biotite ± staurolite schist*

uDMSar — *Rusty weathering black siliceous argillite and argillaceous phyllite*

uDMScg — *Quartz pebble conglomerate*

uDMSas — *Amphibolitic schist: biotite-hornblende±muscovite schist; chorite-sericite schist; locally calcareous*

uDMSv3 — *Calc-alkaline metabasaltic rocks. Massive, fragmental or plagioclase porphyritic textures; commonly with buff carbonate pods*

uDMSbs — *Medium-grained grey biotite-quartz-plagioclase±hornblende schist*

uDMSgcg — *Pebble to cobble paraconglomerate with matrix of biotite-muscovite-chlorite-quartz schist; angular to rounded clasts of crystalline quartz and gritty quartzite*

MIDDLE AND (OR) UPPER DEVONIAN
MOUNT SPROAT ASSEMBLAGE

DMS — *Dark grey, carbonaceous quartz-mica schist to quartzite; grey and brown weathering, fine- to- medium-grained biotite-quartz-feldspar schist and micaceous (muscovite-biotite) quartzite; micaceous grey phyllite; phyllitic greenstone; marble*

Dgn — *Quartzofeldspathic and pelitic paragneiss with or without muscovite, garnet and sillimanite; minor white to grey marble and amphibolitic schist; metamorphosed equivalent of IPMSu?*

DMSm2 — *Differentially weathering light grey to white calc-silicate and marble with abundant cm-scale phyllitic laminations; local tremolite ± grossular ± diopside*

DMSv2 — *Metabasaltic rocks of island arc tholeiite affinity.*

DMSdm — *Buff weathering, fine-grained white or light grey dolomitic marble and (or) calcitic marble; massive and pervasively fractured*

DMSv1 — *Metabasaltic rocks of enriched mid-ocean ridge basalt, or rarely ocean island basalt, affinity*

DMSwq — *Fine-grained white quartzite to light grey phyllitic quartzite with light rusty orange weathering*

DMSm1 — *Medium to dark grey platy marble and argillaceous marble; limy carbonaceous phyllite*

DMScq — *Rusty-weathering, fine-grained carbonaceous quartzite to sooty quartz-mica schist; contorted quartz veinlets (sweats) define transposition foliation, S1*

CAMBRIAN TO DEVONIAN
LARDEAU GROUP
BROADVIEW FORMATION

IPLBgq — *Light green or grey phyllitic quartzite to subarkosic wacke with blue-quartz granules; millimetre-scale phyllitic partings define transposition foliation*

IPLBs — *Graphitic grey quartzose phyllite or schist with common blue-quartz granules; quartz veinlets along undulatory foliation*

FORMATION NOT ASSIGNED

IPLv — *Green phyllite and phyllitic greenstone*

COLUMBIA RIVER FAULT ZONE

ROCKS NORTHEAST OF MOBBS FAULT

CARBONIFEROUS
UPPER MISSISSIPPIAN AND PENNSYLVANIAN
MILFORD GROUP (DAVIS ASSEMBLAGE)

MMD — *Medium and dark grey silty phyllite with minor metasiltstone and metasandstone; locally pyritiferous*

MMDb — *Thinly bedded (<5 m) assemblage of limy phyllite, metasiltstone, metasandstone and limestone*

MMDch — *Grey to black bedded chert and cherty quartzite*

MMDq — *Massive grey quartzite, minor limy quartzite to limestone*

MMDc — *Medium grey to black crystalline limestone; locally fossiliferous*

MMDpcg — *Oligomict, locally polymict, pebble conglomerate with grey or green phyllite matrix*

MMDcg — *Oligomict pebble to cobble orthoconglomerate with quartzitic matrix*

LOWER OR MIDDLE MISSISSIPPIAN
THOMPSON ASSEMBLAGE

MT — *Greenish phyllitic grit with graded bedding; greenish grey phyllite; green and maroon banded phyllite and phyllitic argillite; grey crystalline limestone and limestone-dolostone breccia; sandy marble; rare, thin beds of whitish chert*

MTv — *Purple and dark green amygdaloidal metabasalt of enriched mid-ocean ridge basalt geochemical affinity*

MTm — *Medium to dark grey platy marble and argillaceous marble; limy carbonaceous phyllite; crinoid ossicles on ridge west-southwest of McCrae Peak*

CAMBRIAN TO DEVONIAN
LARDEAU GROUP
BROADVIEW FORMATION

IPLBgq — *Light green or grey phyllitic quartzite to subarkosic wacke with blue-quartz granules; millimetre-scale phyllitic partings define transposition foliation*

IPLBs — *Graphitic grey quartzose phyllite or schist with common blue-quartz granules; quartz veinlets along undulatory foliation*

IPLBc — *Medium or dark grey marble and argillaceous marble*

FORMATION NOT ASSIGNED

IPLv — *Green phyllite and phyllitic greenstone*

ROCKS WEST OF COLUMBIA RIVER FAULT ZONE

DEVONIAN

Dqfb — *Silver Creek Schist?: purplish biotite-feldspar-quartz schist with or without muscovite, garnet and sillimanite; minor white to grey marble and amphibolitic schist*

Dcqm — *Calcareous Quartzite Marker (Chase Quartzite?): pitted, calcareous quartzite; diopside-bearing calcareous quartzite; quartzite; marble*

PROTEROZOIC (TO PALEOZOIC?)

Pqfh — *Biotite-quartz-feldspar schist (with or without sillimanite, garnet); feldspar-quartz-hornblende schist (with or without biotite); amphibolite; calc-silicate gneiss; micaceous quartzite (map units M and F of Reesor and Moore, 1971)*

Pa — *Amphibolite; maybe interlayered with biotite schist and biotite-quartz-feldspar paragneiss (unit M8 of Reesor and Moore, 1971)*

Pcgm — *Marble (unit M7 of Reesor)*

Pm2 — *Biotite-quartz-feldspar paragneiss characterized by lenses and boudins of garnetiferous amphibolite; extensive lenticular masses of pegmatite*

Pm1 — *Biotite-quartz-feldspar paragneiss; sillimanite-biotite-garnet schist; garnet-quartz-feldspar gneiss*

Pq1 — *Quartzite (unit M3a of Reesor and Moore, 1971)*

PROTEROZOIC
PALEOPROTEROZOIC
MONASHEE COMPLEX

IPc1 — *Layered gneisses; biotite-quartz-feldspar gneiss (unit C1 of Reesor and Moore, 1971)*

DESCRIPTIVE NOTES

PHYSIOGRAPHY

TECTONOSTRATIGRAPHIC FRAMEWORK

INTRUSIVE ROCKS

STRUCTURAL GEOLOGY

FAULTING

ECONOMIC GEOLOGY

ACKNOWLEDGEMENTS

OPEN FILE
DOSSIER PUBLIC
6574
GEOLOGICAL SURVEY OF CANADA
COMMISSION GÉOLOGIQUE DU CANADA
2011

Open files are products that have not gone through the GSC formal publication process.

Les dossiers publics sont des produits qui n'ont pas été soumis au processus officiel de publication de la CGC.

Recommended citation:
Kraft, J.L., Thompson, R.I., and Dhesi, P., (compilers), 2011. Geology, Beaton, British Columbia; Geological Survey of Canada, Open File 6574, scale 1:50 000. doi: 10.4095/288009

Canada

Natural Resources Canada / Ressources naturelles Canada

GEOLOGICAL SURVEY OF CANADA — COMMISSION GÉOLOGIQUE DU CANADA

TGI 3 Cordillera / GC 3 Cordillère

MINERAL OCCURRENCE INDEX

MINFILE #	NAME	COMMODITY
082KNW006	TONAWANDA	CU
082KNW007	REVENUE	AG,PB,ZN,AU
082KNW008	SLASH	PB,ZN,AG
082KNW009	IXL (L.8710)	AG,PB,ZN,AU
082KNW010	GYP FR. (L.5691)	AG,PB,ZN
082KNW011	KOOTENAY (L.7247), KOOTENAY	AG,PB,AU,ZN,CU
082KNW012	RAVEN	AG,PB,ZN
082KNW013	FLORENCE (L.7051)	PB,AG
082KNW014	BLACK EAGLE (L.4735)	AG,PB,ZN
082KNW015	FIVE MILE	AG,PB,ZN,AU
082KNW016	GOLD BUG	AG,PB,ZN,AU
082KNW017	DARY	WO,SN
082KNW018	CANADIAN BOY	AG,PB,AU
082KNW019	RAMBLER	AG,PB,ZN,AU,CU
082KNW020	DAVEY (L.2452)	PB
082KNW021	COPPER QUEEN (L.6477)	AU,AG,PB
082KNW022	CALIFORNIA	PB
082KNW023	U AND I (L.7589)	AU,PB,ZN,CU
082KNW024	OKANAGAN (L.9127)	AU,AG,PB,ZN,CU
082KNW025	WINSLOW (L.8680)	AU,AG,PB,ZN,CU
082KNW026	TRIUNE (L.5681)	AG,AU,PB,ZN
082KNW027	SILVER CUP (L.768)	AG,PB,ZN,AU,CU
082KNW028	TOWSER (L.1565)	AG,AU,PB,ZN
082KNW029	MUSKATEER	FE,CU,NI,AU
082KNW030	TRUE FISSURE (L.1097)	AG,PB,ZN,AU,CU
082KNW031	BROADVIEW (L.1550)	PB,ZN,CU,AG,AU
082KNW032	OPHIR LADE	AU,AG,BI,CU,PB,TE
082KNW033	BADSHOT	AG,PB,ZN
082KNW034	BLACK PRINCE (L.755)	PB,AG,ZN
082KNW035	MOHICAN	AG,PB,AU,ZN
082KNW036	MOLLIE MAC	AG,PB,ZN,CU
082KNW037	WHITE QUAIL (L.4577)	PB,AG,ZN,AU
082KNW038	INDEX (L.3956)	AG,PB,ZN
082KNW039	SILVER CHIEF	PB,AG,AU,SN
082KNW050	SHEEP CREEK	AG,AU,PB,ZN
082KNW051	BANNOCKBURN (L.4450)	AG,PB,ZN,CU
082KNW052	SHEILA	AG,PB,ZN
082KNW053	RED ELEPHANT	AU,AG,CU
082KNW054	SUPERIOR (L.12849)	AU,AG,PB,ZN
082KNW055	RENO	BA,PB
082KNW056	ABBOTT (L.765)	AG,AU,PB,ZN
082KNW057	FRANCIS JEWELL (L.3467)	AG,PB,ZN,AU
082KNW058	CROMWELL (L.13046)	AU,AG,PB,CU,AB
082KNW060	BLUE BELL (L.5707)	AG,PB,ZN,AU
082KNW061	GREAT NORTHERN (L.1099)	AG,AU,PB,ZN,CU
082KNW062	ST. ELMO (L.4581)	AG,AU,PB,ZN,CU
082KNW080	SURPRISE (L.8661)	AG,PB,ZN,AU
082KNW086	IRENE (L.7464)	AG,PB,CU
082KNW095	BUTTE	AG,AU,PB,ZN
082KNW098	MORNING STAR	AG,AU,PB,CU
082KNW099	AJAX (L.4955)	AG,AU,PB,ZN,CU,MN
082KNW100	NETTIE L. (L.4954)	AG,AU,PB,ZN,CU
082KNW103	JEWEL	AG,AU,PB,ZN
082KNW104	HERCULES	AU,AG,ZN,PB
082KNW106	HIDDEN TREASURE (L.4718)	AG,PB,ZN
082KNW108	NEW ZONE COPPER	CU,NI
082KNW109	FREE COINAGE (L.1588)	AG,PB,ZN,AU
082KNW111	SILVER PLATE	PB,AG,AU
082KNW112	BONANZA	AU,AG,PB,ZN
082KNW113	SKYLINE	AU,AG,PB
082KNW114	FIDELITY	AU,AG,PB,ZN,SB
082KNW115	ARALLU	PB,ZN,AG
082KNW116	GOLDEN CROWN	AU,AG,PB
082KNW117	FOGGY DAY	AU,AG,PB,ZN
082KNW118	I.X.L.	AU,AG,PB,ZN
082KNW119	CHANCE	AG,AU,PB,ZN,CU
082KNW120	YUILL	AU,AG,PB,ZN
082KNW121	GUS	AU,AG,PB,ZN
082KNW122	YAMHILL	AU,CU
082KNW125	MOLY	AU,AG,PB,ZN
082KNW140	CRESCENT	AU,AG,PB
082KNW142	H.Y.M.	AG,PB
082KNW150	IQ	FS,BS
082KNW151	REVELSTOKE (L.4476)	PB,AG
082KNW153	NOBLE FIVE	AU,AG,PB,ZN,CU
082KNW154	COPPER MOUNTAIN	CU,AG,AU
082KNW155	MABLE	CU,PB
082KNW157	J.C. (L.7263)	PB
082KNW158	SHARON	AG,PB
082KNW159	SILVER BELT (L.5695)	AG,PB,ZN,AU
082KNW160	CANADIAN GIRL (L.4705)	PB,AG,ZN
082KNW165	ALICE (L.7440)	AU,AG
082KNW169	SILVER TRAY	AG,PB
082KNW177	WARD (L.3479)	AG,PB
082KNW178	GUS #3 & 4	PB,ZN,AU,AG
082KNW179	DEATH ON THE TRAIL (L.4986)	AG,PB
082KNW184	GERTRUDE (L.6804)	AU,AG,PB,ZN
082KNW209	ABRAHAMSON	AG,AU
082KNW211	JUMBO (L.7052)	AG,PB,AU
082KNW212	WAGNER	AG,PB,ZN,AU,CU,SN
082KNW214	ALPINE	AG,AU,PB,ZN
082KNW215	GALLANT BOY (L.14179)	AU,AG,PB,ZN
082KNW220	COPPER	CU,PB,AG,AU
082KNW221	CULKEEN	AU
082KNW222	SILVER CUP	TC,AB
082KNW225	PRINCESS MARIE (L.3475)	AG,ZN,PB
082KNW227	RAMBLER (L.6470)	PB

*Abbreviations for commodities: AB - asbestos; AG – silver; AU - gold; BA - barite; BI - bismuth; BS - building stone; CU - copper; FE - iron; FA - flagstone; MN - manganese; NI - nickel; PB - lead; SB - antimony SN - tin; TC - talc; TE - tellurium; W - tungsten; ZN - zinc

Source: British Columbia Ministry of Energy and Mines, MINFILE database available at: http://www.em.gov.bc.ca/Mining/Geolsurv/Minfile/

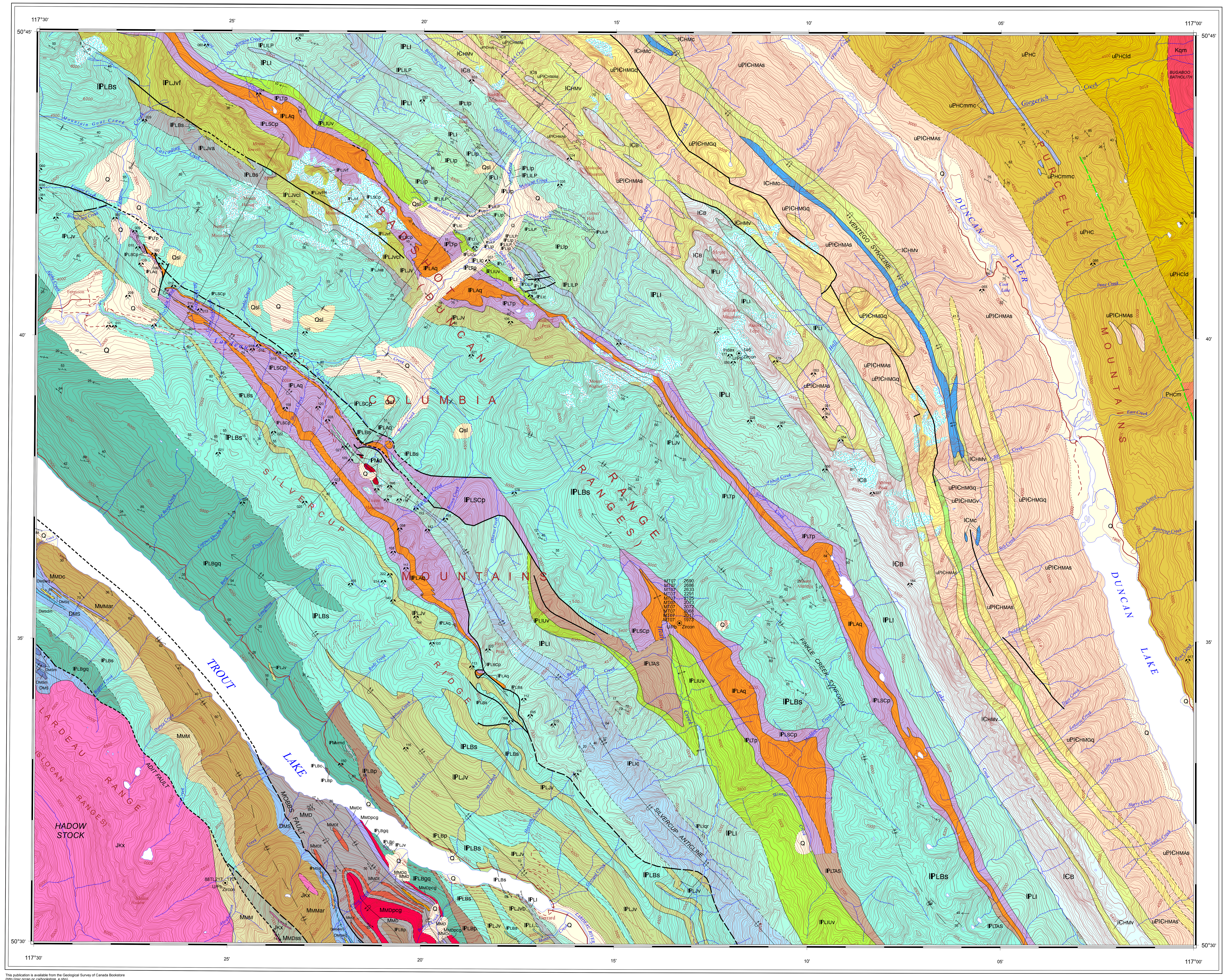


LOCATION MAP

Compilers: J.L. Kraft, R.I. Thompson and P. Dhesi

Geology by: J.T. Fyles, 1960-62; P.B. Read 1962-64, 1971-76; J.O. Wheeler, 1965, 67 J.L. Kraft, 2006-08

Geological compilation by R.I. Thompson, 2002 and J. Kraft, 2010

Digital cartography by P. Dhesi, Geological Survey of Canada, Pacific Division

Any revisions or additional information known to the user would be welcomed by the Geological Survey of Canada

OPEN FILE 6572

GEOLOGY

TROUT LAKE

BRITISH COLUMBIA

Scale 1:50 000/Echelle 1/50 000

kilometres 1 0 1 2 3 4 kilomètres

Universal Transverse Mercator Projection
North American Datum 1983

Projection transverse universelle de Mercator
Système de référence géodésique nord-américain 1983

Digital base map from data compiled by Geomatics Canada, modified by the Geological Survey of Canada - Pacific Division

Magnetic declination 2011, 16°34' E, decreasing 13.3' annually

*Elevations in feet above mean sea level
Contour interval 100 feet*

*Universal Transverse Mercator Grid
North American Datum 1983
Zone 11*

82 K/13	82 K/14	82 K/15
OF6573		
82 K/12 OF6574	82 K/11 OF6572	82 K/10
82 K/5 OF6185	82 K/6 OF6184	82 K/7 OF6183

NATIONAL TOPOGRAPHIC SYSTEM REFERENCE AND INDEX TO ADJOINING GEOLOGICAL SURVEY OF CANADA MAPS

LEGEND

CENOZOIC
QUATERNARY
PLEISTOCENE AND RECENT

- Q — *Unconsolidated sediments; glacial deposits, colluvium and alluvium; few if any outcrops*
- Qsl — *Slide*

MESOZOIC
CRETACEOUS

- Kgm — *Hornblende-biotite granodiorite*

JURASSIC
EARLY AND MIDDLE JURASSIC

- JKx — *Kuskanax Batholith: biotite or augite granodiorite; leuco-quartz monzonite; minor leucosyenite and leucogranite*

PALEOZOIC AND/OR MESOZOIC

- PMd — *Hornblende and pyroxene meta-gabbro or meta-diorite, amphibolite*
- PMvmd — *volcanic rocks*

CARBONIFEROUS
UPPER MISSISSIPPIAN AND PENNSYLVANIAN
MILFORD GROUP (MCHARDY ASSEMBLAGE)

- MMM — *Medium grey to black phyllite and bedded or massive metasiltstone; argillaceous phyllite*
- MMMar — *Carbonaceous and siliceous argillite and metasiltstone weathering rusty brown and orange; pyritiferous*

DEVONIAN
MIDDLE AND (OR) UPPER DEVONIAN
MOUNT SPROAT ASSEMBLAGE

- DMS — *Dark grey, carbonaceous quartz-mica schist to quartzite, grey and brown weathering, fine- to medium-grained biotite-quartz-feldspar schist and micaceous (muscovite-biotite) quartzite; micaceous grey phyllite; phyllitic greenstone; marble*
- DMSq — *Medium grey and white quartzite*
- DMSwq — *Fine-grained white quartzite to light grey phyllitic quartzite with light rusty orange weathering*
- DMSdm — *Buff weathering, fine-grained white or light grey dolomitic marble and (or) calcitic marble, often interbedded at centimetre-scale with phyllite*

CAMBRIAN TO DEVONIAN
LARDEAU GROUP
BROADVIEW FORMATION

- lPLBgq — *Light green or light grey phyllitic quartzite to subarkosic wacke with blue-quartz granules*
- lPLBs — *Graphitic grey quartzose phyllite and schist with common blue-quartz granules; quartz veinlets along undulatory foliation*

CARBONIFEROUS
UPPER MISSISSIPPIAN AND PENNSYLVANIAN
MILFORD GROUP (DAVIS ASSEMBLAGE)

- MMD — *Medium and dark grey silty phyllite. Minor metasiltstone and cream or brown metasandstone; locally pyritiferous*
- MMDss — *Tan and grey, rusty weathering metasandstone*
- MMDq — *Massive grey quartzite; limy quartzite to limestone*
- MMDc — *Grey to black bedded chert and cherty quartzite*
- MMDc — *Medium grey to black crystalline limestone; locally fossiliferous*
- MMDpcg — *Oligomict, locally polymict, pebble conglomerate with grey or green phyllite matrix*

CAMBRIAN TO DEVONIAN
LARDEAU GROUP
BROADVIEW FORMATION

- lPLBgq — *Light green or light grey phyllitic quartzite to subarkosic wacke with blue-quartz granules*
- lPLBs — *Graphitic grey quartzose phyllite and schist with common blue-quartz granules; quartz veinlets along undulatory foliation*

- lPLBp — *Dark grey slaty phyllite*
- lPLBc — *Medium or dark grey marble and argillaceous marble*

JOWETT FORMATION

- lPLJv — *Metamorphosed basaltic tuff and flows, mafic volcanic breccia and pillow basalt; green phyllite and limy green phyllite; phyllitic greenstone*
- lPLJva — *Agglomerate and breccia (Fyles and Eastwood, 1962)*
- lPLJvb — *Meta-andesite and metadiorite, sills and dykes (Read, 1973)*
- lPLJvf — *Mafic lavas (Fyles and Eastwood, 1962)*
- lPLJvcl — *Pyroclastic rocks, argillite and limestone (Fyles and Eastwood, 1962)*

TRIUNE, AJAX AND SHARON CREEK FORMATIONS

- lPLTAS — *undivided*
- lPLSCp — *SHARON CREEK FORMATION: dark grey to black siliceous phyllite and argillite*
- lPLAq — *AJAX FORMATION: massive grey quartzite commonly with extensive quartz veining*
- lPLTp — *TRIUNE FORMATION: grey to black siliceous phyllite and argillite*

INDEX FORMATION

- lPLI — *Grey and light green phyllite; dark grey slaty phyllite; minor phyllitic limestone and quartz grit*
- lPLIuv — *Altered volcanic rocks (Fyles and Eastwood, 1962)*
- lPLIc — *Medium to dark grey crystalline limestone and marble, phyllitic limestone and minor limy grey phyllite*
- lPLIp — *Green phyllite (Fyles and Eastwood, 1962; likely of non-volcanic protolith)*
- lPLILP — *LADE PEAK MEMBER: limestone and argillaceous limestone (Fyles and Eastwood, 1962)*

LOWER CAMBRIAN

- lCB — *BADSHOT FORMATION: grey and white crystalline limestone and marble*

HAMILL GROUP
MOHICAN FORMATION

- lCHMv — *Green phyllite, minor grey phyllite and limestone*
- lCHMc — *White to light grey limestone*

EDIACARAN AND/OR LOWER CAMBRIAN

- uPlCHMAs — *MARSH ADAMS FORMATION: white, grey and brown quartzite, phyllitic quartzite; minor grey and black phyllite*
- uPlCHMGq — *MOUNT GAINER FORMATION: pelite, white quartzite*
- uPlCHMGv — *Green phyllite, greenstone*

NEOPROTEROZOIC (HADRYNIAN)
WINDERMERE SUPERGROUP
HORSETHIEF CREEK GROUP

- uPHC — *Shale, argillite, sandstone and grit (and metamorphosed equivalents); limestone; conglomerate; volcanic and metavolcanic rocks; quartzite*
- uPHCm — *Marker Unit: Thinly bedded tan dolomitic siltstone (upper part) and competent, homogeneous green argillite or green micaceous quartzite (lower part)*
- uPHCmmc — *Limestone*
- uPHCld — *Lower Division: quartzofeldspathic sandstone and grit, grey slate, minor quartz pebble conglomerate, rare limestone*

SYMBOLS

REFERENCES

Bond, G. and Kominz, M.A.
1984: Construction of tectonic subsidence curves for the early Paleozoic miogeocline, southern Canadian Rocky Mountains: Implications for subsidence mechanisms, age of breakup and crustal thinning. Geological Society of America Bulletin, v. 95, pp. 155-173.

Colpron, M., Logan, J.M., and Mortensen, J.K.
2002: U-Pb zircon age constraint for late Neoproterozoic rifting and initiation of the lower Paleozoic passive margin of western Laurentia. Canadian Journal of Earth Sciences, v. 39, pp. 133-143.

Colpron, M., and Price, R.A.
1995: Tectonic significance of the Kootenay terrane, southeastern Canadian Cordillera: An alternative model. Geology, v. 23, pp. 25-28.

Emmens, N.W.
1926: Mineral Resources of the Lardeau and Trout Lake Mining Divisions of British Columbia. Canadian Mining Journal, January 1st, 1926, pp. 5-8.

Fyles, J.T., and Eastwood, G.E.P.
1962: Geology of the Ferguson area, British Columbia. British Columbia Department of Mines and Petroleum Resources, Bulletin 45, 97 pp.

Kraft, J.L., Thompson, R.I., and Dhesi, P., (compilers)
2011: Geology, Beaton, British Columbia; Geological Survey of Canada, Open File 6574, scale 1:50 000.

Klepacki, D.W.
1985: Stratigraphy and structural geology of the Goat Range area, southeastern British Columbia. Unpublished Ph.D. thesis, Massachusetts Institute of Technology, Cambridge, Mass., 268 pp.

Lawley, C.J.M.
2009: Age, Geochemistry, and Fluid Characteristics of the MAX Porphyry Mo Deposit, Southeast British Columbia. Unpublished M.Sc. thesis, University of Alberta, Edmonton, AB, 166 pp.

Read, P. B.
1973: Petrology and structure of Poplar Creek map-area, British Columbia. Geological Survey of Canada, Bulletin 193, 144pp.

Read, P.B. and Wheeler, J.O.
1976: Geology of Lardeau W/2 (82K W/2). Geological Survey of Canada, Open File Map 432, 1: 125,000.

Read, P.B., Psutka, J.F., Fyles, J.T., and MacLeod, R.F.
2009: Geology, MAX Molybdenum Mine area (NTS 82K/12), British Columbia; Geological Survey of Canada, Open File 6215, 2 sheets, 1:10 000 scale, and 1 report, 21 pages.

Roback, R.C.
1993: Late Paleozoic to middle Mesozoic tectonic evolution of the Kootenay Arc. Unpublished Ph.D. thesis, University of Texas at Austin, TX.

Ross, G.M.
1991: Tectonic setting of the Windermere Supergroup revisited. Geology, v. 19, pp.1125-1128.

Smith, M.T.
1990: Stratigraphy, structural, and U-Pb geochronological investigation of lower Paleozoic eugeoclinal strata in the Kootenay Arc, NE Washington and SE British Columbia. Unpublished Ph.D. thesis, University of Arizona, Tucson, AZ.

Smith, M.T. and Gehrels, G.E.
1990: Geology of the Lardeau Group east of Trout Lake, southeastern British Columbia (Silvercup Ridge, Mount Wagner and Mount Aldridge areas); British Columbia Ministry of Energy, Mines and Petroleum Resources, Open File Map 1990-24, 1:25 000.

Smith, M.T., and Gehrels, G.E.
1991: Detrital zircon geochronology of Upper Proterozoic to lower Paleozoic continental margin strata of the Kootenay Arc: implications for the early Paleozoic tectonic development of the eastern Canadian Cordillera. Canadian Journal of Earth Sciences, v. 28, pp. 1271-1284.

Smith, M.T., and Gehrels, G.E.
1992: Structural geology of the Lardeau Group near Trout Lake, British Columbia: implications for the structural evolution of the Kootenay Arc. Canadian Journal of Earth Sciences, v. 29, pp. 1305-1319.

Canadian Geochronology Knowledgebase: http://gdr.nrcan.gc.ca/geochron/index_e.php

DESCRIPTIVE NOTES

The Trout Lake map area (NTS 82K/11) in southeastern British Columbia is underlain by a considerable section of weakly metamorphosed, and locally strongly deformed, continental margin sedimentary strata ranging in age from Neoproterozoic east of the Duncan River to Mississippian west of Trout Lake. The map area lies within the northern Kootenay Arc – an arcuate structural belt characterized by Jurassic-Cretaceous deformation and metamorphism along the transition from Cordilleran foreland to hinterland. All of the map area is mountainous, and much of it is accessible by trail or helicopter only. Excepting a small segment of the Purcell Mountains east of Duncan River, the map area lies within the Selkirk Mountains, which are subdivided into the Badshot and Lardeau ranges east and west of Trout Lake or the Lardeau River, respectively. The nearest incorporated community is Nakusp (76 km), although accommodation and a general store with gasoline can be found at the head of Trout Lake in the homonymous community.

STRATIGRAPHY

The Neoproterozoic (Hadrynian) Horsethief Creek Group (Windermere Supergroup) and Lower Cambrian Hamill Group, which underlie the eastern third of Trout Lake map area, are dominantly psammite and semipelite with rift related mafic volcanic rocks. They are interpreted as continental rift sequences recording opening of the Cordilleran margin (Bond and Kominz, 1984; Ross, 1991; Colpron et al., 2002). The Hamill Group is correlative with other arenaceous Lower Cambrian strata across the southern Canadian Cordillera, such as the Gog Group. In the Trout Lake map area, the Hamill Group comprises the predominantly quartz-arenaceous Mount Gainer and Marsh-Adams formations overlain by phyllite and marble of the Mohican Formation (Fyles and Eastwood, 1962). The overlying Badshot Formation, which represents an extensive Lower Cambrian carbonate platform, is a regionally important stratigraphic marker that forms impressive peaks in the Badshot Range. East of Trout Lake, the Lardeau shear zone juxtaposes the lower Paleozoic Lardeau Group against Badshot Formation marble (Smith and Gehrels, 1992), however the two are considered to be stratigraphically linked (Smith and Gehrels, 1991; Colpron and Price, 1995). The Lardeau Group consists of carbonaceous metasediments, alkaline mafic volcanic rocks, quartzite, marble and grit that were placed into six formations by Fyles and Eastwood (1962). Depositionally overlying the Lardeau Group west of Trout Lake is the Middle to Upper Devonian Mount Sproat assemblage (new term; see Kraft et al., 2011 for more information). A small section of the Mount Sproat assemblage (MSA) occurs on this map sheet southwest of Trout Lake. The lithological and structural style of the MSA in the Trout Lake map area are broadly similar to those of the Lardeau Group, but the assemblage is distinguished by its unique internal stratigraphy and certain distinctive rock types. MSA in the Trout Lake map area is mainly carbonaceous phyllite with quartzite, marble and rare chert. To the west, the MSA contains arc related mafic volcanic rocks of Late Devonian age (Kraft et al., 2011).

An angular unconformity separates the MSA from overlying conglomerate, fossiliferous limestone and fine-grained siliciclastic rocks of the Upper Mississippian Milford Group. The Milford Group near Trout Lake is divided into two lithologically distinct assemblages using the nomenclature of Klepacki (1985). The Davis Assemblage comprises silty grey phyllite with minor chert, limestone and sandstone. Basal conglomerate of the Davis Assemblage east of the Mobbs fault contains clasts and matrix compositionally similar to underlying Broadview and Jowett formations. The McHardy Assemblage is predominantly rusty weathering, black siliceous argillite and phyllite. It unconformably overlies the Mount Sproat assemblage to the northwest (Kraft et al., 2011).

INTRUSIVE ROCKS

Undated, weakly metamorphosed lenses, sheets and small stocks of coarse grained diorite or gabbro intrude the Lardeau Group along the crest of the Silvercup anticline on the east side of Silvercup Ridge (Smith, 1990). Pods of pyroxenite, serpentinite and talc schist occur on the east slope of Silvercup Ridge (not shown on map; Smith, 1990). Isoclinally folded, recrystallized, albitized felsic dykes of unknown age intrude the upper Index Formation near Mount Wagner (Smith, 1990). The Middle Jurassic Hadow stock west of Trout Lake is a satellite of the Kuskanax Batholith, which lies immediately to the west. The Hadow stock comprises biotite or hornblende granodiorite to quartz monzonite. A sliver of hornblende-biotite granodiorite of the Cretaceous Bugaboo Batholith enters the northeast corner of the map area.

STRUCTURAL GEOLOGY

Devonian and older strata in the Selkirk Mountains were strongly deformed at greenschist-facies to form transposition foliation, S1, prior to deposition of Viséan (mid-Mississippian) Milford Group strata. Rootless F1 folds and quartz veinlets along S1 occur in the Lardeau Group and MSA. Map-scale F1 folds are not known in the Trout Lake map area. Regional D2 deformation synchronous with the Early to Middle Jurassic Kuskanax Batholith (Read, 1973; Roback 1993) was approximately coaxial with D1. Jurassic F2 folds are upright to inclined and plunge gently northwest. F2 folds, of which the Silvercup Anticline is the most conspicuous, control the structural grain of the area, and repeat and thicken Lardeau Group strata. F2 folds outlined by Davis Assemblage strata are parasitic to the Silvercup Anticline and are truncated by the Mobbs fault. Belts of the McHardy and Davis assemblages are juxtaposed by the Adit and Mobbs faults, which have been extended from Beaton (NTS 82K/12) and Poplar Creek (NTS 82K/06) map areas, respectively. The Adit fault truncates the ca. 80 Ma MAX Molybdenum Mine deposit to the northwest (Read et al., 2009; Lawley, 2009). To the south, the Adit fault may correspond to the Emmens fault of Roback (1993).

ECONOMIC GEOLOGY

Early 20th century metal exploration and production of the Ferguson camp northeast of Trout Lake was derived from a number of small, high-grade Cu, Pb, Zn, Ag and Au vein hosted deposits concentrated in two northwest trending belts parallel to the structural grain (Emmens, 1926). One belt follows the axis of the Silvercup Anticline from Silvercup Ridge to Broadview Creek. The other belt of mineralization occurs near the Badshot/Index Formation contact in carbonaceous sediments and carbonate. Placer gold mining operations in watercourses of the Badshot Range were also significant early in the 20th century.

ACKNOWLEDGMENTS

This map is largely a compilation of exceptional mapping by J.T. Fyles, P.B. Read, and J.O. Wheeler. Their reconnaissance, and locally detailed mapping provided the geological framework upon which new mapping and interpretations are founded. Support from a variety of sources at the Geological Survey of Canada through the Targeted Geoscience Initiative 3 - Cordillera program enabled this mapping and compilation. R.G. Anderson especially is thanked for his unfailing support in production of these maps. Kraft is grateful for supervisory support from P. Erdmer at University of Alberta during the course of this project. Kraft also wishes to thank Y. Lemieux for introducing him to Cordilleran geology in the Upper Arrow Lake area. Excellent field assistance to Kraft was provided by B. Jablonski, R. Tapping, and K. Laird. This map benefited from careful review by A. Okulitch.

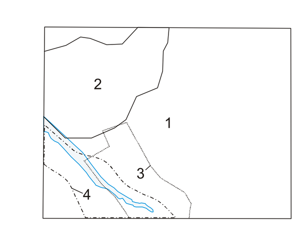

COMPILATION SOURCES:
1. Read and Wheeler (1976)
2. Fyles and Eastwood (1962)
3. Read (1973)
4. Kraft (2011)

OPEN FILE
DOSSIER PUBLIC
6572
GEOLOGICAL SURVEY OF CANADA
COMMISSION GÉOLOGIQUE DU CANADA
2011

Open files are products that have not gone through the GSC formal publication process.

Les dossiers publics sont des produits qui n'ont pas été soumis au processus officiel de publication de la CGC.

Recommended citation:
Kraft, J.L., Thompson, R.I., and Dhesi, P., (compilers), 2011. Geology, Trout Lake, British Columbia; Geological Survey of Canada, Open File 6572, scale 1:50 000. doi:10.4095/288063

Canada

Natural Resources Canada / Ressources naturelles Canada

GEOLOGICAL SURVEY OF CANADA / COMMISSION GÉOLOGIQUE DU CANADA

TGI3 Cordillera / GC3 Cordillère

REFERENCES

Read, P.B., and Wheeler, J.O.
1976: Geology, Lardeau west-half, British Columbia (82K W/2); Geological Survey of Canada, Open File Map 432, 1:250,000.

Sears, J.W.
1979: Tectonic contrasts between the Columbian orogen, Albert Peak area, western Selkirk Mountains, British Columbia; PhD thesis, Queens University, Ontario, Canada, 154 p. (geological maps and cross-sections in pocket).

Thompson, R.I.
1978: Geology of the Akolkolex River area; B.C. Ministry of Energy, Mines and Petroleum Resources, Bulletin 60, 77 p.

Canadian Geochronology Knowledgebase: http://gdr.nrcan.gc.ca/geochron/index_e.php

MINERAL OCCURRENCE INDEX

MINFILE #	NAME	COMMODITY
082KNW001	HOMESTEAD	AG,PB,AU
082KNW041	MOHAWK (L.4571)	AG,ZN,PB
082KNW042	MOSCOW (L.4500)	AG,PB,ZN
082KNW043	EXCISE	AG,PB,ZN
082KNW044	ECLIPSE (L.5170)	AG,PB,ZN
082KNW045	SPIDER (L.15752)	AG,PB,ZN
082KNW046	ST. JOE (L.5675)	PB
082KNW047	CONMORE (L.5677)	PB,ZN,AG
082KNW048	SANDY (L.8719)	AG,PB,ZN
082KNW049	BARCLAY	PB
082KNW063	RED HORSE (L.8718)	AG,AU,PB
082KNW064	MERIDIAN	AU,AG
082KNW065	CRITERION-OYSTER	AU,AG
082KNW066	EVA (L.5172)	AU,AG,PB
082KNW068	WIGWAM	ZN,PB,AG
082KNW069	TEDDY GLACIER	AG,PB,ZN
082KNW070	VIMY RIDGE	AG,PB,ZN
082KNW071	LEAD STAR	AG,PB,ZN
082KNW072	BURNIERE (L.4198)	AU,AG,PB
082KNW074	MORNING STAR	AG,PB,ZN
082KNW075	ASBESTOS	AB,TC,MT
082KNW076	GOLDFINCH (L.5654)	AU,AG,PB
082KNW077	MAMMOTH (L.6473)	AG,PB,AU
082KNW078	BIG SHOWING	AG,PB,ZN
082KNW101	SILVER DOLLAR	AG,PB,ZN
082KNW124	ALMA	AG,PB,ZN
082KNW126	DEL REY (L.10373)	AG,PB,AU
082KNW127	GILLMAN	AU,AG,PB
082KNW129	WIDE WEST (L.6453)	PB,CU,AU
082KNW130	BLACK BEAR (L.5086)	PB,ZN
082KNW131	MOUNTAIN BOY (L. 2495)	AG,PB
082KNW132	AGNES	AU,AG,CU
082KNW133	SUNSET (L.1970)	AG,PB,ZN
082KNW137	HUNTER (L.4495)	AG,PB,ZN
082KNW138	NELSON	AU,AG
082KNW139	SCOUT	AG,PB,ZN
082KNW143	CHOLLA (L.5399)	AU,AG
082KNW146	PIPESTEM (L.15779)	AG,PB,ZN
082KNW148	KITSAP (L.3500)	AG,PB,ZN
082KNW161	LEXINGTON (L.3088)	AG,PB
082KNW162	NELLIE (L.5670)	PB,AG,ZN
082KNW163	BANNER (L.3085)	AG,PB,ZN
082KNW168	KINGSTON (L.6558)	AU
082KNW174	BRUNSWICK (L.4354)	AU
082KNW180	HARVEY (L.5169)	AG,AU,PB
082KNW185	TRILBY	PB,AG
082KNW186	IMPERIAL (L.4778)	AU,AG,PB
082KNW187	LUCKY JACK (L.8715)	AU,AG
082KNW190	LARDEAU-GOLDSMITH	AG,PB
082KNW195	LOST CUP (L.1870)	AG,PB
082KNW196	PAYMASTER	AG,PB,ZN
082KNW197	DAFFODIL	PB,AG
082KNW198	UNITED VICTORY	WO,MO
082KNW199	YELLOWJACKET	PB,CU
082KNW202	ROYAL	AG,PB
082KNW216	ADVENTURE	AU
082KNW232	KELLIE CREEK	WO,MO
082LNE046	GHOST PEAK	ZN,PB

* Abbreviations for commodities: AG – silver; AU - gold; CU - copper; MO - molybdenum; PB - lead; TC - talc WO - tungsten; ZN - zinc

Source: British Columbia Ministry of Energy and Mines, MINFILE database available at: http://www.em.gov.bc.ca/Mining/Geolsurv/Minfile/

ACKNOWLEDGMENTS

This map is largely a compilation of geological mapping by P.B. Read, J.O. Wheeler, and R.I. Thompson. Recent mapping by Kraft in the southwest portion of Camborne map area served to bring out local detail and subtleties of the framework that had been established prior. Contacts on the north flank of McCrae Peak are primarily those of Thompson. Support from a variety of sources at the Geological Survey of Canada through the Targeted Geoscience Initiative 3 - Cordillera program enabled the mapping and compilation. R.G. Anderson especially is thanked for his unfailing support in production of these maps. Kraft is grateful for supervisory support from P. Erdmer at University of Alberta during the course of this project. Excellent field assistance to Kraft was provided by B. Jablonski, R. Tapping, and L. Laird. This map has benefited from careful review by A. Okulitch.

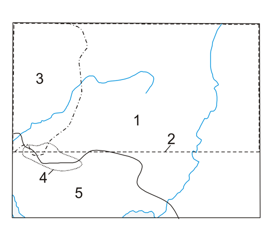

COMPILATION SOURCES:
1. Read and Wheeler (1976)
2. Sears (1979)
3. Thompson (1978)
4. Thompson (2007)
5. Kraft (2011)

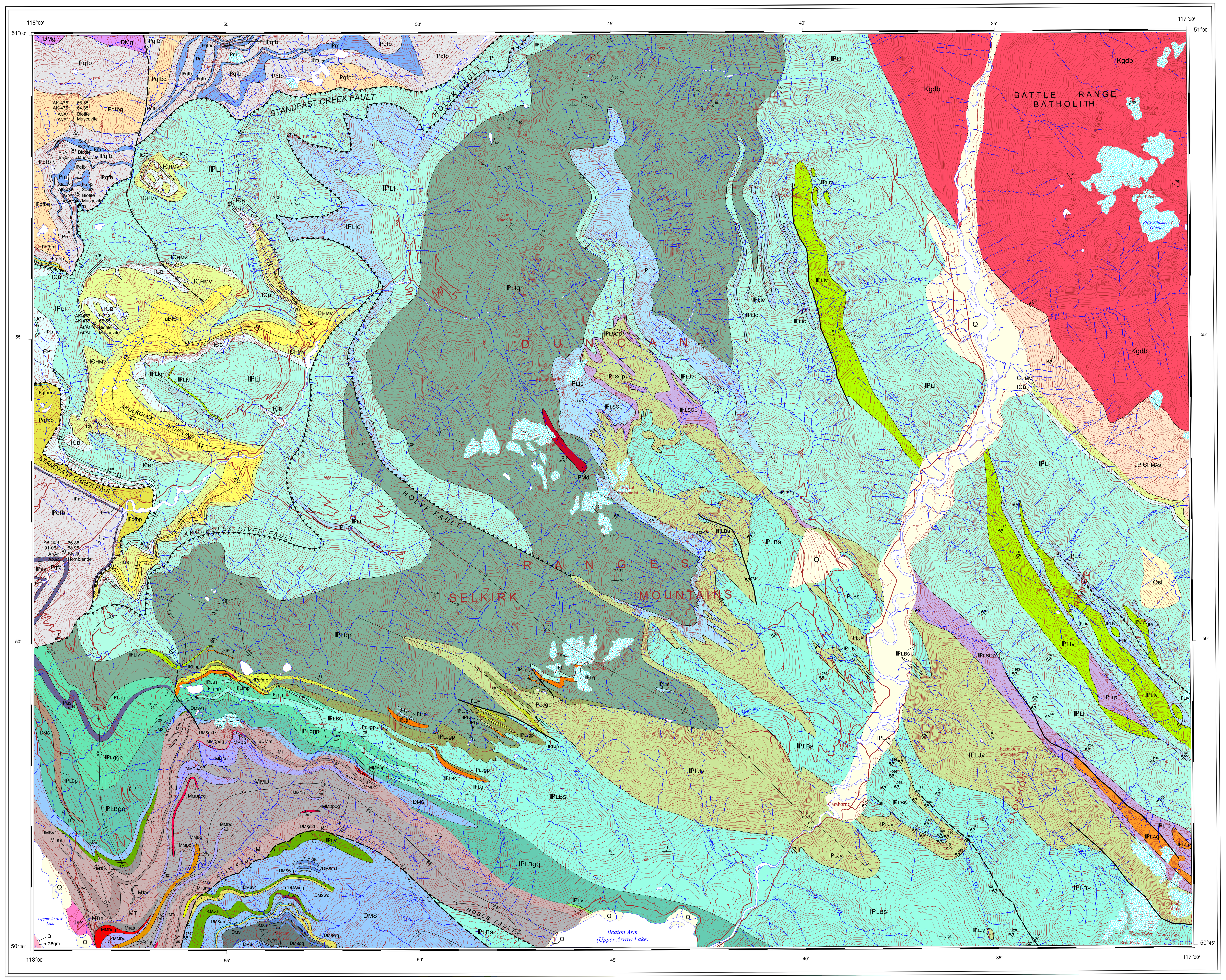

LOCATION MAP

This publication is available from the Geological Survey of Canada Bookstore (http://gsc.nrcan.gc.ca/bookstore_e.php). It can also be downloaded free of charge from GeoPub (http://geopub.nrcan.gc.ca/).

OPEN FILE 6573

GEOLOGY

CAMBORNE

BRITISH COLUMBIA

Scale 1:50 000/Échelle 1/50 000

Kilometres 1 0 1 2 3 4 kilomètres

Universal Transverse Mercator Projection / North American Datum 1983 — Projection transverse universelle de Mercator / Système de référence géodésique nord-américain 1983

Compilers: J.L. Kraft, R.I. Thompson and P. Dhesi

Geology by: J.O. Wheeler, 1965, 67; R.I. Thompson, 1969-70, 2006-07; P.B. Read 1971-76; J.L. Kraft, 2006-08

Geological compilation by R.I. Thompson, 2002 and J.L. Kraft, 2010

Digital cartography by P. Dhesi, Geological Survey of Canada, Pacific Division

Any revisions or additional information known to the user would be welcomed by the Geological Survey of Canada

Digital base map from data compiled by Geomatics Canada, modified by the Geological Survey of Canada - Pacific Division

Magnetic declination 2011, 15°48'E, decreasing 13.5' annually

Elevations in feet above mean sea level
Contour interval 20 metres

Universal Transverse Mercator Grid
North American Datum 1983
Zone 11

82 M/1	82 N/4	82 N/3
82 L/16	82 K/13 OF 6573	82 K/14
82 L/9	82 K/12 OF 6574	82 K/11 OF 6572

NATIONAL TOPOGRAPHIC SYSTEM REFERENCE AND INDEX TO ADJOINING GEOLOGICAL SURVEY OF CANADA MAPS

LEGEND

ROCKS IN FOOTWALL OF STANDFAST CREEK FAULT

PALEOZOIC
DEVONIAN OR CARBONIFEROUS
LATE DEVONIAN OR EARLY MISSISSIPPIAN

- **DMg** — *foliated granitoid rocks*

PALEOZOIC

- **Pqfb** — *Grey and brown garnet-biotite schist; micaceous quartzite; minor amphibolite (Thompson, 1978)*
- **Pm** — *Grey marble*
- **Pqfbp** — *Grey and brown schist; black phyllite; minor limestone (Thompson, 1978)*
- **Pqfbm** — *marble*
- **lPas** — *Medium to coarse grained amphibolite and calcareous amphibolite; amphibolitic schist with or without biotite; minor marble*
- **Pqfbq** — *Grey, white, and brown quartzite and micaceous quartzite; minor schist and amphibolite (Thompson, 1978)*

STANDFAST CREEK FAULT

CENOZOIC

- **Q** — *Unconsolidated sediments; glacial deposits, colluvium and alluvium; few if any outcrops*
- **Qsl** — *Slide*

MESOZOIC
CRETACEOUS

- **Kgdb** — *Pyritiferous alaskite*

JURASSIC
MIDDLE JURASSIC

- **JGBqm** — *Galena Bay Stock: muscovite-biotite quartz monzonite, granodiorite and monzogranite*

EARLY AND MIDDLE JURASSIC

- **JKx** — *Kuskanax Batholith: biotite or augite granodiorite; leuco-quartz monzonite; minor leucosyenite and leucogranite*

PALEOZOIC OR MESOZOIC

- **PMd** — *Hornblende and pyroxene meta-gabbro or meta-diorite; amphibolite*

UPPER MISSISSIPPIAN AND PENNSYLVANIAN
MILFORD GROUP (DAVIS ASSEMBLAGE)

- **MMD** — *Medium and dark grey silty phyllite with minor metasiltstone and metasandstone; locally pyritiferous*
- **MMDc** — *Medium grey to black crystalline limestone; locally fossiliferous*
- **MMDq** — *Massive grey quartzite, minor limy quartzite to limestone*
- **MMDpcg** — *Oligomict, locally polymict, pebble conglomerate with grey or green phyllitic matrix*
- **MMDcg** — *Oligomict pebble to cobble orthoconglomerate with quartzitic matrix*

LOWER OR MIDDLE MISSISSIPPIAN
THOMPSON ASSEMBLAGE

- **MT** — *Calcareous green to grey phyllite, limy grey quartzite and conglomeratic phyllite (at Northeast Arm of Upper Arrow Lake); grey phyllite, conglomeratic quartzite, sandy limestone, crinoidal limestone, talc schist (near Mt. McCrae); rusty-weathering, argillaceous biotite schist, amphibole-biotite schist, metaconglomerate and tremolite-bearing light grey marble (near mouth of Crawford Creek)*
- **MTum** — *Talc-serpentine schist; waxy green talc-bearing phyllite*
- **MTm** — *Medium to dark grey platy marble and argillaceous marble; limy carbonaceous phyllite; crinoid ossicles on ridge west-southwest of McCrae Peak*
- **MTas** — *Amphibolitic schist: biotite-hornblende±muscovite schist; muscovite schist with coarse sprays of black amphibole; locally calcareous*
- **MTcg** — *Oligomict and polymict pebble paraconglomerate with quartzose matrix*

MIDDLE AND (OR) UPPER DEVONIAN
MOUNT SPROAT ASSEMBLAGE

- **DMS** — *Dark grey, carbonaceous quartz-mica schist to quartzite; grey and brown weathering, fine- to- medium-grained biotite-quartz-feldspar schist and micaceous (muscovite-biotite) quartzite; micaceous grey phyllite; phyllitic greenstone; marble*
- **DMSv1** — *Metabasaltic rocks of enriched mid-ocean ridge basalt, or rarely ocean island basalt, affinity*
- **uDMSgcg** — *Pebble to cobble paraconglomerate with matrix of biotite-muscovite-chlorite-quartz schist; angular to rounded clasts of crystalline quartz and gritty quartzite*
- **DMSdm** — *Buff weathering, fine-grained white or light grey dolomitic marble and (or) calcitic marble; massive and pervasively fractured*
- **DMSwq** — *Fine-grained white quartzite to light grey phyllitic quartzite with light rusty orange weathering*
- **DMSm1** — *Medium to dark grey platy marble and argillaceous marble; limy carbonaceous phyllite; banded grey to white coarse crystalline marble to calc-silicate gneiss near Upper Arrow Lake*
- **DMScq** — *Rusty-weathering, fine-grained carbonaceous quartzite to sooty quartz-mica schist; contorted quartz veinlets (sweats) define transposition foliation, S1*

ROCKS IN THE McCRAE PEAK AREA

CAMBRIAN TO DEVONIAN
LARDEAU GROUP
BROADVIEW FORMATION

- **lPLBgq** — *Tan to light grey weathering micaceous quartzite and gritty quartzite with characterisitic phyllitic or micaceous partings; minor grey and green phyllite and gritty phyllite*
- **lPLBp** — *Coarse grained, rusty weathering garnet-biotite-muscovite schist with or without staurolite; minor quartzite and garnetiferous quartzite*

FORMATION NOT ASSIGNED

- **lPLggp** — *Interlayered green and grey phyllite; occasional layers of micaceous and (or) gritty quartzite, rusty weathering ferroan marble and beige to tan weathering phyllite*
- **lPLas** — *Medium to coarse grained amphibolite and calcareous amphibolite; amphibolitic schist with or without biotite; minor marble*
- **lPLgq** — *Grey to dark grey weathering, gritty quartzite marker approximately 20 m thick and forming the structurally upper boundary to the barite-chert-phyllite succession at McCrae Peak*
- **lPLbcp** — *Barite-chert (exhalite?)-phyllite succession (<30 m thick): beige to light rusty brown weathering light grey stratiform barite and chert; gradationally underlain by black siliceous phyllite*
- **lPLfmp** — *Rusty-brown weathering ferroan marble interlayered with tan, grey and green sericitic phyllite and quartzose phyllite*

ROCKS NORTH AND EAST OF McCRAE PEAK AREA

CAMBRIAN TO DEVONIAN
LARDEAU GROUP
BROADVIEW FORMATION

- **lPLBgq** — *Light green or grey phyllitic quartzite to subarkosic wacke with blue-quartz granules*
- **lPLBs** — *Graphitic grey quartzose phyllite or schist with common blue-quartz granules; quartz veinlets along undulatory foliation*
- **lPLBc** — *Medium or dark grey marble and argillaceous marble*
- **lPLv** — *Green phyllite and phyllitic greenstone*

JOWETT FORMATION

- **lPLJv** — *Metamorphosed basaltic tuff and flows, mafic volcanic breccia and pillow basalt; green phyllite and limy green phyllite; phyllitic greenstone*
- **lPLJgp** — *Green phyllite*
- **lPLJp** — *Pale greenish grey phyllite with rusty brown weathered surfaces*

TRIUNE, AJAX AND SHARON CREEK FORMATIONS

- **lPLSCp** — *SHARON CREEK FORMATION: dark grey to black siliceous phyllite and argillite*
- **lPLAq** — *AJAX FORMATION: massive grey quartzite commonly with extensive quartz veining*
- **lPLTp** — *TRIUNE FORMATION: grey to black siliceous phyllite and argillite*

INDEX FORMATION

- **lPLI** — *Grey and light green phyllite; Dark grey slaty phyllite; minor phyllitic limestone and quartz grit*
- **lPLIqr** — *Intercalated quartzofeldspathic grit and grey and green phyllite with or without quartz granules; quartz mica schist; micaceous quartzite*
- **lPLg** — *Light grey to white gritty quartzite; micaceous quartz grit*
- **lPLIc** — *Medium to dark grey crystalline limestone and marble; phyllitic limestone and minor limy grey phyllite*
- **lPLIv** — *Green phyllite, limy green phyllite, greenstone*

LOWER CAMBRIAN

- **lЄB** — *BADSHOT FORMATION: grey and white crystalline limestone and marble*

HAMILL GROUP

- **lЄHMv** — *MOHICAN FORMATION: green phyllite, minor grey phyllite and limestone*

EDIACARAN AND/OR LOWER CAMBRIAN

- **uPlЄH** — *White, pure green, and grey quartzite and micaceous quartzite; dark slate, phyllite, and mica schist; some pebbly and feldspathic quartzite*
- **uPlЄHMAs** — *MARSH ADAMS FORMATION: white, grey and brown quartzite, phyllitic quartzite; minor grey and black phyllite*

SYMBOLS

- Foliation (unclassified): inclined, horizontal, vertical
- Foliation (1st generation): inclined, horizontal, vertical
- Bedding: inclined, horizontal, vertical, overturned
- Fold: axis plane (unknown generation) s-verging, z-verging
- Cleavage
- Mineral lineation
- Geochronology sample (http://gdr.nrcan.gc.ca/geochron/index_e.php): database no., isotopic sys., age, mineral
- Mineral Occurrence
- Geological boundary: defined, approximate, assumed
- Geological boundary: arbitrary
- Quaternary limit
- Fault, reverse (teeth indicate upthrust side): defined, approximate, assumed
- Fault, normal (balls indicate downthrow side): defined, approximate
- Fault, normal (balls indicate downthrow side): assumed
- Fault, sinistral: approximate
- Fault, unclassified: defined, approximate, assumed
- Anticline (unknown generation): recumbent
- Syncline (unknown generation): recumbent
- Anticline (2nd generation): upright, overturned, plunging
- Syncline (2nd generation): upright, overturned, plunging
- Anticline (3rd generation): recumbent
- Syncline (3rd generation): recumbent

OPEN FILE / DOSSIER PUBLIC
6573
GEOLOGICAL SURVEY OF CANADA / COMMISSION GÉOLOGIQUE DU CANADA
2011

Open files are products that have not gone through the GSC formal publication process.

Les dossiers publics sont des produits qui n'ont pas été soumis au processus officiel de publication de la CGC.

Recommended citation:
Kraft, J.L., Thompson, R.I., and Dhesi, P. (compilers), 2011. Geology, Camborne, British Columbia; Geological Survey of Canada, Open File 6573, scale 1:50 000. doi: 10.4095/288064

Canada

Appendix 2: Stratigraphic description and laboratory data

A2-1: Mount Sproat assemblage description

The stratigraphy of the MSA described below comes primarily from strike-normal transects between Galena Pass and Mount Sproat, alpine exposures at Trout Mountain and a ridge traverse between Mobbs and Tenderfoot creeks. Map unit abbreviations correspond to appended Open File maps by Kraft et al. (2011a; 2011b; 2011c).

Carbonaceous member

Distribution

The Carbonaceous member occurs in two belts of polydeformed, greenschist-facies strata that are separated by the post-80 Ma Adit fault (Read et al., 2009). The main belt strikes ~35 km from Mount Sproat to the Jurassic Hadow stock. It forms a tight, gently northwest plunging, upright to overturned Jurassic antiform. An extension of the Adit fault is inferred to truncate the northeast limb of the antiform and juxtapose it with Broadview phyllite and grit. A second, >25 km long belt of Carbonaceous member strata defines the limbs of a post-Carboniferous syncline cored by the McHardy assemblage (Milford Group) in a panel bounded by the Adit-Emmens and Mobbs faults from the head of Trout Lake at least as far south as Tenderfoot Creek. Mapping by Thompson (2006, unpublished data) suggests lateral equivalents of the Carbonaceous member may continue at least as far south as Poplar Creek. Carbonaceous schist that hosts the MAX Molybdenum Mine is included in the Carbonaceous Member.

Description

The Carbonaceous Member of the MSA is a mixed gradation of banded fine-grained carbonaceous quartzite to phyllite, limy carbonaceous phyllite and grey marble, and quartzite. The unique carbonaceous quartzite is relatively resistant and forms the summits of Mount Sproat and Little Trout Mountain. Discontinuous, fine white bands and quartz veins parallel to transposition foliation, S1, are common. Near Beaton Arm, MSA carbonaceous quartzite is gradational with texturally similar, fine-grained white orthoquartzite to phyllitic quartzite, which, at least locally, may lack carbon due to secondary processes. Carbonaceous quartzite is gradational with carbonaceous phyllite that is ubiquitous in both the Carbonaceous and Heterolithic members. Thin sections show the carbonaceous phyllite comprises quartz, fine colourless mica and graphite. Straight to highly contorted, sugary white quartz veinlets in the transposition foliation, S1, are ubiquitous.

Weakly foliated to platy, grey, medium-grained marble interbedded with limy carbonaceous phyllite overlies the lowest carbonaceous quartzite north of Galena Pass. The marble is characteristically uniform and has smooth weathered surfaces that sometimes show decimetre-scale spaced foliation parallel to layering. Strongly deformed cream to light buff coloured veinlets or laminations are locally abundant. Similar thick, and tightly folded, grey marble interbedded with carbonaceous phyllite in a fault-bounded panel on Ethel Ridge above the MAX Mine (Read et al., 2009) is correlated with the Carbonaceous Member of the MSA. Massive, densely fractured white dolomitic marble that weathers orange-buff occurs in strata correlated with the Carbonaceous member up-slope of the MAX Molybdenum Mine. The Carbonaceous member is generally devoid of volcanic rocks except at The Ramparts, where a few metres of actinolite schist occur. Evidence for an extrusive versus intrusive origin of the schist is lacking.

Carbonaceous member (?) east of the Emmens fault

At the southeast limit of mapping along a rocky ridge segment called The Ramparts, a ~300 m thick interval of purple, cream and light grey quartzite bears carbonaceous and micaceous horizons similar to lower MSA quartzite. Several metres of chlorite schist and greenschist with stretched millimetres-sized clots of actinolite in felsic groundmass occur within the varicoloured quartzite. The quartzite is directly overlain by a few metres of medium grained grey marble (unit DMSm1) and buff weathering white marble (unit DMSdm). The marbles are overlain by greater than 100 metres of fine grained carbonaceous quartzite to siliceous argillite (unit DMScq) with several layers of coloured, poorly sorted quartzite similar to Broadview quartzite ~300 metres down section to the east. Another thick varicoloured quartzite above the carbonaceous rocks becomes conglomeratic westward, containing subrounded to subangular pebble-size clasts of white (vein?) quartz. The conglomerate is juxtaposed by the Emmens fault against recessive, silty grey phyllite of the Milford Group to the west.

Contact relations

On the north flank of Trout Mountain, the contact between carbonaceous quartzite of the lowermost MSA and an inlier of gritty quartzite correlated with the Broadview Formation (see Chapter 2) is a mixed gradation across more than 10 m of outcrop (Figure 2-8). At that locality, grey phyllite and delicately laminated fine-grained quartzite and carbonaceous quartzite that typify the carbonaceous member in the area interlayer with white-weathering foliated quartzite and rock types intermediate to the two in a large, well exposed outcrop. Semi-continuous exposures traversing the MSA-Broadview contact in the valley of Asher Creek are consistent with a gradational transition. The upper contact of the Carbonaceous member is conformable and is arbitrarily placed at either the lowest extensive metavolcanic unit or non-carbonaceous grey phyllite that overlie the Carbonaceous member. At The Ramparts ridge transect, rusty weathering quartzite, carbonaceous schist, and marble of the Carbonaceous member are interlayered with poorly sorted quartzite that was previously correlated with the Broadview Formation (Read and Wheeler, 1976); the Jurassic or younger Mobbs fault separates the succession from bona fide Broadview strata to the east (Read and Wheeler, 1976).

Heterolithic member

The Heterolithic member of the MSA is a sharply interbedded assemblage of mafic metavolcanic strata, micaceous phyllite, fine-grained biotite schist, and white marble along with marble and phyllite like those in the Carbonaceous member. It stratigraphically overlies the Carbonaceous member between Mount Sproat and Trout Mountain.

Description

On Mount Sproat's south ridge, the lowest exposures assigned to the Heterolithic member comprise interbedded medium grey and greenish grey slaty phyllite with decametres-thick beds of white to light grey massive marble. The marble weathers orange-buff or white, is fine-grained and ranges from calcitic to dolomitic. Its colour and distinctive, thoroughly fractured texture contrast sharply with the grey marble unit common in the Carbonaceous member. The lower phyllite is conformably overlain by green phyllite with pods of buff marble and local millimetric black amphibole porphyroblasts – the lowest mafic horizon at Mount Sproat. On the forested slopes between Beaton Arm and Trout Mountain, where only resistant units tend to outcrop, the lowest greenstone or green phyllite is taken as the base of the Heterolithic member. Green phyllite and greenstone are commonly interlayered with and (or) contain small pods or lenses of buff to orange weathering carbonate.

Tens of metres of black slaty phyllite with straight cleavage outcrop above white quartzite and buff marble on the north ridge of Mount Sproat. One metre of the slaty phyllite contains quartzite pebbles.

Thick beds of buff marble interlayered with greenstone on the west flank of Trout Mountain locally contains abundant mm-scale tremolite, talc, and rare grossular. Buff weathering marble frequently occurs as cm-scale deformed lenses or pods within green phyllite throughout the Mount Sproat assemblage. Green phyllite and phyllitic greenstone interpreted to be basaltic meta-tuff and flows (unit DMSv1) are abundant in the Heterolithic member. Fyles and Eastwood (1962) reported pillows in metavolcanic rocks near Beaton Creek assigned here to the Heterolithic member. Metavolcanics occur in multiple (or repeated) layers metres to tens of metres thick, of which only the more extensive could be shown at the scale of mapping. Several green phyllite to phyllitic greenstone horizons can be followed kilometres along strike through discontinuous exposures. Near Mount Sproat, the volumetric abundance of green phyllite to greenstone increases significantly above the lower grey marbles. Medium to coarse grained, dark green, and strongly foliated actinolitic greenstone (unit DMSv2) was mapped above phyllitic greenstone within medium grained biotite±garnet and rare muscovite schist at the west end of Galena Pass and at Trout Mountain. The greenstone is interlayered with buff marble, and, at Trout Mountain, also contains intrusions of coarse hornblende gabbro or diorite. The dominant rock type is carbonaceous quartzite to quartzose black biotite ± amphibole ± garnet schist; carbonaceous phyllite is absent. Silver coloured micaceous phyllite to schist occurs at Trout Mountain and near Mount Murray. A resistant, light grey marble with prominent differential weathering (unit DMSm2) forms a stratigraphic marker near the upper limit of the Heterolithic member. The marble is white to light grey on fresh surfaces, commonly contains sprays of tremolite, and has extremely rough, weathered surfaces, which commonly highlight compositional layering. Metres-scale lenses of differential weathering marble are interbedded with fine-grained quartzose biotite schist.

Intermittent exposure of lower MSA lithologies was mapped on the forested slope west of the south end of Trout Lake. Lithological units are on the order of metres to tens of metres thick. Sharply interbedded (cm-scale) buff weathering marble and phyllite (unit 5MSdm) occurs below and above light grey to black flinty quartzite and phyllite. Thin beds of fine grained white quartzite (unit 5MSwq) were observed near the marble. Horizons not greater than tens of metres thick of massive medium grey pyritic quartzite and purplish brown laminated quartzite (unit 5MSq) are unlike quartzite in the northwest belt. The purplish brown quartzite is similar to quartzite interbedded with carbonaceous rocks at The Ramparts.

Contact relations

The western contact with black siliceous argillite of Milford Group is not exposed. The eastern contact truncates folded Milford phyllite, chert and conglomerate and corresponds to the Mobbs fault of Read (1973).

Amphibolitic schist member

Amphibole-plagioclase (± quartz ± calcite ± biotite ± chlorite ± epidote ± titanite) schist gradationally interlayered with biotite-plagioclase schist and finely schistose greenstone form a significant map unit near the shores of Upper Arrow Lake.

Its basal contact with the Heterolithic member is exposed on the north and south flanks of Mount Sproat. Near Blind Bay, the McHardy assemblage (Milford Group) directly overlies the Amphibolitic Schist member with angular unconformity. Upper levels of the member and its gradational transition to the overlying Upper Clastic member are fairly well exposed along Highway 23 and adjacent logging roads near the mouths of St. Leon Creek and Halfway River.

The lowest unit of the Amphibolitic Schist member is conglomerate with a green phyllitic to finely schistose matrix of chlorite-biotite-quartz-feldspar, which gradationally overlies green phyllite with buff carbonate of the Heterolithic member. The same conglomeratic horizon forms the hanging wall of a sub-horizontal brittle fault on the east shore of Blind Bay (Figure A1-1). The green conglomerate is matrix-supported and contains angular to well rounded, pebble to boulder size clasts of grit and pale green and white quartzite. Grit clasts are white to light grey with granules of white quartz and feldspar. Attempts to find foliated or igneous clasts failed. North of Mount Sproat the conglomerate has a phyllitic matrix and also contains diffusely bedded grit to clast-supported pebble conglomerate with flattened clasts of light coloured quartzite and scattered, highly flattened dark grey argillite clasts possibly representing mud rip-ups. Conglomerate exceeds 20 m thickness at Blind Bay and is between ~10 and 30 metres thick on Mount Sproat. The green conglomerate matrix is indistinguishable from directly overlying and underlying strata giving the appearance of a gradational contact. An identical association of phyllitic greenstone with lenses and pods of buff carbonate present in the Amphibolitic Schist member and the Heterolithic member supports a conformable relationship.

On the south flank of Mount Sproat, the conglomerate is overlain by blocky, fine grained biotite-chlorite-sericite(?) schist and schistose greenstone texturally and compositionally similar to the conglomerate matrix. Fragmental horizons in the schist contain strongly flattened and stretched unimodal clasts of felsic to intermediate volcanic rocks. Five metres of porphyritic green schist with cm-size stretched plagioclase phenocrysts outcrop 50-100 metres up-section from the conglomerate. Similar plagioclase porphyritic texture was observed in the same unit up-slope from Whiskey Point and on a closed road above Blind Bay. Plagioclase phenocrysts have altered to sericite, quartz and carbonate.

Greenschist and greenstone grade up-section (and with increasing metamorphism) into medium-grained biotite-amphibole schist, schistose amphibolite, and grey biotite-plagioclase schist referred to collectively as amphibolitic schist (unit uDMSas). It occurs in a range of textures but is consistently composed of black amphibole, plagioclase and fine epidote, and commonly also contains significant amounts of dark biotite. Amphibolitic schist is typically well foliated and platy, and it commonly effervesces in dilute HCl. Coarse sprays or needles of black amphibole occur on micaceous foliation surfaces. A unique unit of porphyritic greenstone with equant, 2-6 mm black phenocrysts, probably amphibole pseudomorphing augite, and intermediate porphyritic and vesicular lapilli occurs within the Amphibolitic Schist member 3 km north of Halfway River on Highway 23. At Halfway River, amphibolitic schist contains clast-supported polymict (mafic to intermediate) volcanic metaconglomerate and matrix supported monomict volcanic breccia with igneous clasts from centimetres to decimetres in size.

Rusty weathering biotite-muscovite ± garnet schist and banded calc-silicate to marble are interlayered with amphibolitic schist near Arrowhead and in the immediate hanging wall of the Columbia River fault zone at Halcyon Hot Springs.

Upper Clastic member

Volcanogenic strata of the Amphibolitic Schist member pass upward into a succession of banded metasiltstone, metasandstone, semipelitic and pelitic schist, and conglomerate referred to here as the Upper Clastic member. The lower contact is a gradation from amphibolitic schist to black argillaceous siltstone, garnet-muscovite schist, and quartz pebble conglomerate where exposed in the Upper Arrow Lake shoreline at Whiskey Point. There the Upper Clastic member occupies the core of a south-plunging Jurassic syncline and its top is not exposed. A similar transition is discontinuously exposed along the same axial trace along an old logging road on the southwest flank of Mount Sproat. Rocks transitional between the Amphibolitic Schist and Upper Clastic members include distinctive medium-grained muscovite schist with coarse porphyroblasts of garnet and black amphibole. At St. Leon Creek, amphibole- and biotite-rich schist are interlayered with pelitic schist and well-bedded metasiltstone and metasandstone across hundreds of metres. Relatively fine-grained staurolite-garnet-biotite schist, locally with cm-size plagioclase porphyroblasts, forms massive rounded grey outcrops unlike any other map unit in the region. Metasandstone and metasiltstone are strongly planar bedded at decimetre to metre scale. Conglomerate clasts are pebble to cobble size, variably rounded vein quartz, quartzite and felsic to mafic igneous rocks. Some clasts resemble rocks of the underlying Amphibolitic Schist member. The upper contact near St. Leon Creek was not observed; it is inferred to correspond with the base of quartzite pebble to cobble conglomerate near the Ione Falls Rest Area, which forms the base of the argillaceous Milford Group.

Rocks on the west shore of Upper Arrow Lake near Nakusp include fine-grained grey biotite ± garnet ± staurolite schist and purplish biotite schist like in the Upper Siliclastic member, and rusty weathering muscovite schist and banded marble to calc-silicate indistinguishable from rocks in the Amphibolitic Schist member. Amphibolitic schist was not observed there. Beaches cover either end of the succession so its context is uncertain, however, lithological similarities strongly suggest a link to upper levels of the Mount Sproat assemblage, especially to the Upper Clastic member. Lemieux (2006) made the same correlation with rocks near St. Leon Creek, which he included in his Unit 3. Although calcareous quartzite does outcrop along strike to the west, correlation of the calc-silicate horizon with the Chase Formation as suggested by Lemieux (2006) is not supported by this investigation. The calc-silicate horizon is more similar to calc-silicate in the

Amphibolitic Schist member near Arrowhead and Halcyon Hot Springs.

A2-2: Geochemical data

Data are grouped by map units of the appended Open File maps by Kraft et al. (2011a; 2011b; 2011c).

Abbreviations and definitions:
Interpreted affinity abbreviations as in the text (see section 2.5); BLANK, analytical background (blank) measurement; DUP, analysis of a second fragment of the same hand sample; LOI, loss on ignition; N.D., no data; SPLIT, duplicate analysis of coarse crush from the sample;

Sample	06TWJK248B	06TWJK176C	06TWJK110A2	06TWJK178C	06TWJK178C	06TWJK323D	06TWJK241B
Rock type	hbl-plag amphibolite	massive metadiorite	massive metadiorite	massive metadiorite	SPLIT	massive metadiorite	foliated metabasalt
Map Unit*	Pd	Pd	Pd	Pd		Pd	PKmv
Interpreted affinity	N-MORB	BABB	N-MORB	N-MORB		N-MORB	E-MORB
Easting	457815	447107	444326	447191		469626	437777
Northing	5593327	5613789	5569053	5613333		5593055	5582517
SiO2 (wt%)	49.81	51.12	49.6	47.04	47.04	47.68	50.02
TiO2 (wt%)	1.54	0.87	1.51	2.59	2.59	0.79	1.42
Al2O3 (wt%)	14.19	14.91	15.67	14.36	14.36	16.32	13.7
Fe2O3 (wt%)	11.56	9.67	10.94	14.05	14.05	8.37	12.49
MnO (wt%)	0.21	0.17	0.16	0.22	0.22	0.14	0.29
MgO (wt%)	7.79	8.96	8.02	8.1	8.10	10.76	7.39
CaO (wt%)	10.48	9.85	10.74	10.63	10.63	13.45	9.97
Na2O (wt%)	3.71	3.66	2.97	2.6	2.60	2.28	3.26
K2O (wt%)	0.69	0.54	0.2	0.31	0.31	0.29	0.9
P2O5 (wt%)	0.14	0.1	0.14	0.08	0.08	0.05	0.17
LOI (wt%)	0.48	0.78	0.87	1.16	1.16	1.12	0.84
Total (wt%)	*100.59*	*100.62*	*100.83*	*101.15*	*101.15*	*101.25*	*100.47*
Cr (ppm)	191.2	>400.00	284.4	17.58		174.86	134.74
Ni (ppm)	90.9	142.17	97.45	66.83		140.99	51.43
Co (ppm)	40.03	36.8	44.18	51.28		44.74	38.8
Sc (ppm)	38.98	36.13	41.39	>50.00		>50.00	37.41
V (ppm)	>300.00	180.11	>300.00	>300.00		230.29	>300.00
Cu (ppm)	10.95	29.94	18.25	10.8		24.38	82.69
Pb (ppm)	6	17.4	0.6	4.8		2.8	11.4
Zn (ppm)	76.74	67.39	76.46	92.74		42.97	94.38
Rb (ppm)	7.66	14.3	6.03	5.85		7.08	21.02
Cs (ppm)	0.185	1.054	0.098	0.171		0.55	1.093
Ba (ppm)	42.02	554.2	32.58	81.56		27.51	673.56
Sr (ppm)	168.3	307	152.1	179.2		120.5	234.8
Ga (ppm)	17.24	15	15.09	17.43		12.89	16.02
Ta (ppm)	N.D.	N.D.	N.D.	N.D.		N.D.	0.48
Nb (ppm)	3.2	1.2	2	1.7		1	8.3
Hf (ppm)	2.3	1.8	2.7	2.1		1.3	2.4
Zr (ppm)	81.4	64.3	97.9	69.3		44.3	86
Y (ppm)	30.49	22.81	31.02	24.29		15.9	28.53
Th (ppm)	0.21	0.16	0.2	0.14		0.1	1.05
U (ppm)	0.316	0.08	0.109	0.059		0.084	0.68
La (ppm)	4.2	2.35	3.86	2.71		1.9	8.27
Ce (ppm)	12.52	7.35	11.79	8.25		5.44	17.6
Pr (ppm)	2.057	1.257	1.952	1.416		0.922	2.751
Nd (ppm)	10.91	6.92	10.57	7.66		5.16	13.3
Sm (ppm)	3.64	2.49	3.46	2.77		1.83	3.7
Eu (ppm)	1.335	0.906	1.224	1.495		0.724	1.161
Gd (ppm)	4.821	3.445	4.72	3.875		2.547	4.673
Tb (ppm)	0.84	0.61	0.841	0.686		0.454	0.786
Dy (ppm)	5.693	4.079	5.582	4.526		3.037	5.258
Ho (ppm)	1.214	0.891	1.188	0.958		0.635	1.11
Er (ppm)	3.536	2.586	3.498	2.783		1.828	3.177
Tm (ppm)	0.511	0.382	0.509	0.399		0.256	0.456
Yb (ppm)	3.33	2.5	3.31	2.57		1.65	3.01
Lu (ppm)	0.497	0.374	0.492	0.373		0.239	0.444
Tl (ppm)	0.07	0.13	0.05	0.04		0.06	0.25
Li (ppm)	14.34	13.34	20.17	15.8		22.28	18.41
Be (ppm)	1.74	0.45	0.51	0.58		0.33	1.18
Bi (ppm)	1	1	1	1		1	1
Cd (ppm)	0.054	0.062	0.058	0.066		0.04	0.122
Mo (ppm)	0.4	0.25	0.92	0.24		0.46	1.8
Sb (ppm)	0.06	0.06	0.09	0.08		0.09	0.08
Sn (ppm)	1.67	0.72	0.86	1.02		0.45	1.03
W (ppm)	0.09	0.11	1.33	0.14		0.24	0.26

Sample	06TWJK338B	07TWJK156	06TWJK111A	06TWJK176E	06TWJK178B	06TWJK324B1	06TWJK008A
Rock type	ep-hbl amphibolite	chloritic greenstone	massive metabasalt	chloritic metabasalt	actinolitic metabasalt	act-chl greenstone	ep-hbl-bt schist
Map Unit*	PKmv	PKmv	PKmv	PKmv	PKmv	PKmv	uDMsas
Interpreted affinity	E-MORB	IAT	N-MORB	N-MORB	N-MORB	N-MORB	CAB
Easting	473839	453187	439631	447148	447191	469100	440391
Northing	5585050	5607988	5573230	5613755	5613333	5593044	5615553
SiO2 (wt%)	53.08	29.55	50.02	45.75	50.35	47.95	50.54
TiO2 (wt%)	1.44	1.58	1.66	1.02	1.68	1.2	1.33
Al2O3 (wt%)	15.79	12.93	15.12	9.59	15.28	9.34	17.31
Fe2O3 (wt%)	12.06	15.57	11.74	11.51	11.5	12.06	9.67
MnO (wt%)	0.25	0.33	0.18	0.19	0.26	0.2	0.18
MgO (wt%)	4.1	10.72	7.03	11.88	7.04	14.78	5.06
CaO (wt%)	9.3	15.5	9.94	14.54	8.99	11.87	10.51
Na2O (wt%)	3.37	0.85	4.01	1.76	4.09	1.88	3.57
K2O (wt%)	0.49	0.17	0.33	0.13	0.64	0.17	1.26
P2O5 (wt%)	0.19	0.25	0.15	0.1	0.19	0.1	0.24
LOI (wt%)	0.43	12.52	0.5	4.03	0.7	0.81	0.83
Total (wt%)	*100.5*	*99.97*	*100.66*	*100.5*	*100.7*	*100.37*	*100.51*
Cr (ppm)	16.61	106	161.47	>400.00	235.08	>400.00	27.71
Ni (ppm)	16.3	47	53.63	295.1	102.03	>300.00	7.91
Co (ppm)	28.22	33.4	35.82	67.25	39.61	64.58	21.91
Sc (ppm)	31.36	37.7	41.42	>50.00	37.88	>50.00	30.86
V (ppm)	>300.00	348	>300.00	249.5	>300.00	298.35	244.84
Cu (ppm)	44.8	65	14.88	79.46	9.07	15.59	9.73
Pb (ppm)	3.8	8.6	4.4	4.3	17	1.9	15
Zn (ppm)	80.88	86	84.23	62.15	90.7	72.64	76.65
Rb (ppm)	11.74	26	5.67	0.71	16.35	2.68	32.37
Cs (ppm)	0.137	2.017	0.377	0.028	1.287	0.189	0.943
Ba (ppm)	81.89	83.2	29.65	56.25	131.45	70.25	413.26
Sr (ppm)	201.6	231	95	136.4	162.9	119.5	709.7
Ga (ppm)	17.63	17.06	18.69	10.63	17.23	11.05	17.81
Ta (ppm)	0.17	<0.2	N.D.	N.D.	0.19	N.D.	0.87
Nb (ppm)	3.1	0.8	2	1.6	3	1.6	16.4
Hf (ppm)	2.7	1.81	2.8	1.8	2.7	2	1.8
Zr (ppm)	97.9	57	102.6	63.2	98	62.7	57.6
Y (ppm)	29.13	24.19	32.32	19.26	34.27	22.86	21.29
Th (ppm)	0.88	0.46	0.16	0.14	0.25	0.14	3.14
U (ppm)	0.362	0.19	0.085	0.058	0.123	0.058	1.056
La (ppm)	8.1	3.28	4	2.92	4.79	2.78	23.36
Ce (ppm)	20.13	10.1	12.14	8.8	14.7	8.39	50.02
Pr (ppm)	2.997	1.51	2.01	1.48	2.404	1.414	6.046
Nd (ppm)	14.53	8.32	10.96	7.86	12.55	7.7	24.54
Sm (ppm)	4.18	2.74	3.74	2.5	4.2	2.7	5.11
Eu (ppm)	1.431	0.979	1.437	1.008	1.465	0.953	1.526
Gd (ppm)	4.964	3.31	5.038	3.255	5.55	3.686	4.727
Tb (ppm)	0.833	0.595	0.896	0.574	0.958	0.647	0.714
Dy (ppm)	5.476	4	5.998	3.756	6.406	4.339	4.233
Ho (ppm)	1.167	0.851	1.278	0.79	1.351	0.911	0.841
Er (ppm)	3.405	2.39	3.776	2.244	3.972	2.607	2.339
Tm (ppm)	0.491	0.377	0.543	0.32	0.566	0.375	0.331
Yb (ppm)	3.22	2.458	3.54	2.08	3.65	2.46	2.12
Lu (ppm)	0.485	0.382	0.525	0.308	0.536	0.364	0.311
Tl (ppm)	0.08	0.215	0.05	N.D.	0.13	0.02	0.23
Li (ppm)	22.27	11.2	13.35	4.46	17.25	15.16	24.37
Be (ppm)	0.99	0.74	0.65	N.D.	0.94	0.4	1.27
Bi (ppm)	1	0.114	1	1	1	1	1
Cd (ppm)	0.061	0.07	0.084	0.056	0.077	0.059	0.037
Mo (ppm)	0.69	6.51	2.88	0.3	4.55	0.74	0.72
Sb (ppm)	0.08	0.36	0.08	0.13	0.06	0.06	N.D.
Sn (ppm)	1.09	0.7	1.17	0.61	1.21	0.63	1.06
W (ppm)	0.26	<0.5	0.3	0.1	0.16	0.33	0.34

Sample	06TWJK144A	06TWJK225B	06TWJK381A	06TWJK382A1	06TWJK382A2	07TWJK389	06TWJK148A1
Rock type	hbl-bt schist	ep-amphibole schist	ep-bt-amphibole schist	ep-bt schist	bt-hbl schist	bt-hbl schist	hbl-plag greenstone
Map Unit*	uDMSas	uDMSas	uDMSas	uDMSas	uDMSas	uDMSas	uDMSas
Interpreted affinity	CAB	CAB	CAB	CAB	CAB	CAB	CAB, depleted
Easting	440738	436416	436296	436324	436324	433889	435416
Northing	5617322	5586835	5619086	5618999	5618999	5619284	5591588
SiO2 (wt%)	54.77	57.94	53.84	53.24	53.02	58.21	56.14
TiO2 (wt%)	0.78	1.12	1.04	1.27	1.12	0.96	0.68
Al2O3 (wt%)	16.55	16.65	19.94	19.69	15.61	16.56	13.03
Fe2O3 (wt%)	8.88	9.08	7.5	8.34	12.98	8.58	9.94
MnO (wt%)	0.15	0.16	0.11	0.12	0.23	0.16	0.19
MgO (wt%)	5.44	4.14	4.02	3.12	5.06	4.04	6.87
CaO (wt%)	5.25	4.5	2.95	5.68	6.94	5.91	8.33
Na2O (wt%)	4.97	4.28	5.53	4.93	2.8	4.52	4.19
K2O (wt%)	2.02	1.47	3.02	2.5	1.29	0.67	0.37
P2O5 (wt%)	0.17	0.2	0.28	0.29	0.35	0.2	0.11
LOI (wt%)	1.34	1.06	2.11	1.38	1.16	1.03	0.51
Total (wt%)	*100.32*	*100.6*	*100.33*	*100.57*	*100.58*	*100.84*	*100.36*
Cr (ppm)	102.26	29.93	19.9	30.42	9.32	103	>400.00
Ni (ppm)	38.98	6.49	11.8	16.51	12.81	19	71.3
Co (ppm)	27.09	20.73	17.04	22.44	36.32	20.8	36.02
Sc (ppm)	29.4	23.26	17.6	22.51	31.41	20.6	33.02
V (ppm)	180.36	95.92	157.48	182.91	>300.00	109	171.38
Cu (ppm)	45.92	17.55	>140.00	124.02	108.43	4	34.42
Pb (ppm)	22.2	19.9	22.3	20.5	11.6	21.9	14.9
Zn (ppm)	87.97	87.33	73.74	77.68	133.73	82	64.43
Rb (ppm)	57.19	49.18	84.91	74.44	28.23	19.7	3.1
Cs (ppm)	2.757	1.548	1.814	1.455	0.524	0.972	0.071
Ba (ppm)	>1400.00	>1400.00	>1400.00	1033.57	767.58	403.2	255.79
Sr (ppm)	422.7	338.8	460.1	503.1	454	251	423.5
Ga (ppm)	17.25	19.74	19.31	19.57	18.78	17.48	13.02
Ta (ppm)	0.48	0.99	0.6	0.72	0.33	1.1	0.3
Nb (ppm)	7.9	16.6	10.1	13.2	6.1	16.35	4.8
Hf (ppm)	2.9	3.9	4.1	4.6	3	4.08	2
Zr (ppm)	104.5	144.8	148.1	175.6	104.4	161	71.2
Y (ppm)	19.2	21.48	21.9	27.62	27.22	23.33	15.43
Th (ppm)	7.07	7.12	10.4	12.03	7.07	7.86	3.49
U (ppm)	3.425	2.149	3.524	4.302	2.339	2.32	0.757
La (ppm)	18.58	25.52	24.18	28.88	23.86	27.39	11.9
Ce (ppm)	37.2	50.43	49.49	59.62	50.7	53.4	23.96
Pr (ppm)	4.446	5.915	5.904	7.184	6.521	6.22	2.915
Nd (ppm)	17.36	22.71	24.15	28.71	28.36	24.16	11.96
Sm (ppm)	3.75	4.69	5.22	6.12	6.59	4.76	2.69
Eu (ppm)	1.069	1.261	1.241	1.467	1.879	1.212	0.753
Gd (ppm)	3.561	4.259	4.793	5.612	6.423	4.38	2.682
Tb (ppm)	0.565	0.641	0.706	0.839	0.926	0.68	0.432
Dy (ppm)	3.599	4.072	4.432	5.199	5.505	3.9	2.784
Ho (ppm)	0.737	0.821	0.893	1.052	1.06	0.811	0.577
Er (ppm)	2.185	2.349	2.511	3.03	2.932	2.26	1.728
Tm (ppm)	0.32	0.345	0.361	0.429	0.403	0.364	0.251
Yb (ppm)	2.15	2.29	2.4	2.84	2.65	2.259	1.65
Lu (ppm)	0.319	0.343	0.357	0.428	0.391	0.349	0.247
Tl (ppm)	0.29	0.28	0.33	0.22	0.12	0.11	0.02
Li (ppm)	18.41	40.86	36.49	30.1	19.67	13.7	7.24
Be (ppm)	1.69	1.46	1.95	2.19	1.58	1.63	0.86
Bi (ppm)	1	1	1	1	1	0.107	1
Cd (ppm)	0.042	0.044	0.038	0.056	0.055	0.07	0.041
Mo (ppm)	0.46	0.52	0.16	0.23	0.69	0.14	0.29
Sb (ppm)	0.16	0.1	0.1	0.43	0.22	0.11	0.1
Sn (ppm)	1.37	1.68	1.65	2.09	1.21	1.58	0.85
W (ppm)	0.22	0.32	0.41	0.51	0.26	0.7	0.12

Sample	06TWJK148A1	06TWJK148A2	06TWJK148A2	06TWJK215A	06TWJK225A	07TWJK173	06TWJK081A1
Rock type	DUP	hbl-plag greenstone	DUP	amphibole-ep schist	amphibole-plag schist	amphibolite schist	bt-act greenstone
Map Unit*		uDMSas		uDMSas	uDMSas	uDMSas	uDMSv3
Interpreted affinity		CAB, depleted		CAB, depleted	CAB, depleted	OIB	CAB
Easting		435416		433187	436416	442358	444053
Northing		5591588		5608015	5586835	5614608	5617244
SiO2 (wt%)	56.14	51.68	51.68	47.75	52.69	49.81	54.08
TiO2 (wt%)	0.68	0.88	0.88	0.98	0.97	0.3	1.35
Al2O3 (wt%)	13.03	15.86	15.86	18.03	17.44	16.06	18.45
Fe2O3 (wt%)	9.94	11.69	11.69	11.94	11.06	8.31	10.19
MnO (wt%)	0.19	0.18	0.18	0.2	0.18	0.14	0.1
MgO (wt%)	6.87	7.11	7.11	4.25	4.45	10.88	4.23
CaO (wt%)	8.33	7.91	7.91	10.93	6.86	11.18	2.68
Na2O (wt%)	4.19	2.91	2.91	1.15	3.37	3.21	2.79
K2O (wt%)	0.37	0.85	0.85	2.89	1.66	0.22	2.44
P2O5 (wt%)	0.11	0.11	0.11	0.09	0.15	<0.01	0.2
LOI (wt%)	0.51	1.07	1.07	2.51	0.78	0.7	3.63
Total (wt%)	*100.36*	*100.24*	*100.24*	*100.71*	*99.63*	*100.81*	*100.15*
Cr (ppm)		145.11		78.05	43.41	126	45.54
Ni (ppm)		28.81		19.35	13.85	73	11.27
Co (ppm)		39.84		37.88	29.66	44.5	26.44
Sc (ppm)		39.08		>50.00	32.36	29.3	26.86
V (ppm)		237.03		>300.00	204.33	249	173.56
Cu (ppm)		41.33		33.93	23.47	81	79.08
Pb (ppm)		19.9		25.1	22.1	1.4	28.6
Zn (ppm)		96.77		93.04	95.6	108	100.6
Rb (ppm)		29.43	29.43	66.35	64.71	3.3	68.25
Cs (ppm)		0.865	0.865	0.497	3.07	0.449	2.085
Ba (ppm)		553.7		>1400.00	>1400.00	49.9	>1400.00
Sr (ppm)		386.8	386.8	471.9	541.3	89	161
Ga (ppm)		16.42		23.12	18.07	19.69	21.28
Ta (ppm)		0.23	0.23	0.18	0.51	2.2	0.95
Nb (ppm)		3.9	3.9	3.6	8.2	34.98	16.1
Hf (ppm)		2	2.0	1.7	2.6	2.9	4.7
Zr (ppm)		68.3	68.3	54.2	94	120	173.3
Y (ppm)		20.3	20.30	21.16	23.11	20.51	25.57
Th (ppm)		2.47	2.47	2.33	3.7	3.29	12.55
U (ppm)		1.03	1.030	1.025	1.046	0.92	4.367
La (ppm)		8.68	8.68	7.5	13.17	24.84	26.06
Ce (ppm)		18.72	18.72	16.44	27.34	46.9	53.5
Pr (ppm)		2.485	2.485	2.214	3.461	5.36	6.354
Nd (ppm)		10.83	10.83	9.98	14.7	21.31	25.35
Sm (ppm)		2.89	2.89	2.82	3.62	4.11	5.37
Eu (ppm)		0.867	0.867	1.005	1.077	1.327	1.363
Gd (ppm)		3.315	3.315	3.264	3.831	3.95	5.087
Tb (ppm)		0.558	0.558	0.575	0.653	0.616	0.804
Dy (ppm)		3.7	3.700	3.924	4.296	3.6	5
Ho (ppm)		0.791	0.791	0.863	0.893	0.721	1.021
Er (ppm)		2.375	2.375	2.587	2.601	1.89	2.939
Tm (ppm)		0.351	0.351	0.391	0.378	0.287	0.428
Yb (ppm)		2.34	2.34	2.66	2.53	1.772	2.77
Lu (ppm)		0.357	0.357	0.401	0.379	0.264	0.408
Tl (ppm)		0.16		0.42	0.29	0.021	0.31
Li (ppm)		45.69		25.62	45.53	60.7	34.17
Be (ppm)		1.02		1.87	1.12	0.27	2.44
Bi (ppm)		1		1	1	0.015	1
Cd (ppm)		0.038		0.053	0.067	0.1	0.044
Mo (ppm)		0.14		0.39	0.43	0.5	0.18
Sb (ppm)		0.08		0.06	0.15	0.05	0.05
Sn (ppm)		0.86		1.07	1.01	1.22	2.1
W (ppm)		0.09		0.36	0.42	<0.5	2.54

Sample	06TWJK081A2	06TWJK200A2	06TWJK200A2	06TWJK351A	07TWJK159	07TWJK299B	08TWJK144A
Rock type	hbl-biotite hornfels	bt-act greenstone	DUP	bt-act greenstone	greenstone	hbl-bt amphibolite	greenstone
Map Unit*	uDMSv3	uDMSv3		uDMSv3	uDMSv3	DMSv2	DMSv2
Interpreted affinity	CAB	CAB		CAB	CAB	Back-arc	E-MORB
Easting	444053	444126		443867	442766	457822	457355
Northing	5617244	5616889		5615801	5611340	5606619	5605798
SiO2 (wt%)	56.92	56.62	56.62	56.44	60.06	53.22	43.88
TiO2 (wt%)	1.46	1.19	1.19	1.21	0.71	2.33	2.29
Al2O3 (wt%)	16.96	16.78	16.78	18.11	14.35	14.69	13.14
Fe2O3 (wt%)	10.71	10.82	10.82	8.72	9.11	11.86	12.38
MnO (wt%)	0.14	0.07	0.07	0.06	0.11	0.36	0.22
MgO (wt%)	2.86	4.52	4.52	4.21	3.59	6.19	7.8
CaO (wt%)	2.99	1.75	1.75	1.72	3.37	4.92	8.51
Na2O (wt%)	6.08	1.85	1.85	2.3	2.25	2.25	3.31
K2O (wt%)	0.39	2.28	2.28	2.92	2.36	0.6	0.27
P2O5 (wt%)	0.42	0.2	0.20	0.18	0.13	0.35	0.21
LOI (wt%)	1.39	3.55	3.55	4.11	3.33	3.07	8.47
Total (wt%)	*100.33*	*99.64*	*99.64*	*100*	*99.35*	*99.84*	*100.48*
Cr (ppm)	9.12	32.35		48.87	23	149	94
Ni (ppm)	7.2	10.12		11.85	11.7	74	77.4
Co (ppm)	24.64	21.6		20.57	16.06	39.6	44
Sc (ppm)	28.84	20.03		26.19	27.6	36.4	40.7
V (ppm)	261.86	140.19		150.39	128.6	234	>370
Cu (ppm)	>140.00	88.72		76.08	17.9	103	41.2
Pb (ppm)	35.1	18		22.3	4.5	11.5	7.8
Zn (ppm)	99.3	109.77		94.26	115	106	108
Rb (ppm)	6.7	66.72	66.72	85.76	46.83	18.7	10.83
Cs (ppm)	1.424	2.187	2.187	2.052	1.027	1.217	1.192
Ba (ppm)	>1400.00	>1400.00		>1400.00	873.9	101.4	35.7
Sr (ppm)	406.7	106.8	106.8	140.9	118	272	162.8
Ga (ppm)	19.07	19.13		20.74	17.25	20.12	19.62
Ta (ppm)	1.05	0.86	0.86	0.87	0.204	1.3	0.884
Nb (ppm)	18	14.9	14.9	14.9	3.199	18.4	14.648
Hf (ppm)	6	4.6	4.6	4.6	3.17	4.26	2.61
Zr (ppm)	216.6	168.9	168.9	166	113	162	96
Y (ppm)	34.64	23.2	23.20	23.44	29.55	36.06	20.13
Th (ppm)	18.39	12.25	12.25	11.54	2.995	3.35	0.903
U (ppm)	7.243	4.323	4.323	3.779	0.803	0.64	0.379
La (ppm)	42.22	21.68	21.68	31.81	11.31	22.51	11.04
Ce (ppm)	82.14	45.65	45.65	64.05	25.7	55.6	24.85
Pr (ppm)	9.518	5.594	5.594	7.439	3.433	7.05	3.412
Nd (ppm)	36.92	22.6	22.60	29.02	15.83	32.19	15.51
Sm (ppm)	7.53	4.84	4.84	5.91	4.432	7.62	4.125
Eu (ppm)	1.535	1.14	1.140	1.31	1.225	2.205	1.292
Gd (ppm)	6.864	4.432	4.432	5.252	4.876	7.8	4.575
Tb (ppm)	1.052	0.695	0.695	0.792	0.807	1.224	0.693
Dy (ppm)	6.529	4.415	4.415	4.863	5.334	7	4.162
Ho (ppm)	1.331	0.9	0.900	0.977	1.139	1.355	0.773
Er (ppm)	3.853	2.665	2.665	2.704	3.486	3.54	2.049
Tm (ppm)	0.575	0.379	0.379	0.392	0.521	0.52	0.264
Yb (ppm)	3.8	2.48	2.48	2.6	3.591	3.268	1.583
Lu (ppm)	0.573	0.363	0.363	0.393	0.552	0.5	0.215
Tl (ppm)	0.06	0.33		0.42	0.221	0.126	0.064
Li (ppm)	21.36	39.08		25.11	49.5	43.4	46.4
Be (ppm)	3.06	2.17		2.09	0.61	1.44	1.05
Bi (ppm)	1	1		1	<0.15	0.08	<0.15
Cd (ppm)	0.056	0.041		0.046	0.072	0.07	0.173
Mo (ppm)	0.34	0.16		0.16	0.68	0.28	0.28
Sb (ppm)	0.28	0.07		0.07	<0.04	0.09	0.06
Sn (ppm)	2.91	1.85		2.16	1.37	2	1.43
W (ppm)	0.86	1.78		3.04	0.45	1.3	0.14

Sample	08TWJK126A	08TWJK126A	08TWJK19A1	07TW118	06TWJK031	06TWJK155D	06TWJK280
Rock type	greenstone	DUP	greenstone	massive amphibolite	phyllitic greenstone	phyllitic metabasalt	mt-bt greenstone
Map Unit*	DMSv2		DMSv2	DMSv2	DMSv2	DMSv1	DMSv1
Interpreted affinity	IAT		IAT	IAT	IAT or MORB	E-MORB	E-MORB
Easting	456622		447505	458078	446842	443261	451971
Northing	5607658		5616471	5604453	5616389	5620482	5614315
SiO2 (wt%)	52.72	52.71	51.8	49.05	45.38	43.49	43.25
TiO2 (wt%)	0.95	0.98	1.46	0.98	0.7	1.46	2
Al2O3 (wt%)	15.71	15.64	15.29	16.7	16.11	14.15	12.08
Fe2O3 (wt%)	12.77	12.69	12.59	11.95	14.03	11.55	15.08
MnO (wt%)	0.22	0.21	0.21	0.2	0.17	0.17	0.23
MgO (wt%)	5.6	5.62	5.15	5.22	8.15	10.79	6
CaO (wt%)	8.41	8.33	8.06	9.89	9.56	7.18	10.11
Na2O (wt%)	3.11	3.12	2.9	3.73	2.84	2.04	2.55
K2O (wt%)	0.2	0.2	0.18	0.79	0.15	0.03	0.45
P2O5 (wt%)	0.1	0.1	0.21	0.11	0.05	0.14	0.24
LOI (wt%)	0.7	0.7	2.08	0.96	2.44	9.36	8.26
Total (wt%)	*100.49*	*100.31*	*99.92*	*99.58*	*99.58*	*100.35*	*100.25*
Cr (ppm)	91	91	22	108	125	282.96	128
Ni (ppm)	40.5	40.1	20.2	49	75	171.3	57
Co (ppm)	39.19	39.4	33.24	34.1	48.3	51.26	35.7
Sc (ppm)	41.1	41.2	41.9	38.2	54.6	33.29	30.2
V (ppm)	>370	386.9	287.8	358	352	258.19	308
Cu (ppm)	77.4	76.4	25.9	67	47	124.87	63
Pb (ppm)	4.4	4.3	5.1	9.1	2.2	1.3	1.7
Zn (ppm)	107	107	102	88	85	70.47	81
Rb (ppm)	2.24	2.22	1.81	25.7	1.2	0.78	6.9
Cs (ppm)	0.209	0.2	0.127	2.005	0.066	0.158	0.991
Ba (ppm)	33.8	32.9	16.8	82.2	43.8	22.06	76
Sr (ppm)	188.7	187.6	222.5	230	178	188.8	215
Ga (ppm)	17.38	17.48	19.27	17.48	15.97	14.88	15.31
Ta (ppm)	0.066	0.065	0.113	<0.2	<0.2	0.46	0.7
Nb (ppm)	1.004	0.993	1.627	0.8	0.66	8.4	12.32
Hf (ppm)	1.99	1.9	2.71	1.84	0.82	2.3	4.75
Zr (ppm)	65	65	104	58	25	90.6	200
Y (ppm)	25.54	25.29	33.46	23.84	27.98	19.59	39
Th (ppm)	0.462	0.439	0.416	0.44	<0.09	0.6	0.59
U (ppm)	0.182	0.168	0.139	0.19	0.19	0.175	0.24
La (ppm)	3.6	3.55	4.34	3.21	0.92	6.8	12.75
Ce (ppm)	10.68	10.41	13.12	10.1	2.6	16.19	31.2
Pr (ppm)	1.661	1.603	2.191	1.54	0.48	2.332	4.43
Nd (ppm)	8.9	8.52	11.77	8.31	3.02	11.43	21.14
Sm (ppm)	2.949	2.85	3.952	2.72	1.41	3.17	5.68
Eu (ppm)	1.07	1.006	1.466	0.944	0.641	1.129	1.79
Gd (ppm)	3.853	3.729	5.174	3.18	2.34	3.677	6.46
Tb (ppm)	0.661	0.636	0.883	0.578	0.507	0.613	1.07
Dy (ppm)	4.508	4.417	5.988	3.8	3.9	3.849	7
Ho (ppm)	0.947	0.935	1.255	0.83	0.911	0.768	1.437
Er (ppm)	2.854	2.717	3.769	2.34	2.74	2.182	3.88
Tm (ppm)	0.414	0.395	0.54	0.375	0.443	0.301	0.585
Yb (ppm)	2.699	2.611	3.496	2.438	2.905	1.93	3.698
Lu (ppm)	0.408	0.39	0.52	0.378	0.45	0.274	0.577
Tl (ppm)	0.013	0.011	0.013	0.219	0.01	N.D.	0.033
Li (ppm)	25.2	25.4	14.1	10.8	22.2	34.39	23.8
Be (ppm)	0.39	0.41	0.54	0.8	0.21	0.68	0.59
Bi (ppm)	<0.15	0.03	<0.15	0.109	0.081	1	0.037
Cd (ppm)	0.141	0.142	0.079	0.07	0.04	0.051	0.1
Mo (ppm)	0.39	0.47	0.63	5.88	0.43	0.18	0.48
Sb (ppm)	0.1	0.1	0.56	0.37	0.21	0.09	0.09
Sn (ppm)	0.84	0.78	0.63	0.7	0.29	0.75	1.07
W (ppm)	0.18	0.17	0.48	<0.5	<0.5	0.11	<0.5

Sample	06TWJK342A1	07TWJK388A	07TWJK407A	08TWJK100A	08TWJK135A	08TWJK20A	08TWJK228
Rock type	hbl-plag amphibolitic schist	massive greenstone	phyllitic greenstone	greenstone	greenstone	greenstone	greenstone
Map Unit*	DMSv1	DMSv1	DMSv1	DMSv1	DMSv1	DMSv1	DMSv1
Interpreted affinity	E-MORB	E-MORB	E-MORB	E-MORB	E-MORB	E-MORB	E-MORB
Easting	474793	433342	438104	458155	457267	447984	430750
Northing	5585555	5620233	5625782	5605322	5607030	5616899	5625732
SiO2 (wt%)	52.28	51.8	44.92	44.49	49.05	46.15	47.65
TiO2 (wt%)	2.1	1.14	1.99	0.97	1.36	1.55	0.83
Al2O3 (wt%)	12.99	13.04	15.38	8.67	15.87	13.67	5.81
Fe2O3 (wt%)	11.05	12.99	15.42	11.8	11.13	13	12.75
MnO (wt%)	0.19	0.21	0.24	0.21	0.14	0.21	0.22
MgO (wt%)	7.67	7.16	7.41	15.65	8.09	12.5	19.37
CaO (wt%)	8.92	10.28	4.98	11.16	9.14	6.58	9.67
Na2O (wt%)	4.31	2.04	2.84	0.79	4.02	2.66	0.16
K2O (wt%)	0.2	0.19	0.46	2.4	0.17	0.18	0.02
P2O5 (wt%)	0.26	0.13	0.17	0.14	0.21	0.19	0.24
LOI (wt%)	0.24	1.68	5.87	2.86	0.98	3.84	3.39
Total (wt%)	*100.21*	*100.66*	*99.68*	*99.14*	*100.17*	*100.53*	*100.11*
Cr (ppm)	369.44	73	195	1570	193	477	712
Ni (ppm)	192.78	71	106	732.3	192.8	225.2	496.5
Co (ppm)	41.27	44.9	53.4	67.19	51.8	59.04	70.18
Sc (ppm)	27.83	39.5	50.4	21.5	35.2	32.5	14.9
V (ppm)	247.81	257	355	196.2	269	275	118.5
Cu (ppm)	87.71	24	9	120	90.9	169.7	7.1
Pb (ppm)	1.8	1.1	1.1	2.6	1.2	1.6	1.7
Zn (ppm)	88.03	77	116	96	87	97	140
Rb (ppm)	2.5	1.6	11.9	105.17	0.87	4.09	<0.23
Cs (ppm)	0.294	0.081	0.821	10.541	0.031	0.374	0.043
Ba (ppm)	67.26	69.5	187.7	218.1	66	15.6	4.9
Sr (ppm)	223.7	137	121	123.3	522.5	106.1	74.8
Ga (ppm)	14.71	13.28	19.94	12.16	16.66	17.26	10.12
Ta (ppm)	1.04	0.4	0.3	0.665	0.634	0.525	1.249
Nb (ppm)	17.5	5.1	4.63	11.382	10.57	8.177	17.45
Hf (ppm)	3.6	1.66	3.17	1.56	2.55	2.75	1.6
Zr (ppm)	140.8	58	112	65	108	113	73
Y (ppm)	21.11	24.5	47.1	12.47	19.5	21.94	15.8
Th (ppm)	1.19	0.41	0.35	0.875	0.744	0.672	1.191
U (ppm)	0.411	0.25	0.19	0.432	0.222	0.191	0.469
La (ppm)	13.37	4.5	5.73	10.01	9.74	7.57	13.07
Ce (ppm)	32.03	10.9	15	20.68	22.39	18.79	26.14
Pr (ppm)	4.41	1.63	2.46	2.679	3.168	2.703	3.287
Nd (ppm)	20.18	8.23	13.82	11.89	14.69	12.7	13.94
Sm (ppm)	4.99	2.58	4.77	2.7	3.649	3.553	3.405
Eu (ppm)	1.515	0.848	1.707	1.142	1.326	1.268	0.78
Gd (ppm)	4.961	3.31	6.12	2.809	3.922	4.23	3.697
Tb (ppm)	0.742	0.601	1.104	0.413	0.606	0.68	0.562
Dy (ppm)	4.5	4.1	7.8	2.493	3.767	4.305	3.31
Ho (ppm)	0.867	0.901	1.715	0.475	0.749	0.865	0.599
Er (ppm)	2.308	2.5	5	1.284	2.098	2.428	1.544
Tm (ppm)	0.316	0.391	0.802	0.173	0.288	0.335	0.2
Yb (ppm)	1.99	2.562	4.968	1.105	1.816	2.143	1.174
Lu (ppm)	0.287	0.398	0.768	0.159	0.267	0.311	0.162
Tl (ppm)	0.01	0.014	0.064	0.638	0.006	0.025	<0.005
Li (ppm)	15.2	9.4	39.2	55.8	23	33.7	6.8
Be (ppm)	1.08	0.37	0.43	0.98	1.21	1	0.56
Bi (ppm)	1	0.011	0.046	0.39	<0.15	<0.15	<0.15
Cd (ppm)	0.078	0.06	0.05	0.26	0.087	0.09	0.171
Mo (ppm)	2.64	0.24	0.13	9.35	0.21	0.22	0.42
Sb (ppm)	0.08	0.09	0.35	0.11	0.07	0.13	<0.04
Sn (ppm)	1.15	0.63	1.11	0.72	1.11	1.1	1.59
W (ppm)	0.27	<0.5	<0.5	1.83	0.09	0.28	0.24

Sample	08TWJK332B1	08TWJK315	08TWJK325B1	06TWJK435A	06TWJK062A	07TWJK359	07TWJK405
Rock type	greenstone	greenstone	greenstone	hbl-bt schist	act-chl phyllite	bt-chl greenstone	massive greenstone
Map Unit*	DMSv1	DMSv1	DMSv1	DMSv1	DMSv1	DMSv1	DMSv1
Interpreted affinity	E-MORB	E-MORB to OIB	E-MORB to OIB	N-MORB	N-MORB	OIB	OIB
Easting	474842	477994	474695	435189	449352	432166	437557
Northing	5585057	5588758	5585506	5618888	5615711	5625078	5624581
SiO2 (wt%)	48.59	48.65	49.9	50.67	50.21	43.41	45.07
TiO2 (wt%)	2.02	1.33	3.39	0.89	1.23	2.98	2.27
Al2O3 (wt%)	12.47	14.51	12.5	13.82	14.43	10.84	13.4
Fe2O3 (wt%)	12.16	9.6	13.55	10.71	12.51	13.15	12.33
MnO (wt%)	0.17	0.13	0.21	0.18	0.21	0.19	0.1
MgO (wt%)	8.84	7.17	6.89	9.85	8.09	11.12	5.19
CaO (wt%)	9.93	8.87	7.59	9.2	8.42	12.02	9.38
Na2O (wt%)	3.74	3.75	4.89	3.43	3.49	2.05	1.27
K2O (wt%)	0.29	0.09	0.24	0.52	0.16	1.29	2.46
P2O5 (wt%)	0.26	0.36	0.48	0.05	0.1	0.4	0.39
LOI (wt%)	1.34	6.02	0.14	0.84	2.03	2.48	8.94
Total (wt%)	*99.81*	*100.49*	*99.78*	*100.16*	*100.86*	*99.93*	*100.8*
Cr (ppm)	365	524	76	345.34	169.21	>600	349
Ni (ppm)	184.2	108	73.2	136.27	70.85	398	206
Co (ppm)	48.39	38.38	43.24	42.5	47	63.8	34.2
Sc (ppm)	31.3	26.3	31.1	41.17	45.7	29	23.9
V (ppm)	281.2	174.9	327.6	>300.00	>300.00	239	186
Cu (ppm)	56.1	71.2	39.1	49.76	68.59	66	44
Pb (ppm)	4.1	4.5	6.2	13	1.2	1.9	2.8
Zn (ppm)	111	97	115	65.2	85.77	110	72
Rb (ppm)	7.64	1.83	7.29	13.19	1.81	26.2	54.1
Cs (ppm)	0.912	0.352	1.785	0.839	0.124	4.164	2.154
Ba (ppm)	253.5	87.7	167.3	106.73	56.14	426.7	498.4
Sr (ppm)	246.2	428	240	177.5	161.1	348	420
Ga (ppm)	16.11	18.82	16.98	14.3	16.16	16.6	16.59
Ta (ppm)	0.96	1.268	2.204	N.D.	N.D.	2.8	2.4
Nb (ppm)	14.909	21.081	32.161	1.7	2.5	43.41	39.27
Hf (ppm)	3.38	2.56	6.74	1.3	1.9	4.42	3.76
Zr (ppm)	134	108	260	41.4	66.6	186	153
Y (ppm)	24.7	16.3	38.02	17.08	28.02	22.78	21.95
Th (ppm)	0.963	1.865	2.34	0.18	0.19	3.1	3.04
U (ppm)	0.45	0.439	1.026	0.626	0.1	0.82	0.77
La (ppm)	11.7	22.26	24.07	2.02	2.91	30.42	26.08
Ce (ppm)	28.6	44.7	60.13	5.76	8.35	63.8	53.6
Pr (ppm)	4.027	5.557	8.228	0.961	1.369	7.87	6.7
Nd (ppm)	18.74	23.48	36.64	5.22	7.54	33.57	28.44
Sm (ppm)	4.913	5.208	8.766	1.86	2.7	6.88	5.98
Eu (ppm)	1.733	1.756	2.624	0.661	1.042	2.095	2.211
Gd (ppm)	5.284	4.866	8.958	2.637	3.939	6.15	5.47
Tb (ppm)	0.805	0.655	1.336	0.469	0.713	0.871	0.821
Dy (ppm)	4.973	3.603	8.064	3.206	4.952	4.6	4.3
Ho (ppm)	0.939	0.627	1.523	0.685	1.068	0.817	0.79
Er (ppm)	2.598	1.597	4.138	2.041	3.273	1.93	1.95
Tm (ppm)	0.351	0.2	0.554	0.29	0.48	0.27	0.276
Yb (ppm)	2.189	1.172	3.523	1.93	3.19	1.591	1.615
Lu (ppm)	0.311	0.162	0.503	0.288	0.489	0.226	0.237
Tl (ppm)	0.055	0.013	0.051	0.11	0.01	0.061	0.166
Li (ppm)	10.8	34.4	18.7	18.64	15.34	50.2	12.4
Be (ppm)	1.17	0.83	1.75	1.14	0.69	2.02	1.42
Bi (ppm)	<0.15	<0.15	<0.15	1	1	0.023	0.048
Cd (ppm)	0.168	0.113	0.106	0.096	0.069	0.08	0.06
Mo (ppm)	0.62	0.25	1.28	0.22	0.28	0.13	0.15
Sb (ppm)	0.1	0.2	<0.04	N.D.	0.3	0.19	0.58
Sn (ppm)	1.97	1.06	2.29	0.5	0.75	1.57	1.36
W (ppm)	0.31	0.42	0.2	0.75	0.22	<0.5	0.7

Sample	08TWJK179	08TWJK387	06TWJK306	06TWJK306B	07TWJK468	07TWJK517	07TWJK605
Rock type	greenstone	greenstone	phyllitic greenstone	phyllitic greenstone	massive greenstone	phenocrystic greenstone	chloritic greenstone
Map Unit*	IPLv	IPLJv	IPLJv	IPLJv	IPLJv	IPLJv	IPLJv
Interpreted affinity	OIB	E-MORB	E-MORB to OIB	E-MORB to OIB	E-MORB to OIB	E-MORB to OIB	E-MORB to OIB
Easting	446213	431442	476588	476588	442899	444839	444996
Northing	5623463	5629236	5614080	5614080	5628693	5630121	5630275
SiO2 (wt%)	47.99	47.94	55.01	54.85	45.97	50.75	43.56
TiO2 (wt%)	1.97	1.3	0.88	0.9	1.56	2.05	2.19
Al2O3 (wt%)	14.66	16.08	9.27	9.02	12.17	13.06	10.52
Fe2O3 (wt%)	12.28	10.44	8.28	9.26	10.47	12.42	13.49
MnO (wt%)	0.12	0.18	0.13	0.14	0.14	0.16	0.21
MgO (wt%)	9.22	5.7	10.43	11.54	6.5	6.89	14.77
CaO (wt%)	4.85	12.26	9.63	9.44	10.06	8.37	7.99
Na2O (wt%)	3.63	3.75	2.41	2.26	2.68	4	1.14
K2O (wt%)	1.05	0.26	1.38	1.06	0.01	0.23	0.92
P2O5 (wt%)	0.49	0.16	0.1	0.09	0.19	0.26	0.4
LOI (wt%)	3.54	2.78	1.6	1.9	10.26	2.52	5.05
Total (wt%)	*99.81*	*100.85*	*99.12*	*100.46*	*100.01*	*100.71*	*100.24*
Cr (ppm)	222	207	374	376	325	205	550
Ni (ppm)	173.5	65.3	227	255	226	91	364
Co (ppm)	43.58	43.47	43.1	51	40.9	40.6	68.3
Sc (ppm)	20.7	41.5	17.8	20	17.2	29.9	25.5
V (ppm)	217	287.1	170	152	119	241	207
Cu (ppm)	21.4	143.3	432	267	48	11	18
Pb (ppm)	1.6	3.5	2.3	2	1.7	1.3	2.6
Zn (ppm)	129	83	55	61	91	105	105
Rb (ppm)	16.36	6.95	21.9	15.3	<0.2	2.3	26.9
Cs (ppm)	0.295	0.397	0.384	0.268	0.056	0.111	7.675
Ba (ppm)	982.6	36.1	>2400	>2400	62.4	141	1161.9
Sr (ppm)	262.4	306.5	165	147	478	167	197
Ga (ppm)	22.28	17.16	8.08	7.64	15.66	12.23	13.76
Ta (ppm)	1.776	0.561	0.7	0.7	1.3	1.3	1.8
Nb (ppm)	27.551	9.102	12.34	12.38	19.28	20.56	28.38
Hf (ppm)	3.87	1.64	1.36	1.44	2.72	3.58	3.28
Zr (ppm)	164	62	52	52	100	140	130
Y (ppm)	20.47	19.91	9.63	9.63	18.25	22.2	20.02
Th (ppm)	2.806	0.718	1.21	1.27	2.25	2.3	2.77
U (ppm)	0.731	0.244	0.26	0.26	0.62	0.58	0.7
La (ppm)	31.9	7.58	10.44	10.96	13.73	17.22	25.46
Ce (ppm)	62.37	17.78	20.4	21.6	27.8	38.5	51.5
Pr (ppm)	7.592	2.517	2.49	2.61	3.53	4.98	6.21
Nd (ppm)	31.72	11.52	10.57	11.04	15.93	21.93	26.63
Sm (ppm)	6.932	3.15	2.27	2.45	4.03	4.96	5.53
Eu (ppm)	2.512	1.197	1.242	1.2	1.333	1.51	1.726
Gd (ppm)	6.136	3.665	2.17	2.28	4.16	4.91	4.97
Tb (ppm)	0.84	0.59	0.328	0.355	0.634	0.754	0.737
Dy (ppm)	4.589	3.759	1.9	2	3.6	4.3	3.9
Ho (ppm)	0.791	0.76	0.359	0.363	0.667	0.806	0.755
Er (ppm)	2.02	2.193	0.91	0.89	1.62	2.06	1.86
Tm (ppm)	0.252	0.315	0.131	0.132	0.222	0.305	0.267
Yb (ppm)	1.537	1.993	0.836	0.853	1.305	1.792	1.544
Lu (ppm)	0.206	0.298	0.116	0.115	0.187	0.258	0.229
Tl (ppm)	0.073	0.05	0.174	0.132	<0.005	0.019	0.298
Li (ppm)	62.6	14.8	4.7	7.1	23.8	15.9	90.6
Be (ppm)	0.98	0.56	2.17	1.23	1.01	0.99	1.45
Bi (ppm)	<0.15	0.24	<0.009	<0.009	0.015	0.012	0.042
Cd (ppm)	0.078	0.112	0.06	0.05	0.07	0.07	0.09
Mo (ppm)	0.17	0.27	0.24	0.3	0.43	0.24	0.41
Sb (ppm)	0.37	<0.04	1.45	1.35	0.16	0.27	0.21
Sn (ppm)	1.69	1.04	0.75	0.57	1.28	1.32	1.28
W (ppm)	0.49	0.66	<0.5	<0.5	<0.5	<0.5	<0.5

Sample	06TWJK312	07TWJK457	07TWJK492	07TWJK492	07TWJK522A	07TWJK522B	07TWJK523
Rock type	phyllitic greenstone	massive greenstone	plag.-phyric greenstone	DUP	massive greenstone	phenocrystic chloritic greenstone	greenstone dyke
Map Unit*	ℙLJv	ℙLJv	ℙLJv		ℙLJv	ℙLJv	ℙLJv
Interpreted affinity	OIB	OIB	OIB		OIB	OIB	OIB
Easting	479096	441545	437745		444656	444656	444746
Northing	5595773	5628406	5630036		5629971	5629971	5630037
SiO2 (wt%)	43.77	46.76	45.33	45.37	48.14	46.13	47.44
TiO2 (wt%)	2.02	2.69	2.14	2.16	2.51	2.54	2.93
Al2O3 (wt%)	14.44	15.03	17.12	17.1	16.67	15.12	14.04
Fe2O3 (wt%)	10.49	12.62	10.53	10.55	13.05	11.91	13.76
MnO (wt%)	0.14	0.22	0.18	0.18	0.16	0.16	0.2
MgO (wt%)	6.36	7.05	6.02	5.93	4.67	6.32	5.23
CaO (wt%)	10.2	9.86	9.97	10.02	7.38	10.99	9.96
Na2O (wt%)	2.9	1.2	3.11	3.17	4.22	2.52	3.26
K2O (wt%)	2.55	0.01	0.06	0.06	0.49	0.62	0.24
P2O5 (wt%)	0.3	0.4	0.33	0.33	0.31	0.36	0.39
LOI (wt%)	7.57	4.5	5.69	5.66	3.04	2.67	2.75
Total (wt%)	*100.74*	*100.34*	*100.48*	*100.53*	*100.64*	*99.34*	*100.2*
Cr (ppm)	75	55	77		28	196	30
Ni (ppm)	61	70	58		39	102	38
Co (ppm)	35.2	46	37.8		34.9	35.4	37.2
Sc (ppm)	25.9	30.3	26.5		25.9	27.3	25.3
V (ppm)	229	296	228		272	258	272
Cu (ppm)	81	87	11		85	56	45
Pb (ppm)	2.5	5.6	5		3.2	3.4	5.4
Zn (ppm)	76	117	85		107	84	104
Rb (ppm)	16.3	0.4	1.6		6.6	8.4	3.7
Cs (ppm)	0.25	0.05	0.059		0.922	0.195	10.816
Ba (ppm)	1959.3	22.2	40.9		385.8	451.2	366.8
Sr (ppm)	451	815	738		417	1397	608
Ga (ppm)	16.35	20.31	18.38		18.56	20.4	19.39
Ta (ppm)	1.8	2.5	2		2.1	2.4	2.2
Nb (ppm)	27.61	39.56	31.46		31.72	35.81	33.61
Hf (ppm)	3.36	4.77	3.59		4.43	4.69	5.22
Zr (ppm)	133	194	144		175	190	204
Y (ppm)	19.93	25.02	19.91		24.99	24.97	27.31
Th (ppm)	3.03	3.93	3.05		3.66	4.06	4.4
U (ppm)	0.72	0.9	0.66		0.91	0.94	1.07
La (ppm)	25.33	31.1	24.46		24.68	28.6	29.35
Ce (ppm)	51.9	65.4	51.8		53.9	60.8	63.6
Pr (ppm)	6.33	7.92	6.29		6.79	7.47	7.98
Nd (ppm)	26.32	33.06	26.14		29.26	31.48	33.4
Sm (ppm)	5.28	6.7	5.31		6.17	6.62	7.12
Eu (ppm)	1.878	2.053	1.699		1.938	2.137	2.141
Gd (ppm)	4.82	5.95	4.88		5.76	6	6.61
Tb (ppm)	0.72	0.903	0.714		0.878	0.9	0.97
Dy (ppm)	3.9	4.8	3.9		4.9	5	5.3
Ho (ppm)	0.749	0.907	0.724		0.929	0.928	0.994
Er (ppm)	1.84	2.24	1.8		2.29	2.31	2.52
Tm (ppm)	0.264	0.324	0.252		0.332	0.34	0.366
Yb (ppm)	1.615	1.946	1.55		1.956	2.091	2.218
Lu (ppm)	0.236	0.283	0.221		0.291	0.301	0.32
Tl (ppm)	0.086	<0.005	0.006		0.055	0.062	0.025
Li (ppm)	33.6	49.7	33.8		19.4	20.3	23.8
Be (ppm)	0.99	1.41	0.91		1.32	1.36	1.19
Bi (ppm)	0.084	0.015	0.02		0.021	0.035	0.045
Cd (ppm)	0.08	0.09	0.06		0.08	0.07	0.11
Mo (ppm)	0.25	0.71	0.43		0.32	0.34	0.41
Sb (ppm)	0.98	1.56	0.82		1.08	2.03	1.38
Sn (ppm)	1.3	1.54	1.23		1.53	1.88	1.88
W (ppm)	<0.5	0.5	<0.5		<0.5	<0.5	<0.5

Sample	07TWJK523B	07TWJK543	08TWJK266A1	08TWJK266A1	06TWJK413B	06TWJK413B	08TWJK307
Rock type	greenstone dyke	greenstone	greenstone	DUP	hbl-biotite-feldspar-titanite schist	SPLIT	greenstone
Map Unit*	lPLJv	lPLJv	lPLJv		qfba		MTv
Interpreted affinity	OIB	OIB	OIB		OIB		E-MORB
Easting	444746	444438	430861		435676		454029
Northing	5630037	5629816	5629854		5602982		5619104
SiO2 (wt%)	47.81	43.12	46.08	46.4	47.83	47.83	41.25
TiO2 (wt%)	2.92	2.66	1.65	1.65	2.97	2.97	1.48
Al2O3 (wt%)	14.22	14.33	15.09	15.23	14.73	14.73	14.82
Fe2O3 (wt%)	13.29	13.1	12.92	12.95	10.83	10.83	13.42
MnO (wt%)	0.2	0.19	0.18	0.18	0.17	0.17	0.16
MgO (wt%)	4.97	4.72	9.74	9.83	7.96	7.96	13.13
CaO (wt%)	10.01	10.84	9.38	9.46	7.97	7.97	4.53
Na2O (wt%)	3.32	2.34	3	3	3.31	3.31	1.81
K2O (wt%)	0.24	0.76	0.18	0.18	2.52	2.52	0.02
P2O5 (wt%)	0.41	0.41	0.28	0.28	0.57	0.57	0.2
LOI (wt%)	2.67	8.09	1.12	1.12	1.11	1.11	9.51
Total (wt%)	*100.06*	*100.56*	*99.62*	*100.3*	*99.98*	*99.98*	*100.33*
Cr (ppm)	31	53	607	590	21.87		763
Ni (ppm)	38	48	259.5	254.4	37.68		471.9
Co (ppm)	34.8	37.6	60.34	59.41	39.7		71.57
Sc (ppm)	24.9	20.7	40.9	39.8	23.99		29.1
V (ppm)	274	243	303.6	297.3	283.73		218.8
Cu (ppm)	46	50	105.7	104.2	17.36		5.7
Pb (ppm)	5	2.9	7.8	7.8	7.3		0.7
Zn (ppm)	101	108	113	110	91.96		164
Rb (ppm)	5	13.7	3.17	3.12	58.05		0.53
Cs (ppm)	15.136	0.625	0.088	0.085	3.508		0.231
Ba (ppm)	440.6	362	17.5	17.1	1106.32		36.6
Sr (ppm)	639	340	659.4	645.2	707.2		79.8
Ga (ppm)	19.68	18.35	18.14	17.66	20.12		20.18
Ta (ppm)	2.3	2.7	1.609	1.569	3.69		0.53
Nb (ppm)	35.09	39.78	28.832	28.04	60.5		8.685
Hf (ppm)	5.39	4.86	2.66	2.62	3.4		2.14
Zr (ppm)	214	191	109	107	124.3		80
Y (ppm)	28.91	24.62	19.75	19.27	23.02		13.82
Th (ppm)	4.56	4.66	2.581	2.559	5.75		0.466
U (ppm)	1.09	1.05	0.623	0.609	1.602		0.167
La (ppm)	31.58	31.79	22.96	22.74	44.21		4.3
Ce (ppm)	66.9	67.1	44.9	44.38	89.12		9.95
Pr (ppm)	8.3	8	5.39	5.323	10.172		1.557
Nd (ppm)	35.39	33.19	21.38	21.33	40.36		8.15
Sm (ppm)	7.48	6.46	4.478	4.429	7.84		2.555
Eu (ppm)	2.268	1.978	1.568	1.528	2.58		0.901
Gd (ppm)	7.14	5.86	4.346	4.312	6.836		2.945
Tb (ppm)	1.037	0.876	0.66	0.638	0.936		0.452
Dy (ppm)	5.7	4.8	3.903	3.855	5.351		2.787
Ho (ppm)	1.079	0.905	0.741	0.734	0.984		0.554
Er (ppm)	2.64	2.36	2.047	1.975	2.51		1.61
Tm (ppm)	0.381	0.347	0.271	0.269	0.34		0.231
Yb (ppm)	2.303	2.159	1.72	1.662	2.12		1.567
Lu (ppm)	0.335	0.312	0.247	0.244	0.291		0.244
Tl (ppm)	0.027	0.112	0.019	0.02	0.39		<0.005
Li (ppm)	23	36.3	23.8	23.4	32.14		126.2
Be (ppm)	1.24	1.34	1.43	1.36	1.56		0.55
Bi (ppm)	0.022	0.054	<0.15	0.07	1		<0.15
Cd (ppm)	0.12	0.09	0.119	0.111	0.084		0.047
Mo (ppm)	0.52	0.24	0.27	0.22	1.37		0.13
Sb (ppm)	1.25	1.04	0.13	0.13	N.D.		<0.04
Sn (ppm)	1.92	1.55	1.19	1.16	1.79		0.86
W (ppm)	<0.5	0.6	0.49	0.48	0.39		0.11

Sample	08TWJK307	08TWJK362	08JKPB1	08JKPB2	08JKPB3	GSR-2-1024	SY-4-0469
Rock type	DUP	conglomeratic greenschist	amphibolite	amphibolite	amphibolite	INTL_STD	INTL_STD
Map Unit*		MMMcg	lCHv	lCHv	lCHv		
Interpreted affinity		OIB	OIB	OIB	OIB		
Easting		477535	-	-	-		
Northing		5594308	-	-	-		
SiO2 (wt%)	41.45	42.49	42.68	38.03	46.89		
TiO2 (wt%)	1.47	4.48	3.64	2.13	2.74		
Al2O3 (wt%)	14.75	10.69	14.67	12.02	15.5		
Fe2O3 (wt%)	13.39	14.91	13.08	10.65	13.64		
MnO (wt%)	0.17	0.2	0.19	0.24	0.19		
MgO (wt%)	13.05	11.84	9.87	3.53	7.22		
CaO (wt%)	4.5	9.02	8.78	19.98	9.73		
Na2O (wt%)	1.78	1.91	3.53	3.02	3.23		
K2O (wt%)	0.02	0.08	1.34	0.9	0.36		
P2O5 (wt%)	0.2	0.74	0.83	0.48	0.4		
LOI (wt%)	9.5	3.93	1.18	9.73	0.41		
Total (wt%)	*100.28*	*100.29*	*99.8*	*100.71*	*100.32*		
Cr (ppm)	786	618	298	68	230		
Ni (ppm)	485.4	373.2	140.1	43.7	103.7		
Co (ppm)	74.18	71.79	47.48	26.28	47.93		
Sc (ppm)	30.3	30.3	26.5	19.2	31.2		
V (ppm)	223.5	309.8	271.9	132.7	298.6		
Cu (ppm)	6.7	88.1	132.6	7.4	12.2		
Pb (ppm)	0.7	2.9	8.6	8.4	5.3		
Zn (ppm)	172	194	99	131	152		
Rb (ppm)	0.55	1.61	52.14	18.04	5.68	>150.00	52.76
Cs (ppm)	0.231	1.083	14.26	0.762	0.977	37.062	1.566
Ba (ppm)	37.1	22.6	747.3	258.4	245.1		
Sr (ppm)	81.4	197.4	296	460	217.2	106.3	1147.0
Ga (ppm)	20.67	24.22	14.31	19.36	20.87		
Ta (ppm)	0.53	3.032	5.189	3.303	2.404	6.35	0.73
Nb (ppm)	8.806	50.041	78.15	56.958	37.726	40.5	13.6
Hf (ppm)	2.11	7.87	4.86	3.23	4.85	5.4	9.3
Zr (ppm)	81	320	194	124	195	150.6	501.8
Y (ppm)	14.71	28.98	26.73	46.86	27.95	63.54	107.91
Th (ppm)	0.469	3.815	4.65	5.887	3.286	54.82	1.38
U (ppm)	0.169	1.083	0.979	3.148	1.112	>20.000	0.964
La (ppm)	4.45	42	57.08	49.6	30.66	51.41	55.01
Ce (ppm)	10.26	93.65	118.95	104.56	62.1	107.63	118.04
Pr (ppm)	1.564	12.461	14.689	13.276	7.837	11.880	14.108
Nd (ppm)	8.39	53.32	57.79	53.41	31.87	43.22	55.45
Sm (ppm)	2.568	11.744	10.453	11.15	6.991	9.28	11.99
Eu (ppm)	0.932	3.476	3.12	3.019	2.324	0.806	1.821
Gd (ppm)	3.015	10.212	8.493	10.295	6.784	8.524	13.008
Tb (ppm)	0.471	1.355	1.116	1.482	0.986	1.520	2.453
Dy (ppm)	2.97	7.152	6.266	8.87	5.867	9.907	17.500
Ho (ppm)	0.584	1.173	1.098	1.704	1.097	2.055	4.162
Er (ppm)	1.656	2.717	2.85	4.736	2.973	6.464	13.768
Tm (ppm)	0.234	0.326	0.368	0.657	0.396	1.042	2.140
Yb (ppm)	1.575	1.761	2.186	4.166	2.441	7.33	14.02
Lu (ppm)	0.244	0.234	0.306	0.595	0.351	1.133	1.962
Tl (ppm)	0.004	0.013	0.339	0.091	0.061		
Li (ppm)	133.6	49	103.6	12.2	18		
Be (ppm)	0.54	3.02	1.63	2.14	1.81		
Bi (ppm)	0.02	<0.15	0.4	0.31	0.15		
Cd (ppm)	0.036	0.158	0.225	0.283	0.303		
Mo (ppm)	0.11	0.32	0.1	0.21	1.49		
Sb (ppm)	0.03	1.04	<0.04	0.31	0.08		
Sn (ppm)	0.87	2.96	1.8	3.25	2.71		
W (ppm)	0.11	1.05	0.8	1.97	0.52		

Sample	BIR-1-1525	GSR-3-0414	RBLK-8268	RBLK-8269	RBLK-8270	RBLK-8271
Rock type	INTL_STD	INTL_STD	BLANK	BLANK	BLANK	BLANK
Map Unit*						
Interpreted affinity						
Easting						
Northing						
SiO2 (wt%)	47.21	43.92				
TiO2 (wt%)	1.01	2.32				
Al2O3 (wt%)	15.30	13.64				
Fe2O3 (wt%)	11.38	13.42				
MnO (wt%)	0.17	0.18				
MgO (wt%)	9.55	7.57				
CaO (wt%)	13.37	8.98				
Na2O (wt%)	1.76	3.21				
K2O (wt%)	0.03	2.31				
P2O5 (wt%)	0.03	1.02				
LOI (wt%)	N.D.	2.09				
Total (wt%)	*99.29*	*98.67*				
Cr (ppm)						
Ni (ppm)						
Co (ppm)						
Sc (ppm)						
V (ppm)						
Cu (ppm)						
Pb (ppm)						
Zn (ppm)						
Rb (ppm)			N.D.	N.D.	N.D.	N.D.
Cs (ppm)			0.015	0.012	0.013	0.014
Ba (ppm)						
Sr (ppm)			N.D.	N.D.	N.D.	N.D.
Ga (ppm)						
Ta (ppm)			N.D.	N.D.	N.D.	N.D.
Nb (ppm)			N.D.	N.D.	N.D.	N.D.
Hf (ppm)			N.D.	N.D.	N.D.	N.D.
Zr (ppm)			N.D.	N.D.	N.D.	N.D.
Y (ppm)			0.02	N.D.	0.02	N.D.
Th (ppm)			N.D.	N.D.	N.D.	N.D.
U (ppm)			N.D.	N.D.	N.D.	N.D.
La (ppm)			0.09	N.D.	0.02	0.02
Ce (ppm)			0.98	0.12	0.11	0.09
Pr (ppm)			0.014	N.D.	N.D.	N.D.
Nd (ppm)			0.05	N.D.	N.D.	N.D.
Sm (ppm)			N.D.	N.D.	N.D.	N.D.
Eu (ppm)			N.D.	N.D.	N.D.	N.D.
Gd (ppm)			N.D.	N.D.	N.D.	N.D.
Tb (ppm)			N.D.	N.D.	N.D.	N.D.
Dy (ppm)			N.D.	N.D.	N.D.	N.D.
Ho (ppm)			N.D.	N.D.	N.D.	N.D.
Er (ppm)			N.D.	N.D.	N.D.	N.D.
Tm (ppm)			N.D.	N.D.	N.D.	N.D.
Yb (ppm)			N.D.	N.D.	N.D.	N.D.
Lu (ppm)			N.D.	N.D.	N.D.	N.D.
Tl (ppm)						
Li (ppm)						
Be (ppm)						
Bi (ppm)						
Cd (ppm)						
Mo (ppm)						
Sb (ppm)						
Sn (ppm)						
W (ppm)						

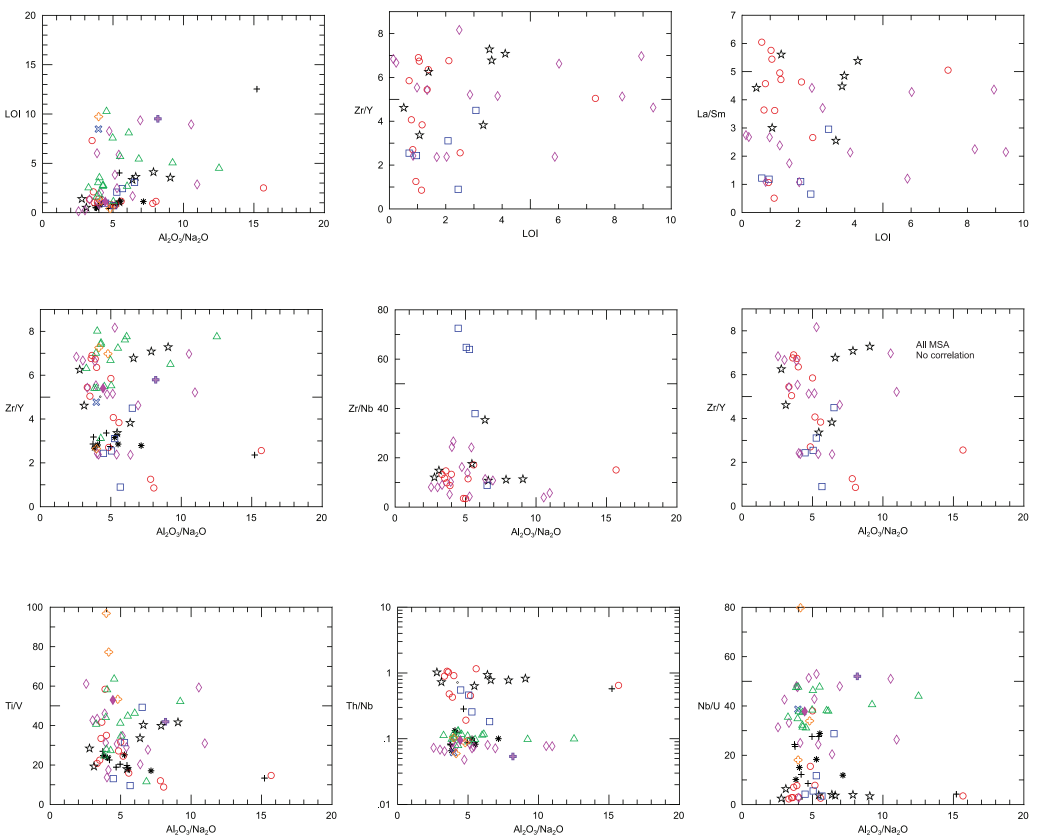

A2-3. Alteration tests of lithogeochemical data.
Scatter plots of Loss on Ignition (LOI) and various trace elements utilized in tectonic discrimination versus the alteration proxy Al_2O_3/Na_2O. The lack of correlation between the various parameters is interpreted to indicate that the concentrations of these parameters were not substantially affected by alteration or metamorphic processes.

U-Pb Results for 06TWJK-200

	Description	Weight (µg)	U (ppm)	Th (ppm)	Pb (ppm)	Th/U	TCPb (pg)	$^{206}Pb/^{204}Pb$	$^{206}Pb/^{238}U$		$^{207}Pb/^{235}U$		$^{207}Pb/^{206}Pb$		Model Ages (Ma) $^{206}Pb/^{238}U$		Model Ages (Ma) $^{207}Pb/^{235}U$		Model Ages (Ma) $^{207}Pb/^{206}Pb$		%Disc
1	1 zircon - colorless irregular fragment	1.8	98	51	44	0.52	4	960	0.37307	0.00086	9.5369	0.0398	0.18540	0.00056	2043.8	4.0	2391.1	3.8	2701.8	4.9	28.3
2	1 zircon - 2:1 colorless prism	0.5	346	105	30	0.30	6	123	0.05861	0.00023	0.4207	0.0134	0.05206	0.00159	367.2	1.4	356.6	9.5	287.9	68.1	-28.3
3	1 zircon - 3:1 colorless prism	0.8	832	75	46	0.09	4	629	0.05464	0.00009	0.4147	0.0022	0.05505	0.00027	342.9	0.6	352.3	1.6	414.2	11.1	17.7
4	1 zircon - 4:1 colorless prism	0.6	323	134	25	0.42	4	184	0.05863	0.00025	0.4547	0.0135	0.05625	0.00157	367.3	1.5	380.6	9.4	462.3	60.7	21.1

A2-4. ID-TIMS U-Pb zircon data.
See section 2.6.1 and Heaman et al. (2002) for methods and data treatment procedures.

A2-5: LA-MC-ICPMS U-Pb geochronology methods

Sample preparation

Samples were cut and hand washed prior to pulverizing in a jaw crusher and disk mill. Mineral separation utilized a Wilfley table, Frantz isodynamic magnetic separator, and methylene iodide techniques. High pyrite content in samples 06TWJK138A, 07TWJK104B, and 07TWJK567 required additional magnetic separation subsequent to use of heavy liquid.

Preparation of mounts for samples 08TWJK357 (Slocan Group), 08TWJK073 (Thompson assemblage), 08JK_TOBY (Toby Formation), and 06TWJK176D (McHardy assemblage) did not involve hand sorting or collection of zircon morphology or colour data. Zircon morphology and (or) colour data were collected for all other detrital zircon samples using the following procedure. Zircons were hand picked in alcohol under a binocular microscope because of large proportions of pyrite, apatite, titanite, rutile and other minerals. To minimize sampling bias due to hand picking, the unsorted heavy minerals were isolated into groups in the picking dish and all zircon greater than ~50 microns (minimum analyzable grain size) were removed from each group until at least ~150 zircon grains (rarely fewer where zircon yields were below 150) were removed from each sample. Subsequent inspection confirmed that all colour and morphological variations were selected. Only cloudy (metamict) grains were removed prior to analysis. Zircons were then sorted by morphology and colour, photographed and set in epoxy grain mounts by group. This procedure aims to maintain approximate proportionality of zircon populations while preserving their morphological context.

Analytical procedure: LA-MC-ICP-MS

U-Pb isotopic dating of detrital zircon was performed by laser ablation multi-collector inductively-coupled plasma mass spectrometry (LA-MC-ICP-MS) at the Radiogenic Isotope Facility, University of Alberta. Grains were hit with a 40 micron beam at grain centre using a Nu Plasma multi-collector inductively-coupled plasma mass spectrometer (MC-ICP-MS) coupled to a frequency quintupled Nd:YAG laser ablation system (New Wave Research). Instrumental mass bias in measured Pb isotopic ratios was corrected using a Tl tracer. Analyses were conducted using a standard-sample-standard protocol after the analytical procedures described in detail by Simonetti et al. (2005) with the following modifications. Background signal was measured between blocks of 24 unknown zircons. Unknowns were analyzed in groups of 12 bracketed by two or three spots on an in-house standard (LH94-15, 1830 ± 1 Ma; Ashton et al., 1998), which was used to correct for mass bias and instrumental drift in the ratios: $^{207}Pb/^{206}Pb$, $^{206}Pb/^{238}U$ and $^{207}Pb/^{235}U$. Common lead corrections were applied to samples 06TWJK138A, 06TWJK104B, 08TWJK043 and 08TWJK309.

Introduction of a secondary zircon standard (GJ1-32, 605.4 ± 0.6 Ma; L. Heaman, unpublished data) in place of every 12th unknown grains as a quality check in eight samples (08JK_TOBY, 08TWJK073, 08TWJK043, 08TWJK309, 06TWJK176D, 08TWJK357, Chase quartzite, and DMF-5s) measured the accuracy of the normalization. An excess of grains were placed in each mount therefore zircon groups were analyzed in their relative proportions.

Notes on data tables

Appended data tables include all usable LA-MC-ICP-MS data. If the "Best age" is not a $^{207}Pb/^{206}Pb$ or $^{206}Pb/^{238}U$ model age as described in Chapter 5, the type of age is indicated by a number according to the following scheme. Only one "Best age" is listed for each grain except for rare instances in which different rim and core ages were identified.

1	weighted mean of $^{207}Pb/^{206}Pb$ ages that are less than 10% discordant
2	weighted mean of $^{206}Pb/^{238}U$ ages that are less than 10% discordant
3	concordia age calculated with Isoplot
4	upper intercept age
5	lower intercept age

A2-6. LA-MC-ICPMS U-Pb detrital zircon data

oby Formation conglomerate Depositional age: Cryogenian n= 109

ircon 40 um Location (Lat., Long.): approx. 116.75°W, 41.42°N

Grain	^{206}Pb cps	^{206}Pb/^{204}Pb	^{207}Pb/^{206}Pb	± (2σ)	^{207}Pb/^{235}U	± (2σ)	^{206}Pb/^{238}U	± (2σ)	rho	Model Ages ^{207}Pb/^{206}Pb	± (2σ)	^{206}Pb/^{238}U	± (2σ)	% disc.	Best Age (Ma)	± (2σ)
GJ1-1	95241	1612	0.0601	0.0006	0.8321	0.0442	0.1003	0.0052	0.9792	609	23	616	31	-1.3		
GJ1-2	71266	1103	0.0600	0.0009	0.8265	0.0421	0.0999	0.0048	0.9521	605	33	614	28	-1.6		
GJ1-3	99198	7762	0.0599	0.0007	0.8299	0.0418	0.1005	0.0049	0.9702	599	26	617	29	-3.1		
GJ1-4	122652	842	0.0601	0.0006	0.8123	0.0325	0.0981	0.0038	0.9706	606	21	603	22	0.5		
GJ1-5	146598	1007	0.0601	0.0007	0.8063	0.0316	0.0973	0.0037	0.9609	607	23	599	22	1.4		
GJ1-6	73402	611	0.0597	0.0011	0.7897	0.0468	0.0960	0.0054	0.9508	592	39	591	32	0.1		
GJ1-7	111462	1133	0.0600	0.0006	0.8353	0.0504	0.1010	0.0060	0.9857	603	22	620	35	-3.0		
Toby-65	36415	327	0.0645	0.0009	1.0720	0.0585	0.1205	0.0064	0.9700	758	28	734	37	3.5	734	37
Toby-12	68751	1611	0.0722	0.0009	1.4245	0.1350	0.1431	0.0134	0.9906	991	26	862	75	13.8	reject	
Toby-78	277383	2167	0.0733	0.0007	1.7735	0.0893	0.1755	0.0087	0.9825	1022	19	1043	47	-2.2	1022	19
Toby-47	267537	7173	0.0738	0.0007	1.6895	0.0808	0.1660	0.0078	0.9818	1037	18	990	43	4.9	1037	18
Toby-44	8994	200	0.0758	0.0015	2.0992	0.1237	0.2009	0.0111	0.9387	1089	40	1180	59	-9.2	1089	40
Toby-6	26176	294	0.0759	0.0012	1.7645	0.1396	0.1687	0.0131	0.9799	1092	31	1005	72	8.6	1092	31
Toby-41	13413	441	0.0761	0.0014	2.1811	0.1211	0.2078	0.0109	0.9435	1098	36	1217	58	-11.9	reject	
Toby-2	44162	496	0.0763	0.0008	1.8059	0.1434	0.1716	0.0135	0.9912	1104	21	1021	74	8.2	1104	21
Toby-22	23627	970	0.0765	0.0011	1.8660	0.1443	0.1768	0.0134	0.9811	1109	30	1050	73	5.8	1109	30
Toby-5	41012	534	0.0766	0.0007	1.8525	0.1451	0.1755	0.0136	0.9922	1110	19	1042	74	6.6	1110	19
Toby-9	79678	765	0.0766	0.0006	1.8060	0.1271	0.1710	0.0120	0.9937	1111	16	1017	65	9.1	1111	16
Toby-21	27684	3734	0.0767	0.0008	1.8946	0.1537	0.1792	0.0144	0.9908	1113	22	1063	78	4.9	1113	22
Toby-16	139983	3226	0.0767	0.0006	1.7507	0.1294	0.1656	0.0122	0.9949	1113	15	988	67	12.2	reject	
Toby-84	22511	303	0.0770	0.0012	2.0923	0.0986	0.1971	0.0088	0.9475	1121	30	1160	47	-3.8	1121	30
Toby-17	52674	1558	0.0773	0.0007	1.9173	0.1404	0.1799	0.0131	0.9933	1129	17	1066	71	6.1	1129	17
Toby-61	9989	71	0.0775	0.0015	2.2618	0.1170	0.2116	0.0101	0.9246	1134	39	1238	54	-10.0	reject	
Toby-14	49592	1917	0.0775	0.0007	1.8848	0.1303	0.1763	0.0121	0.9911	1134	18	1047	66	8.4	1134	18
Toby-60	17655	135	0.0775	0.0013	2.3226	0.1381	0.2172	0.0124	0.9610	1135	32	1267	65	-12.8	reject	
oby-103	72983	2434	0.0776	0.0008	2.0571	0.1056	0.1923	0.0097	0.9807	1136	20	1134	52	0.2	1136	20
Toby-27	65226	3678	0.0776	0.0008	1.9879	0.1400	0.1858	0.0129	0.9882	1137	21	1098	70	3.7	1137	21
oby-111	110604	1415	0.0776	0.0008	2.0729	0.0876	0.1937	0.0079	0.9677	1137	21	1141	43	-0.4	1137	21
Toby-43	16313	233	0.0776	0.0015	2.2416	0.1333	0.2094	0.0118	0.9494	1138	37	1226	63	-8.5	1138	37

Toby Formation conglomerate Depositional age: Cryogenian n= 109

Zircon 40 um Location (Lat., Long.): approx. 116.75°W, 41.42°N

Grain	^{206}Pb cps	^{206}Pb/^{204}Pb	^{207}Pb/^{206}Pb	± (2σ)	^{207}Pb/^{235}U	± (2σ)	^{206}Pb/^{238}U	± (2σ)	rho	Model Ages ^{207}Pb/^{206}Pb	± (2σ)	^{206}Pb/^{238}U	± (2σ)	% disc.	Best Age (Ma)	± (2σ)
Toby-45	16773	341	0.0779	0.0012	2.2126	0.0977	0.2059	0.0085	0.9407	1146	29	1207	46	-5.9	1146	29
Toby-24	500319	13458	0.0780	0.0005	1.9567	0.1459	0.1819	0.0135	0.9957	1148	14	1077	73	6.7	1148	14
Toby-13	44250	919	0.0791	0.0007	2.1839	0.1768	0.2002	0.0161	0.9946	1175	17	1176	86	-0.1	1175	17
Toby-89	121570	1279	0.0792	0.0008	2.1663	0.0892	0.1983	0.0079	0.9707	1178	19	1166	42	1.1	1178	19
Toby-98	28471	243	0.0792	0.0011	2.1318	0.0904	0.1951	0.0079	0.9498	1178	26	1149	42	2.7	1178	26
Toby-38	117926	923	0.0796	0.0011	1.1886	0.0897	0.1082	0.0080	0.9829	1188	27	663	47	46.5	reject	
Toby-15	118046	3354	0.0799	0.0006	2.1354	0.1513	0.1937	0.0137	0.9945	1195	15	1142	73	4.9	1195	15
Toby-96	95653	895	0.0804	0.0008	2.4284	0.1297	0.2190	0.0115	0.9830	1208	19	1276	61	-6.3	1208	19
Toby-95	231621	1879	0.0805	0.0008	2.2196	0.0865	0.2000	0.0076	0.9707	1209	18	1175	41	3.0	1209	18
Toby-76	205901	1315	0.0809	0.0008	2.2768	0.1210	0.2041	0.0107	0.9836	1219	19	1197	57	2.0	1219	19
Toby-52	49677	513	0.0809	0.0009	2.2781	0.1200	0.2041	0.0105	0.9760	1220	22	1198	56	2.0	1220	22
Toby-31	32023	388	0.0819	0.0010	2.2584	0.1075	0.2001	0.0092	0.9670	1242	24	1176	49	5.9	1242	24
Toby-69	69773	532	0.0819	0.0009	2.2789	0.1372	0.2017	0.0120	0.9848	1244	20	1185	64	5.2	1244	20
Toby-62	30090	248	0.0821	0.0011	2.4134	0.1395	0.2132	0.0120	0.9722	1248	26	1246	63	0.1	1248	26
Toby-56	146024	1170	0.0834	0.0008	2.3439	0.1589	0.2037	0.0137	0.9899	1279	19	1195	73	7.2	1279	19
Toby-122	26140	223	0.0841	0.0028	2.1642	0.1101	0.1866	0.0071	0.7488	1295	64	1103	39	16.1	reject	
Toby-108	398651	1698	0.0844	0.0010	2.2048	0.1179	0.1894	0.0099	0.9746	1303	23	1118	53	15.4	reject	
Toby-26	39070	4130	0.0846	0.0009	2.4940	0.1909	0.2138	0.0162	0.9910	1306	20	1249	86	4.8	1306	20
Toby-79	103786	812	0.0853	0.0009	2.6475	0.1218	0.2252	0.0101	0.9759	1321	19	1309	53	1.0	1321	19
Toby-49	41488	683	0.0856	0.0010	2.6401	0.1415	0.2238	0.0117	0.9761	1328	22	1302	61	2.2	1328	22
Toby-116	101539	1031	0.0857	0.0008	2.5313	0.1250	0.2142	0.0104	0.9799	1331	19	1251	55	6.6	1331	19
Toby-75	70223	480	0.0857	0.0009	2.6334	0.1627	0.2228	0.0136	0.9853	1332	20	1297	71	2.9	1332	20
Toby-120	87751	767	0.0858	0.0008	2.6928	0.1290	0.2277	0.0107	0.9797	1333	18	1323	56	0.8	1333	18
Toby-106	48437	1128	0.0858	0.0010	2.7818	0.1565	0.2352	0.0130	0.9787	1333	22	1362	67	-2.4	1333	22
Toby-54	12020	77	0.0864	0.0018	0.2275	0.0113	0.0191	0.0009	0.9135	1348	39	122	5	91.8	reject	
Toby-114	240890	2047	0.0867	0.0008	2.4684	0.1028	0.2064	0.0084	0.9756	1355	18	1210	45	11.8	reject	
Toby-19	204281	222	0.0892	0.0006	2.9693	0.2543	0.2415	0.0206	0.9968	1408	13	1394	106	1.1	1408	13
Toby-70	53325	416	0.0892	0.0012	2.7739	0.1674	0.2256	0.0133	0.9761	1408	25	1311	70	7.6	1408	25
Toby-8	223166	2175	0.0898	0.0006	2.7678	0.2079	0.2235	0.0167	0.9961	1421	13	1300	88	9.4	1421	13
Toby-83	107366	1593	0.0901	0.0009	3.2380	0.1330	0.2607	0.0104	0.9726	1427	18	1493	53	-5.2	1427	18
Toby-25	54571	4342	0.0905	0.0009	2.9739	0.2372	0.2382	0.0189	0.9926	1437	18	1377	97	4.6	1437	18

Toby Formation conglomerate Depositional age: Cryogenian n= 109

Zircon 40 um Location (Lat., Long.): approx. 116.75°W, 41.42°N

Grain	^{206}Pb cps	^{206}Pb/^{204}Pb	^{207}Pb/^{206}Pb	± (2σ)	^{207}Pb/^{235}U	± (2σ)	^{206}Pb/^{238}U	± (2σ)	rho	Model Ages ^{207}Pb/^{206}Pb	± (2σ)	^{206}Pb/^{238}U	± (2σ)	% disc.	Best Age (Ma)	± (2σ)
Toby-91	55565	582	0.0906	0.0010	3.1856	0.1511	0.2550	0.0117	0.9717	1438	21	1464	60	-2.0	1438	21
Toby-126	263554	735	0.0910	0.0013	1.1378	0.1195	0.0907	0.0094	0.9910	1446	27	560	56	63.9	reject	
Toby-123	88122	838	0.0913	0.0009	3.1798	0.1677	0.2525	0.0131	0.9823	1453	19	1452	67	0.1	1453	19
Toby-113	140277	1608	0.0914	0.0009	3.1285	0.1782	0.2481	0.0139	0.9848	1456	19	1429	72	2.1	1456	19
Toby-71	53477	354	0.0918	0.0011	3.0247	0.1895	0.2390	0.0147	0.9807	1463	23	1381	76	6.2	1463	23
Toby-34	94581	1042	0.0921	0.0010	2.8130	0.1705	0.2216	0.0132	0.9829	1469	21	1290	69	13.4	reject	
Toby-109	102689	1816	0.0922	0.0009	3.3352	0.1634	0.2623	0.0126	0.9802	1472	18	1502	64	-2.3	1472	18
Toby-105	68129	1941	0.0922	0.0010	3.2293	0.1451	0.2539	0.0111	0.9725	1472	20	1459	57	1.0	1472	20
Toby-57	11724	85	0.0948	0.0018	0.2509	0.0150	0.0192	0.0011	0.9479	1525	35	123	7	92.8	reject	
Toby-23	225140	10010	0.0999	0.0007	3.8734	0.3012	0.2812	0.0218	0.9960	1622	13	1597	109	1.7	1622	13
Toby-72	104892	690	0.1005	0.0009	3.9917	0.1526	0.2882	0.0107	0.9693	1633	17	1632	53	0.0	1633	17
Toby-64	69523	461	0.1011	0.0010	3.9865	0.1965	0.2861	0.0138	0.9797	1644	18	1622	69	1.5	1644	18
Toby-36	70421	2057	0.1034	0.0011	4.0584	0.2636	0.2847	0.0183	0.9877	1686	19	1615	91	4.7	1686	19
Toby-93	155345	1497	0.1038	0.0009	4.4646	0.2418	0.3119	0.0167	0.9859	1694	17	1750	81	-3.8	1694	17
Toby-112	42347	530	0.1055	0.0012	4.4085	0.3055	0.3032	0.0207	0.9869	1722	20	1707	102	1.0	1722	20
Toby-107	81884	2068	0.1055	0.0011	4.2085	0.2018	0.2892	0.0136	0.9782	1724	18	1638	67	5.7	1724	18
Toby-29	247910	22894	0.1062	0.0007	4.2044	0.3421	0.2872	0.0233	0.9966	1735	12	1628	116	7.0	1735	12
Toby-10	99179	904	0.1067	0.0008	3.9627	0.2817	0.2692	0.0190	0.9940	1745	14	1537	96	13.4	reject	
Toby-90	363764	2745	0.1069	0.0010	4.3007	0.2076	0.2919	0.0138	0.9824	1747	16	1651	69	6.2	1747	16
Toby-85	100685	1190	0.1069	0.0010	4.5579	0.1823	0.3093	0.0120	0.9719	1747	17	1737	59	0.6	1747	17
Toby-42	18982	548	0.1069	0.0018	5.0020	0.3538	0.3394	0.0233	0.9723	1747	30	1884	111	-9.0	1747	30
Toby-104	193171	4845	0.1070	0.0010	4.7240	0.2738	0.3203	0.0183	0.9878	1748	16	1791	89	-2.8	1748	16
Toby-40	69330	4070	0.1070	0.0012	4.1863	0.2286	0.2836	0.0152	0.9800	1750	20	1610	76	9.0	1750	20
Toby-82	127781	2267	0.1073	0.0010	4.4762	0.2120	0.3025	0.0140	0.9794	1754	17	1704	69	3.3	1754	17
Toby-130	83114	780	0.1073	0.0011	4.6090	0.2264	0.3114	0.0150	0.9782	1755	19	1748	73	0.5	1755	19
Toby-28	244462	7145	0.1073	0.0007	4.2167	0.3746	0.2849	0.0252	0.9969	1755	13	1616	125	8.9	1755	13
Toby-18	60332	2094	0.1076	0.0009	4.3364	0.3355	0.2924	0.0225	0.9939	1759	16	1653	111	6.8	1759	16
Toby-117	51289	625	0.1076	0.0011	4.7828	0.2777	0.3223	0.0184	0.9854	1759	18	1801	89	-2.7	1759	18
Toby-73	273067	1724	0.1077	0.0010	4.4093	0.2164	0.2969	0.0143	0.9827	1761	17	1676	71	5.5	1761	17
Toby-68	122487	978	0.1078	0.0010	4.4271	0.2522	0.2978	0.0167	0.9853	1763	18	1680	82	5.3	1763	18
Toby-3	205230	2695	0.1079	0.0008	4.2550	0.3066	0.2861	0.0205	0.9948	1764	13	1622	102	9.1	1764	13

Toby Formation conglomerate Depositional age: Cryogenian n= 109

Zircon 40 um Location (Lat., Long.): approx. 116.75°W, 41.42°N

Grain	^{206}Pb cps	$^{206}Pb/^{204}Pb$	$^{207}Pb/^{206}Pb$	± (2σ)	$^{207}Pb/^{235}U$	± (2σ)	$^{206}Pb/^{238}U$	± (2σ)	rho	Model Ages $^{207}Pb/^{206}Pb$	± (2σ)	$^{206}Pb/^{238}U$	± (2σ)	% disc.	Best Age (Ma)	± (2σ)
Toby-55	145823	1434	0.1079	0.0010	4.7507	0.2202	0.3193	0.0145	0.9792	1764	17	1787	70	-1.5	1764	17
Toby-74	204173	1277	0.1080	0.0010	4.7663	0.2554	0.3201	0.0169	0.9847	1766	17	1790	82	-1.6	1766	17
Toby-100	242894	2364	0.1080	0.0010	4.9694	0.2571	0.3336	0.0170	0.9841	1767	17	1856	82	-5.8	1767	17
Toby-35	75660	967	0.1081	0.0012	4.6633	0.1889	0.3130	0.0122	0.9620	1767	20	1755	60	0.8	1767	20
Toby-46	108067	2160	0.1083	0.0011	4.6168	0.2498	0.3092	0.0164	0.9831	1771	18	1737	80	2.2	1771	18
Toby-53	117310	1172	0.1084	0.0010	4.6675	0.2307	0.3124	0.0151	0.9808	1772	18	1752	74	1.3	1772	18
Toby-121	257198	2684	0.1084	0.0010	4.8586	0.2381	0.3251	0.0157	0.9825	1773	17	1815	76	-2.7	1773	17
Toby-77	263856	1805	0.1085	0.0010	4.5993	0.2102	0.3076	0.0138	0.9794	1774	17	1729	68	2.9	1774	17
Toby-88	260654	2284	0.1085	0.0010	4.8880	0.2034	0.3268	0.0133	0.9759	1774	16	1823	64	-3.2	1774	16
Toby-20	362077	1432	0.1089	0.0010	3.2814	0.4067	0.2185	0.0270	0.9970	1782	17	1274	141	31.4	reject	
Toby-59	175790	2056	0.1092	0.0010	5.0501	0.3203	0.3353	0.0210	0.9889	1787	17	1864	101	-5.0	1787	17
Toby-32	111639	1230	0.1093	0.0010	4.7326	0.2977	0.3141	0.0195	0.9885	1787	17	1761	95	1.7	1787	17
Toby-119	69740	543	0.1099	0.0010	4.8894	0.2133	0.3227	0.0137	0.9761	1798	17	1803	67	-0.3	1798	17
Toby-115	135591	1320	0.1101	0.0011	4.8387	0.2074	0.3188	0.0133	0.9737	1801	18	1784	65	1.1	1801	18
Toby-1	237758	3130	0.1101	0.0008	4.5539	0.3167	0.2999	0.0208	0.9950	1801	13	1691	102	7.0	1801	13
Toby-4	93003	1659	0.1103	0.0008	4.6208	0.3356	0.3038	0.0219	0.9947	1805	14	1710	108	6.0	1805	14
Toby-48	56886	2061	0.1104	0.0012	4.6010	0.2432	0.3023	0.0156	0.9780	1806	20	1703	77	6.5	1806	20
Toby-87	129460	1214	0.1109	0.0013	4.7385	0.2308	0.3098	0.0146	0.9703	1815	21	1740	72	4.7	1815	21
Toby-80	261989	1854	0.1113	0.0010	4.5372	0.2245	0.2958	0.0144	0.9825	1820	17	1670	71	9.3	1820	17
Toby-92	485336	1418	0.1114	0.0012	4.2583	0.2247	0.2773	0.0143	0.9805	1822	19	1578	72	15.1	reject	
Toby-97	108796	989	0.1115	0.0011	5.0005	0.2422	0.3254	0.0154	0.9795	1823	18	1816	75	0.5	1823	18
Toby-102	94738	2674	0.1115	0.0011	5.1772	0.1952	0.3366	0.0122	0.9629	1825	18	1870	59	-2.9	1825	18
Toby-7	113924	1250	0.1127	0.0009	4.6482	0.3245	0.2992	0.0208	0.9941	1843	14	1688	102	9.6	1843	14
Toby-81	147124	1175	0.1128	0.0028	5.0236	0.2324	0.3231	0.0127	0.8488	1844	44	1805	62	2.5	1844	44
Toby-39	62881	2505	0.1128	0.0012	5.0565	0.3671	0.3252	0.0234	0.9894	1845	19	1815	113	1.8	1845	19
Toby-94	218626	2162	0.1130	0.0010	5.2723	0.2211	0.3385	0.0139	0.9764	1848	16	1879	66	-2.0	1848	16
Toby-86	105773	1160	0.1133	0.0011	5.2575	0.2523	0.3366	0.0158	0.9791	1853	18	1870	76	-1.1	1853	18
Toby-67	61708	526	0.1135	0.0011	4.9691	0.2503	0.3174	0.0157	0.9809	1857	18	1777	76	4.9	1857	18
Toby-127	310773	2264	0.1136	0.0010	4.8737	0.2721	0.3112	0.0172	0.9870	1858	16	1747	84	6.8	1858	16
Toby-128	281356	2152	0.1178	0.0011	5.2350	0.3296	0.3222	0.0201	0.9894	1924	16	1801	97	7.3	1924	16
Toby-110	193501	2363	0.1249	0.0012	5.6286	0.2749	0.3269	0.0157	0.9819	2027	16	1823	76	11.5	reject	

Toby Formation conglomerate Depositional age: Cryogenian n= 109

Zircon 40 um Location (Lat., Long.): approx. 116.75°W, 41.42°N

										Model Ages						
Grain	**^{206}Pb cps**	**^{206}Pb/^{204}Pb**	**^{207}Pb/^{206}Pb**	**± (2σ)**	**^{207}Pb/^{235}U**	**± (2σ)**	**^{206}Pb/^{238}U**	**± (2σ)**	**rho**	**^{207}Pb/^{206}Pb**	**± (2σ)**	**^{206}Pb/^{238}U**	**± (2σ)**	**% disc.**	**Best Age (Ma)**	**± (2σ)**
Toby-99	3084	27	0.1307	0.0070	0.4162	0.0351	0.0231	0.0015	0.7713	2108	91	147	9	94.0	reject	
Toby-129	212314	1941	0.1545	0.0014	9.4418	0.4311	0.4432	0.0198	0.9791	2397	16	2365	88	1.6	2397	16
Toby-11	579069	8453	0.1592	0.0011	8.9393	0.6410	0.4073	0.0291	0.9957	2447	11	2203	132	11.8	reject	
Toby-101	329361	7563	0.1723	0.0015	12.0501	0.5073	0.5072	0.0209	0.9775	2580	15	2645	89	-3.0	2580	15
Toby-37	120616	3974	0.1801	0.0017	11.9533	0.6679	0.4814	0.0265	0.9862	2654	15	2533	114	5.5	2654	15
Toby-30	34203	2559	0.1816	0.0015	11.7658	1.0522	0.4700	0.0418	0.9955	2667	14	2483	181	8.3	2667	14
Toby-124	17388	158	0.1828	0.0023	14.3846	0.6719	0.5707	0.0257	0.9624	2678	21	2911	104	-10.8	reject	
Toby-118	398029	3966	0.1829	0.0016	13.2935	0.7840	0.5271	0.0307	0.9884	2679	15	2729	128	-2.3	2679	15
Toby-58	65291	768	0.1842	0.0017	13.0310	0.6592	0.5131	0.0255	0.9823	2691	16	2670	108	1.0	2691	16
Toby-63	77278	689	0.1846	0.0018	13.4698	0.7087	0.5292	0.0274	0.9830	2695	16	2738	114	-2.0	2695	16
Toby-50	24077	241	0.1850	0.0020	12.9385	0.8749	0.5073	0.0338	0.9865	2698	18	2645	143	2.4	2698	18
Toby-33	80472	1099	0.1862	0.0018	12.9640	0.7836	0.5049	0.0301	0.9872	2709	16	2635	128	3.3	2709	16
Toby-125	210525	2031	0.1874	0.0017	13.5267	0.6718	0.5235	0.0256	0.9836	2719	15	2714	107	0.2	2719	15
Toby-51	99065	871	0.1961	0.0019	14.8511	1.8060	0.5492	0.0666	0.9970	2794	15	2822	271	-1.2	2794	15
Toby-66	305870	92	0.2675	0.0299	13.8567	2.7938	0.3757	0.0630	0.8322	3291	165	2056	289	43.6	reject	

Mount Forster Fm, Dmf-5s Depositional age: Middle Devonian (Eifelian) n= 76

Zircon 40 um Location (UTM): unknown

Grain	colour	shape	^{206}Pb cps	^{206}Pb/^{204}Pb	^{207}Pb/^{206}Pb	± (2σ)	^{207}Pb/^{235}U	± (2σ)	^{206}Pb/^{238}U	± (2σ)	rho	Model Ages ^{207}Pb/^{206}Pb	± (2σ)	^{206}Pb/^{238}U	± (2σ)	% disc.	Best Age (Ma)	± (2σ)	*interp type*
GJ1-32-1			173847	infinite	0.0603	0.0012	0.7902	0.0345	0.0951	0.0037	0.8874	613	43	586	22	4.7			
GJ1-32-2			168895	infinite	0.0600	0.0011	0.7706	0.0348	0.0931	0.0039	0.9188	604	39	574	23	5.2			
GJ1-32-3			176795	infinite	0.0608	0.0012	0.8095	0.0345	0.0965	0.0037	0.8916	633	42	594	22	6.4			
GJ1-32-4			184591	infinite	0.0609	0.0012	0.8064	0.0360	0.0961	0.0038	0.8884	635	44	591	22	7.2			
GJ1-32-5			342478	3723	0.0608	0.0013	0.7846	0.0352	0.0936	0.0037	0.8704	633	48	577	21	9.3			
GJ1-32-6			190725	infinite	0.0608	0.0012	0.8019	0.0348	0.0956	0.0037	0.8984	634	41	589	22	7.4			
GJ1-32-7			211681	infinite	0.0589	0.0009	0.7931	0.0330	0.0977	0.0038	0.9252	562	34	601	22	-7.3			
GJ1-32-8			95557	infinite	0.0595	0.0009	0.7956	0.0329	0.0970	0.0037	0.9234	584	34	597	22	-2.3			
80	cll	rnd	41362	infinite	0.0660	0.0044	1.5508	0.1169	0.1704	0.0060	0.4659	806	140	1014	33	-27.9		reject	
88a	cll	rnd	148525	infinite	0.0729	0.0017	1.7679	0.0755	0.1758	0.0062	0.8292	1012	48	1044	34	-3.4	994	35	
88b	cll	rnd	140701	infinite	0.0716	0.0017	1.7690	0.0758	0.1792	0.0063	0.8265	974	49	1063	35	-9.8		reject	
45a	cll	rnd	51321	infinite	0.0791	0.0036	2.0687	0.1188	0.1896	0.0067	0.6143	1176	90	1119	36	5.3	1177	65	*1*
45b	cll	rnd	44864	infinite	0.0792	0.0039	2.0997	0.1253	0.1922	0.0064	0.5593	1178	98	1133	35	4.1			
65	ylw	rnd	207138	968	0.0978	0.0055	2.8739	0.2611	0.2131	0.0153	0.7880	1583	105	1245	81	23.4		reject	
5	pnk	rnd	131495	1906	0.1027	0.0019	4.0827	0.1611	0.2884	0.0100	0.8818	1673	34	1634	50	2.7	1673	34	
70	pnk	rnd	108599	3879	0.1031	0.0017	4.6805	0.1725	0.3292	0.0108	0.8881	1681	31	1835	52	-10.5		reject	
54	cll	rnd	63646	1414	0.1039	0.0041	4.3887	0.2678	0.3063	0.0142	0.7602	1695	73	1723	70	-1.9	1695	73	
32	pnk	frag	294213	2829	0.1042	0.0012	4.5525	0.1631	0.3169	0.0108	0.9511	1700	20	1775	53	-5.0	1700	20	
60	cll	frag	168468	2762	0.1046	0.0013	4.0171	0.1566	0.2784	0.0102	0.9439	1708	24	1583	51	8.2	1708	24	
85	cll	rnd	34901	infinite	0.1048	0.0014	4.6868	0.1634	0.3243	0.0104	0.9223	1711	25	1810	51	-6.6	1711	25	
11	pnk	rnd	176514	1919	0.1057	0.0016	4.0537	0.1683	0.2781	0.0108	0.9315	1727	28	1582	54	9.5	1727	28	
77	cll	subrnd	204181	4004	0.1060	0.0014	4.5649	0.1738	0.3125	0.0111	0.9334	1731	25	1753	54	-1.4	1731	25	
56	cll	rnd	107840	1586	0.1060	0.0022	4.7943	0.1996	0.3280	0.0119	0.8704	1732	38	1829	57	-6.4	1732	38	
48	cll	rnd	86567	2278	0.1061	0.0020	4.5707	0.1806	0.3126	0.0108	0.8755	1733	35	1753	53	-1.4	1733	35	
24	pnk	rnd	124882	2191	0.1062	0.0017	4.6662	0.1767	0.3188	0.0110	0.9074	1735	29	1784	53	-3.2	1735	29	
26	pnk	rnd	169674	3535	0.1064	0.0014	3.7521	0.1437	0.2559	0.0092	0.9381	1738	24	1469	47	17.3		reject	
71	pnk	rnd	230584	6588	0.1064	0.0013	4.6510	0.1679	0.3170	0.0108	0.9452	1739	22	1775	53	-2.4	1739	22	
29	pnk	frag	369066	4012	0.1067	0.0012	4.2442	0.1895	0.2884	0.0125	0.9689	1744	20	1634	62	7.2	1744	20	
31	pnk	frag	135092	infinite	0.1085	0.0018	4.7629	0.1894	0.3184	0.0115	0.9113	1774	30	1782	56	-0.5	1774	30	
37	pnk	frag	438831	9973	0.1087	0.0012	4.6364	0.2162	0.3092	0.0140	0.9732	1779	20	1737	69	2.7	1779	20	
7	pnk	rnd	291507	3555	0.1087	0.0013	4.9710	0.1774	0.3315	0.0111	0.9421	1779	22	1846	54	-4.3	1779	22	
8	pnk	rnd	234338	3083	0.1090	0.0013	4.9887	0.1845	0.3320	0.0116	0.9478	1782	21	1848	56	-4.2	1782	21	
23	pnk	rnd	136933	3260	0.1090	0.0016	4.8228	0.1881	0.3209	0.0116	0.9273	1782	27	1794	56	-0.8	1782	27	
64	cll	frag	397771	3315	0.1096	0.0014	4.5941	0.1983	0.3039	0.0125	0.9526	1793	24	1711	61	5.3	1793	24	
74	cll	subrnd	76633	infinite	0.1098	0.0028	4.9952	0.2076	0.3300	0.0108	0.7846	1796	47	1839	52	-2.8	1796	47	
69	pnk	rnd	158460	3961	0.1098	0.0016	5.1286	0.1830	0.3386	0.0110	0.9142	1797	26	1880	53	-5.4	1797	26	

Mount Forster Fm, Dmf-5s
Zircon 40 um

Depositional age: Middle Devonian (Eifelian)
Location (UTM): unknown

n= 76

Grain	colour	shape	^{206}Pb cps	^{206}Pb/^{204}Pb	^{207}Pb/^{206}Pb	± (2σ)	^{207}Pb/^{235}U	± (2σ)	^{206}Pb/^{238}U	± (2σ)	rho	Model Ages ^{207}Pb/^{206}Pb	± (2σ)	Model Ages ^{206}Pb/^{238}U	± (2σ)	% disc.	Best Age (Ma)	± (2σ)	*interp type*
87	cll	rnd	67994	infinite	0.1099	0.0027	5.0581	0.2151	0.3338	0.0115	0.8130	1798	45	1857	56	-3.8	1798	45	
84	cll	rnd	166867	4172	0.1101	0.0020	5.1455	0.1927	0.3389	0.0111	0.8710	1801	33	1881	53	-5.1	1801	33	
73	pnk	rnd	233245	4859	0.1109	0.0014	4.1173	0.2022	0.2691	0.0128	0.9682	1815	22	1536	65	17.2	reject		
35	pnk	frag	378851	7577	0.1111	0.0012	4.9948	0.1745	0.3261	0.0109	0.9538	1818	19	1819	53	-0.1	1818	19	
55	cll	rnd	150170	4844	0.1111	0.0014	5.0754	0.1931	0.3313	0.0119	0.9425	1818	23	1845	57	-1.7	1818	23	
49	cll	rnd	155841	4870	0.1113	0.0017	5.0905	0.1922	0.3318	0.0114	0.9100	1820	28	1847	55	-1.7	1820	28	
25	pnk	rnd	141558	6155	0.1115	0.0013	4.8510	0.1815	0.3156	0.0112	0.9496	1824	21	1768	55	3.5	1824	21	
57	cll	rnd	25975	infinite	0.1118	0.0058	4.8830	0.3120	0.3168	0.0117	0.5776	1829	95	1774	57	3.4	1829	95	
1	ylw	subrnd	121227	2165	0.1118	0.0017	5.2549	0.1917	0.3408	0.0114	0.9141	1830	27	1890	54	-3.8	1830	27	
36	pnk	frag	307515	5695	0.1119	0.0012	4.9480	0.1935	0.3207	0.0121	0.9626	1830	19	1793	59	2.3	1830	19	
16	pnk	rnd	73658	infinite	0.1121	0.0026	4.8556	0.2269	0.3142	0.0127	0.8672	1834	42	1761	62	4.5	1834	42	
68	pnk	rnd	47357	infinite	0.1121	0.0035	5.3503	0.2457	0.3461	0.0117	0.7332	1834	57	1916	56	-5.2	1834	57	
67	ylw	subrnd	318025	3457	0.1122	0.0013	5.0747	0.1869	0.3280	0.0115	0.9515	1836	21	1829	56	0.4	1836	21	
4	ylw	subrnd	98810	infinite	0.1126	0.0022	4.6283	0.1959	0.2980	0.0112	0.8878	1842	35	1682	55	9.9	1842	35	
6	pnk	rnd	158755	2835	0.1131	0.0013	5.3426	0.1883	0.3425	0.0114	0.9413	1850	22	1899	54	-3.0	1850	22	
10	pnk	rnd	191594	3041	0.1131	0.0016	5.2549	0.1947	0.3369	0.0116	0.9273	1850	25	1872	56	-1.3	1850	25	
39	pnk	frag	429147	4877	0.1131	0.0012	5.0690	0.2047	0.3249	0.0127	0.9645	1851	19	1814	61	2.3	1851	19	
40	pnk	frag	422209	6921	0.1132	0.0012	5.3074	0.1925	0.3402	0.0118	0.9554	1851	19	1887	56	-2.3	1851	19	
62	cll	frag	153468	infinite	0.1140	0.0018	5.1724	0.1849	0.3292	0.0106	0.9008	1864	28	1834	51	1.8	1864	28	
59	cll	frag	139326	infinite	0.1140	0.0016	5.3788	0.1948	0.3422	0.0114	0.9225	1864	25	1897	55	-2.0	1864	25	
15	pnk	rnd	219851	3997	0.1143	0.0017	5.2874	0.2187	0.3356	0.0130	0.9340	1868	27	1865	62	0.2	1868	27	
53	cll	rnd	70793	infinite	0.1143	0.0035	5.1996	0.2326	0.3299	0.0109	0.7372	1869	55	1838	53	1.9	1869	55	
81	cll	rnd	52969	infinite	0.1150	0.0032	5.4760	0.2480	0.3453	0.0123	0.7853	1880	51	1912	59	-1.9	1880	51	
79	cll	rnd	91838	infinite	0.1152	0.0022	5.4769	0.2090	0.3449	0.0113	0.8618	1882	35	1910	54	-1.7	1882	35	
34	pnk	frag	172672	3674	0.1154	0.0014	5.5274	0.2016	0.3473	0.0120	0.9458	1887	21	1921	57	-2.1	1887	21	
86	cll	rnd	281120	4325	0.1157	0.0013	5.6170	0.1896	0.3522	0.0112	0.9449	1890	20	1945	53	-3.3	1890	20	
27	pnk	rnd	161859	7037	0.1173	0.0014	5.0511	0.1798	0.3124	0.0105	0.9420	1915	21	1752	51	9.7	1915	21	
42	pnk	frag	223941	4868	0.1206	0.0014	6.2057	0.2199	0.3732	0.0125	0.9421	1965	21	2045	58	-4.7	1965	21	
82	cll	rnd	183917	3753	0.1210	0.0018	6.2507	0.2288	0.3748	0.0126	0.9157	1970	26	2052	59	-4.8	1970	26	
19	pnk	rnd	124284	1855	0.1224	0.0019	6.1732	0.2486	0.3658	0.0136	0.9230	1992	28	2010	64	-1.1	1992	28	
3	ylw	subrnd	179316	2456	0.1232	0.0017	6.2473	0.2290	0.3679	0.0125	0.9292	2003	24	2019	59	-1.0	2003	24	
2	ylw	subrnd	83502	1113	0.1251	0.0026	6.4676	0.2730	0.3750	0.0139	0.8755	2030	36	2053	65	-1.3	2030	36	
83	cll	rnd	198903	infinite	0.1255	0.0015	6.4888	0.2323	0.3749	0.0126	0.9420	2036	21	2053	59	-0.9	2036	21	
47	cll	rnd	133544	3816	0.1262	0.0018	6.6543	0.2615	0.3823	0.0140	0.9325	2046	25	2087	65	-2.4	2046	25	
63	cll	frag	431213	4539	0.1299	0.0014	6.9152	0.2393	0.3862	0.0127	0.9506	2096	19	2105	59	-0.5	2096	19	
52	cll	rnd	70793	infinite	0.1400	0.0023	8.2673	0.3089	0.4283	0.0144	0.8973	2227	29	2298	64	-3.8	2227	29	

Mount Forster Fm, Dmf-5s

Zircon 40 um

Depositional age: Middle Devonian (Eifelian)

Location (UTM): unknown

n= 76

Grain	colour	shape	^{206}Pb cps	$^{206}Pb/^{204}Pb$	$^{207}Pb/^{206}Pb$	± (2σ)	$^{207}Pb/^{235}U$	± (2σ)	$^{206}Pb/^{238}U$	± (2σ)	rho	Model Ages $^{207}Pb/^{206}Pb$	± (2σ)	Model Ages $^{206}Pb/^{238}U$	± (2σ)	% disc.	Best Age (Ma)	± (2σ)	*interp type*
17	pnk	rnd	277577	3855	0.1422	0.0017	8.1209	0.2973	0.4142	0.0144	0.9470	2254	20	2234	65	1.0	2254	20	
46	cll	rnd	220616	8171	0.1434	0.0016	8.0503	0.2776	0.4071	0.0133	0.9470	2269	19	2202	61	3.5	2269	19	
33	pnk	frag	368252	3876	0.1516	0.0016	9.3494	0.3946	0.4472	0.0182	0.9662	2364	19	2383	81	-0.9	2364	19	
21	pnk	rnd	219109	2608	0.1560	0.0017	9.3521	0.3629	0.4348	0.0162	0.9612	2413	18	2327	72	4.2	2413	18	
78	cll	rnd	360675	5725	0.1571	0.0018	8.0092	0.3174	0.3698	0.0141	0.9596	2425	19	2028	66	19.0	reject		
12	pnk	rnd	221810	4266	0.1672	0.0018	10.7941	0.3910	0.4681	0.0162	0.9531	2530	18	2475	71	2.6	2530	18	
51	cll	rnd	103671	1547	0.1688	0.0019	9.3508	0.3640	0.4018	0.0150	0.9574	2546	19	2177	68	17.0	reject		
14	pnk	rnd	299790	4612	0.1695	0.0018	10.8965	0.4200	0.4664	0.0173	0.9632	2552	17	2468	76	4.0	2552	17	
9	pnk	rnd	251138	1495	0.1722	0.0023	7.7249	0.4929	0.3253	0.0203	0.9784	2579	22	1816	98	33.9	reject		
44	pnk	frag	871404	19805	0.1727	0.0018	9.6466	0.3669	0.4050	0.0148	0.9633	2584	17	2192	68	17.9	reject		
43	pnk	frag	802252	5943	0.1734	0.0018	7.0127	0.3022	0.2934	0.0123	0.9712	2590	17	1658	61	40.7	reject		
58	cll	frag	178613	2101	0.1764	0.0021	12.1229	0.4588	0.4983	0.0179	0.9488	2620	20	2606	77	0.6	2620	20	
66	ylw	subrnd	235100	2612	0.1778	0.0019	12.3168	0.4205	0.5025	0.0163	0.9493	2632	18	2624	70	0.4	2632	18	
18	pnk	rnd	136015	2519	0.1786	0.0021	12.5289	0.4628	0.5088	0.0178	0.9491	2640	19	2651	76	-0.5	2640	19	
22	pnk	rnd	241041	2940	0.1838	0.0021	13.1005	0.4631	0.5168	0.0173	0.9467	2688	19	2686	73	0.1	2688	19	
30	pnk	frag	347797	4092	0.1845	0.0019	12.8096	0.4682	0.5035	0.0176	0.9586	2694	17	2629	75	2.9	2694	17	
41	pnk	frag	376925	5626	0.1855	0.0019	13.6353	0.5055	0.5332	0.0190	0.9611	2702	17	2755	79	-2.4	2702	17	
72	pnk	rnd	341877	10055	0.1860	0.0019	13.4469	0.4531	0.5243	0.0168	0.9515	2707	17	2717	71	-0.4	2707	17	
13	pnk	rnd	537895	14538	0.1869	0.0019	12.5812	0.4225	0.4883	0.0156	0.9529	2715	17	2563	67	6.8	2715	17	
38	pnk	frag	139986	1707	0.1921	0.0023	14.2650	0.5221	0.5385	0.0186	0.9459	2760	20	2777	78	-0.8	2760	20	
50	cll	rnd	288528	3242	0.1969	0.0021	14.6355	0.4929	0.5390	0.0173	0.9509	2801	17	2779	72	0.9	2801	17	
28	pnk	frag	269081	3450	0.2015	0.0021	16.0298	0.5941	0.5769	0.0205	0.9603	2839	17	2936	83	-4.3	2839	17	
20	pnk	rnd	231721	2759	0.2128	0.0023	15.3863	0.5468	0.5245	0.0178	0.9538	2927	17	2718	75	8.7	2927	17	
76	cll	subrnd	476656	8512	0.2169	0.0022	17.5878	0.6376	0.5882	0.0205	0.9599	2957	16	2982	83	-1.0	2957	16	
75	cll	subrnd	307380	6682	0.2582	0.0027	20.4412	0.9547	0.5742	0.0262	0.9753	3236	16	2925	106	11.9	reject		

Akolkolex Fm, 07TWJK567
Zircon 40 um

Depositional age: Cambrian-Devonian
Location (UTM): 445097E, 5630450N

n= 75

												Model Ages							
Grain	**colour**	**shape**	**^{206}Pb cps**	**^{206}Pb/^{204}Pb**	**^{207}Pb/^{206}Pb**	**± (2σ)**	**^{207}Pb/^{235}U**	**± (2σ)**	**^{206}Pb/^{238}U**	**± (2σ)**	**rho**	**^{207}Pb/^{206}Pb**	**± (2σ)**	**^{206}Pb/^{238}U**	**± (2σ)**	**% disc.**	**Best Age (Ma)**	**± (2σ)**	*interp type*
16a		subhed	164040	5468	0.0643	0.0028	1.1551	0.0536	0.1301	0.0021	0.5910	753	94	788	27	-5.1	789	18	2
16c		subhed	105756	infinite	0.0670	0.0003	1.2047	0.0143	0.1303	0.0014	0.9396	839	23	789	25	6.3			
16b		subhed	117780	infinite	0.0679	0.0005	1.1935	0.0132	0.1273	0.0011	0.9280	866	25	773	24	11.4			
21		subhed	219998	334	0.0887	0.0371	2.0785	0.8730	0.1684	0.0065	0.1141	1398	802	1003	49	30.5		reject	
46			871438	5810	0.0904	0.0026	1.5804	0.0488	0.1267	0.0012	0.6959	1433	59	769	24	49.1		reject	
9		prism	1607779	4674	0.0908	0.0017	2.2276	0.3472	0.1726	0.0267	0.9909	1442	41	1026	162	31.2		reject	
41	op		2460714	349	0.0930	0.0021	1.1145	0.0299	0.0849	0.0012	0.7906	1488	47	525	17	67.3		reject	
13		subhed	125813	350	0.0964	0.0176	2.5206	0.5141	0.1911	0.0174	0.4629	1556	343	1127	108	30.0		reject	
24		subhed	165911	959	0.0974	0.0017	4.2662	0.1004	0.3199	0.0052	0.8566	1574	37	1789	61	-15.7		reject	
12		prism	157275	1123	0.0992	0.0018	4.4000	0.1101	0.3224	0.0056	0.8488	1610	39	1801	62	-13.6		reject	
80	pink	subang	451780	1580	0.1010	0.0006	4.4331	0.0767	0.3190	0.0052	0.9429	1643	22	1785	61	-9.9	1643	22	
37			1431337	28627	0.1015	0.0006	2.4459	0.1558	0.1747	0.0111	0.9869	1651	21	1038	73	40.1		reject	
82	pink	subang	686073	1933	0.1023	0.0003	4.5243	0.0690	0.3195	0.0048	0.9513	1666	19	1787	60	-8.3	1666	19	
23		subhed	444650	2088	0.1052	0.0020	4.3913	0.1752	0.3023	0.0106	0.9026	1717	40	1703	79	1.0	1717	40	
35	op		898419	infinite	0.1054	0.0002	3.3415	0.0517	0.2308	0.0035	0.9542	1722	19	1339	45	24.6		reject	
40	op		703103	18028	0.1057	0.0009	3.3670	0.1158	0.2302	0.0077	0.9595	1727	24	1335	60	25.1		reject	
58	pink	rnd	859886	3412	0.1061	0.0004	4.6217	0.0751	0.3160	0.0050	0.9494	1733	20	1770	60	-2.4	1733	20	
52	pink	rnd	705112	3473	0.1063	0.0004	4.6361	0.1102	0.3189	0.0075	0.9600	1738	20	1784	68	-3.1	1738	20	
34	op		851004	7151	0.1065	0.0004	3.7489	0.0965	0.2563	0.0065	0.9624	1740	20	1471	58	17.3		reject	
38	op		493830	infinite	0.1066	0.0004	3.3192	0.0479	0.2262	0.0031	0.9466	1743	20	1315	43	27.1		reject	
4		prism	1060664	6507	0.1068	0.0003	4.1641	0.1292	0.2830	0.0088	0.9714	1745	19	1607	69	9.0	1745	19	
36	op		1263144	10269	0.1068	0.0004	4.0489	0.1064	0.2775	0.0072	0.9645	1746	19	1579	63	10.8		reject	
67	pink	rnd	901756	12186	0.1072	0.0004	4.1712	0.0783	0.2821	0.0052	0.9544	1753	20	1602	56	9.7	1753	20	
20		subhed	766974	7670	0.1077	0.0020	4.2481	0.1020	0.2857	0.0043	0.8367	1761	39	1620	54	9.0	1761	39	
76	pink	subang	774579	3014	0.1078	0.0005	4.4802	0.1167	0.2994	0.0077	0.9626	1762	20	1689	67	4.7	1762	20	
83	pink	subang	729407	182352	0.1078	0.0002	4.5184	0.0735	0.3036	0.0049	0.9556	1763	19	1709	58	3.5	1763	19	
10		prism	727223	7991	0.1079	0.0005	4.3353	0.0891	0.2915	0.0058	0.9545	1765	20	1649	60	7.4	1765	20	
6		prism	399622	8503	0.1082	0.0005	4.7440	0.0995	0.3181	0.0065	0.9541	1770	20	1780	65	-0.7	1770	20	
105	pink	subang	767329	9592	0.1083	0.0004	4.6269	0.0930	0.3102	0.0062	0.9575	1770	19	1742	63	1.8	1770	19	
44	op		1123692	11237	0.1084	0.0014	3.0246	0.0926	0.2015	0.0056	0.9274	1772	29	1184	48	36.3		reject	
14		subhed	183979	infinite	0.1087	0.0005	4.0275	0.0479	0.2668	0.0030	0.9428	1778	20	1524	49	16.0		reject	
98	cll	subang	492457	24623	0.1088	0.0007	4.2982	0.0730	0.2862	0.0045	0.9414	1779	21	1623	55	9.9	1779	21	
74	pink	rnd	578060	2862	0.1089	0.0005	4.8932	0.0828	0.3270	0.0053	0.9467	1782	20	1824	62	-2.7	1782	20	
32a	op		1317561	infinite	0.1116	0.0004	3.2616	0.0372	0.2116	0.0023	0.9448	1826	19	1237	39	35.4		reject	
32b	op		665017	47501	0.1091	0.0002	4.6208	0.0806	0.3071	0.0053	0.9568	1784	19	1726	60	3.7	1784	19	
87	pink	subang	276790	14568	0.1093	0.0006	4.7939	0.0660	0.3180	0.0040	0.9408	1787	21	1780	58	0.5	1787	21	
42	op		494929	4267	0.1094	0.0017	3.4287	0.2777	0.2247	0.0178	0.9762	1790	34	1307	111	29.8		reject	
90	cll	subang	294426	24536	0.1098	0.0005	4.9500	0.1047	0.3268	0.0068	0.9560	1796	20	1823	66	-1.7	1796	20	

Akolkolex Fm, 07TWJK567
Zircon 40 um

Depositional age: Cambrian-Devonian
Location (UTM): 445097E, 5630450N

n= 75

Grain	colour	shape	^{206}Pb cps	^{206}Pb/^{204}Pb	^{207}Pb/^{206}Pb	± (2σ)	^{207}Pb/^{235}U	± (2σ)	^{206}Pb/^{238}U	± (2σ)	rho	Model Ages ^{207}Pb/^{206}Pb	± (2σ)	^{206}Pb/^{238}U	± (2σ)	% disc.	Best Age (Ma)	± (2σ)	*interp type*
31		sub-rnd	212444	infinite	0.1098	0.0003	4.8672	0.0848	0.3211	0.0055	0.9546	1796	19	1795	62	0.1	1796	19	
3		prism	117358	11736	0.1101	0.0014	5.1179	0.1052	0.3371	0.0055	0.9005	1802	29	1873	64	-4.5	1802	29	
92	cll	subang	80296	8922	0.1106	0.0025	5.2254	0.1612	0.3450	0.0071	0.8141	1809	45	1910	70	-6.5	1809	45	
96	cll	subang	259203	infinite	0.1107	0.0002	5.0879	0.1193	0.3337	0.0078	0.9638	1811	19	1856	71	-2.9	1811	19	
75	pink	rnd	373844	infinite	0.1108	0.0002	5.0558	0.0794	0.3321	0.0052	0.9546	1813	19	1849	62	-2.3	1813	19	
59	pink	rnd	150263	1503	0.1109	0.0102	5.2228	0.4980	0.3433	0.0091	0.3889	1815	167	1903	76	-5.6	1815	167	
5		prism	281228	infinite	0.1110	0.0006	4.6645	0.0387	0.3039	0.0019	0.9327	1817	21	1711	52	6.6	1817	21	
60	pink	rnd	363574	infinite	0.1111	0.0003	4.7734	0.0934	0.3114	0.0060	0.9580	1818	19	1748	62	4.4	1818	19	
68	pink	rnd	359207	1497	0.1116	0.0007	5.5330	0.0677	0.3598	0.0037	0.9307	1825	22	1981	63	-9.9	1825	22	
77	pink	subang	580167	infinite	0.1121	0.0002	4.9524	0.0817	0.3195	0.0052	0.9552	1833	19	1787	61	2.9	1833	19	
104	pink	subang	582651	infinite	0.1122	0.0003	4.8779	0.0962	0.3155	0.0062	0.9591	1836	19	1768	63	4.2	1836	19	
93	cll	subang	141757	70879	0.1122	0.0005	4.7017	0.2079	0.3040	0.0134	0.9786	1836	20	1711	91	7.8	1836	20	
1		prism	593097	26959	0.1126	0.0004	4.5958	0.1557	0.2960	0.0100	0.9723	1842	19	1671	75	10.5	reject		
84	pink	subang	731767	365883	0.1130	0.0002	4.9907	0.0878	0.3212	0.0056	0.9567	1847	19	1796	62	3.2	1847	19	
94	cll	subang	367825	6688	0.1136	0.0011	4.5699	0.1360	0.2919	0.0082	0.9435	1858	25	1651	68	12.6	reject		
69	pink	rnd	438581	infinite	0.1136	0.0002	5.1869	0.0804	0.3311	0.0051	0.9546	1858	18	1844	62	0.9	1858	18	
7		prism	564707	28235	0.1137	0.0006	4.9272	0.1766	0.3144	0.0112	0.9709	1859	20	1762	82	6.0	1859	20	
71	pink	rnd	292890	infinite	0.1139	0.0003	5.2985	0.0628	0.3373	0.0039	0.9484	1863	19	1874	60	-0.7	1863	19	
65	pink	rnd	257270	infinite	0.1147	0.0004	5.3500	0.0710	0.3376	0.0043	0.9485	1875	19	1875	61	0.0	1875	19	
91	cll	subang	343230	24516	0.1148	0.0004	5.7068	0.1146	0.3603	0.0071	0.9560	1877	19	1984	71	-6.6	1877	19	
97	cll	subang	143137	7157	0.1149	0.0022	5.5540	0.1443	0.3477	0.0063	0.8452	1878	38	1924	67	-2.8	1878	38	
55	pink	rnd	752467	3071	0.1153	0.0004	5.4629	0.1137	0.3435	0.0071	0.9587	1885	19	1903	69	-1.1	1885	19	
100	cll	subang	154574	infinite	0.1155	0.0004	5.7447	0.0981	0.3617	0.0060	0.9514	1887	19	1990	68	-6.3	1887	19	
95	cll	subang	76252	infinite	0.1156	0.0007	5.6565	0.1381	0.3553	0.0084	0.9528	1890	21	1960	75	-4.3	1890	21	
26		subrnd	191674	infinite	0.1158	0.0003	5.5123	0.0948	0.3451	0.0059	0.9547	1892	19	1911	66	-1.2	1892	19	
54	pink	rnd	210480	infinite	0.1162	0.0004	5.4900	0.0997	0.3425	0.0061	0.9542	1898	19	1899	66	0.0	1898	19	
64	pink	rnd	183989	infinite	0.1165	0.0006	5.6661	0.0473	0.3507	0.0023	0.9332	1904	20	1938	59	-2.1	1904	20	
17		subhed	967026	1525	0.1177	0.0010	5.5909	0.1386	0.3477	0.0081	0.9414	1921	24	1924	73	-0.2	1921	24	
51	pink	rnd	193476	infinite	0.1189	0.0005	5.9502	0.0936	0.3631	0.0055	0.9497	1940	19	1997	67	-3.4	1940	19	
109	cll	rnd	40297	infinite	0.1218	0.0011	6.2093	0.1053	0.3715	0.0053	0.9211	1983	24	2036	68	-3.1	1983	24	
48	op		173913	infinite	0.1264	0.0007	5.0028	0.1348	0.2874	0.0076	0.9596	2048	20	1629	65	23.1	reject		
78	pink	subang	220191	infinite	0.1281	0.0004	6.7250	0.1249	0.3801	0.0070	0.9565	2073	18	2077	73	-0.2	2073	18	
70	pink	rnd	965228	3317	0.1330	0.0010	6.5468	0.0973	0.3614	0.0046	0.9268	2138	22	1989	65	8.1	2138	22	
45	op		1286624	9674	0.1426	0.0005	7.4175	0.2281	0.3764	0.0115	0.9691	2259	18	2059	88	10.3	reject		
19		subhed	1028544	2286	0.1500	0.0028	8.6037	0.4773	0.4178	0.0218	0.9418	2346	36	2250	136	4.8	2346	36	
79	pink	subang	1082622	4180	0.1539	0.0004	8.9389	0.1957	0.4209	0.0092	0.9614	2390	18	2265	84	6.2	2390	18	
39	op		766243	8239	0.1576	0.0007	7.0300	0.2211	0.3228	0.0101	0.9682	2430	19	1803	78	29.5	reject		
72	pink	rnd	557659	2145	0.1583	0.0005	10.2236	0.1886	0.4688	0.0085	0.9551	2437	18	2478	87	-2.0	2437	18	
8		prism	109997	infinite	0.1627	0.0005	10.6046	0.2261	0.4728	0.0100	0.9594	2483	18	2496	92	-0.6	2483	18	

Akolkolex Fm, 07TWJK567 Depositional age: Cambrian-Devonian n= 75

Zircon 40 um Location (UTM): 445097E, 5630450N

Grain	colour	shape	^{206}Pb cps	^{206}Pb/^{204}Pb	^{207}Pb/^{206}Pb	± (2σ)	^{207}Pb/^{235}U	± (2σ)	^{206}Pb/^{238}U	± (2σ)	rho	Model Ages ^{207}Pb/^{206}Pb	± (2σ)	^{206}Pb/^{238}U	± (2σ)	% disc.	Best Age (Ma)	± (2σ)	*interp type*
2		prism	325165	6774	0.1631	0.0009	7.5725	0.1087	0.3372	0.0044	0.9394	2488	19	1873	61	28.4	reject		
22		subhed	241933	880	0.1639	0.0086	10.1017	0.6605	0.4453	0.0172	0.6658	2496	90	2375	116	5.8	2496	90	
18		subhed	1068323	10683	0.1655	0.0014	5.4732	0.3535	0.2391	0.0153	0.9826	2513	22	1382	98	49.8	reject		
99	cll	subang	920392	infinite	0.1657	0.0001	10.7658	0.2363	0.4708	0.0103	0.9636	2515	17	2487	92	1.4	2515	17	
102	pink	subang	795022	9938	0.1665	0.0005	9.8092	0.1883	0.4258	0.0081	0.9570	2523	18	2287	81	11.1	reject		
28		sub-rnd	857004	11427	0.1684	0.0005	9.4260	0.1871	0.4054	0.0079	0.9574	2542	18	2194	79	16.1	reject		
30		sub-rnd	526632	5429	0.1694	0.0017	10.7120	0.2094	0.4580	0.0077	0.9199	2552	24	2431	84	5.7	2552	24	
43	op		1156638	6885	0.1699	0.0007	9.0975	0.3303	0.3875	0.0140	0.9734	2557	18	2111	99	20.4	reject		
56	pink	rnd	906418	3555	0.1711	0.0006	6.6521	0.0935	0.2820	0.0039	0.9493	2568	18	1602	53	42.4	reject		
15		subhed	136178	4539	0.1723	0.0033	11.7103	0.3341	0.4922	0.0104	0.8530	2580	36	2580	95	0.0	2580	36	
101	pink	subang	1126335	8731	0.1739	0.0003	11.9592	0.1726	0.4975	0.0071	0.9530	2596	17	2603	87	-0.3	2596	17	
11		prism	386925	2909	0.1754	0.0007	10.3608	0.3417	0.4308	0.0141	0.9703	2610	18	2309	103	13.7	reject		
29		sub-rnd	441434	5808	0.1756	0.0004	11.7006	0.2282	0.4847	0.0094	0.9584	2612	17	2548	91	3.0	2612	17	
66	pink	rnd	837887	12506	0.1758	0.0004	11.9695	0.2067	0.4938	0.0085	0.9565	2614	17	2587	89	1.2	2614	17	
85	pink	subang	565314	22613	0.1768	0.0004	11.7873	0.2246	0.4828	0.0091	0.9586	2623	17	2539	90	3.9	2623	17	
50a	pink	rnd	395270	913	0.1777	0.0029	9.9657	0.8080	0.4064	0.0323	0.9755	2632	32	2198	187	19.4	reject		
50b	pink	rnd	644333	3068	0.1822	0.0005	11.4899	0.3607	0.4571	0.0143	0.9712	2673	17	2427	105	11.0	reject		
47	op		884710	4058	0.1782	0.0005	11.1244	0.1865	0.4522	0.0075	0.9543	2636	17	2405	82	10.5	reject		
86	pink	subang	807444	12051	0.1786	0.0004	11.8618	0.1836	0.4814	0.0074	0.9541	2640	17	2533	85	4.9	2640	17	
53	pink	rnd	665120	3293	0.1789	0.0005	9.3349	0.0919	0.3769	0.0035	0.9453	2643	17	2062	65	25.6	reject		
25		sub-rnd	334100	2115	0.1802	0.0009	12.7992	0.3216	0.5151	0.0127	0.9594	2654	18	2679	104	-1.1	2654	18	
89	cll	subang	158215	5456	0.1805	0.0011	12.7107	0.2514	0.5105	0.0096	0.9456	2658	20	2659	94	-0.1	2658	20	
107	pink	subang	769906	6416	0.1810	0.0005	9.8013	0.1072	0.3932	0.0041	0.9466	2662	17	2137	68	23.1	reject		
81	pink	subang	629169	infinite	0.1815	0.0003	11.8623	0.3011	0.4729	0.0120	0.9668	2667	17	2496	98	7.7	2667	17	
33	op		710215	1835	0.1820	0.0005	12.4886	0.1811	0.4968	0.0071	0.9520	2671	17	2600	86	3.2	2671	17	
73	pink	rnd	287864	5757	0.1834	0.0026	13.4349	0.2902	0.5314	0.0087	0.8846	2684	29	2747	94	-2.9	2684	29	
49	pink	rnd	1267328	6466	0.1841	0.0003	13.7655	0.2010	0.5418	0.0078	0.9535	2690	17	2791	93	-4.6	2690	17	
103	pink	subang	384223	4629	0.1852	0.0006	13.3139	0.2805	0.5217	0.0108	0.9581	2700	17	2706	99	-0.3	2700	17	
57	pink	rnd	1046985	4106	0.1860	0.0004	13.2165	0.3111	0.5149	0.0121	0.9639	2707	17	2678	102	1.3	2707	17	
110			223722	3242	0.1905	0.0011	13.9488	0.2813	0.5292	0.0102	0.9477	2746	19	2738	98	0.4	2746	19	
106	pink	subang	385067	7859	0.1911	0.0011	13.8444	0.3400	0.5251	0.0125	0.9554	2752	19	2721	104	1.4	2752	19	
88	pink	subang	760488	760488	0.1978	0.0004	13.9931	0.2653	0.5107	0.0096	0.9589	2808	17	2659	94	6.5	2808	17	
27		sub-rnd	253127	1145	0.2012	0.0012	15.3401	0.7758	0.5538	0.0278	0.9806	2836	19	2841	166	-0.2	2836	19	
108	cll	rnd	96021	infinite	0.2219	0.0007	18.6054	0.2995	0.6076	0.0096	0.9528	2994	17	3061	104	-2.8	2994	17	

Broadview Fm, 08TWJK043

Zircon 40 um

Depositional age: (Ordovician?-)Devonian

Location (UTM): 475774E, 5612834N

n= 108

Grain	colour	shape	^{206}Pb cps	^{206}Pb/^{204}Pb	^{207}Pb/^{206}Pb	± (2σ)	^{207}Pb/^{235}U	± (2σ)	^{206}Pb/^{238}U	± (2σ)	rho	Model Ages ^{207}Pb/^{206}Pb	± (2σ)	^{206}Pb/^{238}U	± (2σ)	% disc.	Best Age (Ma)	± (2σ)
GJ1-32-1			263043	infinite	0.0603	0.0007	0.8105	0.0331	0.0974	0.0038	0.9636	615	24	599	22	2.7		
GJ1-32-2			249849	infinite	0.0602	0.0006	0.7873	0.0317	0.0948	0.0037	0.9636	611	23	584	22	4.7		
GJ1-32-3			259849	infinite	0.0594	0.0007	0.7955	0.0317	0.0972	0.0037	0.9601	581	24	598	22	-3.0		
GJ1-32-4			291083	infinite	0.0591	0.0009	0.8144	0.0333	0.0999	0.0038	0.9323	571	32	614	22	-7.9		
GJ1-32-5			290136	infinite	0.0608	0.0010	0.8074	0.0336	0.0963	0.0037	0.9213	632	35	593	22	6.4		
GJ1-32-6			303767	infinite	0.0605	0.0011	0.8141	0.0350	0.0975	0.0038	0.9140	623	38	600	22	3.8		
GJ1-32-7			295741	infinite	0.0608	0.0009	0.8135	0.0339	0.0971	0.0038	0.9283	632	33	597	22	5.7		
GJ1-32-8			282955	infinite	0.0607	0.0008	0.8246	0.0336	0.0985	0.0038	0.9477	630	28	605	22	4.1		
GJ1-32-9			264108	infinite	0.0610	0.0010	0.7876	0.0340	0.0936	0.0037	0.9269	641	35	577	22	10.5		
GJ1-32-10			267445	infinite	0.0609	0.0013	0.8113	0.0365	0.0967	0.0038	0.8857	634	45	595	23	6.4		
GJ1-32-11			185134	1202	0.0605	0.0010	0.7875	0.0326	0.0944	0.0036	0.9241	621	34	582	21	6.7		
GJ1-32-12			568949	5080	0.0604	0.0011	0.7751	0.0335	0.0931	0.0036	0.8978	617	41	574	21	7.4		
116	cll	subrnd	434243	2399	0.0659	0.0009	1.6250	0.3592	0.1787	0.0066	0.9093	805	35	1060	36	-6.9	805	35
66	pnk	rnd	336563	2650	0.0689	0.0005	1.5881	0.0350	0.1672	0.0058	0.9399	895	26	997	32	3.8	895	26
30	ylw	rnd	105847	infinite	0.0709	0.0007	1.6301	0.0317	0.1667	0.0061	0.9320	955	29	994	33	-3.0	955	29
65	pnk	rnd	194369	1676	0.0715	0.0010	1.9057	0.1855	0.1932	0.0072	0.9057	973	35	1139	39	-5.0	973	35
1	cll	rnd	122640	3833	0.0756	0.0011	2.0526	0.0799	0.1970	0.0068	0.8852	1084	36	1159	36	-7.6	1084	36
19	cll	subrnd	195380	8881	0.0773	0.0008	1.7564	0.1465	0.1648	0.0072	0.9527	1129	28	983	40	19.4	reject	
72	pnk	rnd	458386	7903	0.0773	0.0005	1.8845	0.0587	0.1768	0.0059	0.9406	1130	24	1049	32	-12.2	reject	
36	pnk	rnd	238813	39802	0.0775	0.0004	2.1039	0.1870	0.1970	0.0069	0.9494	1133	23	1159	37	-1.5	1133	23
24	cll	subrnd	237809	infinite	0.0779	0.0004	2.2166	0.2687	0.2063	0.0071	0.9500	1145	22	1209	38	-1.7	1145	22
115	cll	subrnd	279393	infinite	0.0810	0.0006	2.4434	0.1583	0.2188	0.0075	0.9392	1221	25	1276	39	-9.9	1221	25
31	ylw	rnd	115621	infinite	0.0818	0.0007	2.1700	0.4788	0.1925	0.0070	0.9425	1240	25	1135	38	2.7	1240	25
101	cll	rnd	255421	4561	0.0841	0.0008	2.5941	0.1648	0.2237	0.0086	0.9435	1295	26	1301	45	1.5	1295	26
103	cll	rnd	130509	2663	0.0842	0.0015	2.6550	0.1736	0.2287	0.0082	0.8694	1297	40	1328	43	2.8	1297	40
110	cll	rnd	289141	3012	0.0871	0.0005	3.0199	0.1060	0.2516	0.0088	0.9505	1362	22	1446	45	-0.6	1362	22
76	pnk	rnd	275663	4672	0.0881	0.0010	2.8016	0.3056	0.2307	0.0090	0.9352	1384	29	1338	47	4.0	1384	29
14	cll	subrnd	344102	infinite	0.0883	0.0003	2.6859	0.1620	0.2205	0.0079	0.9606	1390	20	1284	42	6.4	1390	20
85	pnk	subrnd	282731	4220	0.0936	0.0007	3.1265	0.3618	0.2423	0.0084	0.9419	1500	23	1399	44	6.9	1500	23
105	cll	rnd	134625	716	0.0943	0.0021	3.7860	0.1733	0.2911	0.0099	0.8162	1515	46	1647	49	6.5	1515	46
49	pnk	prism	117286	798	0.0966	0.0014	4.3088	0.1663	0.3236	0.0104	0.8809	1559	33	1807	51	-4.3	1559	33

Broadview Fm, 08TWJK043
Zircon 40 um

Depositional age: (Ordovician?-)Devonian
Location (UTM): 475774E, 5612834N

n= 108

Grain	colour	shape	^{206}Pb cps	$^{206}Pb/^{204}Pb$	$^{207}Pb/^{206}Pb$	± (2σ)	$^{207}Pb/^{235}U$	± (2σ)	$^{206}Pb/^{238}U$	± (2σ)	rho	Model Ages $^{207}Pb/^{206}Pb$	± (2σ)	Model Ages $^{206}Pb/^{238}U$	± (2σ)	% disc.	Best Age (Ma)	± (2σ)
61	pnk	rnd	229420	1639	0.1013	0.0019	4.4583	0.1840	0.3193	0.0120	0.8668	1648	40	1786	58	-6.5	1648	40
119	cll	subrnd	176944	1361	0.1017	0.0012	4.4973	0.1929	0.3206	0.0113	0.9160	1656	29	1792	55	-7.8	1656	29
41	pnk	prism	50233	1570	0.1027	0.0039	4.6576	0.1696	0.3290	0.0110	0.6489	1673	73	1834	53	-0.2	1673	73
27	cll	prism	47314	infinite	0.1027	0.0012	4.3436	0.1921	0.3066	0.0110	0.9163	1674	29	1724	54	-6.4	1674	29
117	cll	subrnd	221838	1395	0.1029	0.0017	4.6969	0.2137	0.3310	0.0106	0.8594	1678	35	1843	51	1.3	1678	35
63	pnk	rnd	135234	1166	0.1030	0.0015	4.6633	0.1629	0.3285	0.0111	0.8851	1678	33	1831	54	-3.0	1678	33
111	cll	rnd	289141	3012	0.1039	0.0013	4.7671	0.4394	0.3327	0.0110	0.9013	1695	29	1852	53	-2.9	1695	29
50	pnk	rnd	149518	1359	0.1040	0.0014	4.6584	0.1649	0.3248	0.0112	0.9017	1697	31	1813	54	-3.5	1697	31
129	pnk	rnd	247665	infinite	0.1041	0.0009	3.9711	0.3914	0.2766	0.0119	0.9577	1699	24	1574	60	-1.0	1699	24
58	pnk	rnd	196963	1669	0.1052	0.0011	4.5609	0.1803	0.3145	0.0102	0.9117	1718	27	1763	50	-2.4	1718	27
108	cll	rnd	142688	1413	0.1052	0.0014	4.7393	0.3821	0.3267	0.0106	0.8912	1718	30	1823	51	3.5	1718	30
71	pnk	rnd	199650	2017	0.1053	0.0011	4.6498	0.0782	0.3201	0.0104	0.9123	1720	27	1790	50	-18.6	reject	
113	cll	rnd	303590	2153	0.1054	0.0010	4.9831	0.3592	0.3430	0.0117	0.9296	1721	25	1901	56	-12.5	reject	
81	pnk	subrnd	133841	1761	0.1057	0.0011	4.5532	0.1790	0.3125	0.0109	0.9261	1726	26	1753	53	-1.7	1726	26
91	pnk	subrnd	287923	3063	0.1058	0.0007	3.5276	0.4317	0.2417	0.0098	0.9594	1729	22	1396	51	5.5	1729	22
125	pnk	rnd	299899	3190	0.1059	0.0009	4.5861	0.0326	0.3141	0.0105	0.9323	1730	24	1761	51	6.7	1730	24
120	cll	subrnd	149592	1160	0.1060	0.0008	4.6694	0.1110	0.3196	0.0109	0.9385	1731	23	1788	53	-6.9	1731	23
54	pnk	rnd	136601	1076	0.1060	0.0012	4.9749	0.0336	0.3404	0.0115	0.9157	1732	27	1889	55	6.4	1732	27
56	pnk	rnd	223197	1908	0.1061	0.0010	4.8036	0.4702	0.3285	0.0118	0.9342	1733	25	1831	57	1.8	1733	25
53	pnk	rnd	219670	1815	0.1061	0.0007	4.6180	0.1578	0.3157	0.0117	0.9498	1733	22	1769	57	-18.3	reject	
100	cll	rnd	154565	1593	0.1066	0.0013	4.8128	0.1344	0.3274	0.0119	0.9192	1742	29	1826	58	20.5	reject	
62	pnk	rnd	256895	1976	0.1072	0.0008	4.6739	0.1744	0.3163	0.0112	0.9450	1752	22	1771	55	-7.0	1752	22
46	pnk	prism	352252	2669	0.1073	0.0005	4.7849	0.1833	0.3236	0.0105	0.9459	1753	20	1807	51	4.6	1753	20
97	pnk	subrnd	205635	2120	0.1073	0.0010	4.5735	0.1807	0.3092	0.0098	0.9199	1754	25	1737	48	3.9	1754	25
20	cll	subrnd	59031	7379	0.1073	0.0019	4.8420	0.4780	0.3271	0.0124	0.8848	1755	37	1824	60	0.9	1755	37
26	cll	prism	291964	22459	0.1075	0.0005	4.4166	0.0803	0.2980	0.0104	0.9529	1757	20	1682	51	-6.2	1757	20
130	pnk	rnd	175792	2021	0.1075	0.0012	4.6533	0.1736	0.3139	0.0104	0.9143	1758	27	1760	51	-9.4	1758	27
88	pnk	subrnd	401731	6809	0.1079	0.0006	4.4929	0.1718	0.3019	0.0099	0.9460	1765	21	1701	49	-1.8	1765	21
25	cll	subrnd	200536	infinite	0.1081	0.0005	5.0001	0.4401	0.3356	0.0124	0.9580	1767	20	1865	59	9.2	1767	20
39	pnk	rnd	220640	4163	0.1082	0.0006	4.6570	0.0773	0.3123	0.0101	0.9411	1769	21	1752	49	-2.5	1769	21
92	pnk	subrnd	215577	2450	0.1084	0.0007	3.7660	0.4058	0.2519	0.0084	0.9402	1773	22	1448	43	5.3	1773	22
109	cll	rnd	145877	1758	0.1085	0.0010	5.1069	0.1910	0.3415	0.0120	0.9318	1774	25	1894	58	-5.5	1774	25
77	pnk	rnd	289323	2704	0.1087	0.0006	4.8465	0.1649	0.3235	0.0109	0.9453	1777	21	1807	53	-4.7	1777	21
57	pnk	rnd	305445	3117	0.1089	0.0006	5.1077	0.1799	0.3403	0.0110	0.9435	1780	21	1888	53	0.1	1780	21
45	pnk	prism	395088	3265	0.1089	0.0006	4.9812	0.2408	0.3318	0.0104	0.9419	1781	20	1847	50	-11.1	reject	

Broadview Fm, 08TWJK043 | Depositional age: (Ordovician?-)Devonian | n= 108

Zircon 40 um | Location (UTM): 475774E, 5612834N

Grain	colour	shape	^{206}Pb cps	^{206}Pb/^{204}Pb	^{207}Pb/^{206}Pb	± (2σ)	^{207}Pb/^{235}U	± (2σ)	^{206}Pb/^{238}U	± (2σ)	rho	Model Ages ^{207}Pb/^{206}Pb	± (2σ)	^{206}Pb/^{238}U	± (2σ)	% disc.	Best Age (Ma)	± (2σ)
121	pnk	rnd	182316	1558	0.1091	0.0006	4.7625	0.1757	0.3166	0.0107	0.9486	1785	21	1773	52	-10.6	reject	
131	pnk	rnd	282081	2411	0.1093	0.0007	4.8904	0.1703	0.3244	0.0111	0.9442	1788	22	1811	54	-4	1788	22
74	pnk	rnd	226159	3231	0.1094	0.0008	4.9117	0.2741	0.3255	0.0112	0.9430	1790	22	1816	54	4.1	1790	22
47	pnk	prism	462904	3404	0.1095	0.0007	5.0773	0.1655	0.3362	0.0110	0.9418	1792	21	1868	53	7.1	1792	21
60	pnk	rnd	185167	1556	0.1097	0.0010	5.0914	0.5276	0.3367	0.0113	0.9250	1794	25	1871	54	-3.9	1794	25
79	pnk	subrnd	562462	5257	0.1097	0.0004	4.4208	0.0663	0.2924	0.0096	0.9524	1794	19	1653	48	7.7	1794	19
69	pnk	rnd	275602	2841	0.1099	0.0010	4.8799	0.1788	0.3220	0.0111	0.9315	1798	25	1800	54	-10.5	reject	
80	pnk	subrnd	404229	3642	0.1100	0.0007	4.6065	0.4158	0.3038	0.0102	0.9430	1799	22	1710	50	15.3	reject	
93	pnk	subrnd	430181	4345	0.1104	0.0004	4.8436	0.1155	0.3183	0.0103	0.9501	1805	19	1781	50	7.5	1805	19
38	pnk	rnd	576996	12822	0.1107	0.0003	4.9624	0.1873	0.3251	0.0106	0.9527	1811	19	1814	51	3.1	1811	19
4	cll	rnd	170819	18980	0.1109	0.0012	5.5544	0.2918	0.3632	0.0183	0.9591	1814	27	1997	86	-11.7	reject	
13	cll	subrnd	220124	infinite	0.1110	0.0004	4.6641	0.3993	0.3047	0.0101	0.9530	1816	19	1714	50	7.4	1816	19
96	pnk	subrnd	164697	1771	0.1111	0.0008	4.6619	0.1558	0.3044	0.0107	0.9445	1817	22	1713	53	4.1	1817	22
94	pnk	subrnd	549674	6176	0.1115	0.0006	4.8884	0.1936	0.3180	0.0107	0.9492	1824	20	1780	52	3.6	1824	20
123	pnk	rnd	0	infinite	0.1115	0.0014	5.1424	0.1826	0.3344	0.0110	0.8989	1824	29	1860	53	-12.1	reject	
43	pnk	prism	687021	27481	0.1115	0.0003	4.6761	0.1594	0.3040	0.0103	0.9552	1825	19	1711	51	1.1	1825	19
33	cll	prism	233999	infinite	0.1117	0.0003	5.1223	0.0636	0.3325	0.0116	0.9582	1828	19	1851	56	-4.4	1828	19
126	pnk	rnd	196316	2181	0.1117	0.0015	4.9423	0.0889	0.3208	0.0114	0.9074	1828	30	1794	55	-4.9	1828	30
95	pnk	subrnd	587408	6249	0.1118	0.0004	4.8531	0.1643	0.3147	0.0121	0.9636	1830	19	1764	59	6.5	1830	19
87	pnk	subrnd	662766	12050	0.1121	0.0004	4.7538	0.1647	0.3076	0.0101	0.9524	1834	19	1729	50	5.6	1834	19
16	cll	subrnd	146542	infinite	0.1121	0.0003	4.9851	0.4191	0.3224	0.0109	0.9566	1834	19	1802	53	5.3	1834	19
52	pnk	rnd	641717	5303	0.1122	0.0003	5.0934	0.4574	0.3292	0.0111	0.9557	1836	19	1834	54	-5.2	1836	19
17	cll	subrnd	151049	infinite	0.1126	0.0004	4.1409	0.1768	0.2666	0.0090	0.9534	1842	19	1524	46	2.0	1842	19
10	cll	rnd	116958	infinite	0.1127	0.0004	5.1098	0.3875	0.3289	0.0112	0.9553	1843	19	1833	54	1.7	1843	19
8	cll	rnd	122006	infinite	0.1129	0.0004	5.2548	0.1995	0.3375	0.0122	0.9596	1847	19	1874	59	0.3	1847	19
44	pnk	prism	196442	infinite	0.1138	0.0009	4.9362	0.3215	0.3146	0.0101	0.9277	1861	23	1763	49	34.0	reject	
42	pnk	prism	140081	8240	0.1141	0.0009	5.0392	0.0333	0.3202	0.0109	0.9345	1866	23	1791	53	-7.9	1866	23
29	ylw	prism	159180	14471	0.1154	0.0005	5.3270	0.1700	0.3349	0.0119	0.9554	1885	20	1862	57	-3.4	1885	20
128	pnk	rnd	209292	2093	0.1155	0.0005	5.3924	0.1748	0.3387	0.0112	0.9487	1887	20	1881	54	-11.3	reject	
89	pnk	subrnd	679684	7724	0.1157	0.0003	5.2302	0.4045	0.3278	0.0108	0.9547	1891	18	1828	52	17.1	reject	
35	pnk	rnd	409616	31509	0.1175	0.0004	5.4400	0.4626	0.3359	0.0110	0.9529	1918	19	1867	53	1.6	1918	19
86	pnk	subrnd	549685	9994	0.1176	0.0003	5.4229	0.1531	0.3345	0.0114	0.9576	1920	18	1860	55	8.9	1920	18
11	cll	rnd	124203	infinite	0.1182	0.0003	5.6690	0.1828	0.3478	0.0118	0.9563	1930	19	1924	56	0.6	1930	19
7	cll	rnd	187632	infinite	0.1186	0.0004	5.7063	0.4248	0.3490	0.0116	0.9543	1935	19	1930	55	-1.0	1935	19
127	pnk	rnd	384523	3924	0.1213	0.0006	6.0479	0.0655	0.3617	0.0122	0.9486	1975	20	1990	58	-34.4	reject	

Broadview Fm, 08TWJK043
Zircon 40 um

Depositional age: (Ordovician?-)Devonian
Location (UTM): 475774E, 5612834N

n= 108

Grain	colour	shape	^{206}Pb cps	$^{206}Pb/^{204}Pb$	$^{207}Pb/^{206}Pb$	± (2σ)	$^{207}Pb/^{235}U$	± (2σ)	$^{206}Pb/^{238}U$	± (2σ)	rho	Model Ages $^{207}Pb/^{206}Pb$	± (2σ)	$^{206}Pb/^{238}U$	± (2σ)	% disc.	Best Age (Ma)	± (2σ)
107	cll	rnd	216194	2300	0.1237	0.0008	6.1578	0.4245	0.3611	0.0118	0.9376	2010	21	1987	55	9.1	2010	21
104	cll	rnd	43672	607	0.1246	0.0042	7.1231	0.1944	0.4147	0.0151	0.7208	2023	62	2236	68	4.1	2023	62
22	cll	subrnd	66969	4186	0.1296	0.0019	6.9763	0.2079	0.3903	0.0133	0.8841	2093	32	2124	61	-4.6	2093	32
34	pnk	rnd	930858	24496	0.1380	0.0006	5.4814	0.0832	0.2882	0.0096	0.9502	2202	19	1632	48	9.2	2202	19
102	cll	rnd	46945	533	0.1382	0.0053	7.9947	0.0340	0.4195	0.0161	0.6981	2205	68	2258	73	10.5	reject	
112	cll	rnd	122687	1105	0.1406	0.0007	8.0716	0.1095	0.4165	0.0142	0.9509	2234	19	2245	64	-2.7	2234	19
68	pnk	rnd	337278	4497	0.1407	0.0006	7.7112	0.1755	0.3975	0.0135	0.9530	2236	19	2158	62	-1.3	2236	19
106	cll	rnd	141163	1384	0.1409	0.0033	8.6212	0.1583	0.4437	0.0146	0.7911	2238	44	2367	65	1.1	2238	44
70	pnk	rnd	280106	3012	0.1532	0.0006	9.0653	0.4035	0.4293	0.0137	0.9490	2382	18	2302	62	6.4	2382	18
37	pnk	rnd	817089	58364	0.1559	0.0003	8.7528	0.1924	0.4071	0.0136	0.9565	2412	17	2202	62	29.2	reject	
75	pnk	rnd	352933	5430	0.1559	0.0007	8.8303	0.1807	0.4107	0.0137	0.9503	2412	19	2218	62	-0.1	2412	19
6	cll	rnd	595334	infinite	0.1654	0.0002	10.9771	0.0331	0.4812	0.0180	0.9653	2512	17	2533	78	2.7	2512	17
99	pnk	subrnd	411183	7907	0.1665	0.0005	10.6106	0.1489	0.4621	0.0159	0.9564	2523	18	2449	70	21.4	reject	
118	cll	subrnd	128504	938	0.1669	0.0012	11.1539	0.1732	0.4847	0.0159	0.9361	2527	21	2548	69	-7.0	2527	21
9	cll	rnd	161743	infinite	0.1670	0.0003	10.8639	0.1979	0.4719	0.0161	0.9582	2527	17	2492	70	-1.7	2527	17
40	pnk	rnd	1025130	5177	0.1697	0.0013	7.5072	0.3065	0.3209	0.0131	0.9568	2555	21	1794	64	10.3	reject	
78	pnk	subrnd	767258	6394	0.1715	0.0004	10.7933	0.0339	0.4565	0.0146	0.9525	2572	17	2424	64	5.7	2572	17
55	pnk	rnd	232719	1521	0.1732	0.0010	12.2523	0.1786	0.5132	0.0213	0.9628	2588	19	2670	90	-7.9	2588	19
84	pnk	subrnd	343057	5278	0.1738	0.0005	11.2369	0.1721	0.4690	0.0162	0.9580	2594	17	2479	71	-1.9	2594	17
48	pnk	prism	104080	765	0.1741	0.0013	12.5310	0.1709	0.5221	0.0179	0.9382	2597	21	2708	75	6.0	2597	21
90	pnk	subrnd	599303	8099	0.1753	0.0004	11.4228	0.0336	0.4727	0.0163	0.9587	2608	17	2495	71	4.1	2608	17
32	ylw	rnd	176094	infinite	0.1778	0.0005	12.1637	0.1984	0.4962	0.0182	0.9622	2632	17	2597	78	1.4	2632	17
59	pnk	rnd	188552	1366	0.1783	0.0010	12.2579	0.1830	0.4986	0.0176	0.9515	2637	19	2608	75	-10.5	reject	
114	cll	rnd	157502	1141	0.1792	0.0009	12.7556	0.0365	0.5163	0.0184	0.9536	2645	19	2684	78	6.4	2645	19
12	cll	subrnd	209330	infinite	0.1792	0.0011	11.6081	0.2004	0.4697	0.0152	0.9407	2646	19	2482	66	0.3	2646	19
3	cll	rnd	121407	6070	0.1792	0.0010	12.2793	0.4339	0.4968	0.0166	0.9460	2646	19	2600	71	2.1	2646	19
21	cll	subrnd	363042	16502	0.1800	0.0005	11.5774	0.0806	0.4664	0.0156	0.9546	2653	17	2468	68	13.9	reject	
51	pnk	rnd	407507	3638	0.1805	0.0004	12.4680	0.1763	0.5011	0.0182	0.9620	2657	17	2619	78	-4.9	2657	17
124	pnk	rnd	0	infinite	0.1815	0.0005	12.3870	0.4774	0.4949	0.0177	0.9600	2667	17	2592	76	-1.8	2667	17
64	pnk	rnd	483275	3805	0.1818	0.0006	12.0444	0.4549	0.4804	0.0153	0.9498	2670	17	2529	66	1.3	2670	17
23	cll	subrnd	785713	98214	0.1823	0.0003	11.7362	0.4049	0.4669	0.0169	0.9625	2674	17	2470	74	8.4	2674	17
83	pnk	subrnd	689400	7924	0.1828	0.0003	12.2746	0.1175	0.4870	0.0164	0.9574	2678	17	2558	71	3.7	2678	17
28	cll	subrnd	180928	infinite	0.1834	0.0004	12.7030	0.1617	0.5024	0.0182	0.9620	2684	17	2624	78	4.9	2684	17
98	pnk	subrnd	842486	10531	0.1851	0.0003	12.0526	0.4102	0.4724	0.0159	0.9576	2699	17	2494	69	5.2	2699	17
15	cll	subrnd	349004	infinite	0.1856	0.0003	12.6178	0.1006	0.4931	0.0156	0.9524	2703	17	2584	67	8.4	2703	17

Broadview Fm, 08TWJK043
Zircon 40 um

Depositional age: (Ordovician?-)Devonian
Location (UTM): 475774E, 5612834N

n= 108

Grain	colour	shape	^{206}Pb cps	$^{206}Pb/^{204}Pb$	$^{207}Pb/^{206}Pb$	± (2σ)	$^{207}Pb/^{235}U$	± (2σ)	$^{206}Pb/^{238}U$	± (2σ)	rho	Model Ages $^{207}Pb/^{206}Pb$	± (2σ)	$^{206}Pb/^{238}U$	± (2σ)	% disc.	Best Age (Ma)	± (2σ)
82	pnk	subrnd	496442	7522	0.1856	0.0004	11.0565	0.3090	0.4321	0.0152	0.9601	2703	17	2315	68	9.5	2703	17
5	cll	rnd	159283	infinite	0.1859	0.0005	13.3126	0.5272	0.5193	0.0198	0.9648	2707	17	2696	84	0.5	2707	17
73	pnk	rnd	761567	9890	0.1867	0.0004	11.4021	0.5816	0.4430	0.0155	0.9599	2713	17	2364	69	6.4	2713	17
18	cll	subrnd	145454	infinite	0.1876	0.0005	13.4662	0.0317	0.5205	0.0177	0.9567	2722	17	2701	75	4.7	2722	17
2	cll	rnd	340957	8742	0.1971	0.0007	11.6802	0.6158	0.4298	0.0222	0.9796	2802	17	2305	99	21.1	reject	
122	pnk	rnd	0	infinite	0.1988	0.0007	13.2061	0.2901	0.4818	0.0168	0.9570	2816	17	2535	73	-0.6	2816	17
67	pnk	rnd	351039	4179	0.2255	0.0006	17.3807	0.1932	0.5591	0.0178	0.9510	3020	17	2863	73	-9.6	3020	17

Broadview Fm, 07TWJK516
Zircon 40 um

Depositional age: (Ordovician?-)Devonian
Location (UTM): 430676E, 5626451N

n= 128

											Model Ages						
Grain	**shape**	**^{206}Pb cps**	**$^{206}Pb/^{204}Pb$**	**$^{207}Pb/^{206}Pb$**	**± (2σ)**	**$^{207}Pb/^{235}U$**	**± (2σ)**	**$^{206}Pb/^{238}U$**	**± (2σ)**	**rho**	**$^{207}Pb/^{206}Pb$**	**± (2σ)**	**$^{206}Pb/^{238}U$**	**± (2σ)**	**% disc.**	**Best Age (Ma)**	**± (2σ)**
44	subrnd	877637	3483	0.0700	0.0005	1.1022	0.0299	0.1141	0.0030	0.9557	927	25	697	28	26.2	reject	
125	rnd	393545	13118	0.0702	0.0012	1.5291	0.0326	0.1571	0.0020	0.8456	936	40	941	31	-0.6	936	40
58	rnd	448060	8961	0.0706	0.0004	1.5018	0.0268	0.1528	0.0026	0.9467	946	23	917	32	3.3	946	23
121	rnd	423649	21182	0.0711	0.0007	1.5166	0.0210	0.1540	0.0014	0.8994	959	30	923	29	4.0	959	30
77	rnd	71183	infinite	0.0716	0.0005	1.5825	0.0233	0.1590	0.0021	0.9347	975	24	951	31	2.7	975	24
110	rnd	177299	infinite	0.0716	0.0004	1.5113	0.0287	0.1518	0.0028	0.9497	975	23	911	32	7.1	975	23
94	rnd	124710	6236	0.0720	0.0025	1.5930	0.0607	0.1595	0.0025	0.6692	987	73	954	32	3.6	987	73
64	rnd	176973	3539	0.0724	0.0044	1.6937	0.1125	0.1682	0.0046	0.5385	997	125	1002	41	-0.6	997	125
69	rnd	563394	28170	0.0724	0.0006	1.5640	0.0299	0.1559	0.0027	0.9349	998	26	934	32	6.9	998	26
66	rnd	992681	5117	0.0725	0.0003	1.5643	0.0326	0.1560	0.0032	0.9562	1001	22	935	34	7.1	1001	22
148	subrnd	152970	infinite	0.0726	0.0004	1.6323	0.0177	0.1614	0.0016	0.9387	1002	23	965	30	4	1002	23
86	rnd	716951	infinite	0.0729	0.0002	1.5175	0.0231	0.1501	0.0023	0.9535	1012	21	902	30	11.7	reject	
70	rnd	89925	8993	0.0729	0.0017	1.6702	0.0569	0.1643	0.0040	0.8207	1012	53	981	38	3.3	1012	53
17	frag	717593	3292	0.0730	0.0015	1.6623	0.0882	0.1660	0.0082	0.9300	1015	45	990	57	2.6	1015	45
82	rnd	715166	3804	0.0731	0.0004	1.6787	0.0298	0.1662	0.0028	0.9479	1016	23	991	34	2.6	1016	23
65	rnd	504485	infinite	0.0731	0.0002	1.5472	0.0397	0.1529	0.0039	0.9657	1016	21	917	36	10.4	reject	
100	rnd	536506	infinite	0.0731	0.0001	1.6472	0.0280	0.1623	0.0027	0.9561	1018	21	970	33	5.1	1018	21
12	prism	294838	infinite	0.0732	0.0002	1.5294	0.0345	0.1509	0.0034	0.9605	1019	21	906	34	11.8	reject	
53	subrnd	246976	infinite	0.0732	0.0002	1.6784	0.0354	0.1652	0.0034	0.9591	1019	21	986	36	3.5	1019	21
160	rnd	255098	infinite	0.0733	0.0002	1.8050	0.0366	0.1783	0.0036	0.9586	1023	21	1058	38	-4	1023	21
107	rnd	158266	infinite	0.0737	0.0003	1.6978	0.0350	0.1651	0.0033	0.9559	1033	22	985	36	5.0	1033	22
117	rnd	361842	infinite	0.0738	0.0002	1.7143	0.0210	0.1672	0.0020	0.9471	1035	21	997	32	3.9	1035	21
47	subrnd	659788	6598	0.0738	0.0024	1.6411	0.0586	0.1609	0.0025	0.6958	1035	68	962	33	7.6	1035	68
112	rnd	97085	infinite	0.0739	0.0005	1.8495	0.0480	0.1781	0.0045	0.9543	1037	24	1057	41	-2.0	1037	24
152	frag	209573	infinite	0.0739	0.0003	1.6821	0.0383	0.1633	0.0037	0.9605	1040	21	975	37	7	1040	21
134	rnd	286465	infinite	0.0741	0.0002	1.8686	0.0427	0.1818	0.0041	0.9609	1043	21	1077	40	-3	1043	21
1	subrnd	883784	6313	0.0741	0.0003	1.7900	0.0463	0.1751	0.0045	0.9635	1044	22	1040	41	0.4	1044	22
153	frag	220890	infinite	0.0741	0.0002	1.7088	0.0147	0.1660	0.0013	0.9439	1045	21	990	31	6	1045	21
101	rnd	86487	infinite	0.0742	0.0005	1.8096	0.0272	0.1743	0.0024	0.9367	1047	24	1036	34	1.1	1047	24
97	rnd	360320	infinite	0.0742	0.0002	1.7632	0.0321	0.1711	0.0031	0.9560	1047	21	1018	36	3.0	1047	21
132	rnd	211944	infinite	0.0744	0.0002	1.8092	0.0252	0.1747	0.0024	0.9504	1051	21	1038	34	1	1051	21
74	rnd	79347	39673	0.0744	0.0005	1.7179	0.0316	0.1663	0.0028	0.9379	1054	25	992	34	6.4	1054	25

Broadview Fm, 07TWJK516
Zircon 40 um

Depositional age: (Ordovician?-)Devonian
Location (UTM): 430676E, 5626451N

n= 128

Grain	shape	^{206}Pb cps	$^{206}Pb/^{204}Pb$	$^{207}Pb/^{206}Pb$	± (2σ)	$^{207}Pb/^{235}U$	± (2σ)	$^{206}Pb/^{238}U$	± (2σ)	rho	Model Ages $^{207}Pb/^{206}Pb$	± (2σ)	Model Ages $^{206}Pb/^{238}U$	± (2σ)	% disc.	Best Age (Ma)	± (2σ)
108	rnd	220949	infinite	0.0745	0.0003	1.7438	0.0309	0.1682	0.0029	0.9534	1054	21	1002	35	5.3	1054	21
115	rnd	131891	infinite	0.0746	0.0004	1.6193	0.0284	0.1554	0.0026	0.9473	1058	23	931	32	12.9	reject	
133	rnd	125257	infinite	0.0747	0.0004	1.9013	0.0449	0.1829	0.0042	0.9570	1059	22	1083	41	-2	1059	22
127	rnd	142181	infinite	0.0747	0.0004	1.8670	0.0268	0.1791	0.0024	0.9440	1060	22	1062	35	-0.2	1060	22
85	rnd	451190	infinite	0.0747	0.0002	1.6532	0.0385	0.1593	0.0037	0.9620	1061	21	953	36	10.9	reject	
116	rnd	739449	infinite	0.0750	0.0001	1.7615	0.0323	0.1695	0.0031	0.9589	1070	20	1009	35	6.1	1070	20
40	subrnd	417405	2130	0.0752	0.0007	1.9707	0.0402	0.1893	0.0034	0.9282	1074	27	1117	39	-4.4	1074	27
144	rnd	376815	infinite	0.0752	0.0002	1.8125	0.0251	0.1743	0.0024	0.9510	1074	21	1036	34	4	1074	21
122	rnd	757219	3522	0.0752	0.0005	2.0340	0.0390	0.1955	0.0036	0.9457	1075	23	1151	40	-7.8	1075	23
38	subrnd	128481	12848	0.0753	0.0012	1.7603	0.0418	0.1684	0.0029	0.8654	1075	39	1003	35	7.2	1075	39
9	frag	133244	infinite	0.0757	0.0006	1.7927	0.0451	0.1702	0.0041	0.9479	1086	25	1013	39	7.3	1086	25
13	frag	178592	infinite	0.0760	0.0004	1.8208	0.0453	0.1731	0.0042	0.9595	1094	22	1029	40	6.4	1094	22
8	frag	23486	infinite	0.0760	0.0014	1.9456	0.0721	0.1826	0.0058	0.8968	1094	42	1081	47	1.3	1094	42
158	subrnd	261824	infinite	0.0762	0.0002	1.9268	1.0000	0.1840	0.0038	25.2999	1101	6	1089	22	1	1101	6
89	rnd	102689	infinite	0.0764	0.0005	1.8369	0.0302	0.1721	0.0026	0.9417	1107	23	1024	34	8.1	1107	23
14	frag	104141	infinite	0.0766	0.0004	1.8787	0.0429	0.1768	0.0040	0.9566	1112	22	1050	39	6.0	1112	22
3	subrnd	135769	infinite	0.0767	0.0004	1.8656	0.0549	0.1750	0.0051	0.9656	1113	22	1040	43	7.1	1113	22
161	rnd	708303	35415	0.0768	0.0005	1.9888	0.0417	0.1880	0.0038	0.9490	1116	23	1111	40	1	1116	23
79	rnd	590672	2773	0.0768	0.0004	1.9306	0.0412	0.1815	0.0038	0.9534	1117	22	1075	39	4.0	1117	22
102	rnd	401217	infinite	0.0769	0.0002	1.8170	0.0325	0.1703	0.0030	0.9570	1118	20	1014	35	10.1	reject	
78	rnd	30570	infinite	0.0773	0.0007	1.9754	0.0319	0.1822	0.0024	0.9191	1130	27	1079	35	4.9	1130	27
130	rnd	224456	infinite	0.0775	0.0003	2.0391	0.0383	0.1892	0.0035	0.9534	1133	21	1117	39	1.6	1133	21
50	subrnd	50162	infinite	0.0775	0.0002	1.6752	0.0395	0.1560	0.0037	0.9638	1134	20	935	36	18.9	reject	
135	rnd	493111	infinite	0.0776	0.0002	2.0613	0.0351	0.1917	0.0032	0.9559	1137	20	1130	39	1	1137	20
5	frag	46643	infinite	0.0777	0.0011	1.7974	0.0483	0.1665	0.0038	0.8988	1140	35	993	37	13.9	reject	
56	rnd	390380	infinite	0.0778	0.0016	1.8780	0.0418	0.1744	0.0015	0.7944	1141	45	1036	32	9.9	1141	45
103	rnd	283701	28370	0.0780	0.0006	2.0161	0.0493	0.1860	0.0043	0.9473	1146	25	1100	42	4.4	1146	25
72	rnd	571584	3248	0.0781	0.0010	1.5165	0.0523	0.1408	0.0045	0.9347	1151	32	849	37	28.0	reject	
105	rnd	172431	infinite	0.0783	0.0004	2.1099	0.0410	0.1941	0.0037	0.9523	1153	22	1144	41	0.9	1153	22
126	rnd	588171	infinite	0.0783	0.0001	2.1291	0.0384	0.1965	0.0035	0.9583	1154	20	1156	40	-0.3	1154	20
88	rnd	94079	infinite	0.0783	0.0004	1.9992	0.0381	0.1826	0.0034	0.9514	1154	22	1081	38	6.9	1154	22
6	prism	74423	infinite	0.0783	0.0005	2.0646	0.0514	0.1884	0.0045	0.9513	1154	24	1113	43	3.9	1154	24

Broadview Fm, 07TWJK516 Depositional age: (Ordovician?-)Devonian n= 128

Zircon 40 um Location (UTM): 430676E, 5626451N

Grain	shape	^{206}Pb cps	$^{206}Pb/^{204}Pb$	$^{207}Pb/^{206}Pb$	± (2σ)	$^{207}Pb/^{235}U$	± (2σ)	$^{206}Pb/^{238}U$	± (2σ)	rho	Model Ages $^{207}Pb/^{206}Pb$	± (2σ)	$^{206}Pb/^{238}U$	± (2σ)	% disc.	Best Age (Ma)	± (2σ)
62	rnd	246886	12344	0.0783	0.0013	1.9641	0.0439	0.1807	0.0028	0.8616	1155	38	1071	36	7.9	1155	38
109	rnd	186436	infinite	0.0784	0.0004	2.0469	0.0368	0.1887	0.0033	0.9505	1156	22	1114	39	3.9	1156	22
98	rnd	267231	infinite	0.0785	0.0002	2.0345	0.0316	0.1866	0.0028	0.9521	1160	21	1103	37	5.4	1160	21
22	frag	224366	22437	0.0787	0.0007	2.0047	0.0509	0.1841	0.0044	0.9390	1164	27	1089	42	7.0	1164	27
2	subrnd	243705	infinite	0.0787	0.0002	2.0202	0.0491	0.1852	0.0045	0.9634	1165	21	1095	42	6.5	1165	21
123	rnd	163210	infinite	0.0788	0.0002	2.1597	0.0352	0.1969	0.0032	0.9529	1166	21	1159	39	0.7	1166	21
162	rnd	459725	9194	0.0794	0.0017	2.2372	0.1837	0.2076	0.0165	0.9631	1182	46	1216	103	-3	1182	46
36	subrnd	1064	infinite	0.0796	0.0272	0.0972	0.0333	0.0081	0.0003	0.1280	1188	674	52	2	96.0	reject	
29	subrnd	142017	infinite	0.0797	0.0004	1.9980	0.0412	0.1799	0.0036	0.9541	1189	22	1066	39	11.2	reject	
54	subrnd	383369	infinite	0.0802	0.0006	2.2799	0.0554	0.2026	0.0047	0.9498	1203	24	1189	45	1.2	1203	24
41	subrnd	70141	infinite	0.0803	0.0006	1.9980	0.0653	0.1781	0.0057	0.9605	1204	24	1057	46	13.3	reject	
118	rnd	74551	infinite	0.0804	0.0005	2.3305	0.0338	0.2085	0.0028	0.9389	1206	23	1221	40	-1.4	1206	23
76	rnd	840259	infinite	0.0804	0.0002	1.9942	0.0310	0.1801	0.0028	0.9544	1208	20	1068	36	12.6	reject	
32	subrnd	24791	infinite	0.0805	0.0013	2.1160	0.0560	0.1877	0.0039	0.8782	1208	38	1109	40	8.9	1208	38
92	rnd	448706	3205	0.0806	0.0006	2.2515	0.0622	0.2014	0.0053	0.9523	1211	25	1183	47	2.6	1211	25
21	frag	39165	infinite	0.0814	0.0008	2.2309	0.0848	0.1974	0.0072	0.9562	1232	0	1161	55	6.2	1232	0
165	rnd	311575	infinite	0.0824	0.0002	2.4380	0.0525	0.2131	0.0045	0.9601	1255	20	1245	46	1	1255	20
30	subrnd	440221	1873	0.0829	0.0005	2.4678	0.0544	0.2156	0.0045	0.9475	1266	23	1259	46	0.7	1266	23
84	rnd	968867	4465	0.0835	0.0004	2.1414	0.0520	0.1854	0.0044	0.9588	1281	22	1096	42	15.7	reject	
154	frag	121575	4053	0.0836	0.0038	2.4853	0.1187	0.2135	0.0030	0.5603	1283	91	1247	41	3	1283	91
139	rnd	258307	12915	0.0836	0.0012	2.5240	0.0642	0.2173	0.0045	0.8945	1283	34	1268	46	1	1283	34
25	subrnd	379397	2432	0.0838	0.0006	2.4871	0.0989	0.2144	0.0084	0.9685	1288	24	1252	62	3.1	1288	24
150	frag	113292	infinite	0.0841	0.0004	2.5068	0.0531	0.2120	0.0044	0.9533	1295	22	1239	45	5	1295	22
147	subrnd	77668	infinite	0.0844	0.0004	2.5422	0.0340	0.2157	0.0027	0.9445	1301	21	1259	41	4	1301	21
136	rnd	64168	infinite	0.0845	0.0004	2.6637	0.0363	0.2250	0.0028	0.9418	1305	22	1308	43	0	1305	22
140	rnd	473420	infinite	0.0849	0.0002	2.6582	0.0525	0.2258	0.0044	0.9594	1313	20	1312	47	0	1313	20
141	rnd	764086	infinite	0.0852	0.0001	2.5594	0.0306	0.2169	0.0026	0.9505	1320	20	1266	41	5	1320	20
128	rnd	271442	infinite	0.0852	0.0002	2.6524	0.0463	0.2250	0.0039	0.9561	1321	20	1308	45	1.1	1321	20
95	rnd	72473	infinite	0.0853	0.0005	2.5199	0.0343	0.2114	0.0026	0.9402	1322	22	1236	40	7.1	1322	22
99	rnd	248862	4880	0.0861	0.0009	2.7243	0.0795	0.2274	0.0062	0.9381	1341	28	1321	53	1.7	1341	28
166	rnd	179450	infinite	0.0865	0.0003	2.7194	0.0510	0.2272	0.0042	0.9549	1350	20	1320	46	2	1350	20
131	rnd	375903	12530	0.0868	0.0012	2.8636	0.0522	0.2378	0.0027	0.8682	1357	34	1375	44	-2	1357	34

Broadview Fm, 07TWJK516 Depositional age: (Ordovician?-)Devonian n= 128

Zircon 40 um Location (UTM): 430676E, 5626451N

Grain	shape	^{206}Pb cps	$^{206}Pb/^{204}Pb$	$^{207}Pb/^{206}Pb$	± (2σ)	$^{207}Pb/^{235}U$	± (2σ)	$^{206}Pb/^{238}U$	± (2σ)	rho	Model Ages $^{207}Pb/^{206}Pb$	± (2σ)	$^{206}Pb/^{238}U$	± (2σ)	% disc.	Best Age (Ma)	± (2σ)
129	rnd	350486	35049	0.0874	0.0005	2.8217	0.0585	0.2328	0.0047	0.9506	1369	22	1349	49	1.6	1369	22
124	rnd	297513	infinite	0.0874	0.0003	2.8050	0.0541	0.2312	0.0044	0.9566	1370	20	1341	48	2.3	1370	20
37	subrnd	751542	15031	0.0884	0.0010	2.6265	0.0496	0.2150	0.0032	0.9015	1392	30	1255	42	10.8	reject	
138	rnd	1134409	8466	0.0888	0.0003	2.4969	0.0525	0.2035	0.0042	0.9585	1400	20	1194	44	16	reject	
7	frag	250798	infinite	0.0892	0.0006	2.6122	0.0645	0.2112	0.0050	0.9519	1408	23	1235	47	13.5	reject	
43	subrnd	87343	8734	0.0893	0.0018	2.8442	0.0784	0.2290	0.0043	0.8343	1410	43	1329	47	6.4	1410	43
96	rnd	334071	3341	0.0893	0.0046	2.9129	0.1558	0.2356	0.0031	0.5087	1411	101	1364	45	3.7	1411	101
146	frag	287215	57443	0.0901	0.0003	2.9496	0.0453	0.2365	0.0035	0.9493	1428	20	1368	46	5	1428	20
143	rnd	125081	infinite	0.0902	0.0004	3.1236	0.0547	0.2487	0.0042	0.9494	1429	21	1432	49	0	1429	21
163	rnd	363020	4034	0.0903	0.0013	2.7704	0.1170	0.2225	0.0088	0.9387	1431	34	1295	64	10	reject	
45	subrnd	105089	infinite	0.0906	0.0003	2.8782	0.0328	0.2281	0.0025	0.9447	1437	20	1325	42	8.7	1437	20
104	rnd	443071	infinite	0.0918	0.0002	3.0896	0.0635	0.2422	0.0049	0.9600	1463	20	1398	51	4.9	1463	20
119	rnd	1000532	100053	0.0922	0.0002	3.0291	0.0497	0.2376	0.0039	0.9553	1470	19	1374	47	7.3	1470	19
26	subrnd	184179	infinite	0.0927	0.0004	2.8190	0.0913	0.2174	0.0070	0.9694	1482	21	1268	56	15.9	reject	
24	prism	280476	infinite	0.0928	0.0003	2.8522	0.1239	0.2225	0.0096	0.9800	1483	20	1295	68	14.0	reject	
46	subrnd	261983	1101	0.1002	0.0010	4.0955	0.0751	0.2949	0.0046	0.9205	1629	26	1666	56	-2.6	1629	26
19	prism	183366	1060	0.1031	0.0014	4.5101	0.1518	0.3158	0.0097	0.9287	1681	31	1769	76	-6.0	1681	31
20	frag	359228	1529	0.1048	0.0009	4.1374	0.1280	0.2874	0.0085	0.9524	1710	24	1628	69	5.4	1710	24
63	rnd	825740	8257	0.1054	0.0019	4.0880	0.1026	0.2816	0.0050	0.8547	1722	37	1599	56	8.0	1722	37
23	frag	337376	1730	0.1066	0.0006	4.6783	0.1397	0.3173	0.0093	0.9625	1742	21	1777	74	-2.3	1742	21
87	rnd	676456	3505	0.1081	0.0006	4.2772	0.1021	0.2857	0.0067	0.9566	1767	21	1620	62	9.4	1767	21
81	rnd	491850	infinite	0.1081	0.0002	3.9158	0.0587	0.2614	0.0039	0.9541	1768	19	1497	50	17.2	reject	
159	subrnd	359264	4129	0.1086	0.0006	4.7897	0.1463	0.3196	0.0096	0.9631	1776	21	1788	76	-1	1776	21
34	subrnd	102600	2052	0.1098	0.0075	4.6133	0.3194	0.3015	0.0038	0.4110	1797	125	1699	55	6.2	1797	125
15	frag	98954	infinite	0.1099	0.0005	4.6546	0.1388	0.3048	0.0090	0.9653	1798	20	1715	72	5.2	1798	20
52	subrnd	187179	9359	0.1102	0.0003	4.5155	0.1033	0.2933	0.0067	0.9618	1803	19	1658	62	9.1	1803	19
28	subrnd	465470	2412	0.1102	0.0006	4.5898	0.1137	0.3029	0.0073	0.9583	1803	20	1706	66	6.1	1803	20
55	rnd	51822	infinite	0.1104	0.0003	4.3287	0.0726	0.2824	0.0047	0.9554	1806	19	1604	55	12.6	reject	
111	rnd	482183	48218	0.1106	0.0004	4.6003	0.0894	0.2998	0.0057	0.9564	1810	19	1690	60	7.5	1810	19
67	rnd	840214	infinite	0.1112	0.0001	4.2568	0.0871	0.2770	0.0057	0.9615	1818	18	1576	57	15.0	reject	
59	rnd	102995	infinite	0.1114	0.0003	4.6566	0.1221	0.3016	0.0079	0.9667	1822	19	1699	68	7.7	1822	19
60	rnd	439148	infinite	0.1114	0.0003	4.6566	0.1221	0.3016	0.0079	0.9667	1822	19	1699	68	7.7	1822	19

Broadview Fm, 07TWJK516
Zircon 40 um

Depositional age: (Ordovician?-)Devonian
Location (UTM): 430676E, 5626451N

n= 128

Grain	shape	^{206}Pb cps	$^{206}Pb/^{204}Pb$	$^{207}Pb/^{206}Pb$	± (2σ)	$^{207}Pb/^{235}U$	± (2σ)	$^{206}Pb/^{238}U$	± (2σ)	rho	Model Ages $^{207}Pb/^{206}Pb$	± (2σ)	$^{206}Pb/^{238}U$	± (2σ)	% disc.	Best Age (Ma)	± (2σ)
142	rnd	701287	6679	0.1114	0.0003	4.7781	0.0920	0.3098	0.0059	0.9578	1823	19	1740	62	5	1823	19
83	rnd	501088	infinite	0.1129	0.0002	3.9253	0.0707	0.2496	0.0045	0.9578	1847	18	1436	50	24.8	reject	
39	subrnd	98084	infinite	0.1134	0.0006	4.8148	0.0918	0.3039	0.0056	0.9491	1854	20	1711	60	8.8	1854	20
155	subrnd	137257	13726	0.1144	0.0012	5.3655	0.1125	0.3349	0.0061	0.9217	1870	26	1862	65	0	1870	26
91	rnd	156183	infinite	0.1145	0.0004	4.8915	0.0964	0.3069	0.0060	0.9570	1872	19	1725	62	8.9	1872	19
33	subrnd	102412	infinite	0.1152	0.0005	4.7546	0.0691	0.2956	0.0041	0.9454	1883	20	1669	55	12.9	reject	
80	rnd	110465	infinite	0.1169	0.0005	5.1621	0.0940	0.3165	0.0056	0.9528	1910	19	1773	62	8.2	1910	19
164	rnd	361269	4817	0.1172	0.0006	5.4075	0.0995	0.3358	0.0059	0.9476	1913	20	1866	65	3	1913	20
137	rnd	869816	8206	0.1172	0.0003	5.1530	0.1245	0.3179	0.0076	0.9635	1913	19	1779	68	8	1913	19
11	frag	187451	infinite	0.1183	0.0004	5.4485	0.1202	0.3304	0.0072	0.9592	1931	19	1840	68	5.4	1931	19
35	subrnd	480346	2053	0.1190	0.0007	4.9775	0.2244	0.3028	0.0135	0.9766	1942	21	1705	92	13.9	reject	
68	rnd	125952	infinite	0.1210	0.0005	5.6499	0.1229	0.3355	0.0072	0.9581	1971	19	1865	69	6.2	1971	19
157	frag	57190	11438	0.1235	0.0014	6.1009	0.1377	0.3556	0.0069	0.9131	2007	27	1961	70	3	2007	27
93	rnd	170576	1122	0.1362	0.0016	7.0762	0.1395	0.3761	0.0060	0.9052	2179	27	2058	70	6.5	2179	27
106	rnd	894266	10906	0.1417	0.0006	6.2654	0.1642	0.3193	0.0082	0.9619	2248	19	1786	71	23.5	reject	
156	subrnd	143124	infinite	0.1459	0.0010	8.7174	0.1664	0.4273	0.0076	0.9420	2299	21	2293	80	0	2299	21
51	subrnd	717546	infinite	0.1460	0.0016	6.1830	0.1746	0.3035	0.0079	0.9312	2300	26	1709	68	29.2	reject	
113	rnd	98508	infinite	0.1480	0.0005	8.5301	0.1498	0.4127	0.0071	0.9540	2322	18	2227	77	4.8	2322	18
16	prism	332278	1426	0.1614	0.0036	6.2631	0.6827	0.2752	0.0293	0.9759	2471	42	1567	174	41.1	reject	
145	rnd	202168	1271	0.1629	0.0012	10.7517	0.2600	0.4740	0.0109	0.9466	2486	21	2501	95	-1	2486	21
149	prism	630396	5342	0.1727	0.0007	6.9978	0.1692	0.2919	0.0070	0.9600	2584	18	1651	63	41	reject	
120	rnd	854085	8627	0.1750	0.0006	7.4186	0.3604	0.3060	0.0148	0.9829	2606	18	1721	98	38.6	reject	
73	rnd	739024	36951	0.1772	0.0004	11.3443	0.1882	0.4628	0.0076	0.9546	2627	17	2452	84	8.0	2627	17
49	subrnd	74708	427	0.1775	0.0011	11.7993	0.3019	0.4750	0.0118	0.9545	2630	20	2505	98	5.7	2630	20
42	subrnd	171243	3425	0.1782	0.0044	11.6192	0.3442	0.4693	0.0078	0.7795	2636	44	2480	85	7.1	2636	44
10	frag	1457188	21119	0.1796	0.0003	11.2951	0.3396	0.4568	0.0137	0.9714	2649	17	2426	103	10.1	reject	
75	rnd	613345	4868	0.1797	0.0005	11.3192	0.2891	0.4553	0.0116	0.9650	2650	17	2419	95	10.4	reject	
114	rnd	679758	11521	0.1803	0.0004	11.9925	0.2283	0.4800	0.0091	0.9586	2656	17	2527	90	5.9	2656	17
151	frag	342206	6984	0.1822	0.0007	12.3184	0.2969	0.4863	0.0116	0.9611	2673	18	2555	98	5	2673	18
90	rnd	618552	3417	0.1837	0.0007	9.9473	0.4018	0.3899	0.0157	0.9772	2687	18	2122	106	24.6	reject	
27	subrnd	200741	1134	0.1842	0.0011	12.1525	0.2703	0.4763	0.0102	0.9505	2691	19	2511	93	8.1	2691	19
57	rnd	490050	9801	0.1846	0.0017	12.0547	0.2615	0.4711	0.0093	0.9318	2694	22	2488	89	9.2	2694	22

Broadview Fm, 07TWJK516 Depositional age: (Ordovician?-)Devonian n= 128

Zircon 40 um Location (UTM): 430676E, 5626451N

											Model Ages						
Grain	**shape**	**^{206}Pb cps**	**^{206}Pb/^{204}Pb**	**^{207}Pb/^{206}Pb**	**± (2σ)**	**^{207}Pb/^{235}U**	**± (2σ)**	**^{206}Pb/^{238}U**	**± (2σ)**	**rho**	**^{207}Pb/^{206}Pb**	**± (2σ)**	**^{206}Pb/^{238}U**	**± (2σ)**	**% disc.**	**Best Age (Ma)**	**± (2σ)**
18	frag	142082	infinite	0.1852	0.0005	12.7409	0.3720	0.4960	0.0144	0.9697	2700	17	2597	109	4.7	2700	17
71	rnd	450899	3607	0.1885	0.0009	12.1227	0.6586	0.4641	0.0251	0.9841	2729	18	2458	152	12.0	reject	
31	subrnd	202927	4059	0.1923	0.0037	12.7738	0.3887	0.4817	0.0114	0.8640	2762	35	2535	97	9.9	2762	35
4	subrnd	400686	2414	0.2069	0.0006	15.6708	0.3440	0.5475	0.0119	0.9602	2881	17	2815	104	2.9	2881	17
61	rnd	817036	5795	0.2105	0.0004	14.8507	0.3347	0.5101	0.0115	0.9630	2909	17	2657	100	10.6	reject	

Mount Sproat assemblage, 06TWJK138A Depositional age: Late Devonian or Early Mississippian n= 120

Zircon 40 um Location (UTM): 441773E, 5617473N

Grain	colour	shape	^{206}Pb cps	^{206}Pb/^{204}Pb	^{207}Pb/^{206}Pb	± (2σ)	^{207}Pb/^{235}U	± (2σ)	^{206}Pb/^{238}U	± (2σ)	rho	Model Ages ^{207}Pb/^{206}Pb	± (2σ)	^{206}Pb/^{238}U	± (2σ)	% disc.	Best Age (Ma)	± (2σ)	*interp type*
33	cll	frag	63485	infinite	0.0580	0.0005	0.6267	0.0071	0.0780	0.0005	0.9058	530	30	484	15	8.6	484	15	
10	pnk	frag	458503	infinite	0.0699	0.0002	1.5052	0.0177	0.1563	0.0018	0.9482	927	21	936	30	-1.0	927	21	
138	cll	subrnd	94927	4746	0.0703	0.0004	1.4734	0.0109	0.1519	0.0007	0.9297	939	24	912	28	3	939	24	
93	cll	rnd	407969	infinite	0.0709	0.0002	1.5391	0.0199	0.1575	0.0020	0.9503	954	21	943	31	1.2	954	21	
23	ylw	rnd	74777	infinite	0.0733	0.0006	1.5993	0.0176	0.1585	0.0013	0.9204	1022	26	949	29	7.2	1022	26	
52	cll	prism	108014	5685	0.0734	0.0027	1.8773	0.0742	0.1855	0.0024	0.6256	1024	78	1097	36	-7.1	1024	78	
121	ylw	subrnd	58450	infinite	0.0743	0.0006	1.7350	0.0215	0.1699	0.0016	0.9227	1050	25	1011	32	3.7	1050	25	
76	cll	subrnd	180880	infinite	0.0744	0.0003	1.7155	0.0205	0.1666	0.0019	0.9429	1053	22	993	32	5.6	1053	22	
7	pnk	rnd	333702	infinite	0.0744	0.0002	1.7841	0.0207	0.1744	0.0020	0.9485	1053	21	1036	33	1.6	1053	21	
75	cll	subrnd	81939	infinite	0.0746	0.0004	1.7610	0.0205	0.1716	0.0018	0.9398	1058	22	1021	32	3.5	1058	22	
135	cll	subrnd	29636	infinite	0.0748	0.0006	1.4925	0.0196	0.1451	0.0015	0.9198	1062	26	873	28	18	reject		
43	cll	subrnd	142897	infinite	0.0748	0.0003	1.8228	0.0225	0.1765	0.0021	0.9450	1062	22	1048	34	1.4	1062	22	
84	cll	subrnd	92307	infinite	0.0752	0.0005	1.7492	0.0162	0.1690	0.0012	0.9288	1074	0	1007	31	6.3	1074	0	
91	cll	rnd	76931	infinite	0.0756	0.0003	1.7856	0.0228	0.1710	0.0021	0.9442	1084	22	1018	33	6.1	1084	22	
97	cll	rnd	84487	3379	0.0757	0.0004	1.4791	0.1016	0.1417	0.0097	0.9881	1087	23	854	64	21.4	reject		
35	cll	frag	28728	infinite	0.0763	0.0010	1.9635	0.0323	0.1889	0.0020	0.8828	1102	32	1115	35	-1.2	1102	32	
28	ylw	subrnd	335307	30482	0.0766	0.0004	1.7947	0.0227	0.1700	0.0019	0.9361	1110	23	1012	32	8.8	1110	23	
115	pnk	frag	292178	infinite	0.0767	0.0003	1.9286	0.0224	0.1827	0.0020	0.9450	1113	21	1082	35	2.8	1113	21	
42	cll	subrnd	39480	infinite	0.0769	0.0004	2.0865	0.0252	0.1960	0.0021	0.9361	1118	23	1154	37	-3.2	1118	23	
2	pnk	rnd	155140	infinite	0.0770	0.0005	1.9562	0.0255	0.1848	0.0020	0.9291	1122	24	1093	35	2.6	1122	24	
106	cll	rnd	106316	infinite	0.0772	0.0003	1.8714	0.0221	0.1763	0.0019	0.9424	1126	22	1047	33	7.0	1126	22	
101	cll	rnd	22169	infinite	0.0772	0.0008	1.8576	0.0284	0.1749	0.0020	0.9072	1126	28	1039	33	7.7	1126	28	
133	cll	subrnd	27424	infinite	0.0773	0.0007	1.8503	0.0231	0.1732	0.0015	0.9109	1128	27	1030	32	9	1128	27	
118	pnk	subrnd	52930	infinite	0.0775	0.0004	1.8609	0.0263	0.1737	0.0023	0.9398	1134	23	1032	34	9.0	1134	23	
74	cll	subrnd	146906	infinite	0.0776	0.0003	1.9341	0.0234	0.1810	0.0021	0.9466	1137	21	1072	34	5.7	1137	21	
16	ylw	prism	106850	infinite	0.0778	0.0004	1.9333	0.0249	0.1797	0.0021	0.9414	1142	22	1065	34	6.7	1142	22	
31	ylw	rnd	53315	infinite	0.0780	0.0008	2.0471	0.0309	0.1888	0.0021	0.9039	1146	29	1115	36	2.7	1146	29	
11A	pnk	rnd	58740	infinite	0.0781	0.0005	2.0163	0.0207	0.1881	0.0014	0.9246	1150	24	1111	34	3.4	1139	16	*1*
11B	pnk	rnd	136754	infinite	0.0773	0.0003	1.9547	0.0298	0.1835	0.0027	0.9472	1130	22	1086	36	3.9			
79	cll	subrnd	19693	infinite	0.0784	0.0009	1.9587	0.0340	0.1797	0.0022	0.8925	1156	31	1066	35	7.8	1156	31	
32	cll	subrnd	12929	infinite	0.0785	0.0015	1.9138	0.0427	0.1761	0.0021	0.8212	1158	42	1045	34	9.8	1158	42	
125	ylw	rnd	68836	infinite	0.0786	0.0005	1.9730	0.0262	0.1819	0.0021	0.9344	1161	23	1077	35	7.2	1161	23	
8	pnk	rnd	337481	infinite	0.0789	0.0002	2.1501	0.0252	0.1980	0.0023	0.9476	1169	21	1164	37	0.4	1169	21	
80	cll	subrnd	91040	infinite	0.0795	0.0003	2.0508	0.0250	0.1860	0.0021	0.9440	1185	0	1099	35	7.2	1185	0	
102	cll	rnd	73913	infinite	0.0799	0.0005	2.0690	0.0274	0.1879	0.0022	0.9325	1196	24	1110	36	7.2	1196	24	
128	cll	frag	26574	infinite	0.0800	0.0013	1.2502	0.0685	0.1128	0.0059	0.9521	1196	38	689	42	42.4	reject		

Mount Sproat assemblage, 06TWJK138A
Zircon 40 um

Depositional age: Late Devonian or Early Mississippian
Location (UTM): 441773E, 5617473N

n= 120

Grain	colour	shape	^{206}Pb cps	$^{206}Pb/^{204}Pb$	$^{207}Pb/^{206}Pb$	± (2σ)	$^{207}Pb/^{235}U$	± (2σ)	$^{206}Pb/^{238}U$	± (2σ)	rho	Model Ages $^{207}Pb/^{206}Pb$	± (2σ)	$^{206}Pb/^{238}U$	± (2σ)	% disc.	Best Age (Ma)	± (2σ)	*interp type*
60	cll	subrnd	45856	infinite	0.0802	0.0015	1.6551	0.0330	0.1494	0.0011	0.8141	1203	41	898	28	25.4		reject	
90	cll	rnd	61804	infinite	0.0803	0.0006	2.1248	0.0179	0.1915	0.0009	0.9207	1203	24	1130	34	6.1	1203	24	
89	cll	rnd	73411	infinite	0.0803	0.0004	2.1017	0.0252	0.1905	0.0021	0.9387	1203	22	1124	36	6.6	1203	22	
66	cll	frag	137209	infinite	0.0804	0.0004	2.2765	0.0302	0.2058	0.0026	0.9437	1206	22	1206	39	0.0	1206	22	
95	cll	rnd	259842	infinite	0.0806	0.0004	2.1511	0.0219	0.1935	0.0017	0.9381	1213	22	1140	36	6.0	1213	22	
82	cll	subrnd	15355	infinite	0.0807	0.0013	2.1039	0.0406	0.1871	0.0020	0.8468	1214	37	1106	35	8.9	1214	37	
69	cll	rnd	28786	infinite	0.0808	0.0009	2.1808	0.0380	0.1949	0.0027	0.9071	1218	29	1148	38	5.7	1218	29	
105	cll	rnd	73237	infinite	0.0813	0.0004	2.2056	0.0363	0.1969	0.0031	0.9486	1229	21	1159	39	5.7	1229	21	
44	cll	subrnd	176736	3273	0.0817	0.0011	2.3742	0.0414	0.2103	0.0023	0.8769	1239	33	1231	39	0.7	1239	33	
127	cll	frag	13718	infinite	0.0821	0.0020	2.0289	0.0578	0.1824	0.0028	0.7762	1247	51	1080	36	13.4		reject	
73	cll	ı-subhed	53445	infinite	0.0825	0.0008	2.2853	0.0266	0.2002	0.0015	0.9089	1258	26	1176	36	6.5	1258	26	
21	ylw	rnd	18376	infinite	0.0836	0.0022	2.2606	0.0620	0.1971	0.0015	0.7213	1284	55	1160	36	9.7	1284	55	
72	cll	prism	75555	infinite	0.0853	0.0021	2.3044	0.0651	0.1951	0.0028	0.7693	1322	0	1149	38	13.1		reject	
20	ylw	rnd	311965	infinite	0.0856	0.0003	2.6165	0.0270	0.2224	0.0022	0.9458	1329	20	1294	41	2.6	1329	20	
22	ylw	rnd	135640	infinite	0.0865	0.0004	2.6939	0.0241	0.2266	0.0017	0.9363	1349	21	1317	41	2.4	1349	21	
87	cll	rnd	53104	infinite	0.0866	0.0006	2.6445	0.0258	0.2219	0.0014	0.9205	1352	24	1292	40	4.4	1352	24	
134	cll	rnd	234977	infinite	0.0867	0.0004	2.6737	0.0388	0.2240	0.0031	0.9473	1353	21	1303	43	4	1353	21	
111	op		604209	2466	0.0867	0.0012	2.0585	0.1082	0.1721	0.0087	0.9590	1354	33	1024	60	24.4		reject	
132	cll	subrnd	112691	infinite	0.0869	0.0006	2.5844	0.0232	0.2160	0.0012	0.9225	1358	24	1261	38	7	1358	24	
117	pnk	subrnd	185054	infinite	0.0871	0.0004	2.6913	0.0330	0.2242	0.0026	0.9440	1363	21	1304	42	4.3	1363	21	
141	cll	rnd	117920	infinite	0.0882	0.0004	2.6579	0.0318	0.2185	0.0024	0.9404	1386	21	1274	41	8	1386	21	
78	cll	subrnd	76757	infinite	0.0913	0.0005	3.0597	0.0450	0.2423	0.0033	0.9428	1453	21	1399	46	3.7	1453	21	
26	ylw	subrnd	88037	infinite	0.0927	0.0004	2.9888	0.0265	0.2349	0.0018	0.9367	1481	21	1360	42	8.2	1481	21	
108	cll	rnd	87504	infinite	0.0928	0.0004	3.1343	0.0272	0.2450	0.0018	0.9376	1483	21	1413	44	4.8	1483	21	
9	pnk	frag	229217	infinite	0.0928	0.0004	3.2032	0.0374	0.2507	0.0027	0.9435	1485	20	1442	46	2.9	1485	20	
104	cll	rnd	141108	infinite	0.0932	0.0003	3.1182	0.0401	0.2426	0.0030	0.9476	1492	20	1400	45	6.1	1492	20	
40	cll	subrnd	146428	infinite	0.0935	0.0003	3.2406	0.0397	0.2518	0.0030	0.9471	1497	20	1448	47	3.3	1497	20	
92	cll	rnd	224969	infinite	0.0937	0.0002	3.3254	0.0710	0.2576	0.0055	0.9610	1503	19	1478	54	1.7	1503	19	
142	cll	rnd	115811	infinite	0.0939	0.0004	3.2918	0.0573	0.2551	0.0043	0.9486	1507	21	1465	50	3	1507	21	
94	cll	rnd	259842	2598	0.0950	0.0005	3.3562	0.0264	0.2568	0.0015	0.9338	1527	21	1473	45	3.5	1527	21	
3	pnk	rnd	147376	infinite	0.1016	0.0004	4.0208	0.0499	0.2874	0.0034	0.9441	1654	20	1628	52	1.6	1654	20	
48	cll	subrnd	93126	infinite	0.1028	0.0004	3.8127	0.0378	0.2688	0.0024	0.9400	1676	20	1535	48	8.4	1676	20	
71	cll	subrnd	146312	1951	0.1043	0.0003	4.2065	0.0942	0.2936	0.0065	0.9602	1702	19	1659	62	2.5	1702	19	
63	cll	subrnd	300413	1533	0.1051	0.0009	4.3721	0.0513	0.3018	0.0025	0.9167	1716	24	1700	53	0.9	1716	24	
15a	ylw	prism	343949	infinite	0.1117	0.0004	4.1714	0.0388	0.2717	0.0023	0.9414	1827	19	1550	48	15.2		reject	
15b	ylw	prism	253637	infinite	0.1056	0.0005	3.1913	0.1207	0.2193	0.0082	0.9738	1725	20	1278	61	25.9		reject	

Mount Sproat assemblage, 06TWJK138A

Zircon 40 um

Depositional age: Late Devonian or Early Mississippian

Location (UTM): 441773E, 5617473N

n= 120

												Model Ages							
Grain	colour	shape	^{206}Pb cps	^{206}Pb/^{204}Pb	^{207}Pb/^{206}Pb	± (2σ)	^{207}Pb/^{235}U	± (2σ)	^{206}Pb/^{238}U	± (2σ)	rho	^{207}Pb/^{206}Pb	± (2σ)	^{206}Pb/^{238}U	± (2σ)	% disc.	Best Age (Ma)	± (2σ)	*interp type*
5	pnk	frag	511721	9476	0.1074	0.0004	4.7140	0.0579	0.3184	0.0037	0.9451	1756	20	1782	57	-1.4	1756	20	
120	ylw	rnd	91293	infinite	0.1076	0.0006	4.4827	0.0609	0.3044	0.0038	0.9409	1759	21	1713	56	2.6	1759	21	
38	cll	subrnd	112071	3296	0.1103	0.0016	4.9248	0.0953	0.3230	0.0040	0.8661	1805	33	1804	59	0.0	1805	33	
6	pnk	frag	417015	infinite	0.1112	0.0002	5.0293	0.0574	0.3282	0.0037	0.9502	1819	18	1830	59	-0.6	1819	18	
143	cll	rnd	52082	infinite	0.1121	0.0008	4.9075	0.0599	0.3168	0.0032	0.9287	1834	22	1774	56	3	1834	22	
34	cll	frag	77711	infinite	0.1130	0.0005	5.0693	0.0530	0.3242	0.0030	0.9396	1848	20	1810	57	2.1	1848	20	
14	ylw	frag	267895	infinite	0.1131	0.0003	5.1393	0.0464	0.3299	0.0028	0.9450	1849	19	1838	57	0.6	1849	19	
144	cll	rnd	84916	84916	0.1132	0.0006	4.9930	0.0714	0.3188	0.0042	0.9400	1851	21	1784	58	4	1851	21	
62	cll	rnd	100070	infinite	0.1133	0.0004	5.1350	0.0627	0.3292	0.0038	0.9458	1853	19	1834	59	1.0	1853	19	
17	ylw	prism	179554	infinite	0.1133	0.0010	3.0487	0.3236	0.1939	0.0205	0.9929	1853	24	1142	126	38.3	reject		
24	ylw	rnd	98499	infinite	0.1136	0.0005	4.9774	0.0571	0.3178	0.0033	0.9402	1858	20	1779	57	4.3	1858	20	
124	ylw	subrnd	200529	infinite	0.1137	0.0004	4.3447	0.0559	0.2770	0.0034	0.9475	1859	19	1576	51	15.2	reject		
123	ylw	rnd	107965	infinite	0.1140	0.0004	5.0681	0.0417	0.3220	0.0024	0.9410	1865	19	1800	56	3.5	1865	19	
59	cll	prism	172308	infinite	0.1141	0.0004	4.9324	0.0671	0.3143	0.0041	0.9471	1865	19	1762	58	5.5	1865	19	
116	pnk	frag	269794	infinite	0.1141	0.0003	5.1375	0.0765	0.3262	0.0048	0.9527	1865	19	1820	61	2.4	1865	19	
77	cll	subrnd	72676	infinite	0.1141	0.0005	5.2818	0.0689	0.3370	0.0042	0.9455	1866	19	1872	61	-0.3	1866	19	
4	pnk	rnd	83938	infinite	0.1142	0.0004	5.1054	0.0571	0.3245	0.0034	0.9440	1867	19	1811	58	3.0	1867	19	
119	pnk	subrnd	228323	infinite	0.1143	0.0003	4.8994	0.0572	0.3106	0.0035	0.9485	1868	19	1744	56	6.7	1868	19	
131	cll	prism	77836	38918	0.1148	0.0009	5.1489	0.0637	0.3246	0.0032	0.9233	1877	23	1812	57	3	1877	23	
103	cll	rnd	180268	12018	0.1149	0.0007	5.1536	0.0799	0.3254	0.0046	0.9373	1878	21	1816	60	3.3	1878	21	
114	pnk	frag	158767	infinite	0.1152	0.0004	5.2728	0.0535	0.3326	0.0031	0.9429	1883	19	1851	58	1.7	1883	19	
83	cll	rnd	46513	infinite	0.1154	0.0005	5.2089	0.0588	0.3290	0.0034	0.9398	1886	20	1834	58	2.8	1886	20	
107	cll	rnd	31316	infinite	0.1154	0.0011	4.6504	0.0587	0.2915	0.0024	0.9059	1886	25	1649	51	12.6	reject		
86	cll	rnd	147423	infinite	0.1157	0.0005	5.1552	0.0623	0.3228	0.0037	0.9431	1891	20	1803	58	4.6	1891	20	
126	cll	prism	71909	infinite	0.1158	0.0016	5.1252	0.1006	0.3233	0.0046	0.8857	1893	30	1806	60	4.6	1893	30	
30	ylw	rnd	126819	infinite	0.1160	0.0005	4.6783	0.0860	0.2917	0.0052	0.9527	1895	19	1650	58	12.9	reject		
12	pnk	frag	431067	13063	0.1166	0.0004	5.1862	0.0669	0.3226	0.0040	0.9462	1905	19	1803	58	5.4	1905	19	
13	ylw	frag	122756	infinite	0.1168	0.0004	5.5420	0.0461	0.3443	0.0027	0.9432	1907	19	1907	59	0.0	1907	19	
25	ylw	rnd	87126	43563	0.1178	0.0007	5.1021	0.0616	0.3137	0.0033	0.9331	1922	21	1759	56	8.5	1922	21	
109	op		416516	5018	0.1182	0.0012	4.9543	0.1870	0.3028	0.0110	0.9549	1930	26	1705	80	11.6	reject		
36	cll	subrnd	116394	infinite	0.1186	0.0004	5.6521	0.0906	0.3447	0.0054	0.9520	1935	19	1909	65	1.3	1935	19	
67	cll	rnd	210639	infinite	0.1192	0.0006	3.9876	0.1634	0.2427	0.0099	0.9760	1944	20	1401	71	28.0	reject		
98	cll	rnd	109324	infinite	0.1195	0.0005	5.4532	0.0685	0.3311	0.0040	0.9454	1949	19	1844	60	5.4	1949	19	
53	cll	prism	66680	infinite	0.1196	0.0006	5.4153	0.1036	0.3328	0.0061	0.9488	1950	20	1852	65	5.0	1950	20	
113	pnk	frag	120907	infinite	0.1199	0.0005	5.6422	0.0665	0.3413	0.0037	0.9423	1955	19	1893	60	3.2	1955	19	
51	cll	prism	35642	infinite	0.1206	0.0007	5.5779	0.0800	0.3353	0.0044	0.9404	1965	20	1864	61	5.1	1965	20	

Mount Sproat assemblage, 06TWJK138A
Zircon 40 um

Depositional age: Late Devonian or Early Mississippian
Location (UTM): 441773E, 5617473N

n= 120

Grain	colour	shape	^{206}Pb cps	$^{206}Pb/^{204}Pb$	$^{207}Pb/^{206}Pb$	± (2σ)	$^{207}Pb/^{235}U$	± (2σ)	$^{206}Pb/^{238}U$	± (2σ)	rho	Model Ages $^{207}Pb/^{206}Pb$	± (2σ)	Model Ages $^{206}Pb/^{238}U$	± (2σ)	% disc.	Best Age (Ma)	± (2σ)	*interp type*
110	op		326353	infinite	0.1223	0.0002	4.9742	0.1040	0.2945	0.0061	0.9613	1991	18	1664	61	16.4	reject		
61	cll	rnd	109499	1217	0.1236	0.0008	6.0304	0.0935	0.3554	0.0050	0.9368	2009	21	1960	65	2.4	2009	21	
130	cll	prism	124812	41604	0.1248	0.0006	5.5454	0.1059	0.3217	0.0059	0.9508	2026	20	1798	63	11	reject		
47	cll	subrnd	60205	infinite	0.1260	0.0009	6.1777	0.0992	0.3567	0.0051	0.9332	2043	22	1966	65	3.8	2043	22	
129	cll	frag	105701	infinite	0.1274	0.0009	5.1935	0.1081	0.2954	0.0058	0.9430	2063	22	1669	60	19	reject		
88	cll	rnd	41745	infinite	0.1319	0.0005	6.6985	0.0909	0.3698	0.0048	0.9480	2124	19	2029	66	4.5	2124	19	
50	cll	subrnd	166406	infinite	0.1331	0.0004	7.1428	0.1235	0.3897	0.0066	0.9538	2139	18	2122	73	0.8	2139	18	
99	cll	rnd	118005	infinite	0.1379	0.0004	7.5530	0.0861	0.3980	0.0044	0.9467	2201	18	2160	69	1.9	2201	18	
70	cll	prism	216243	2162	0.1418	0.0006	7.9725	0.2031	0.4104	0.0103	0.9618	2249	19	2217	87	1.5	2249	19	
54	cll	subrnd	172074	382	0.1439	0.0013	5.5126	0.1055	0.2831	0.0048	0.9285	2275	23	1607	55	29.4	reject		
1	pnk	rnd	408234	4918	0.1457	0.0004	8.6306	0.1104	0.4309	0.0054	0.9485	2297	18	2310	75	-0.6	2297	18	
41	cll	prism	122923	infinite	0.1524	0.0003	8.7922	0.1169	0.4168	0.0055	0.9513	2373	17	2246	74	5.3	2373	17	
46	cll	subrnd	121647	3924	0.1527	0.0014	8.7545	0.1051	0.4144	0.0032	0.9079	2376	23	2235	69	5.9	2376	23	
81	cll	subrnd	190302	952	0.1596	0.0005	9.6295	0.2219	0.4374	0.0100	0.9610	2452	18	2339	88	4.6	2452	18	
65	cll	frag	29862	infinite	0.1609	0.0013	9.7660	0.1828	0.4410	0.0075	0.9328	2465	22	2355	81	4.5	2465	22	
19	ylw	subrnd	293665	infinite	0.1726	0.0003	11.4560	0.0992	0.4819	0.0041	0.9467	2583	17	2536	79	1.8	2583	17	
96	cll	rnd	337959	6759	0.1726	0.0005	11.8111	0.1297	0.4964	0.0053	0.9470	2583	17	2598	83	-0.6	2583	17	
27	ylw	frag	446307	446307	0.1775	0.0003	11.6369	0.0980	0.4743	0.0039	0.9468	2630	17	2503	78	4.8	2630	17	
140	cll	rnd	113183	1132	0.1802	0.0133	12.3125	0.9181	0.4942	0.0059	0.3824	2655	123	2589	84	2	2655	123	
55	cll	subrnd	232769	895	0.1804	0.0013	12.2959	0.1610	0.4946	0.0054	0.9278	2656	20	2591	83	2.5	2656	20	
137	cll	prism	106325	infinite	0.1817	0.0011	12.6908	0.1963	0.5076	0.0072	0.9380	2669	20	2646	88	1	2669	20	
112	pnk	frag	378723	3293	0.1830	0.0006	12.4839	0.2100	0.4946	0.0081	0.9527	2681	17	2591	89	3.4	2681	17	
29	ylw	subrnd	329104	109701	0.1843	0.0003	10.6520	0.1678	0.4183	0.0065	0.9551	2692	17	2253	76	16.3	reject		
100	cll	rnd	128110	5124	0.1851	0.0005	12.9428	0.1973	0.5070	0.0076	0.9521	2699	17	2644	89	2.1	2699	17	
57	cll	prism	181427	infinite	0.1859	0.0004	12.8867	0.1798	0.5048	0.0069	0.9516	2706	17	2635	87	2.6	2706	17	
136	cll	subrnd	267341	1782	0.1862	0.0004	13.3644	0.1420	0.5201	0.0054	0.9486	2709	17	2699	86	0	2709	17	
139	cll	rnd	117144	infinite	0.1873	0.0004	12.8698	0.1533	0.4974	0.0058	0.9499	2719	17	2603	84	4	2719	17	
18	ylw	subrnd	83433	infinite	0.1884	0.0009	13.4287	0.1151	0.5157	0.0037	0.9369	2728	18	2681	83	1.7	2728	18	
37	cll	subrnd	104689	infinite	0.1901	0.0006	13.2894	0.2026	0.5056	0.0076	0.9517	2743	17	2638	88	3.9	2743	17	
64	cll	frag	130876	infinite	0.1903	0.0007	14.0845	0.1497	0.5379	0.0054	0.9434	2744	18	2775	88	-1.1	2744	18	
45	cll	subrnd	285311	infinite	0.1987	0.0004	12.8855	0.1585	0.4677	0.0057	0.9503	2816	17	2473	80	12.2	reject		
58	cll	prism	138991	infinite	0.2002	0.0006	14.1923	0.1973	0.5158	0.0070	0.9499	2828	17	2681	88	5.2	2828	17	
39	cll	subrnd	245039	infinite	0.2186	0.0003	17.0503	0.1310	0.5656	0.0043	0.9466	2971	16	2890	89	2.7	2971	16	
85	cll	subrnd	1068361	18420	0.2551	0.0002	21.9779	0.2413	0.6251	0.0068	0.9505	3217	16	3130	100	2.7	3217	16	

Thompson assemblage, 08TWJK073 Depositional age: Mississippian n= 98

Zircon 40 um Location (UTM): 454397E, 5618697N

Grain	^{206}Pb cps	^{206}Pb/^{204}Pb	^{207}Pb/^{206}Pb	± (2σ)	^{207}Pb/^{235}U	± (2σ)	^{206}Pb/^{238}U	± (2σ)	rho	Model Ages ^{207}Pb/^{206}Pb	± (2σ)	^{206}Pb/^{238}U	± (2σ)	% disc.	Best Age (Ma)	± (2σ)
GJ1-1	81743	5279	0.0603	0.0004	0.8169	0.0454	0.0983	0.0054	0.9910	614	16	604	32	1.6		
GJ1-2	85889	5236	0.0604	0.0005	0.8358	0.0500	0.1003	0.0059	0.9900	619	18	616	35	0.5		
GJ1-3	91818	5359	0.0600	0.0005	0.8001	0.0448	0.0968	0.0053	0.9876	603	19	595	31	1.3		
GJ1-4	94080	1907	0.0603	0.0005	0.8288	0.0416	0.0996	0.0049	0.9882	616	16	612	29	0.6		
GJ1-5	103847	1539	0.0603	0.0005	0.8176	0.0376	0.0983	0.0044	0.9833	615	18	604	26	1.8		
GJ1-6	86117	1560	0.0598	0.0005	0.7982	0.0399	0.0967	0.0048	0.9874	598	17	595	28	0.5		
GJ1-7	75687	1484	0.0600	0.0006	0.8383	0.0475	0.1013	0.0057	0.9867	604	20	622	33	-3.1		
GJ1-8	67225	1090	0.0603	0.0006	0.8415	0.0540	0.1012	0.0064	0.9869	614	22	622	37	-1.3		
GJ1-9	66293	827	0.0605	0.0006	0.8222	0.0444	0.0986	0.0052	0.9856	621	20	606	31	2.5		
GJ1-10	58779	4610	0.0601	0.0007	0.8525	0.0506	0.1029	0.0060	0.9826	606	24	632	35	-4.4		
'JK073-87	42869	761	0.0615	0.0007	0.9401	0.0649	0.1109	0.0076	0.9876	656	23	678	44	-3.6	678	44
K073-124	196638	1161	0.0716	0.0019	0.7274	0.0719	0.0737	0.0070	0.9619	974	54	458	42	54.8		reject
'JK073-50	15815	601	0.0781	0.0009	2.2904	0.1243	0.2126	0.0113	0.9757	1150	23	1243	60	-8.9	1150	23
'JK073-31	68720	1834	0.0851	0.0007	2.6082	0.1660	0.2223	0.0140	0.9915	1318	16	1294	74	2.0	1318	16
'JK073-38	44150	974	0.0859	0.0013	2.4491	0.1634	0.2067	0.0134	0.9743	1336	29	1211	71	10.3		reject
K073-108	322580	2493	0.0894	0.0007	2.0902	0.1358	0.1696	0.0110	0.9937	1412	14	1010	60	30.7		reject
'JK073-43	74373	923	0.0912	0.0008	1.5369	0.0994	0.1222	0.0078	0.9898	1452	17	743	45	51.6		reject
'JK073-25	39031	885	0.0914	0.0009	3.2181	0.2423	0.2552	0.0191	0.9917	1456	18	1465	97	-0.7	1456	18
'JK073-81	76482	1139	0.0920	0.0008	3.2322	0.2102	0.2547	0.0164	0.9919	1468	16	1463	84	0.4	1468	16
'JK073-96	34511	692	0.0920	0.0008	3.1127	0.2174	0.2453	0.0170	0.9919	1468	17	1414	87	4.1	1468	17
'JK073-40	91989	2818	0.0926	0.0006	3.2778	0.1764	0.2567	0.0137	0.9918	1480	13	1473	70	0.5	1480	13
K073-121	87263	2610	0.0978	0.0010	2.1650	0.1676	0.1605	0.0123	0.9917	1583	19	960	68	42.3		reject
'JK073-83	155395	2205	0.1025	0.0007	4.0434	0.2894	0.2862	0.0204	0.9949	1669	13	1623	101	3.1	1669	13
K073-105	611309	7022	0.1061	0.0010	3.5503	0.2858	0.2426	0.0194	0.9937	1734	16	1400	100	21.4		reject
K073-116	209092	1850	0.1062	0.0016	1.7592	0.1420	0.1201	0.0095	0.9829	1736	27	731	55	61.1		reject
'JK073-55	680401	6648	0.1065	0.0008	3.9465	0.2641	0.2688	0.0179	0.9942	1740	13	1535	90	13.3		reject
'JK073-61	73099	1215	0.1073	0.0008	4.5979	0.2501	0.3108	0.0167	0.9895	1754	14	1745	82	0.6	1754	14
'JK073-70	260839	4579	0.1077	0.0007	4.2715	0.2349	0.2875	0.0157	0.9926	1762	12	1629	78	8.5	1762	12
'JK073-33	174112	4794	0.1085	0.0007	4.7676	0.2621	0.3186	0.0174	0.9927	1775	12	1783	84	-0.5	1775	12
'JK073-66	703906	8102	0.1086	0.0007	4.0573	0.2233	0.2710	0.0148	0.9927	1776	12	1546	75	14.6		reject
'JK073-16	95326	3360	0.1087	0.0008	4.7830	0.3476	0.3192	0.0231	0.9946	1777	14	1786	112	-0.6	1777	14

Thompson assemblage, 08TWJK073 Depositional age: Mississippian n= 98

Zircon 40 um Location (UTM): 454397E, 5618697N

Grain	^{206}Pb cps	$^{206}Pb/^{204}Pb$	$^{207}Pb/^{206}Pb$	± (2σ)	$^{207}Pb/^{235}U$	± (2σ)	$^{206}Pb/^{238}U$	± (2σ)	rho	Model Ages $^{207}Pb/^{206}Pb$	± (2σ)	$^{206}Pb/^{238}U$	± (2σ)	% disc.	Best Age (Ma)	± (2σ)
JK073-52	87177	8144	0.1089	0.0008	4.7211	0.2383	0.3143	0.0157	0.9897	1782	13	1762	77	1.3	1782	13
JK073-47	67408	1391	0.1091	0.0010	5.0729	0.2850	0.3372	0.0187	0.9861	1785	17	1873	89	-5.7	1785	17
K073-128	253288	12828	0.1097	0.0008	5.2076	0.3714	0.3444	0.0244	0.9944	1794	14	1908	116	-7.4	1794	14
K073-123	73313	4549	0.1097	0.0009	4.4703	0.3406	0.2954	0.0224	0.9941	1795	15	1669	110	8.0	1795	15
K073-107	106536	1488	0.1099	0.0008	4.7647	0.2743	0.3145	0.0180	0.9921	1797	13	1763	88	2.2	1797	13
JK073-53	150381	3727	0.1100	0.0007	5.0242	0.3197	0.3312	0.0210	0.9945	1800	12	1844	101	-2.9	1800	12
K073-117	160304	3062	0.1103	0.0008	4.9748	0.2876	0.3271	0.0188	0.9917	1804	13	1824	90	-1.3	1804	13
JK073-20	60503	1463	0.1105	0.0008	3.6403	0.2023	0.2388	0.0132	0.9909	1808	14	1381	68	26.2	reject	
JK073-59	141012	3244	0.1106	0.0007	4.4585	0.3386	0.2923	0.0221	0.9961	1809	12	1653	109	9.8	1809	12
JK073-63	402646	7739	0.1111	0.0007	4.9297	0.2793	0.3219	0.0181	0.9938	1817	11	1799	88	1.1	1817	11
JK073-78	144188	8807	0.1112	0.0007	4.9054	0.2974	0.3199	0.0193	0.9941	1819	12	1789	94	1.9	1819	12
JK073-44	61678	2088	0.1114	0.0009	5.1547	0.4157	0.3355	0.0269	0.9951	1823	14	1865	129	-2.6	1823	14
JK073-77	232924	9270	0.1115	0.0007	5.0796	0.2786	0.3305	0.0180	0.9932	1824	12	1841	87	-1.1	1824	12
JK073-13	120311	7011	0.1117	0.0008	4.9679	0.2856	0.3226	0.0184	0.9926	1827	13	1802	89	1.6	1827	13
JK073-28	212137	2676	0.1119	0.0008	4.3316	0.3491	0.2809	0.0225	0.9962	1830	13	1596	112	14.4	reject	
JK073-14	56433	1588	0.1120	0.0010	4.8404	0.2743	0.3134	0.0175	0.9871	1833	16	1757	85	4.7	1833	16
K073-129	73356	5087	0.1122	0.0010	4.1834	0.3334	0.2705	0.0214	0.9932	1835	17	1543	108	17.9	reject	
JK073-37	297205	4745	0.1123	0.0007	4.7798	0.3080	0.3087	0.0198	0.9948	1837	12	1734	97	6.4	1837	12
WJK073-2	118415	5634	0.1123	0.0008	4.9306	0.2775	0.3183	0.0178	0.9925	1838	12	1781	86	3.5	1838	12
JK073-42	126198	2594	0.1124	0.0008	5.4502	0.3843	0.3515	0.0247	0.9948	1839	13	1942	117	-6.5	1839	13
JK073-93	29694	726	0.1125	0.0011	4.8875	0.3994	0.3151	0.0256	0.9922	1840	18	1766	124	4.6	1840	18
K073-104	157465	3626	0.1126	0.0008	5.0215	0.3123	0.3235	0.0200	0.9932	1841	13	1807	97	2.2	1841	13
JK073-85	346081	5148	0.1126	0.0010	4.5108	0.4259	0.2904	0.0273	0.9952	1843	17	1644	135	12.2	reject	
K073-119	78050	2071	0.1127	0.0009	5.3918	0.3634	0.3471	0.0232	0.9930	1843	14	1921	110	-4.9	1843	14
JK073-54	101754	2412	0.1127	0.0008	5.2212	0.3103	0.3360	0.0198	0.9923	1843	13	1867	95	-1.5	1843	13
WJK073-9	227243	3327	0.1128	0.0011	4.5214	0.4561	0.2907	0.0292	0.9950	1845	18	1645	144	12.3	reject	
JK073-68	48674	973	0.1128	0.0009	5.1134	0.2998	0.3287	0.0191	0.9906	1845	14	1832	92	0.8	1845	14
K073-125	74044	6430	0.1129	0.0009	4.8971	0.2831	0.3146	0.0180	0.9896	1847	15	1763	88	5.2	1847	15
JK073-58	443537	6735	0.1130	0.0007	4.3069	0.2354	0.2763	0.0150	0.9929	1849	12	1573	75	16.8	reject	
JK073-92	101336	2185	0.1132	0.0009	5.1967	0.3007	0.3331	0.0191	0.9901	1851	15	1853	92	-0.2	1851	15
K073-112	106582	3872	0.1132	0.0009	5.1737	0.3434	0.3316	0.0219	0.9932	1851	14	1846	105	0.3	1851	14

Thompson assemblage, 08TWJK073 Depositional age: Mississippian n= 98

Zircon 40 um Location (UTM): 454397E, 5618697N

Grain	^{206}Pb cps	$^{206}Pb/^{204}Pb$	$^{207}Pb/^{206}Pb$	± (2σ)	$^{207}Pb/^{235}U$	± (2σ)	$^{206}Pb/^{238}U$	± (2σ)	rho	Model Ages $^{207}Pb/^{206}Pb$	± (2σ)	$^{206}Pb/^{238}U$	± (2σ)	% disc.	Best Age (Ma)	± (2σ)
JK073-17	49351	1594	0.1134	0.0010	5.3773	0.3608	0.3439	0.0229	0.9922	1855	15	1905	109	-3.2	1855	15
K073-110	22617	373	0.1134	0.0016	4.9978	0.3115	0.3196	0.0194	0.9753	1855	25	1788	94	4.2	1855	25
K073-113	68990	3447	0.1136	0.0010	5.2038	0.2933	0.3321	0.0185	0.9887	1858	15	1849	89	0.6	1858	15
JK073-71	126189	2440	0.1138	0.0008	5.3711	0.4186	0.3423	0.0266	0.9959	1861	13	1898	126	-2.3	1861	13
JK073-79	99672	4155	0.1139	0.0008	5.2295	0.2563	0.3331	0.0162	0.9895	1862	13	1854	78	0.5	1862	13
K073-103	150157	3529	0.1139	0.0008	5.1027	0.3242	0.3250	0.0205	0.9938	1862	13	1814	99	3.0	1862	13
K073-114	55923	1968	0.1141	0.0011	5.1605	0.3204	0.3279	0.0201	0.9888	1866	17	1828	97	2.3	1866	17
JK073-94	107229	2097	0.1143	0.0010	5.1364	0.3944	0.3260	0.0249	0.9941	1868	15	1819	120	3.0	1868	15
JK073-29	70463	1120	0.1146	0.0009	5.3712	0.3689	0.3398	0.0232	0.9929	1874	15	1886	111	-0.7	1874	15
K073-126	38693	2475	0.1149	0.0010	4.9999	0.3818	0.3155	0.0239	0.9933	1879	16	1768	116	6.8	1879	16
K073-109	123091	1922	0.1150	0.0009	5.1184	0.3195	0.3229	0.0200	0.9922	1879	14	1804	97	4.6	1879	14
JK073-32	221176	5152	0.1152	0.0007	4.6841	0.2931	0.2949	0.0184	0.9948	1883	11	1666	91	13.0	reject	
JK073-56	175053	4512	0.1172	0.0008	5.4696	0.2902	0.3386	0.0178	0.9922	1913	12	1880	85	2.0	1913	12
JK073-35	242201	3221	0.1173	0.0008	4.5988	0.3449	0.2843	0.0212	0.9956	1916	13	1613	106	17.8	reject	
JK073-22	124837	5071	0.1177	0.0008	5.5882	0.3016	0.3443	0.0184	0.9914	1922	13	1907	88	0.9	1922	13
JK073-60	57248	886	0.1181	0.0008	5.3933	0.3331	0.3312	0.0203	0.9934	1928	13	1844	98	5.0	1928	13
JK073-15	198598	1857	0.1189	0.0009	2.8551	0.2806	0.1742	0.0171	0.9973	1939	13	1035	93	50.4	reject	
JK073-45	117917	2737	0.1189	0.0009	4.3648	0.3180	0.2662	0.0193	0.9946	1940	13	1521	97	24.2	reject	
K073-102	19963	640	0.1207	0.0016	6.9762	0.5112	0.4192	0.0302	0.9840	1967	23	2257	136	-17.5	reject	
JK073-11	129220	23695	0.1209	0.0009	5.9753	0.4061	0.3586	0.0242	0.9945	1969	13	1975	114	-0.4	1969	13
WJK073-8	53785	2278	0.1210	0.0009	6.0425	0.4821	0.3623	0.0288	0.9953	1970	14	1993	135	-1.3	1970	14
K073-120	147306	722	0.1213	0.0011	2.4710	0.1927	0.1478	0.0115	0.9935	1975	16	888	64	58.8	reject	
JK073-89	36849	578	0.1222	0.0010	5.9684	0.3701	0.3543	0.0218	0.9907	1988	15	1955	103	1.9	1988	15
WJK073-3	81611	3352	0.1224	0.0009	5.9417	0.3049	0.3521	0.0179	0.9907	1991	12	1945	85	2.7	1991	12
JK073-67	44802	1259	0.1224	0.0011	5.7401	0.3444	0.3400	0.0202	0.9887	1992	16	1887	96	6.1	1992	16
JK073-72	49892	1476	0.1225	0.0010	6.5771	0.6096	0.3893	0.0359	0.9960	1993	15	2120	165	-7.4	1993	15
K073-100	39539	1056	0.1227	0.0012	5.7991	0.3628	0.3428	0.0212	0.9885	1996	17	1900	101	5.6	1996	17
JK073-39	51019	1396	0.1228	0.0012	6.0086	0.3161	0.3550	0.0184	0.9830	1997	17	1958	87	2.2	1997	17
JK073-23	33685	1005	0.1228	0.0012	6.0958	0.3426	0.3600	0.0199	0.9843	1997	18	1982	94	0.9	1997	18
JK073-80	127763	3904	0.1230	0.0009	5.9020	0.3573	0.3480	0.0209	0.9933	2000	12	1925	99	4.3	2000	12
JK073-62	57551	1270	0.1231	0.0011	6.2335	0.3346	0.3674	0.0194	0.9861	2001	16	2017	91	-0.9	2001	16

Thompson assemblage, 08TWJK073 Depositional age: Mississippian n= 98

Zircon 40 um Location (UTM): 454397E, 5618697N

Grain	^{206}Pb cps	^{206}Pb/^{204}Pb	^{207}Pb/^{206}Pb	± (2σ)	^{207}Pb/^{235}U	± (2σ)	^{206}Pb/^{238}U	± (2σ)	rho	Model Ages ^{207}Pb/^{206}Pb	± (2σ)	^{206}Pb/^{238}U	± (2σ)	% disc.	Best Age (Ma)	± (2σ)
JK073-97	40166	867	0.1233	0.0013	6.0658	0.3903	0.3568	0.0227	0.9873	2005	18	1967	107	2.2	2005	18
JK073-64	72662	1238	0.1237	0.0009	6.6763	0.4592	0.3916	0.0268	0.9949	2010	12	2130	123	-7.0	2010	12
K073-118	128749	2400	0.1237	0.0009	5.5062	0.3694	0.3228	0.0215	0.9936	2010	13	1803	104	11.8	reject	
K073-122	68127	3561	0.1238	0.0011	6.2355	0.4201	0.3653	0.0244	0.9914	2012	16	2007	114	0.2	2012	16
JK073-26	212288	987	0.1276	0.0009	6.1872	0.4333	0.3516	0.0245	0.9954	2065	12	1942	116	6.9	2065	12
JK073-82	84794	1436	0.1277	0.0010	6.3612	0.4009	0.3614	0.0226	0.9925	2066	14	1989	106	4.4	2066	14
JK073-46	211534	4370	0.1326	0.0009	6.3225	0.3825	0.3457	0.0208	0.9931	2133	12	1914	99	11.8	reject	
K073-111	152333	2363	0.1401	0.0035	3.0114	0.2662	0.1559	0.0132	0.9602	2229	42	934	73	62.3	reject	
JK073-34	154411	1070	0.1414	0.0012	5.3492	0.3555	0.2743	0.0181	0.9915	2245	15	1563	91	34.1	reject	
JK073-10	185342	4411	0.1470	0.0010	7.7567	0.6032	0.3827	0.0296	0.9962	2311	12	2089	137	11.3	reject	
JK073-98	27771	594	0.1483	0.0014	8.4833	0.5731	0.4150	0.0278	0.9901	2326	16	2238	125	4.5	2326	16
JK073-88	161298	2334	0.1502	0.0011	8.3412	0.5826	0.4028	0.0280	0.9941	2348	13	2182	127	8.3	2348	13
JK073-30	99980	1968	0.1509	0.0010	9.3600	0.5954	0.4500	0.0285	0.9944	2356	11	2395	125	-2.0	2356	11
JK073-24	46749	944	0.1522	0.0012	9.1425	0.8491	0.4356	0.0403	0.9963	2371	14	2331	179	2.0	2371	14
K073-101	77082	1480	0.1595	0.0012	9.7945	0.6374	0.4455	0.0288	0.9934	2450	13	2375	127	3.6	2450	13
JK073-90	126046	1501	0.1694	0.0012	6.5937	0.4875	0.2823	0.0208	0.9950	2552	12	1603	104	41.9	reject	
JK073-49	231705	5903	0.1704	0.0016	10.2248	0.5917	0.4353	0.0248	0.9860	2561	16	2329	111	10.8	reject	
JK073-19	143715	3239	0.1717	0.0011	11.5672	0.8158	0.4887	0.0343	0.9959	2574	11	2565	147	0.4	2574	11
JK073-21	138296	4090	0.1719	0.0011	11.1298	0.6374	0.4695	0.0267	0.9934	2576	11	2481	116	4.4	2576	11
JK073-51	191412	4810	0.1728	0.0016	5.9447	1.2563	0.2495	0.0527	0.9991	2585	15	1436	266	49.4	reject	
JK073-65	96869	1717	0.1751	0.0011	11.4050	0.5498	0.4723	0.0226	0.9910	2607	11	2494	98	5.2	2607	11
JK073-86	213936	1323	0.1815	0.0016	7.3247	0.6771	0.2927	0.0269	0.9957	2667	14	1655	133	42.9	reject	
JK073-48	169344	3978	0.1817	0.0011	12.5376	0.6106	0.5005	0.0242	0.9917	2668	10	2616	103	2.4	2668	10
JK073-41	85840	2319	0.1821	0.0014	13.2264	0.7408	0.5268	0.0292	0.9910	2672	12	2728	122	-2.6	2672	12
JK073-36	65508	1423	0.1824	0.0013	12.3762	0.8121	0.4920	0.0321	0.9940	2675	12	2579	137	4.3	2675	12
JK073-73	204481	8077	0.1824	0.0011	12.8897	0.6305	0.5124	0.0249	0.9919	2675	10	2667	105	0.4	2675	10
JK073-57	389093	6595	0.1829	0.0011	12.8028	0.7575	0.5077	0.0299	0.9948	2679	10	2647	127	1.5	2679	10
JK073-76	99567	3965	0.1836	0.0012	13.3159	1.0512	0.5260	0.0414	0.9965	2686	11	2725	172	-1.8	2686	11
JK073-84	441380	6656	0.1839	0.0013	13.3484	0.9252	0.5263	0.0363	0.9947	2689	12	2726	151	-1.7	2689	12
JK073-69	40168	642	0.1842	0.0013	12.5862	0.7192	0.4955	0.0281	0.9920	2691	12	2594	120	4.4	2691	12
K073-106	99517	2074	0.1845	0.0014	13.0653	0.8896	0.5137	0.0348	0.9938	2694	12	2672	146	1.0	2694	12

Thompson assemblage, 08TWJK073 Depositional age: Mississippian n= 98

Zircon 40 um Location (UTM): 454397E, 5618697N

Grain	^{206}Pb cps	^{206}Pb/^{204}Pb	^{207}Pb/^{206}Pb	± (2σ)	^{207}Pb/^{235}U	± (2σ)	^{206}Pb/^{238}U	± (2σ)	rho	Model Ages ^{207}Pb/^{206}Pb	± (2σ)	^{206}Pb/^{238}U	± (2σ)	% disc.	Best Age (Ma)	± (2σ)
'JK073-18	62920	1060	0.1845	0.0014	13.5177	1.1722	0.5313	0.0459	0.9963	2694	12	2747	190	-2.4	2694	12
K073-130	194562	17731	0.1848	0.0013	13.5665	1.0308	0.5323	0.0403	0.9957	2697	12	2751	167	-2.5	2697	12
K073-127	17500	1450	0.1855	0.0021	14.5692	1.1973	0.5695	0.0463	0.9902	2703	19	2906	188	-9.3	2703	19
WJK073-4	55096	2591	0.1855	0.0015	13.3464	1.0512	0.5217	0.0409	0.9948	2703	13	2706	171	-0.2	2703	13
'JK073-95	150260	2305	0.1864	0.0013	13.5080	1.0453	0.5257	0.0405	0.9957	2710	12	2723	169	-0.6	2710	12
'JK073-27	33113	565	0.1869	0.0016	14.2746	0.8982	0.5540	0.0345	0.9904	2715	14	2842	142	-5.8	2715	14
'JK073-74	338287	145	0.1870	0.0108	1.6004	0.2089	0.0621	0.0073	0.8961	2716	92	388	44	88.2	reject	
'JK073-99	86149	1752	0.1871	0.0015	12.3360	0.8607	0.4782	0.0331	0.9936	2717	13	2519	143	8.8	2717	13
K073-115	40940	1327	0.1896	0.0016	14.0423	0.9364	0.5373	0.0355	0.9922	2738	14	2772	147	-1.5	2738	14
WJK073-6	47460	1758	0.1897	0.0014	14.1768	0.8134	0.5421	0.0308	0.9916	2739	12	2792	128	-2.4	2739	12
'JK073-91	125363	2848	0.1907	0.0014	13.0191	1.0267	0.4952	0.0389	0.9957	2748	12	2593	166	6.8	2748	12
WJK073-5	52362	1720	0.1950	0.0014	13.7189	0.8816	0.5102	0.0326	0.9933	2785	12	2657	138	5.6	2785	12
'JK073-12	22876	infinite	0.1962	0.0021	14.2490	1.3392	0.5267	0.0492	0.9938	2795	17	2727	204	3.0	2795	17
WJK073-7	43525	1793	0.2015	0.0015	15.2969	1.1825	0.5506	0.0424	0.9954	2838	12	2828	174	0.5	2838	12
WJK073-1	199300	4072	0.2017	0.0013	15.5470	0.9060	0.5591	0.0324	0.9940	2840	10	2863	133	-1.0	2840	10
'JK073-75	695808	78	0.2691	0.0164	1.8533	0.2113	0.0500	0.0048	0.8441	3301	93	314	29	92.5	reject	

Davis assemblage, 07TWJK104B
Zircon 40 um

Depositional age: Late Mississippian
Location (UTM): 459310E, 5611179N

n= 96

Grain	colour	shape	^{206}Pb cps	$^{206}Pb/^{204}Pb$	$^{207}Pb/^{206}Pb$	± (2σ)	$^{207}Pb/^{235}U$	± (2σ)	$^{206}Pb/^{238}U$	± (2σ)	rho	Model Ages $^{207}Pb/^{206}Pb$	± (2σ)	Model Ages $^{206}Pb/^{238}U$	± (2σ)	% disc.	Best Age (Ma)	± (2σ)	*interp type*
23a	pnk	subrnd	267143	infinite	0.0596	0.0002	0.7161	0.0141	0.0869	0.0017	0.9560	590	23	537	19	9.4	489	140	*5*
23b	pnk	subrnd	213897	infinite	0.0609	0.0003	0.7580	0.0123	0.0904	0.0014	0.9434	635	25	558	19	12.7			
66a		prism	387712	infinite	0.1242	0.0003	5.8775	0.1212	0.3428	0.0070	0.9602	2017	18	1900	69	6.7	520	150	*5*
66b		prism	117209	543	0.1056	0.0049	2.8054	0.2635	0.1902	0.0155	0.8756	1725	87	1122	98	38.0	2045	49	*4*
89a	incl.		19597	infinite	0.0585	0.0010	0.8904	0.0208	0.1103	0.0018	0.8543	550	43	674	23	-23.8	reject		
89b	incl.		18628	infinite	0.0600	0.0009	1.0339	0.0188	0.1244	0.0012	0.8552	604	39	756	24	-26.7	reject		
89c	incl.	subrnd	35345	infinite	0.0619	0.0008	0.8864	0.0182	0.1035	0.0017	0.9022	672	34	635	22	5.8	635	22	
80	pnk	rnd	675915	infinite	0.0732	0.0002	1.7310	0.0323	0.1715	0.0032	0.9577	1020	21	1020	36	0.0	1020	21	
76	pnk	rnd	680517	18392	0.0741	0.0004	1.8179	0.0360	0.1779	0.0034	0.9519	1044	22	1055	38	-1.1	1044	22	
111	pnk	rnd	618574	30929	0.0748	0.0005	1.8790	0.0432	0.1818	0.0040	0.9475	1064	24	1077	40	-1.3	1067	18	*1*
111a	pnk	rnd	406471	20324	0.0750	0.0008	1.8929	0.0482	0.1828	0.0043	0.9311	1070	29	1082	41	-1.2			
65		prism	114461	10406	0.0761	0.0006	1.9091	0.0370	0.1826	0.0032	0.9310	1099	26	1081	38	1.7	1099	26	
56	cll	subrnd	69373	infinite	0.0764	0.0007	1.8232	0.0345	0.1714	0.0029	0.9268	1106	27	1020	35	8.5	1106	27	
70	cll	rnd	149946	infinite	0.0766	0.0003	1.8913	0.0326	0.1786	0.0030	0.9513	1110	22	1059	36	4.9	1110	22	
58	cll	subrnd	90473	infinite	0.0776	0.0004	1.8902	0.0422	0.1762	0.0038	0.9525	1137	23	1046	39	8.6	1137	23	
74	cll	rnd	49430	infinite	0.0785	0.0006	2.3666	0.0398	0.2202	0.0032	0.9281	1160	26	1283	43	-11.6	reject		
99	pnk	rnd	252139	63035	0.0790	0.0004	2.2288	0.0377	0.2054	0.0033	0.9440	1171	23	1204	41	-3.1	1171	23	
93	incl.	rnd	172552	86276	0.0803	0.0009	2.3000	0.0385	0.2076	0.0026	0.9005	1205	30	1216	39	-1.0	1205	30	
50	cll	subrnd	35857	1494	0.0808	0.0094	1.9772	0.2344	0.1678	0.0042	0.3081	1218	229	1000	39	19.3	reject		
51	cll	subrnd	100552	infinite	0.0809	0.0003	2.2310	0.0422	0.1997	0.0037	0.9539	1218	21	1174	41	4.0	1218	21	
53	cll	subrnd	183434	5395	0.0825	0.0010	2.3418	0.0530	0.2067	0.0040	0.9103	1257	31	1211	43	4.0	1257	31	
101	pnk	rnd	111696	22339	0.0828	0.0008	2.5966	0.0595	0.2275	0.0048	0.9337	1264	27	1321	48	-5.0	1264	27	
52	cll	subrnd	31781	infinite	0.0832	0.0009	2.1134	0.0444	0.1811	0.0033	0.9205	1274	28	1073	38	17.1	reject		
26	pnk	subrnd	389200	24325	0.0874	0.0004	2.7490	0.0474	0.2289	0.0038	0.9469	1370	22	1329	45	3.4	1370	22	
88	incl.	rnd	124222	124222	0.0877	0.0005	3.0480	0.0461	0.2525	0.0035	0.9402	1376	22	1451	48	-6.1	1376	22	
14	pnk	subrnd	557546	22302	0.0893	0.0005	2.8756	0.0858	0.2333	0.0068	0.9637	1411	22	1352	57	4.6	1411	22	
11	pnk	subrnd	858153	85815	0.0910	0.0003	3.1034	0.0483	0.2467	0.0037	0.9507	1446	20	1422	48	1.9	1446	20	
35	cll	subrnd	1126819	563410	0.0911	0.0003	2.6275	0.0597	0.2092	0.0047	0.9615	1448	20	1224	46	17.0	reject		
49	cll	subrnd	426909	213454	0.0920	0.0003	3.1377	0.0548	0.2469	0.0042	0.9542	1467	20	1422	49	3.4	1467	20	
61	cll	subrnd	55625	infinite	0.0923	0.0006	2.9406	0.0619	0.2294	0.0046	0.9463	1473	23	1331	48	10.6	reject		
18	pnk	subrnd	644156	infinite	0.0927	0.0002	3.0585	0.0392	0.2394	0.0030	0.9505	1482	19	1383	45	7.4	1482	19	
40	cll	subrnd	189053	infinite	0.0941	0.0005	3.3533	0.0385	0.2582	0.0026	0.9360	1509	22	1481	47	2.1	1509	22	
63		prism	760631	6978	0.0981	0.0005	3.6008	0.1018	0.2677	0.0075	0.9634	1588	21	1529	63	4.1	1588	21	
90	incl.		244008	22183	0.1003	0.0010	3.4248	0.0832	0.2478	0.0055	0.9321	1629	26	1427	53	13.8	reject		
68	cll	rnd	298656	infinite	0.1024	0.0007	3.9227	0.0750	0.2782	0.0049	0.9400	1668	23	1582	55	5.8	1668	23	
69a	cll	rnd	169994	525	0.1048	0.0013	4.5887	0.5008	0.3195	0.0346	0.9902	1711	29	1787	201	-5.1	1711	29	

Davis assemblage, 07TWJK104B Depositional age: Late Mississippian n= 96

Zircon 40 um Location (UTM): 459310E, 5611179N

Grain	colour	shape	^{206}Pb cps	$^{206}Pb/^{204}Pb$	$^{207}Pb/^{206}Pb$	± (2σ)	$^{207}Pb/^{235}U$	± (2σ)	$^{206}Pb/^{238}U$	± (2σ)	rho	Model Ages $^{207}Pb/^{206}Pb$	± (2σ)	$^{206}Pb/^{238}U$	± (2σ)	% disc.	Best Age (Ma)	± (2σ)	*interp type*
69b	cll	rnd	35423	148	0.0835	0.0533	1.9954	1.2905	0.1673	0.0176	0.1680	1281	1244	997	109	23.9	reject		
30	pnk	subrnd	845894	84589	0.1063	0.0003	4.4717	0.1039	0.3049	0.0070	0.9621	1737	19	1716	65	1.4	1737	19	
103	pnk	rnd	930136	103348	0.1091	0.0002	4.7885	0.0723	0.3183	0.0048	0.9542	1785	19	1781	60	0.2	1785	19	
77	pnk	rnd	317265	infinite	0.1095	0.0002	4.7064	0.0986	0.3113	0.0065	0.9608	1791	19	1747	64	2.8	1791	19	
47	cll	subrnd	121492	121492	0.1101	0.0006	4.9448	0.1067	0.3257	0.0068	0.9506	1801	21	1817	66	-1.1	1801	21	
100	pnk	rnd	958090	47905	0.1101	0.0004	4.2448	0.0697	0.2794	0.0045	0.9527	1802	19	1588	54	13.3	reject		
94	incl.	rnd	162946	infinite	0.1102	0.0004	4.9099	0.0945	0.3233	0.0061	0.9565	1803	19	1806	64	-0.2	1803	19	
3	pnk	subrnd	491030	infinite	0.1107	0.0003	4.6374	0.0548	0.3036	0.0035	0.9473	1811	19	1709	55	6.4	1811	19	
28	pnk	subrnd	756645	151329	0.1118	0.0002	4.9534	0.1708	0.3213	0.0111	0.9756	1828	18	1796	82	2.0	1828	18	
21	pnk	subrnd	388131	13384	0.1120	0.0006	4.7708	0.1227	0.3091	0.0078	0.9588	1832	20	1736	68	5.9	1832	20	
31	pnk	subrnd	923501	65964	0.1123	0.0002	4.8831	0.1377	0.3153	0.0089	0.9694	1837	18	1767	73	4.4	1837	18	
92	incl.	subrnd	436150	145383	0.1124	0.0004	4.9400	0.0837	0.3175	0.0053	0.9534	1839	19	1777	61	3.8	1839	19	
83	pnk	rnd	314847	31485	0.1125	0.0006	5.3593	0.1396	0.3452	0.0088	0.9605	1841	20	1912	75	-4.4	1841	20	
32	pnk	subrnd	270470	135235	0.1126	0.0003	5.1444	0.1060	0.3313	0.0068	0.9587	1841	19	1845	67	-0.2	1841	19	
20	pnk	subrnd	443243	8363	0.1127	0.0006	4.7651	0.0814	0.3087	0.0050	0.9467	1843	20	1734	59	6.7	1843	20	
22	pnk	subrnd	441994	infinite	0.1127	0.0002	5.0774	0.0973	0.3269	0.0062	0.9591	1843	18	1823	65	1.2	1843	18	
29	pnk	subrnd	433105	61872	0.1127	0.0004	5.2703	0.1454	0.3390	0.0093	0.9654	1844	19	1882	76	-2.4	1844	19	
7	pnk	subrnd	739280	infinite	0.1127	0.0002	4.9500	0.1003	0.3180	0.0064	0.9608	1844	18	1780	64	4.0	1844	18	
43	cll	subrnd	169358	infinite	0.1129	0.0004	5.4364	0.0885	0.3491	0.0055	0.9512	1847	19	1930	66	-5.2	1847	19	
36	cll	subrnd	166993	infinite	0.1129	0.0004	5.2583	0.1420	0.3376	0.0090	0.9645	1847	19	1875	75	-1.7	1847	19	
78	pnk	rnd	357696	35770	0.1132	0.0005	5.2061	0.1123	0.3332	0.0070	0.9565	1852	20	1854	68	-0.1	1852	20	
46	cll	subrnd	164753	82376	0.1132	0.0005	5.2223	0.1176	0.3344	0.0074	0.9576	1852	20	1860	69	-0.5	1852	20	
104	pnk	rnd	538823	44902	0.1135	0.0003	5.1757	0.0849	0.3305	0.0053	0.9535	1857	19	1841	63	1.0	1857	19	
10	pnk	subrnd	184967	36993	0.1135	0.0009	4.5721	0.1117	0.2903	0.0067	0.9456	1857	23	1643	62	13.0	reject		
59	cll	subrnd	194479	27783	0.1138	0.0007	4.7462	0.0514	0.3022	0.0027	0.9316	1861	21	1702	53	9.7	1861	21	
42	cll	subrnd	377997	infinite	0.1138	0.0005	5.1088	0.1795	0.3259	0.0113	0.9713	1861	20	1818	84	2.6	1861	20	
33	pnk	subrnd	570721	63413	0.1139	0.0003	5.2311	0.1278	0.3331	0.0081	0.9636	1862	19	1853	71	0.5	1862	19	
81	pnk	rnd	496934	infinite	0.1142	0.0002	5.4589	0.1077	0.3463	0.0068	0.9594	1867	18	1917	69	-3.1	1867	18	
12	pnk	subrnd	109483	infinite	0.1142	0.0004	4.2813	0.3233	0.2716	0.0205	0.9916	1867	19	1549	126	19.2	reject		
25	pnk	subrnd	533860	66732	0.1144	0.0004	5.1886	0.1003	0.3290	0.0063	0.9560	1870	19	1834	65	2.2	1870	19	
9	pnk	subrnd	214826	71609	0.1145	0.0004	5.2132	0.1195	0.3299	0.0075	0.9605	1872	19	1838	69	2.1	1872	19	
17	pnk	subrnd	312492	4167	0.1145	0.0010	5.1494	0.1343	0.3292	0.0081	0.9425	1873	24	1835	71	2.3	1873	24	
82	pnk	rnd	555526	18518	0.1146	0.0009	5.3655	0.0996	0.3377	0.0057	0.9364	1874	22	1876	65	-0.1	1874	22	
54	cll	subrnd	287838	28784	0.1151	0.0005	5.4317	0.1113	0.3414	0.0068	0.9553	1882	20	1893	68	-0.7	1882	20	
60	cll	subrnd	231756	23176	0.1153	0.0007	5.3640	0.1286	0.3367	0.0078	0.9524	1885	21	1871	71	0.9	1885	21	
5	pnk	subrnd	167781	infinite	0.1156	0.0006	5.3829	0.1212	0.3385	0.0074	0.9556	1889	20	1879	70	0.6	1889	20	

Davis assemblage, 07TWJK104B
Zircon 40 um

Depositional age: Late Mississippian
Location (UTM): 459310E, 5611179N

n= 96

Grain	colour	shape	^{206}Pb cps	^{206}Pb/^{204}Pb	^{207}Pb/^{206}Pb	± (2σ)	^{207}Pb/^{235}U	± (2σ)	^{206}Pb/^{238}U	± (2σ)	rho	Model Ages ^{207}Pb/^{206}Pb	± (2σ)	^{206}Pb/^{238}U	± (2σ)	% disc.	Best Age (Ma)	± (2σ)	*interp type*
6	pnk	subrnd	185071	infinite	0.1160	0.0003	5.3194	0.0801	0.3322	0.0049	0.9516	1895	19	1849	62	2.8	1895	19	
37	cll	subrnd	115032	115032	0.1180	0.0005	5.7956	0.0925	0.3560	0.0055	0.9482	1927	20	1963	66	-2.2	1927	20	
13	pnk	subrnd	594578	1824	0.1182	0.0010	4.9499	0.1210	0.3022	0.0070	0.9434	1929	23	1702	64	13.4	reject		
57	cll	subrnd	357099	32464	0.1190	0.0006	5.5864	0.1313	0.3398	0.0078	0.9559	1941	20	1886	71	3.3	1941	20	
110	pnk	rnd	529488	16045	0.1193	0.0005	5.3783	0.1158	0.3264	0.0069	0.9561	1946	20	1821	67	7.4	1946	20	
38	cll	subrnd	157796	22542	0.1198	0.0009	5.9708	0.1271	0.3632	0.0073	0.9422	1954	22	1997	72	-2.6	1954	22	
55	cll	subrnd	292800	12200	0.1206	0.0007	5.9434	0.1415	0.3564	0.0083	0.9555	1965	20	1965	75	0.0	1965	20	
107	pnk	rnd	754915	11614	0.1207	0.0009	5.8409	0.1470	0.3502	0.0084	0.9468	1967	23	1936	74	1.8	1967	23	
106	pnk	rnd	208537	infinite	0.1210	0.0005	5.9557	0.0868	0.3570	0.0050	0.9472	1971	19	1968	65	0.2	1971	19	
102	pnk	rnd	85253	42627	0.1210	0.0008	6.0807	0.1426	0.3662	0.0083	0.9517	1971	21	2011	76	-2.4	1971	21	
19a	pnk	subrnd	399787	5794	0.1215	0.0008	6.0504	0.0562	0.3610	0.0025	0.9283	1978	21	1987	61	-0.5	1995	40	*3*
19b	pnk	subrnd	258316	infinite	0.1240	0.0003	6.0401	0.0880	0.3526	0.0050	0.9515	2014	18	1947	65	3.9			
15	pnk	subrnd	789695	46453	0.1219	0.0003	5.7444	0.0923	0.3418	0.0054	0.9533	1984	18	1895	64	5.2	1984	18	
97	pnk	rnd	209918	9542	0.1246	0.0010	6.5525	0.1170	0.3816	0.0061	0.9306	2023	23	2084	71	-3.5	2023	23	
79	pnk	rnd	296757	29676	0.1258	0.0006	6.4573	0.1310	0.3706	0.0073	0.9536	2040	19	2032	73	0.4	2040	19	
91	incl.	frag	572155	infinite	0.1284	0.0002	6.3707	0.1383	0.3601	0.0078	0.9625	2076	18	1982	73	5.2	2076	18	
95	incl.	rnd	285619	95206	0.1299	0.0003	6.8491	0.1228	0.3825	0.0068	0.9563	2096	18	2088	73	0.5	2096	18	
39	cll	subrnd	233592	infinite	0.1305	0.0003	6.9516	0.1357	0.3863	0.0075	0.9585	2105	18	2106	75	0.0	2105	18	
24	pnk	subrnd	709743	5633	0.1326	0.0005	7.0544	0.1485	0.3860	0.0080	0.9582	2132	18	2104	77	1.5	2132	18	
71	cll	rnd	76704	infinite	0.1338	0.0005	7.4049	0.1288	0.4020	0.0068	0.9514	2148	19	2178	75	-1.6	2148	19	
16	pnk	subrnd	445265	7299	0.1359	0.0013	7.0557	0.1901	0.3762	0.0095	0.9398	2176	24	2059	81	6.3	2176	24	
64		prism	815186	3607	0.1448	0.0033	2.7402	0.2621	0.1376	0.0128	0.9682	2285	43	831	81	67.7	reject		
85	pnk	rnd	818230	9405	0.1477	0.0003	9.2006	0.1873	0.4514	0.0091	0.9601	2319	18	2402	87	-4.2	2319	18	
87	incl.	subrnd	629415	69935	0.1480	0.0006	6.9509	0.0710	0.3405	0.0032	0.9421	2323	18	1889	59	21.5	reject		
45	cll	subrnd	788754	78875	0.1511	0.0006	8.6010	0.1920	0.4127	0.0091	0.9587	2359	18	2227	83	6.6	2359	18	
41	cll	subrnd	379968	19998	0.1611	0.0080	9.3886	0.6613	0.4795	0.0239	0.7485	2468	86	2525	147	-2.8	2468	86	
62	cll	subrnd	295690	4620	0.1657	0.0052	12.2795	1.0653	0.5481	0.0444	0.9341	2515	55	2817	243	-14.9	reject		
86	incl.	frag	104548	infinite	0.1673	0.0009	11.6105	0.1946	0.5063	0.0080	0.9446	2531	19	2641	90	-5.3	2531	19	
75	cll	rnd	232000	1589	0.1754	0.0075	7.1401	0.6012	0.2940	0.0213	0.8713	2610	73	1662	130	41.1	reject		
67		prism	145090	797	0.1755	0.0166	12.6299	2.2662	0.5164	0.0786	0.8515	2611	159	2684	417	-3.4	2611	159	
34	cll	subrnd	413674	51709	0.1795	0.0005	12.2394	0.1786	0.4939	0.0071	0.9520	2648	17	2587	86	2.8	2648	17	
2	pnk	subrnd	1247224	infinite	0.1828	0.0002	12.5358	0.2909	0.4969	0.0115	0.9646	2678	17	2600	99	3.5	2678	17	
1	pnk	subrnd	854738	7305	0.1830	0.0006	12.2933	0.3078	0.4894	0.0121	0.9635	2680	17	2568	100	5.1	2680	17	
96	pnk	rnd	528580	528580	0.1834	0.0004	12.9529	0.2518	0.5123	0.0099	0.9588	2683	17	2667	95	0.8	2683	17	
27	pnk	subrnd	564467	141117	0.1847	0.0005	12.8904	0.3065	0.5061	0.0120	0.9636	2696	17	2640	101	2.5	2696	17	
4	pnk	subrnd	561727	28086	0.1848	0.0006	11.3359	0.4716	0.4447	0.0184	0.9791	2696	17	2371	121	14.4	reject		

Davis assemblage, 07TWJK104B
Zircon 40 um

Depositional age: Late Mississippian
Location (UTM): 459310E, 5611179N

n= 96

												Model Ages							
Grain	**colour**	**shape**	**^{206}Pb cps**	**^{206}Pb/^{204}Pb**	**^{207}Pb/^{206}Pb**	**± (2σ)**	**^{207}Pb/^{235}U**	**± (2σ)**	**^{206}Pb/^{238}U**	**± (2σ)**	**rho**	**^{207}Pb/^{206}Pb**	**± (2σ)**	**^{206}Pb/^{238}U**	**± (2σ)**	**% disc.**	**Best Age (Ma)**	**± (2σ)**	*interp type*
84	pnk	rnd	1019857	8792	0.1852	0.0003	14.2995	0.3140	0.5599	0.0123	0.9625	2700	17	2866	106	-7.6	2700	17	
105	pnk	rnd	683073	34154	0.1854	0.0004	12.9844	0.2755	0.5100	0.0108	0.9616	2702	17	2657	97	2.0	2702	17	
44	cll	subrnd	289644	infinite	0.1871	0.0006	13.3017	0.2851	0.5156	0.0109	0.9598	2717	17	2680	99	1.6	2717	17	
48	cll	subrnd	225868	infinite	0.1875	0.0005	12.9857	0.3504	0.5052	0.0136	0.9669	2721	17	2636	106	3.8	2721	17	
8	pnk	subrnd	212993	infinite	0.1883	0.0005	13.8193	0.3541	0.5316	0.0135	0.9652	2727	17	2748	108	-1.0	2727	17	
109	pnk	rnd	334192	22279	0.1896	0.0004	12.1178	0.2713	0.4632	0.0103	0.9624	2738	17	2454	92	12.5	reject		
98	pnk	rnd	201542	40308	0.1902	0.0005	14.0428	0.1712	0.5354	0.0063	0.9482	2744	17	2764	89	-0.9	2744	17	
72	cll	rnd	223311	4466	0.1905	0.0033	13.9634	0.3549	0.5310	0.0098	0.8592	2747	33	2746	97	0.0	2747	33	
73	cll	rnd	247166	13009	0.1923	0.0010	13.2829	0.2096	0.4978	0.0074	0.9450	2762	18	2604	87	6.9	2762	18	
108a	pnk	rnd	378033	34367	0.2832	0.0006	27.9593	0.6714	0.7153	0.0171	0.9647	3381	16	3479	133	-3.8	3381	11	*1*
108b	pnk	rnd	386724	27623	0.2833	0.0009	26.2293	0.5801	0.6673	0.0146	0.9604	3381	16	3296	122	3.2			

Davis assemblage, 08TWJK309
Zircon 40 um

Depositional age: Late Mississippian
Location (UTM): 453667E, 5618627N

n= 87

Grain	colour	shape	^{206}Pb cps	^{206}Pb/^{204}Pb	^{207}Pb/^{206}Pb	± (2σ)	^{207}Pb/^{235}U	± (2σ)	^{206}Pb/^{238}U	± (2σ)	rho	Model Ages ^{207}Pb/^{206}Pb	± (2σ)	^{206}Pb/^{238}U	± (2σ)	% disc.	Best Age (Ma)	± (2σ)	*interp type*
GJ1-32-1			216106	infinite	0.0609	0.0011	0.8268	0.0326	0.0985	0.0035	0.8972	635	37	606	20	4.9			
GJ1-32-2			201191	infinite	0.0606	0.0011	0.8300	0.0322	0.0993	0.0034	0.8890	626	38	610	20	2.6			
GJ1-32-3			197903	infinite	0.0607	0.0010	0.8160	0.0308	0.0975	0.0033	0.8894	628	37	600	19	4.6			
GJ1-32-4			181874	infinite	0.0607	0.0011	0.8165	0.0326	0.0976	0.0035	0.8991	628	38	600	21	4.6			
GJ1-32-5			217613	infinite	0.0620	0.0013	0.8339	0.0334	0.0975	0.0033	0.8541	675	45	600	20	11.6			
GJ1-32-6			199598	infinite	0.0613	0.0011	0.8195	0.0321	0.0969	0.0034	0.8871	650	39	596	20	8.7			
GJ1-32-7			215554	infinite	0.0605	0.0010	0.8203	0.0312	0.0984	0.0034	0.9013	621	36	605	20	2.7			
GJ1-32-8			192666	infinite	0.0608	0.0007	0.8168	0.0300	0.0974	0.0034	0.9429	633	26	599	20	5.6			
GJ1-32-9			187411	infinite	0.0609	0.0010	0.8079	0.0325	0.0963	0.0035	0.9081	634	36	593	21	6.9			
GJ1-32-10			181461	infinite	0.0603	0.0012	0.8136	0.0323	0.0978	0.0033	0.8621	616	43	601	20	2.5			
101	pnk	frag	23690	infinite	0.0533	0.0089	0.4571	0.0784	0.0622	0.0024	0.2235	341	379	389	14	-14.6	reject		
43		facet	32201	infinite	0.0546	0.0045	0.5236	0.0477	0.0696	0.0027	0.4205	395	186	434	16	-10.1	reject		
36		facet	186713	infinite	0.0555	0.0012	0.4967	0.0232	0.0649	0.0027	0.8833	433	49	405	16	6.6	405	16	
102a	pnk	frag	125696	infinite	0.0567	0.0018	0.5145	0.0260	0.0658	0.0026	0.7730	481	71	411	16	15.2	415	11	*3*
102b	pnk	frag	173762	infinite	0.0558	0.0011	0.5090	0.0226	0.0662	0.0026	0.8874	444	45	413	16	7.3			
42		facet	59264	infinite	0.0549	0.0027	0.5125	0.0322	0.0677	0.0026	0.6168	408	111	422	16	-3.7	422	16	
26		facet	65852	infinite	0.0557	0.0030	0.5211	0.0345	0.0678	0.0026	0.5676	441	121	423	15	4.2	423	15	
48		subhed	96702	infinite	0.0558	0.0018	0.5224	0.0268	0.0679	0.0027	0.7751	446	72	423	16	5.2	423	16	
49a		subhed	98732	infinite	0.0560	0.0026	0.5310	0.0321	0.0688	0.0027	0.6385	452	103	429	16	5.4	427	9	*2*
49b		subhed	83740	infinite	0.0558	0.0025	0.5261	0.0312	0.0684	0.0026	0.6462	444	101	427	16	4.0			
49c		subhed	48378	infinite	0.0558	0.0050	0.5267	0.0507	0.0684	0.0025	0.3807	445	198	427	15	4.2			
33		facet	151398	infinite	0.0560	0.0022	0.4359	0.0252	0.0564	0.0024	0.7208	454	89	354	14	22.6	reject		
32		facet	84238	infinite	0.0567	0.0023	0.5107	0.0288	0.0653	0.0025	0.6923	481	90	408	15	15.7	reject		
92	cll	frag	31585	535	0.0621	0.0045	1.8504	0.1457	0.2160	0.0069	0.4086	679	154	1260	37	-94.4	reject		
63	cll	rnd	370851	4075	0.0685	0.0010	1.4357	0.0530	0.1519	0.0052	0.9249	885	29	912	29	-3.3	885	29	
91	cll	frag	91376	1603	0.0700	0.0024	1.8265	0.0878	0.1892	0.0064	0.7050	929	70	1117	35	-22.1	reject		
5	pnk	frag	298487	4326	0.0710	0.0012	1.6875	0.0625	0.1723	0.0057	0.8893	959	35	1025	31	-7.4	959	35	
109			183646	3673	0.0719	0.0012	1.7592	0.0679	0.1775	0.0062	0.8987	983	34	1053	34	-7.7	983	34	
47		facet	198084	3195	0.0725	0.0011	1.6340	0.0615	0.1634	0.0056	0.9156	1000	31	976	31	2.6	1000	31	
74	cll	rnd	29652	3295	0.0733	0.0030	1.8671	0.0985	0.1846	0.0063	0.6442	1024	82	1092	34	-7.3	1024	82	
59	cll	rnd	119718	1814	0.0738	0.0026	1.8774	0.0937	0.1846	0.0064	0.6954	1035	72	1092	35	-6.0	1035	72	
11	pnk	frag	94937	2637	0.0738	0.0016	2.0390	0.0802	0.2003	0.0065	0.8256	1037	45	1177	35	-14.8	reject		
2	pnk	frag	393638	6056	0.0739	0.0010	1.8040	0.0686	0.1770	0.0063	0.9407	1040	26	1050	35	-1.1	1040	26	
78	pnk	rnd	205657	20566	0.0749	0.0009	1.6535	0.0589	0.1602	0.0054	0.9396	1065	25	958	30	10.8	reject		
56a		subhed	36357	infinite	0.0793	0.0076	1.9390	0.1972	0.1773	0.0062	0.3413	1180	189	1052	34	11.7	1060	23	*3*

Davis assemblage, 08TWJK309
Zircon 40 um

Depositional age: Late Mississippian
Location (UTM): 453667E, 5618627N

n= 87

Grain	colour	shape	^{206}Pb cps	^{206}Pb/^{204}Pb	^{207}Pb/^{206}Pb	± (2σ)	^{207}Pb/^{235}U	± (2σ)	^{206}Pb/^{238}U	± (2σ)	rho	Model Ages ^{207}Pb/^{206}Pb	± (2σ)	^{206}Pb/^{238}U	± (2σ)	% disc.	Best Age (Ma)	± (2σ)	*interp type*
56b		subhed	26416	infinite	0.0773	0.0094	1.9118	0.2417	0.1794	0.0060	0.2649	1129	243	1064	33	6.2			
83	cll	frag	243652	infinite	0.0761	0.0009	1.8585	0.0694	0.1772	0.0063	0.9520	1097	23	1051	34	4.5	1097	23	
99	pnk	frag	93702	1616	0.0765	0.0024	2.2095	0.1065	0.2094	0.0076	0.7532	1109	63	1226	40	-11.6	reject		
82	cll	frag	61558	7695	0.0770	0.0014	1.9706	0.0751	0.1857	0.0063	0.8863	1121	35	1098	34	2.2	1121	35	
79	pnk	rnd	108616	12068	0.0772	0.0013	2.0213	0.0722	0.1900	0.0060	0.8909	1126	32	1121	33	0.4	1126	32	
81	pnk	rnd	29397	infinite	0.0775	0.0032	2.0203	0.1066	0.1891	0.0063	0.6346	1134	81	1116	34	1.7	1134	81	
96	ylw	frag	47092	infinite	0.0795	0.0047	2.0322	0.1363	0.1853	0.0061	0.4895	1185	116	1096	33	8.2	1185	116	
84	cll	frag	272924	infinite	0.0799	0.0009	2.0765	0.0695	0.1885	0.0060	0.9436	1194	22	1113	32	7.3	1194	22	
70	cll	rnd	113407	infinite	0.0800	0.0018	2.0874	0.0845	0.1892	0.0063	0.8232	1197	45	1117	34	7.3	1197	45	
77	cll	rnd	56320	3520	0.0808	0.0021	2.4015	0.1016	0.2157	0.0073	0.7954	1216	50	1259	38	-3.9	1216	50	
55a		subhed	135525	infinite	0.0890	0.0018	2.7533	0.1050	0.2244	0.0073	0.8520	1404	38	1305	38	7.8	1232	180	*5*
55b		subhed	134152	infinite	0.0888	0.0015	2.7598	0.1015	0.2253	0.0074	0.8885	1401	32	1310	39	7.2			
55c		subhed	359575	4181	0.0858	0.0010	2.5874	0.1041	0.2187	0.0084	0.9583	1334	22	1275	44	4.8			
69	cll	rnd	76848	infinite	0.0818	0.0033	2.2076	0.1158	0.1957	0.0067	0.6518	1241	78	1152	36	7.8	1241	78	
44		facet	67597	infinite	0.0820	0.0028	2.3399	0.1118	0.2071	0.0068	0.6905	1245	68	1213	36	2.8	1245	68	
65	cll	rnd	54123	459	0.0823	0.0041	3.4350	0.2093	0.3027	0.0107	0.5820	1253	97	1705	53	-41.1	reject		
66	cll	rnd	136770	infinite	0.0830	0.0014	2.2966	0.0902	0.2006	0.0071	0.8969	1270	34	1178	38	7.9	1270	34	
75	cll	rnd	81229	infinite	0.0865	0.0012	2.5956	0.1003	0.2176	0.0079	0.9371	1350	26	1269	42	6.6	1350	26	
76	cll	rnd	159567	infinite	0.0873	0.0010	2.5414	0.0874	0.2112	0.0069	0.9439	1367	22	1235	36	10.6	reject		
71	cll	rnd	191245	2516	0.0885	0.0015	3.0332	0.1162	0.2487	0.0085	0.8919	1392	33	1432	44	-3.1	1392	33	
13	pnk	frag	1328674	12079	0.0988	0.0011	3.7661	0.1286	0.2766	0.0089	0.9440	1601	21	1574	45	1.9	1601	21	
104	pnk	frag	463512	9656	0.1000	0.0011	3.6682	0.1293	0.2661	0.0089	0.9480	1624	21	1521	45	7.1	1624	21	
61	cll	rnd	289934	674	0.1018	0.0014	2.4322	0.1067	0.1733	0.0072	0.9491	1657	26	1030	40	40.9	reject		
57	cll	rnd	300179	2832	0.1026	0.0013	2.1219	0.1092	0.1500	0.0075	0.9714	1671	23	901	42	49.3	reject		
52		subhed	204798	1575	0.1032	0.0015	3.3022	0.1228	0.2321	0.0080	0.9218	1682	27	1346	41	22.1	reject		
97	ylw	frag	135985	2893	0.1032	0.0016	4.0657	0.1454	0.2857	0.0092	0.8993	1683	29	1620	46	4.2	1683	29	
50		subhed	126165	760	0.1035	0.0025	4.3787	0.1917	0.3068	0.0112	0.8355	1688	44	1725	55	-2.5	1688	44	
100	pnk	frag	116569	1325	0.1042	0.0025	4.6084	0.1998	0.3208	0.0116	0.8318	1700	44	1793	56	-6.3	1700	44	
4	pnk	frag	556967	3376	0.1046	0.0013	2.4813	0.1172	0.1720	0.0078	0.9623	1707	24	1023	43	43.3	reject		
30		facet	528906	7147	0.1061	0.0012	4.6747	0.1608	0.3196	0.0104	0.9453	1733	21	1788	51	-3.6	1733	21	
72	cll	rnd	140877	1830	0.1085	0.0016	4.6816	0.1710	0.3130	0.0105	0.9182	1774	26	1756	51	1.2	1774	26	
34		facet	114318	2722	0.1089	0.0019	4.9989	0.1917	0.3328	0.0114	0.8900	1782	32	1852	55	-4.5	1782	32	
45		facet	305084	4179	0.1093	0.0012	5.0683	0.1745	0.3364	0.0110	0.9454	1787	20	1869	53	-5.3	1787	20	
1	pnk	frag	160359	2864	0.1097	0.0019	5.0479	0.1876	0.3339	0.0110	0.8845	1794	32	1857	53	-4.1	1794	32	
31		facet	295915	3401	0.1098	0.0013	5.0188	0.1748	0.3315	0.0109	0.9401	1796	22	1846	52	-3.2	1796	22	
73	cll	rnd	116495	6472	0.1103	0.0018	4.6178	0.1816	0.3036	0.0109	0.9149	1805	29	1709	54	6.0	1805	29	

Davis assemblage, 08TWJK309 Depositional age: Late Mississippian n= 87

Zircon 40 um Location (UTM): 453667E, 5618627N

Grain	colour	shape	^{206}Pb cps	^{206}Pb/^{204}Pb	^{207}Pb/^{206}Pb	± (2σ)	^{207}Pb/^{235}U	± (2σ)	^{206}Pb/^{238}U	± (2σ)	rho	Model Ages ^{207}Pb/^{206}Pb	± (2σ)	Model Ages ^{206}Pb/^{238}U	± (2σ)	% disc.	Best Age (Ma)	± (2σ)	*interp type*
103	pnk	frag	122244	3704	0.1104	0.0017	4.8279	0.1715	0.3172	0.0101	0.8983	1806	28	1776	49	1.9	1806	28	
46		facet	341625	4166	0.1106	0.0015	4.9966	0.2240	0.3275	0.0140	0.9535	1810	25	1826	68	-1.0	1810	25	
111			287702	2877	0.1107	0.0014	5.0037	0.1827	0.3279	0.0112	0.9381	1810	23	1828	54	-1.1	1810	23	
37		facet	25457	infinite	0.1107	0.0065	4.9049	0.3323	0.3213	0.0111	0.5082	1811	106	1796	54	0.9	1811	106	
7	pnk	frag	116794	3768	0.1109	0.0014	4.9769	0.1681	0.3256	0.0102	0.9314	1814	22	1817	50	-0.2	1814	22	
106	pnk	frag	239166	5979	0.1109	0.0013	4.9507	0.1726	0.3236	0.0106	0.9406	1815	21	1807	51	0.5	1815	21	
10	pnk	frag	505933	9920	0.1110	0.0012	4.2168	0.1633	0.2755	0.0103	0.9613	1816	19	1569	52	15.3	reject		
80	pnk	rnd	69443	11574	0.1110	0.0018	4.8026	0.1717	0.3137	0.0100	0.8879	1817	30	1759	49	3.6	1817	30	
28		facet	464970	8157	0.1112	0.0012	5.1966	0.1755	0.3388	0.0108	0.9437	1820	20	1881	52	-3.9	1820	20	
40		facet	217322	10349	0.1114	0.0013	5.1021	0.1761	0.3322	0.0108	0.9388	1822	22	1849	52	-1.7	1822	22	
17	pnk	frag	316455	12171	0.1114	0.0012	5.0371	0.1729	0.3279	0.0107	0.9491	1823	20	1828	52	-0.4	1823	20	
3	pnk	frag	445541	7304	0.1116	0.0013	4.9985	0.1734	0.3249	0.0107	0.9459	1825	20	1814	52	0.7	1825	20	
89	cll	frag	51628	1076	0.1117	0.0036	5.3249	0.2462	0.3457	0.0115	0.7166	1828	58	1914	55	-5.5	1828	58	
19	pnk	frag	168666	7028	0.1119	0.0013	5.2535	0.1784	0.3406	0.0108	0.9355	1830	22	1889	52	-3.7	1830	22	
62	cll	rnd	177319	2216	0.1119	0.0015	5.1437	0.1752	0.3333	0.0104	0.9204	1831	24	1854	50	-1.5	1831	24	
25	pnk	frag	227103	5047	0.1121	0.0014	5.3468	0.1797	0.3460	0.0108	0.9246	1834	23	1915	51	-5.2	1834	23	
21	pnk	frag	346003	15727	0.1121	0.0012	4.9764	0.1682	0.3219	0.0103	0.9488	1834	19	1799	50	2.2	1834	19	
18	pnk	frag	108601	6033	0.1121	0.0015	5.1447	0.1778	0.3327	0.0106	0.9221	1834	24	1852	51	-1.1	1834	24	
29		facet	113683	infinite	0.1123	0.0020	5.1884	0.1946	0.3352	0.0111	0.8796	1836	32	1863	53	-1.7	1836	32	
6	pnk	frag	508882	8342	0.1124	0.0012	5.2424	0.1741	0.3384	0.0106	0.9474	1838	19	1879	51	-2.6	1838	19	
87	cll	frag	32724	infinite	0.1128	0.0013	5.1337	0.1886	0.3302	0.0115	0.9519	1844	20	1839	56	0.3	1844	20	
16	pnk	frag	96094	3003	0.1133	0.0020	5.2534	0.1932	0.3362	0.0108	0.8718	1853	33	1869	52	-0.9	1853	33	
23	pnk	frag	209835	9538	0.1134	0.0014	5.2016	0.1794	0.3326	0.0107	0.9339	1855	22	1851	52	0.2	1855	22	
41		facet	210427	11690	0.1140	0.0012	5.3013	0.1882	0.3374	0.0114	0.9518	1863	20	1874	55	-0.7	1863	20	
35		facet	209824	4464	0.1152	0.0014	5.4920	0.1923	0.3459	0.0113	0.9351	1882	22	1915	54	-2.0	1882	22	
105	pnk	frag	468517	13780	0.1161	0.0012	5.2486	0.1801	0.3278	0.0107	0.9503	1897	19	1828	52	4.2	1897	19	
67	cll	rnd	172963	2621	0.1172	0.0017	5.6813	0.2042	0.3515	0.0116	0.9180	1915	26	1942	55	-1.6	1915	26	
98	ylw	frag	122927	2509	0.1185	0.0017	5.5794	0.1972	0.3416	0.0110	0.9116	1933	26	1894	53	2.3	1933	26	
24	pnk	frag	206475	4802	0.1221	0.0016	6.2032	0.2101	0.3685	0.0115	0.9245	1987	23	2022	54	-2.1	1987	23	
27		facet	94938	1556	0.1231	0.0021	6.3749	0.2366	0.3756	0.0124	0.8929	2002	30	2055	58	-3.1	2002	30	
88	cll	frag	91133	infinite	0.1247	0.0014	6.0676	0.2044	0.3530	0.0112	0.9457	2024	19	1949	53	4.3	2024	19	
93	cll	frag	56074	1020	0.1279	0.0064	6.4255	0.4194	0.3644	0.0151	0.6365	2069	89	2003	71	3.7	2069	89	
95	ylw	frag	362809	5759	0.1287	0.0014	6.3708	0.2157	0.3591	0.0115	0.9459	2080	19	1978	54	5.7	2080	19	
22	pnk	frag	225880	6454	0.1303	0.0016	5.3245	0.2274	0.2963	0.0121	0.9563	2102	22	1673	60	23.1	reject		
107			179663	5284	0.1356	0.0016	7.0498	0.2410	0.3772	0.0121	0.9373	2171	21	2063	56	5.8	2171	21	
9	pnk	frag	191261	6170	0.1408	0.0020	7.4202	0.2515	0.3824	0.0118	0.9117	2236	24	2087	55	7.8	2236	24	

Davis assemblage, 08TWJK309
Zircon 40 um

Depositional age: Late Mississippian
Location (UTM): 453667E, 5618627N

n= 87

Grain	colour	shape	^{206}Pb cps	$^{206}Pb/^{204}Pb$	$^{207}Pb/^{206}Pb$	± (2σ)	$^{207}Pb/^{235}U$	± (2σ)	$^{206}Pb/^{238}U$	± (2σ)	rho	Model Ages $^{207}Pb/^{206}Pb$	± (2σ)	Model Ages $^{206}Pb/^{238}U$	± (2σ)	% disc.	Best Age (Ma)	± (2σ)	*interp type*
58	cll	rnd	164628	2457	0.1423	0.0021	7.9514	0.2744	0.4053	0.0127	0.9046	2255	25	2193	58	3.3	2255	25	
110			201799	3363	0.1471	0.0020	8.3019	0.3235	0.4094	0.0149	0.9364	2312	23	2212	68	5.1	2312	23	
12	pnk	frag	758096	3928	0.1505	0.0016	7.9371	0.2886	0.3825	0.0133	0.9586	2352	18	2088	62	13.1	reject		
15	pnk	frag	211626	5039	0.1511	0.0019	9.2988	0.3151	0.4463	0.0140	0.9253	2358	22	2379	62	-1.0	2358	22	
38		facet	323716	14075	0.1576	0.0016	9.8064	0.3550	0.4514	0.0156	0.9574	2430	18	2401	69	1.4	2430	18	
8	pnk	frag	230867	10038	0.1733	0.0018	11.7202	0.3897	0.4905	0.0155	0.9491	2590	17	2573	67	0.8	2590	17	
51		subhed	484090	3936	0.1734	0.0018	11.3482	0.4048	0.4748	0.0162	0.9569	2590	17	2504	70	4.0	2590	17	
20	pnk	frag	273074	10923	0.1737	0.0019	11.9166	0.3926	0.4975	0.0155	0.9457	2594	18	2603	66	-0.4	2594	18	
53		subhed	132398	1439	0.1769	0.0022	11.9024	0.4345	0.4881	0.0167	0.9389	2624	21	2562	72	2.8	2624	21	
108			250219	3850	0.1781	0.0020	10.6818	0.4721	0.4350	0.0186	0.9686	2635	18	2328	83	13.9	reject		
54		subhed	243441	3121	0.1789	0.0021	5.6979	0.1953	0.2310	0.0074	0.9404	2642	19	1340	39	54.4	reject		
90	cll	frag	156971	3019	0.1807	0.0021	12.2728	0.4090	0.4927	0.0154	0.9390	2659	19	2582	66	3.5	2659	19	
14	pnk	frag	303814	7995	0.1842	0.0019	13.3425	0.4718	0.5253	0.0178	0.9556	2691	17	2722	75	-1.4	2691	17	
94	ylw	frag	186618	3110	0.1846	0.0022	12.6425	0.4342	0.4966	0.0160	0.9393	2695	19	2599	69	4.3	2695	19	
64	cll	rnd	234485	2369	0.1934	0.0022	13.8987	0.4757	0.5211	0.0169	0.9455	2772	18	2704	71	3.0	2772	18	
68	cll	rnd	130670	1867	0.2038	0.0026	15.1392	0.5215	0.5389	0.0173	0.9309	2857	20	2779	72	3.4	2857	20	
39		facet	658722	20585	0.2048	0.0021	13.0363	0.4455	0.4617	0.0150	0.9538	2865	17	2447	66	17.5	reject		

Davis assemblage, 08TWJK309
Zircon 40 um

Depositional age: Late Mississippian
Location (UTM): 453667E, 5618627N

n= 87

Grain	colour	shape	^{206}Pb cps	$^{206}Pb/^{204}Pb$	$^{207}Pb/^{206}Pb$	± (2σ)	$^{207}Pb/^{235}U$	± (2σ)	$^{206}Pb/^{238}U$	± (2σ)	rho	Model Ages $^{207}Pb/^{206}Pb$	± (2σ)	Model Ages $^{206}Pb/^{238}U$	± (2σ)	% disc.	Best Age (Ma)	± (2σ)	*interp type*
GJ1-32-1			216106	infinite	0.0609	0.0011	0.8268	0.0326	0.0985	0.0035	0.8972	635	37	606	20	4.9			
GJ1-32-2			201191	infinite	0.0606	0.0011	0.8300	0.0322	0.0993	0.0034	0.8890	626	38	610	20	2.6			
GJ1-32-3			197903	infinite	0.0607	0.0010	0.8160	0.0308	0.0975	0.0033	0.8894	628	37	600	19	4.6			
GJ1-32-4			181874	infinite	0.0607	0.0011	0.8165	0.0326	0.0976	0.0035	0.8991	628	38	600	21	4.6			
GJ1-32-5			217613	infinite	0.0620	0.0013	0.8339	0.0334	0.0975	0.0033	0.8541	675	45	600	20	11.6			
GJ1-32-6			199598	infinite	0.0613	0.0011	0.8195	0.0321	0.0969	0.0034	0.8871	650	39	596	20	8.7			
GJ1-32-7			215554	infinite	0.0605	0.0010	0.8203	0.0312	0.0984	0.0034	0.9013	621	36	605	20	2.7			
GJ1-32-8			192666	infinite	0.0608	0.0007	0.8168	0.0300	0.0974	0.0034	0.9429	633	26	599	20	5.6			
GJ1-32-9			187411	infinite	0.0609	0.0010	0.8079	0.0325	0.0963	0.0035	0.9081	634	36	593	21	6.9			
GJ1-32-10			181461	infinite	0.0603	0.0012	0.8136	0.0323	0.0978	0.0033	0.8621	616	43	601	20	2.5			
101	pnk	frag	23690	infinite	0.0533	0.0089	0.4571	0.0784	0.0622	0.0024	0.2235	341	379	389	14	-14.6	reject		
43		facet	32201	infinite	0.0546	0.0045	0.5236	0.0477	0.0696	0.0027	0.4205	395	186	434	16	-10.1	reject		
36		facet	186713	infinite	0.0555	0.0012	0.4967	0.0232	0.0649	0.0027	0.8833	433	49	405	16	6.6	405	16	
102a	pnk	frag	125696	infinite	0.0567	0.0018	0.5145	0.0260	0.0658	0.0026	0.7730	481	71	411	16	15.2	415	11	*3*
102b	pnk	frag	173762	infinite	0.0558	0.0011	0.5090	0.0226	0.0662	0.0026	0.8874	444	45	413	16	7.3			
42		facet	59264	infinite	0.0549	0.0027	0.5125	0.0322	0.0677	0.0026	0.6168	408	111	422	16	-3.7	422	16	
26		facet	65852	infinite	0.0557	0.0030	0.5211	0.0345	0.0678	0.0026	0.5676	441	121	423	15	4.2	423	15	
48		subhed	96702	infinite	0.0558	0.0018	0.5224	0.0268	0.0679	0.0027	0.7751	446	72	423	16	5.2	423	16	
49a		subhed	98732	infinite	0.0560	0.0026	0.5310	0.0321	0.0688	0.0027	0.6385	452	103	429	16	5.4	427	9	*2*
49b		subhed	83740	infinite	0.0558	0.0025	0.5261	0.0312	0.0684	0.0026	0.6462	444	101	427	16	4.0			
49c		subhed	48378	infinite	0.0558	0.0050	0.5267	0.0507	0.0684	0.0025	0.3807	445	198	427	15	4.2			
33		facet	151398	infinite	0.0560	0.0022	0.4359	0.0252	0.0564	0.0024	0.7208	454	89	354	14	22.6	reject		
32		facet	84238	infinite	0.0567	0.0023	0.5107	0.0288	0.0653	0.0025	0.6923	481	90	408	15	15.7	reject		
92	cll	frag	31585	535	0.0621	0.0045	1.8504	0.1457	0.2160	0.0069	0.4086	679	154	1260	37	-94.4	reject		
63	cll	rnd	370851	4075	0.0685	0.0010	1.4357	0.0530	0.1519	0.0052	0.9249	885	29	912	29	-3.3	885	29	
91	cll	frag	91376	1603	0.0700	0.0024	1.8265	0.0878	0.1892	0.0064	0.7050	929	70	1117	35	-22.1	reject		
5	pnk	frag	298487	4326	0.0710	0.0012	1.6875	0.0625	0.1723	0.0057	0.8893	959	35	1025	31	-7.4	959	35	
109			183646	3673	0.0719	0.0012	1.7592	0.0679	0.1775	0.0062	0.8987	983	34	1053	34	-7.7	983	34	
47		facet	198084	3195	0.0725	0.0011	1.6340	0.0615	0.1634	0.0056	0.9156	1000	31	976	31	2.6	1000	31	
74	cll	rnd	29652	3295	0.0733	0.0030	1.8671	0.0985	0.1846	0.0063	0.6442	1024	82	1092	34	-7.3	1024	82	
59	cll	rnd	119718	1814	0.0738	0.0026	1.8774	0.0937	0.1846	0.0064	0.6954	1035	72	1092	35	-6.0	1035	72	
11	pnk	frag	94937	2637	0.0738	0.0016	2.0390	0.0802	0.2003	0.0065	0.8256	1037	45	1177	35	-14.8	reject		
2	pnk	frag	393638	6056	0.0739	0.0010	1.8040	0.0686	0.1770	0.0063	0.9407	1040	26	1050	35	-1.1	1040	26	
78	pnk	rnd	205657	20566	0.0749	0.0009	1.6535	0.0589	0.1602	0.0054	0.9396	1065	25	958	30	10.8	reject		
56a		subhed	36357	infinite	0.0793	0.0076	1.9390	0.1972	0.1773	0.0062	0.3413	1180	189	1052	34	11.7	1060	23	*3*

Davis assemblage, 08TWJK309
Zircon 40 um

Depositional age: Late Mississippian
Location (UTM): 453667E, 5618627N

n= 87

Grain	colour	shape	^{206}Pb cps	^{206}Pb/^{204}Pb	^{207}Pb/^{206}Pb	± (2σ)	^{207}Pb/^{235}U	± (2σ)	^{206}Pb/^{238}U	± (2σ)	rho	Model Ages ^{207}Pb/^{206}Pb	± (2σ)	^{206}Pb/^{238}U	± (2σ)	% disc.	Best Age (Ma)	± (2σ)	*interp type*
56b		subhed	26416	infinite	0.0773	0.0094	1.9118	0.2417	0.1794	0.0060	0.2649	1129	243	1064	33	6.2			
83	cll	frag	243652	infinite	0.0761	0.0009	1.8585	0.0694	0.1772	0.0063	0.9520	1097	23	1051	34	4.5	1097	23	
99	pnk	frag	93702	1616	0.0765	0.0024	2.2095	0.1065	0.2094	0.0076	0.7532	1109	63	1226	40	-11.6	reject		
82	cll	frag	61558	7695	0.0770	0.0014	1.9706	0.0751	0.1857	0.0063	0.8863	1121	35	1098	34	2.2	1121	35	
79	pnk	rnd	108616	12068	0.0772	0.0013	2.0213	0.0722	0.1900	0.0060	0.8909	1126	32	1121	33	0.4	1126	32	
81	pnk	rnd	29397	infinite	0.0775	0.0032	2.0203	0.1066	0.1891	0.0063	0.6346	1134	81	1116	34	1.7	1134	81	
96	ylw	frag	47092	infinite	0.0795	0.0047	2.0322	0.1363	0.1853	0.0061	0.4895	1185	116	1096	33	8.2	1185	116	
84	cll	frag	272924	infinite	0.0799	0.0009	2.0765	0.0695	0.1885	0.0060	0.9436	1194	22	1113	32	7.3	1194	22	
70	cll	rnd	113407	infinite	0.0800	0.0018	2.0874	0.0845	0.1892	0.0063	0.8232	1197	45	1117	34	7.3	1197	45	
77	cll	rnd	56320	3520	0.0808	0.0021	2.4015	0.1016	0.2157	0.0073	0.7954	1216	50	1259	38	-3.9	1216	50	
55a		subhed	135525	infinite	0.0890	0.0018	2.7533	0.1050	0.2244	0.0073	0.8520	1404	38	1305	38	7.8	1232	180	*5*
55b		subhed	134152	infinite	0.0888	0.0015	2.7598	0.1015	0.2253	0.0074	0.8885	1401	32	1310	39	7.2			
55c		subhed	359575	4181	0.0858	0.0010	2.5874	0.1041	0.2187	0.0084	0.9583	1334	22	1275	44	4.8			
69	cll	rnd	76848	infinite	0.0818	0.0033	2.2076	0.1158	0.1957	0.0067	0.6518	1241	78	1152	36	7.8	1241	78	
44		facet	67597	infinite	0.0820	0.0028	2.3399	0.1118	0.2071	0.0068	0.6905	1245	68	1213	36	2.8	1245	68	
65	cll	rnd	54123	459	0.0823	0.0041	3.4350	0.2093	0.3027	0.0107	0.5820	1253	97	1705	53	-41.1	reject		
66	cll	rnd	136770	infinite	0.0830	0.0014	2.2966	0.0902	0.2006	0.0071	0.8969	1270	34	1178	38	7.9	1270	34	
75	cll	rnd	81229	infinite	0.0865	0.0012	2.5956	0.1003	0.2176	0.0079	0.9371	1350	26	1269	42	6.6	1350	26	
76	cll	rnd	159567	infinite	0.0873	0.0010	2.5414	0.0874	0.2112	0.0069	0.9439	1367	22	1235	36	10.6	reject		
71	cll	rnd	191245	2516	0.0885	0.0015	3.0332	0.1162	0.2487	0.0085	0.8919	1392	33	1432	44	-3.1	1392	33	
13	pnk	frag	1328674	12079	0.0988	0.0011	3.7661	0.1286	0.2766	0.0089	0.9440	1601	21	1574	45	1.9	1601	21	
104	pnk	frag	463512	9656	0.1000	0.0011	3.6682	0.1293	0.2661	0.0089	0.9480	1624	21	1521	45	7.1	1624	21	
61	cll	rnd	289934	674	0.1018	0.0014	2.4322	0.1067	0.1733	0.0072	0.9491	1657	26	1030	40	40.9	reject		
57	cll	rnd	300179	2832	0.1026	0.0013	2.1219	0.1092	0.1500	0.0075	0.9714	1671	23	901	42	49.3	reject		
52		subhed	204798	1575	0.1032	0.0015	3.3022	0.1228	0.2321	0.0080	0.9218	1682	27	1346	41	22.1	reject		
97	ylw	frag	135985	2893	0.1032	0.0016	4.0657	0.1454	0.2857	0.0092	0.8993	1683	29	1620	46	4.2	1683	29	
50		subhed	126165	760	0.1035	0.0025	4.3787	0.1917	0.3068	0.0112	0.8355	1688	44	1725	55	-2.5	1688	44	
100	pnk	frag	116569	1325	0.1042	0.0025	4.6084	0.1998	0.3208	0.0116	0.8318	1700	44	1793	56	-6.3	1700	44	
4	pnk	frag	556967	3376	0.1046	0.0013	2.4813	0.1172	0.1720	0.0078	0.9623	1707	24	1023	43	43.3	reject		
30		facet	528906	7147	0.1061	0.0012	4.6747	0.1608	0.3196	0.0104	0.9453	1733	21	1788	51	-3.6	1733	21	
72	cll	rnd	140877	1830	0.1085	0.0016	4.6816	0.1710	0.3130	0.0105	0.9182	1774	26	1756	51	1.2	1774	26	
34		facet	114318	2722	0.1089	0.0019	4.9989	0.1917	0.3328	0.0114	0.8900	1782	32	1852	55	-4.5	1782	32	
45		facet	305084	4179	0.1093	0.0012	5.0683	0.1745	0.3364	0.0110	0.9454	1787	20	1869	53	-5.3	1787	20	
1	pnk	frag	160359	2864	0.1097	0.0019	5.0479	0.1876	0.3339	0.0110	0.8845	1794	32	1857	53	-4.1	1794	32	
31		facet	295915	3401	0.1098	0.0013	5.0188	0.1748	0.3315	0.0109	0.9401	1796	22	1846	52	-3.2	1796	22	
73	cll	rnd	116495	6472	0.1103	0.0018	4.6178	0.1816	0.3036	0.0109	0.9149	1805	29	1709	54	6.0	1805	29	

Davis assemblage, 08TWJK309
Zircon 40 um

Depositional age: Late Mississippian
Location (UTM): 453667E, 5618627N

n= 87

Grain	colour	shape	^{206}Pb cps	$^{206}Pb/^{204}Pb$	$^{207}Pb/^{206}Pb$	± (2σ)	$^{207}Pb/^{235}U$	± (2σ)	$^{206}Pb/^{238}U$	± (2σ)	rho	Model Ages $^{207}Pb/^{206}Pb$	± (2σ)	Model Ages $^{206}Pb/^{238}U$	± (2σ)	% disc.	Best Age (Ma)	± (2σ)	*interp type*
103	pnk	frag	122244	3704	0.1104	0.0017	4.8279	0.1715	0.3172	0.0101	0.8983	1806	28	1776	49	1.9	1806	28	
46		facet	341625	4166	0.1106	0.0015	4.9966	0.2240	0.3275	0.0140	0.9535	1810	25	1826	68	-1.0	1810	25	
111			287702	2877	0.1107	0.0014	5.0037	0.1827	0.3279	0.0112	0.9381	1810	23	1828	54	-1.1	1810	23	
37		facet	25457	infinite	0.1107	0.0065	4.9049	0.3323	0.3213	0.0111	0.5082	1811	106	1796	54	0.9	1811	106	
7	pnk	frag	116794	3768	0.1109	0.0014	4.9769	0.1681	0.3256	0.0102	0.9314	1814	22	1817	50	-0.2	1814	22	
106	pnk	frag	239166	5979	0.1109	0.0013	4.9507	0.1726	0.3236	0.0106	0.9406	1815	21	1807	51	0.5	1815	21	
10	pnk	frag	505933	9920	0.1110	0.0012	4.2168	0.1633	0.2755	0.0103	0.9613	1816	19	1569	52	15.3	reject		
80	pnk	rnd	69443	11574	0.1110	0.0018	4.8026	0.1717	0.3137	0.0100	0.8879	1817	30	1759	49	3.6	1817	30	
28		facet	464970	8157	0.1112	0.0012	5.1966	0.1755	0.3388	0.0108	0.9437	1820	20	1881	52	-3.9	1820	20	
40		facet	217322	10349	0.1114	0.0013	5.1021	0.1761	0.3322	0.0108	0.9388	1822	22	1849	52	-1.7	1822	22	
17	pnk	frag	316455	12171	0.1114	0.0012	5.0371	0.1729	0.3279	0.0107	0.9491	1823	20	1828	52	-0.4	1823	20	
3	pnk	frag	445541	7304	0.1116	0.0013	4.9985	0.1734	0.3249	0.0107	0.9459	1825	20	1814	52	0.7	1825	20	
89	cll	frag	51628	1076	0.1117	0.0036	5.3249	0.2462	0.3457	0.0115	0.7166	1828	58	1914	55	-5.5	1828	58	
19	pnk	frag	168666	7028	0.1119	0.0013	5.2535	0.1784	0.3406	0.0108	0.9355	1830	22	1889	52	-3.7	1830	22	
62	cll	rnd	177319	2216	0.1119	0.0015	5.1437	0.1752	0.3333	0.0104	0.9204	1831	24	1854	50	-1.5	1831	24	
25	pnk	frag	227103	5047	0.1121	0.0014	5.3468	0.1797	0.3460	0.0108	0.9246	1834	23	1915	51	-5.2	1834	23	
21	pnk	frag	346003	15727	0.1121	0.0012	4.9764	0.1682	0.3219	0.0103	0.9488	1834	19	1799	50	2.2	1834	19	
18	pnk	frag	108601	6033	0.1121	0.0015	5.1447	0.1778	0.3327	0.0106	0.9221	1834	24	1852	51	-1.1	1834	24	
29		facet	113683	infinite	0.1123	0.0020	5.1884	0.1946	0.3352	0.0111	0.8796	1836	32	1863	53	-1.7	1836	32	
6	pnk	frag	508882	8342	0.1124	0.0012	5.2424	0.1741	0.3384	0.0106	0.9474	1838	19	1879	51	-2.6	1838	19	
87	cll	frag	32724	infinite	0.1128	0.0013	5.1337	0.1886	0.3302	0.0115	0.9519	1844	20	1839	56	0.3	1844	20	
16	pnk	frag	96094	3003	0.1133	0.0020	5.2534	0.1932	0.3362	0.0108	0.8718	1853	33	1869	52	-0.9	1853	33	
23	pnk	frag	209835	9538	0.1134	0.0014	5.2016	0.1794	0.3326	0.0107	0.9339	1855	22	1851	52	0.2	1855	22	
41		facet	210427	11690	0.1140	0.0012	5.3013	0.1882	0.3374	0.0114	0.9518	1863	20	1874	55	-0.7	1863	20	
35		facet	209824	4464	0.1152	0.0014	5.4920	0.1923	0.3459	0.0113	0.9351	1882	22	1915	54	-2.0	1882	22	
105	pnk	frag	468517	13780	0.1161	0.0012	5.2486	0.1801	0.3278	0.0107	0.9503	1897	19	1828	52	4.2	1897	19	
67	cll	rnd	172963	2621	0.1172	0.0017	5.6813	0.2042	0.3515	0.0116	0.9180	1915	26	1942	55	-1.6	1915	26	
98	ylw	frag	122927	2509	0.1185	0.0017	5.5794	0.1972	0.3416	0.0110	0.9116	1933	26	1894	53	2.3	1933	26	
24	pnk	frag	206475	4802	0.1221	0.0016	6.2032	0.2101	0.3685	0.0115	0.9245	1987	23	2022	54	-2.1	1987	23	
27		facet	94938	1556	0.1231	0.0021	6.3749	0.2366	0.3756	0.0124	0.8929	2002	30	2055	58	-3.1	2002	30	
88	cll	frag	91133	infinite	0.1247	0.0014	6.0676	0.2044	0.3530	0.0112	0.9457	2024	19	1949	53	4.3	2024	19	
93	cll	frag	56074	1020	0.1279	0.0064	6.4255	0.4194	0.3644	0.0151	0.6365	2069	89	2003	71	3.7	2069	89	
95	ylw	frag	362809	5759	0.1287	0.0014	6.3708	0.2157	0.3591	0.0115	0.9459	2080	19	1978	54	5.7	2080	19	
22	pnk	frag	225880	6454	0.1303	0.0016	5.3245	0.2274	0.2963	0.0121	0.9563	2102	22	1673	60	23.1	reject		
107			179663	5284	0.1356	0.0016	7.0498	0.2410	0.3772	0.0121	0.9373	2171	21	2063	56	5.8	2171	21	
9	pnk	frag	191261	6170	0.1408	0.0020	7.4202	0.2515	0.3824	0.0118	0.9117	2236	24	2087	55	7.8	2236	24	

Davis assemblage, 08TWJK309
Zircon 40 um

Depositional age: Late Mississippian
Location (UTM): 453667E, 5618627N

n= 87

Grain	colour	shape	^{206}Pb cps	^{206}Pb/^{204}Pb	^{207}Pb/^{206}Pb	± (2σ)	^{207}Pb/^{235}U	± (2σ)	^{206}Pb/^{238}U	± (2σ)	rho	Model Ages ^{207}Pb/^{206}Pb	± (2σ)	^{206}Pb/^{238}U	± (2σ)	% disc.	Best Age (Ma)	± (2σ)	*interp type*
58	cll	rnd	164628	2457	0.1423	0.0021	7.9514	0.2744	0.4053	0.0127	0.9046	2255	25	2193	58	3.3	2255	25	
110			201799	3363	0.1471	0.0020	8.3019	0.3235	0.4094	0.0149	0.9364	2312	23	2212	68	5.1	2312	23	
12	pnk	frag	758096	3928	0.1505	0.0016	7.9371	0.2886	0.3825	0.0133	0.9586	2352	18	2088	62	13.1	reject		
15	pnk	frag	211626	5039	0.1511	0.0019	9.2988	0.3151	0.4463	0.0140	0.9253	2358	22	2379	62	-1.0	2358	22	
38		facet	323716	14075	0.1576	0.0016	9.8064	0.3550	0.4514	0.0156	0.9574	2430	18	2401	69	1.4	2430	18	
8	pnk	frag	230867	10038	0.1733	0.0018	11.7202	0.3897	0.4905	0.0155	0.9491	2590	17	2573	67	0.8	2590	17	
51		subhed	484090	3936	0.1734	0.0018	11.3482	0.4048	0.4748	0.0162	0.9569	2590	17	2504	70	4.0	2590	17	
20	pnk	frag	273074	10923	0.1737	0.0019	11.9166	0.3926	0.4975	0.0155	0.9457	2594	18	2603	66	-0.4	2594	18	
53		subhed	132398	1439	0.1769	0.0022	11.9024	0.4345	0.4881	0.0167	0.9389	2624	21	2562	72	2.8	2624	21	
108			250219	3850	0.1781	0.0020	10.6818	0.4721	0.4350	0.0186	0.9686	2635	18	2328	83	13.9	reject		
54		subhed	243441	3121	0.1789	0.0021	5.6979	0.1953	0.2310	0.0074	0.9404	2642	19	1340	39	54.4	reject		
90	cll	frag	156971	3019	0.1807	0.0021	12.2728	0.4090	0.4927	0.0154	0.9390	2659	19	2582	66	3.5	2659	19	
14	pnk	frag	303814	7995	0.1842	0.0019	13.3425	0.4718	0.5253	0.0178	0.9556	2691	17	2722	75	-1.4	2691	17	
94	ylw	frag	186618	3110	0.1846	0.0022	12.6425	0.4342	0.4966	0.0160	0.9393	2695	19	2599	69	4.3	2695	19	
64	cll	rnd	234485	2369	0.1934	0.0022	13.8987	0.4757	0.5211	0.0169	0.9455	2772	18	2704	71	3.0	2772	18	
68	cll	rnd	130670	1867	0.2038	0.0026	15.1392	0.5215	0.5389	0.0173	0.9309	2857	20	2779	72	3.4	2857	20	
39		facet	658722	20585	0.2048	0.0021	13.0363	0.4455	0.4617	0.0150	0.9538	2865	17	2447	66	17.5	reject		

McHardy assemblage, 07TWJK153
Zircon 40 um

Depositional age: Late Mississippian or Pennsylvanian
Location (UTM): 453524E, 5608660N

n= 115

												Model Ages							
Grain	colour	shape	^{206}Pb cps	^{206}Pb/^{204}Pb	^{207}Pb/^{206}Pb	± (2σ)	^{207}Pb/^{235}U	± (2σ)	^{206}Pb/^{238}U	± (2σ)	rho	^{207}Pb/^{206}Pb	± (2σ)	^{206}Pb/^{238}U	± (2σ)	% disc.	Best Age (Ma)	± (2σ)	*interp type*
138	pnk	sub-rnd	86243	infinite	0.0611	0.0013	0.8199	0.0215	0.0981	0.0016	0.8162	644	50	603	21	7	644	50	
13	pnk	ang	14155	infinite	0.0575	0.0008	0.8912	0.0165	0.1118	0.0014	0.8773	512	37	683	22	-35.3			
13a	pnk	ang	618035	7725	0.0619	0.0011	0.8939	0.0201	0.1046	0.0015	0.8502	670	42	641	21	4.5	646	15	*2*
13b	pnk	ang	391257	2608	0.0616	0.0006	0.9032	0.0156	0.1063	0.0015	0.9099	662	31	651	21	1.7			
47	cll	sub-rnd	61091	infinite	0.0625	0.0005	0.9459	0.0191	0.1094	0.0021	0.9410	691	26	669	24	3.4	669	24	
137	pnk	sub-rnd	218493	infinite	0.0621	0.0003	0.8790	0.0208	0.1027	0.0024	0.9557	677	24	630	24	7	677	24	
135	cll	sub-rnd	285451	infinite	0.0615	0.0010	0.9560	0.0194	0.1127	0.0013	0.8423	657	42	689	22	-5	689	22	
131	cll	sub-rnd	363960	2426	0.0625	0.0003	0.9101	0.0309	0.1056	0.0035	0.9693	692	24	647	29	7	692	24	
37	cll	sub-rnd	347563	2483	0.0622	0.0014	0.9906	0.0277	0.1139	0.0018	0.7906	682	54	695	24	-2.1	695	24	
45	cll	sub-rnd	589392	4912	0.0640	0.0010	0.9422	0.0193	0.1072	0.0015	0.8655	741	39	656	22	12.0	reject		
140a	pnk	sub-rnd	1595419	10636	0.0819	0.0002	2.2653	0.0378	0.2004	0.0033	0.9544	1242	20	1178	40	6	1239	14	*1*
140b	pnk	sub-rnd	456283	infinite	0.0816	0.0002	2.2566	0.0376	0.2006	0.0033	0.9542	1236	20	1178	40	5			
30	cll	ang	427773	28518	0.0853	0.0013	2.9462	0.0516	0.2125	0.0019	0.8553	1322	35	1242	39	6.7	1322	35	
44	cll	sub-rnd	22537	infinite	0.1011	0.0184	4.6212	0.8430	0.3285	0.0058	0.1807	1645	337	1831	64	-13.0	reject		
81	pnk	sub-rnd	438507	8770	0.1047	0.0022	3.2738	0.2705	0.2266	0.0181	0.9642	1708	43	1317	112	25.3	reject		
33	cll	ang	299487	infinite	0.1053	0.0057	3.5904	0.2213	0.2472	0.0075	0.6038	1720	100	1424	61	19.2	reject		
24	pnk	ang	596316	infinite	0.1065	0.0012	4.8784	0.1062	0.3325	0.0061	0.9104	1741	28	1851	65	-7.2	1741	28	
21	pnk	ang	257620	infinite	0.1066	0.0044	4.8408	0.2260	0.3296	0.0073	0.6488	1742	77	1836	69	-6.2	1742	77	
105	pnk	sub-rnd	832422	5549	0.1066	0.0016	2.9852	0.3086	0.2026	0.0207	0.9859	1743	33	1189	127	34.7	reject		
114	pnk	rnd	595543	5955	0.1069	0.0040	4.3355	0.1869	0.2940	0.0064	0.6810	1747	70	1661	62	5.5	1747	70	
116	pnk	rnd	1306057	7915	0.1076	0.0034	4.5255	0.1666	0.3047	0.0059	0.7219	1760	60	1714	61	2.9	1760	60	
112	pnk	rnd	1223492	4190	0.1077	0.0003	4.1804	0.1061	0.2812	0.0071	0.9656	1761	19	1597	63	10.5	reject		
22	pnk	ang	387660	1399	0.1078	0.0035	4.7847	0.1943	0.3238	0.0077	0.7326	1762	63	1808	69	-3.0	1762	63	
2	pnk	rnd	240540	4811	0.1078	0.0032	5.0361	0.1727	0.3389	0.0058	0.7276	1763	57	1881	65	-7.7	1763	57	
62	pnk	sub-rnd	1015755	8258	0.1080	0.0004	3.9154	0.1809	0.2626	0.0121	0.9812	1766	19	1503	83	16.7	reject		
107	pnk	sub-rnd	1480722	6761	0.1081	0.0028	4.5465	0.1435	0.3049	0.0056	0.7744	1767	50	1715	60	3.3	1767	50	
121	pnk	rnd	355864	8897	0.1081	0.0004	4.6782	0.1162	0.3123	0.0077	0.9620	1768	20	1752	68	1.0	1768	20	
57	pnk	sub-rnd	424693	2831	0.1081	0.0021	4.7426	0.1204	0.3185	0.0053	0.8361	1768	39	1782	61	-0.9	1768	39	
16	pnk	ang	375301	3753	0.1081	0.0043	4.7676	0.1975	0.3186	0.0033	0.5888	1768	76	1783	57	-0.9	1768	76	
91	pnk	sub-rnd	659309	infinite	0.1085	0.0037	4.7692	0.1962	0.3190	0.0073	0.7151	1775	65	1785	67	-0.7	1775	65	
40	cll	sub-rnd	215187	4304	0.1086	0.0026	4.4353	0.3046	0.2962	0.0191	0.9389	1775	47	1672	119	6.6	1775	47	
90	pnk	sub-rnd	621005	4140	0.1090	0.0027	4.6457	0.1426	0.3093	0.0058	0.7904	1783	48	1737	61	2.9	1783	48	
61	pnk	sub-rnd	1460097	9360	0.1090	0.0004	4.6665	0.1470	0.3107	0.0097	0.9698	1783	19	1744	76	2.5	1783	19	
106	pnk	sub-rnd	774369	5531	0.1090	0.0028	4.5881	0.1449	0.3049	0.0057	0.7804	1783	50	1715	61	4.3	1783	50	
14	pnk	ang	353945	3539	0.1090	0.0020	4.7250	0.1258	0.3131	0.0061	0.8554	1783	38	1756	63	1.7	1783	38	
123	pnk	rnd	241381	infinite	0.1096	0.0003	4.7595	0.0954	0.3149	0.0063	0.9588	1792	19	1765	63	1.7	1792	19	

McHardy assemblage, 07TWJK153

Zircon 40 um

Depositional age: Late Mississippian or Pennsylvanian

Location (UTM): 453524E, 5608660N

n= 115

												Model Ages							
Grain	colour	shape	^{206}Pb cps	^{206}Pb/^{204}Pb	^{207}Pb/^{206}Pb	± (2σ)	^{207}Pb/^{235}U	± (2σ)	^{206}Pb/^{238}U	± (2σ)	rho	^{207}Pb/^{206}Pb	± (2σ)	^{206}Pb/^{238}U	± (2σ)	% disc.	Best Age (Ma)	± (2σ)	*interp type*
55	pnk	sub-rnd	703980	4693	0.1096	0.0014	4.7434	0.0812	0.3132	0.0037	0.8870	1793	29	1756	57	2.3	1793	29	
103	pnk	sub-rnd	766970	19174	0.1097	0.0005	3.9601	0.1586	0.2612	0.0104	0.9754	1795	20	1496	75	18.6	reject		
98	pnk	sub-rnd	764959	15299	0.1099	0.0017	4.7161	0.1265	0.3110	0.0069	0.8945	1797	33	1746	65	3.3	1797	33	
82	pnk	sub-rnd	759029	6121	0.1099	0.0018	5.0714	0.1231	0.3345	0.0061	0.8730	1798	34	1860	65	-4.0	1798	34	
9	pnk	rnd	151200	7560	0.1100	0.0021	4.8554	0.1054	0.3201	0.0036	0.8218	1800	38	1790	57	0.6	1800	38	
54	pnk	sub-rnd	227653	11383	0.1102	0.0048	4.2093	0.2121	0.2774	0.0072	0.6536	1803	81	1578	62	14.0	reject		
74	pnk	sub-rnd	657977	16449	0.1102	0.0020	4.8452	0.1385	0.3182	0.0071	0.8705	1803	37	1781	67	1.4	1803	37	
15	pnk	ang	609854	6099	0.1102	0.0059	4.9971	0.2782	0.3289	0.0051	0.5095	1803	99	1833	62	-1.9	1803	99	
8	pnk	rnd	320143	32014	0.1102	0.0005	4.9039	0.0906	0.3215	0.0057	0.9500	1803	20	1797	63	0.4	1803	20	
38	cll	sub-rnd	315512	3155	0.1103	0.0062	4.4175	0.2801	0.2903	0.0087	0.5869	1804	103	1643	70	10.1	reject		
6	pnk	rnd	177340	17734	0.1105	0.0009	4.9589	0.1033	0.3275	0.0063	0.9355	1808	24	1826	65	-1.1	1808	24	
86	pnk	sub-rnd	1591394	15914	0.1108	0.0003	4.8848	0.1004	0.3184	0.0065	0.9593	1813	19	1782	65	2.0	1813	19	
89	pnk	sub-rnd	866800	5779	0.1108	0.0005	5.1278	0.1247	0.3358	0.0080	0.9598	1813	20	1867	72	-3.4	1813	20	
70	pnk	sub-rnd	1042563	10426	0.1114	0.0004	5.0552	0.0882	0.3294	0.0056	0.9532	1822	19	1836	63	-0.8	1822	19	
59	pnk	sub-rnd	825715	4915	0.1117	0.0035	5.1627	0.1903	0.3324	0.0063	0.7176	1828	60	1850	66	-1.4	1828	60	
53x	pnk	sub-rnd	483830	3226	0.1118	0.0092	4.9603	0.4278	0.3223	0.0085	0.4239	1828	150	1801	72	1.7	1828	150	
115	pnk	rnd	683203	4555	0.1121	0.0026	4.9188	0.1434	0.3164	0.0057	0.8012	1833	45	1772	62	3.8	1833	45	
109	pnk	rnd	1276799	7980	0.1122	0.0030	4.8982	0.1554	0.3163	0.0056	0.7636	1835	51	1772	62	4.0	1835	51	
26	cll	ang	655406	131081	0.1124	0.0004	4.8687	0.1049	0.3143	0.0067	0.9580	1839	19	1762	65	4.8	1839	19	
41	cll	sub-rnd	291619	5832	0.1125	0.0036	5.1796	0.2022	0.3337	0.0076	0.7374	1839	60	1856	70	-1.1	1839	60	
28	cll	ang	112406	infinite	0.1125	0.0004	4.7404	0.0938	0.3056	0.0059	0.9559	1841	19	1719	61	7.5	1841	19	
125	pnk	rnd	402064	40206	0.1127	0.0006	5.0380	0.1079	0.3219	0.0067	0.9512	1843	21	1799	66	2.8	1843	21	
119	pnk	rnd	415713	8314	0.1127	0.0034	5.1189	0.2067	0.3291	0.0087	0.7690	1844	58	1834	73	0.6	1844	58	
18	pnk	ang	1047147	2692	0.1131	0.0041	5.3305	0.2130	0.3437	0.0058	0.6613	1849	68	1904	66	-3.4	1849	68	
78	pnk	sub-rnd	366154	7323	0.1131	0.0015	5.1282	0.1505	0.3259	0.0086	0.9218	1850	30	1819	73	2.0	1850	30	
101	pnk	sub-rnd	906203	5846	0.1138	0.0003	5.1045	0.1533	0.3249	0.0097	0.9702	1861	19	1814	77	2.9	1861	19	
79	pnk	sub-rnd	526415	8774	0.1144	0.0021	5.3654	0.1505	0.3400	0.0072	0.8615	1871	38	1887	69	-1.0	1871	38	
118	pnk	rnd	534712	4456	0.1147	0.0004	5.1036	0.0991	0.3222	0.0062	0.9557	1876	19	1801	64	4.6	1876	19	
126	pnk	ang	381101	38110	0.1148	0.0004	5.2519	0.1399	0.3314	0.0087	0.9644	1877	19	1845	74	2.0	1877	19	
99	pnk	sub-rnd	756903	9461	0.1154	0.0010	5.0583	0.1128	0.3175	0.0065	0.9353	1886	24	1777	65	6.6	1886	24	
94	pnk	sub-rnd	1248350	6712	0.1161	0.0043	5.5568	0.2272	0.3474	0.0059	0.6512	1897	69	1922	66	-1.5	1897	69	
36	cll	sub-rnd	14260	infinite	0.1163	0.0006	5.6876	0.1007	0.3549	0.0060	0.9470	1901	20	1958	67	-3.5	1901	20	
27	cll	ang	829805	4048	0.1165	0.0008	3.2416	0.1000	0.2018	0.0060	0.9581	1903	22	1185	50	41.2	reject		
51	cll	rnd	480976	3207	0.1167	0.0004	5.2594	0.1325	0.3271	0.0082	0.9637	1906	19	1824	71	4.9	1906	19	
95	pnk	sub-rnd	1332538	6904	0.1168	0.0003	5.4038	0.0774	0.3368	0.0047	0.9518	1907	19	1871	62	2.2	1907	19	
84	pnk	sub-rnd	937450	6127	0.1172	0.0020	5.2548	0.1487	0.3252	0.0073	0.8763	1913	36	1815	68	5.9	1913	36	
128	pnk	ang	1290185	7289	0.1178	0.0005	4.2655	0.2217	0.2624	0.0136	0.9840	1922	19	1502	90	24	reject		

McHardy assemblage, 07TWJK153 Depositional age: Late Mississippian or Pennsylvanian n= 115

Zircon 40 um Location (UTM): 453524E, 5608660N

Grain	colour	shape	^{206}Pb cps	^{206}Pb/^{204}Pb	^{207}Pb/^{206}Pb	± (2σ)	^{207}Pb/^{235}U	± (2σ)	^{206}Pb/^{238}U	± (2σ)	rho	Model Ages ^{207}Pb/^{206}Pb	± (2σ)	^{206}Pb/^{238}U	± (2σ)	% disc.	Best Age (Ma)	± (2σ)	*interp type*
130	pnk	ang	549261	54926	0.1183	0.0009	5.6156	0.0890	0.3459	0.0048	0.9299	1931	23	1915	63	1	1931	23	
108	pnk	rnd	777119	5181	0.1185	0.0003	5.5990	0.1186	0.3407	0.0072	0.9603	1934	18	1890	69	2.6	1934	18	
43	cll	sub-rnd	100306	836	0.1185	0.0009	5.7032	0.1193	0.3518	0.0069	0.9408	1934	22	1943	70	-0.5	1934	22	
133	cll	sub-rnd	19439	infinite	0.1189	0.0009	3.8191	0.3070	0.2324	0.0186	0.9894	1939	22	1347	115	34	reject		
97	pnk	sub-rnd	466716	9334	0.1195	0.0004	5.6573	0.1073	0.3444	0.0064	0.9551	1949	19	1908	67	2.5	1949	19	
56	pnk	sub-rnd	372723	7454	0.1197	0.0033	5.6442	0.1994	0.3424	0.0077	0.7801	1952	52	1898	71	3.2	1952	52	
19	pnk	ang	350941	3509	0.1198	0.0003	5.9192	0.0822	0.3583	0.0049	0.9506	1954	19	1974	65	-1.2	1954	19	
124	pnk	rnd	507591	25380	0.1200	0.0003	5.7234	0.1329	0.3476	0.0080	0.9625	1956	19	1923	73	1.9	1956	19	
87	pnk	sub-rnd	635373	4538	0.1212	0.0010	5.6793	0.0886	0.3398	0.0046	0.9269	1974	23	1886	62	5.2	1974	23	
77	pnk	sub-rnd	423977	10599	0.1212	0.0006	4.6122	0.1454	0.2760	0.0086	0.9670	1974	20	1571	68	23.0	reject		
50	cll	rnd	257317	infinite	0.1221	0.0005	6.1068	0.0836	0.3632	0.0047	0.9454	1988	19	1997	65	-0.6	1988	19	
117	pnk	rnd	808089	40404	0.1230	0.0003	6.0526	0.1151	0.3550	0.0067	0.9585	2001	18	1959	69	2.4	2001	18	
100	pnk	sub-rnd	992853	5641	0.1234	0.0016	6.0048	0.1495	0.3527	0.0075	0.9066	2005	29	1947	71	3.3	2005	29	
25	cll	ang	732107	18303	0.1240	0.0006	6.5110	0.1045	0.3808	0.0058	0.9451	2014	20	2080	70	-3.8	2014	20	
73	pnk	sub-rnd	314167	7854	0.1240	0.0012	5.9236	0.1302	0.3444	0.0068	0.9266	2014	25	1908	68	6.1	2014	25	
104	pnk	sub-rnd	368025	2178	0.1241	0.0008	6.0832	0.1223	0.3549	0.0067	0.9445	2016	21	1958	70	3.4	2016	21	
92	pnk	sub-rnd	1273866	6923	0.1243	0.0002	5.4416	0.1392	0.3175	0.0081	0.9670	2018	18	1778	70	13.6	reject		
7	pnk	rnd	170652	17065	0.1252	0.0010	6.4557	0.0968	0.3742	0.0048	0.9281	2031	22	2049	67	-1.0	2031	22	
23	pnk	ang	72973	infinite	0.1252	0.0004	6.4159	0.0847	0.3715	0.0048	0.9495	2031	18	2036	66	-0.3	2031	18	
83	pnk	sub-rnd	1141025	7607	0.1267	0.0005	6.6789	0.1513	0.3846	0.0086	0.9599	2053	19	2098	78	-2.6	2053	19	
139	pnk	sub-rnd	125073	12507	0.1270	0.0004	6.2658	0.1233	0.3551	0.0069	0.9571	2057	19	1959	70	6	2057	19	
88	pnk	sub-rnd	415987	2650	0.1276	0.0034	6.5344	0.2053	0.3714	0.0063	0.7612	2065	50	2036	70	1.7	2065	50	
69	pnk	sub-rnd	228164	infinite	0.1279	0.0003	6.1182	0.1469	0.3472	0.0083	0.9639	2069	18	1921	74	8.3	2069	18	
46	cll	sub-rnd	58116	infinite	0.1289	0.0031	6.8165	0.2053	0.3851	0.0071	0.7951	2083	45	2100	74	-0.9	2083	45	
120	pnk	rnd	839056	7111	0.1299	0.0018	6.6091	0.1856	0.3686	0.0089	0.9065	2097	31	2023	78	4.1	2097	31	
72	pnk	sub-rnd	136269	infinite	0.1317	0.0048	5.7743	0.2535	0.3180	0.0079	0.7080	2121	66	1780	69	18.4	reject		
132	cll	sub-rnd	18652	infinite	0.1348	0.0063	6.3988	0.3323	0.3478	0.0080	0.6080	2161	83	1924	73	13	reject		
68	pnk	sub-rnd	897618	6699	0.1401	0.0005	7.4406	0.1277	0.3850	0.0064	0.9515	2229	19	2100	72	6.8	2229	19	
58	pnk	sub-rnd	522609	4355	0.1429	0.0054	7.9424	0.3389	0.4056	0.0082	0.6682	2263	67	2195	80	3.5	2263	67	
29	cll	ang	110228	infinite	0.1463	0.0091	6.1968	0.6489	0.3127	0.0264	0.8169	2303	108	1754	157	27.2	reject		
80	pnk	sub-rnd	793648	4434	0.1481	0.0017	8.8430	0.1733	0.4328	0.0068	0.9038	2325	26	2318	79	0.3	2325	26	
1	pnk	rnd	457816	6540	0.1563	0.0006	9.6648	0.2568	0.4514	0.0119	0.9644	2416	18	2401	96	0.7	2416	18	
10	pnk	rnd	1102773	11858	0.1586	0.0003	10.1832	0.2477	0.4658	0.0113	0.9651	2441	17	2465	95	-1.2	2441	17	
122	pnk	rnd	786634	60510	0.1630	0.0017	10.5405	0.2450	0.4689	0.0097	0.9250	2487	24	2479	90	0.4	2487	24	
3	pnk	rnd	231114	2358	0.1649	0.0027	10.8124	0.3260	0.4748	0.0120	0.8912	2506	33	2504	98	0.1	2506	33	
49	cll	rnd	78599	infinite	0.1671	0.0006	11.0503	0.1627	0.4801	0.0068	0.9488	2529	18	2528	84	0.1	2529	18	
113	pnk	rnd	580745	3872	0.1679	0.0010	8.1919	0.3364	0.3534	0.0144	0.9737	2537	20	1951	99	26.7	reject		

McHardy assemblage, 07TWJK153
Zircon 40 um

Depositional age: Late Mississippian or Pennsylvanian
Location (UTM): 453524E, 5608660N

n= 115

Grain	colour	shape	^{206}Pb cps	$^{206}Pb/^{204}Pb$	$^{207}Pb/^{206}Pb$	± (2σ)	$^{207}Pb/^{235}U$	± (2σ)	$^{206}Pb/^{238}U$	± (2σ)	rho	Model Ages $^{207}Pb/^{206}Pb$	± (2σ)	$^{206}Pb/^{238}U$	± (2σ)	% disc.	Best Age (Ma)	± (2σ)	*interp type*
11	pnk	rnd	1059172	8682	0.1687	0.0008	10.9283	0.2084	0.4703	0.0087	0.9501	2545	19	2485	87	2.8	2545	19	
20	pnk	ang	433287	4333	0.1689	0.0008	10.7170	0.2095	0.4627	0.0088	0.9516	2546	19	2451	87	4.5	2546	19	
71	pnk	sub-rnd	320244	3202	0.1700	0.0014	11.0778	0.2099	0.4726	0.0080	0.9299	2557	22	2495	86	2.9	2557	22	
60	pnk	sub-rnd	1045714	7578	0.1703	0.0006	11.1384	0.2624	0.4747	0.0110	0.9606	2561	18	2504	95	2.7	2561	18	
4	pnk	rnd	297720	14886	0.1708	0.0011	11.6998	0.3344	0.4965	0.0139	0.9595	2566	20	2599	106	-1.6	2566	20	
129	pnk	ang	195792	infinite	0.1713	0.0004	11.2715	0.2068	0.4770	0.0087	0.9571	2570	17	2514	88	3	2570	17	
85	pnk	sub-rnd	1034140	7334	0.1714	0.0004	11.2323	0.2082	0.4755	0.0087	0.9575	2571	17	2508	88	3.0	2571	17	
65	pnk	sub-rnd	376455	9411	0.1719	0.0007	8.4508	0.3510	0.3564	0.0147	0.9780	2576	18	1965	100	27.4	reject		
110	pnk	rnd	940296	5804	0.1722	0.0004	10.3661	0.1515	0.4362	0.0063	0.9520	2580	17	2334	78	11.3	reject		
39	cll	sub-rnd	220600	1232	0.1726	0.0047	11.4677	0.4984	0.4806	0.0162	0.8335	2583	49	2530	114	2.5	2583	49	
17	pnk	ang	676822	2982	0.1732	0.0025	11.1801	0.5472	0.4680	0.0219	0.9532	2588	29	2475	138	5.3	2588	29	
141	--	--	713672	infinite	0.1734	0.0006	11.0761	0.2397	0.4635	0.0099	0.9586	2590	18	2455	90	6	2590	18	
93	pnk	sub-rnd	426335	3553	0.1744	0.0004	11.3176	0.4359	0.4708	0.0181	0.9779	2600	17	2487	121	5.2	2600	17	
96	pnk	sub-rnd	928826	6731	0.1745	0.0005	11.9059	0.2995	0.4951	0.0124	0.9640	2602	17	2593	101	0.4	2602	17	
66	pnk	sub-rnd	300294	6006	0.1750	0.0016	12.1968	0.2819	0.5057	0.0107	0.9340	2606	23	2638	97	-1.5	2606	23	
111	pnk	rnd	1087288	4666	0.1750	0.0003	11.6254	0.2243	0.4813	0.0093	0.9596	2606	17	2533	90	3.4	2606	17	
53	pnk	sub-rnd	251421	1676	0.1756	0.0095	12.3109	0.7154	0.5072	0.0104	0.5351	2612	92	2644	96	-1.5	2612	92	
31	cll	ang	427565	28504	0.1773	0.0006	12.1891	0.2436	0.4984	0.0098	0.9572	2628	17	2607	94	1.0	2628	17	
35	cll	ang	74602	infinite	0.1801	0.0010	9.3889	0.3785	0.3781	0.0151	0.9740	2654	19	2067	103	25.8	reject		
67	pnk	sub-rnd	562900	4050	0.1807	0.0025	12.8725	0.3045	0.5165	0.0099	0.8950	2659	28	2684	96	-1.2	2659	28	
76	pnk	sub-rnd	1047812	3866	0.1809	0.0033	12.8110	0.3742	0.5135	0.0118	0.8712	2661	34	2672	101	-0.5	2661	34	
12	pnk	rnd	359985	12000	0.1822	0.0013	12.6662	0.2481	0.5043	0.0092	0.9411	2673	20	2632	92	1.9	2673	20	
42	cll	sub-rnd	38327	infinite	0.1825	0.0026	11.3419	0.5693	0.4550	0.0219	0.9555	2675	29	2417	137	11.6	reject		
102	pnk	sub-rnd	868337	5461	0.1826	0.0004	12.3036	0.3326	0.4882	0.0132	0.9677	2677	17	2563	103	5.2	2677	17	
52	cll	rnd	155521	1555	0.1834	0.0046	9.4157	0.3295	0.3722	0.0090	0.8082	2684	45	2040	79	27.9	reject		
64	pnk	sub-rnd	1765267	10087	0.1848	0.0011	12.3925	0.4166	0.4863	0.0161	0.9666	2696	19	2555	114	6.4	2696	19	
75	pnk	sub-rnd	641670	4583	0.1861	0.0009	13.3028	0.2660	0.5160	0.0100	0.9516	2708	18	2682	96	1.1	2708	18	
34	cll	ang	405510	2519	0.1862	0.0004	13.0216	0.1801	0.5069	0.0069	0.9514	2709	17	2643	87	3.0	2709	17	
134	cll	sub-rnd	76416	infinite	0.1893	0.0006	13.9127	0.2387	0.5336	0.0090	0.9533	2736	17	2757	95	-1	2736	17	
136	pnk	sub-rnd	14747	infinite	0.1901	0.0004	13.9802	0.3142	0.5305	0.0119	0.9628	2743	17	2743	103	0	2743	17	
48	cll	sub-rnd	163651	infinite	0.1917	0.0008	14.7758	0.3449	0.5588	0.0128	0.9596	2757	18	2861	108	-4.7	2757	18	
5	pnk	rnd	222815	11141	0.2002	0.0014	15.2632	0.2614	0.5532	0.0087	0.9371	2828	20	2838	96	-0.4	2828	20	
63	pnk	sub-rnd	332828	2869	0.2586	0.0006	18.9689	0.6326	0.5318	0.0177	0.9739	3238	16	2749	123	18.5	reject		

McHardy assemblage, 07TWJK176D
Zircon 40 um

Depositional age: Late Carboniferous or Early Permian
Location (UTM): 447105E, 5613795N

n= 7

Grain	^{206}Pb cps	$^{206}Pb/^{204}Pb$	$^{207}Pb/^{206}Pb$	± (2σ)	$^{207}Pb/^{235}U$	± (2σ)	$^{206}Pb/^{238}U$	± (2σ)	rho	Model Ages $^{207}Pb/^{206}Pb$	± (2σ)	$^{206}Pb/^{238}U$	± (2σ)	% disc.	Best Age (Ma)	± (2σ)
GJ1-32-1	276744	191	0.0605	0.0005	0.8402	0.0835	0.1007	0.0100	0.9965	622	18	619	58	0.5		
GJ1-32-2	257701	183	0.0602	0.0004	0.7733	0.0761	0.0932	0.0091	0.9978	610	14	574	54	6.2		
JK176D-12start	127837	939	0.0528	0.0004	0.3806	0.0398	0.0523	0.0054	0.9972	320	18	328	33	-2.6	328	33
JK176D-12end	19786	219	0.0597	0.0031	0.7943	0.0894	0.0964	0.0097	0.8908	594	111	593	57	0.1	593	57
JK176D-16	468570	4190	0.0772	0.0004	2.1745	0.2134	0.2043	0.0200	0.9985	1126	11	1198	106	-7.1	1126	11
JK176D-10	178915	2275	0.0787	0.0005	1.9712	0.1962	0.1817	0.0180	0.9982	1164	12	1076	98	8.2	1164	12
JK176D-11	247824	2382	0.0993	0.0007	3.9278	0.4059	0.2869	0.0296	0.9979	1611	13	1626	147	-1.1	1611	13
JK176D-5	271695	2086	0.1128	0.0005	5.8570	0.5778	0.3765	0.0371	0.9990	1845	8	2060	171	-13.6	1845	8
JK176D-15	713726	5679	0.1220	0.0011	5.1982	0.5451	0.3089	0.0323	0.9965	1986	15	1735	157	14.4	1986	15

Chase Formation, Chase quartzite Depositional age: Late Devonian n= 86

Zircon 40 um Location (UTM): 431540E, 5554274N

Grain	shape	^{206}Pb cps	$^{206}Pb/^{204}Pb$	$^{207}Pb/^{206}Pb$	± (2σ)	$^{207}Pb/^{235}U$	± (2σ)	$^{206}Pb/^{238}U$	± (2σ)	rho	Model Ages $^{207}Pb/^{206}Pb$	± (2σ)	Model Ages $^{206}Pb/^{238}U$	± (2σ)	% disc.	Best Age (Ma)	± (2σ)	*interp type*
GJ1-32-1		26761	41	0.0603	0.0011	0.7518	0.0237	0.0904	0.0024	0.8279	614	38	558	14	9.5			
GJ1-32-1a		69668	105	0.0604	0.0025	0.7753	0.0429	0.0931	0.0034	0.6556	618	90	574	20	7.4			
GJ1-32-2		56799	184	0.0566	0.0022	0.7152	0.0353	0.0917	0.0027	0.6066	475	87	566	16	-19.9			
GJ1-32-3		180434	193	0.0586	0.0005	0.7271	0.0246	0.0900	0.0029	0.9648	551	19	556	17	-0.8			
GJ1-32-4		222485	413	0.0602	0.0006	0.7493	0.0262	0.0902	0.0030	0.9569	612	22	557	18	9			
GJ1-32-5		78688	483	0.0581	0.0013	0.7115	0.0390	0.0888	0.0045	0.9169	534	48	548	26	-3			
GJ1-32-6		167914	355	0.0597	0.0014	0.7657	0.0451	0.0931	0.0050	0.9198	591	50	574	30	3.0			
GJ1-32-7		416688	infinite	0.0595	0.0003	0.7767	0.0256	0.0947	0.0031	0.9915	585	9	583	18	0.4			
GJ1-32-8		416973	18570	0.0592	0.0004	0.8116	0.0250	0.0995	0.0030	0.9733	573	15	611	17	-7.0			
GJ1-32-9		432248	18420	0.0595	0.0004	0.8068	0.0253	0.0983	0.0030	0.9750	586	15	605	18	-3.4			
GJ1-32-10		440188	10541	0.0594	0.0003	0.8260	0.0300	0.1009	0.0036	0.9908	581	11	620	21	-7.1			
GJ1-32-11		416377	2603	0.0598	0.0003	0.8092	0.0301	0.0981	0.0036	0.9906	597	11	603	21	-1.1			
GJ1-32-12		445785	1890	0.0599	0.0003	0.8415	0.0286	0.1019	0.0034	0.9923	600	9	626	20	-4.6			
GJ1-32-13		373817	748370	0.0595	0.0002	0.8107	0.0250	0.0988	0.0030	0.9910	585	9	607	18	-3.9			
GJ1-32-14		430372.9	5104	0.0597	0.0004	0.8257	0.0213	0.1003	0.0025	0.9680	593	14	616	15	-4			
GJ1-32-15		414526.1	2759	0.0601	0.0004	0.8322	0.0223	0.1004	0.0026	0.9730	608	13	617	15	-2			
117	rnd-subrnd	218952.5	1257.391707	0	0.0004	0.3792	0.0096	0.0517	0.0013	0.9566	338.9361	17	325	8	4	325	8	
43	rnd-subrnd	189222.9	2291105.104	0	0.0005	0.4615	0.0166	0.0624	0.0022	0.9721	354.9175	19	390	13	-10	reject		
8	prism	340496	2250	0.0538	0.0003	0.4464	0.0126	0.0601	0.0017	0.9853	364	11	377	10	-3.5	375	6	*2*
8b	prism	531871	3573	0.0541	0.0002	0.4437	0.0115	0.0595	0.0015	0.9879	375	9	373	9	0.6			
8c	prism	235480	1081	0.0548	0.0005	0.4555	0.0127	0.0603	0.0016	0.9507	404	19	377	10	6.9			
58	prism	93475	2826	0.0539	0.0005	0.4802	0.0142	0.0647	0.0018	0.9590	365	19	404	11	-10.9	reject		
62	prism	257660	8306	0.0550	0.0006	0.4799	0.0162	0.0633	0.0020	0.9488	412	24	396	12	4.2	396	12	
123a	prism	100706	753	0.0549	0.0004	0.5113	0.0158	0.0675	0.0020	0.9726	409	16	421	12	-3	420	9	*2*
123b	prism	106387	900	0.0552	0.0004	0.5101	0.0158	0.0670	0.0020	0.9696	421	17	418	12	1			
87a	rnd-subrnd	242925	1346	0.0552	0.0003	0.5065	0.0171	0.0665	0.0022	0.9884	422	11	415	13	1.8	420	6	*2*
87b	rnd-subrnd	425586	2274	0.0549	0.0002	0.5074	0.0169	0.0670	0.0022	0.9938	409	8	418	13	-2.3			
87d	rnd-subrnd	296684	1684	0.0550	0.0002	0.5128	0.0166	0.0676	0.0022	0.9919	413	9	422	13	-2.1			
87c	rnd-subrnd	153593	869	0.0551	0.0004	0.5121	0.0168	0.0674	0.0022	0.9806	415	14	421	13	-1.4			
87e	rnd-subrnd	677612	3612	0.0551	0.0002	0.5160	0.0170	0.0679	0.0022	0.9942	416	8	424	13	-1.8			
67a	prism	469284	8204	0.0553	0.0003	0.5122	0.0189	0.0672	0.0025	0.9893	422	12	419	15	0.7	420	10	*2*
67b	prism	348004	5195	0.0554	0.0003	0.5141	0.0198	0.0673	0.0026	0.9885	429	13	420	15	2.1			
75a	rnd-subrnd	273355	2090	0.0553	0.0003	0.5117	0.0203	0.0671	0.0026	0.9907	424	12	419	16	1.4	421	8	*3*
75b	rnd-subrnd	253527	1979	0.0556	0.0005	0.5062	0.0184	0.0660	0.0023	0.9713	436	19	412	14	5.7			

Chase Formation, Chase quartzite Depositional age: Late Devonian n= 86

Zircon 40 um Location (UTM): 431540E, 5554274N

Grain	shape	^{206}Pb cps	$^{206}Pb/^{204}Pb$	$^{207}Pb/^{206}Pb$	± (2σ)	$^{207}Pb/^{235}U$	± (2σ)	$^{206}Pb/^{238}U$	± (2σ)	rho	Model Ages $^{207}Pb/^{206}Pb$	± (2σ)	$^{206}Pb/^{238}U$	± (2σ)	% disc.	Best Age (Ma)	± (2σ)	*interp type*
127	prism	77968	779	0.0554	0.0006	0.5178	0.0131	0.0678	0.0015	0.9018	429	24	423	9	1	423	9	
60a	prism	368921	16492	0.0554	0.0004	0.4912	0.0145	0.0643	0.0018	0.9700	429	16	402	11	6.5	443	42	*1*
60b	prism	308992	9755	0.0561	0.0004	0.5383	0.0157	0.0696	0.0020	0.9688	457	16	434	12	5.2			
69a	prism	246736	8650	0.0545	0.0003	0.5048	0.0189	0.0672	0.0025	0.9857	391	14	419	15	-7.5	reject		
69b	prism	205265	2472	0.0556	0.0007	0.5495	0.0247	0.0717	0.0031	0.9652	434	26	447	19	-2.9	447	19	
111a	rnd-subrnd	279620	1962	0.0576	0.0004	0.6465	0.0217	0.0814	0.0027	0.9783	515	15	505	16	2.0	508	9	*2*
111b	rnd-subrnd	274331	1383	0.0576	0.0004	0.6547	0.0158	0.0824	0.0019	0.9593	516	15	510	11	1.3			
112a	rnd-subrnd	38992	323	0.0610	0.0008	0.1890	0.0056	0.0225	0.0006	0.8922	638	29	143	4	78.4	reject		
112b	rnd-subrnd	46026	232	0.0960	0.0033	0.3266	0.0150	0.0247	0.0008	0.6636	1548	65	157	5	90.9	reject		
112c	rnd-subrnd	48303	255	0.0895	0.0012	0.2967	0.0083	0.0241	0.0006	0.8783	1414	25	153	4	90.2	reject		
14	prism	327470	3641	0.0701	0.0003	1.4091	0.0397	0.1459	0.0041	0.9909	930	8	878	23	6.1	930	8	
104	rnd-subrnd	327644	2794	0.0707	0.0005	1.5204	0.0467	0.1559	0.0047	0.9747	949	14	934	26	1.7	949	14	
113	rnd-subrnd	76447	581	0.0711	0.0006	1.5266	0.0398	0.1557	0.0038	0.9473	961	17	933	21	3.1	961	17	
74	rnd-subrnd	304933	2201	0.0712	0.0004	1.2483	0.0453	0.1272	0.0046	0.9900	963	10	772	26	21.1	reject		
7	prism	139753	1153	0.0713	0.0004	1.5520	0.0491	0.1579	0.0049	0.9807	966	13	945	27	2.3	966	13	
16	rnd-subrnd	74904	754	0.0715	0.0007	1.1273	0.0328	0.1143	0.0031	0.9458	973	19	698	18	29.8	reject		
17	rnd-subrnd	333954	4311	0.0717	0.0003	1.5102	0.0420	0.1528	0.0042	0.9861	977	9	917	23	6.6	977	9	
35	rnd-subrnd	137275	108796	0.0719	0.0004	1.5797	0.0545	0.1594	0.0054	0.9836	982	13	954	30	3.1	982	13	
64	prism	288120	23828	0.0719	0.0003	1.6069	0.0573	0.1620	0.0057	0.9910	984	10	968	32	1.8	984	10	
72	rnd-subrnd	585550	5070	0.0721	0.0003	1.6229	0.0623	0.1632	0.0062	0.9930	989	9	975	34	1.6	989	9	
45	rnd-subrnd	620668	36249	0.0726	0.0005	1.6023	0.0456	0.1601	0.0044	0.9718	1003	14	957	25	4.9	1003	14	
103	rnd-subrnd	954632	32756	0.0728	0.0004	1.6075	0.0462	0.1602	0.0045	0.9783	1008	12	958	25	5.3	1008	12	
88	rnd-subrnd	378321	2128	0.0728	0.0003	1.6559	0.0550	0.1649	0.0054	0.9936	1009	8	984	30	2.7	1009	8	
114	rnd-subrnd	491680	3305	0.0734	0.0005	1.6608	0.0572	0.1642	0.0056	0.9832	1024	13	980	31	4.6	1024	13	
52	rnd-subrnd	191176	2929	0.0736	0.0006	1.7547	0.0570	0.1730	0.0054	0.9629	1029	18	1029	30	0.1	1029	18	
29	rnd-subrnd	253924	125046	0.0743	0.0004	1.6639	0.0658	0.1624	0.0064	0.9910	1049	11	970	35	8.1	1049	11	
59	prism	292415	9746	0.0744	0.0005	1.6420	0.0501	0.1602	0.0048	0.9725	1051	14	958	26	9.5	1051	14	
70	prism	884534	8982	0.0744	0.0004	1.6865	0.0602	0.1645	0.0058	0.9887	1052	11	981	32	7.2	1052	11	
56	rnd-subrnd	521932	19083	0.0744	0.0006	1.7382	0.0515	0.1694	0.0048	0.9560	1053	18	1009	26	4.5	1053	18	
57	rnd-subrnd	149581	8490	0.0747	0.0006	1.6842	0.0481	0.1635	0.0045	0.9568	1061	17	976	25	8.6	1061	17	
91	rnd-subrnd	547649	infinite	0.0751	0.0003	1.8057	0.0651	0.1743	0.0063	0.9947	1072	7	1036	34	3.6	1072	7	
96	rnd-subrnd	679073	infinite	0.0752	0.0003	1.7591	0.0571	0.1697	0.0055	0.9938	1074	7	1010	30	6.4	1074	7	
22	rnd-subrnd	182011	17562	0.0754	0.0005	1.7245	0.0632	0.1658	0.0060	0.9866	1080	12	989	33	9.1	1080	12	
21	rnd-subrnd	108161	1033	0.0755	0.0005	1.7963	0.0690	0.1725	0.0065	0.9857	1083	13	1026	36	5.7	1083	13	
63	prism	151677	12570	0.0764	0.0004	1.9504	0.0721	0.1853	0.0068	0.9903	1104	10	1096	37	0.9	1104	10	

Chase Formation, Chase quartzite
Zircon 40 um

Depositional age: Late Devonian
Location (UTM): 431540E, 5554274N

n= 86

											Model Ages							
																Best Age		*interp*
Grain	**shape**	**^{206}Pb cps**	**$^{206}Pb/^{204}Pb$**	**$^{207}Pb/^{206}Pb$**	**± (2σ)**	**$^{207}Pb/^{235}U$**	**± (2σ)**	**$^{206}Pb/^{238}U$**	**± (2σ)**	**rho**	**$^{207}Pb/^{206}Pb$**	**± (2σ)**	**$^{206}Pb/^{238}U$**	**± (2σ)**	**% disc.**	**(Ma)**	**± (2σ)**	*type*
78	rnd-subrnd	330663	1716	0.0766	0.0004	1.8953	0.0726	0.1794	0.0068	0.9927	1111	9	1064	37	4.6	1111	9	
81	rnd-subrnd	318314	1728	0.0770	0.0004	1.9259	0.0736	0.1813	0.0069	0.9926	1122	9	1074	37	4.6	1122	9	
84	rnd-subrnd	248563	1301	0.0772	0.0003	1.9709	0.0670	0.1853	0.0062	0.9928	1125	8	1096	34	2.9	1125	8	
109	rnd-subrnd	910993	12760	0.0773	0.0005	1.8972	0.0569	0.1780	0.0052	0.9799	1129	12	1056	29	7.0	1129	12	
2	prism	579647	3739	0.0777	0.0002	1.9941	0.0624	0.1860	0.0058	0.9952	1140	6	1100	31	3.9	1140	6	
61	prism	385516	13792	0.0778	0.0005	1.9078	0.0733	0.1777	0.0067	0.9848	1143	13	1055	37	8.4	1143	13	
1	prism	279837	1959	0.0785	0.0003	2.0218	0.0538	0.1867	0.0049	0.9871	1160	8	1104	27	5.3	1160	8	
5	prism	1069251	7291	0.0793	0.0002	2.0735	0.0643	0.1896	0.0058	0.9955	1180	6	1119	32	5.6	1180	6	
15	rnd-subrnd	665800	6171	0.0795	0.0003	2.0115	0.0738	0.1834	0.0067	0.9958	1185	7	1086	36	9.1	1185	7	
42	rnd-subrnd	776177	543943	0.0801	0.0005	2.1451	0.0624	0.1942	0.0055	0.9742	1200	13	1144	30	5.1	1200	13	
89	rnd-subrnd	252272	infinite	0.0809	0.0003	2.2348	0.0759	0.2003	0.0068	0.9928	1220	8	1177	36	3.8	1220	8	
122	prism	397756	2741	0.0840	0.0004	2.3018	0.0719	0.1988	0.0061	0.9857	1292	10	1169	33	10		reject	
124	prism	466131	3400	0.0840	0.0020	1.9410	0.2094	0.1675	0.0176	0.9754	1294	46	998	97	25		reject	
68	prism	562610	12747	0.0846	0.0009	1.4840	0.0898	0.1273	0.0076	0.9860	1305	20	772	43	43.3		reject	
66	prism	497824	16136	0.0850	0.0004	2.5266	0.0941	0.2155	0.0080	0.9911	1317	10	1258	42	4.9	1317	10	
4	prism	594022	3944	0.0852	0.0003	2.4703	0.0739	0.2102	0.0062	0.9933	1321	7	1230	33	7.5	1321	7	
93	rnd-subrnd	166886	infinite	0.0854	0.0003	2.5416	0.1021	0.2157	0.0086	0.9954	1326	7	1259	46	5.5	1326	7	
24	rnd-subrnd	405618	48853	0.0860	0.0004	2.5308	0.0895	0.2134	0.0075	0.9931	1339	8	1247	40	7.6	1339	8	
65	prism	358875	15080	0.0870	0.0004	2.7073	0.1006	0.2258	0.0083	0.9920	1360	9	1312	44	3.8	1360	9	
37	rnd-subrnd	1868762	156308	0.0874	0.0003	2.6342	0.1023	0.2187	0.0084	0.9950	1369	7	1275	45	7.6	1369	7	
36	rnd-subrnd	419840	190879	0.0877	0.0004	2.6568	0.0971	0.2197	0.0080	0.9922	1376	9	1280	42	7.7	1376	9	
105	rnd-subrnd	299994	4287	0.0879	0.0006	2.7454	0.0710	0.2267	0.0057	0.9693	1379	12	1317	30	5.0	1379	12	
92	rnd-subrnd	385105	infinite	0.0903	0.0003	2.9747	0.1132	0.2388	0.0090	0.9958	1433	7	1381	47	4.0	1433	7	
94	rnd-subrnd	860196	infinite	0.0918	0.0003	2.9486	0.0967	0.2328	0.0076	0.9946	1464	6	1349	40	8.7	1467	17	***4***
94b	rnd-subrnd	884483	629813	0.0919	0.0003	3.0646	0.0988	0.2419	0.0078	0.9950	1465	6	1396	40	5.2			
97	rnd-subrnd	361071	145046	0.0927	0.0003	2.9260	0.1135	0.2290	0.0089	0.9966	1481	6	1329	46	11.3		reject	
86	rnd-subrnd	166147	884	0.0929	0.0004	3.2090	0.1115	0.2505	0.0086	0.9921	1486	8	1441	44	3.3	1486	8	
120	prism	1728237	10217	0.0929	0.0005	3.2486	0.0868	0.2535	0.0067	0.9823	1487	9	1457	34	2	1487	9	
108	rnd-subrnd	54389	594	0.0936	0.0008	3.1733	0.0848	0.2460	0.0062	0.9448	1499	17	1418	32	6.0	1499	17	
116	rnd-subrnd	1388179	7246	0.0940	0.0006	3.1226	0.0757	0.2409	0.0057	0.9689	1508	11	1391	29	8.6	1508	11	
106	rnd-subrnd	806700	6671	0.0946	0.0006	3.2995	0.1214	0.2531	0.0092	0.9863	1519	11	1454	47	4.8	1519	11	
77	rnd-subrnd	523621	2151	0.0960	0.0007	3.3501	0.1511	0.2530	0.0113	0.9873	1549	13	1454	58	6.8	1549	13	
23	rnd-subrnd	149623	62331	0.0981	0.0005	3.5075	0.1192	0.2594	0.0087	0.9876	1588	10	1487	44	7.1	1588	10	
102	rnd-subrnd	29811	435	0.0985	0.0017	0.3288	0.0105	0.0242	0.0006	0.8393	1597	32	154	4	91.4		reject	
115	rnd-subrnd	162294	927	0.0989	0.0011	2.7941	0.1279	0.2050	0.0091	0.9706	1603	21	1202	49	27.4		reject	

Chase Formation, Chase quartzite Depositional age: Late Devonian n= 86

Zircon 40 um Location (UTM): 431540E, 5554274N

Grain	shape	^{206}Pb cps	^{206}Pb/^{204}Pb	^{207}Pb/^{206}Pb	± (2σ)	^{207}Pb/^{235}U	± (2σ)	^{206}Pb/^{238}U	± (2σ)	rho	Model Ages ^{207}Pb/^{206}Pb	± (2σ)	^{206}Pb/^{238}U	± (2σ)	% disc.	Best Age (Ma)	± (2σ)	*interp type*
53	rnd-subrnd	1781500	11945	0.0990	0.0007	2.8240	0.1033	0.2068	0.0074	0.9803	1606	13	1212	40	26.9		reject	
6	prism	222496	1615	0.0991	0.0004	3.6512	0.1115	0.2673	0.0081	0.9912	1606	8	1527	41	5.5	1606	8	
101	rnd-subrnd	1303605	17098	0.0995	0.0007	3.6823	0.1106	0.2685	0.0079	0.9747	1614	13	1533	40	5.6	1614	13	
46	rnd-subrnd	483161	21804	0.0995	0.0007	3.6766	0.1121	0.2680	0.0080	0.9763	1615	12	1531	40	5.8	1615	12	
83	rnd-subrnd	1069421	4680	0.0996	0.0004	3.6057	0.1335	0.2626	0.0097	0.9937	1616	8	1503	49	7.8	1616	8	
33	rnd-subrnd	548627	infinite	0.1005	0.0004	3.7471	0.1428	0.2704	0.0102	0.9945	1634	7	1543	52	6.3	1634	7	
126	prism	469920	4409	0.1005	0.0005	3.7920	0.0946	0.2735	0.0067	0.9769	1634	10	1559	34	5	1634	10	
85	rnd-subrnd	1069676	4636	0.1007	0.0003	3.7523	0.1268	0.2703	0.0091	0.9957	1637	6	1542	46	6.5	1637	6	
107	rnd-subrnd	566859	7009	0.1008	0.0006	3.8600	0.0994	0.2778	0.0070	0.9726	1638	11	1580	35	4.0	1638	11	
41	rnd-subrnd	473150	842458	0.1009	0.0004	3.5299	0.1172	0.2537	0.0084	0.9927	1641	7	1457	43	12.5		reject	
90	rnd-subrnd	437635	infinite	0.1009	0.0003	3.8743	0.1485	0.2784	0.0106	0.9959	1641	6	1583	53	4.0	1641	6	
31	rnd-subrnd	345280	infinite	0.1033	0.0005	3.9484	0.1474	0.2771	0.0103	0.9920	1685	9	1577	52	7.2	1685	9	
18	rnd-subrnd	316329	3798	0.1048	0.0003	4.0069	0.1268	0.2773	0.0087	0.9953	1711	6	1578	44	8.7	1711	6	
10	prism	522852	3251	0.1049	0.0004	3.7647	0.0949	0.2604	0.0065	0.9894	1712	7	1492	33	14.4		reject	
125	prism	814863	2812	0.1051	0.0010	3.7937	0.0973	0.2619	0.0063	0.9320	1715	17	1500	32	14		reject	
118	rnd-subrnd	388657	3359	0.1052	0.0005	4.2436	0.1315	0.2925	0.0089	0.9861	1718	9	1654	44	4	1718	9	
38	rnd-subrnd	625458	266360	0.1053	0.0004	3.5296	0.1331	0.2432	0.0091	0.9936	1719	8	1403	47	20.4		reject	
119	rnd-subrnd	77992	608	0.1055	0.0007	4.1616	0.1160	0.2860	0.0077	0.9682	1724	13	1622	39	7	1724	13	
99	rnd-subrnd	679263	37586	0.1059	0.0006	4.2613	0.1391	0.2919	0.0094	0.9831	1730	11	1651	47	5.2	1730	11	
30	rnd-subrnd	964191	38552	0.1061	0.0004	3.9525	0.1462	0.2701	0.0099	0.9946	1734	7	1541	50	12.5		reject	
12	prism	485928	12599	0.1074	0.0003	4.0672	0.1135	0.2746	0.0076	0.9938	1756	6	1564	38	12.3		reject	
40	rnd-subrnd	312319	808540	0.1078	0.0005	4.3839	0.1586	0.2950	0.0106	0.9931	1762	8	1667	53	6.1	1762	8	
79	rnd-subrnd	1225255	5791	0.1087	0.0005	4.4129	0.2222	0.2944	0.0148	0.9963	1778	8	1664	73	7.3	1778	8	
19	rnd-subrnd	537971	4787	0.1089	0.0003	4.1611	0.1352	0.2771	0.0090	0.9951	1781	6	1577	45	12.9		reject	
54	rnd-subrnd	62245	204	0.1092	0.0027	0.3744	0.0155	0.0249	0.0008	0.8084	1785	44	158	5	92.2		reject	
20	rnd-subrnd	1118804	7747	0.1107	0.0005	4.4650	0.1582	0.2926	0.0103	0.9931	1810	8	1655	51	9.7	1810	8	
73	rnd-subrnd	1773755	13771	0.1121	0.0005	4.7783	0.1836	0.3091	0.0118	0.9934	1834	8	1736	58	6.1	1834	8	
11	prism	569967	13480	0.1133	0.0004	4.2125	0.1173	0.2696	0.0075	0.9935	1853	6	1539	38	19.0		reject	
110	rnd-subrnd	2038860	11896	0.1139	0.0007	4.1015	0.1266	0.2612	0.0079	0.9818	1862	11	1496	40	22.0		reject	
50	rnd-subrnd	2246272	34003	0.1158	0.0008	4.7306	0.1368	0.2963	0.0083	0.9743	1892	12	1673	41	13.2		reject	
3	prism	918357	7417	0.1172	0.0003	4.9598	0.1579	0.3069	0.0097	0.9963	1914	5	1725	48	11.2		reject	
82	rnd-subrnd	2204895	9276	0.1190	0.0003	4.8491	0.1916	0.2956	0.0117	0.9973	1941	5	1670	58	15.8		reject	
27	rnd-subrnd	566227	38937	0.1198	0.0005	5.2430	0.1847	0.3175	0.0111	0.9937	1953	7	1777	54	10.3		reject	
44	rnd-subrnd	692850	81069	0.1200	0.0008	5.2824	0.1644	0.3193	0.0097	0.9776	1956	12	1786	47	9.9	1956	12	
76	rnd-subrnd	157417	1177	0.1214	0.0006	5.6578	0.2232	0.3380	0.0132	0.9919	1977	9	1877	63	5.8	1977	9	

Chase Formation, Chase quartzite Depositional age: Late Devonian n= 86

Zircon 40 um Location (UTM): 431540E, 5554274N

											Model Ages							
Grain	**shape**	**^{206}Pb cps**	**^{206}Pb/^{204}Pb**	**^{207}Pb/^{206}Pb**	**± (2σ)**	**^{207}Pb/^{235}U**	**± (2σ)**	**^{206}Pb/^{238}U**	**± (2σ)**	**rho**	**^{207}Pb/^{206}Pb**	**± (2σ)**	**^{206}Pb/^{238}U**	**± (2σ)**	**% disc.**	**Best Age (Ma)**	**± (2σ)**	*interp type*
121	prism	963236	5443	0.1228	0.0008	5.8886	0.1459	0.3478	0.0083	0.9632	1997	12	1924	40	4	1997	12	
9	prism	611925	3633	0.1251	0.0004	5.8241	0.1435	0.3376	0.0083	0.9921	2031	5	1875	40	8.8	2031	5	
49	rnd-subrnd	39109	158	0.1377	0.0107	0.4927	0.0429	0.0259	0.0010	0.4556	2199	135	165	6	93.6		reject	
95	rnd-subrnd	327551	290912	0.1492	0.0006	8.1854	0.2783	0.3979	0.0134	0.9939	2337	6	2159	62	8.9	2337	6	
55	rnd-subrnd	47893	132	0.1586	0.0100	0.5703	0.0410	0.0261	0.0009	0.4868	2441	106	166	6	94.3		reject	
71	rnd-subrnd	799880	445596	0.1695	0.0007	9.4572	0.4752	0.4046	0.0203	0.9963	2553	7	2190	92	16.7		reject	
25	rnd-subrnd	483492	12350	0.1837	0.0008	11.8326	0.4037	0.4672	0.0158	0.9927	2686	7	2471	69	9.6	2686	7	
100	rnd-subrnd	506993	13558	0.1842	0.0011	12.3270	0.3559	0.4854	0.0137	0.9780	2691	10	2551	59	6.3	2691	10	
34	rnd-subrnd	684662	infinite	0.1855	0.0008	11.0287	0.4917	0.4312	0.0191	0.9949	2703	7	2311	86	17.2		reject	
13	prism	1553525	24739	0.1890	0.0005	11.5434	0.3100	0.4430	0.0118	0.9943	2733	5	2364	53	16.1		reject	
48	rnd-subrnd	1274880	50961	0.1922	0.0013	11.1082	0.4513	0.4192	0.0168	0.9859	2761	11	2257	76	21.6		reject	
26	rnd-subrnd	204001	6236	0.1952	0.0010	10.8148	0.8291	0.4018	0.0307	0.9978	2787	8	2177	140	25.7		reject	
98	rnd-subrnd	324483	infinite	0.1974	0.0008	13.6495	0.4696	0.5014	0.0171	0.9936	2805	6	2620	73	8.0	2805	6	
80	rnd-subrnd	190016	987	0.2019	0.0011	14.4837	0.5857	0.5202	0.0208	0.9903	2842	9	2700	88	6.1	2842	9	
39	rnd-subrnd	252736	24767	0.2109	0.0009	14.5619	0.5777	0.5007	0.0198	0.9943	2913	7	2617	84	12.3		reject	
28	rnd-subrnd	210479	15255	0.2172	0.0008	15.9656	0.6292	0.5332	0.0209	0.9951	2960	6	2755	87	8.5	2960	6	
32	rnd-subrnd	520980	infinite	0.2208	0.0009	16.1695	0.5620	0.5312	0.0184	0.9938	2986	6	2747	77	9.8	2986	6	
51	rnd-subrnd	164491	7893	0.2226	0.0015	16.7014	0.5479	0.5443	0.0175	0.9794	2999	11	2801	73	8.1	2999	11	
47	rnd-subrnd	280759	19343	0.2542	0.0018	19.3391	0.6526	0.5518	0.0182	0.9779	3211	11	2833	75	14.5		reject	

Slocan Group, 08TWJK357
Zircon 40 um

Depositional age: Late Triassic
Location (UTM): 438591E, 5574507N

Grain	^{206}Pb cps	$^{206}Pb/^{204}Pb$	$^{207}Pb/^{206}Pb$	± (2σ)	$^{207}Pb/^{235}U$	± (2σ)	$^{206}Pb/^{238}U$	± (2σ)	rho	Model Ages $^{207}Pb/^{206}Pb$	± (2σ)	$^{206}Pb/^{238}U$	± (2σ)	% disc.	n= 67 -10%<disc.<10% age (Ma)	± (2σ)	n= 42 disc. <-10% age (Ma)	± (2σ)
GJ1-3	64161	3048	0.0601	0.0010	0.8077	0.0500	0.0975	0.0058	0.9615	606	36	600	34	1.2				
GJ1-4	56819	2583	0.0603	0.0011	0.8321	0.0558	0.1001	0.0065	0.9622	614	39	615	38	-0.1				
GJ1-5	56673	1736	0.0606	0.0013	0.8163	0.0459	0.0977	0.0051	0.9264	624	45	601	30	3.8				
GJ1-6	53331	1234	0.0603	0.0011	0.7903	0.0594	0.0951	0.0069	0.9681	614	40	586	41	4.8				
GJ1-7	62719	1279	0.0602	0.0012	0.8020	0.0537	0.0966	0.0062	0.9565	612	42	594	36	3.0				
GJ1-8	59330	5479	0.0597	0.0011	0.7632	0.0415	0.0927	0.0047	0.9407	594	39	571	28	3.9				
GJ1-9	97974	2089	0.0599	0.0010	0.8241	0.0475	0.0997	0.0055	0.9576	602	36	613	32	-1.9				
GJ1-10	87446	2353	0.0597	0.0010	0.7724	0.0481	0.0939	0.0056	0.9628	592	36	578	33	2.5				
GJ1-11	114573	1640	0.0606	0.0012	0.7914	0.0494	0.0947	0.0056	0.9503	626	41	583	33	7.3				
GJ1-12	104122	1331	0.0597	0.0011	0.7641	0.0515	0.0929	0.0060	0.9651	592	38	572	36	3.5				
08TWJK357-48	30989	2001	0.0491	0.0011	0.2329	0.0179	0.0344	0.0025	0.9598	151	50	218	16	-44.9		reject	218	16
08TWJK357-45	33635	1323	0.0493	0.0010	0.2348	0.0159	0.0345	0.0022	0.9529	163	47	219	14	-34.5		reject	219	14
08TWJK357-119	142213	2384	0.0498	0.0004	0.2390	0.0133	0.0348	0.0019	0.9871	187	21	220	12	-18.1		reject	220	12
08TWJK357-110	41022	1130	0.0488	0.0007	0.2390	0.0162	0.0355	0.0024	0.9788	140	32	225	15	-62.2		reject	225	15
08TWJK357-66	52583	1640	0.0488	0.0006	0.2413	0.0271	0.0358	0.0040	0.9945	140	27	227	25	-63.6		reject	227	25
08TWJK375-81	32095	805	0.0473	0.0010	0.2413	0.0151	0.0370	0.0022	0.9386	67	50	234	13	-254.8		reject	234	13
08TWJK357-60	64149	4871	0.0513	0.0012	0.2720	0.0189	0.0385	0.0025	0.9386	253	54	243	16	3.9	243	16		
08TWJK357-69	50419	2250	0.0490	0.0005	0.2625	0.0151	0.0388	0.0022	0.9852	148	23	246	14	-66.7		reject	246	14
08TWJK357-10	14596	418	0.0479	0.0016	0.2572	0.0205	0.0389	0.0028	0.9112	95	76	246	18	-163.3		reject	246	18
08TWJK357-54	85324	4892	0.0502	0.0008	0.2704	0.0204	0.0391	0.0029	0.9766	204	37	247	18	-21.8		reject	247	18
08TWJK357-4	31246	920	0.0496	0.0013	0.2725	0.0549	0.0399	0.0080	0.9910	174	62	252	49	-45.7		reject	252	49
08TWJK357-44	10249	611	0.0461	0.0023	0.2631	0.0216	0.0414	0.0027	0.7911	4	117	261	17	-6534.2		reject	261	17
08TWJK357-2	12797	410	0.0490	0.0012	0.2815	0.0208	0.0416	0.0029	0.9444	149	56	263	18	-78.2		reject	263	18
08TWJK357-68	75520	2562	0.0499	0.0005	0.2921	0.0186	0.0424	0.0027	0.9869	191	24	268	16	-41.0		reject	268	16
08TWJK357-57	28306	1844	0.0509	0.0010	0.2981	0.0205	0.0425	0.0028	0.9555	235	46	268	17	-14.6		reject	268	17
08TWJK357-1	16747	535	0.0494	0.0011	0.2943	0.0253	0.0432	0.0036	0.9637	168	53	273	22	-63.2		reject	273	22
08TWJK357-92	99645	2169	0.0507	0.0005	0.3029	0.0179	0.0433	0.0025	0.9847	228	24	273	16	-20.4		reject	273	16
08TWJK357-116	95253	1733	0.0506	0.0005	0.3071	0.0161	0.0440	0.0023	0.9848	221	21	278	14	-26.0		reject	278	14
08TWJK357-34	47831	2238	0.0508	0.0009	0.3090	0.0281	0.0441	0.0039	0.9790	231	42	278	24	-21.0		reject	278	24
08TWJK375-89	37535	799	0.0500	0.0009	0.3223	0.0231	0.0467	0.0032	0.9666	196	42	294	20	-51.0		reject	294	20
08TWJK375-84	61821	1019	0.0504	0.0006	0.3269	0.0203	0.0470	0.0029	0.9809	216	28	296	18	-38.2		reject	296	18
08TWJK357-9	57011	2322	0.0512	0.0009	0.3324	0.0316	0.0471	0.0044	0.9828	252	40	296	27	-18.2		reject	296	27
08TWJK375-88	55239	736	0.0592	0.0021	0.3885	0.0356	0.0476	0.0040	0.9241	573	74	300	25	48.7		reject		
08TWJK357-51	112583	7994	0.0520	0.0009	0.3525	0.0221	0.0492	0.0030	0.9636	285	38	309	18	-8.7	309	18		

Slocan Group, 08TWJK357

Zircon 40 um

Depositional age: Late Triassic

Location (UTM): 438591E, 5574507N

Grain	^{206}Pb cps	^{206}Pb/^{204}Pb	^{207}Pb/^{206}Pb	± (2σ)	^{207}Pb/^{235}U	± (2σ)	^{206}Pb/^{238}U	± (2σ)	rho	Model Ages ^{207}Pb/^{206}Pb	± (2σ)	^{206}Pb/^{238}U	± (2σ)	% disc.	n= 67 -10%<disc.<10% age (Ma)	± (2σ)	n= 42 disc. <-10% age (Ma)	± (2σ)
08TWJK357-122	127561	2167	0.0518	0.0005	0.3514	0.0203	0.0492	0.0028	0.9870	275	21	310	17	-13.0		reject	310	17
08TWJK357-101	78982	1234	0.0517	0.0006	0.3660	0.0209	0.0514	0.0029	0.9799	270	26	323	18	-20.0		reject	323	18
08TWJK375-72	43227	948	0.0515	0.0007	0.4125	0.0256	0.0581	0.0035	0.9784	263	29	364	21	-39.4		reject	364	21
08TWJK357-105	46034	634	0.0517	0.0007	0.4172	0.0245	0.0585	0.0033	0.9702	272	32	367	20	-35.7		reject	367	20
08TWJK357-42	60909	2210	0.0531	0.0009	0.4323	0.0255	0.0591	0.0033	0.9570	333	38	370	20	-11.4		reject	370	20
08TWJK375-79	180606	3838	0.0532	0.0005	0.4353	0.0267	0.0593	0.0036	0.9874	338	22	372	22	-10.3		reject	372	22
08TWJK357-64	58780	1431	0.0515	0.0007	0.4238	0.0259	0.0597	0.0036	0.9757	263	31	374	22	-43.1		reject	374	22
08TWJK357-128	17748	251	0.0471	0.0013	0.4058	0.0255	0.0624	0.0035	0.9047	56	63	390	21	-611.1		reject	390	21
08TWJK357-63	92301	503	0.0552	0.0016	0.4852	0.0462	0.0638	0.0058	0.9523	419	64	399	35	5.0	399	35		
08TWJK375-85	12334	222	0.0456	0.0025	0.4177	0.0344	0.0665	0.0040	0.7347	-25	130	415	24	1802.1		reject		
08TWJK357-114	161450	5961	0.0544	0.0005	0.5030	0.0293	0.0670	0.0039	0.9894	389	19	418	23	-7.7	418	23		
08TWJK357-103	7992	110	0.0338	0.0068	0.3398	0.0789	0.0730	0.0084	0.4951	-809	495	454	50	161.9		reject		
08TWJK357-111	21227	820	0.0514	0.0012	0.5360	0.0309	0.0757	0.0040	0.9097	258	54	470	24	-85.6		reject	470	24
08TWJK357-93	44021	970	0.0535	0.0011	0.5777	0.0355	0.0783	0.0046	0.9453	350	45	486	27	-40.5		reject	486	27
08TWJK357-22	58906	2513	0.0555	0.0011	0.6118	0.0449	0.0799	0.0057	0.9652	433	42	496	34	-15.1		reject	496	34
08TWJK357-130	96211	1406	0.0568	0.0005	0.6330	0.0522	0.0809	0.0066	0.9940	482	20	501	39	-4.2	501	39		
08TWJK357-36	64881	4161	0.0573	0.0010	0.6564	0.0620	0.0831	0.0077	0.9844	503	36	515	46	-2.5	515	46		
08TWJK357-113	118865	3245	0.0577	0.0005	0.6767	0.0436	0.0851	0.0054	0.9915	518	18	526	32	-1.6	526	32		
08TWJK375-71	29336	609	0.0551	0.0010	0.6532	0.0379	0.0859	0.0048	0.9522	417	39	531	28	-28.4		reject	531	28
08TWJK357-115	80058	1557	0.0566	0.0005	0.6884	0.0432	0.0882	0.0055	0.9883	476	21	545	32	-15.1		reject	545	32
08TWJK357-37	39059	1598	0.0564	0.0010	0.6881	0.0563	0.0884	0.0071	0.9751	470	40	546	42	-17.0		reject	546	42
08TWJK357-17	129728	6920	0.0582	0.0010	0.7255	0.0509	0.0904	0.0062	0.9723	538	35	558	36	-3.8	558	36		
08TWJK357-31	34754	995	0.0583	0.0010	0.7282	0.0553	0.0906	0.0067	0.9756	541	36	559	40	-3.4	559	40		
08TWJK357-11	25457	813	0.0580	0.0011	0.7529	0.0562	0.0942	0.0068	0.9689	529	40	580	40	-10.1		reject	580	40
08TWJK357-35	46398	2617	0.0591	0.0010	0.7757	0.0475	0.0953	0.0056	0.9605	569	37	587	33	-3.2	587	33		
08TWJK357-40	14082	530	0.0540	0.0014	0.7102	0.0465	0.0954	0.0057	0.9171	372	58	587	34	-60.8		reject	587	34
08TWJK357-106	125146	1629	0.0598	0.0005	0.7917	0.0539	0.0960	0.0065	0.9925	597	18	591	38	1.1	591	38		
08TWJK357-50	37818	2007	0.0589	0.0012	0.8146	0.0631	0.1003	0.0075	0.9664	563	43	616	44	-9.9	616	44		
08TWJK357-99	33654	641	0.0592	0.0009	0.8541	0.0601	0.1046	0.0072	0.9764	576	33	641	42	-11.9		reject	641	42
08TWJK375-77	194967	4159	0.0612	0.0005	0.9510	0.0609	0.1127	0.0072	0.9927	646	17	689	41	-7.0	689	41		
08TWJK357-12	250937	7428	0.0659	0.0012	1.0655	0.1003	0.1172	0.0108	0.9821	804	37	715	62	11.7		reject		
08TWJK357-16	33991	1249	0.0762	0.0013	1.2435	0.0792	0.1184	0.0073	0.9644	1099	33	721	42	36.3		reject		
08TWJK357-41	61627	2874	0.0664	0.0011	1.1301	0.0919	0.1235	0.0098	0.9772	818	36	751	56	8.8	818	36		
08TWJK375-83	137966	617	0.0812	0.0050	1.4423	0.1424	0.1289	0.0099	0.7808	1225	117	782	56	38.4		reject		
08TWJK357-15	159998	7500	0.0686	0.0011	1.3936	0.0888	0.1473	0.0091	0.9692	887	32	886	51	0.1	887	32		
08TWJK357-97	9999	167	0.0586	0.0033	1.2081	0.1338	0.1495	0.0142	0.8584	552	119	898	79	-67.3		reject	898	79
08TWJK357-96	11158	198	0.0691	0.0020	1.8105	0.1151	0.1900	0.0107	0.8885	902	59	1121	58	-26.5		reject	902	59

Slocan Group, 08TWJK357

Zircon 40 um

Depositional age: Late Triassic

Location (UTM): 438591E, 5574507N

Grain	^{206}Pb cps	$^{206}Pb/^{204}Pb$	$^{207}Pb/^{206}Pb$	± (2σ)	$^{207}Pb/^{235}U$	± (2σ)	$^{206}Pb/^{238}U$	± (2σ)	rho	Model Ages $^{207}Pb/^{206}Pb$	± (2σ)	$^{206}Pb/^{238}U$	± (2σ)	% disc.	n= 67 -10%<disc.<10% age (Ma)	± (2σ)	n= 42 disc. <-10% age (Ma)	± (2σ)
08TWJK357-30	51639	1722	0.0702	0.0012	1.5753	0.1198	0.1628	0.0121	0.9756	934	34	972	67	-4.4	934	34		
08TWJK357-53	103593	3513	0.0711	0.0011	1.5318	0.0879	0.1562	0.0086	0.9602	961	32	936	48	2.8	961	32		
08TWJK357-120	75726	1358	0.0719	0.0007	1.6302	0.1167	0.1645	0.0117	0.9898	982	21	982	64	0.1	982	21		
08TWJK357-18	55139	3224	0.0720	0.0013	1.6801	0.1266	0.1693	0.0124	0.9719	986	36	1008	68	-2.5	986	36		
08TWJK375-73	100424	2879	0.0721	0.0006	1.5387	0.1009	0.1547	0.0101	0.9919	990	17	927	56	6.8	990	17		
08TWJK357-94	74159	1614	0.0731	0.0008	1.6969	0.1075	0.1684	0.0105	0.9850	1016	22	1003	58	1.4	1016	22		
08TWJK357-7	38031	1356	0.0731	0.0013	1.7233	0.1612	0.1709	0.0157	0.9811	1017	36	1017	86	0.0	1017	36		
08TWJK357-5	34261	1145	0.0731	0.0014	1.6618	0.1216	0.1648	0.0116	0.9659	1018	38	983	64	3.6	1018	38		
08TWJK357-49	91184	7246	0.0738	0.0012	1.7598	0.1278	0.1729	0.0122	0.9752	1036	32	1028	67	0.8	1036	32		
08TWJK357-127	21045	283	0.0753	0.0013	1.6660	0.1157	0.1605	0.0108	0.9703	1077	33	959	60	11.7	reject			
08TWJK357-38	98631	3672	0.0753	0.0012	1.8861	0.1133	0.1816	0.0105	0.9645	1077	32	1076	57	0.2	1077	32		
08TWJK375-74	60549	1572	0.0760	0.0007	1.9672	0.1617	0.1878	0.0153	0.9939	1095	18	1109	83	-1.4	1095	18		
08TWJK357-104	69311	1359	0.0770	0.0006	2.1233	0.1717	0.2001	0.0161	0.9948	1120	16	1176	86	-5.4	1120	16		
08TWJK357-59	32909	2421	0.0776	0.0014	1.9921	0.1318	0.1863	0.0119	0.9636	1136	35	1101	64	3.3	1136	35		
08TWJK357-27	55180	1596	0.0791	0.0014	2.0970	0.1544	0.1924	0.0138	0.9724	1174	34	1134	74	3.7	1174	34		
08TWJK357-28	114064	2227	0.0792	0.0012	2.1561	0.1607	0.1975	0.0144	0.9776	1176	31	1162	77	1.3	1176	31		
08TWJK375-87	13445	226	0.0793	0.0021	2.7014	0.1740	0.2471	0.0145	0.9087	1180	52	1423	74	-23.1	reject		1180	52
08TWJK357-26	90141	2160	0.0794	0.0013	2.2104	0.1682	0.2019	0.0150	0.9773	1182	32	1185	80	-0.3	1182	32		
08TWJK357-102	243618	3450	0.0800	0.0007	2.1197	0.1307	0.1922	0.0117	0.9901	1197	17	1133	63	5.8	1197	17		
08TWJK357-118	217012	2426	0.0810	0.0008	1.8494	0.1027	0.1656	0.0091	0.9854	1222	18	988	50	20.7	reject			
08TWJK357-91	100501	2130	0.0820	0.0010	2.2864	0.1828	0.2023	0.0160	0.9890	1244	23	1188	85	5.0	1244	23		
08TWJK357-129	124042	1700	0.0823	0.0007	2.2754	0.1655	0.2006	0.0145	0.9939	1252	16	1179	77	6.4	1252	16		
08TWJK357-67	82017	2738	0.0843	0.0006	2.6383	0.1555	0.2269	0.0133	0.9914	1301	15	1318	69	-1.5	1301	15		
08TWJK375-90	29233	526	0.0872	0.0013	2.7370	0.1608	0.2276	0.0129	0.9669	1365	29	1322	68	3.5	1365	29		
08TWJK357-125	283618	2671	0.0882	0.0007	1.9357	0.2088	0.1592	0.0171	0.9973	1386	15	953	95	33.6	reject			
08TWJK357-23	69278	2271	0.0884	0.0015	2.6492	0.2716	0.2175	0.0220	0.9853	1390	33	1268	115	9.6	1390	33		
08TWJK375-78	159443	3533	0.0884	0.0008	2.8642	0.2232	0.2349	0.0182	0.9939	1392	16	1360	94	2.6	1392	16		
08TWJK357-52	33679	2215	0.0885	0.0015	2.9848	0.2112	0.2447	0.0168	0.9713	1393	32	1411	87	-1.5	1393	32		
08TWJK357-121	135615	1783	0.0886	0.0007	2.8416	0.1979	0.2326	0.0161	0.9937	1395	15	1348	84	3.7	1395	15		
08TWJK357-124	306766	4685	0.0891	0.0006	2.8217	0.1645	0.2298	0.0133	0.9926	1406	14	1333	69	5.7	1406	14		
08TWJK357-62	206404	5659	0.0892	0.0006	3.0001	0.1880	0.2440	0.0152	0.9939	1408	13	1407	78	0.0	1408	13		
08TWJK357-13	130147	6363	0.0893	0.0014	2.9013	0.1939	0.2355	0.0153	0.9724	1412	30	1363	79	3.8	1412	30		
08TWJK375-80	151779	2719	0.0894	0.0007	2.7970	0.2199	0.2270	0.0178	0.9950	1412	15	1319	93	7.3	1412	15		
08TWJK357-24	40897	1297	0.0895	0.0015	3.0116	0.2509	0.2439	0.0199	0.9806	1416	31	1407	102	0.7	1416	31		
08TWJK357-56	254734	19032	0.0896	0.0014	3.0063	0.2354	0.2435	0.0187	0.9805	1416	29	1405	96	0.9	1416	29		
08TWJK357-112	276404	6469	0.0897	0.0016	2.2399	0.2659	0.1810	0.0212	0.9883	1420	34	1073	115	26.5	reject			
08TWJK375-76	117077	2049	0.0898	0.0007	2.9363	0.1682	0.2373	0.0135	0.9908	1420	15	1373	70	3.7	1420	15		

Slocan Group, 08TWJK357 Depositional age: Late Triassic

Zircon 40 um Location (UTM): 438591E, 5574507N

Grain	^{206}Pb cps	$^{206}Pb/^{204}Pb$	$^{207}Pb/^{206}Pb$	± (2σ)	$^{207}Pb/^{235}U$	± (2σ)	$^{206}Pb/^{238}U$	± (2σ)	rho	Model Ages $^{207}Pb/^{206}Pb$	± (2σ)	$^{206}Pb/^{238}U$	± (2σ)	% disc.	n= 67 -10%<disc.<10% age (Ma)	± (2σ)	n= 42 disc. <-10% age (Ma)	± (2σ)
08TWJK357-123	158917	2457	0.0899	0.0007	3.0239	0.2037	0.2438	0.0163	0.9933	1424	15	1407	84	1.4	1424	15		
08TWJK357-46	249723	10935	0.0900	0.0016	2.5393	0.2199	0.2046	0.0173	0.9784	1426	34	1200	92	17.4		reject		
08TWJK357-6	140981	5310	0.0906	0.0014	3.2445	0.2187	0.2597	0.0170	0.9726	1438	30	1488	87	-3.9	1438	30		
08TWJK357-109	633143	12040	0.0908	0.0006	2.9807	0.1868	0.2381	0.0148	0.9944	1442	13	1377	77	5.0	1442	13		
08TWJK357-25	189143	7396	0.0935	0.0015	2.9821	0.2957	0.2312	0.0226	0.9873	1499	30	1341	117	11.6		reject		
08TWJK357-43	77449	2713	0.0955	0.0018	2.9493	0.2797	0.2241	0.0208	0.9799	1537	35	1303	109	16.8		reject		
08TWJK357-98	469549	7931	0.0961	0.0007	3.4956	0.1982	0.2638	0.0148	0.9906	1550	15	1509	75	3.0	1550	15		
08TWJK357-95	51124	863	0.0992	0.0008	3.4424	0.2235	0.2518	0.0162	0.9913	1609	16	1448	83	11.2		reject		
08TWJK357-8	5042	241	0.0998	0.0031	4.6241	0.4349	0.3362	0.0299	0.9455	1620	56	1868	143	-17.7		reject	1620	56
08TWJK357-3	30719	887	0.0999	0.0017	3.8581	0.3150	0.2802	0.0224	0.9768	1621	32	1592	112	2.0	1621	32		
08TWJK357-32	152112	4105	0.1006	0.0016	4.0052	0.2834	0.2889	0.0199	0.9751	1634	29	1636	99	-0.1	1634	29		
08TWJK375-86	216088	3773	0.1006	0.0007	3.8140	0.2579	0.2749	0.0185	0.9941	1636	14	1566	93	4.8	1636	14		
08TWJK357-58	189095	11630	0.1007	0.0016	4.0849	0.2889	0.2943	0.0203	0.9755	1636	29	1663	100	-1.9	1636	29		
08TWJK357-108	162161	3701	0.1010	0.0007	3.7449	0.2437	0.2690	0.0174	0.9936	1642	14	1536	88	7.3	1642	14		
08TWJK357-55	158877	5221	0.1010	0.0017	4.0178	0.2261	0.2886	0.0155	0.9562	1642	30	1634	77	0.5	1642	30		
08TWJK357-20	99672	4665	0.1027	0.0016	4.1265	0.2830	0.2913	0.0194	0.9728	1674	29	1648	96	1.8	1674	29		
08TWJK357-117	497532	6374	0.1033	0.0007	3.3530	0.3098	0.2354	0.0217	0.9970	1685	13	1363	112	21.2		reject		
08TWJK357-65	151870	4004	0.1037	0.0007	4.2309	0.2617	0.2959	0.0182	0.9934	1692	13	1671	90	1.4	1692	13		
08TWJK357-29	139154	2897	0.1040	0.0016	4.2712	0.2799	0.2979	0.0190	0.9715	1697	28	1681	94	1.1	1697	28		
08TWJK357-33	116315	4805	0.1041	0.0016	4.3728	0.2548	0.3047	0.0171	0.9637	1698	28	1715	84	-1.1	1698	28		
08TWJK357-61	382967	9131	0.1062	0.0007	4.6957	0.2585	0.3207	0.0175	0.9920	1735	13	1793	85	-3.8	1735	13		
08TWJK375-75	235296	4781	0.1085	0.0007	4.5992	0.3014	0.3074	0.0200	0.9946	1774	12	1728	98	3.0	1774	12		
08TWJK357-14	94618	4201	0.1090	0.0017	4.6364	0.3375	0.3085	0.0219	0.9769	1783	28	1733	107	3.2	1783	28		
08TWJK375-82	41247	998	0.1213	0.0017	4.9928	0.3600	0.2985	0.0211	0.9818	1976	24	1684	104	16.8		reject		
08TWJK357-126	57214	801	0.1217	0.0018	4.1140	0.3127	0.2451	0.0183	0.9805	1981	26	1413	94	31.9		reject		
08TWJK357-19	76020	3043	0.1251	0.0029	5.2825	0.5022	0.3063	0.0282	0.9701	2030	40	1723	138	17.2		reject		
08TWJK357-47	232706	11944	0.1268	0.0031	5.9641	0.6604	0.3412	0.0368	0.9753	2054	43	1892	175	9.1	2054	43		
08TWJK357-39	62946	2861	0.1375	0.0022	7.0795	0.5437	0.3733	0.0280	0.9773	2196	28	2045	130	8.0	2196	28		
08TWJK357-21	199314	5309	0.1646	0.0025	10.7286	0.7391	0.4729	0.0317	0.9745	2503	26	2496	137	0.3	2503	26		
08TWJK357-107	431411	4653	0.2395	0.0031	17.9236	1.0588	0.5428	0.0313	0.9750	3117	21	2795	129	12.7		reject		